



HAL
open science

Modeling intestinal glucose absorption with oral D-Xylose test for the study of its contribution on postprandial glucose response: studies in minipigs and in humans

Rébecca Goutchtat

► **To cite this version:**

Rébecca Goutchtat. Modeling intestinal glucose absorption with oral D-Xylose test for the study of its contribution on postprandial glucose response: studies in minipigs and in humans. Tissues and Organs [q-bio.TO]. Université de Lille, 2023. English. NNT : 2023ULILS051 . tel-04426309

HAL Id: tel-04426309

<https://theses.hal.science/tel-04426309>

Submitted on 30 Jan 2024

HAL is a multi-disciplinary open access archive for the deposit and dissemination of scientific research documents, whether they are published or not. The documents may come from teaching and research institutions in France or abroad, or from public or private research centers.

L'archive ouverte pluridisciplinaire **HAL**, est destinée au dépôt et à la diffusion de documents scientifiques de niveau recherche, publiés ou non, émanant des établissements d'enseignement et de recherche français ou étrangers, des laboratoires publics ou privés.

Thèse de doctorat d'université
Pour l'obtention du titre de
DOCTEUR DE L'UNIVERSITÉ DE LILLE

Discipline : Physiologie

Présentée par

Rébecca GOUTCHTAT

Modeling intestinal glucose absorption with oral D-Xylose test for
the study of its contribution on postprandial glucose response:
studies in minipigs and in humans

Présentée et soutenue publiquement le 1^{er} décembre 2023

JURY

Président :

Monsieur le Docteur David VAL-LAILLET

Rapporteurs :

Madame le Professeur Fanny STORCK

Madame le Docteur Maude LE GALL

Examineurs :

Madame le Docteur Julie-Anne NAZARE

Monsieur le Professeur Jean-François GAUTIER

Directeurs de thèse :

Monsieur le Docteur Thomas HUBERT

Monsieur le Professeur François PATTOU

Remerciements

A mes directeurs de thèse,

Je suis très honorée de vous avoir eu comme encadrants de thèse et mentors. Vous m'avez permis de me projeter réellement en tant que chercheuse et de trouver ma voie. Je tiens à vous exprimer toute ma gratitude et mon profond respect et j'espère que nous aurons l'occasion d'établir de belles collaborations dans le futur.

Au Dr Thomas HUBERT, Maître de Conférences en Chirurgie à l'Université de Lille : je te remercie grandement pour avoir donné ces fameux enseignements à l'EnvA au moment où j'étais en pleine phase de questionnement, pour m'avoir intégrée au sein du laboratoire et pour avoir encadré mon travail depuis le Master 2 avec pragmatisme et bienveillance. Je souhaiterais t'exprimer ma gratitude pour m'avoir permis de m'épanouir au sein de l'U1190 et du Dhure, scientifiquement et personnellement, pour m'avoir donné ta confiance sur ton sujet de recherche et pour les nombreuses opportunités d'échanges et de réseaux professionnels au sein de congrès nationaux et internationaux relatifs à l'utilisation des animaux à des fins scientifiques.

Au Pr François PATTOU, directeur de l'U1190 et chef du service de Chirurgie Générale et Endocrinienne du CHU de Lille : je vous remercie grandement d'avoir souhaité intégrer ma direction de thèse, pour m'avoir accordé votre confiance sur ce sujet transdisciplinaire et pour m'avoir encadrée avec intuition et enthousiasme. Je souhaiterais vous témoigner ma gratitude pour avoir su discerner mon potentiel, pour m'avoir permis de donner le meilleur de moi-même, pour votre charisme et votre vision passionnée de la recherche et de la médecine, et pour les nombreuses opportunités de présentations lors de congrès internationaux prestigieux.

A mes juges,

Je vous remercie très chaleureusement de me faire l'honneur de juger mon travail et d'assister à ma soutenance de thèse.

Au Pr Fanny STORCK, Professeure à VetAgro Sup Lyon, que je ne pourrai jamais suffisamment remercier pour ses précieux conseils tout au long de mon parcours vétérinaire, pour m'avoir guidée judicieusement vers la voie de la recherche et pour son soutien pour la suite de ma carrière.

Au Dr Maude LE GALL, Directrice de Recherche Inserm au département d'hépatogastroentérologie du Centre de Recherche sur l'Inflammation de Paris Cité, pour sa rigueur, la qualité de son expertise sur le sujet et les échanges constructifs que nous avons pu avoir lors de notre première rencontre.

Au Dr David VAL-LAILLET, Directeur de Recherche Inrae en Neurosciences Comportementales et Nutrition de l'Institut NuMeCan à Rennes, pour sa maîtrise du modèle porcin, ses connaissances en nutrition et ses présentations toujours très pertinentes et inspirantes. Merci de m'avoir suivie tout au long de ce travail.

Au Dr Julie-Anne NAZARE, Maîtresse de Conférences à l'Université de Lyon 1 et directrice du Centre de Recherche en Nutrition Humaine Rhône-Alpes, pour la collaboration fructueuse que nous avons ensemble, pour sa gentillesse, pour son expertise sur le turnover du glucose, pour m'avoir accueillie à Lyon le temps de quelques jours et pour avoir guidé mes réflexions sur le sujet.

Au Pr Jean-François GAUTIER, chef du service de Diabétologie, Endocrinologie et Nutrition du Centre Universitaire du Diabète et de ses complications à l'Hôpital Lariboisière et chercheur Inserm à l'Institut

Necker Enfants Malades à Paris, pour son invitation au 26^{ème} Oxford Workshop de l'EASD, son regard de clinicien aguerri et sa sympathie.

A mes financeurs,

Je tiens à remercier les institutions ayant permis de financer ce projet, en particulier l'Institut National de la Santé et de la Recherche Médicale (Inserm), m'ayant généreusement attribué un Poste d'Accueil comme bourse de doctorat, ainsi que l'Agence Nationale de Recherche (n°ANR-18-CE14-0028-01) et l'European Genomic Institute for Diabetes (ANR-10-LABX-46).

Aux membres de l'U1190,

4 ans et demi avec vous, le temps est passé si vite... Un immense merci pour votre sympathie et votre aide durant tout ce travail. Que de bons moments passés avec vous, je retiendrai tout particulièrement le congrès de la SFD de Montpellier en 2023. Remerciements spécifiques :

A Julie KERR-CONTE, pour m'avoir permis de mener à bien ma thèse au sein du laboratoire, pour ses précieux conseils, ses nombreuses idées et pour m'avoir désinhibée en anglais.

A Violeta RAVERDY, pour m'avoir orientée sur ce sujet, pour ses conseils tout au long de l'avancement de ma thèse, pour sa connaissance de la littérature et pour sa faculté à trouver des articles que personne d'autre n'arrive à trouver.

A Mehdi MAANAOUÏ et Pierre BAUVIN, mes grands frères de labo, pour les nombreuses discussions et conseils statistiques. Heureusement que je n'étais pas dans votre bureau, on aurait beaucoup trop parlé !

A Chiara SAPONARO, pour sa patience, sa disponibilité, ses conseils et ses qualités scientifiques indéniables. A Ana ACOSTA-MONTALVO, « mi amiguita », fue un placer de hacer la thesis contigo. Buena suerte por la proxima parte de tu vida en Alemania. To Caroline BONNER, thank you for your support, especially during the ADA's travel! A Isabel GONZALEZ-MARISCAL, muchas gracias por todos los consejos.

À la team « islets » : Nathalie pour les « islets » de cochon, Anaïs pour les dosages d'insuline et les légumes, Valéry GMYR pour les conseils en tout genre et les réparations de vélo, Julien pour les tips rongeurs, Gianni pour les quelques manip' de biologie moléculaire, Morgane le scan des lames.

Aux ARC, le bureau d'en face : Aurélie, Gessica et Léïla, pour leur grande gentillesse, les petits gâteaux, et les réponses éclairées à mes nombreuses questions sur ABOS (souvent les mêmes). Et à Jérôme bien sûr, parti beaucoup trop tôt...

Aux jeunes, la relève : Valentin, Maria, Isaline, Omolara, Priya, Elise, Tiffany. C'est vous les prochains, accrochez vous !

Et à Rofigua, Alexandre et Benjamin, pour toutes les sollicitations administratives, et pas toujours anticipées...

Aux membres du Dhure,

« Parce-qu'au Dhure on est très durs ! » Que dire car tellement de souvenirs... Des manip' aux post-it en passant par les barbecues... Ce projet n'aurait pas pu aboutir sans vous, clairement.

A Audrey, ma binôme de pancréatectomie : merci pour tout ce que tu m'as appris. Je n'oublierai jamais tes compétences techniques, ton enthousiasme à mettre au point de nouvelles manip' et ta capacité à optimiser les plannings.

A Titi : tu as été mon partenaire technique pendant toute la durée de la thèse. Merci pour ton soutien, les débuts de repas tests maïzena à 7h30 et pour les refixations de sondes jéjunales le dimanche après-midi ! A bientôt en région parisienne.

A Julie : merci pour toute l'aide que tu m'as apportée, ta sensibilité et ta détermination. Bonne continuation pour la suite, je suis certaine que tu iras loin.

A Sarah, la reine des animations manuelles ! Merci également pour tout ton soutien, ton regard très apaisé et apaisant sur les choses, et les bons moments que nous avons passés à Marseille.

A Sabrina, ma binôme de sport ! « Un esprit sain dans un corps sain », et c'est aussi grâce à toi. Un grand merci pour toutes ces séances le midi (souvent câlées entre deux prélèvements de repas test).

Mais aussi à Arnold, merci pour ton expérience et nos conversations sur le sens de la vie ; à Martin, pour ta gentillesse et ta pédagogie ; à Michel, pour ta rigueur et ton dévouement envers les animaux ; à Frank, pour les tartes au maroilles et l'humour pinçant et merci aussi à Marion et Lorenzo pour leur gentillesse et à Micael pour ton aide précieuse lors de ton année avec nous.

Au service de Chirurgie Générale et Endocrinienne,

Un immense merci à Robert CAIAZZO, Grégory BAUD, Camille MARCINIAK, Mikael CHETBOUN, Vincent VENGELDER et Hélène VERKINDT, dont les travaux et conversations m'ont grandement inspirés. Grâce à vous, j'ai pu bénéficier d'une belle matière première ayant permis de rendre mes analyses robustes.

Dédicace toute particulière à Mathilde GOBERT, Agathe RÉMOND et Sarah BENHALIMA, qui ont parcouru un bout de chemin avec moi au cours de leur M2. Je sais qu'il y a eu des hauts et des bas pour chacune (inhérents à chaque M2) mais j'ai particulièrement apprécié l'esprit d'entraide qui vous a animé et nos brainstorming autour de nos résultats respectifs.

Aux collaborations,

A Valérie SAUVINET, Laure MEILLER et Corinne LOUCHE-PÉLISSIER du CRNH de Lyon. Merci beaucoup pour votre expertise avec le spectromètre de masse, votre générosité, votre bonne humeur, et pour m'avoir expliqué quelques rudiments de physique/chimie sous-jacents aux analyses.

Au membres de CRISAL, en particulier Cédric LHOSSAINE, Maxime FOLSCHETTE et DANILO DURSONIAH, pour notre collaboration, toutes les réunions MIGAD et les outils de modélisation dont j'ai pu bénéficier.

Au service de glycobiologie, pour tous les dosages de D-Xylose, mais également à Arnaud BRUNEEL et son équipe pour les réflexions sur son métabolisme et à Patrice MABOUDOU pour la biochimie.

A mes proches,

A mes parents, votre soutien indéfectible et inconditionnel durant toutes ces années, je ne vous remercierai jamais assez. A mes grands-parents, sans qui je n'aurai pas pu accomplir tout ce parcours aujourd'hui. J'espère pouvoir vous rendre fiers d'où vous êtes.

A Fred, devenu expert en chirurgie bariatrique et en D-Xylose, pour ton amour et pour me soutenir au quotidien. A Arielle et Frédéric Sr, pour leur gentillesse et leur accueil toujours chaleureux.

A tous mes amis : les Lillois, les Parisiens, les Vétos, Claire et Muriel, et Margotte ma souris. Merci d'avoir toujours été là, pour les moments festifs passés ensemble et ceux à venir !

Table of contents

Table of contents.....	4
List of abbreviations	8
Résumé.....	10
Abstract	11
General Introduction	12
Part 1 – Intestinal Glucose Absorption: A Critical Pathophysiological Mechanism for Type 2 Diabetes	16
I. Glucose absorption and metabolism in health	17
1. Glucose homeostasis	17
2. Physiology of intestinal glucose absorption: determinants	18
3. Glucose metabolism in the postprandial period	22
4. Glucose metabolism in fasting period	26
5. Regulations of glucose metabolism.....	28
6. Role of the kidney in glucose metabolism.....	36
II. Type 2 diabetes and implication of intestinal glucose absorption in its pathophysiology	37
1. Definition and classification	37
2. Epidemiology	39
3. Complications	41
4. Well-described pathophysiology	42
5. Implication of intestinal glucose absorption on postprandial glucose response.....	51
III. Intestinal glucose absorption: a therapeutic target in type 2 diabetes management.....	62
1. Nutritional approaches.....	62
2. Medical therapy.....	67
3. Interventional therapy: metabolic surgery	74
IV. Conclusion	86
Part 2 – Metabolic Syndrome and Early Signs of Impaired Glucose Tolerance in a Minipig Model of Glucose and Lipid Overabsorption	88
I. Introduction.....	89
1. The minipig: a preclinical model with a high translational value for metabolism research	89
2. Diabetogenic interventions in pigs: existing approaches and limits	91
3. Parenteral nutrition as a potential strategy for type 2 diabetes induction?.....	95
4. Aim and hypothesis	97
II. Materials and Methods	98
1. Ethical statement.....	98
2. Animals and housing	98

3. Study design	99
4. Surgical procedures	100
5. Energetic overload.....	101
6. Metabolic evaluations	103
7. Biological analyses.....	103
8. Calculations and statistical analyses.....	104
III. Results	105
1. Choice of the Göttingen-like minipig strain after comparison with Ossabaw	105
2. Reduction of Acute Insulin Response after subtotal pancreatectomy in Göttingen-like minipigs	108
3. No significant change in glucose metabolism following the combination of a subtotal pancreatectomy with a 2-month HFHSD in Göttingen-like minipigs	110
4. Alterations of insulin secretion pattern and insulin resistance after long-term intraportal glucose and lipids infusions in Göttingen-like minipigs.....	112
IV. Discussion.....	116
1. Summary of the obtained results	116
2. Ossabaw strain	117
3. Subtotal pancreatectomy and combination with high-fat high-sucrose diet	118
4. Long-term intraportal glucose and lipid infusions, preceded or not with a subtotal pancreatectomy	118
5. Changes of lipid profile.....	120
6. Early signs of impaired glucose tolerance and insulin resistance only after interventions mimicking intestinal glucose and lipid overabsorption.....	121
7. Limitations of the study.....	121
V. Conclusion	123
Part 3 – Validation of D-Xylose Test as a Relevant Biomarker of Intestinal Glucose Absorption	124
I. Introduction.....	125
1. Existing methods of in vivo intestinal glucose absorption assessment and limits	125
2. D-Xylose: a proposed biomarker to assess intestinal glucose absorption in vivo.....	130
3. Aims and hypothesis.....	135
III. Materials and Methods	135
1. Ethical statement.....	135
2. Study design	135
3. Animals and housing	137
4. Surgical procedures	137
5. Pharmacokinetic and standard metabolic tests	138
6. Gold-standard glucose labeled Meal Test with D-Xylose	140

7. Postprandial glucose turnover evaluation from isotopic enrichment assessment.....	140
8. Other biological procedures.....	141
9. Intestinal Glucose Absorption modeling with D-Xylose.....	142
10. Calculations and statistics.....	145
III. Results.....	146
1. Elements of pharmacokinetics of D-Xylose.....	146
2. Comparison of the Rate of Appearance of D-Xylose obtained by the proposed models with the Rate of Appearance of Exogenous Glucose obtained by the glucose labeled method in healthy minipigs.....	150
3. Sensibility of each model of systemic appearance of D-Xylose to reflect correctly the differences of Ra Exogenous glucose observed between two minipigs.....	157
IV. Discussion.....	159
1. Pharmacokinetic characteristics.....	159
2. Intestinal glucose absorption modeling.....	162
3. Comparison of Ra D-Xylose obtained by each model with RaE Glucose obtained by the gold-standard.....	163
4. Limitations of the study.....	164
V. Conclusion.....	165
Part 4 – Challenge of the Relevance of D-Xylose Test in Experimental Models.....	166
I. Introduction.....	167
II. Materials and methods.....	168
1. Ethical statement.....	168
2. Study design.....	168
3. Animals and housing.....	169
4. Surgical procedures.....	169
5. High-Fat High-Sucrose Diet (HFHSD).....	171
6. Mixed Meal Test (MMT) with D-Xylose.....	171
7. Biological procedures.....	172
8. Intestinal glucose absorption modeling with D-Xylose.....	172
9. Calculations and statistics.....	172
III. Results.....	173
1. No variation of the systemic appearance of D-Xylose following subtotal pancreatectomy and 2-months High-Fat High-Sucrose Diet.....	173
2. Variations of the systemic appearance of D-Xylose consequently to a rapid gastric emptying.....	177
IV. Discussion.....	178
1. Summary of the obtained results.....	178

2. Interpretation framework	179
3. Intestinal resection and decrease of systemic appearance of D-Xylose	179
4. No modification of the systemic appearance of D-Xylose after subtotal pancreatectomy and high-fat high-sucrose diet.....	181
5. Intestinal glucose absorption and gastric emptying	182
6. Limitations of the study.....	183
V. Conclusion	185
Part 5 – Exploration of D-Xylose Clinical Value in Glucose Metabolic Disorders	186
I. Introduction.....	187
II. Materials and methods	188
1. Ethical statement.....	188
2. Animals and housing	188
3. Study design	189
4. Biological procedures	189
5. Intestinal glucose absorption modeling with D-Xylose	190
6. Calculations and statistics	190
III. Results	191
1. Variation of intestinal D-Xylose absorption according to glycemic status.....	191
2. Time-dependent association between D-Xylose absorption and postprandial glucose response	196
V. Discussion.....	200
1. Summary of the obtained results.....	200
2. Consistency with the literature data	200
3. Intestinal D-Xylose absorption and splanchnic uptake of D-Xylose	201
4. Rate of absorption and gastric emptying	202
5. Intestinal glucose absorption: an early/causal factor in type 2 diabetes onset?.....	202
6. Limitations of the study.....	203
V. Conclusion	204
General Conclusion	206
References.....	210
List of communications	262

List of abbreviations

ABOS = Atlas Biologique de l'Obésité Sévère
AIR = Acute Insulin Response
AMPc = Adenosine Monophosphate
AMPK = AMP-activated protein kinase
ATP = Adenosine Triphosphate
BA = Bile Acids
BMI = Body Mass Index
BPD = Biliopancreatic Diversion
BPD-DS = Biliopancreatic Diversion with Duodenal Switch
BW = Body Weight
CCK = Cholecystokinin
ChREBP = Carbohydrate Responsive-Element-Binding Protein
CRISPR = Clustered Regularly Interspaced Short Palindromic Repeats
CVC = Central Venous Catheter
DNA = Deoxyribonucleic Acid
EN = Enteral Nutrition
EGP = Endogenous Glucose Production
EWL = Excess Weight Loss
F = bioavailability
FXR = Farnesoid X Receptor
GI = Glycemic Index
GIP = Gastric Inhibitory Polypeptide
GL = Göttingen-Like
GLP-1 = Glucagon-Like Peptide-1
GLUT = Glucose Transporter
GNG = Gluconeogenesis
GSIS = Glucose-Stimulated Insulin Secretion
HbA_{1c} = glycated hemoglobin
HDL = High-Density Lipoprotein
HFHSD = High-Fat High-Sucrose Diet
HGP = Hepatic Glucose Production
HIRI = Hepatic Insulin Resistance Index
HNF1- α = Hepatocyte Nuclear Factor 1 homeobox alpha
HOMA-IR = Homeostasis Model Assessment of Insulin Resistance
IAAP = Islet Amyloid Polypeptide
ICC = Interstitial Cells of Cajal
(i)AUC = (incremental) Area Under Curve
IGA = Intestinal Glucose Absorption
IGT = Impaired Glucose Tolerance
INS = insulin
INSR = Insulin Receptor
IRS = Insulin Receptor Substrate
IVGTT = Intravenous Glucose Tolerance Test
IVXTT = Intravenous D-Xylose Tolerance Test
Km = Michaelis constant
KO = Knot-Out
LAGB/AGB = (Laparoscopic) Adjustable Gastric Band
LDL = Low-Density Lipoprotein
LDLR = Low-Density Lipoprotein Receptor

LETO = Long-Evans Tokushima
MARD = Mild Age-Related Diabetes
Me-4FDG = α -methyl-4- ^{18}F fluoro-4-deoxy-D-glucopyranoside
MMT = Mixed Meal Test
MOD = Mild Obesity-Related Diabetes
MODY = Maturity-Onset Diabetes of the Young
NASH = Non-Alcoholic Steatohepatitis
NEFA = Non-Esterified Fatty Acids
NG/NGT = Normal Glucose Tolerance
O = Ossabaw
OAGB = One Anastomosis Gastric Bypass
OGTT = Oral Glucose Tolerance Test
OTLEF = Otsuka Long-Evans Tokushima
OXY = Oxyntomodulin
PCSK9 = Proprotein Convertase Subtilisin/Kexin 9
PDX1 = Pancreatic and duodenal homeobox 1
PET = Positron Emission Tomography
PGR = Postprandial Glucose Response
PI3K = Phosphatidyl Inositol triphosphate
POP = Persistent Organic Pollutants
PPAR γ = Peroxisome Proliferator-activated Receptor gamma
Px = Pancreatectomy
PYY = Peptide Tyrosine-Tyrosine
Ra D-Xylose = Rate of Appearance of D-Xylose
RaE = Rate of Appearance of Exogenous glucose
RaT = Rate of Appearance of Total glucose
RdE = Rate of Disappearance of Exogenous glucose
RdT = Rate of Disappearance of Total glucose
RNA = Ribonucleic Acid
RYGB = Roux-en-Y Gastric Bypass
SADI-S = Single-Anastomosis Duodeno Ileal-Switch
SAID = Severe Autoimmune Diabetes
SCFAs = Short-Chain Fatty Acids
SIDD = Severe Insulin-Deficient Diabetes
SIRD = Severe Insulin-Resistant Diabetes
SG-TB = Sleeve Gastrectomy with Transit Bipartition
SG/VSG = Sleeve Gastrectomy
SGLT = Sodium Glucose Transporter
SNPs = Single Nucleotide Polymorphisms
STRs = Sweet Taste Receptors
STZ = Streptozotocin
TG = Triglycerides
TGR5 = Takeda-G-protein-membrane receptor-5
TNF- α = Tumor Necrosis Factor alpha
TPN = Total Parenteral Nutrition
T2D/T2DM = Type 2 Diabetes
Vd = Volume of Distribution
WHO = World Health Organization
2-FDG = 2-deoxy-2- ^{18}F fluoro-D-glucose
3-OMG = 3-O-methylglucose
4-FDG = 4-deoxy-4- ^{18}F fluoro-D-glucose
95 % CI = 95 % Confidence Interval

Résumé

La réponse glycémique postprandiale (RGP) est reconnue comme un facteur prédictif précoce de l'apparition du diabète de type 2 (DT2), indépendamment de la glycémie à jeun. Si l'implication de la diminution de la sensibilité et de la sécrétion d'insuline sur la RPG, et par conséquent sur la physiopathologie du DT2, a été bien étudiée, celle de l'absorption intestinale du glucose (AIG) reste partiellement comprise. La RGP est sous l'influence de nombreux mécanismes dont les principaux sont l'apparition du glucose exogène, l'utilisation du glucose par les tissus et la production endogène de glucose. L'AIG, l'insulinosécrétion et la sensibilité à l'insuline gouvernent ainsi la RGP.

Les données de la littérature laissent supposer que l'évaluation en routine de l'AIG permettrait une médecine de précision pour améliorer la prévention et le traitement du DT2. Cependant, l'AIG est une variable difficile à mesurer *in vivo*, ce qui implique la nécessité d'un biomarqueur facile à utiliser en pratique clinique.

L'objectif de ce travail a été de mieux comprendre la contribution de l'AIG sur la RPG, particulièrement par la validation d'une nouvelle méthode de quantification de l'absorption. Ce travail a été conduit par des approches expérimentales sur modèle porcin et par une approche transversale à partir de données cliniques.

Dans un premier temps, nous avons montré que l'élaboration d'un modèle de miniporc mimant une hyper-absorption de glucose et de lipides était, chez cette espèce, la seule stratégie efficace permettant l'induction d'un syndrome métabolique avec des signes précoces d'intolérance au glucose. Deuxièmement, nous avons élaboré un modèle fiable, spécifique et simple d'utilisation de quantification de l'AIG en utilisant le test oral au D-Xylose. Troisièmement, nous avons montré que l'apparition systémique du D-Xylose ne dépendait ni de l'insulinosensibilité, ni de l'insulinosécrétion, mais que son mécanisme d'absorption était modifié par la vitesse de vidange gastrique dans les temps précoces du repas. Enfin, les études transversales ont mis en évidence l'association entre l'AIG et le statut glycémique ainsi que sa contribution positive sur la RGP, aussi bien précoce que globale, et quel que soit le statut glycémique.

Après avoir validé l'apparition systémique du D-Xylose comme biomarqueur fiable de quantification de l'AIG, notre étude a permis également de confirmer l'association entre une AIG augmentée et une hyperglycémie postprandiale. L'AIG serait donc un prédicteur précoce permettant le phénotypage des patients et leur prise en charge personnalisée dans l'optique d'une médecine de précision. Moduler l'absorption intestinale du glucose, par les inhibiteurs de SGLT1 ou la chirurgie métabolique représente donc une stratégie thérapeutique pertinente pour l'amélioration de la réponse glycémique postprandiale.

Abstract

Intestinal glucose absorption (IGA), insulin secretion, and insulin sensitivity are the main explicative factors of postprandial glucose response (PGR). PGR is also recognized as a predictive factor of type 2 diabetes (T2D) onset, independently of fasting glycemia. If the implication of decreased insulin sensitivity and secretion on PGR, and consequently on T2D progression, have been well described, the one of IGA remains partially understood. PGR is influenced by numerous mechanisms such as the appearance of exogenous glucose, the uptake of glucose by the organs, and the endogenous glucose production.

Literature data let suppose that the routine assessment of IGA would allow precision medicine for a better prevention and treatment of T2D. However, IGA is a variable difficult to assess *in vivo*, involving the necessity of a biomarker easier to use in clinical practice.

The aim of this work was to better understand the contribution of IGA on PGR, particularly thanks to the validation of a new method of quantification of absorption. For this purpose, we used experimental approaches in a preclinical porcine model and a cross-sectional approach with clinical data.

First, we demonstrated that the development of a minipig model that mimics intestinal overabsorption of glucose and lipids was the only method for inducing a metabolic syndrome with early signs of impaired glucose tolerance in this species. Second, using oral D-Xylose test, we developed a model for evaluating intestinal glucose absorption *in vivo* that is accurate, specific, and simple to use. Thirdly, we showed that systemic appearance of D-Xylose is independent of insulin sensitivity and secretion, but that the rate of gastric emptying plays a key role in the acceleration of the intestinal glucose absorption's pattern during the early phases of a meal. Finally, the cross-sectional studies highlighted the positive correlation between intestinal glucose absorption and glycemic status as well as its contribution to early and global postprandial glucose responses.

After validation of the systemic appearance of D-Xylose as a reliable biomarker for IGA quantification, our research enabled us to confirm the association between increased IGA and postprandial hyperglycemia. In order to ensure precision medicine, IGA would be an early biomarker allowing to phenotype patients and to set up individualized treatment plan. Modulating intestinal glucose absorption, especially with SGLT1 inhibitors or metabolic surgery, thus represents a relevant approach for postprandial glucose response improvement.

General Introduction

“Let food be thy medicine, and let medicine be thy food”, as supposed stated by Hippocrate. This quotation is particularly true when talking about diabetes mellitus. Diabetes mellitus is a complex disease characterized by dysregulation of glucose homeostasis and usually classified into two main forms: type 1 and type 2 diabetes. The complications of diabetes are pleiotropic, often severe, and difficult to control after their occurrence.

Numerous studies have noted the extreme heterogeneity of type 2 diabetes, and new subtypes of the disease have been identified with vastly different patient characteristics and risks for complications (Ahlqvist et al., 2018; Raverdy et al., 2022). As a result, the idea of "Precision Medicine" seems to be particularly pertinent for the prediction, diagnosis, and therapy of type 2 diabetes.

One of the goals of type 2 diabetes research is to find early predictors that could make the disease easily reversible (**Figure 1**). For this reason, the targets of intervention of type 2 diabetes, such as fasting glycemia, HbA_{1c}, and the 2-hour blood glucose concentration following a 75-g Oral Glucose Tolerance Test (OGTT) are currently questioned because they are not early enough (Bergman et al., 2018). Current screening and diagnostic guidelines should thus be redefined.

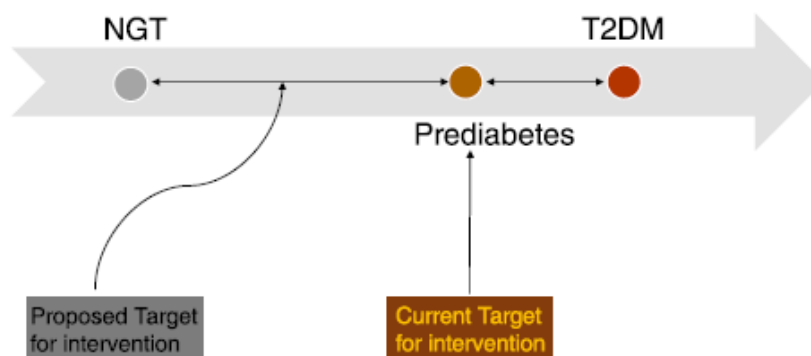


Figure 1: Proposed target for intervention compared to current target occurring at prediabetes stage (Bergman et al., 2018)
NGT = Normal Glucose Tolerance. T2DM = Type 2 Diabetes Mellitus.

The early postprandial glucose response (particularly the 1-hour postload level) has been proposed as a new target of intervention (Bergman et al., 2018; Buysschaert et al., 2022; Peddinti et al., 2019) and is by the way a topic discussed during the 2023 Hamburg Congress of the European Association for the Study of Diabetes (EASD).

In fact, the 1-hour cut-off value of 155 mg/dL during an OGTT stratifies people into high and low risk groups for developing type 2 diabetes in the future (Abdul-Ghani et al., 2008), independently of impaired fasting glucose (Fiorentino et al., 2015), beta cell function impairment and insulin resistance among adults (Bianchi et al., 2013) and obese youth from multiple ethnic origins (Kim et al., 2013; Oh et al., 2017; Tricò et al., 2019a). Additionally, it has been shown as an indicator of mortality (Bergman

et al., 2016), non-alcoholic steatohepatitis (NASH) (Fiorentino et al., 2016), as well as cardiovascular disease risk (Bianchi et al., 2013; Fiorentino et al., 2019; Tanaka et al., 2014). Furthermore, the 1-hour cut-off value of 11.6 mmol/L (209 mg/dL) was also suggested by a recent meta-analysis for the diagnosis of type 2 diabetes (Ahuja et al., 2021).

Thus, early postprandial glycemic response is suggested as a universal tool for the early management of metabolic diseases. The contribution of insulin sensitivity and secretion on postprandial glycemic response, which aims to increase plasma glucose clearance and decrease endogenous glucose production, has been well described, but it is currently not enough to fully explain all the pathophysiological mechanisms underlying postprandial glucose response (DeFronzo, 2009).

Following the consumption of a meal, intestinal glucose absorption enables glucose to enter the plasmatic compartment. This mechanism is the only one that permits the organism to receive exogenous glucose and its contribution on postprandial glucose response in health and dysglycemia onset was largely neglected. Interestingly, it was not part to the ominous octet presented in the Banting Lecture of DeFronzo (DeFronzo, 2009). But now, increasing evidence suggests that intestinal glucose absorption is an important determinant of early postprandial glucose response (Tricò et al., 2019b) and its routine assessment may inform precision medicine for the prevention and treatment of type 2 diabetes.

The aim of this work is thus to better understand the association between intestinal glucose absorption to postprandial glycemic response by using the systemic appearance of D-Xylose as a biomarker for in vivo measure of intestinal glucose absorption.

This thesis was constituted of one bibliographic section (Part 1), three longitudinal studies (Parts 2, 3, and 4), and one cross-sectional study (Part 5). In Part 1, we discussed the documented evidence for the association between intestinal glucose absorption and postprandial glucose response, in health and metabolic disorders. In Part 2, using a Minipig model of glucose and lipid overabsorption, we created a metabolic syndrome with early indications of impaired glucose tolerance. In Part 3, we validated D-Xylose test as biomarker of intestinal glucose absorption. In Part 4, we challenged the systemic appearance of D-Xylose in experimental models. In Part 5, we finally validated the clinical relevance of D-Xylose by confirming the association between intestinal glucose absorption and postprandial glycemic response, in health and impaired glucose tolerance.

Part 1

Intestinal Glucose Absorption: A Critical Pathophysiological Mechanism for Type 2 Diabetes

I. Glucose absorption and metabolism in health

1. Glucose homeostasis

For many species, especially non-ruminant mammals, glucose serves as their primary energy source. Glucose does not naturally occur in food but is released after complex carbohydrates have been digested. Glucose enters the liver through the portal vein after being transported across the intestinal wall and is then distributed to other tissues. By using different catabolic pathways, glucose can be transformed into fatty acids or amino acids, stored as glycogen, or oxidized inside cells.

Some organs and tissues, particularly the brain, require a steady supply of glucose. Low blood glucose levels can cause a coma, seizures, or even death. In contrast, high blood glucose levels can be toxic to organs and increase the risk of retinopathy, vascular diseases, neuropathy, and renal failure. For this reason, glycemia must be kept within a very small range. Homeostasis is the process of maintaining steady-state blood glucose levels within predetermined limits (**Figure 2**).

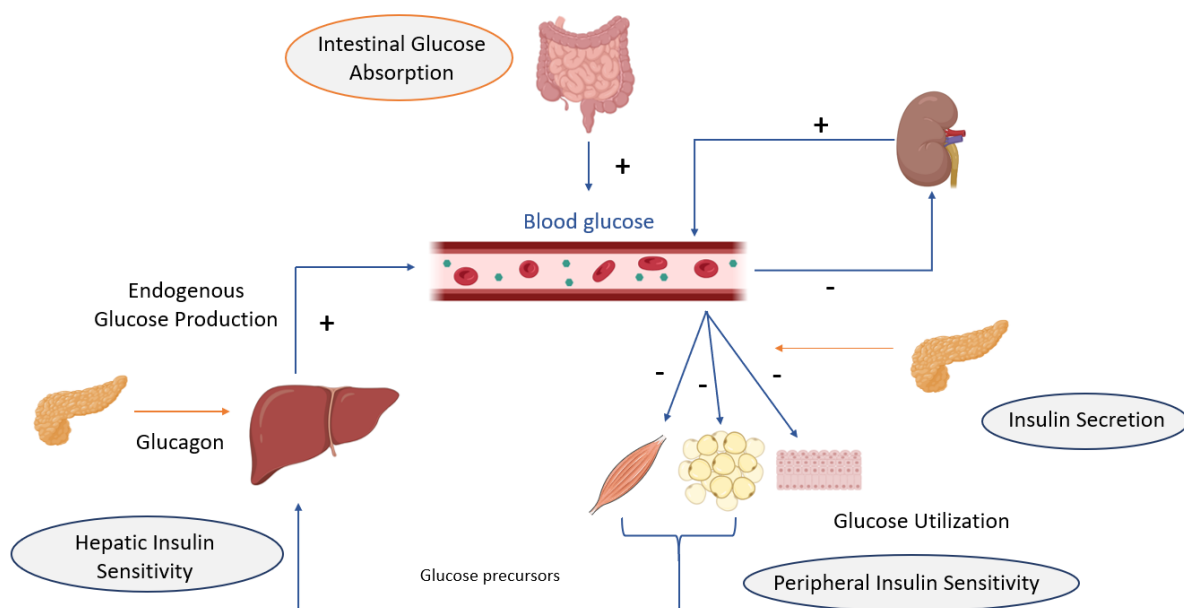


Figure 2: Glucose homeostasis despite the fluxes of glucose between the blood compartment of the other tissues

The blood compartment can be viewed as a type of system with glucose fluxes at the entrance and exit. The entrance fluxes consist in intestinal glucose absorption and endogenous glucose production, whereas the exit fluxes consist in the oxidation or storage of glucose by peripheral tissues and its elimination through the kidney tubules. The body controls blood glucose levels through physiological mechanisms, particularly hormonal ones, to prevent hyperglycemia after eating and hypoglycemia after exercise or during a fast (Szablewski, 2011).

Metabolic abnormalities can happen if the regulation system is not working properly or if there is an imbalance in the flux of glucose entering and leaving the body. Thus, the clinical outcome of the dysfunctional glucose homeostasis is diabetes mellitus. Although there may be several initial imbalances, the end result in the later stages of the disease is chronic hyperglycemia that is linked to a variety of difficult-to-control complications.

2. Physiology of intestinal glucose absorption: determinants

The movement of glucose as monosaccharides through the intestinal wall, from the lumen to the portal vein, is referred to as intestinal glucose absorption (Gerich, 2000), and it is essential for consuming energy. Using perfusion systems, some studies in humans assessed the maximum ability of the proximal jejunum to absorb glucose at a rate of 0.5 g/min/30cm² (Duchman et al., 1997; Modigliani and Bernier, 1971).

According to the meal's composition, the circadian cycle, or the anatomy of the intestine itself, blood glucose concentrations inside the intestinal lumen can vary greatly; levels can range from 0.2 to 48 mmol/L while oscillating in the blood compartment around the setpoint value of 5 mmol/L (Ferraris et al., 1990). The intestine thus exhibits the ability to act as a barrier by controlling glucose transport and limiting its passage to ensure glucose homeostasis.

According to this theory, every factor that changes intestinal functionality can subsequently have an impact on glucose homeostasis. There are numerous factors that affect how much glucose is absorbed from the intestine, including nutrient exposure to the mucosa of the digestive tract, conversion of complex carbohydrates to monosaccharides, and glucose transport through the enterocytes.

2.1 Exposure to the intestinal mucosa

The rate at which nutrients are delivered to the intestine and, as a result, are digested and absorbed depends on the motility of the gastrointestinal tract. The main contributor to nutrient exposure is gastric emptying.

2.1.1 Gastric emptying

The three primary functions of the stomach are to store food before duodenal transit, to mix food with gastric secretion to liquefy the chyme, and to control the rate of food delivery to the intestine for proper rate of digestion and absorption (Holst et al., 2016; Lema-Perez et al., 2019).

The stomach enables an initial lag phase between 20 and 40 minutes before the delivery of food in the intestine and it has been demonstrated that the rate of gastric emptying is normally little affected by the size of the chyme but more by the nature, the energetic load of meal and its viscosity: in case of a viscous chyme, gastric emptying would be delayed (Marciani et al., 2000; Sakamoto et al., 2011;

Wolever et al., 2020). In healthy subjects, this rate has been measured at 1-4 kcal/min (Brener et al., 1983), and gastric emptying is controlled so that this rate is maintained regardless of the type of chyme. Although intraindividual variability for the same conditions appears to be negligible in humans, interindividual variability of this rate has been demonstrated (Lartigue et al., 1994). Following gastric emptying, incretin hormones are released, and they remain active for the duration of the gut's delivery of nutrients.

Multiple mechanisms, including the nervous system as well as gastric and intestinal hormones, are involved in the regulation of gastric emptying. The main hormones responsible for the slowing of gastric emptying are known as incretins, which refers to Gastric Inhibitory Polypeptide (GIP) and Glucagon-Like Peptide-1 (GLP-1). Cholecystokinin (CCK) and Peptide Tyrosine-Tyrosine (PYY) are also involved in the regulation of gastric emptying. Gastric emptying is also delayed by pancreatic and duodenal hormones like glucagon, amylin, and motilin. On the other hand, the rate is sped up by the orexigenic hormones ghrelin and motilin from the stomach. The effect of these hormones on delayed gastric emptying is also related to their satiety effect (Camilleri, 2019). In terms of nervous regulation, vagal nerve branches implanted in the pylorus control local hormonal mechanisms for controlling gastric emptying in addition to short reflexes (Holst et al., 2016). According to the prandial or interprandial period, two parallel nervous circuits—one inhibitory and one excitatory—were found to mediate the inhibition or stimulation of gastric emptying, respectively (Goyal et al., 2019b).

2.1.2 Intestinal motility

If gastric emptying is the primary factor affecting how nutrients are exposed into the intestine, small intestinal motility also influences how quickly glucose is absorbed (Thazhath et al., 2014). In fact, an increase in small intestine motility causes a higher exposure of glucose along the intestinal tract, increasing the rate at which the transporters can absorb glucose (Kuo et al., 2010a; Schwartz et al., 2002). The rate of absorption, on the other hand, is decreased by lowered intestinal motility (Chaikomin et al., 2007; Ogawa et al., 2011).

2.2 Digestion of complex carbohydrates

Digestion is the process by which complex carbohydrates, which cannot be absorbed directly, are converted to monosaccharides, which enterocytes can transport. A quick and complete absorption of glucose is facilitated by an efficient and rapid digestion. The nature of the carbohydrate itself and the digestive enzymes that affect its cleavage are two factors that affect how quickly it breaks down.

2.2.1 The main carbohydrates

According to their degree of polymerization, carbohydrates can be divided into 3 main categories: 1/ monosaccharides (glucose, fructose and galactose, form absorbable by the intestine) and

disaccharides (saccharose, lactose and maltose); 2/ oligosaccharides, constituted of 3 to 9 monosaccharides; 3/ polysaccharides (from 10 unities), including starch, a mix of amylose and amylopectin, and other carbohydrates as cellulose for example, digestible only for herbivorous species. The size and the morphology of starch granules and the proportion of amylose and amylopectin depends on the origin plants of starch and determine its digestibility.

2.2.2 Degradation by the digestive enzymes

Disaccharides and oligosaccharides from food are hydrolyzed directly by enterocytes at the brush border while starch digestion is first made up of preparatory steps in the mouth by salivary α -amylase, in the stomach and in the intestinal lumen by pancreatic α -amylase, to be transformed into oligosaccharides later.

The presence of lactase, maltase, and isomaltase along the enterocyte brush border enables the formation of all monosaccharide units that are directly absorbed by the enterocytes. We refer to the intestinal wall as the "digestive-absorptive interface" because the action of these enzymes and the transport of monosaccharides are closely integrated (Levin, 1994). However, it appears that sucrose absorption is not rate-limited by the hydrolysis of oligosaccharides, implying that these two processes are independent (Gray and Ingelfinger, 1966).

2.2.3 Fermentation in the large intestine

The non-absorbed fraction of carbohydrates comes then into the large intestine. In fact, some carbohydrates, such as cellulose, that are derived from fruits, vegetables, or synthetic compounds are insufficiently digestible by endogenous enzymes and consequently only partially absorbed in the small intestine. The microbiota in the large intestine then ferments them there into Short-Chain Fatty Acids (SCFAs), such as acetate, propionate, and butyrate (Makki et al., 2018). SCFAs then passively diffuse across the large intestinal barrier. As a result, the type of carbohydrates consumed can have an impact on the nature and diversity of the microbiota (Xie et al., 2020).

2.3 Monosaccharides transportation across the intestinal barrier

2.3.1 By specific transporters through the enterocytes

Specific transporters are primarily responsible for moving glucose, galactose, and fructose, monosaccharides, released during the digestion of complex carbohydrates, across the enterocytes. Sodium Glucose Transporter 1 (SGLT1, gene *slc5a1*) is responsible for transporting glucose and galactose across the apical membrane, while Glucose Transporter 5 (GLUT5, gene *slc2a5*) is responsible for transporting fructose. All monosaccharides take the Glucose Transporter 2 (GLUT2, gene *slc2a2*) at the basolateral membrane to connect to the blood system (**Figure 3**).

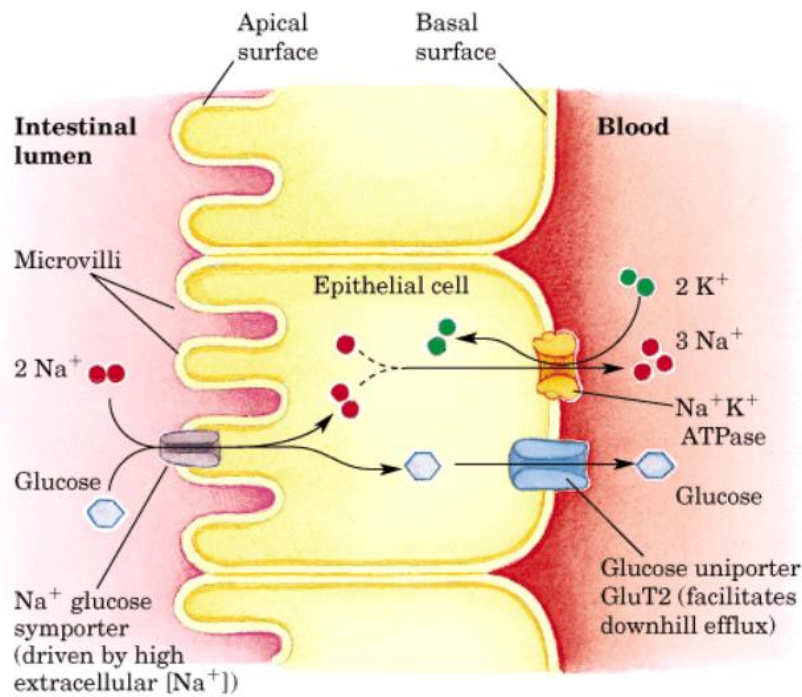


Figure 3: Active transport of glucose by SGLT1 (apical pole) and GLUT 2 (basal pole) across the intestinal wall (Saikat, 2016)

One molecule of glucose is co-absorbed with two molecules of sodium ion (Na^+) during the active cotransport of glucose and galactose from the intestinal lumen into the cells. The sodium/potassium active adenosine triphosphatase pump (Na^+/K^+ ATPase), which is located at the basal pole and is responsible for removing intracellular Na^+ , maintains the Na^+ concentration gradient. Even though intraluminal glucose levels are lower than blood ones, there is still a strong and efficient transport of glucose across the enterocyte (Thazhath et al., 2014). Each monosaccharide has a different affinity for SGLT1, with glucose being more affine than galactose (Michaelis constants (K_m) of 0.5 and 1 mM, respectively) and 3-O-methylglucose, a glucose analogue (Gromova et al., 2021; Koepsell, 2020). Phlorizin, a naturally occurring substance found in fruit trees, is the primary competitive inhibitor of the SGLT1 transporter. Since its discovery 150 years ago, phlorizin has been used as a therapeutic target and as a pharmacological tool for preclinical research (Ehrenkranz et al., 2005). Phloretin and cytochalasin B, two additional glucose transporter inhibitors, do not have any inhibitory effects on SGLT1 in contrast to phlorizin (Koepsell, 2020).

By facilitating diffusion through GLUT5, fructose enterocyte entry happens. In knock-out (KO) *slc2a5* mouse models, fructose uptake across the apical membrane is abolished, indicating that GLUT5 is mainly responsible for fructose enterocyte uptake (Ferraris et al., 2018).

The exit of glucose, galactose and fructose from the enterocyte occurs at the basolateral membrane by facilitating diffusion thanks to GLUT2, independently from Na^+ . With apparent K_m values of 17 mM

for glucose, 76 mM for galactose, and 92 mM for fructose, respectively, glucose has the highest affinity for GLUT2. Phloretin and cytochalasin B, but not phlorizin, inhibit GLUT2 (Koepsell, 2020).

2.3.2 Paracellular transport

In addition to the transport of monosaccharides by particular transporters, some evidence also suggested that paracellular transport occurred (Pappenheimer, 1990). The Pappenheimer's group founds differences between studies using isolated cells conducted in vivo and in vitro. In vivo studies revealed a linear increase in glucose uptake beyond the highest intraluminal glucose concentrations, in contrast to in vitro observations of intestinal glucose transport that revealed complete SGLT1 transporter saturation in the case of high glucose levels. Along with the paracellular glucose transport, an increase in water absorption across the epithelium was also noted, causing morphological changes in the tight junctions between enterocytes and facilitating the permeation of other hydrophilic molecules (Madara and Pappenheimer, 1987). According to Gromova and Gruzdkov, less than 15 % of all glucose transport occurs paracellularly (Gromova and Gruzdkov, 1993).

2.3.3 Glucose sensing by Sweet Taste Receptors

In contrast to SGLT1 transporters, a process involving Sweet Taste Receptors (STRs) enables the small intestine to sense glucose (Dyer et al., 2003). The two dimers T1R2 and T1R3 are combined to form STRs, which are coupled to G-protein and expressed at the epithelial pole of enteroendocrine K and L cells (Renwick and Molinary, 2010). The G-protein α -gustducin and the subunit T1R3 enable glucose sensing and the control of SGLT1 expression in enterocytes (Margolskee et al., 2007). The enteroendocrine cell detects glucose via STRs, which causes the release of GIP and GLP-1, which serves as a signal for SGLT1 enterocyte expression and subsequent glucose absorption (Egan and Margolskee, 2008). STRs are supposed to participate to the release of incretin hormones in postprandial state.

3. Glucose metabolism in the postprandial period

3.1 Fate of glucose after meal ingestion

Glucose enters the portal vein following its absorption. According to studies (Dimitriadis et al., 2021), the liver directly absorbs between 40 and 70 % of glucose. After this first pass effect, the remaining absorbed glucose enters the systemic circulation and is swiftly absorbed by the other tissues in order to preserve its homeostasis and be used as a source of energy.

Skeletal muscle is thought to take up 26 %, the brain 15 %, the kidney 10 %, the adipose tissue 3 %, and the remaining organs (heart, blood cells, skin...) 7 %. The liver, skeletal muscle, and brain thus account for 80% of the total load absorbed (Kelley et al., 1988) (**Figure 4**).

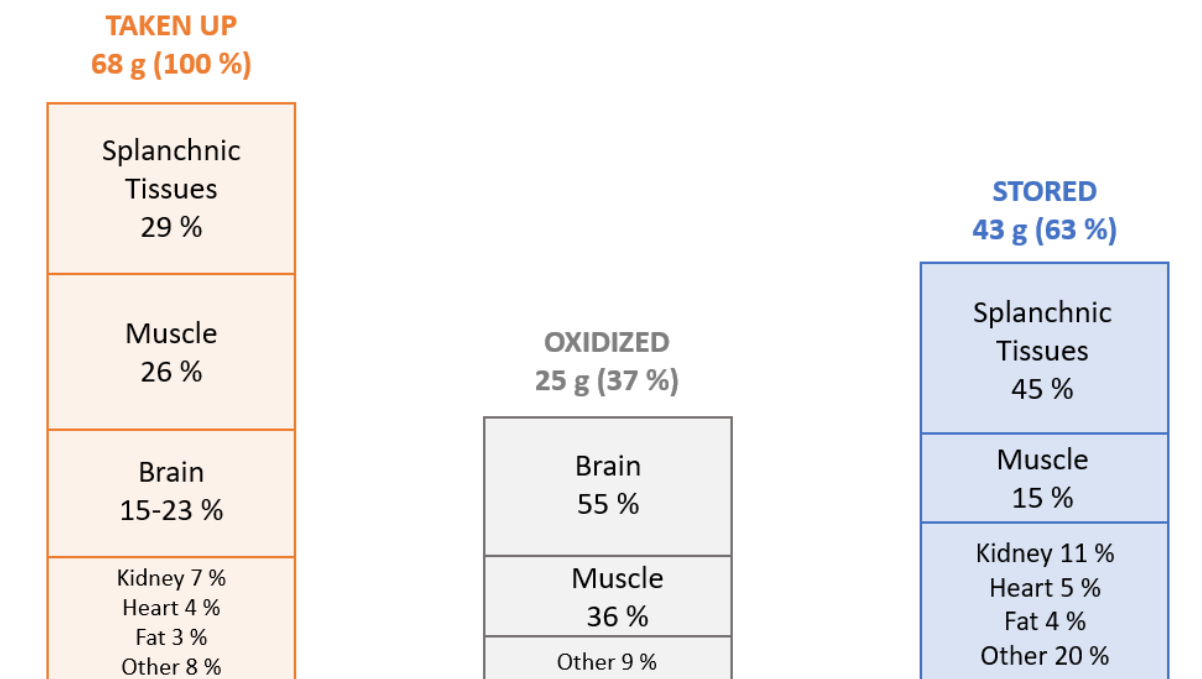


Figure 4: Overview of metabolic fate of 68-g oral glucose load in normal human volunteers. Adapted from (Kelley et al., 1988).

Values for kidney storage actually represent net uptake and may include glucose that was metabolized.

For glucose uptake, two categories of tissues can be distinguished:

- non-insulin dependent tissues, such as the brain, blood cells or retina. Their consumption of glucose is constant and continue and glucose represents their exclusive energy supply.

- insulin dependent tissues, such as the liver, skeletal muscle and adipose tissue, in which insulin stimulates glucose storage and utilization by increasing its uptake or its metabolic pathways.

Glycolysis, the Krebs cycle, oxidative phosphorylations, and the pentose phosphate pathway are the glucose cellular metabolism pathways that allow glucose to be directly oxidized after entering cells. Glycogen synthetase, an enzyme found in the liver and muscles, converts glucose into glycogen, the primary form of glucose storage.

3.2 Glucose transporters

The transport of glucose by transmembrane proteins is necessary for it to be metabolized by the cells. Two kinds of transporters can be distinguished: glucose transporters by facilitating diffusion (GLUT family) (Thorens and Mueckler, 2010) and sodium-glucose transporters, also known as cotransporters (SGLT family) (Wright et al., 2011).

14 GLUT proteins (GLUT1 to 14) have been discovered so far, but only half of them have well-understood functions. GLUT proteins differ according to the tissues in which they are expressed, in their kinetic characteristics, and in the monosaccharides transported. The main GLUT proteins responsible for glucose transport are GLUT1, GLUT2, GLUT3, GLUT4 and GLUT5.

The well-studied protein GLUT1 is highly expressed in the membranes of erythrocytes. It is also present in nerve, endothelial, placental, and adipose tissue cells.

GLUT2 is highly expressed in pancreatic beta cells, enterocyte basal membranes, hepatocytes, and kidney epithelial cells. It has a high affinity for transporting glucose (K_m of 17 mM). GLUT2 allows a quick glucose balance between extracellular and intracellular space.

The nervous system is the primary site of GLUT3 expression. Widespread in dendrites and axons, this transporter's expression levels vary depending on the cerebral area and are correlated with the local cerebral glucose uptake. Leukocytes and platelets also contain GLUT3. The amount of GLUT3 expressed at the cell membrane would regulate the uptake of glucose.

GLUT4 is primarily expressed in tissues that respond to insulin, like skeletal muscle and adipose tissue. The translocation of GLUT4 from the cytosol to the cell membrane is regulated by the action of insulin, but the pathway responsible for this translocation, from insulin binding to its receptor, remains incompletely understood.

For its part, GLUT5 has a very high level of fructose transport specificity and is widely expressed in the apical membrane of enterocytes. Other tissues such as the kidney, brain, muscle, and adipose tissue also express it. However, the physiological relevance of its extraintestinal expression remains unclear.

Robert Crane made the initial discovery of the sodium-glucose transporters in 1960 with the identification of the intestinal SGLT1, which is found at the apical pole of enterocytes. The two primary glucose cotransporters are SGLT1 and SGLT2, which are primarily found in the intestine and the kidney, respectively. However, SGLT3 (an intestinal glucose sensor), SGLT4 (in the small intestine and brain), SGLT5 (in the kidney), and SGLT6 (in the spinal cord, kidney, and brain) have also been identified.

3.3 Role of the liver

The liver is a crucial component of the homeostasis of glucose. Its primary function following a meal is to convert glucose into glycogen. Insulin is not required for glucose entry into hepatocytes because GLUT2 transporters have a high affinity for glucose, allowing glucose to enter the cells proportionally to extracellular glucose levels. This unregulated mechanism of entrance allows glucose clearance after a meal (Thorens, 2015).

When glucose enters the hepatocyte, it is phosphorylated to form glucose-6-phosphate, which is then used in metabolic glucose pathways like glycolysis, the Krebs cycle, or oxidative phosphorylation. It can also be stored as glycogen or used as an energy source. The liver synthesizes about 50 % of the portal glucose into glycogen. However, because aminoacids and non-esterified fatty acids are the most significant energy sources, the liver only oxidizes a small amount of glucose.

Following a meal, hyperglycemia and hyperinsulinemia ensure the nearly complete suppression of the normally constant endogenous glucose production, which is primarily carried out by the liver and kidney during fasting. This suppression, which includes both gluconeogenesis and glycogenolysis abolition, takes place within the first 30 to 60 minutes after the oral carbohydrate challenge.

3.4 Role of the skeletal muscle and adipose tissue

The quantity of glucose uptake after a meal by the skeletal muscle is estimated at 26 % (Dimitriadis et al., 2021). The entry of glucose into the muscular cells is facilitated by the insulin-regulated translocation of GLUT4 from the cytosol to the membrane, which serves as a limiting step in the metabolism of glucose. After eating a meal, the muscle begins to absorb glucose within the first 15 to 30 minutes and reaches its peak 60 to 90 minutes later. The peak of uptake is in synchronization with the peak of plasma insulin levels (Ferrannini et al., 1985; Taylor et al., 1993). After that, glucose is either oxidized or stored as glycogen in the muscle.

It has been established that oxidation, which accounts for 50 % of the glucose taken up, is the major outcome of glucose in muscular cells. Glycogen synthesis begins only 90 minutes after meal ingestion and accounts for about 35 % of the glucose uptake by the muscle (Kelley et al., 1988; Taylor et al., 1993). Glycogen synthesis occurs in the muscle in the later postprandial period, when the glucose oxidation pathway reaches saturation point. The remaining 15 % are related to glucose being metabolized into lactate, alanine, or pyruvate (Kelley et al., 1988).

According to some studies, the skeletal muscle plays a secondary role to the liver in the process of disposing of glucose. Because the liver has a higher insulin sensitivity than muscle, it would be used to regulate small amounts of ingested glucose before turning to skeletal muscle as a backup mechanism if the capacities of the liver were to be exceeded (Kowalski et al., 2017). In fact, it was demonstrated that endogenous glucose production was completely inhibited at plasma insulin concentrations of 60 μ IU/mL, whereas maximal glucose disposal occurred at insulin concentrations of 200–700 μ IU/mL, confirming the greater insulin sensitivity of the liver and the secondary action of the muscle (Rizza et al., 1981).

For its part, adipose tissue is extremely sensitive to insulin, as only 13 $\mu\text{IU/mL}$ of plasma insulin are required to suppress 50 % of lipolysis (Nurjhan et al., 1986). However, since only 3 % of oral glucose is taken up by adipocytes, adipose tissue does not play a significant role in the disposal of glucose.

3.5 Role of the brain

The brain uptakes about 15-23 % of glucose. Thanks to GLUT1, glucose can pass through the blood–brain barrier. The primary transporters found in the brain, GLUT1 and GLUT3, facilitate diffusion within the neurons and enable rapid glucose transport. Glucose essentially supplies the energy for neurotransmission. The only energy reserve for the brain in astrocytes is glycogen, but it is synthesized at a much lower level than other types of conventional energy reserves (Mergenthaler et al., 2013).

4. Glucose metabolism in fasting period

4.1 Glucose disposal and production

The time period from 6 to 12 hours after the last meal to the next is referred to as the fasting period. Blood glucose levels must be kept between 80 and 90 mg/dL even if there is no glucose entry into the body, while insulin concentrations must stay below 10 $\mu\text{IU/mL}$. In a fasted state, non-insulin dependent tissue glucose uptake primarily affects the brain (50 %), skeletal muscle (15 %), blood cells (10 %), and kidneys (5 %). There is no storage, and the rate of glucose production from endogenous sources is roughly equal to the rate of glucose consumption, which is estimated at 2 mg/kg/min (Gerich, 1993).

The liver is essential for the production of endogenous glucose and accounts for 80 % of the glucose produced and released into the bloodstream (Gerich, 2000). The kidney comes in second place with 20 % of the contribution, and the intestine contributes very little (Gerich, 2000). There are two main mechanisms that permit endogenous production:

- glycogenolysis by the liver, that accounts for 50 % of the glucose produced and consists of the release of glucose from glycogen, its main form of storage.

- gluconeogenesis, essentially by the liver and the kidney (respectively 30 % and 20 % of total glucose release), consisting of the *de novo* synthesis of glucose from precursors.

4.2 Glycogenolysis

The first mechanism for releasing glucose in the fasting state is the depletion of liver glycogen stores. After a 24-hour fast, the entire glycogen reserve is used up, and as a backup mechanism, gluconeogenesis increases concurrently (**Figure 5**). When fasting for the typical length of time, liver glycogenolysis contributes to 50 % of the production of glucose; however, if the fast is prolonged, gluconeogenesis can overtake this percentage. Skeletal muscle can also store glycogen, but unlike the

liver, muscle lacks the enzyme glucose-6-phosphatase and is unable to release free glucose. Only emergency situations result in brain glycogenolysis (Kanungo et al., 2018).

The total amount of glycogen stored is influenced by the quantity of carbohydrates consumed at the previous meal, the length of starvation (Rothman et al., 1991), and the level of physical activity (Hearris et al., 2018).

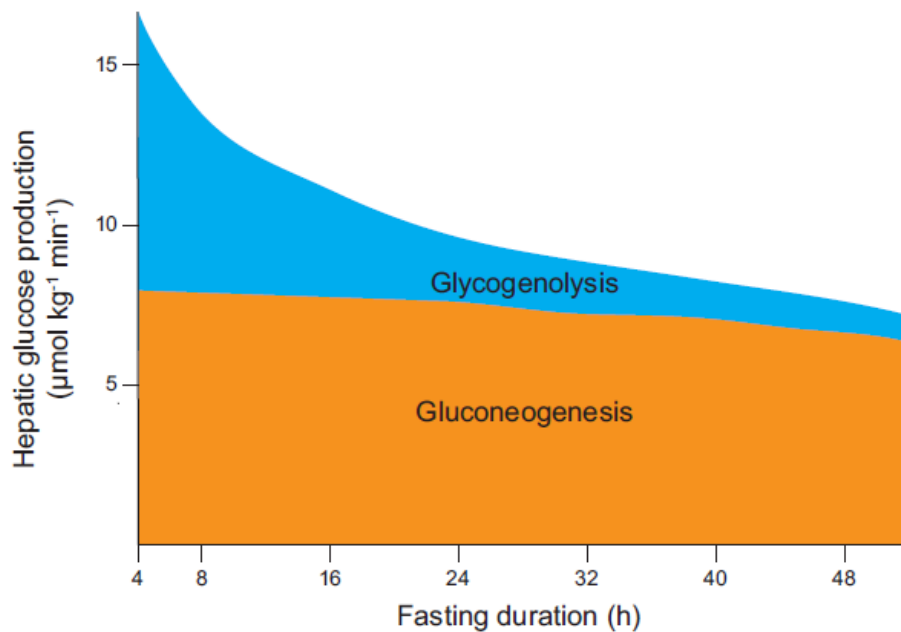


Figure 5: Sources of hepatic glucose production during fasting in humans (Petersen and Shulman, 2018)

Data from Rothman et al., 1991

One glucose-1-phosphate molecule can be released during the breakdown of glycogen thanks to the glycogen phosphorylase. Insulin and intracellular glucose concentration inhibit this enzyme while glucagon and adrenaline activate it (Stalmans et al., 1987). After that, glucose-1-phosphate is changed into glucose-6-phosphate and then glucose, before being released into the bloodstream (Paredes-Flores and Mohiuddin, 2023).

4.3 Gluconeogenesis

Parallel to glycogenolysis, gluconeogenesis emerges as the primary mechanism of glucose synthesis following the depletion of glycogen stores. The liver enables the synthesis of glucose from precursors other than carbohydrates. These precursors can include glycerol, lactate, alanine, glutamine, and other aminoacids. Lactate is the main precursor of gluconeogenesis (about 45 %), followed by alanine (20 %) and glutamine (15 %). Glycerol represents only 12 % (Gerich, 2000).

Skeletal muscle is the major source of these substrates and allows the supply of lactate and alanine from glycogenolysis and glutamine directly from proteolysis once glycogen is depleted. Muscle is thus

responsible for 70 % of the alanine released in the systemic circulation, 40 % of the lactate and 45 % of the glutamine (Dimitriadis et al., 2021).

The hormone-sensitive lipase catalyzes the breakdown of triglycerides into glycerol and non-esterified fatty acids (NEFA) in adipose tissue. The liver then transforms glycerol into glucose. Skeletal muscle can use NEFA as energetic substrates for oxidation, and as NEFA production rises, glucose uptake and oxidation by the muscle decrease. NEFA also permit the liver and kidney to stimulate gluconeogenesis (Ferrannini et al., 1983).

5. Regulations of glucose metabolism

5.1 Action of insulin

5.1.1 Synthesis, secretion and signalization

The most significant hormone in the control of glucose metabolism is insulin. It is a peptide hormone made up of 2 chains alpha and beta, each containing 21 and 30 amino acids, and linked by another peptide, the C-peptide, which has 31 amino acids and is found in the proinsulin state. Proinsulin is broken down into insulin on the one hand and C-peptide on the other during maturation in the Golgi Body. Pancreatic beta cells secrete insulin and C-peptide in equimolar amounts. The half-lives of insulin and C-peptide are 6-8 and 15 minutes, respectively.

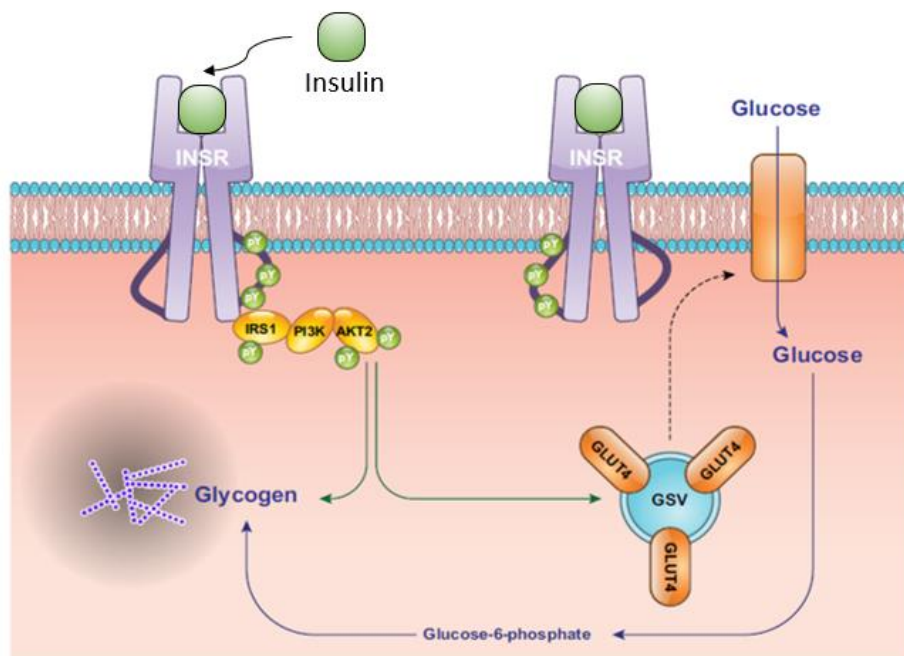


Figure 6: The insulin signaling cascade in skeletal muscle. Adapted from (Petersen and Shulman, 2018).

The main target tissues of insulin are the skeletal muscle, the liver and the white adipose tissue. In skeletal muscle, insulin promotes glucose utilization and storage by increasing glucose transport and

net glycogen synthesis. In liver, insulin activates glycogen synthesis, increases lipogenic gene expression, and decreases gluconeogenic gene expression. In white adipocyte tissue, insulin suppresses lipolysis and increases glucose transport and lipogenesis (Petersen and Shulman, 2018).

The insulin receptor is a transmembrane receptor with tyrosine kinase activity. Following the fixation of insulin, the receptor dimerizes, which causes autophosphorylation and activates signal transduction. A phosphorylation cascade involving the IRS and AKT proteins constitutes the signal transduction.

After insulin binds to its receptor in the skeletal muscle, a transduction signal causes GLUT4 to move from the cytosol to the cell membrane, where it then allows glucose to enter the cell (**Figure 6**). In the liver, the entrance of glucose into the hepatocytes via GLUT2 is independent from insulin but the AKT signaling leads to fast effects such as activation of the glycogen and protein synthetic machinery and slower transcriptionally mediated effects include upregulation of glucokinase, diminution of gluconeogenic capacity, and stimulation of de novo lipogenic capacity. In the adipose tissue, insulin signaling allows the translocation of GLUT4 to the membrane for glucose entrance. The most critical physiological functions of insulin action in white adipose tissue are suppression of lipolysis (required by the action of the phosphodiesterase 3B) and stimulation of glucose uptake (Petersen and Shulman, 2018).

The release of insulin from pancreatic beta cells is a controlled process that is influenced by a variety of variables, including blood glucose levels, hormonal levels, and nervous system activity. Glucose is absorbed into the portal vein during meal assimilation and joins the beta cells in entry by GLUT2 transporters. When glucose enters a beta cell, the glycolysis pathway is activated, which results in ATP synthesis and, ultimately, the closure of potassium ATP-dependent channels, depolarization of the cell membrane, and opening of calcium channels. The final cause of the insulin exocytosis from vesicles translocation to the membrane is the rise of intracellular calcium content, from extracellular liquid but also from the endoplasmic reticulum (**Figure 7**).

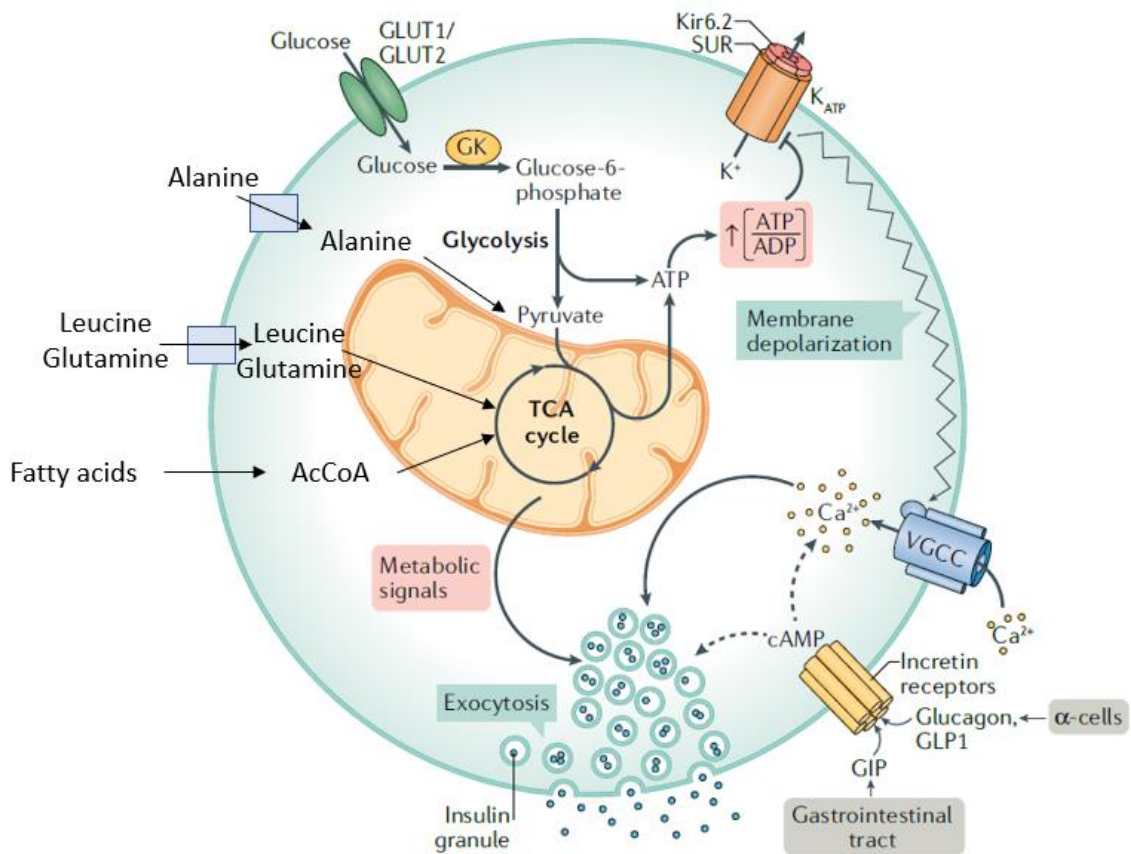


Figure 7: Mechanism of insulin release by beta cell. Adapted from (Campbell and Newgard, 2021)

Thus, the insulin secretion is biphasic; the first phase is a brief peak that lasts for no longer than five minutes and involves the use up of the insulin that had been previously stored in the vesicles. The second phase is characterized by a more gradual rise, with a later peak that persists throughout the postprandial glycaemic excursions. An intravenous glucose tolerance test can reveal the two secretion phases, and research has shown that maintaining a healthy glucose tolerance depends on the kinetics of insulin secretion, or more specifically, the presence of the first peak of insulin secretion. Thus, a change in this initial peak is one of the first indications of impaired glucose tolerance (Del Prato and Tiengo, 2001).

Several mechanisms control insulin secretion in a healthy individual (Fu et al., 2014):

- nutrients: glucose is the main stimulator of insulin secretion, but amino acids and NEFA can also stimulate insulin release. After passive diffusion through the cell, fatty acids are transformed into acetyl coenzyme A, which enters into the Krebs cycle, at the initiation of insulin granules exocytosis. Alanine is transformed into pyruvate and other amino acids such as leucine or glutamine are transformed into other substrates of the Krebs cycle.

- gastrointestinal hormones that stimulate insulin secretion include GIP and GLP-1 (incretin hormones), but they also include gastrin, secretin, and cholecystokinin. Due to the intestinal detection and absorption of nutrients, incretin hormones are released from the enteroendocrine cells. This mechanism participates to the control of postprandial glucose excursions, improving glucose tolerance.

- other pancreatic hormones: glucagon stimulates insulin secretion whereas somatostatin decrease it.

- nervous system: the parasympathetic system activates insulin secretion, whereas the othosympathetic system, especially via the action of adrenaline, decreases it.

- catecholamines: their action inhibits insulin secretion.

5.1.2 Physiological effects

Insulin affects the metabolism of glucose, lipids, and proteins, which primarily take place in the liver, skeletal muscles, and adipose tissue. Insulin is considered the hormone of anabolism.

Effect on glucose metabolism

Insulin is the principal hormone involved in glucose regulation. Its action consists of modulating blood glucose in (**Figure 8**):

- suppressing endogenous glucose production by the liver and the kidney. The expression and activity levels of the limiting enzymes involved in gluconeogenesis, particularly the glucose-6-phosphatase and the phosphoenolpyruvate carboxykinase, are modulated, enabling this potent suppression. It was demonstrated that the increase in insulin concentrations in the portal vein directly mediated the suppression of hepatic glucose production (Lewis et al., 1996). But according to some studies (Cherrington et al., 1998; Mittelman et al., 1997), the primary mechanism by which insulin suppresses endogenous glucose production is an indirect, systemic effect that is mediated by substrates precursors of gluconeogenesis such as glycerol, lactate of amino acids, but also free fatty acids. Consequently, gluconeogenesis is lowered when the systemic levels of these precursors are reduced.

- stimulating glucose disposal (oxidation and storage) by the insulin-sensitive tissues. The recruitment of GLUT4 to the membranes of skeletal muscles, the heart, and adipose tissue is made possible by the insulin signaling pathway, greatly facilitating the entry of glucose. Additionally, insulin enables the activation of the glucose phosphorylation into glucose-6-phosphate, enabling the initiation of the glycolysis pathway and the maintenance of the gradient of glucose concentration between intracellular and extracellular fluid. Because GLUT2 is insulin-independent, insulin has no effect on the

entrance of glucose into hepatocytes in the liver. On the other hand, insulin has a favorable impact on the phosphorylation of glucose-6-phosphate. Lastly, insulin stimulates glycogen synthesis in the liver and muscles by activating glycogen synthase. Insulin inhibits glycogen phosphorylase, which stops glycogenolysis.

Effect on lipid and protein metabolism

80 % of the energy reserves of the body are found in adipose tissue, which allows for the storage of energy in the form of triglycerides. Insulin promotes the synthesis and activity of lipoprotein lipase, which enables the uptake and esterification of NEFA from blood lipoproteins. Insulin is a key hormone that inhibits the action of the hormone sensitive lipase, which is the main hormone responsible for lipolysis. Insulin also stimulates the accumulation of triglycerides in adipose tissue.

Regarding the metabolism of proteins, insulin promotes the active transport of aminoacids into cells, speeds up protein synthesis, and lowers proteolysis. When eating a meal with an increased protein content, the liver and muscles use the extra aminoacids for fatty acid synthesis.

The postprandial inhibition of lipolysis and proteolysis by insulin results in a fall in the levels of amino acids, glycerol, and fatty acids in the blood, constituting the indirect insulin effect of endogenous production (Mittelman and Bergman, 2000; Rebrin et al., 1996).

5.2 Action of glucagon

The main hyperglycemic hormone that functions as an insulin counterregulator is glucagon. It is a 29-aminoacid peptide hormone that is released by pancreatic alpha cells following the maturation of its precursor proglucagon. The half-life of glucagon is only 5–6 minutes. This hormone promotes catabolism and permits the maintenance of glucose release in the bloodstream during periods of fasting (Müller et al., 2017).

In healthy individuals, alpha cells secrete glucagon in situations involving decreased blood glucose levels, prolonged fasting, physical activity, and protein-rich meals. Endocrine or paracrine factors may also affect glucagon release. Globally, insulin, somatostatin, amylin, or GLP-1 inhibit glucagon secretion while ghrelin or GIP activate it. The autonomic nervous system also stimulates its release (Janah et al., 2019).

Glucagon levels typically range from 60 to 200 pg/mL, but they can rise above 1 ng/mL under fasting or stressful circumstances (Müller et al., 2017). Due to significant liver degradation, which directs the action of glucagon to the liver, the level of glucagon in the portal vein during a fast is generally 1.7-fold higher than in the systemic circulation. Blood glucose levels affect the blood levels of glucagon and insulin: when blood glucose levels are low, glucagon levels rise, while when blood glucose levels are

high, insulin levels rise. Therefore, the effect of glucagon on the liver is determined by the insulin/glucagon ratio (Unger, 1971).

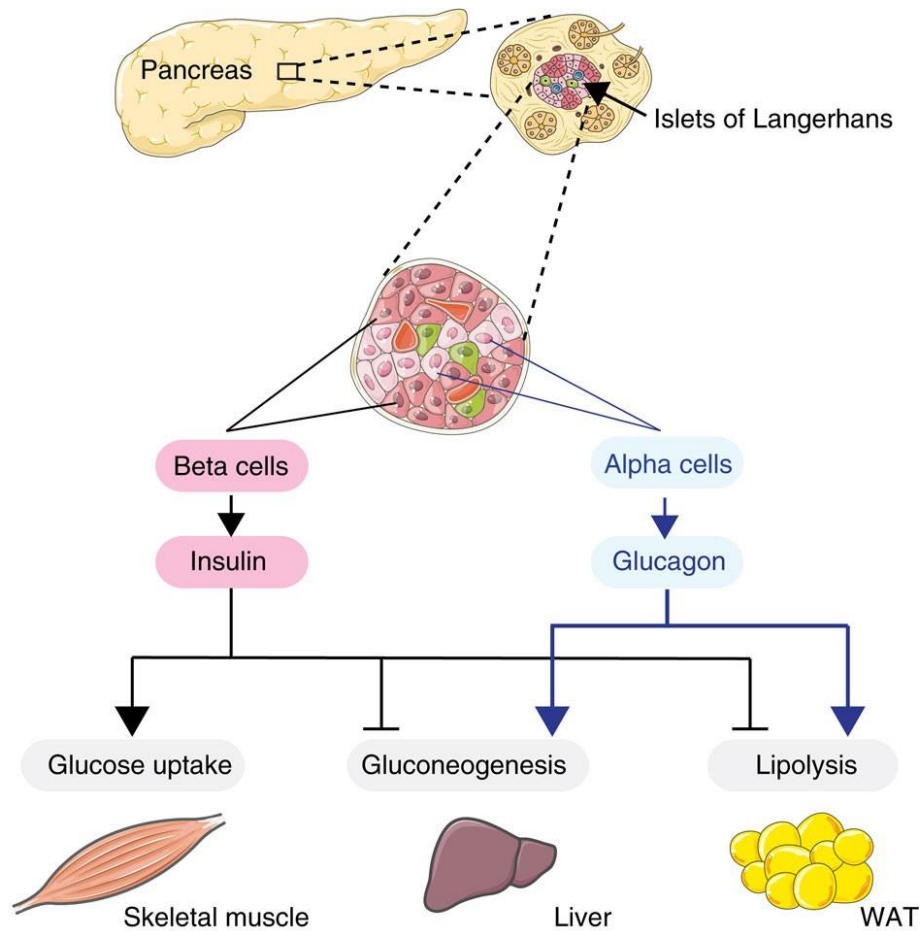


Figure 8: Glucoregulatory roles of the pancreatic-derived hormones insulin and glucagon (Ruud et al., 2017)

The primary effects of glucagon are on the liver, where they include stimulation of gluconeogenesis and glycogenolysis as well as inhibition of glycogenogenesis due to its effects on the key enzymes in these metabolic pathways. In order to release the precursors of endogenous glucose production in the systemic circulation, glucagon increases protein catabolism and amino acid release from muscles (Quesada et al., 2008). It also stimulates lipolysis and inhibits lipogenesis in adipose tissue (**Figure 8**).

5.3 Action of other mechanisms

The other mechanisms involved in glucose metabolism regulation have essentially a hyperglycemic effect and concern:

- the orthosympathetic system: via the action of adrenaline in stimulating glucagon and inhibiting insulin secretion. The orthosympathetic system thus has a similar effect as glucagon on the liver, skeletal muscle, and adipose tissue. It is a regulatory pathway that acute stress activates.

- glucocorticoids: they have a positive effect on gene transcription coding for enzymes involved in gluconeogenesis, lipolysis, and proteolysis, independently of blood glucose levels. Their action also leads to an increase in hepatic glycogen storage.

- growth hormone, which has an anti-insulin effect, directly or indirectly via growth factors. Growth hormone also has an anabolic function in protein metabolism and stimulates lipolysis.

Complex hormonal regulation is needed to maintain the postprandial glycemic response. A delicate balance between the actions of insulin and all other catabolic hormones protects glucose homeostasis.

5.4 Incretin effect

Insulin is released in greater amounts in response to an oral glucose challenge than it is in response to an intravenous glucose challenge. This event is called “incretin effect” and highlights the release of intestinal hormones from enteroendocrine cells jointly with intestinal glucose absorption, which does not occur after intravenous glucose administration (Nauck and Meier, 2018).

GIP and GLP-1 hormones increase the release of insulin and the suppression of glucagon secretion by fixation on their own receptor located in islets. When compared to intravenous administration, the insulin secretory response to oral glucose administration is at least two fold higher (Seino, 2011). GLP-1 is released from L-cells, which are found lower in the small and large intestine, whereas GIP is produced in enteroendocrine K cells, epithelial cells of the intestinal mucosa located in the duodenum and proximal jejunum (**Figure 9**).

In human subjects who are fasting, GIP and GLP-1 basal levels are in the low pmol/L range. The release of GIP and GLP-1 begins shortly after the beginning of food intake, peaks at 15–50 pmol/L between 40–60 minutes after ingestion, and returns to basal levels several hours later (Holst, 2007).

The release of incretin hormones remains yet partially known. It is triggered by glucose detection (even if the contribution of sweet taste receptor is controversial) and other complex carbohydrates, triglycerides, proteins, and aminoacids to a lesser extent. The rate of nutrients entering the intestinal lumen, due to the rate of gastric emptying, basically affects the secretion of GLP-1 and GIP; therefore, a minimum rate is required to start the release. The rate of duodenal glucose delivery needed to stimulate GLP-1 secretion was estimated to be 1.4 kcal/min (Schirra et al., 1996). Intestinal absorption of glucose by SGLT1 (Gorboulev et al., 2012) would appear as a major contributor of incretin release and the presence of a neural transmission is also supposed. Additional factors, such as bile acids or the microbiome, can also promote the release of incretin hormones (Pais et al., 2016).

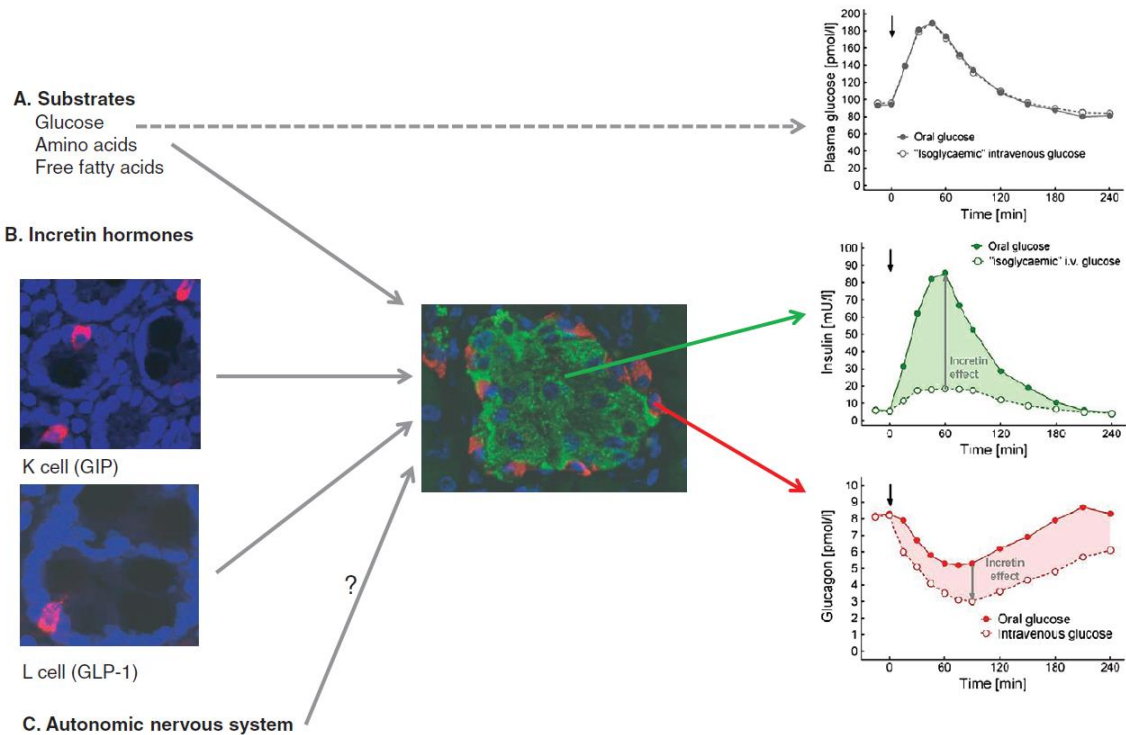


Figure 9: Incretin effect (Nauck and Meier, 2018)

Contribution of (A) metabolic substrates, as well as (B) the incretin hormones glucose-dependent insulinotropic polypeptide (GIP) and glucagon-like peptide-1 (GLP-1), and, potentially, (C) neural transmission (left panels) to the stimulation of insulin secretion (“insulinotropic incretin effect”) and the suppression of glucagon secretion (“glucagonostatic incretin effect”) in healthy human subjects (islet of Langerhans with α cells (red) and β cells (green); central panel).

It is interesting to note that GIP and GLP-1 secretion almost occur simultaneously, whereas L-cells are located more distally, suggesting the existence of a neural signal from the proximal gut to the distal part of the gut, anticipating GLP-1 release before nutrients reached the L-cells (Brubaker, 1991). Under most physiological circumstances, the levels of active incretin hormones are below their total levels because the dipeptidyl peptidase-4 (DPP4) enzyme degrades and inactivates both GIP and GLP-1. Although an interindividual variation in GIP and GLP-1 levels has been noted, it is still unknown whether this variation results from the quantity of enteroendocrine cells or from the efficiency of the mechanisms that control the release of these hormones (Nauck et al., 2004).

Incretin hormones have an insulinotropic effect, but this effect depends on blood glucose levels; it can only be induced by hyperglycemia, so incretin hormones cannot cause hypoglycemia events. The lowest blood sugar level at which the incretin effect can occur was determined to be 66 mg/dL. From this point on, there is a positive correlation between the incremental blood glucose concentrations and the amount of increased insulin secretion (Nauck et al., 2002).

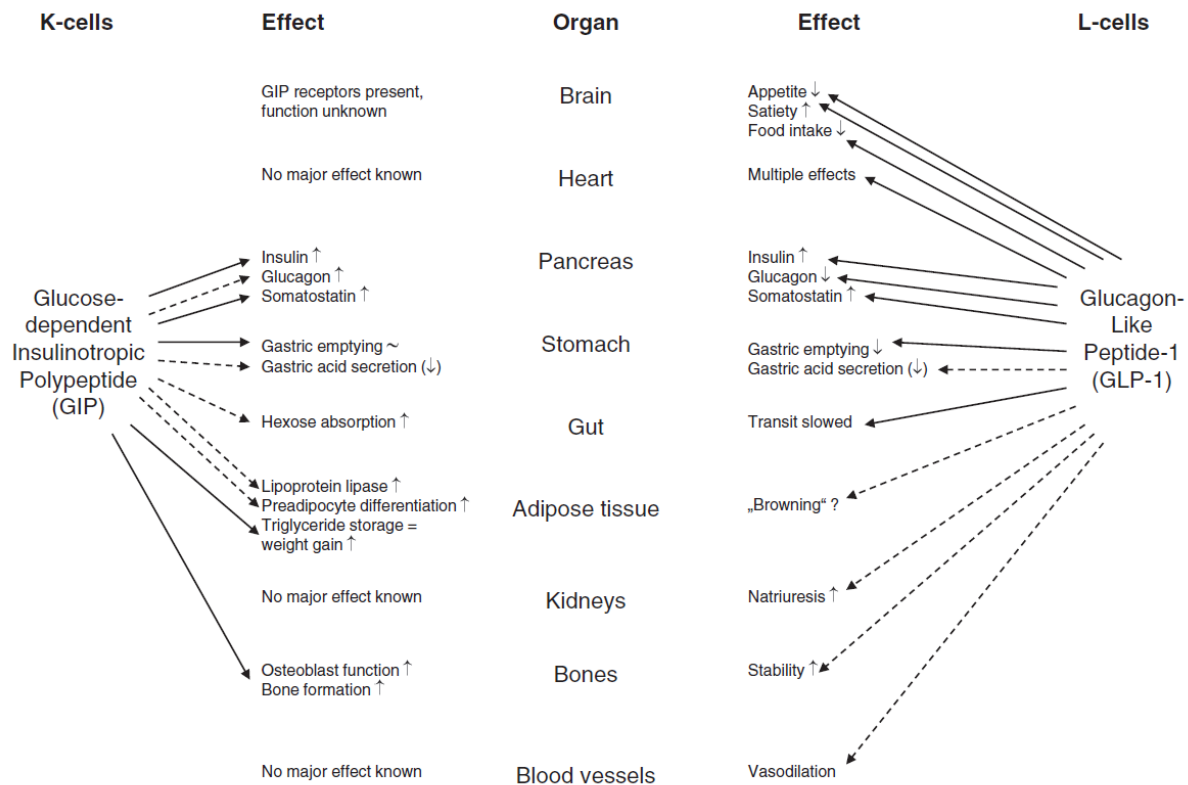


Figure 10: Biological effects of the incretin hormones glucose-dependent insulinotropic polypeptide (GIP) and glucagon-like peptide-1 (GLP-1) on various organs (Nauck and Meier, 2018)

In addition to their impact on beta cells, GIP and GLP-1 also have pleiotropic effects. They target the central nervous system by reducing appetite and food intake and increasing satiety (Flint et al., 1998). Through the activation of the lipoprotein lipase, GIP can also promote the storage of triglycerides in adipose tissue (Yip and Wolfe, 2000). On a physiological and pharmacological level, GLP-1 slows gastric emptying in the gastrointestinal tract, whereas GIP is unable to do so. As a result, the rate of nutrients reaching the intestinal mucosa is delayed. This delays the rate of absorption, which in turn delays the rate at which exogenous glucose and triglycerides appear after eating (Deane et al., 2010). Additionally, GIP and GLP-1 play a role in bones metabolism by promoting bone formation and preventing bone resorption. GLP-1 has been shown to have a variety of positive effects, including those on cardiac blood supply, substrate uptake, ischemia tolerance, and the development of atherosclerosis (Nauck and Meier, 2018) (**Figure 10**).

6. Role of the kidney in glucose metabolism

Although it is not a glucose storage organ, the kidney is crucial to maintain glucose homeostasis. Like all other organs, the kidney uses glucose as fuel for operation. It has been estimated that during the postprandial period, the kidney uses about 10 % of the total amount of glucose taken in by the body.

During fasting, the kidney also contributes to the production of endogenous glucose and is responsible for 20 % of the total glucose released (Gerich, 2000).

In addition to producing and consuming glucose, the kidney also has the capacity to reabsorb glucose following glomerular filtration of the plasma, acting as a mechanism for glucose homeostasis. The amount of glucose that is filtered under normal circumstances is 180 g, or about 180 liters of plasma per day (the amounts of glucose that are metabolized and produced by the kidney after gluconeogenesis are estimated to be 25-35 g and 15-55 g, respectively). The kidneys reabsorb almost all of the 180 g of filtered glucose, depriving the urine of glucose in most cases. The reabsorption of filtered glucose is linearly correlated with blood glucose levels. The point at which the reabsorption process is saturated occurs at a blood glucose level of 11 mmol/L (200 mg/dL) (Gerich, 2010).

Glucose is reabsorbed in the proximal convoluted tubule via SGLT cotransporters. The main player, SGLT2, a high-capacity low-affinity glucose transporter, accounts for 90 % of the total glucose reabsorbed, with SGLT1 (high-affinity and low-capacity) handling the remaining 10 %. SGLT2 allows the cotransport of 1 molecule of sodium and 1 molecule of glucose (Wright et al., 2011).

II. Type 2 diabetes and implication of intestinal glucose absorption in its pathophysiology

1. Definition and classification

Type 2 diabetes consists of dysregulation of glucose homeostasis control and is defined by the World Health Organization (WHO) as a glycemia ≥ 1.26 g/L (7 mmol/L) after an 8-hour fasting and verified twice, a glycemia ≥ 2 g/L (11.1 mmol/L) 2 hours after an oral glucose challenge of 75 g or a glycemia ≥ 2 g/L (11.1 mmol/L) whatever the time of measurement associated with clinical signs (American Diabetes Association, 2014; World Health Organization and International Diabetes Federation, 2006).

The state of progressively worsening glucose homeostasis between the "healthy" and the "type 2 diabetes" states is referred as "prediabetes." Subjects with a glycemia included in the range of 1.10 g/L (6.1 mmol/L) and 1.25 g/L (7 mmol/L) after an 8-hour fasting, verified twice, or a glycemia in the range of 1.40 g/L (4.8 mmol/L) and 2 g/L (11.1 mmol/L) 2 hours after a 75 g oral glucose challenge are considered prediabetics (American Diabetes Association, 2014; World Health Organization and International Diabetes Federation, 2006). People who are prediabetic have impaired glucose tolerance, which results in higher-than-normal blood sugar levels after meals or under other physiological circumstances. If prediabetes is an intermediate phenotype before the onset of type 2 diabetes, then not all prediabetic subjects will inevitably go on to develop type 2 diabetes. The

conversion rate of subjects from prediabetes to type 2 diabetes depends on their characteristics (Bansal, 2015) and this rate has been estimated at 4-6 % for subjects with only impaired glucose tolerance, at 6-9 % for subjects with only impaired fasting glycemia, and at 15-19 % for those with both characteristics (Gerstein et al., 2007).

Since 90 % of diabetes cases are type 2 cases, type 2 diabetes is the predominant etiologic classification for diabetes. Type 1 diabetes is a form of diabetes with beta cell destruction by autoantibodies, leading to a severe insulin deficiency. This destruction is usually immune mediated but can also be idiopathic. Type 2 diabetes is, for its part, characterized first by a predominantly insulin resistance with relative troubles in insulin secretion and then by a predominantly deficiency in insulin secretion associated with insulin resistance. Insulin resistance is thus associated with a set of polymorphic symptoms related to obesity. Thus, six metabolic disorders—visceral obesity, fasting glycemia greater than 1.10 g/L, insulin resistance, dyscholesterolemia, hypertriglyceridemia, and high blood pressure—have been used to define the term metabolic syndrome. Someone who meets at least 3 out of 6 criteria is considered to suffer from metabolic syndrome (DeFronzo and Ferrannini, 1991). Other distinct types of diabetes have also been identified; these include iatrogenic diabetes brought on by drug use, diseases of the exocrine pancreas, endocrinopathies, genetic defects in insulin action, genetic defects in beta cell function, as seen in Maturity-Onset Diabetes of the Young (MODY), and neonatal diabetes. The list also includes gestational diabetes mellitus (American Diabetes Association, 2014).

The type 2 diabetes group is particularly heterogeneous, and type 2 diabetes is distinguished from the other forms more by exclusion criteria than by actual inclusion criteria. The development of more accurate classification systems is a future goal for type 2 diabetes definition: new adult-onset diabetes subgroups have been suggested (Ahlqvist et al., 2018) and used subsequently (Raverdy et al., 2022). Ahlqvist et al. determined 5 sub-clusters of type 2 diabetes based on six defined parameters: glutamate decarboxylase antibodies, age at diagnosis, Body Mass Index (BMI), glycated hemoglobin (HbA1c) and homeostatic model assessment 2 estimated for beta cell function and insulin resistance. The 5 subgroups were the following: Cluster 1: Severe Autoimmune Diabetes (SAID), overlapped with type 1 diabetes; Cluster 2: Severe Insulin-Deficient Diabetes (SIDD); Cluster 3: Severe Insulin-Resistant Diabetes (SIRD); Cluster 4: Mild Obesity-Related Diabetes (MOD); Cluster 5: Mild Age-Related Diabetes (MARD) (**Figure 11**). The aim of this classification is to improve the medical care of patients suffering from type 2 diabetes.

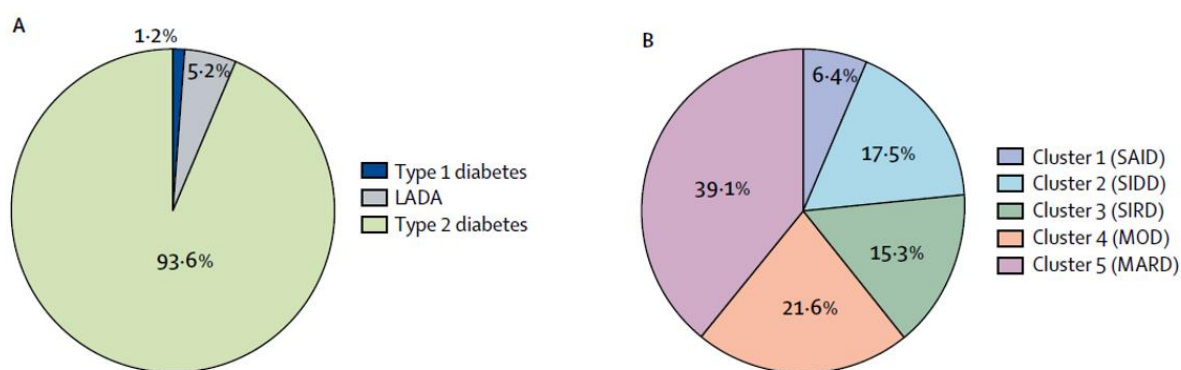


Figure 11: Patient distribution according to method of classification. Adapted from (Ahlqvist et al., 2018).

(A) Distribution of patients (n=8980) according to traditional classification. (B) Distribution of patients (n=8980) according to the proposed clustering.

LADA=latent autoimmune diabetes in adults. SAID=severe autoimmune diabetes. SIDD=severe insulin-deficient diabetes. SIRD=severe insulin-resistant diabetes. MOD=mild obesity-related diabetes. MARD=mild age-related diabetes.

2. Epidemiology

Over 90 % of all cases of diabetes are type 2, which is more common than any other type and affects people of all ages, genders, and socioeconomic backgrounds.

The International Diabetes Federation (IDF) predicts that more than one in ten adults worldwide now have diabetes. In adults aged 20 to 79, diabetes affected 537 million people worldwide (10.5 % of the world's population) in 2021. Predictions announced 643 million (11.3 %) by 2030 and 783 million (12.2 %) by 2045, corresponding to a rate of increase of 46 %. However, this rate of increase predicted by 2045 differs according to the area of the world: it is estimated at 13 % for Europe, 24 % for North America, 27 % for the Western Pacific, 50 % for South and Central America, 68 % for South-East Asia, and finally 87 % and 134 % for South-East Asia/North Africa and Africa, the two areas where the highest rate of prevalence is expected in the coming years. Concerning the number of cases, the most affected countries by diabetes are (in millions of cases): China (140.9), India (74.2), Pakistan (33.0) and the United States of America (32.2). In terms of prevalence, they are: Pakistan (30.8 %), Kuwait (24.9 %) and New Caledonia (23.4 %). It is estimated that approximately 240 million people are living with undiagnosed diabetes worldwide, and almost 90 % of these people live in low- and middle-income countries. In over 70 % of mainly high-income populations, the incidence of diabetes was stable or declined during the 2006-2017 period, that explains the differential rate of progression of the disease predicted to 2045 according to area of the world (International Diabetes Federation, 2021) (**Figure 12**).

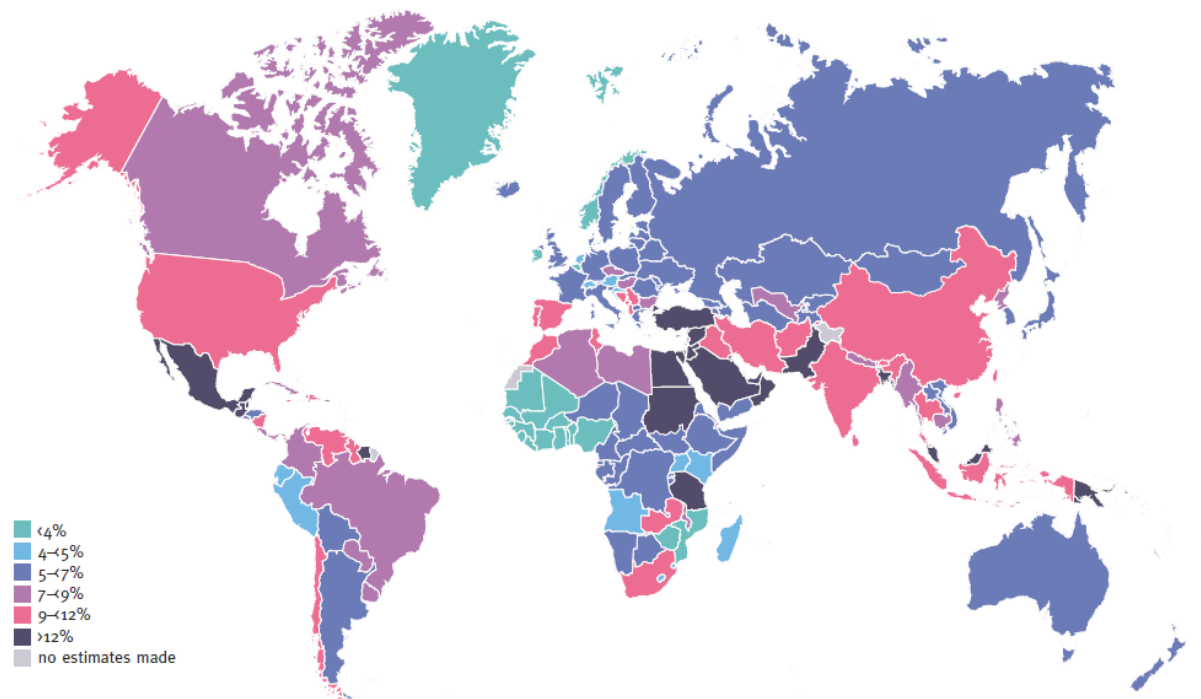


Figure 12: Estimated age-adjusted comparative prevalence of diabetes in adults (20-79 years) in 2021 (International Diabetes Federation, 2021)

In Europe, 1 in 11 adults (61 million) have diabetes, which corresponds to a prevalence of 9.2 %. The countries with the highest number of cases (in millions) are Turkey (9.0), Russia (7.4), Germany (6.2) and Spain (5.1). In terms of prevalence, they are: Turkey (14.5 %), Spain (10.3 %), Andorra (9.7 %) and Portugal (9.1 %) (International Diabetes Federation, 2021).

In France in 2020, more than 3.5 million people (5.3 % of the total population) were diagnosed with diabetes and benefited from pharmacological treatment, with a disparity concerning sex because it affected 6 % of men compared to 4.5 % of women. Territorial disparities were very marked because diabetes prevalence is particularly high in overseas (“Outremer”) territories (more than 9 % in La Réunion and Guadeloupe and more than 7.5 % in Guyane and Martinique), Seine-Saint-Denis (8.1 %) and the Nord-East of France (more than 6 %) whereas the western France is less impacted (Santé publique France, 2021).

The increase in the prevalence of type 2 diabetes followed the increase of obesity. In fact, the prevalence of obesity worldwide increased by three between 1975 and 2016. In 2016, the number of adult subjects suffering from obesity (Body Mass Index (BMI) over 30 kg/m²) was estimated at 650 million and overweight at 1.9 billion (BMI between 25 and 30 kg/m²), corresponding respectively to a prevalence of 13 % and 39 %. Concerning children, 39 million under the age of 5 were overweight or obese in 2020, and over 340 million were aged 5–19 (World Health Organization, 2021).

3. Complications

About 1.5 million deaths per year are directly related to diabetes, according to the World Health Organization, and the International Diabetes Federation estimated that 6.7 million people would die from the disease in 2021 (International Diabetes Federation, 2021). The crude and age-standardized rates of diabetes-related mortality in France are 53.1 and 30.0/100 000, respectively, with men experiencing a higher rate than women (40.7 versus 22.6/100 000) (Santé publique France, 2019).

The mortality rate in diabetes is caused by the numerous complications brought on by chronic hyperglycemia. The production of mitochondrial superoxide causes tissue damage as a result of hyperglycemia. Endothelial cells in the retinal capillaries, mesangial cells in the renal glomerulus, and neurons and Schwann cells in peripheral nerves are among the cells that are particularly sensitive to hyperglycemia (Stolar, 2010). Consequently, the retina, the kidney and the peripheral nerves are organs particularly affected by hyperglycemia-related complications.

Concerning the retina, diabetic retinopathy constitutes the leading cause of blindness in the world. Macular edema or the development of neo-vessels as a result of a retinal split are thought to be the causes of the vision loss that worsens over time. In a systematic review, the annual incidence of diabetic retinopathy was estimated to be between 2.2 and 12.7 % (Sabanayagam et al., 2019).

Kidney disease in diabetes is identified by either a rise in albumin excretion in urines or a fall in glomerular filtration rate (Gembillo et al., 2021). Type 2 diabetic patients are thought to develop chronic kidney disease in nearly 50 % of cases (Thomas et al., 2015). Kidney inflammatory lesions, cell damage, and apoptosis, as well as tissue remodeling and fibrosis, are all caused by hyperglycemia.

Concerning the peripheral nerves, over 50 % of diabetes patients are predicted to experience symptoms of neuropathy as their diabetes progresses, and neuropathy is estimated at 30 % in diabetic subjects. Neuropathy is described by symptoms of numbness, tingling, pain, or weakness that appear generally in the feet before spreading more proximally. Additionally, patients with severe neuropathy run the risk of developing ulcerations, which in the worst cases can result in lower-extremity amputations. According to estimates, 15 % of diabetic patients will experience ulceration as the disease progresses (Callaghan et al., 2012).

Additionally, macrovascular complications from hyperglycemia include atherosclerosis, myocardial infarction, arteriopathy, and stroke. When compared to subjects without diabetes, subjects with diabetes had significantly higher levels of vascular inflammation, neovascularization, intraplaque hemorrhage, and reparative collagen (Purushothaman et al., 2011). In a Finnish study, HbA_{1c} > 7.9 % was linked to 12 % of cardiovascular event mortality and 21 % incidence of coronary heart disease events (Kuusisto et al., 1994). According to the Paris Prospective Study, people with type 2 diabetes or

impaired glucose tolerance have a 2.5-fold higher risk of dying from coronary heart disease compared to healthy people (Eschwege et al., 1985).

According to several epidemiological studies, patients with type 2 diabetes are more likely to develop cancers of the liver, pancreas, stomach, colorectum, kidney, and breast. The onset of cancer would be caused by the hyperglycemic condition (Abudawood, 2019).

Thus, many serious comorbidities are caused by type 2 diabetes. This is why improving glycemic control through medical or interventional treatments, as well as early disease diagnosis, is crucial for lowering complications from long-term hyperglycemia.

4. Well-described pathophysiology

Dysregulation of the energetic metabolism, and particularly of glycemic control, characterizes type 2 diabetes. In other words, there is a change in how the glucose from the alimentation is stored or used. The environmental factors that contribute to type 2 diabetes include obesity, sedentary behavior, and a genetic predisposition. It is well known that the pathophysiological causes of diabetes onset include insulin resistance and inadequate insulin secretion.

4.1 Insulin resistance

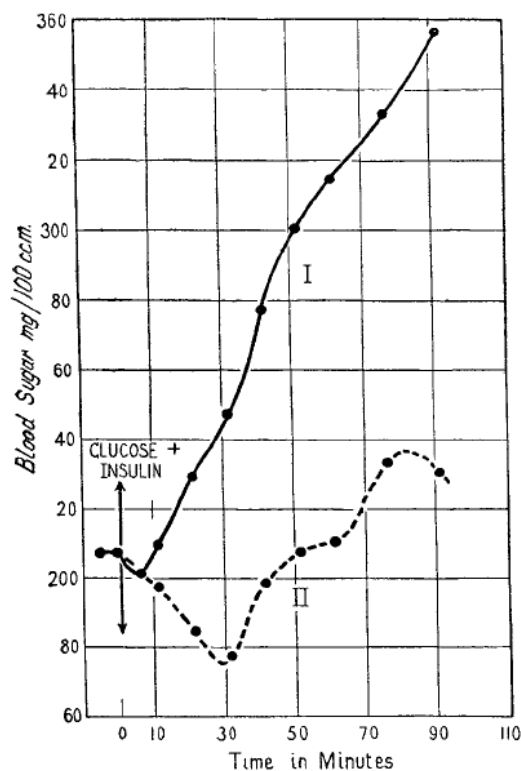


Figure 13: Simultaneous glucose and insulin test (Himsworth, 1936).

Patient I = insulin-insensitive; Patient II = insulin-sensitive

After simultaneous injections of glucose and insulin in type 2 diabetic patients, some subjects responded by continuously lowering blood glucose levels, while others showed a noticeably rising blood glucose level; these were therefore deemed to be insulin-insensitive (Himsworth, 1936). It means that tissues sensitive to insulin are unable to lower blood sugar levels to the same extent at the usual plasma insulin concentration (**Figure 13**).

In other words, the efficiency of the suppression of endogenous glucose production and lipolysis, the cellular glucose uptake, and the glucose storage into glycogen are decreased. Beta cells release more insulin to make up for the decreased responsiveness of their tissues, which raises fasting plasma insulin levels and delays the time it takes for blood glucose levels to return to baseline after a meal. The main factors influencing the development of insulin resistance are excessive glucose and lipid intake before the onset of the illness. Thus, insulin resistance and hyperinsulinemia are the driving forces behind a vicious cycle that, when it reaches its peak, could result in beta cell failure from gluco- and lipotoxicity and type 2 diabetes (Petersen and Shulman, 2018).

Insulin resistance is a significant polymorphic metabolic disorder that involves numerous pathways. It is now understood that obesity-related insulin resistance is a result of a decrease in the content of insulin receptors as well as impaired cellular insulin signal transduction (Petersen and Shulman, 2018). The pathogenesis of insulin resistance has been linked to cellular mechanisms including the accumulation of ectopic lipids, activation of the unfolded protein response, cytokine release, and inflammation (Samuel and Shulman, 2012).

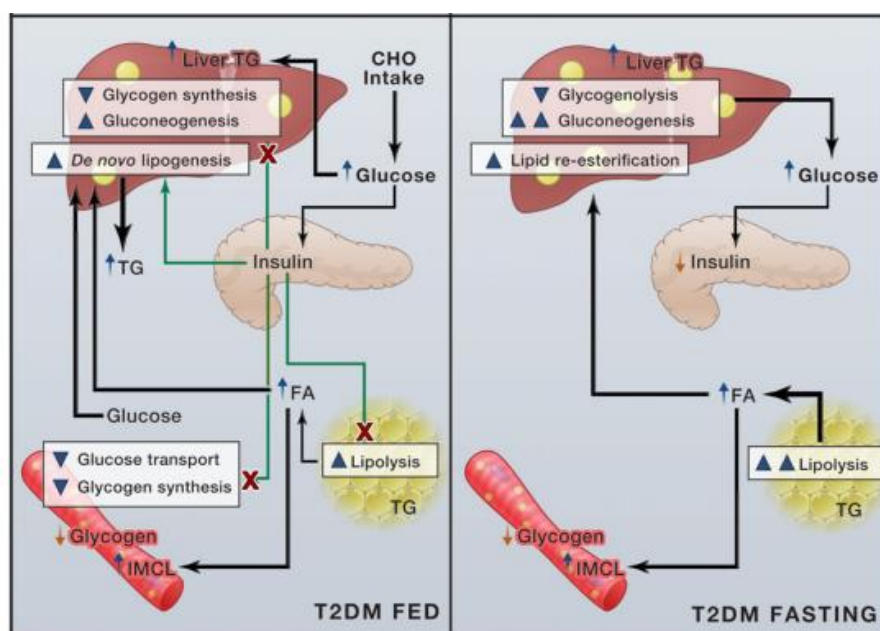


Figure 14: Mechanisms of liver, skeletal muscle and adipose tissue insulin resistance in fed and fasting state (Samuel and Schulman, 2012)

Since various tissues are insulin-sensitive and each has unique functional effects, different types of insulin resistance have been described for these various tissues, including the liver, the skeletal muscle and the white adipose tissue.

4.1.1 In the liver

The physiological effects of insulin on the liver during the postprandial state include the inhibition of gluconeogenesis and glycogenolysis and the stimulation of glycogen synthesis. Hepatic insulin resistance can have acute, chronic, intrahepatic, or extrahepatic components. It has also been reported that hepatic insulin resistance can be selective for glucose or lipids handling (Petersen and Shulman, 2018).

Acute components

In type 2 diabetes, the lack of suppression of hepatic gluconeogenesis is the primary indicator of hepatic insulin resistance and is the cause of fasting hyperglycemia (Dinneen et al., 1992). It occurs shortly after insulin is released and also has an extrahepatic origin because it is made possible by the inhibition of lipolysis in adipose tissue, which lowers the turnover of NEFA and glycerol (Rebrin et al., 1996). However, to a lesser extent, there may also be a decrease in the intrahepatic lipolysis suppression. Although it varies depending on the species or the length of the fast, the glycogen content is also a sign of hepatic insulin resistance. In insulin resistance states, there is less suppression of glycogenolysis and less net hepatic glycogen synthesis, which results in a smaller daily variation in the amount of glycogen in the liver and a globally constant level of glycogen due to a lack of insulin control of both glycogen synthesis and utilization (Basu et al., 2005; Krssak et al., 2004).

Defects of hepatic insulin receptor tyrosine kinase activation and actors of the insulin signaling pathway (especially IRS and AKT) phosphorylation have been identified, similar to those in skeletal muscle and adipose tissue.

Chronic components

Chronic indicators of hepatic insulin resistance include changes to the genes responsible for gluconeogenesis and *de novo* lipogenesis. Gluconeogenesis-related genes exhibit increased expression levels, whereas lipogenesis-related genes exhibit decreased expression levels (Petersen and Shulman, 2018). Additionally, an increase in fasting plasma insulin level represents a rough indicator of hepatic insulin resistance. This indicator is particularly helpful in studies with a large cohort of patients because it enables the calculation of indexes (Singh, 2010).

Insulin resistance is now widely acknowledged to be a common early sign in type 2 diabetes patients. If insulin resistance is the first disorder that many people notice, it is undeniably proven that a defect in beta cell insulin secretion causes type 2 diabetes to develop. Due to both insulin action and secretion

defects, which can be acquired either genetically or environmentally, type 2 diabetes can progress (DeFronzo and Tripathy, 2009).

4.1.2 In the skeletal muscle

The skeletal muscle is the primary actor for the uptake of glucose from the blood system. This uptake is regulated by insulin and then GLUT4 translocation. Because muscle accounts for about 25 % of total postprandial glucose uptake and 80 % of glucose disposal during an insulin-stimulated glucose disposal test (measured by hyperinsulinemic euglycemic clamp, the gold standard technique of insulin resistance measurement in vivo), muscle insulin resistance is a major contributor to whole body obesity-related insulin resistance (DeFronzo and Tripathy, 2009).

Insulin resistance therefore primarily refers to a defect in glucose transport into the cell in skeletal muscle. The synthesis of glycogen has been found to be significantly impaired (by about 50 %) in both type 2 diabetic patients and lean subjects with insulin resistance, suggesting that a primary blockade in the glycogen synthesis pathway could eventually result in a reduction in glucose transport (Shulman, 2014).

However, other data suggested that glucose transport would be the main rate-regulating step and that individuals with insulin resistance would initially have defective GLUT4 translocation to the membrane. In fact, defects of insulin resistance receptors have been identified, including defects in insulin receptor tyrosine kinase activity and content, which impairs the phosphorylation of IRS1, PI3K, and AKT, the key players in the insulin signaling pathway, resulting in a reduction in GLUT4 translocation and glycogen synthesis (Galuska et al., 1998) (**Figure 14**). In order to assess the relative contribution of each specific signaling defect to the final pattern of skeletal muscle insulin resistance, the actual research perspectives are focused on computational modeling of signaling pathways (Petersen and Shulman, 2018).

4.1.3 In the adipose tissue

In comparison to the mechanisms affecting skeletal muscle and the liver, the ones causing insulin resistance in adipose tissue are more complicated and poorly understood. Similar to skeletal muscle, insulin-stimulated glucose uptake is permitted by adipocytes, and this function is compromised by obesity-related insulin resistance. White adipose tissue, however, is much less quantitatively significant than skeletal muscle because it accounts for less than 5 % of the overall total glucose disposal by the body in the postprandial state (Kelley et al., 1988). Because of this, the insulin resistance of adipose tissue is more indirect than direct, with implications for the insulin sensitivity of skeletal muscle and the liver. Insulin has an impact on adipose tissue by suppressing lipolysis and promoting fatty acid esterification. As a result, adipose tissue insulin resistance causes a poor suppression of

lipolysis that is accompanied by a decrease in lipogenesis, and ultimately results in the release of NEFA and glycerol into the blood, preventing the liver from suppressing its endogenous glucose production.

The specific molecular players coordinating the impairment of adipocyte insulin sensitivity are poorly understood, in contrast to the skeletal muscle and the liver. These defects in pathway signaling seem to involve the insulin receptor content and tyrosine kinase activity as in the muscle and the liver (Freidenberg et al., 1987; Kolterman et al., 1979), the carbohydrate responsive-element-binding protein (ChREBP) transcription factor promoting lipogenesis (Herman et al., 2012), but also autocrine or paracrine substances, such as TNF- α , adiponectin, resistin or leptin, that may impair insulin signaling (Arner, 2003).

4.2 Deficiency of insulin secretion

Both a defect in beta cell mass and a defect in beta cell function may contribute to the lack of insulin secretion that characterizes type 2 diabetes, and both conditions appear to be linked to glucose intolerance prior to the development of type 2 diabetes.

4.2.1 Loss of beta cell mass

About 70 % of the islet volume and 3-5 % of the total pancreatic mass are made up of beta cells. Beta cell mass has been quantitatively estimated in postmortem pancreas from both type 2 diabetes patients and healthy volunteers in some studies. According to the findings, type 2 diabetic subjects had a 30 % (Clark et al., 1998) or 60 % (Butler et al., 2003) lower beta cell mass than lean subjects. In addition to the islet amyloid deposit, a slight increase in the number of alpha cells was also noted.

The loss of beta cell mass is related to glucose tolerance, and some evidences suggest that glucose intolerance occurs after a beta cell mass decrease of 50 % in humans: if in rodents a pancreatectomy over 90 % is required to induce a deficit in insulin secretion (Ebrahimi et al., 2020), a reduction of 50 % of the beta cell mass following an administration of streptozotocin, a beta cell toxic, is sufficient to induce hyperglycemia in non-human primates (McCulloch et al., 1991). These findings suggest that, in contrast to other species, relatively small changes in the beta cell population can affect insulin secretion in humans (Clark et al., 2001). Patients with impaired glucose tolerance and impaired fasting glycemia were also reported to have 20 % and 40 % less beta cell mass, respectively (Butler et al., 2003; Meier et al., 2012). Additionally, a link between beta cell mass and HbA_{1c} was shown in both diabetic and non-diabetic subjects (Saisho, 2015), supporting the hypothesis that beta cell mass declines before the onset of type 2 diabetes. But in this study, the loss of beta cell mass in type 2 diabetes was seen independently of the length of diabetes, indicating that this loss may not be the only factor contributing to the onset of insulin secretion deficiency.

4.2.2 Loss of beta cell function

The beta cell mass is not entirely responsible for the insulin release from beta cells in response to a glucose stimulation. The heterogeneity of beta cell response to a glucose stimulus has been clearly identified (Miranda et al., 2021). It was proposed that less than 50 % of the total mass of in vivo beta cells would be required to achieve a correct responsiveness to glucose at any time, and that the remaining percentage would constitute a large storage of secretory ability that can be recruited in case of insulin resistance. The point at which the secretory ability is surpassed causes insulin resistance to change into type 2 diabetes (Clark et al., 2001). This suggests that type 2 diabetes-related beta cell dysfunction results in a complex network of relationships between the environment of the beta cells and the intracellular pathway of insulin secretion.

Assessment of beta cell function in vivo remains a challenge because it is difficult to separate beta cell function *per se* from insulin sensitivity. Effective predictors of changes in glucose tolerance independent of insulin resistance are models of secretion parameters that attempt to capture the dynamic of insulin release in response to variations in blood glucose levels over time (Ferrannini and Mari, 2014). In this perspective, abnormalities of beta cell function described in the pathogenesis of type 2 diabetes concern: an increase in fasting plasma insulin and total insulin release after a glucose challenge; an important impairment of beta cell glucose sensitivity, evaluated at 20-30 % compared to healthy subjects (**Figure 15**), and described as the most important predictive factor of the diabetes progression, independently of age, sex and obesity (Ferrannini et al., 2011); a reduction of insulin secretion rate, reflecting the incompetence of beta cell to correctly respond to incremental glucose stimulations (Mari et al., 2008); and a reduction of the incretin effect, due to a defect of release from the intestine or a GLP-1 resistance of the beta cells (Aulinger et al., 2015).

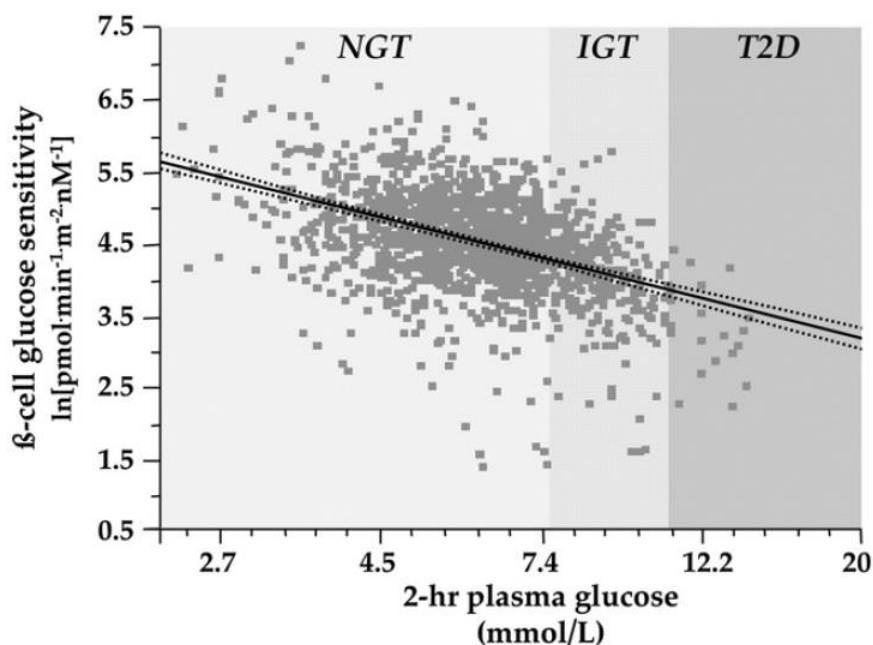


Figure 15: Reciprocal association between β -cell glucose sensitivity and the 2-hour plasma glucose concentration on the OGTT in 1480 individuals spanning the range from normal glucose tolerance (NGT) to impaired glucose tolerance (IGT) to overt type 2 diabetes (T2D) (Ferrannini and Mari, 2014)

The full line is the best fit (and its 95% confidence intervals, dotted lines) adjusted for sex, age, and body mass index (BMI).

The alteration of the insulin secretion pattern is one of the earliest observable *in vivo* signs of beta cell function loss. The Acute Insulin Response (AIR), which refers to the first phase of insulin secretion, is constantly decreasing in patients with impaired glucose tolerance or in the early stages of type 2 diabetes, even if the second phase is generally enhanced (**Figure 16**). Lots of data highlighted the critical role of the first phase of insulin secretion in postprandial glycemic control. Its action is particularly important for the liver (more than the peripheral tissues), especially for the suppression of endogenous glucose production (Del Prato and Tiengo, 2001; Marcelli-Tourvieille et al., 2006). In a longitudinal study conducted in the Pima Indian population, it has yet been conclusively shown that a defect in AIR manifests early in the spontaneous progression of the disease and that this defect can initiate people transition from a healthy state to one of impaired glucose tolerance and, eventually, type 2 diabetes (Weyer et al., 1999).

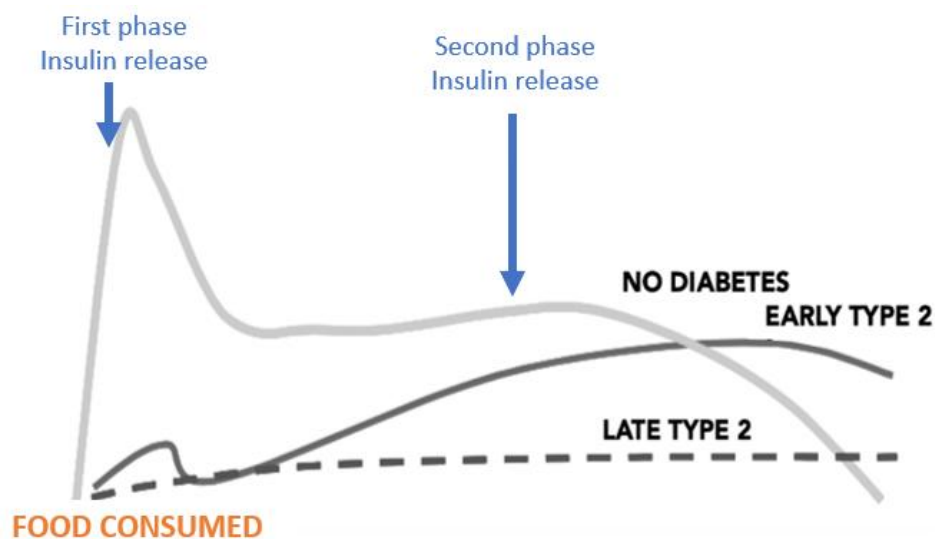


Figure 16: Phases of insulin secretion of a healthy pancreas compared with patients with type 2 diabetes. Adapted from (Luna and Mercado-Asis, 2022).

The relationship between beta cell function and glucose metabolism and between beta cell mass and glucose metabolism has been shown to be very clear. Furthermore, the evidence suggests a relationship between beta cell mass and function. In a study conducted by our group, there was a positive correlation between the maximum AIR measured following intravenous glucose or arginine administration *in vivo* and the pancreatic beta cell mass that was subsequently isolated (Hubert et al., 2008, 2005). Furthermore, it appears that the *in vivo* C-peptide-to-glucose ratio following an oral

glucose tolerance test is a good indicator of beta cell area (Meier et al., 2009). Even though beta cell mass and function can sometimes be separated, it is actually challenging to do so. Because of this, we now refer to "beta cell functional mass" more frequently, and it is now known that beta cell functional mass is impaired as type 2 diabetes progresses (Saisho, 2015).

4.2.3 Cellular mechanisms of beta cell insulin secretion deficiency

When there is an energetic overload, hyperglycemia and hyperlipidemia events frequently occur, which can result in insulin resistance and inflammatory mechanisms. Thus, beta cells are exposed to a variety of harmful pressures, including inflammatory, endoplasmic reticulum, oxidative, and amyloid stress, which start the loss of islets integrity and function. In fact, the unfolded protein response (UPR) or oxidative stress pathway is activated by the gluco- and lipotoxicity brought on by obesity. Additionally, a high glucose concentration promotes the ability of beta cells to produce reactive oxygen species by increasing the production of misfolded insulin and islet amyloid polypeptide (IAAP). All of these stress signals have an impact on the calcium mobilization of the endoplasmic reticulum, which is a mediator of the migration and degranulation of insulin vesicles at beta cell membranes. They also encourage the release of proapoptotic signals and cytokines, which attract macrophages and promote the inflammatory response. These pathophysiological processes eventually result in a dysregulation of glycemia by impairing islet integrity and functionality or paracrine communication within the pancreas (Galicia-Garcia et al., 2020) (Figure 17).

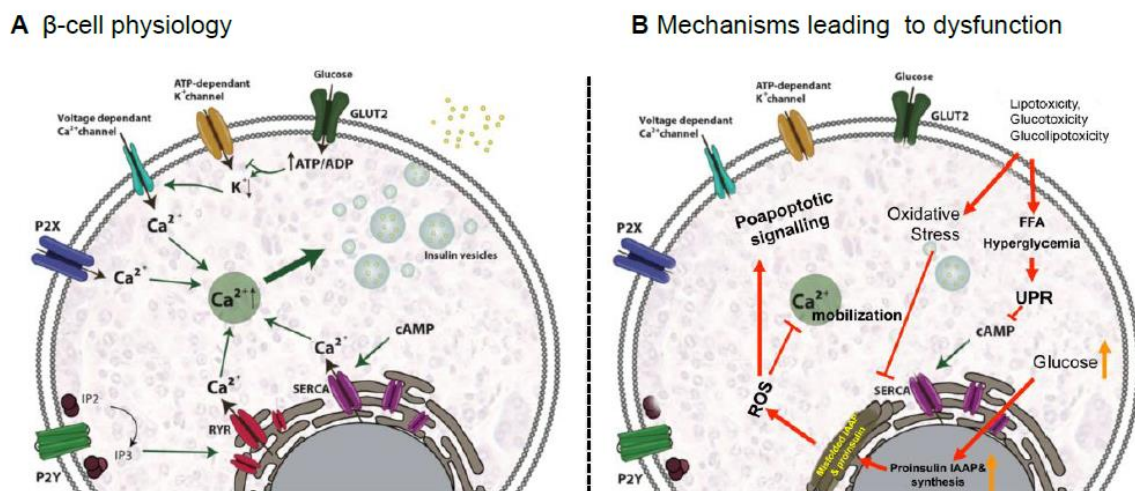


Figure 17: Signaling pathways involved in insulin secretion in beta cells in physiological conditions (A) and mechanisms leading to dysfunction (B) (Galicia-Garcia et al., 2020)

Because human beta cells have a limited capacity for regeneration, the loss of beta cell mass and function represents a pathophysiological mechanism that is particularly harmful. If beta cell replication phenomena were seen in the first five years of life, beta cell mass would remain constant throughout

childhood (Meier et al., 2008). However, this plasticity is constrained, resulting in a beta cell workload saturation that can be exceeded if excessive caloric intake persists, followed by a final beta cell failure (Saisho et al., 2013). Obesity can cause a small expansion of beta cell mass, but this plasticity is also constrained. However, these processes are reversible, and in type 2 diabetic patients, restoring appropriate insulin secretion is a key therapeutic approach.

4.3 Environmental and genetic risk factors for type 2 diabetes

4.3.1 Environmental factors

Today, it is widely accepted that a number of factors, including lifestyle choices, diet, socioeconomic status, environmental toxins, genetics, and epigenetics, are linked to type 2 diabetes. Insufficient beta cells and insulin resistance are both influenced by all of these factors (Mambiya et al., 2019).

Since decades, certain behaviors, such as drinking alcohol, smoking, or being sedentary, have been definitively linked to type 2 diabetes. Because stress contributes to the activation of the hypothalamic-pituitary-adrenal axis, which causes insulin resistance and beta cell dysfunction, it plays a role in the regulation of glucose homeostasis. A significant weight gain that could lead to obesity is triggered by insomnia, which also leads to the dysregulation of the hormones that control appetite. Additionally, insomnia can lead to an increase in blood pressure and the orthosympathetic nervous system, which are risk factors for insulin resistance. Additionally, the intracellular diffusion of some antibiotics, such as fluoroquinolones, has been linked to type 2 diabetes (Spruijt-Metz et al., 2014). These effects include the genesis of oxidative stress and magnesium deficiency.

The consumption of a diet high in sucrose or saturated fats contributes significantly to the development of metabolic disorders. Beyond the macronutrient makeup of food, some micronutrient deficiencies have been identified as type 2 diabetes risk factors: deficiencies in vitamin K, vitamin D, vitamin E, magnesium, and antioxidants like beta-carotene or alpha-tocopherol have been positively linked to the onset of the disease (Ärnlöv et al., 2009; Yahaya et al., 2021).

Persistent Organic Pollutants (POPs) are certain environmental chemicals that exhibit resistance to all forms of inactivation processes and complete their cycle in food. POP can be found in animal products such as meat, fish, or dairy products. It was demonstrated that their ingestion led to their accumulation into lipid droplets in the adipose tissue or to their binding to circulating lipids in the blood system. In the organism, POP has a deleterious effect on the insulin synthesis process and release by beta cells as for as its signaling in the liver, skeletal muscle and adipose tissue (Carpenter, 2008).

4.3.2 Genetic and epigenetic factors

It has been noted that the hereditary component of type 2 diabetes plays a significant role in the progression of the condition. There are numerous candidate genes and Single Nucleotide Polymorphisms (SNPs) that have been discovered, some of which are involved in the process of insulin secretion, such as *kcnj11* (KIR6.2), *slc2a2* (GLUT2) or *hnf1* (HNF1), and others which are involved in the action of insulin, such as *insr*, *ppar*, or *pik3r1* (Mambiya et al., 2019).

Many other genetic factors can also be involved in type 2 diabetes pathophysiology. For example, 3 missense variants of SGLT1 have been identified as protective from diabetes and cardiovascular diseases (Seidelmann et al., 2018), letting us suppose the potential existence of other variants of these transporter of glucose that could be associated to a higher risk of developing type 2 diabetes.

Epigenetics appears to play an important complementary role for the explanation of type 2 diabetes heredity, though the explicative portion of genetic variants in type 2 diabetes onset has only been evaluated at 10–30 % (Brunetti et al., 2014). Despite not involving changes in the nucleotide gene sequence, epigenetics, which includes micro RNAs, DNA methylation, and histone modifications, can partially explain the occurrence of type 2 diabetes because changes in gene expression that appear in one generation of cells can be passed on to the following one. For instance, some environmental factors, like the diet during pregnancy or a starvation period, can cause irreversible hypermethylation of DNA, which can affect genes involved in insulin secretion or signaling and promote the onset of metabolic disorders. The insulin sensitivity gene was hypermethylated and downregulated in children born from mothers who had gestational diabetes mellitus during pregnancy (Ding et al., 2012).

5. Implication of intestinal glucose absorption on postprandial glucose response

The rate of gastric emptying, the efficacy of digestion and the transport of glucose through the enterocytes are the main determinants of intestinal glucose absorption. Thus, every change in each of these determinants can influence the pattern of absorption, and consequently the postprandial glucose response. This is why all these mechanisms are supposed to be implicated in type 2 diabetes pathophysiology.

5.1 Variations in the rate of gastric emptying

Gastric emptying determines the exposure of the nutrients into the intestinal lumen (**Figure 18**), consequently the rate of appearance of exogenous glucose into the systemic circulation, and finally the postprandial glucose excursion (Ryan J. Jalleh et al., 2022; Wu et al., 2020).

One of the pioneer studies conducted by the group of Horowitz evaluated in healthy subjects that gastric emptying accounts for about 34 % of the variance in peak plasma glucose after a 75-g oral

glucose load, that the plasma glucose level at 120 min is inversely rather than directly related to gastric emptying and that the distal stomach influences gastric emptying of glucose (Horowitz et al., 1993). In patients with early type 2 diabetes, the correlation between gastric emptying and postprandial glucose response was also confirmed (Jones et al., 1996).

Using intraduodenal glucose infusions at different rates of delivery, the postprandial glucose, insulin, and incretin responses were the highest consequently to the highest rates of delivery in healthy (Chaikomin et al., 2005; C. S. Marathe et al., 2015) and obese subjects (Trahair et al., 2017). In patients with well-controlled type 2 diabetes, blood glucose, insulin and GLP-1 responses were also critically dependent on the small intestinal glucose load (Ma et al., 2012).

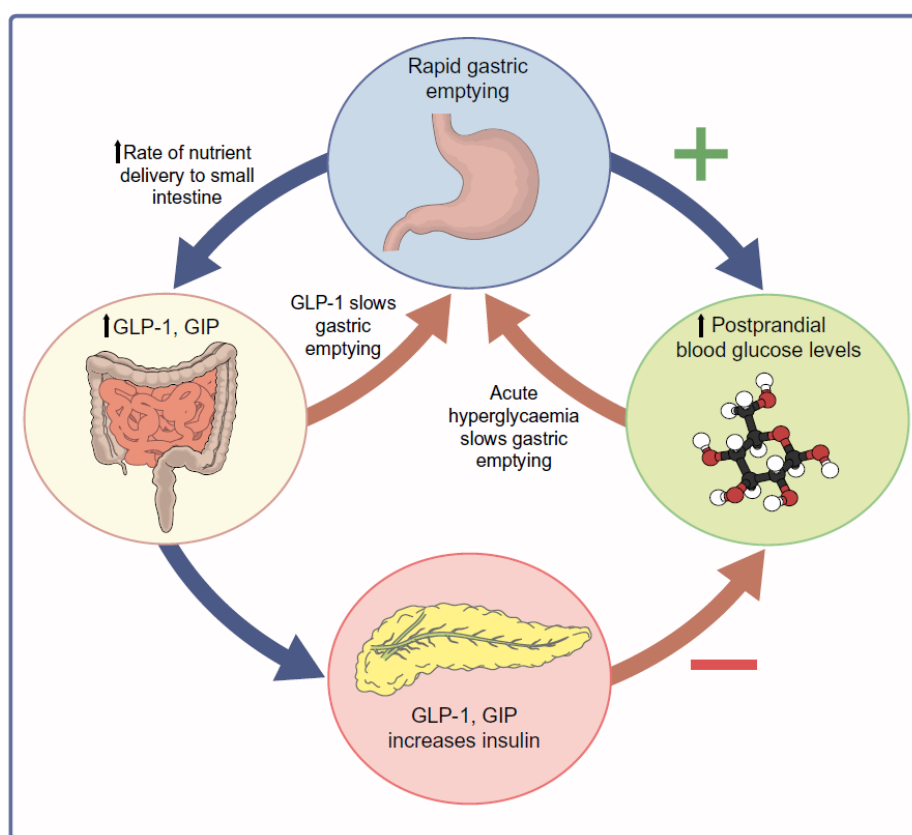


Figure 18: Schema of the interdependent relationships of gastric emptying, incretin hormones and blood glucose (Ryan J. Jalleh et al., 2022)

Gastric emptying is both a determinant of, and determined by, blood glucose.

Conversely, with delayed gastric emptying rates, the peak rate of meal glucose appearance was delayed (Woerle et al., 2008), associated with a greater total insulin sensitivity, decreased total beta cell responsiveness and lower endogenous glucose production (Hinshaw et al., 2014).

Acute changes in blood glucose can modulate the rate of gastric emptying, as kind of feedback mechanism (Phillips et al., 2015). Hyperglycemia delays gastric emptying in healthy humans (Kuo et al.,

2010b) whereas insulin-induced hypoglycemia accelerated it in normal individuals (Berne, 1996) and subjects with diabetes (Russo et al., 2005).

The correlation between gastric emptying and postprandial glucose response was shown time-dependent according to the glycemic status. In healthy individuals as for as patients with type 2 diabetes, the AUC of postprandial glucose between 0 and 30 minutes was positively related to the amount emptied at 30 min (Horowitz et al., 1993; Chinmay S. Marathe et al., 2015). In patients with type 2 diabetes or glucose intolerance, but not in healthy people, gastric emptying was identify as a significant determinant of the first 60 minutes of postprandial glycemic response (Jones et al., 1996; Chinmay S. Marathe et al., 2015). Moreover, the relationship of the plasma glucose at 120 minutes with gastric emptying is inverse in healthy subjects and direct in type 2 diabetes (Horowitz et al., 1993; Ryan J Jalleh et al., 2022). The later peak of postprandial glycemia profile associated to a delay in insulin release and impaired insulin sensitivity commonly described in glucose intolerant and type 2 diabetic patients versus normoglycemic individuals could explain this time-dependent association (**Figure 19**).

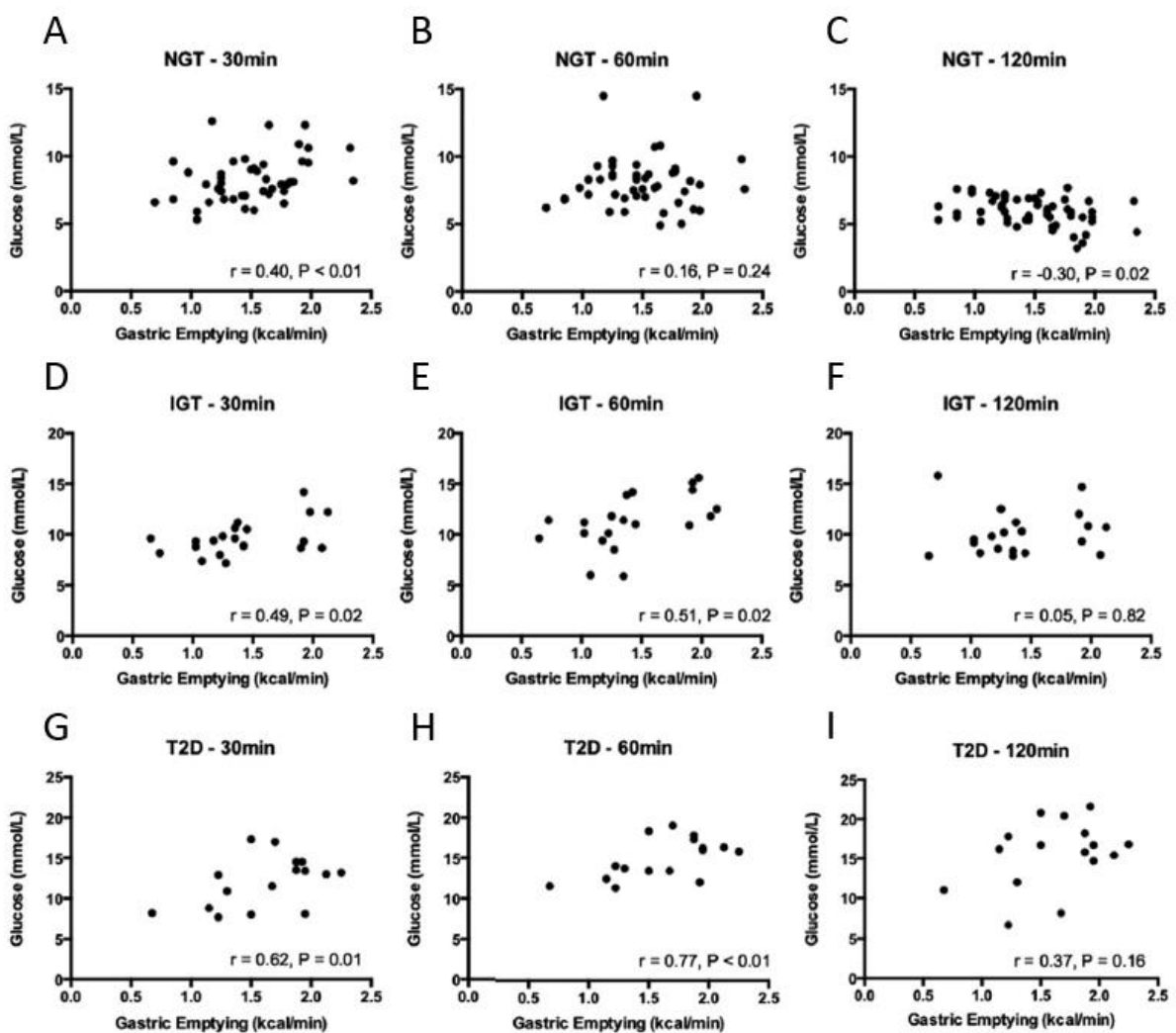


Figure 19: Relationships between blood glucose at 30, 60, 120 min with gastric emptying expressed as kcal/min in subjects with normal glucose tolerance (NGT) (A-C), impaired glucose tolerance (IGT) (D-F) and type 2 diabetes (T2D) (G-I). Adapted from (Chinmay S. Marathe et al., 2015).

The rate of gastric emptying was also related to the ethnicity (Phillips, 2006). Non-diabetic Mexican American exhibited a more rapid glucose gastric emptying compared to non-Hispanic whites, associated with hyperinsulinemia (Schwartz et al., 1995). This characteristic was proposed as a contributing factor for the increased risk of obesity and type 2 diabetes in this population. Moreover, Han Chinese with relatively well-controlled T2D have more rapid gastric emptying compared to Caucasians, which is associated with a greater postprandial glycemic excursion (Wang et al., 2020).

Finally, a lot of studies listed in some reviews (Goyal et al., 2019a; Marathe et al., 2013; Phillips et al., 2015; Skytte et al., 2021) support the existence of a rapid gastric emptying in early stages of type 2 diabetes and proposed it as a potential pathophysiological mechanism in type 2 diabetes occurrence.

The most severe complication of gastric motility in the later stages of type 2 diabetes is gastroparesis. Gastroparesis is characterized by a persistent delay in gastric emptying without mechanical obstruction (Goyal, 2021; Ryan J. Jalleh et al., 2022). The rate of prevalence of gastroparesis among type 2 diabetic patients is evaluated at 32-47 % and concerns alteration of the nervous mechanisms involved in gastric emptying control (Goyal, 2021). Additionally, a kind of pacemaker, constituted by the Interstitial Cells of Cajal (ICC), plays a key role in gastrointestinal motility. The pathophysiological mechanisms underlying gastroparesis are complex and polymorphic, but at later stages of the disease, dysfunction due to glucotoxicity of chronic blood glucose levels occurs. A deficiency of the ICC is typically linked to a compromised inflammatory response that results in a shift in the population of macrophages from M2 to M1 expression. Increased oxidative stress, abnormalities in vagal innervation, intrinsic nerves, and inhibitory neurons are all caused by an increase in M1 macrophages (Ryan J. Jalleh et al., 2022). Gastroparesis is frequently accompanied by gastro-intestinal symptoms like nausea, vomiting, or abdominal distension, but no causal relationship between the symptoms and the motor defects could be established (Goyal, 2021).

In conclusion, it has now been amply shown that the rate of gastric emptying affects the postprandial glycemic response in both healthy people and people with impaired glucose tolerance. Although there is plenty of evidence showing that gastric emptying is sped up in the early stages of the disease, it is still unknown whether rapid gastric emptying associated with higher postprandial glycemic excursion is primarily abnormal (Goyal et al., 2019a). Regularly high postprandial glycemic excursions cause oxidative stress, which alters inhibitory neuromuscular transmission. This increases gastric contractility, which accelerates gastric emptying and creates a vicious cycle (Goyal, 2021).

5.2 Variations in the availability of glucose

5.2.1 The Glycemic Index

The Glycemic Index (GI) was developed in 1981 as a classification indicator for naturally occurring carbohydrates (Jenkins et al., 1981). The goal of this indicator is to predict the postprandial glycemic response based on the type of carbohydrate, and to measure a food's hyperglycemic potential in comparison to a reference carbohydrate (typically glucose or white bread). It allows foods to be ranked on the basis of the rate of digestion and absorption of the carbohydrates that they contain

The Glycemic Index is determined by comparing the incremental Area Under Curve (iAUC) of postprandial glycemia following oral administration of a standard amount (50 g) of a particular carbohydrate to the iAUC obtained after ingesting an equivalent amount of glucose (Wolever et al., 1991). Glucose is thus considered as the carbohydrate with the maximal Glycemic Index of 100.

Therefore, a carbohydrate that has been highly processed will have a high GI (> 70) and, as a result, a high postprandial glycemia peak (**Figure 20**). Conversely, low-GI foods lead (< 55) to lower postprandial glycemic response (Augustin et al., 2015). The glycemic indexes of more than 4000 foods have already been determined. The vast majority of fruits and vegetables, legumes, and wholegrain bread are foods with low glycemic indexes. On the other hand, foods with a high Glycemic Index include white bread, rice, potatoes, and all refined cereal products (Atkinson et al., 2021).

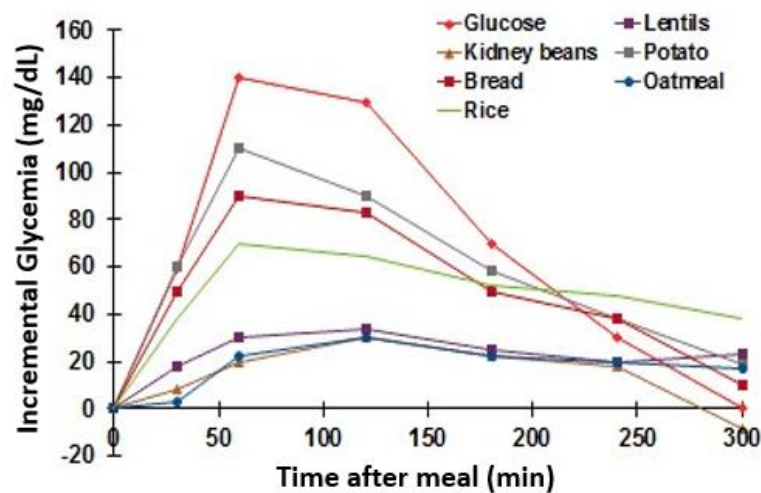


Figure 20: Blood glucose levels during a meal following the ingestion of carbohydrates with diverse Glycemic Index. Adapted from (Jenkins et al., 1981).

The GI presents also some limitations. Only a certain number of food items have officially tested values and the number of participants used for evaluation is often limited (Pasmans et al., 2022). Considerable interindividual variability (differences in iAUC between 15 and 139 mg/dL) in postprandial glycemic responses in healthy individuals were also observed following the ingestion of a same GI-meal (Vega-

López et al., 2007). Additionally, some subjects exhibit a much larger postprandial glycemic response after banana (low GI) than after cookies (high GI) ingestion (Zeevi et al., 2015). This finding is thus particularly evocative of the complexity of the interindividual variability of the postprandial glucose response and the GI remains a useful tool to standardize the nutritional recommendation.

5.2.2 The rate of starch digestion

The rate of starch digestion is moreover an indicator, established *in vitro*, allowing to classify the carbohydrates from *in vitro* measurement according to their availability. Three major fractions are thus defined: rapidly digestible starch (RDS), slowly digestible starch (SDS) and resistant starch (RS). In consequence, rapidly available glucose (RAG) includes RDS, free glucose and the glucose moiety of sucrose. Positive correlations were thus observed *in vitro* between GI and both RDS and RAG (Englyst et al., 1996).

5.2.3 Abundance of intestinal disaccharidases

Additionally, in parallel to the nature of the carbohydrate itself, the activity and the abundance of intestinal disaccharidases influence the rate of digestion. In fact, a study found an increase in sucrase and isomaltase by 1.5- to 2-fold in the small intestine of diabetic patients compared to controls (Dyer et al., 2002). In experimental diabetic animals, these levels were also increased (Deng et al., 2011; Liu et al., 2010). These elements suggest that the increase in the disaccharidase activity could exacerbate postprandial glucose excursions. The adaptative or causal component of this finding in the pathophysiology of type 2 diabetes, however, is still unclear (Liu et al., 2011).

5.2.4 Pathophysiological consequences of a high rate of carbohydrates digestion

The rate of availability of glucose highly influences the physiological mechanisms underlying the postprandial glucose response. In early postprandial period (0-2h after the meal ingestion), the consumption of a high GI meal leads to a rapid absorption of carbohydrate and to a relatively high blood glucose level and a high insulin-to-glucagon ratio that would tend to exaggerate the normal anabolic response to eating. During the middle postprandial period (2-4h), blood glucose concentrations decrease to below preprandial level but the biological effects of the high insulin and low glucagon levels persist. And during the late postprandial period, an increase of counterregulatory hormones after a high GI meal restore euglycemia and cause a marked increase in free fatty acid levels by stimulation of glycogenolytic and gluconeogenic pathways. After a low GI meal consumption, the insulin-to-glucagon ratio is lower and thus the postprandial hypoglycemia and its hormonal consequences do not occur (Ludwig, 2002) (**Figure 21**).

A lot of research has been performed to elucidate the relation between the nature of the carbohydrates intake and the consequent outcome on postprandial glucose response (Pasmans et al.,

2022; Vlachos et al., 2020). A series of systematic reviews and meta-analyses demonstrated that the consumption of high-GI diets were associated with a increase of the metabolic risk compared with low-GI meal (Reynolds et al., 2019). Dietary high glycemic index and load have even been clearly identify as causal factor of type 2 diabetes onset (Livesey et al., 2019).

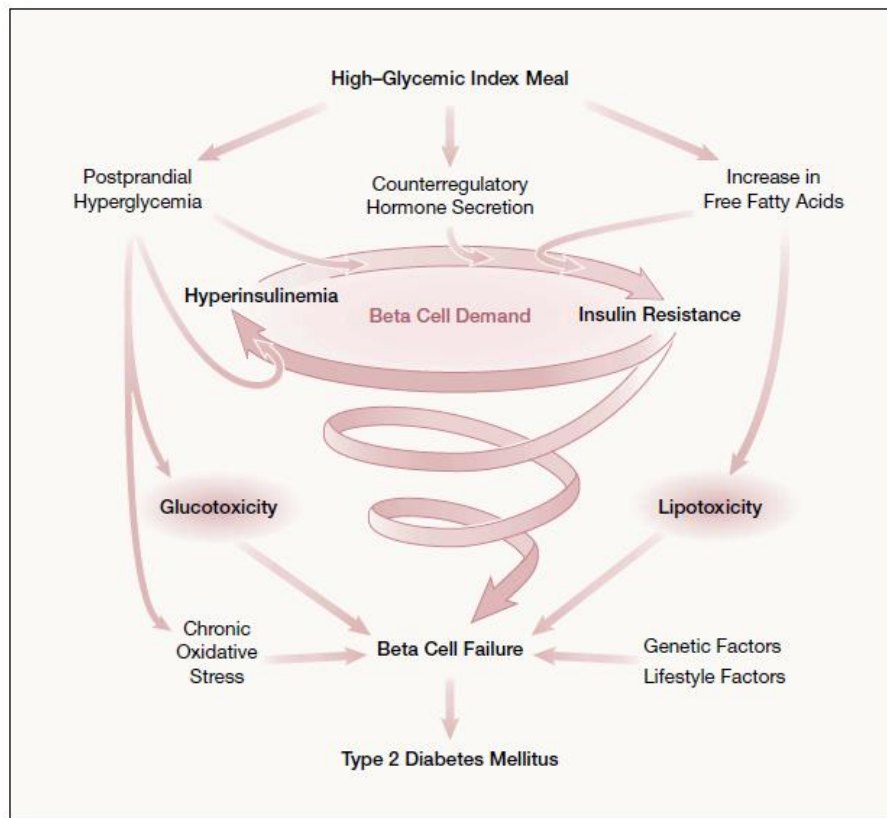


Figure 21: The hypothetical model relates a high-glycemic index diet to increased risk for type 2 diabetes mellitus (Ludwig, 2002)

5.2.5 Microbiota alterations: consequences for fermentation, systemic inflammation, and glucose absorption

The human gastrointestinal tract is home to trillions of bacteria, and numerous studies have examined the relationship between the microbiota and host health, particularly in terms of diet, metabolism, immunity, drug bioavailability, and behavior. The nature of the ingested carbohydrates influences the rate of digestion and consequently the total fraction of glucose absorbed by the small intestine. The nature of the non-absorbed fraction is recognized to influence the nature of the microbiota. Microbiota has now been definitively linked to a wide range of illnesses, particularly human metabolic diseases like obesity or type 2 diabetes (Wu et al., 2015).

The regular consumption of a western diet, which has a low fiber content and a high sugar and protein content, has been shown to impair the diversity of bacterial species in the intestine. The two major bacterial groups in the human gut are *Bacteroidetes* and *Firmicutes*. Depending on the subject's

metabolic state, differences in the *Bacteroidetes/Firmicutes* ratio have been noted: obese subjects appear to have a lower Bacteroidetes proportion than lean subjects (Jandhyala, 2015; Karlsson et al., 2013; Ley et al., 2006). This shift observed in people with obesity seems to also be associated with a reduction in the global microbiota ability to produce SCFAs and an increased incidence of chronic inflammatory diseases. According to Makki et al., the production of SCFA by the microbiota is crucial for the stimulation of mucus and the production of anti-microbial peptides, which in turn increases the expression of tight junction proteins and ensures the well-being of the intestinal barrier (Makki et al., 2018). Therefore, every change or imbalance in the microbiota may impair the health of the intestinal barrier, which will then allow bacteria and their fragments and substrates to move around. The process, known as "metabolic endotoxemia," is a key factor in the systemic inflammation that results in insulin resistance and is well-described in the onset of disease (Festi et al., 2014).

Even though the relationship between the microbiota, inflammation, insulin sensitivity, and secretion has been well documented, it is still unclear whether the diversity of bacterial species has a direct impact on intestinal glucose absorption. Some studies support the ability of the microbiota to influence intestinal glucose absorption (Anhê et al., 2023; Ota et al., 2022) but alterations of microbiota seem more to be the result of variations of intestinal glucose absorption than the contrary.

5.3 Variations in the number and functionality of glucose transporters

5.3.1 Association between SGLT1 level and postprandial glucose response

The transport of the unities of glucose, previously released, across the enterocytes constitutes the main determinant of intestinal glucose absorption. The number and functionality of the glucose transporters is thus clearly associated with postprandial glucose response.

In humans, duodenal SGLT1 expression level correlates with early postprandial glucose since it is increased in individuals with 1-hour postload hyperglycemia or impaired glucose tolerance, as well as in subjects with type 2 diabetes (Fiorentino et al., 2017). In particular, subject with a 1-hour postprandial glucose higher than 155 mg/dL exhibits higher SGLT1 levels than subjects with 1-hour glucose postload lower than this value (**Figure 22**). Conversely, a value of 1-hour postprandial glucose over 155 mg/dL combined with HbA1c-defined normal or prediabetes conditions identifies individuals with increased duodenal levels of SGLT1 (Fiorentino et al., 2021).

5.3.2 Acute changes of transporters levels following the ingestion of a high-carbohydrate meal

The amount of functional transporters changes as a result of the carbohydrate composition of the diet. Following a diet rich in carbohydrates, intraluminal glucose levels can rise quickly to high values (more than 30 mM), which causes a saturation phenomenon of the transporters already in place. Thus, more mechanisms are set up for this reason. An increase in SGLT1 exocytosis is seen at the apical pole as a

short-term process (a few minutes), and GLUT2 recruitment is seen at the basal pole. The expression of SGLT1 and GLUT2 has been shown to increase after several meals rich in carbohydrates, for example, in rodents (Diamond et al., 1984; Miyamoto et al., 1993), piglets (Moran et al., 2010) and humans (Dyer et al., 2002; Fiorentino et al., 2017; Nguyen et al., 2015).

Furthermore, in cases of high intraluminal glucose concentrations, the GLUT2 transporter, which is typically found basolaterally during standard meals, can also be transitory found at the apical membrane after a high carbohydrate diet. In a mouse study, after giving a simple sugar meal orally, GLUT2 was massively recruited to the meal-facing membrane. High intraluminal glucose levels stimulated this recruitment, which increased glucose transport, which was not observed in GLUT2 KO mice (Gouyon et al., 2003). According to several studies (Ait-Omar et al., 2011; Kellett et al., 2008; Kellett and Brot-Laroche, 2005), GLUT2 translocates from the cytosol to the apical pole and allows the entrance of monosaccharides in enterocytes by facilitate diffusion.

5.3.3 Chronic adaptations of SGLT1 and GLUT2 in metabolic disease development

In case of a regular consumption of meals with a high carbohydrate content, the acute changes of the levels of the transporters observed can become permanent.

The association between SGLT1 and dysglycemia has been yet well described in some reviews (Koepsell, 2020; Lehmann and Hornby, 2016). Subjects with type 2 diabetes or impaired glucose tolerance showed a higher SGLT1 level of expression compared to healthy individuals (Dyer et al., 2002; Fiorentino et al., 2017).

Moreover, Fiorentino and coworkers showed a similar increase in SGLT1 content in subjects with type 2 diabetes and glucose intolerance compared to healthy subjects (Fiorentino et al., 2017) (**Figure 22**).

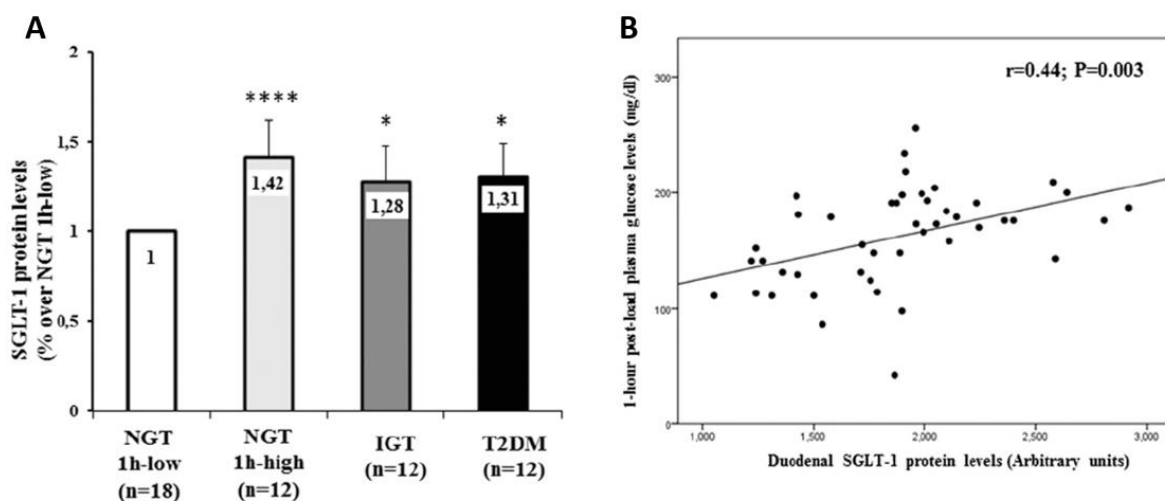


Figure 22: Relationship between duodenal SGLT-1 abundance and the glycemic status. Adapted from (Fiorentino et al., 2017)

(A) SGLT-1 protein levels in subjects with normal glucose tolerance and a low 1-hour postprandial glycemia (NGT 1h-low), in subjects with normal glucose tolerance and a high 1-hour postprandial glycemia (NGT 1h-high), in subjects with impaired glucose tolerance (IGT) and in subjects with type 2 diabetes (T2DM).

(B) Correlation between duodenal SGLT-1 protein levels and 1-hour post-load plasma glucose levels.

If the contribution of SGLT1 on intestinal glucose absorption, postprandial glucose response and diabetes clearly established, the one of the basal GLUT2 transporter remains incompletely understood. GLUT2 is also able to translocate from the cytosol to the apical membrane in case of high carbohydrate content in the intestinal lumen (Kellett et al., 2008), and this translocation can become permanent if the high-sucrose intake endure, as shown in obese subjects and mice, leading to an increase in intestinal glucose absorption (**Figure 23**). However, in fasting state, this accumulation seems to lead more to a release of glucose into the intestinal lumen than to an increase in intestinal glucose absorption, as a kind of protective mechanism (Ait-Omar et al., 2011).

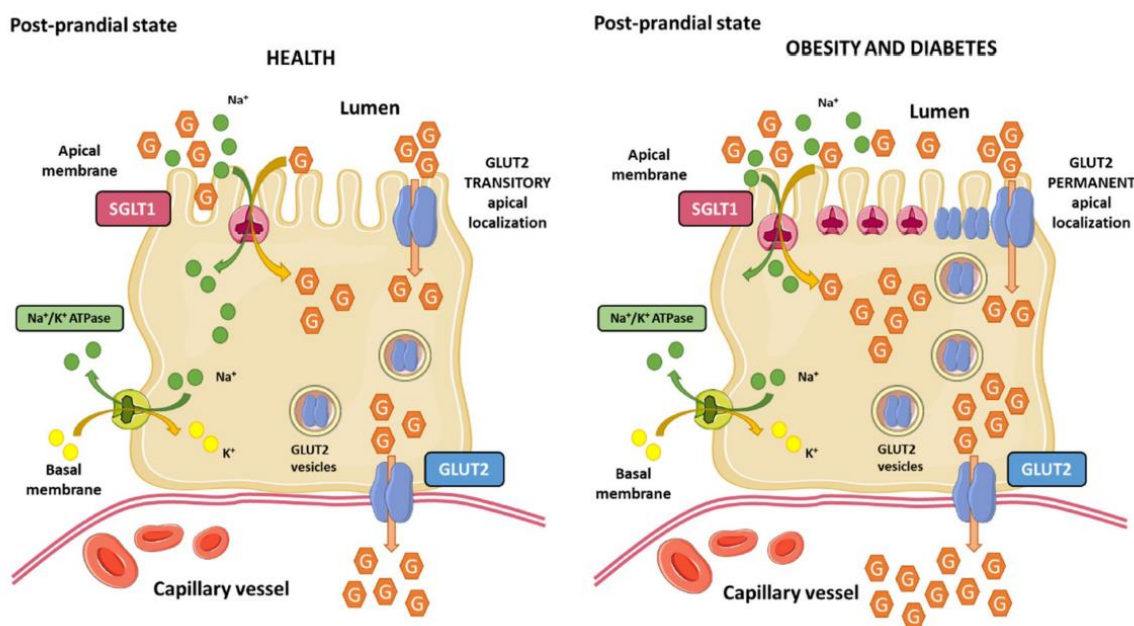


Figure 23: Glucose transport in enterocytes in health and disease (Merino et al., 2019)

5.3.4 Causal relationship between SGLT1 level and postprandial glucose response

According to the previous presented data, it has remained unclear whether the modifications in the SGLT1 levels observed are simply mechanisms brought on by a prolonged exposure to high-carbohydrate foods or if they are structurally linked to the genetic background of a subject, which would make them the primary cause of the disorders. In fact, the positive association between the apical intestinal transport of glucose and postprandial glucose response is supposed causal.

Mouse model without the regulator gene Rsc1A1 of SGLT1 expression exhibited increased SGLT1 protein levels in the small intestine and then developed metabolic disorders (Osswald et al., 2005).

Moreover, a study performed in Otsuka Long-Evans Tokushima Fatty rats showed that an increased in SGLT1 expression, concomitant with intestinal hypertrophy, is partly associated with postprandial hyperglycemia before the onset of insulin resistance and dysglycemia (Fujita et al., 1998). Increased intestinal glucose absorption is thus presented here as a principle cause of postprandial hyperglycemia, and consequently type 2 diabetes.

Finally, using mendelian randomization, Seidelmann and coworkers have supported the causal relationship between intestinal glucose absorption and early postprandial glucose response, by discovering SGLT1 variants protective for cardiometabolic diseases and associated with better glucose tolerance (Seidelmann et al., 2018). In fact, three damaging missense variants of SGLT1 (prevalence rate of 6.7 % in this cohort) were identified and associated with a lower 2-hour postprandial glycemia and a better glucose tolerance compared to subjects deprived of these variants. According to this study, a 20 mg/dL drop in 2-hour postprandial glycemia over a period of 25 years would significantly lower the incidence of type 2 diabetes and obesity. However, the existence of other SGLT1 variants with higher efficiency has not been highlighted so far.

5.3.5 Glucose sensing and intestinal glucose absorption

Evidence for the connection between intestinal glucose transporters, glucose absorption, incretin release, and glucose detection has grown significantly. Glucose detection seems thus to stimulate glucose absorption.

This mechanism can be stimulated by low-calorie artificial sweeteners, largely prevalent in soft drinks. In fact, evidences, support that artificial sweeteners like saccharin, sucralose, acesulfame K, or steviol glycosides stimulate STRs and lead to upregulation of SGLT1 in wild-type mice (Egan and Margolskee, 2008). Additionally, subjects with type 2 diabetes have higher levels of expression of T1R2, one of the subunits of the sweet-taste receptor, than did control subjects. Moreover, the level and the functionality of the sweet taste receptors was associated with a rise in intestinal glucose absorption (Young et al., 2013).

These data let suggest the ability of the stimulation of the sweet taste receptor to increase postprandial glucose excursions, but to our knowledge, it has not been clearly demonstrated sofar. The implication of the low-calories artificial sweeteners on dysglycemia remained controversial and there are not enough data on low-calorie artificial sweeteners globally to declare them unsafe.

III. Intestinal glucose absorption: a therapeutic target in type 2 diabetes management

There are many therapeutic options for managing type 2 diabetes. Due to the polymorphic nature of type 2 diabetes, choosing the most individualized and appropriate treatment is one of the most crucial aspects of managing the disease.

Dietary and hygienic approaches are frequently taken into consideration first. Anti-diabetic medications can be used alone or in combination to enhance insulin secretion, insulin sensitivity, limit intestinal glucose absorption, or prevent kidney reabsorption. If they are unsuccessful in maintaining glycemic control, interventional therapy as metabolic surgery can also be recommended under stricter eligibility requirements. Intestinal glucose absorption, as one of the main actors in glucose homeostasis, represents a particularly appropriate therapeutic target.

1. Nutritional approaches

1.1 Nutritional approaches limiting intestinal glucose absorption

According to the majority of meta-analyses and clinical trials (Vlachos et al., 2020; Zafar et al., 2019), using dietary strategies to reduce the appearance of exogenous glucose during meals is important for improving postprandial glycemic control.

1.1.1 Influencing the rate of gastric emptying

The rate of gastric emptying positively affects the postprandial glucose response. Consequently, the nature of the meal can influence the rate of delivery of the nutrients inside the intestinal lumen, then the rate of absorption and finally the postprandial glucose response. The rate of gastric emptying is impacted only by the composition of food since neither the speed of ingestion (Alsalim and Ahrén, 2019), nor the intensity of a previous physical exercise (Mattin et al., 2018), and nor the posture (Jones et al., 2006) seem to affect it.

Basically, the slowly digestible carbohydrates significantly delay gastric emptying and decrease postprandial glucose and insulin response, as demonstrated in rats (Hasek et al., 2020). However, the cereal composition itself seems not to be impacting because the gastric rates observed respectively after ingestion of different types of cereal (Hlebowicz et al., 2009; Najjar et al., 2009) or bread processing (Bondia-Pons et al., 2011; Hlebowicz et al., 2009) did not differ. The enrichment of the meal in fibers appears in contrast to be particularly relevant in slowing gastric emptying (Benini et al., 1995; Hlebowicz et al., 2007), with beneficial consequences on postprandial glycemia.

The texture of the meal plays a key role in the rate of gastric emptying since a chyme with a high viscosity slows it (Hamad et al., 2021; Kung et al., 2019). In fact, viscous fibers, including beta-glucan

(Nazare et al., 2010a) in oat bran (Juvonen et al., 2009; Wolever et al., 2020) and guar gum (Torsdottir et al., 1989), favorably affect satiety as well as postprandial carbohydrate and lipid metabolism. They delay gastric emptying and strongly affect short-term gut hormone responses by increasing the levels of satiety hormones and decreasing the ghrelin one.

The pre-administration of some aminoacids before a meal leads to a decrease in gastric emptying rate, with consequent decrease of postprandial glucose response. It was clearly shown for glutamine (Du et al., 2018) and tryptophan (Ullrich et al., 2018) but not for leucine, isoleucine or phenylalanine (Elovaris et al., 2021; Fitzgerald et al., 2020). In healthy humans, the addition of protein to oral glucose lowers postprandial blood glucose concentrations acutely, predominantly by slowing gastric emptying, although protein also stimulates incretin hormones and non-glucose-dependent insulin release (Karamanlis et al., 2007). This effect was particularly noticeable after the administration of a whey protein preload (Hutchison et al., 2015; Pham et al., 2019; Smith et al., 2021).

The coadministration of lipids with the meal was also a strategy particularly described in diabetes to decrease postprandial glucose excursions by delaying gastric emptying (Bozzetto et al., 2019; Collier et al., 1984; Gentilcore et al., 2006).

1.1.2 Influencing the rate of digestion

A lot of nutritional approaches were tested in order to decrease the availability of glucose, and consequently the rate of digestion and then the one of absorption. Reducing the glycemic index of the meals have appeared efficient to decrease postprandial glucose excursions and improve glycemic control. A systematic review and meta-analysis of randomized controlled trials demonstrated that the low-GI diet is more effective in controlling glycated hemoglobin and fasting blood glucose compared with a higher-GI diet or control in patients with type 2 diabetes (Ojo et al., 2018).

Co-administration of protein and lipid substrates

First, adding protein or lipid substrates in a carbohydrate meal leads to a reduction of the postprandial glucose response. This is why the glycemic index (GI) of a carbohydrate component has to be recalculated according to if it co-ingested with a lipid or protein load (Wolever et al., 1985).

Replacing glucose by low-calorie sweeteners

One of another option to decrease the GI consists in replacing glucose or sucrose by low-calorie sweeteners, such as stevia, aspartame, trehalose, and isomaltulose. Artificial sweeteners represent a group of various components with important differences in their pharmacokinetics parameters (absorption, distribution, metabolization, elimination, digestion by the microbiota...). This is why the biological fate following their administration is as different as their biochemical properties (Magnuson et al., 2016). Studies demonstrated the beneficial substitution of sucrose-meal by low-GI meals with

trehalose and isomaltulose in healthy subjects (Henry et al., 2009; Yoshizane et al., 2017) and patients with impaired glucose tolerance (van Can et al., 2012). However, the use of artificial sweeteners is controversial because some are suspected to stimulate sweet taste receptors, and consequently upregulating SGLT1 (Margolskee et al., 2007) as for as creating a paradoxical increase of appetite (Blundell, 1986; Pierce et al., 2007). However, there are globally not enough evidences about low caloric artificial sweeteners to qualify them as unsafe and they represent currently more a useful tool in the management of postprandial glucose response.

Addition of fibers

The addition of fibers into the meal is clearly a way to decrease the availability of glucose. The fibers include a heterogeneity of compounds which highly differ in water solubility, viscosity, binding and bulking ability and fermentability (Pasmans et al., 2022). Prebiotic, insoluble and viscous soluble fibers are the main types with beneficial effect on postprandial glucose response.

Inulin-type fructans are nonviscous soluble fibers that have prebiotic properties. It means that they can be selectively used by the intestinal microbiota to confer a health benefit (Hughes et al., 2021). In healthy subjects, the partial replacement of sucrose by oligofructose from chicory or inulin resulted in a reduction of postprandial blood glucose response compared to the full-carbohydrate equivalent (Lightowler et al., 2018). A microbiota shift to an increase in bifidobacterial would be an underlying mechanism contributing to the beneficial effect observed on postprandial glucose response (Vandeputte et al., 2017). Additionally, a meta-analysis conducted on 33 randomized controlled trials showed the improvement of glycemic control in subject with prediabetes or diabetes following supplementation in inulin-type fructans (Wang et al., 2019).

Insoluble fibers contained in foods with whole grains, fruits and vegetables cannot be dissolved in water and lead to fecal bulking (McRorie and McKeown, 2017). The consumption of insoluble fibers allows an improvement of postprandial glucose response by altering nutrient absorption, delaying the time of the gastrointestinal transit (Pantophlet et al., 2017) and inducing a beneficial microbiota shift (Ranaivo et al., 2022)

Viscous soluble fibers (gel-forming fibers such as beta glucan, psyllium or guar gum) are now well-known for their ability to form a non-digestible non-fermentable gel into the gastrointestinal tract, leading to a delay of gastric emptying and reduction of amylolysis (Repin et al., 2017) and finally lowering postprandial glucose response (Giuntini et al., 2022; Telle-Hansen et al., 2022).

Increasing the content of slowly digestible starch (SDS)

Increasing the content of SDS in foods has beneficial consequences on postprandial glucose response. Substituting extruded cereals with biscuits enriched in SDS slows down the availability of glucose from

the breakfast and its appearance in peripheral circulation, blunts the changes in plasma glucose kinetics and homeostasis, reduces excursions in plasma glucose, and possibly distributes the glucose ingested over a longer period following the meal (Péronnet et al., 2015). A recent meta-analysis provides moreover evidence that SDS intake is positively correlated with a reduction of postprandial glucose response (Wang et al., 2022). The quantitative relationship of the reduction in the postprandial glycemic response and SDS consumption was used in these studies to quantify the slow digestion property on an extended time scale, and supplement the in vitro concept of SDS.

Foods with natural inhibitors of the digestive enzymes

Plants are an important source of natural compounds presenting the ability of inhibiting α -glucosidase.

Many of these compounds belong to the family of polyphenols and can be found in some fruits and berries (Castro-Acosta et al., 2016). For example, the administration of kiwifruit resulted in an attenuated glycemic response in healthy individuals (Monro et al., 2022). The α -glucosidase inhibitory effect of anthocyanin, a specific polyphenol found in blueberry, blackcurrant, apple, red grape or cinnamon, was demonstrated in vitro (Ercan and El, 2021; Kong et al., 2018), with associated beneficial consequences on postprandial glucose and insulin lowering (Bell et al., 2017).

Other substrates, such as L-arabinose, D-sorbose (Oku et al., 2014) or inulin-type fructans (Neyrinck et al., 2016), also target the digestive enzymes. The inhibiting effect of L-arabinose on simple carbohydrates but also starch was demonstrated in healthy humans, with a consequent lowering effect of glycemic response (Pol et al., 2022), and the enrichment of 4 % in beverage was established in vitro and confirmed in vivo (Krog-Mikkelsen et al., 2011) to reach this effect.

1.1.3 Influencing glucose transport

Dietary compounds are able to enhance or decrease intestinal glucose uptake by the enterocyte glucose transporters.

The consumption of meal rich in carbohydrates created an adaptation of the enterocytes and a recruitment of SGLT1 at the apical pole (Koepsell, 2020). It was particularly studied in rats models, in which the chronical intake of dietary sugars (Miyamoto et al., 1993), fructose (Kishi et al., 1999) but also high-medium-chain triacylglycerols (Yasutake et al., 1995) increases the expression of jejunal SGLT1, leading to enhancement of intestinal glucose transport for the following meals. The SGLT1 up-regulative capacity of the low-calories artificial sweeteners was also shown in animal models (Margolskee et al., 2007; Moran et al., 2010).

On the contrary, some natural plants compounds, beyond their inhibitory effect on α -glucosidases, are also able to decrease intestinal glucose uptake.

It is the case for phenolic compounds (natural phlorizin from apple or anthocyanin from blackcurrant extracts, cardamomin...) for which the inhibitory effect was demonstrated in vitro for SGLT1 and GLUT2 in Caco-2 cells (Alzaid et al., 2013; Farrell et al., 2013; Zhouyao et al., 2022). Their effect on the inhibition of intestinal glucose absorption was also confirmed in vivo in mice (Satsu et al., 2021) and healthy humans, with a subsequent decrease of postprandial glucose response in randomized, controlled, double-blinded cross-over trial (Castro-Acosta et al., 2017; König et al., 2019). Apple kale extracts administration during several weeks allowed moreover the improvement of postprandial hyperglycemia in mice submitted to an high-fat high-sucrose diet (Schloesser et al., 2017), highlighting the relevance of dietary approaches containing SGLT1 inhibitors for type 2 diabetes management.

Such an effect was also shown with terpenoids, extracted from cinnamon, clove, or ginger. Their antihyperglycemic effect was demonstrated in vitro and in mouse model, as for as their selective inhibition of SGLT1 and α -glucosidases (Ortega et al., 2022; Valdés et al., 2020).

Finally, if beta glucans delay gastric emptying and limit amylolysis thanks to their viscosity, they seem also to inhibit intestinal glucose uptake, by creating a physical barrier limiting the interactions between glucose and SGLT1 and GLUT2 (Abbasi et al., 2016; Malunga et al., 2021).

1.2 Other approaches

In the DiRECT trial, the team of Taylor conducted an open-label, cluster randomized trial in British patients with type 2 diabetes. The dietary intervention involved replacing the entire diet: for 3 to 5 months, the energetic content of the diet was fixed at 850 kcal/day, and then, over the course of 8 weeks, food was gradually reintroduced. Anti-diabetic and anti-hypertensive medications were completely suppressed during the course of this diet (Lean et al., 2018). A remission of type 2 diabetes without the use of medication was achieved by approximately half of the trial participants, proving the viability of this strategy. However, the drastic diet as set up in the DiRECT trial is frustrating for the patients and difficult to conserve in the long-term (Forouhi et al., 2018).

Additionally, the daily context of meal consumption has also become important in nutritional therapy. In fact, the postprandial glycemic response that occurs after consuming a standardized meal varies depending on the time of day. In cross-sectional and experimental studies, the advantages of eating more at breakfast versus at dinner were amply shown to reduce postprandial glucose excursions (Henry et al., 2020). In this light, various intermittent fasting techniques have been tried. Intermittent fasting involves either a regular interruption of energy consumption for a set amount of time each day or a drastic reduction in food intake on one or two days per week (Klempel et al., 2012). Time Restriction Eating is the name of this last strategy, which involves eating only during a window of 4–8 hours and fasting for 16–20 hours in between (Carlson et al., 2007). Some meta-analyses showed that

these diets were not inferior to alternatives that involved restricting caloric intake, but they were more patient-friendly in the long term (Borgundvaag et al., 2021; Wang et al., 2021).

2. Medical therapy

2.1 Molecules limiting intestinal glucose absorption

2.1.1 *Influencing the rate of gastric emptying*

Pharmacological molecules are able to alter gastric emptying, with the corresponding consequences on postprandial glucose response. Pharmacologic acceleration of gastric emptying with prokinetic molecules such as erythromycin (Gonlachanvit et al., 2003) resulted in higher postprandial glucose concentrations whereas delaying it, via opioids (Gonlachanvit et al., 2003) or GLP-1 (Deane et al., 2010; Jones et al., 2019) or amylin analogs (Samsom et al., 2000; Young and Denaro, 1998), results in lower postprandial glucose concentration after a physiological meal in healthy subjects and type 2 diabetes.

GLP-1 has a particularly pleiotropic effect and GLP-1 receptor agonists have taken a leading role in type 2 diabetes management, particularly through their effect on satiety and weight loss and their augmentation of hyperglycemia-induced insulin secretion (Nauck et al., 2021). Several molecules have yet been developed, with a short- or long-term action and variable physiological effects (Ryan J. Jalleh et al., 2022; Trujillo et al., 2021). GLP-1 receptor agonists present the ability to delay the rate of gastric emptying, symptom considered initially by the European Medicine Agency as a side effect (European Medicines Agency, 2022). This characteristic was particularly highlighted for short-acting exenatide (Linnebjerg et al., 2008) and lixisenatide (Jones et al., 2019; Rayner et al., 2020) and for long-acting dulaglutide (Barrington et al., 2011), liraglutide (Meier et al., 2015) and semaglutide (Hjerpsted et al., 2018). The effect on delaying gastric emptying of dual GLP-1 and GIP receptor agonist tirzepatide has also been observed (Jastreboff et al., 2022; Urva et al., 2020). However, this effect seemed to be positively associated with the decrease of postprandial glucose excursions, that proposed the rate of gastric emptying as a mechanism that would be particularly relevant to target in type 2 diabetes management.

2.1.2 *Influencing the rate of digestion*

The pharmacological approach aiming at decreasing the rate of digestion of carbohydrates consists in the inhibition of α -glucosidases, such as acarbose, voglibose or miglitol.

A recent meta-analysis provided quantitative estimation of reductions of postprandial glucose response following α -glucosidases inhibitors in diabetes (-1.5 mmol/L) but also non-diabetes (-0.5 mmol/L) individuals, associated with a reduction of postprandial insulin excursion (Alssema et al., 2021). Acarbose has been associated with a reduction of the risk of cardiovascular disease (Chiasson et al.,

2003) and a reduction of diabetes progression in patients with impaired glucose tolerance (Holman et al., 2017). However, gastrointestinal side effects, as for as flatulence, diarrhea or abdominal pain were frequently reported, limiting its use (Rosak and Mertes, 2012).

This is why the current preclinical research in α -glucosidases inhibitors consist in identifying natural compounds with α -glucosidases inhibitory profile isolated from plant sources with a superior benefice and lower side effects (Elhady et al., 2023; Kęska et al., 2023).

2.1.3 Influencing intestinal glucose uptake

SGLT1 inhibitors

The main approaches consist in targeting SGLT1 for intestinal glucose uptake inhibition. The actual molecules are inspired by the famous polyphenol phlorizin, naturally found in apple. Phlorizin was first used in experimental biology and then medical research after its discovery in 1835. Its ability to improve postprandial glycemic response without affecting insulin action was what made its use interesting (Ehrenkranz et al., 2005). However, the first description of its effects were essentially renal and selective SGLT2 inhibitors were developed at the beginning (Dominguez Rieg and Rieg, 2019).

More recently, there have been studies to develop dual SGLT1/SGLT2 and selective SGLT1 inhibitors. As dual inhibitors, sotagliflozin (20-fold higher potency for SGLT2 than SGLT1) (Cefalo et al., 2019; D. R. Powell et al., 2020; Sano et al., 2020) but also LIK066 (He et al., 2019) and LX4211 (Powell et al., 2013; Zambrowicz et al., 2012) block both enterocyte glucose uptake and kidney glucose reabsorption. These uses are associated with a delayed and blunted intestinal glucose absorption after meals, with also a net increase of GLP-1 and PYY release and a decrease of GIP release and consequently a lower postprandial blood glucose. After administration, the effective regional SGLT1 inhibition of sotagliflozin persists for at least 5 hours (D. R. Powell et al., 2020).

Several molecules with selective SGLT1 inhibition have also been developed. Mizagliflozin is currently the most selective SGLT1 inhibitor (with 300-fold more selective to SGLT1 than SGLT2). It is a non-absorbable compounds (availability of 0.02 %), which guarantee its local action (Ohno et al., 2019). Other compounds presenting a locally acting selective SGLT1 inhibition have been discovered (Goodwin et al., 2017; Kuroda et al., 2020). The action of selective SGLT1 inhibitors results thus in a potent blocking of intestinal glucose uptake, a delayed intestinal glucose absorption, an increase in GLP-1 release and a decrease in GIP secretion, leading finally to a decrease of postprandial glucose response, as demonstrated in humans and diabetic rats (Dobbins et al., 2015; Oguma et al., 2015). An increase of GLP-2 release was also highlighted in another study performed in diabetic rats (Io et al., 2019).

To resume, intestinal inhibition of SGLT1 has numerous beneficial effects on postprandial glucose response. This action is direct, by inhibiting intestinal glucose uptake and consequently delaying and decreasing intestinal glucose absorption, and also indirect, by inducing a prolonged increase in GLP-1 levels.

Metformin

One of the primary first-line medications for lowering glycemia in type 2 diabetes is metformin. Metformin has a pleiotropic effect and is recognized to decrease hepatic endogenous glucose production (Hunter et al., 2018) and increase insulin sensitivity (Stumvoll et al., 1995). Additionally, recent data suggests that metformin primary acts on the intestine instead of via the systemic circulation (Buse et al., 2016). Gastric emptying (Sato et al., 2017), bile acid trafficking (Sansome et al., 2020), GLP-1 release (Bahne et al., 2018), or reshaping in the gut microbiota (Bauer et al., 2018) seem to be involved.

An inhibitory action of metformin on intestinal glucose absorption has also been suggested in rodent models using ex vivo models of perfused intestine (Ikeda et al., 2000; Wilcock and Bailey, 1991) but remained controversial for a long time (Horakova et al., 2019; Lenzen et al., 1996; Sakar et al., 2010).

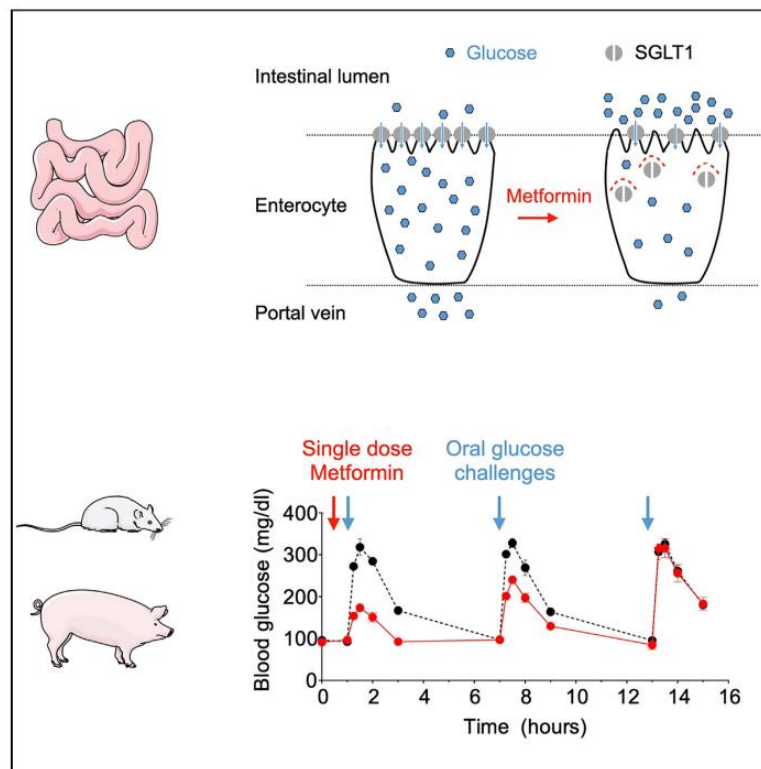


Figure 24: Oral metformin decrease postprandial glucose response by reducing the apical expression of SGLT1 in enterocytes (Zubiaga et al., 2023)

In this recent study from our group, the implication of metformin on intestinal glucose absorption and postprandial glucose response was clearly established. Zubiaga and coworkers demonstrated the ability of oral metformin to transiently lower postprandial glucose response by preventing the translocation of SGLT1 to the apical pole of enterocytes (**Figure 24**). They moreover have insisted on the necessity to administer this drug before a meal, to guarantee this inhibitory effect on absorption, and not after or at bedtime, thus challenging the current recommendation (Zubiaga et al., 2023).

2.2 Incretino-mimetics

Inhibitors of dipeptidyl-peptidase-4 (DPP-4)

The GIP and GLP-1 incretin hormones are quickly inactivated in the blood system. The dipeptidyl-peptidase-4 inhibitors, also known as gliptins, prevented the breakdown of GIP and GLP-1, which indirectly increased incretin levels in the bloodstream. As a result, they help to improve the biological actions of incretins, which results in increased insulin release as well as decreased glucagon and hepatic glucose production and increased satiety.

DPP-4 inhibitors significantly improve fasting and postprandial glycemia, reduce HbA_{1c} by 0.8 %, and inhibit DPP-4 activity by 80 % in vivo. They have good tolerance, and neither weight gain nor hypoglycemic events have been reported (Duez et al., 2012).

GLP-1 receptor agonists

In 2005, exenatide became the first GLP-1 receptor agonist to be approved for the treatment of type 2 diabetes. The first challenge was to create other molecules or formulations that could overcome their rapid elimination without requiring twice-daily injections.

Nowadays, GLP-1 receptor agonists have been developed, with different half-life time: short acting agents (exenatide twice daily or lixisenatide) or long-acting agents (liraglutide, once-weekly exenatide, dulaglutide, albiglutide and semaglutide). Since GLP-1 has a pleiotropic effect, GLP-1 receptor agonists share also the same properties in allowing: an augmentation of hyperglycemia-induced insulin secretion; suppression of glucagon secretion; delaying gastric emptying (as described previously); prevention of high postprandial glycaemic excursions; and decrease of appetite and body weight.

Because they have a similar impact on HbA_{1c} reduction and weight loss without the risk of hypoglycemic events, GLP-1 receptor agonists are preferred as the first-line injectable treatment over insulin. They may be combined with insulin or additional diabetes medications. More recently, the protective action of GLP-1 receptor agonists against myocardial infarction or stroke (and the associated mortality) has been particularly reported (Nauck et al., 2021).

2.3 Other molecules

The therapeutic arsenal is large and includes molecules targeting several pathophysiological pathways (Figure 25). The drugs can be used as mono- or multimodal therapy, in first or second intention. Their efficacy is variable according to the phenotype of each patient and they are often associated with side effects, such as weight gain.

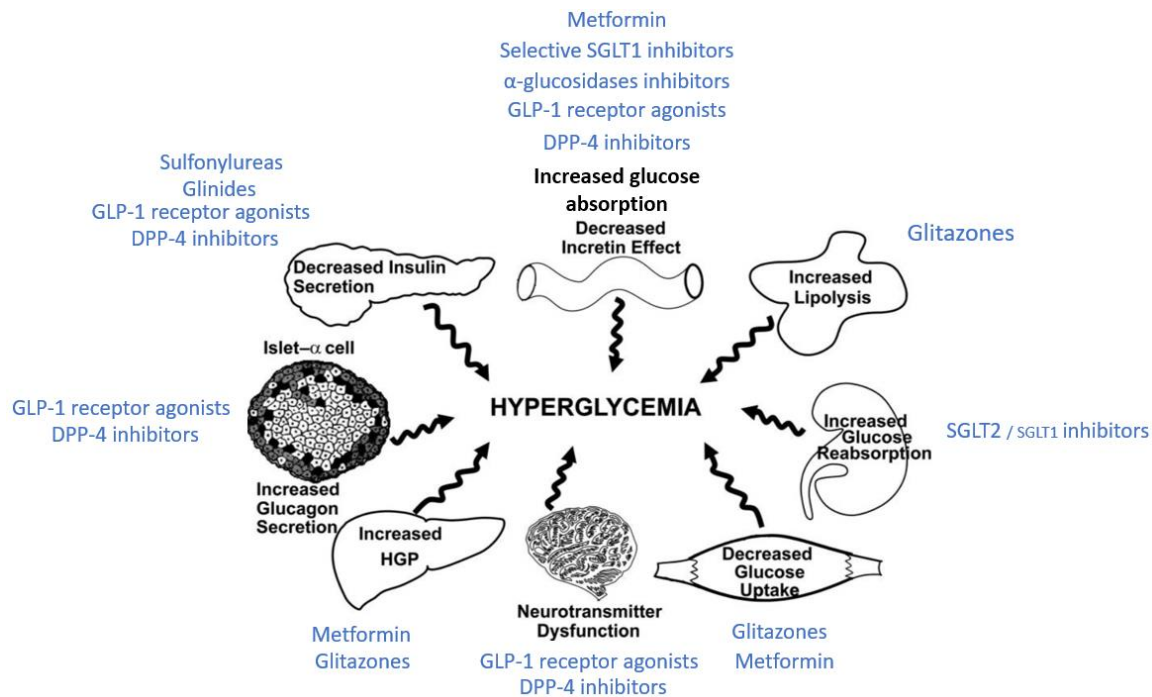


Figure 25: Sites of action of glucose-lowering agents. Adapted from (DeFronzo, 2009).

2.3.1 Stimulating insulin release: sulfonylureas and glinides

The stimulation of glucose-induced insulin release was the first pharmacological approach for type 2 diabetes management, leading to the introduction of sulfonylureas as an anti-diabetic drug more than 50 years ago. Sulfonylurea use has remained the primary pharmacological strategy for patients with newly diagnosed type 2 diabetes since its introduction due to its consistent ability to stimulate insulin secretion while having few unwanted side effects. The American Diabetes Association regarded sulfonylureas as a first-line diabetes monotherapy, as well as in conjunction with other anti-diabetic medications (American Diabetes Association, 2004). Sulfonylureas enhance insulin release thanks to their binding to the sulfonylurea receptor, one of the subunits of the K_{ATP} channel, leading to the closure of the channel, a membrane depolarization, and consequently an influx of calcium ions causing exocytosis of the granules of insulin. Glinides, such as repaglinide, nateglinide and mitiglinide, have the same action mechanism and a similar hyperglycemic power as sulfonylurea but a different binding site on the K_{ATP} channel subunit. The action of these two types of molecules can help to mimic the early phase of insulin release, via enhancing the exocytosis of granules.

In fact, sulfonylureas have been linked to an increased risk of hypoglycemia, body weight gain, beta-cell exhaustion, and limited specificity for closing pancreatic K_{ATP} channels. As a result, new concerns about their recommendations have emerged over the past few decades. Hypoglycemia represents a major therapeutic issue since hypoglycemia events were reported in 11-30 % of diabetic patients treated with sulfonylureas, according to studies (Jennings et al., 1989; The Diabetes Control and Complications Trial Research Group, 1993). As with many other anti-diabetic medications, body weight gain is also a side effect brought on by the increased insulin release. Additionally, sulfonylurea treatment has been shown to increase beta cell apoptosis in rodent and human islets (Efanova et al., 1998; Maedler et al., 2005). Finally, some molecules have a cross-reactivity with the K_{ATP} channel of the cardiovascular system, resulting in a deleterious effect on cardiac function, especially under ischemic conditions (Scognamiglio et al., 2002).

However, their beneficial effect on glucose-stimulated insulin secretion is especially helpful when given in conjunction with other antidiabetic medications, as a multimodal therapy, in order to maximize its potential for reducing the risk of side effects (Del Prato and Pulizzi, 2006).

2.3.2 Stimulating insulin sensitivity

Biguanides

As the only medication in the biguanides family currently in use, metformin (1,1-dimethylbiguanide) is regarded as the first-line therapy for type 2 diabetes. It has a good safety profile because it does not induce an increased risk of hypoglycemia events and does not lead to weight gain, although gastrointestinal symptoms, such as abdominal pain, nausea, or diarrhea are common side effects. Metformin allows a reduction of hyperglycemia thanks to a decrease of HbA_{1c} up to 1.5 %, independently of Body Mass Index, age and duration of diabetes (Holman et al., 2008).

Metformin does not stimulate insulin secretion and does not act directly on the pancreas; instead, it seems to have more of an impact on insulin-sensitive tissue. Understanding of every mechanism underlying the improvement in glucose homeostasis under metformin therapy is still lacking. In fact, the pleiotropic action of metformin suggests a large diversity of mechanisms of action according to each tissue rather than a singly mode of action. The primary antidiabetic action of metformin involves an exacerbation of the suppression of hepatic glucose production by almost 40 % (Hundal et al., 2000) and a stimulation of systemic glucose disposal (Inzucchi et al., 1998). These mechanisms seem underlying an activation of the cellular metabolism via the phosphorylation of the AMP-activated protein kinase (AMPK), leading to an inhibition of the mitochondrial respiratory chain complex 1. This inhibition results in alterations in cellular energy charge and redox state, making the cells more responsive to insulin. Emerging evidence reported a beneficial action of metformin on the systemic

inflammation induced by obesity thanks to direct and indirect effects on tissue-resident immune cells in organs involved in metabolism regulation, especially the adipose tissue, the liver and the gastrointestinal tract (Foretz et al., 2019). Additionally, metformin appears to have a significant impact on the digestive tract through its effects on GLP-1 secretion, bile acid remodeling, microbiota reshaping and intestinal glucose absorption (Bauer et al., 2018; Sansome et al., 2020; Zubiaga et al., 2023).

Glitazones

Glitazones, also known as thiazolidinediones, are a class of medications used as a second-line treatment for type 2 diabetes with the goal of reducing insulin resistance. Troglitazone, rosiglitazone, and pioglitazone are the three main molecules, and they were introduced to the market for the first time in 2000 in Europe.

The mechanism of action of glitazones involves its binding to the nuclear receptor Peroxisome Proliferator-Activated Receptor gamma (PPAR γ), essentially found in adipocytes but also in the liver and the skeletal muscle in a lesser extent. PPAR γ is a transcription factor of genes involved in cellular differentiation or metabolic pathway signaling, so that the binding of glitazones to PPAR γ leads to an enhancement of insulin action in the adipose tissue, but also in the liver and the skeletal muscle. According to Stenkula and Erlanson-Albertsson, glitazones also appear to decrease the number of large adipocytes while promoting the development of smaller, less inflammatory, and consequently more insulin-sensitive adipocytes (Stenkula and Erlanson-Albertsson, 2018). Thus, glitazones help to increase insulin sensitivity and are thought to lower levels of free fatty acids and triglycerides (Bradley, 2002).

But using glitazones is linked to a number of negative side effects, including an increase in body weight, an increased risk of fractures, fluid retention, heart failure, hypercholesterolemia, and a risk of carcinogenesis (in the urinary bladder for pioglitazone). They are not regarded as a rational monotherapy in the general management of type 2 diabetes because of this (Lindberg and Astrup, 2007).

2.3.3 Inhibiting renal glucose reabsorption

Since almost all of the glucose filtered by the kidney at euglycemia is reabsorbed by SGLT2 in the tubules, the kidney is crucial for maintaining glucose homeostasis. In this light, pharmacological inhibitors of SGLT2 (with also an action on SGLT1) have recently been created in order to raise urinary excretion without requiring the action of insulin, thereby lowering plasma glucose levels. Canagliflozin, dapagliflozin, empagliflozin, and ertugliflozin are the molecules that are offered in the United States and Europe (Hasan et al., 2014; Lupsa and Inzucchi, 2018).

The beneficial effect of SGLT2 inhibitors as monotherapy or bitherapy on glucose lowering allows a reduction in HbA_{1c} of between 0.4 and 1.1 % compared to before treatment. Due to its action of

intestinal SGLT1 inhibition, canagliflozin permits a particularly significant decrease (Roden et al., 2013; Stenlöf et al., 2013). Beyond improving glucose homeostasis, SGLT2 inhibitors also induce weight loss, decrease in blood pressure, and a reduction in the occurrence of cardiovascular events and nephropathic risk. They are also associated with a low incidence of hypoglycemia events.

Although the SGLT2 inhibitors are typically well tolerated, they can cause well-described adverse events, such as infections of the genitourinary tract, diabetic ketoacidosis, skeletal fracture, volume depletion, acute kidney injury, or an increased risk of bladder and breast cancer (Lupsa and Inzucchi, 2018).

Due to their protective effect against the occurrence of major cardiac events, SGLT2 inhibitors have been recommended as a second-line treatment after metformin by the American Diabetes Association since 2018 (American Diabetes Association, 2017).

3. Interventional therapy: metabolic surgery

3.1 Introduction

To control postprandial glycemic response, a wide range of dietary strategies have been developed, and they serve as the first-line treatment for diabetes remission. However, for the vast majority of type 2 diabetes patients, they do not enable significant weight loss, glycemic control improvement, or a decrease in cardiovascular morbidity. The second option is to use medical therapy, with the possibility of using a variety of drugs that target various pathophysiological aspects of type 2 diabetes, including insulin secretion, insulin resistance, kidney glucose reabsorption, and intestinal glucose absorption. However, medical therapy only partially achieves the desired glycemic control and cardiovascular mortality reductions (Mingrone et al., 2012). Additionally, the majority of medical treatments have side effects, such as weight gain, which can be detrimental to glycemic control, hypoglycemic incidents, digestive issues, or an increased risk of cardiovascular events.

Bariatric surgery represents an interventional approach to obesity management. It was initially developed as a weight-reduction therapy but has been reported to allow type 2 diabetes remission (Sjöström et al., 2004) and to improve glycemic control independently of weight loss (Umeda et al., 2011) associated with a reduction in the rate of severe cardiovascular disease events (Sjöström et al., 2004). This is why the term “metabolic surgery” also emerged.

In France, the Haute Autorité de Santé (HAS) strictly regulates metabolic surgery, which is currently accepted as a treatment for extreme obesity. Patients eligible for metabolic surgery must have a Body Mass Index (BMI) over 40 kg/m² or a BMI over 35 kg/m² with associated comorbidities susceptible to improvement after surgery, such as: type 2 diabetes, high blood pressure, osteoarticular disorders, or

sleep apnea. Patients must have tried hygienic therapy prior to surgery in order to lose weight during a few months of medical follow-up, and they must be healthy enough to undergo surgery and receive anesthesia (Haute Autorité de Santé, 2009). Informing the patients of the possible outcomes of this care is especially important because surgical interventions are associated with complications. But thanks to laparoscopic surgery, the increased experience of the surgeons, and the creation of specialized centers, the morbidity associated to the procedure has dramatically decreased in recent years, reaching 0.1 % of mortality and 5 % of severe morbidity. The prevalence of rehospitalization or surgical revision can reach 10 % in the first year following surgery, and the postoperative complications, particularly the digestive ones, are still not negligible (Halimi, 2019).

Despite having a relatively low prevalence of obesity in comparison to other nations, France follows the United States and Brazil in terms of the number of bariatric surgery interventions, averaging about 60 000 per year (in 2018). This is probably related to a healthcare system taking totally charge of these surgeries for all the patients. The number of interventions rose significantly because there were 24 000 interventions in 2008 compared to only 5 000 in 1998. More than 80 % of the patients benefiting from bariatric surgery are women, prevalence that has remained relatively constant since 1998.

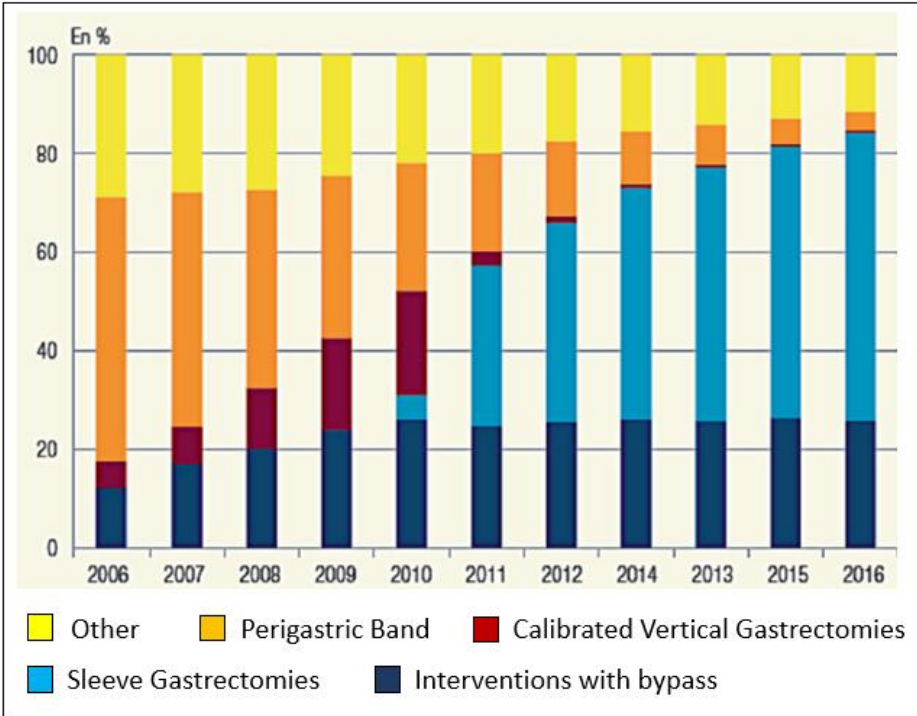


Figure 26: Evolution of the rate of the different interventions of bariatric surgery in France, between 2000 and 2016. Adapted from (Halimi, 2019).

The laparoscopic adjustable gastric band (LAGB), sleeve gastrectomy (SG), and gastric bypass (GBP; Roux-en-Y gastric bypass or biliopancreatic diversion) are the bariatric surgery procedures that are

permitted in France. SG is the most commonly practiced intervention and concerned 57 % of surgeries in 2013, whereas the prevalence of GBP was evaluated at 31 % and at 13 % for LAGB (Figure 26). However, these rates are submitted to national disparities because GPB are more performed in the Ile-de-France, North and Rhône-Alpes area (Halimi, 2019).

There are still being developed additional cutting-edge bariatric/metabolic surgery methods. Research in metabolic surgery is primarily focused on developing the interventions that will have the greatest clinical benefit in reducing the risk of both short- and long-term complications. Even though the clinical benefits of interventions today are well known, the physiological mechanisms underlying these benefits, particularly the improvement of glucose homeostasis, are still not fully understood. Additionally, one of the current perspectives is to identify the type 2 diabetes patients for whom surgery will be especially effective and to best tailor each surgical intervention to each patient's phenotype.

3.2 Different interventions

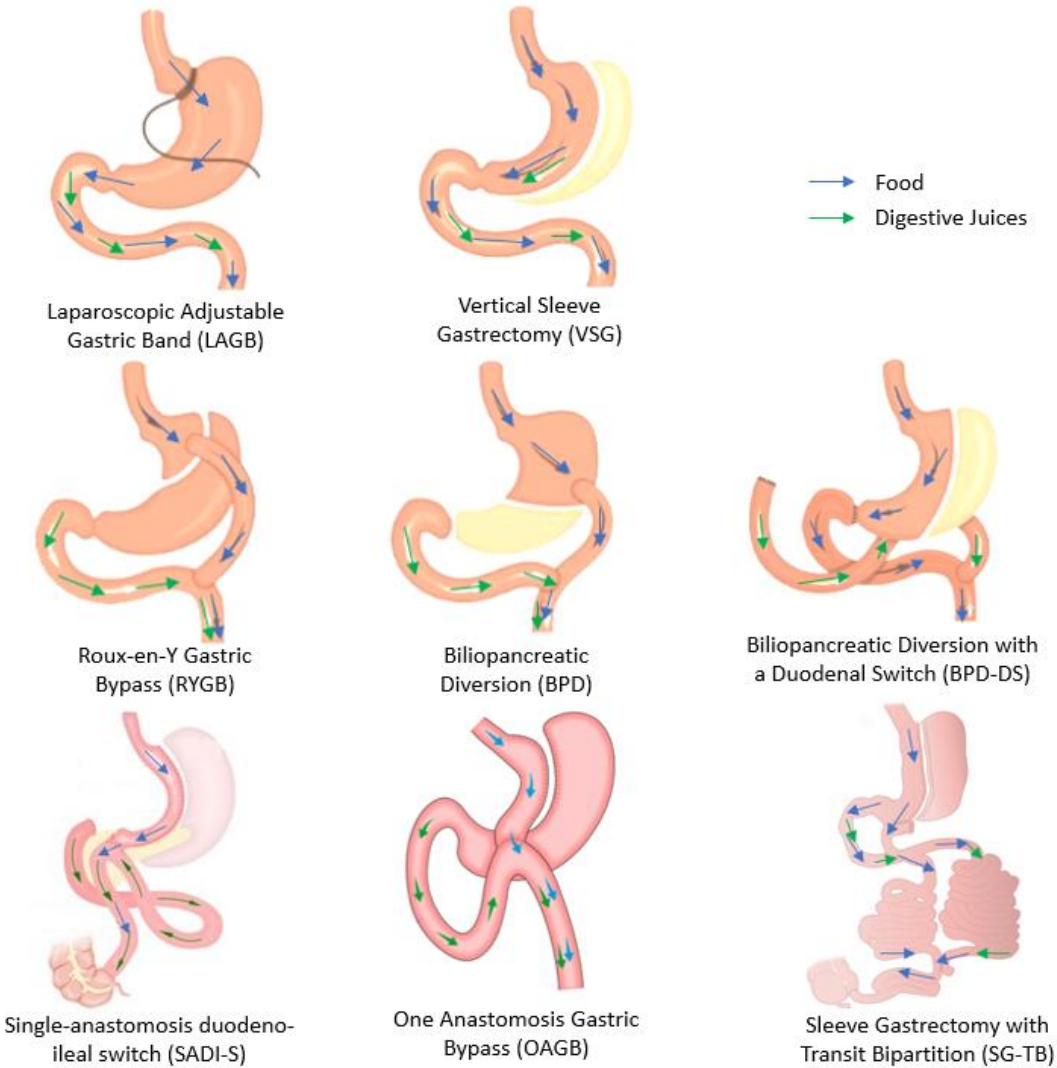


Figure 27: The main interventions of bariatric surgery. Adapted from (Bariatric Clinic, 2021), (Puhalla, 2020), (Mauranui Clinic, 2023) and (Bilecik, 2019).

Among all the interventions of bariatric surgery (**Figure 27**), only the Laparoscopic Adjustable Gastric Band (LAGB), the Vertical Sleeve Gastrectomy (VSG), the Roux-en-Y Gastric Bypass (RYGB) and the Biliopancreatic Diversion (BPD) are allowed in France. The most practiced interventions are the sleeve gastrectomy and the Roux-en-Y Gastric Bypass.

Sleeve Gastrectomy (SG)

Sleeve gastrectomy (SG) consists of a subtotal vertical gastrectomy in which the pylorus is preserved. The fundus, corpus, and antrum are resealed in order to create a tubular duct along the small curvature of the stomach. The resection included 80 % of the stomach, and the remaining gastric pouch has a capacity of 60-100 mL.

Due to the absence of multiple intestinal anastomosis, SG is regarded as a simpler procedure than gastric bypass. Some variations of SG have been described, but no comparative study has been done to determine the benefits of these variations. To maximize metabolic effects, SG is sometimes combined with other intestinal bypass procedures, such as biliopancreatic diversion or SG transit with bipartition (Benaiges et al., 2015).

Roux-en-Y gastric bypass

The Roux-en-Y gastric bypass (RYGB) consists of the elaboration of a gastric pouch of 15-30 mL without extracting the remaining stomach. The upper intestinal segment is affected by the bypass and includes the duodenum and the proximal jejunum. Two anastomoses are performed: a gastro-jejunal and a jejuno-jejunal. Consequently, the portion of the intestine that receives bile and pancreatic enzymes is completely excluded from the route of the chyme. Gastro-intestinal tract is thus reshaping in "Y", leading to the elaboration of 3 different limbs: the bilio-pancreatic limb (measuring about 50 cm), the alimentary limb (about 100 cm) and the common limb, the most distal (between 300 and 400 cm). These dimensions are valid for standard RYGB because some variations concerning the length of each limb have been described (Miras et al., 2021).

3.3 Remission of type 2 diabetes

The clinical benefits of metabolic surgery are multiple and include weight loss (O'Brien et al., 2019), reduction of cardiovascular risk (van Veldhuisen et al., 2022), reduction of hypertension (Schiavon et al., 2018), improvement of dyslipidemia (Liu et al., 2021), improvement of hepatic steatosis and NASH (Caiazzo et al., 2014; Lassailly et al., 2020) and improvement of glycemic control.

One of the earliest and most striking effects of metabolic surgery is effectively an improvement in postprandial glucose response in patients with obesity and type 2 diabetes. The restoration of a tightly

regulated glucose homeostasis appears to be unrelated to weight loss and has been replicated worldwide. Many randomized controlled trials confirmed that metabolic surgery allows a better improvement of postprandial glucose control compared to medical therapy (**Figure 28**) (Aminian et al., 2021; Kirwan et al., 2022; Mingrone et al., 2021, 2015). In the randomized controlled trial conducted by Mingrone et al., the 10-year type 2 diabetes remission rate was 5.5 % for medical therapy compared to 50.0 % for BPD and 25.0 % for RYGB group (Mingrone et al., 2021).

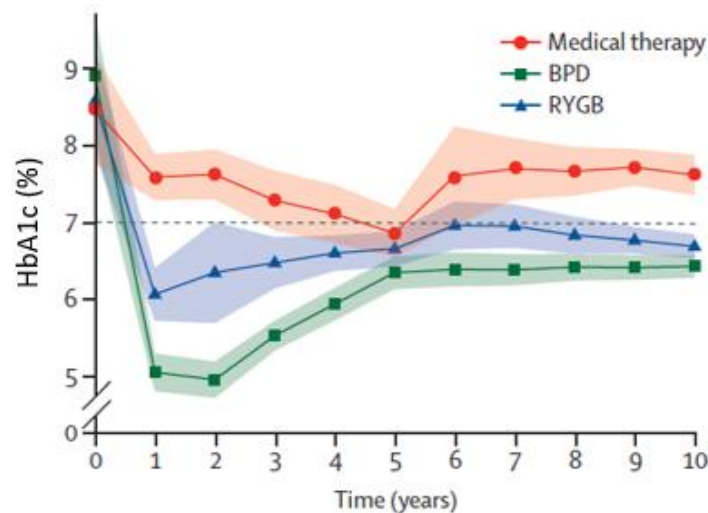


Figure 28: Improvement of glycaemic control following medical therapy, biliopancreatic diversion (BPD) and Roux-en-Y Gastric Bypass (RYGB). Adapted from (Mingrone et al., 2021).

Time course of glycaemic control expressed as glycated haemoglobin (%). The dotted line indicates the target concentration of 7.0% considered to be adequate glycaemic control and the shaded area represents the SD.

Higher rates of type 2 diabetes remission following RYGB were confirmed at 1, 3, and 5 years in a recent meta-analysis that was conducted on 7 randomized controlled trials and included 477 patients who received either RYGB surgery or medical therapy (Cui et al., 2021).

Some meta-analyzed comparative studies between different treatments revealed that RYGB had a better impact on type 2 diabetes remission than SG (Fatima et al., 2022; Hayoz et al., 2018). According to a meta-analysis comparing RYGB and BPD, BPD tends to result in greater diabetes resolution than RYGB (Hedberg et al., 2014).

3.4 Mechanisms involved in postprandial glucose response improvement

The improvement of postprandial glucose response following metabolic surgery remains incompletely unknown but seems to involve a large range of mechanisms, dependent or independent of weight loss, and involving intestinal rearrangement (Laferrère and Pattou, 2018) (**Figure 29**).

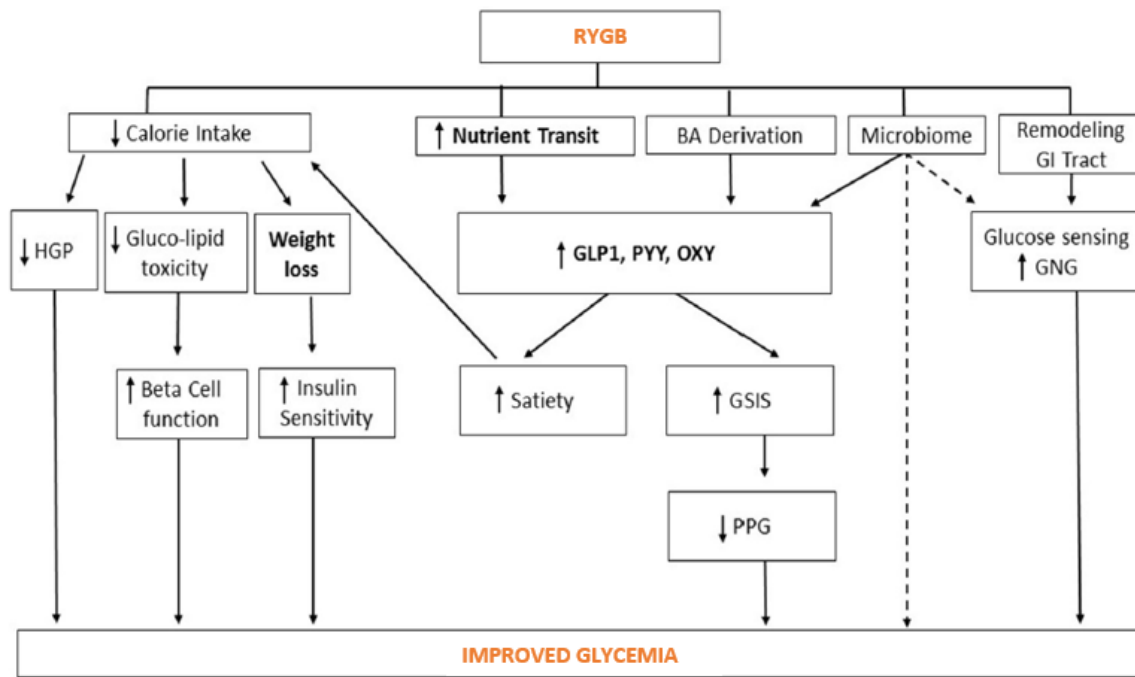


Figure 29: Mechanistic model of improved glycemia after RYGB. RYGB improves glucose metabolism via weight loss, and via weight-independent mechanisms, including stimulation of gut peptides, alteration of bile acids enterohepatic cycle, remodeling of the gastrointestinal track, and alteration of the microbiome. Adapted from (Laferrère and Pattou, 2018).

Solid lines: evidence-based mechanisms; dashed lines: possible mechanisms. RYGB, Roux-en-Y gastric bypass surgery; HGP, hepatic glucose production; BA derivation, bile acids derivation; GI, gastro intestinal; GNG, gluconeogenesis; GLP-1, glucagon-like-peptide 1; PYY, peptide YY; OXY, oxyntomodulin; GSIS, glucose-stimulated insulin secretion; PPG, post-prandial glucose.

Clearly, caloric restriction is crucial for enhancing glucose homeostasis. Following bariatric surgery, limiting food intake reduces the gluco- and lipotoxicity that had previously resulted from nutrient overconsumption (Livingstone et al., 2022). As a result, there is a decrease in inflammation, visceral fat mass, and ectopic deposits, which enhances insulin sensitivity (Flynn et al., 2022). The reduction in stomach volume (the gastric pouch), along with hormonal components that control satiety and insulin secretion, is what causes the caloric restriction. After SG and RYGB, there is a reduced retention of the food in the gastric pouch, resulting in accelerated gastric emptying (Garay et al., 2018; Svane et al., 2019). As a result, the nutrients enter the intestinal lumen more quickly, causing the release of gastrointestinal hormones like GLP-1, cholecystokinin (CCK), peptide YY (PYY), and oxyntomodulin. The key role of these hormones in the central nervous system and specifically in the regulation of satiety has been clearly demonstrated (Steinert et al., 2017), which could explain the decrease of food intake following bariatric surgery.

The increased release of GLP-1 after a meal after SG or RYGB stimulates beta cell insulin secretion in addition to postprandial regulation of satiety. However, beta cell function after RYGB is only minimally improved, especially if beta cell function is severely impacted in the type 2 diabetes phenotype (Dutia

et al., 2014). The increased postprandial insulin secretion after metabolic surgery would seem to depend more on the enteric stimulation than a real improvement of beta cell sensitivity to glucose (Laferrère and Pattou, 2018).

Another suggested mechanism for improving glycemic control is a change in bile acid metabolism. The liver produces bile acids, which are then stored in the gallbladder and released in the duodenum after meals (Di Ciaula et al., 2017). The mix of bile acids with pancreatic exocrine secretion and nutrients from the stomach allows the intestinal absorption of glucose and lipids, mechanism that occurs in the common limb for subjects operated from RYGB surgery (Albaugh et al., 2017). In addition to playing a critical role in lipid absorption, bile acids also function as signaling molecules that control inflammation and metabolism (Oscar Chávez-Talavera et al., 2017; Trabelsi et al., 2017). They bind to two different types of receptors, the nuclear receptor farnesoid X receptor (FXR) and the Takeda-G-protein-membrane receptor-5 (TGR5), which are located in pleiotropic organs involved in glucose homeostasis. While activation of TGR5 on the L-cell stimulates GLP-1 release, intestinal-specific activation of FXR reduces insulin resistance, lipid levels, inflammation, and atherosclerosis (Mazuy et al., 2015). Increased postprandial GLP-1, better glucose tolerance, and weight loss have all been linked to increased circulating levels of bile acids after bariatric surgery. These high levels of circulating bile acids could be explained by an increase in hepatic synthesis, intestinal reabsorption, or decreased hepatic uptake (O. Chávez-Talavera et al., 2017) and could contribute to the increased GLP-1 secretion and decreased insulin resistance observed after surgery.

Additionally, a reshaping of the microbiota in terms of diversity and function is a suggested mechanism for improving glucose homeostasis following bariatric surgery. Modifications to glucose transport and sensing, GLP-1 release, short-chain fatty acid absorption, lipogenesis, dietary intake, energy expenditure, and bile acid metabolism are some of the suggested mechanisms (Anhê et al., 2023; Bauer et al., 2018; Coimbra et al., 2022).

3.5 Alteration of intestinal glucose absorption pattern after metabolic surgery

Beyond the intestinal endocrine functions and their consequences on insulin sensitivity and secretion, modification in intestinal glucose absorption and metabolism seems to also play a key role in the postprandial glucose response improvement following metabolic surgery (**Figure 30**).

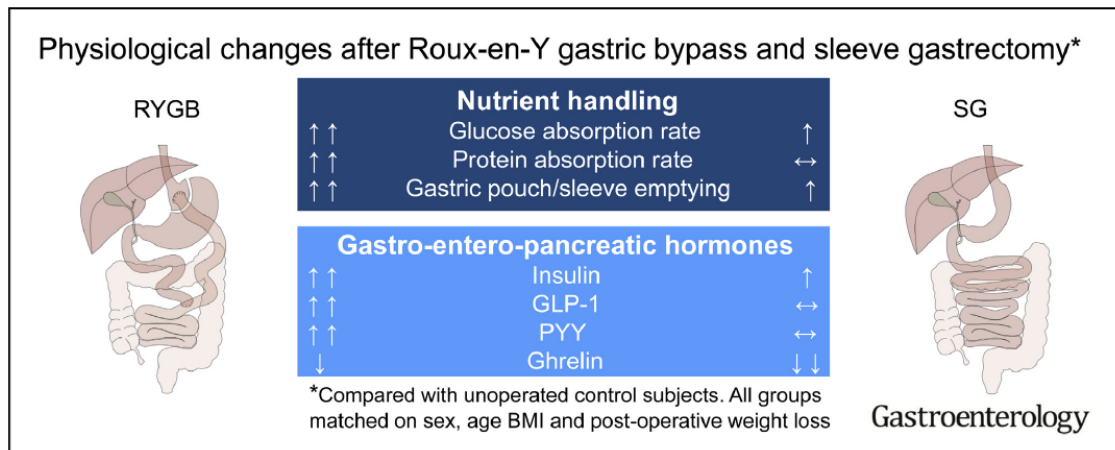


Figure 30: Physiological changes after Roux-en-Y gastric bypass and sleeve gastrectomy (Svane et al., 2019)

3.5.1 Acceleration of gastric emptying

Sleeve Gastrectomy (SG) and Roux-en-Y Gastric Bypass (RYGB) are the two most practiced interventions of bariatric surgery. Both includes redesigns in the gastrointestinal tract, via a removal of 80 % of the stomach for SG, and via the elaboration of a small gastric pouch, associated with the exclusion of the duodenum and the proximal jejunum for the RYGB.

Due to the intervention on the stomach, the gastric retention is strongly suppressed, leading to a clearly highlighted acceleration of the rate of gastric emptying for both SG (Chambers et al., 2014; Melissas et al., 2013; Svane et al., 2019; Vigneshwaran et al., 2016a) and RYGB surgeries (Camastra et al., 2013; Svane et al., 2019; Wang et al., 2012).

The rapid gastric emptying and intestinal transit induced by SG and RYGB was proposed as a major determinant of changes in glucose absorption, incretin release and action, and postprandial glucose response (Laferrère, 2011; Nguyen et al., 2014a). Incretin levels are drastically increased after surgery. The postprandial incretin effect on insulin secretion, blunted in diabetes, improves rapidly after the surgery, with a significant decrease in postprandial glucose levels. The favorable metabolic changes after RYGB are in part GLP-1 dependent because the insulin release and the postprandial glucose response improvement were blocked by the administration of a GLP-1 antagonist (Kindel et al., 2009). The rapid gastric emptying induced by the surgery is thus the main determinant of incretin release since limiting intestinal glucose delivery to the physiological value of 4 kcal/min after RYGB prevented the important release of incretins, the enhancement of insulin release and the improvement of postprandial glucose response (Nguyen et al., 2014a).

The velocity of gastric emptying represents a relevant therapeutic target for postprandial glucose excursions management: if dietary and pharmacological approaches focus on slowing it to decrease the glycemic excursions, the surgical strategy, in contrast, leads to an acceleration of the delivery of

the chyme into the intestine, resulting in a particularly efficient effect on postprandial glucose response improvement.

3.5.2 Bypass surgeries slow the digestion of carbohydrates

Contrary to the sleeve gastrectomy, the bypass procedures involved a redesign of the intestinal tract that affects its physiology. A study in Goto-Kakizaki rats revealed the key role of the duodeno-jejunal bypass (DJB) on the improvement of postprandial glucose response, independently of gastric emptying, food intake, and body weight (Rubino et al., 2006).

The exclusion of the proximal intestine clearly affects the breakdown of carbohydrates into glucose and consequently delays the digestion of carbohydrates since after RYGB, pancreatic α -amylase could act on starch only distally, in the common limb. It is also suggested that this mechanism participate to the enhancement of the GLP-1 release, classically observed (Martinussen et al., 2019). However, no real carbohydrate malabsorption seems to occur after RYGB despite the delay of digestion (Wang et al., 2012).

Consequently, the exclusion of the proximal intestine set up in bypass surgeries can be viewed as producing the same effect on the intestinal availability of glucose as the ingestion of slowly digestible starch.

3.5.3 Gastric bypass decreases overall intestinal glucose absorption

Studies performed in humans with glucose labeled OGTT have shown a clear acceleration of intestinal glucose absorption after RYGB (Bradley et al., 2012; Camastra et al., 2013; Magkos et al., 2016; Svane et al., 2019). A significant 60-min peak of exogenous glucose appearance, which quickly returns to baseline, is typically seen and is associated with a similar postprandial glucose and insulin response. The amount of glucose absorbed during the first hour following ingestion has thus been shown increased by 20 % in operated patients compared to non-operated (Camastra et al., 2022; Svane et al., 2019). This modification was observed in both short-term (16 weeks) (Bradley et al., 2012) and long-term studies (12 months) (Camastra et al., 2013).

Concerning the total amount of glucose absorbed, only a slight reduction (about 5 %) of the total exogenous glucose appearance after meal ingestion has been quantify in some studies after RYGB compared to the pre-surgery state (Camastra et al., 2013; Magkos et al., 2016). According to the authors, the mechanism allowing a significant improvement in postprandial glucose response after metabolic surgery seems to involve more the drastic release of intestinal hormones allowed by the accelerated gastric emptying than a significant decrease in total glucose absorption. In this line, the slight reduction of the total amount of glucose absorbed observed in these studies would thus have a minor contribution to the postprandial glycemic control improvement compared to the other

physiological mechanisms. However, the design of these studies does not take in consideration the considerably altered rate of digestion after RYGB since OGTT, in which glucose is not digested but directly absorbed, is not a physiological meal.

In fact, bypass surgeries seem to decrease the total amount of glucose absorbed during a meal, by influencing both the rate of digestion and also intestinal glucose transport.

A preclinical study in rats has shown that duodenal exclusion significantly influences both intestinal structure and glucose transport function, with glucose absorptive capacity reduced (by 68 %) after RYGB (Stearns et al., 2009). Another investigation using obese Zucker rats showed a reduction in portal glucose levels after RYGB during an OGTT or directly after glucose intra-duodenal administration (Pal et al., 2019).

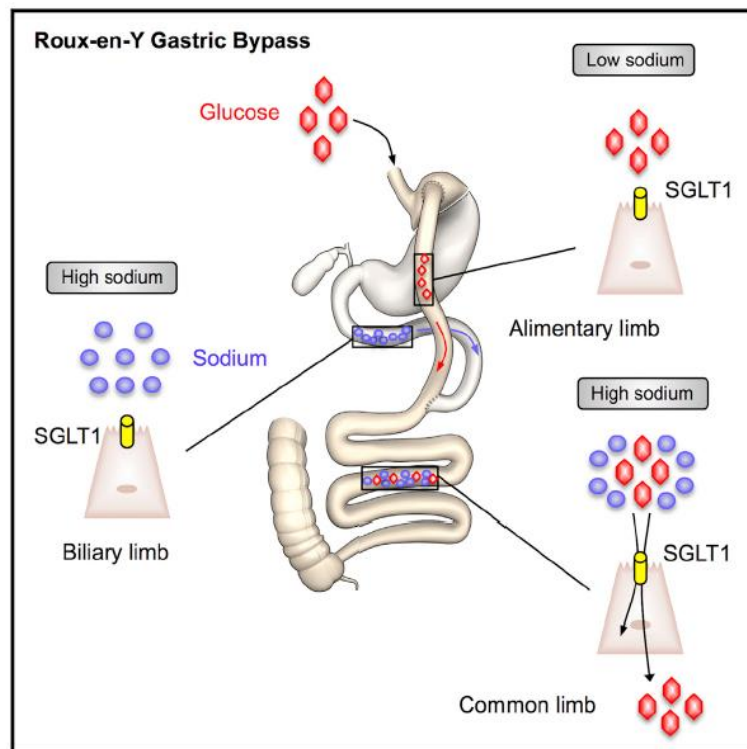


Figure 31: Bile Diversion in Roux-en-Y Gastric Bypass Modulates Sodium-Dependent Glucose Intestinal Uptake (Baud et al., 2016)

In the same line, a study conducted by our team in healthy minipigs showed that bile diversion caused by RYGB modulates intestinal glucose uptake in the small intestine (Baud et al., 2016). In this study, glucose was only absorbed in the common limb, whereas sodium-glucose co-transport did not take place in the bile-deprived alimentary limb. The addition of bile in the alimentary limb, however, restored intestinal glucose uptake. Since glucose can only be efficiently absorbed in the presence of bile (which provides sodium), and since the common limb of the intestine measuring approximately

300–400 cm instead of the entire 700 cm length of a normal non-operated intestine, the fraction of the intestine that can efficiently absorb glucose is significantly decreased after gastric bypass (**Figure 31**).

In this perspective, more recent studies (Anhê et al., 2023; Meng et al., 2022) support a decrease of intestinal glucose absorption following RYGB, in particular by a inhibition of SGLT1.

3.5.4 Implication of the number and functionality of SGLT1 after gastric bypass

If overall intestinal glucose absorption is decreased after RYGB, participating to the improvement of postprandial glucose response, it still remains unclear whether the level of expression and functionality of SGLT1 is involved.

Lower intestinal glucose absorption observed after RYGB seems effectively to be SGLT1-mediated (Anhê et al., 2023) and SGLT1 and GLUT2 levels have been shown decreased in the alimentary and the common limb (Meng et al., 2022). Additionally, a study performed in a mouse model of duodenojejunal bypass showed a decrease in SGLT1 expression, associated with an electrogenic reduction of intestinal glucose absorption (Yan et al., 2013).

On the contrary, a study performed in a type 2 diabetes rat model of ileal interposition showed a weight independent improvement of glucose tolerance and insulin sensitivity despite a 2-fold increased of SGLT1-mediated glucose uptake, suggesting that the improvement of glycemic control after bariatric surgery does not require decreased intestinal glucose absorption. An increased length of villi, hyperplasia of the epithelial layer and increased number of L-cells was also noticed (Jurowich et al., 2015).

Hypertrophy of the gut mucosa was demonstrated in other rat studies, particularly in the common and alimentary limbs (Cavin et al., 2016; Mumphrey et al., 2015). This hypertrophy was associated with a proliferation of the crypt cells (Le Roux et al., 2010) and an increase in the number and size of villi (Stearns et al., 2009), which was not observed after SG (Mumphrey et al., 2015). Mucosa hyperplasia has also been found in humans (Franquet et al., 2019). Additionally to hyperplasia, an increase in the expression of glucose transporters (Cavin et al., 2016; Mumphrey et al., 2015; Nguyen et al., 2014b), as well as of the genes and proteins involved in glucose metabolism (Saeidi et al., 2013) was also noticed. As shown in rats (Cavin et al., 2016) and in patients (Cavin et al., 2016; Franquet et al., 2019), these changes were linked to an increased glucose uptake in the alimentary limb. However, rather than an increase in intestinal glucose absorption, the increase in glucose uptake by the enterocytes in the alimentary limb appears to be the result of an adaptation to meet the increased bioenergetic demands caused by hyperplasia in response to exposure to non-digested nutrients (Saeidi et al., 2013).

Increased intestinal glucose uptake in the alimentary limb would translate into increased enterocyte glucose disposal.

In conclusion, glucose transport across the enterocyte barrier appears to be reduced after RYGB. Bypassing the proximal small intestine may deprive the alimentary limb of bile, which would reduce the efficiency of the absorption process efficiency. After RYGB, all limbs exhibited mucosa hyperplasia, which appears to be a compensatory mechanism in response to a reduction in nutrient digestibility and leads to a higher relative glucose uptake by the enterocytes in order to meet the rise in energetic demands brought on by the hyperproliferation. The improvement in glycemic control following RYGB would be in part caused by the quantitative reduction of glucose absorption by bile deprivation coupled with an increase in glucose disposal by the enterocyte.

3.6 Influence of bypass techniques on the improvement of postprandial glucose response

All bypass procedures improve glucose homeostasis, but not all of them do so as effectively. According to Laferrère and Pattou, BPD improves postprandial glucose response more than RYGB (Laferrère and Pattou, 2019). This improvement seems to be due to an increase in insulin sensitivity but also to a decrease of intestinal glucose absorption and plasma glucose excursion (Harris et al., 2019). Additionally, the technique of OAGB would be linked to higher incidences of side effects like diarrhea, steatorrhea, and nutritional adverse events, suggesting a higher malabsorptive effect (Robert et al., 2019; Ruiz-Tovar et al., 2019). These findings suggest that the nature of the redesign of the gastrointestinal tract would influence the subsequent intestinal glucose absorption.

The modification of the postprandial glycemic response seems to be due to the length of the respective limbs (Laferrère and Pattou, 2019). The long-term results on improvement of metabolic parameters after gastric bypass with a long bilio-pancreatic limb (200 cm) and a short alimentary limb (60 centimeters) versus a long alimentary limb (150 cm) and a short bilio-pancreatic limb (60 cm) were evaluated. Better weight loss was possible with a gastric bypass with a long bilio-pancreatic limb compared to one with a long alimentary limb. However, no difference was observed on postprandial glycemic excursions between these two techniques (Nergaard et al., 2014).

Additionally, the length of the common limb seems to be particularly implicated in postprandial glucose excursions. Because the common limb in BPD-DS is only 50 cm long as opposed to 300–400 cm in RYGB, the efficiency of the intestinal absorption in BPD-DS is significantly reduced when compared to RYGB. As a result, the length of the common limb is inversely related to the distinct impact of gastrointestinal diversion on postprandial glucose excursion (Laferrère and Pattou, 2019). This is why interventions with a shorter common limb like BPD-DS (Harris et al., 2019; Mingrone et al., 2015), long-

limb RYGB (Risstad et al., 2016) or OAGB (Robert et al., 2019) would have an increased effect on glucose metabolism than classical RYGB, explained Laferrère and Pattou.

To resume, all of these findings suggest that after gastric bypass, intestinal glucose absorption decreased globally. This decrease would be one of the main contributors to postprandial glycemic control improvement since the longer the excluded intestine, the greater the remission. The main current issues in bariatric surgery consist in developing two techniques of bypass, or medical devices of gastroenteroanastomosis aiming at mimicking gastric bypass (Caiazzo et al., 2017), to achieve the improvement of postprandial glucose response in decreasing the incidence of complications.

IV. Conclusion

The variability of postprandial glucose response has been now well described in healthy individual and a lot of genetic or environmental determinants are responsible for this variability. Lots of research is now focused on the understanding of interindividual variability in nutrition-related issues and on the development of tools to achieve precision nutrition for the prevention and management of metabolic diseases (Berry et al., 2020; Zeevi et al., 2015).

Intestinal glucose absorption allows the providing of exogenous glucose into the blood system and contributes to the interindividual variability of postprandial glucose response, in healthy individual and those with impaired glucose tolerance.

Gastric emptying, nature and context of the diet, as for as genetics, are as many determinants of postprandial glucose response. Every alteration of these determinants leads to modification of intestinal glucose absorption and finally postprandial glucose response.

Intestinal glucose absorption seems to correlate with postprandial glucose response and to be involved in type 2 diabetes pathophysiology. Moreover, the therapeutic approaches aiming at blunting intestinal glucose absorption, seems to be particularly relevant to manage type 2 diabetes. In particular, a decrease in intestinal glucose absorption seems to represent one of the main mechanisms leading to postprandial glycemic control improvement following bypass surgeries.

The following parts of this work constitute experimental approaches to better understand the contribution of intestinal glucose absorption on postprandial glucose response, particularly through the validation of D-Xylose test, as a new method of in vivo intestinal glucose absorption measurement.

Part 2

Metabolic Syndrome and Early Signs of Impaired Glucose Tolerance in a Minipig Model of Glucose and Lipid Overabsorption

I. Introduction

The impact of various diabetogenic interventions on minipigs was the main topic of this second section. The goal of this project was to develop a minipig model of type 2 diabetes using a combination of current methodologies or cutting-edge techniques. This model would be especially useful for advancing our understanding of how intestinal glucose absorption affects postprandial glucose response, type 2 diabetes pathophysiology, as well as changes in intestinal glucose absorption pattern after bariatric surgery. It has never been done before and it continues to be difficult to induce type 2 diabetes in pigs in accordance with the World Health Organization's definition (World Health Organization and International Diabetes Federation, 2006).

1. The minipig: a preclinical model with a high translational value for metabolism research

Due to its societal acceptability as an alternative to non-human primates and dogs, the pig, also known as *Sus scrofa domesticus*, is a large mammal used in biomedical research (1 % of the all species). Because it shares many anatomical and physiological traits with humans, the pig, a member of the Suidae family, has a particularly high translational value (Kleinert et al., 2018). The cardiovascular, urinary, integumentary, and digestive systems are among the cited systems for which the pig is especially well-suited (Swindle et al., 2012). Pigs are also one of the most common species used in preclinical toxicological testing (Bode et al., 2010; Helke and Swindle, 2013).

The small size of rodents and rabbits is advantageous in terms of maintenance costs but also restrictive when it comes to collecting biomaterial samples (Renner et al., 2016). Minipigs, such as the Göttingen or Yucatan, which were bred specifically for their small size, have the unique ability to weigh up to 80 kg at maturity, whereas domestic pigs raised for human consumption can reach more than 300 kg at maturity (**Figure 32**), making them very difficult to handle and house. Minipigs make it possible to create adult models that are the same size and have the same anatomy as humans, whereas a domestic pig of these proportions would be a juvenile (Bollen and Ellegaard, 1997; Panepinto et al., 1982). For this reason, the size and anatomy of minipigs frequently suggest the direct translation of preclinical studies to clinical application in humans of medical devices like bioartificial pancreas (Ludwig et al., 2012), surgical techniques like bariatric surgery (Verhaeghe et al., 2014), central catheter implantation, or imaging techniques (Ochoa et al., 2014).

Pigs are social animals as well. Minipigs are simple to handle, train, and evaluate in terms of behavior and welfare (Royal et al., 2013).

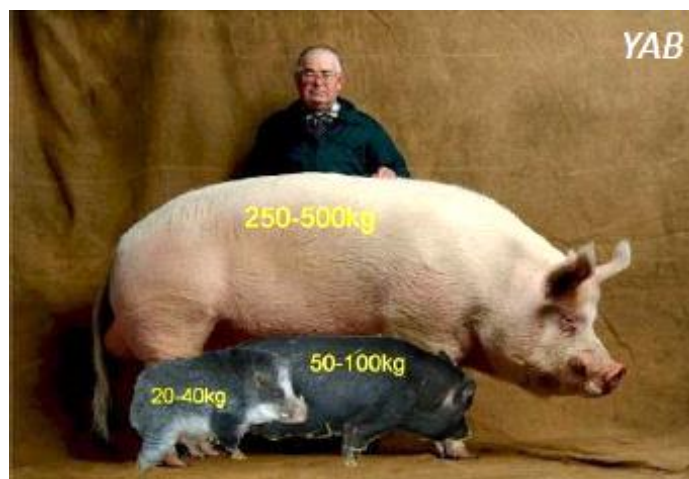


Figure 32: Comparison of the size and weight of a micropig, a minipig, a domestic pig and a human. Adapted from a picture of Yann Arthus Bertrand.

In studies examining metabolism, the pig has been used and described frequently (Kleinert et al., 2018; Koopmans and Schuurman, 2015; Litten-Brown et al., 2010). Pigs are omnivorous (non-rodents), in contrast to rats and mice, and their diet is primarily composed of carbohydrates (60 %). Even though erythrocytes are not permeable to glycosylated compounds (the HbA_{1c} is therefore not a relevant marker) (Higgins et al., 1982), fasting blood glucose, insulin and C-peptide levels, and postprandial glycemic response are similar to those in humans (Larsen and Rolin, 2004). As for humans, insulin sensitivity decreases with age, and females are naturally more insulin resistant than males (Larsen et al., 2001). However, pigs have better oral glucose tolerance and glucose disposal than humans (Larsen and Rolin, 2004). Pigs share similarities with humans in terms of their propensity for obesity, sedentary lifestyle, and eating habits (Val-Laillet, 2019), as well as the potential for visceral adiposity genesis and ectopic triglyceride deposition (Al-Mashhadi et al., 2018). Pigs have a similar plasma concentration of total cholesterol, LDL, HDL, and triglycerides to humans, as well as signs of atherosclerosis and NASH induction (Al-Mashhadi et al., 2018; Dyson et al., 2006; Uceda et al., 2020).

However, there are some anatomical differences in the pig pancreas (**Figure 33**), including the presence of a connecting lobe (Winslow pancreas) that connects the head (duodenal lobe) to the tail (splenic lobe) and is situated beneath the portal vein (Ferrer et al., 2008). Beta cells are located more radially in the architecture of islets compared to that of humans (Cabrera et al., 2006; Steiner et al., 2010). Although the pig pancreas is not naturally amyloid-deposit-free, it is still sensitive to oxidative stress (Betsholtz et al., 1989). Additionally, the sequence of the insulin in pigs and humans only differs by one amino acid (Larsen and Rolin, 2004). Although the liver functions similarly to that of humans, it produces more glucose during fasting (4 mg/kg/min as opposed to 2 mg/kg/min) (DeFronzo et al., 1983; Müller et al., 1983). The anatomy, physiology, and microbiota diversity of the intestine are

comparable to those of humans, and it also absorbs glucose with the same sensitivity. The length of the small intestine in the pig is higher than in humans (11 meters compared to 7) (Gonzalez et al., 2015; Halaihel et al., 1999; Huntley and Patience, 2018a).

All these characteristics make the minipig particularly suitable for studies in metabolic research.

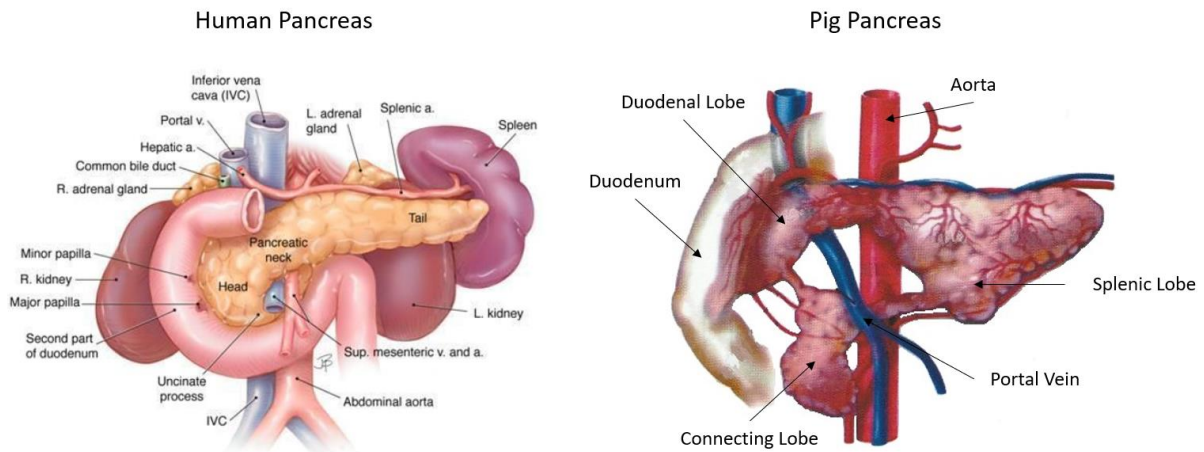


Figure 33: Anatomical variations between human and minipig pancreas. Adapted from (Longnecker, 2021) and (Ferrer et al., 2008).

2. Diabetogenic interventions in pigs: existing approaches and limits

If the pig is a preclinical model that is particularly suitable for studies in metabolic research, then the induction of type 2 diabetes itself is the main problem of this model. In pigs, type 2 diabetes does not occur naturally. Additionally, the pig was chosen for its capacity to store energy and has been dedicated to human consumption since its domestication (which began in - 9 000 years). As a result, this species has evolved in an environment that is obesogenic and diabetogenic, favoring the emergence of metabolic diseases. Since these illnesses also affect the ability of a subject to reproduce, only animals that can withstand diabetes have been selected. Due to this, modern commercial pigs raised for meat production are likely shielded from the negative effects of a "diabetogenic" environment (Gerstein, 2006).

2.1 Different strains of minipigs

Minipigs were chosen for their small size rather than for human consumption; as a result, some strains, like the Göttingen, Ossabaw, or Yucatan minipigs, which are the most widely used types, appear to be more susceptible to metabolic disorders than commercial pigs.

As a result of cross-breeding between Vietnamese pigs, Hormel and Minesota minipigs, and German Landrace, Göttingen minipigs were created in 1962 at the institute of Animal Breeding and Genetics of the University of Göttingen. The parameters of lipid and glucose metabolism were examined and found

to be similar to those in humans. It was hypothesized that some animals of the Göttingen strain might be more at risk to develop abnormal glucose tolerance and metabolic syndrome (Larsen et al., 2001) because they are very similar to humans in terms of the physiology of insulin secretion (M. Larsen et al., 2002; Larsen and Rolin, 2004).

According to several studies (Dyson et al., 2006; Gutierrez et al., 2015; Sturek et al., 2007), Ossabaw minipigs are the strain that is most susceptible to the metabolic syndrome. Due to the intense selection pressure put on it by the dry climate of the Ossabaw island, this strain originated from the "Ossabaw Georgia island" and developed a "thrifty genotype" that allowed it to store energy from low-nutritive substrates with ease. Thus, Ossabaw minipigs are regarded as a natural model of metabolic syndrome and type 2 diabetes, similar to populations that are currently predisposed to these diseases naturally (DeFronzo et al., 2015).

Originally from the Mexican Yucatan peninsula (Panepinto et al., 1978), Yucatan minipigs have been found to be particularly susceptible to obesity (Low Wang et al., 2013), atherosclerosis, hypercholesterolemia (Al-Mashhadi et al., 2018), and glucose intolerance (McKnight et al., 2012).

The Chinese Bama miniature pig was created more recently as a result of long-term inbred selection and demonstrated specific propensities for impaired glucose tolerance (Zhang et al., 2019; Zou et al., 2019).

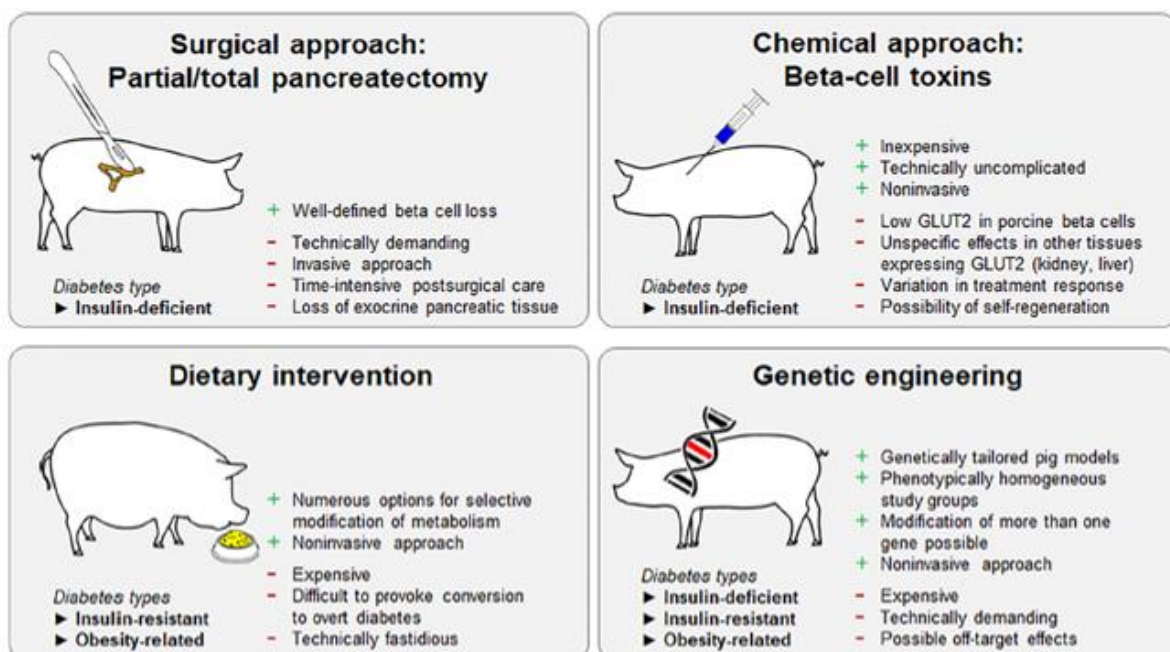


Figure 34: Existing strategies previously attempted to elaborate a minipig with type 2 diabetes. Adapted from (Renner et al., 2020).

There have been numerous attempts in the past to create a minipig model of type 2 diabetes from these strains (**Figure 34**), considering that minipigs have phenotypes that are better adapted to the development of metabolic diseases than commercial pigs.

2.2 Surgical approaches: partial or total pancreatectomy

One of the experimental methods for bringing on diabetes involved performing a pancreatectomy. The total pancreatectomy makes it simple and quick to achieve fasting hyperglycemia, but it has poor medium-term viability (Heinke et al., 2016). Additionally, partial pancreatectomies were set up. The extent of the excision determines how severe the induced phenotype will be; a 40%-pancreatectomy has little effect, whereas an 80%-excision permits significant changes but is technically more challenging to perform and necessitates lengthy postoperative care (Litten-Brown et al., 2010).

Thus, surgical techniques enable the development of insulin-deficient diabetes with a clearly defined loss of exocrine pancreatic tissue, though they are not entirely suited to a type 2 diabetes caused by obesity (Renner et al., 2020).

2.3 Chemical approaches targeting beta cells

The induction of diabetes chemically was also investigated. Streptozotocin (STZ, 2-deoxy-2-(3-methyl-3-nitrosourea)-1-D-glucopyranose) is the most frequently used cytotoxic glucose analogue that enters cells via GLUT2 transporters. Nitric oxide and free radicals are produced as a result of DNA damage caused by STZ, which then causes necrosis and beta cell death (Lenzen, 2008). A single high-dose injection of 150 mg/kg or multiple low-dose injections of 50 mg/kg were two different STZ injection protocols that were used (Dufrane et al., 2006; Gerrity et al., 2001). When used at high doses, STZ causes a severe form of diabetes with a high mortality risk due to hypoglycemia after acute hyperinsulinemia, which leads to beta cell death. To prevent the beta cells from suffering excessive damage, nicotinamide was also used before the injection of STZ (M. O. Larsen et al., 2002; Lee et al., 2012). In these studies, the use of nicotinamide provided a pig model with fasting and postprandial hyperglycemia associated with maintained insulin secretion and beta cell mass.

The main drawback of this approach is the lack of beta cell specificity of STZ since GLUT2 expression is required for STZ efficacy. A significant hepato- and nephrotoxicity is seen after STZ injection at 150 mg/kg because GLUT2 is actually expressed in hepatocytes and nephrocytes (Hara et al., 2008). The response after STZ administration also exhibits significant interindividual and interspecies variation, and the sensitivity of beta cells to STZ is correlated with the degree of GLUT2 expression. Accordingly, porcine beta cells have a low level of GLUT2 compared to other species like rats and primates, which accounts for the lack of sensitivity of this species (Dufrane et al., 2006). The existence of a polymorphism of the *tcf7l2* gene, the most important gene of type 2 diabetes susceptibility in

humans, was proposed as an explicative factor of interindividual variation in pigs (Grant, 2019; Tu et al., 2018).

The use of alloxan as a beta cell toxin was also documented. Alloxan and dialuric acid, which are created as a result of its reduction, cause the production of superoxide radicals, which greatly increase the intracellular calcium content and swiftly kill beta cells (Szkudelski, 2001). Alloxan must be administered at high doses (100–175 mg/kg), just like STZ, and the response to chemical induction of diabetes is also extremely heterogeneous (Badin et al., 2018).

In conclusion, using beta cell toxins is a non-expensive, simple, and noninvasive way to treat insulin-deficient diabetes. However, the low expression of GLUT2 in porcine beta cells is generally associated with a high interindividual variation of response. The requirement for high STZ doses results in elevated toxicity for the liver and kidneys due to the lack of specificity of STZ for the pancreas. Additionally, there is only a weak possibility of controlling the exact mass of beta cells damaged, and the probability of self-regeneration cannot be excluded (Renner et al., 2020).

2.4 Dietary interventions

Thanks to non-invasive methods that mimic the "Western lifestyle," dietary approaches offer a variety of opportunities to change the metabolism. The typical diets are usually high in energy and enriched with saturated fat or high glycemic index carbohydrates, like sucrose or fructose (Koopmans and Schuurman, 2015; Renner et al., 2020, 2016). Pigs fed a high-fat, high-sucrose diet for several months exhibited general obesity, insulin resistance, and dyslipidemia (Christoffersen et al., 2013; Johansen et al., 2001; Lim et al., 2018; Liu et al., 2007). Pure cholesterol supplementation makes dyslipidemia worse (Neeb et al., 2010), whereas a high-fat diet defined by choline-deficient amino acids causes NASH to develop (Duvivier et al., 2022; Lützhøft et al., 2022).

However, even in the case of a high-fat, high-fructose, and high-cholesterol feeding for 9 months, dietary interventions alone do not allow the induction of a real type 2 diabetes phenotype with significant fasting hyperglycemia (Panasevich et al., 2018). To emphasize impaired glucose tolerance and produce hyperglycemia, high-energy diets have been combined with chemical therapies that are toxic to beta cells (Larsen et al., 2005; Otis et al., 2003; Schumacher-Petersen et al., 2019; von Wilmsky et al., 2016). Because the use of this combined approach faces the same challenges as those described after using STZ or alloxan alone, the hyperglycemia brought on by this strategy is very variable.

2.5 Genetic engineering

Genetic engineering allows the elaboration of tailored pig models that can be phenotypically homogenous after genetic alteration. One or more genes can also be targeted through genetic

engineering. Thus, altering the genotype is a non-invasive strategy that may result in insulin-deficient, insulin-resistant, or diabetes brought on by obesity (Renner et al., 2020).

Pronuclear DNA microinjection into fertilized oocytes produced the first transgenic pigs (Hammer et al., 1985), but this method was poorly effective and was later replaced by lentiviral vectors (Hofmann et al., 2003). Although very efficient at producing transgenic piglets, lentiviral vectors have some significant drawbacks, including a limited insert size and the potential for independent integration at multiple sites throughout the genome (Jakobsen et al., 2011). Finally, the use of targeted nucleases for genome editing emerged as a significant technological advance in the advancement of pig genetic modification. These techniques allow a specific gene deletion at a desired locus and include the methods of zinc finger nucleases, transcription activator-like effector nucleases, and the CRISPR/Cas9 system (Hai et al., 2014).

Consequently, many genes were targeted. For example: the insulin promoter (INS), leading to a substantial insulin deficiency, associated-hyperglycemia and severe complications (Cho et al., 2018; Renner et al., 2013); the PDX1 promoter, responsible of the identity of beta cells, leading to a pancreas agenesis (Kang et al., 2017); the proprotein convertase subtilisin/kexin type 9 (PCSK9), mainly expressed in the liver and involved in the cholesterol uptake, leading to hypercholesterolemia and other lipid disorders (Al-Mashhadi et al., 2013); the promoters of the low-density lipoprotein receptor (LDLR) (Davis et al., 2014) and of the apolipoprotein C-III (Wei et al., 2012), responsible respectively for LDL uptake and transport in the blood system, leading to mild to severe hypercholesterolemia. Another study created a genetically altered Bama minipig model with a humanized gene that permits the formation of amyloid deposits, whereas amyloid deposition is initially impossible in pigs (Zou et al., 2019). Although the researchers in this study were successful in obtaining fasting hyperglycemia, no information regarding postprandial insulin was provided.

Even though genetic engineering enables the development of customized pig models with metabolic disorders, this method is still costly, technically challenging, and may have unintended side effects (Renner et al., 2020). The genetic approach is better suited to create a monogenic diabetes model than a polygenic type 2 diabetes model with epigenetic components, even if multiple genes can be targeted.

3. Parenteral nutrition as a potential strategy for type 2 diabetes induction?

Nearly half of patients receiving parenteral nutrition after hospitalization have reported having postprandial hyperglycemia (Gosmanov and Umpierrez, 2013). The addition of insulin during parenteral nutrition procedures is recommended for patients who have pre-existing diabetes or metabolic disease-related insulin resistance (McCulloch et al., 2018; Schönenberger et al., 2022). Additionally, patients receiving total parenteral nutrition were found to have higher fasting insulin

levels and insulin resistance (Sun et al., 2018). By altering the gut microbiome, total parenteral nutrition was also demonstrated to be a causal factor in impairments of glucose metabolism. In a study involving 256 participants, parenteral nutrition that constituted more than 80 % of total energy intake resulted in altered microbiota, impaired gut barrier function and mucosal immunity, insulin resistance, and ultimately disorders of glucose metabolism.

Total parenteral nutrition increased random blood glucose levels, hepatic glycogen deposition, and systemic and molecular insulin resistance in rodent models (Sun et al., 2018). In other studies performed in rodents, chronic parenteral infusions of glucose led to metabolic adaptations such as transient hyperglycemia, as observed in humans during parenteral nutrition, and an increase in beta cell function (Alonso et al., 2007; Hoy et al., 2007). This also caused rats to develop skeletal muscle insulin resistance (Hoy et al., 2007). Additionally, alternate cyclic glucose and lipid infusions in rats led to inhibition of insulin synthesis in pancreatic islets (Hagman et al., 2008).

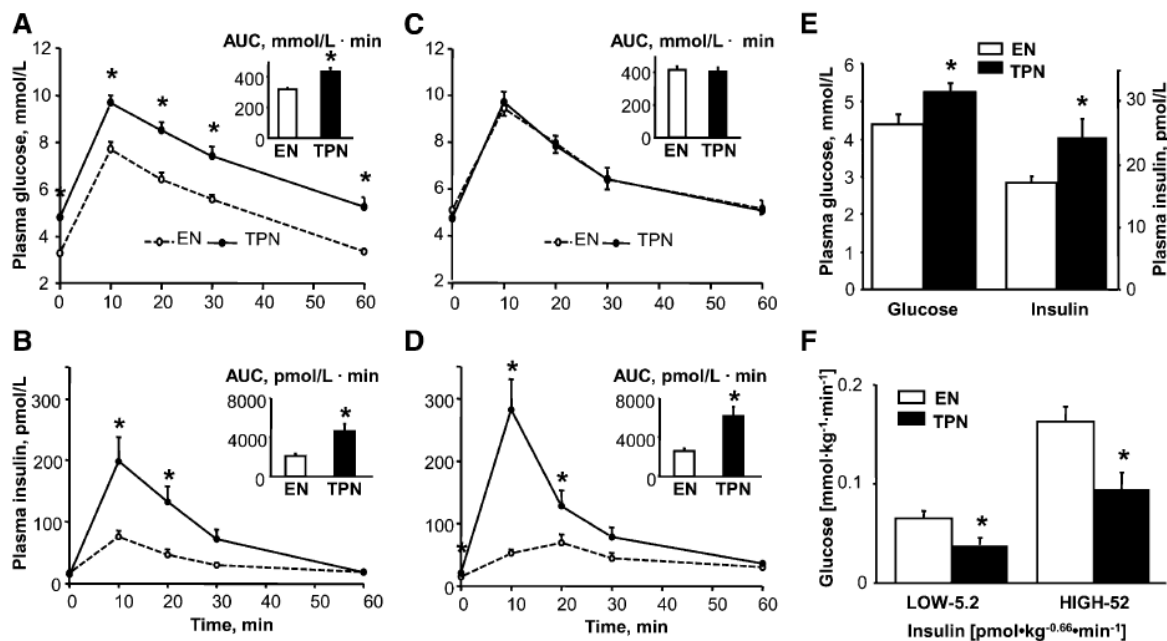


Figure 35: Plasma glucose and insulin concentrations and respective AUC values during IVGTT on d 7 (n = 6) (A, B) and on d 13 (n = 8) (C, D) in TPN and EN pigs. (E) Fasting (12-h) plasma glucose and insulin concentrations in TPN and EN pigs on d 15 (n = 6). (F) Glucose and insulin infusion rates during CLAMP on d 15 in TPN (n = 5) and EN (n = 7) pigs (Stoll et al., 2010).

Results are expressed as mean ± SEM. *p<0.05. TPN = Total Parenteral Nutrition. EN = Enteral Nutrition.

According to Stoll et al., total parenteral nutrition administered to neonatal piglets increased fasting glycemia, insulin resistance, systemic inflammation, and hepatic steatosis in the pig (Stoll et al., 2010) (**Figure 35**). The causal relationship between parenteral nutrition and liver diseases was particularly well described in piglets (Burrin et al., 2020).

Even though parenteral nutrition-related metabolic disorders were amply documented in the literature, this method was not previously thought of as a way to cause the phenotype of type 2 diabetes in pigs. This is why we thought about it as a possible strategy for type 2 diabetes induction.

4. Aim and hypothesis

Because the pig is a species that is particularly resistant to type 2 diabetes, the goal of this experimental part was to cause type 2 diabetes in a minipig model. This model would be especially interesting to better understand how intestinal glucose absorption affects postprandial glycemic response in type 2 diabetes onset and progression, as well as how intestinal glucose absorption patterns change after metabolic surgery.

In order to achieve this, we first identified which minipig variety, between Göttingen and Ossabaw, was especially well suited for this project. To change glucose homeostasis, we also carried out a number of diabetogenic interventions, either individually or in combination.

Some of these interventions were previously described in the literature, such as:

- a subtotal pancreatectomy, in order to decrease the insulin secretion abilities of the pancreas
- a High-Fat, High-Sucrose Diet (HFHSD) for two months, to simulate a diet high in meals with a high Glycemic Index
- as an innovative combination of pre-existing techniques, a subtotal pancreatectomy followed by a 2-month HFHSD, in order to primarily decrease the insulin secretion abilities of the pancreas and then mimic a diet with high Glycemic Index meals for consequently outperforming the regulatory capabilities of the pancreas.

Other interventions were totally innovative, such as:

- long-term intraportal glucose and lipid infusions instead of physiological meals, in order to mimic intestinal glucose and lipid overabsorption
- subtotal pancreatectomy followed by long-term intraportal glucose and lipid infusions instead of physiological meals, in order to primarily decrease the insulin secretion abilities of the pancreas and then mimic intestinal glucose and lipid overabsorption.

The descriptions of the detrimental effects of parenteral nutrition on glucose metabolism in the literature led us to hypothesize that this experimental design might result in the phenotype of type 2 diabetes. Additionally, we designed this model of parenteral nutrition using intraportal glucose and lipid administration in order to best replicate intestinal glucose and lipid overabsorption. Therefore,

we predicted that the organs involved in glucose homeostasis would be particularly harmed by the high gluco- and lipotoxicity caused by these intraportal infusions.

To the best of our knowledge, these methods have never been put to the test on an adult pig model in the literature.

II. Materials and Methods

The Materials and Methods presented hereafter was previously described (Goutchtat et al., 2023). Some precisions were nevertheless added compared to this publication for a better understanding.

1. Ethical statement

The local French Committee of Animal Research and Ethics (CEEA-75, n°#18915), in accordance with European law (2010/63/EU directive), accepted the protocol by approving it in accordance with the widely accepted ARRIVE guidelines. All the procedures were carried out in the agreed-upon (n°D59-35010) Département Hospitalo-Universitaire de Recherche et d'Enseignement (Dhure) in the Faculty of Medicine in Lille, France.

2. Animals and housing

The study included a total of 21 healthy 1-year-old minipigs: 4 Ossabaw minipigs (DTU, Lyngby, Denmark) and 17 Göttingen-like (Pannier, Wylder, France), weighing respectively 48.2 ± 1.9 kg and 31.7 ± 11.0 kg. The variation observed in the body weight between the two strains were probably due to differences in the diet of the animals during their first year of life, that we were not able to control, rather than proper strain differences. Our local minipig strain, called Göttingen-like, was created more than 30 years ago as a consequence of a crossing with the Göttingen strain.

To limit the metabolic differences related to the female hormonal cycle, only males were included. At the start of the protocol, animals were either surgically castrated or delivered castrated in the animal facility.

All animals were housed and enriched in individual boxes in conventional conditions. Water was provided *ad libitum* and 400 g of standard food (Swine Engrais-F S25/T, Uneal Cooperative) was given twice a day. The composition of the standard diet was detailed in **Table 1**. The light/dark cycle was 12 hours of light and 12 hours of darkness with a temperature between 19 and 24 °C. Pigs benefited from a 15-day acclimatization period.

3. Study design

In this study, we wanted to create a preclinical pig model of type 2 diabetes that corresponds to the WHO definition (World Health Organization and International Diabetes Federation, 2006). This led to the combination of a subtotal pancreatectomy, a surgical method of insulin deprivation, with methods of energetic overload, via oral or intraportal administration.

In order to determine which strain of minipigs was most suited for our strategy, we first assessed how both the Göttingen-like strain (n=3) and the Ossabaw one (n=4) responded to a 2-month high-fat, high-sucrose diet (HFHSD). We decided thereafter to discard the Ossabaw strain because Göttingen-like showed a phenotype closer to our expectations.

Following this choice, we combined a subtotal pancreatectomy with 2 months of HFHSD in Göttingen-like minipigs (n=6). Finally, we explored a different strategy by infusing intraportal glucose and lipids for 3 weeks as a parenteral energetic overload, mimicking intestinal glucose and lipid overabsorption, in two groups of Göttingen-like minipigs: in Group 1 (n=4), no subtotal pancreatectomy was initially performed; in Group 2 (n=4), a subtotal pancreatectomy was performed prior to the energetic overload. The impact of the subtotal pancreatectomy on glucose metabolism in the Göttingen-like strain was simultaneously examined (n=10), including the animals subjected to the HFHSD regime following the pancreatectomy (n=6) and those of Group 2 (n=4).

Figure 36 displays the general design of this research.

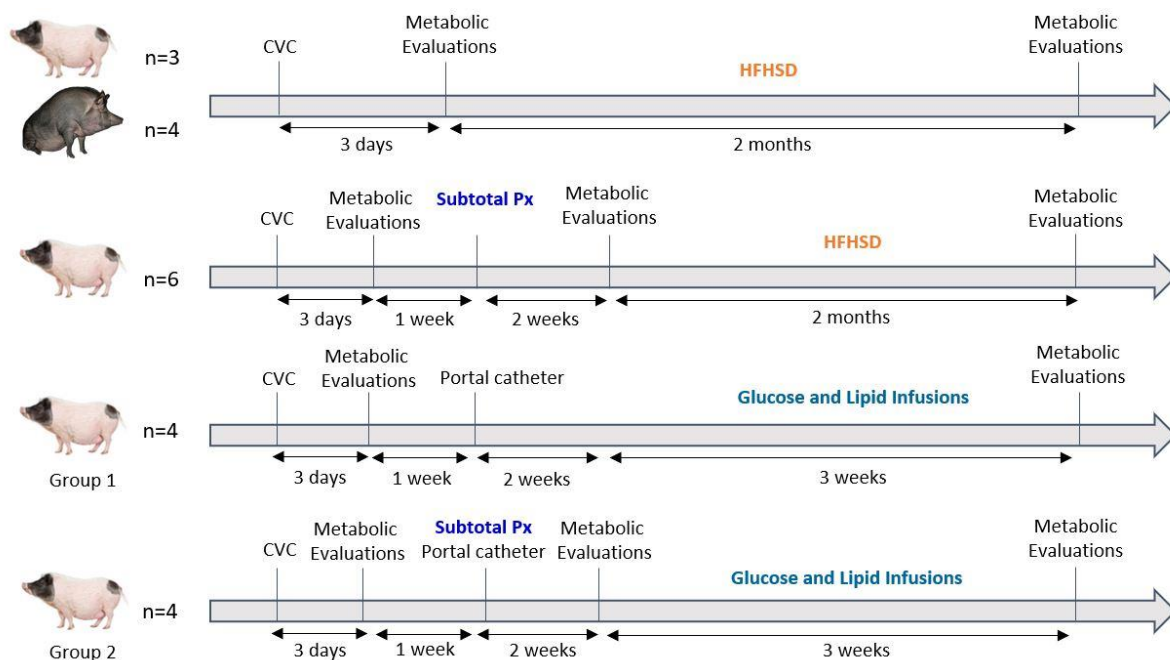


Figure 36: Overall Study Design for each Group of Animals.

CVC = Central Venous Catheter. HFHSD = High Fat High Sucrose Diet. Px = Pancreatectomy. The black minipig represents the Ossabaw strain, while the pink and black ones indicate the Göttingen-like strain. A Mixed Meal Test and an Intravenous Glucose Tolerance Test constitute metabolic assessments. Metabolic tests were performed on all minipigs (n = 10) subjected to the subtotal pancreatectomy 2 weeks after the intervention.

4. Surgical procedures

4.1 Anesthesia and analgesia

Following an overnight fast, all surgical procedures were performed under general anesthesia. Premedication included intramuscular injections of xylazine (3 mg/kg; Sedaxylan®; Dechra Pharmaceutical PLC, France) and ketamine (5 mg/kg; Ketamine 1000®; Virbac, France), followed by isoflurane after endotracheal intubation (0.5 to 2 %; IsoFlo; Zoetis, France). During the laparotomy procedures, animals were ventilated with assistance at 20 mpm or left with spontaneous ventilation in case of surgeries not involving a laparotomy. To ensure analgesia, an intramuscular injection of buprenorphine (15 µg/kg, Bupaq®, Virbac, France) for the insertion of a central venous catheter or a single transdermal application of fentanyl (1.3 mg/kg, Recuvyra®, Lilly-Elanco, France) for laparotomy procedures were used, as previously described (Goutchtat et al., 2021).

4.2 Implantation of a Central Venous Catheter (CVC)

This procedure was performed to allow the collection of large volumes of blood samples during metabolic evaluations.

The external jugular vein was exposed in the neck region after a skin and muscle 5-cm-incision in front of the tip of the scapula. After venotomy, the catheter (Hickman® 9.6F Single-Lumen CV Catheter, Bard Access System, USA) was inserted and linked to the vein with two ligatures (Vicryl® Bobine 2/0, Ethicon, France). The catheter was tunnelized via the subcutaneous tissue from the incision zone to the dorsal area of the neck. Muscular and cutaneous layers were then closed by simple overlock (respectively Polysorb® 2/0, Medtronic, France and Mersilene® 1, Ethicon, France) and its external part fixed on the skin by simple stitches.

This catheter remained throughout the duration of the procedure and was kept operational by administering 5 mL of physiological serum that had been heparinized (1 mL heparin at 5000 UI/mL for 250 mL NaCl 0,9 %) after each usage or every two days if it was not. During longer periods of non-use, catheters were “locked” with a mix solution of 0.5 mL heparin and 4.5 mL of 50-% glucose (G50®, B. Braun, France).

4.3 Subtotal pancreatectomy

By reclining the stomach cranially and the intestinal system caudally, the pancreas was made accessible. From the tail (splenic lobe) to the head (duodenal lobe), the dissection was carried out. In

the retro-portal region, the Winslow pancreas (connecting lobe) was similarly dissected and largely removed. Before section and extraction, ligatures between the splenic and the duodenal lobes as well as at the connecting lobe were tightened. As previously stated (Ferrer et al., 2008), the subtotal pancreatectomy involved removing 75 % of the total organ weight.

4.4 Portal catheter implantation

This procedure was performed to allow long-term glucose and lipid intraportal infusions.

The spleen was removed from the abdominal cavity after median laparotomy of the supra umbilical region, and the splenic vein was dissected on 2 cm. On the left flank, behind the final rib, the catheter (Hickman® 9.6F Single-Lumen CV Catheter, Bard Access System, USA) was tunneled across the abdominal wall. The catheter was placed following the splenic vein venotomy, advanced through the spleno-mesaraic confluence into the portal vein, and secured to the splenic vein with two ligatures. The layers of the peritoneum, muscles and skin were closed by a simple overlock and the external part of the catheter was fixed to the skin on the left flank by simple stitches.

This catheter remained until the end of the intraportal infusions and was kept functional thanks to the same measures as previously described above for the CVC.

4.5 Surgical castration

The surgical castration was performed under general anesthesia during the laparotomy procedure for the animals that were provided non-castrated in our animal facility in order to homogenize all the groups, and to decrease the energetic expenditure related to the synthesis of the reproduction hormones.

Medially between the scrotum and the penile region, cutaneous and subcutaneous tissues were incised after testicles were compressed cranially. Additionally, the tunica vaginalis was cut open to reveal the testis. The cauda epididymis ligament was cut after extraction. Two ligatures were used to ligate the spermatic lead, and it was then sectioned. Simple overlock was used to seal the tunica vaginalis and scrotum.

5. Energetic overload

The energetic overload was performed in two different ways according to groups: via the set up of a high-fat high sucrose diet, as pre-existing diabetogenic approach in pigs, in order to mimic a diet with high Glycemic Index meals; and via intraportal glucose and lipid infusions, as innovative diabetogenic approach, in order to “bypass” the intestine and mimic glucose and lipid overabsorption.

5.1 High-Fat High-Sucrose Diet (HFHSD)

Animals were fed with an HFHSD for two months for the appropriate groups. The Institut National de Recherche pour l'Agriculture, l'Alimentation et l'Environnement (Inrae, France) determined the composition of the food. The quantity of 750 g of HFHSD were administered twice a day and contained 61.7 % of carbohydrates, 23.2 % of fats, and 15.1 % of protein. The composition of the HFHSD was detailed in **Table 1**.

Composition	Standard Diet	HFHS Diet
Wheat	10.00	6.25
Barley	34.00	12.00
Wheat bran	25.00	11.14
Soybean cake	6.00	12.00
Sunflower cake	10.00	8.00
Soybean hulls	12.00	8.86
Cornstarch		6.50
Saccharose		20.00
Calcium carbonate	1.30	1.30
Sodium phosphate	0.60	0.60
Sodium chloride	0.60	0.60
Vitamins and minerals	0.50	0.75
Lard		12.00
Energetic density	12.5 kJ/g	20.9 kJ/g

Table 1: Composition (in %) of the standard diet and the high-fat high-sucrose (HFHS) diet

5.2 Intraportal glucose and lipid infusions

Over the period of three weeks, the intraportal catheter was used to administer lipid and glucose infusions twice daily for two hours, instead of physiological meals. A two-hour gap between the bi-daily infusions was observed.

A mix of 50-% glucose (G50®, B. Braun, France) and lipid solution (Intralipid20®, Fresenius Kabi, France) was administered using infusion pumps (SK 600II®, Mano Medical, France) at respective flow rates of 125 mL/h and 63 mL/h. These flow rates were selected in order to maintain the glycemia of infusions above 500 mg/dL. This threshold of 500 mg/dL was chosen to induce a high glucotoxicity effect. Each infusion was preceded by a 500 mg/kg bolus of 50-% glucose solution to raise blood glucose levels to more than 500 mg/dL within one minute. All the infusions were performed in an awake animal.

Each animal received each day 500 mL of the 50-% glucose solution and 250 mL of the lipid solution, corresponding respectively to 250 g of glucose and 20 g of soybean oil and consequently 4707 kJ (1125 kcal) provided by the 50-%-glucose solution and 837 kJ (200 kcal) provided by the lipid solution. In total, each animal thus received parenterally 5544 kJ (1325 kcal) per day, associated with 1109 kJ

(265 kcal) per day of standard diet during each delivery of infusions. The small quantity (100 g per day) of standard diet was administered to minipigs in order to guarantee their welfare and represented less than 20 % of the total energy intake, as previously reported in studies evaluating the deleterious effect of long-term parental nutrition on metabolism (Wang et al., 2023).

6. Metabolic evaluations

6.1 Mixed Meal Tests (MMT)

After a 12-hour fast, a 20-g solid energy bar (Ovomaltine®, Nestlé, France) and 200 mL of liquid (Fortimel Energy®, Nutricia, France) were mixed and given *via* a nasogastric tube of 16 Fr that had previously been implanted under general anesthesia during the CVC implantation procedure for the first MMT or the day before for the others MMT.

The meal had a 990-kJ (237-kcal) energy density and contained 49 g of total carbohydrates, 13 g of fat, and 15 g of proteins. On EDTA and heparinized tubes, blood samples were obtained before the MMT was administered (t=0 min) and at various time intervals afterwards (t=15, t=30, t=60, t=90, t=120, and t=180 min).

6.2 Intravenous Glucose Tolerance Tests (IVGTT)

Following an overnight fast, a 50-% glucose solution (G50®, B. Braun, France) was intravenously administered into the CVC at a dose of 500 mg/kg. On EDTA tubes, blood samples were taken in the awake animal before (t=0 min) and following the administration of glucose at t=1, t=3, t=5, t=10, t=15, and t=30 minutes.

For each metabolic evaluation, plasma was collected from each tube, centrifuged at 4000 rpm for 10 min at 4 °C, and then stored at -80 °C until analyses.

7. Biological analyses

The amperometric glucose oxidase method was used to measure the level of glucose in blood (glucometer Accu-Chek Performa®, Roche, France, or Nova Biomedical StatStrip Xpress®, DSI, USA). Blood glucose levels were determined instantaneously during each metabolic evaluation.

A DXI Access Immunoassay System (Beckman Coulter) with an assay range between 0.3 and 300 µIU/mL was used to measure the plasma insulin concentrations, as previously mentioned (Cook et al., 2010). Plasma lipid profile (total cholesterol, LDL, HDL and triglycerides) was assessed at the Centre de Biologie-Pathologie of Lille University Hospital, by the group of Patrice Maboudou, using an Abbott Architect C4000® clinical chemistry analyzer.

8. Calculations and statistical analyses

For data analysis and graphical representation, GraphPad Prism v8[®] software was employed. For curves, the results were expressed as mean \pm SEM, and for histograms, as mean \pm SD. Depending on the situation, paired or unpaired Student's t-tests were used to analyze the variables. A Two-Way ANOVA and Sidak post-hoc tests were used to compare blood glucose and plasma insulin levels during the MMT and IVGTT between the different strains of minipigs or between baseline and after diabetogenic interventions. For each comparison of blood glucose or insulin evolution during metabolic test, the effect of time of the metabolic test (called "time") and strain (Göttingen-like or Ossabaw, called "strain") or diabetogenic intervention ("HFHSD", "pancreatectomy", or "infusions") was systematically assessed. The presence of interaction between "time" and "strain" or "time" and "intervention" was also evaluated.

The postprandial glycemic excursion was estimated by the calculation of the incremental area under the curve (iAUC) of glycemia using the trapezoidal method.

The calculation of Insulinogenic Index was performed to evaluate the postprandial early insulin secretion as described (Singh, 2010): $[\text{Plasma Insulin (t = 30)} - \text{Plasma Insulin (t = 0)}] / [\text{Blood Glucose (t = 30)} - \text{Blood Glucose (t = 0)}]$, with plasma insulin in $\mu\text{IU/mL}$ and blood glucose in mg/dL . It corresponds to the ability of the pancreas to release insulin reported to plasma glucose concentration.

The hepatic insulin resistance was evaluated thanks to the Hepatic Insulin Resistance Index (HIRI) calculation as previously described (Abdul-Ghani et al., 2007), by multiplication of the first 30-min area under the curve between glucose and insulin concentration during MMT. The early postprandial area under curve of glucose and insulin directly depends on the suppression of endogenous glucose production by the liver in response to a meal ingestion: the higher the HIRI, the lower the suppression of glucose production and then the higher the hepatic insulin resistance.

The peripheral insulin sensitivity was assessed by the calculation of the Matsuda Index, as previously described (Matsuda and DeFronzo, 1999). The calculation of the Matsuda Index considers fasting glycemia and insulin (markers of central insulin sensitivity) but also the mean of glycemia and the mean of insulinemia during the whole time of the postprandial period (related to peripheral glucose disposal and thus markers of peripheral insulin sensitivity). The Matsuda Index is thus a marker of overall insulin sensitivity.

The Acute Insulin Response (AIR), which describes the initial first phase of insulin production following intravenous glucose stimulation, was computed by subtracting fasting insulin levels from the mean evaluation of plasma insulin levels at 1, 3 and 5 minutes (Hubert et al., 2008, 2005).

III. Results

The Results presented hereafter was previously described (Goutchtat et al., 2023). The figures were arranged differently but are relative to the same results. Some additional calculations were also indicated and the description of the results was reformulated.

1. Choice of the Göttingen-like minipig strain after comparison with Ossabaw

The glucose metabolism of Göttingen-like (GL, n=3) and Ossabaw (O, n=4) minipigs was compared before and after a 2-month High Fat High Sucrose Diet (HFHSD) in order to determine which strain was best suited for our procedure (**Figure 37, 38 and 39**).

Following the regimen, both strains notably gained weight (55.1 ± 4.3 after versus 43.4 ± 6.4 kg before for GL, $p < 0.05$ and 62.8 ± 4.8 after versus 48.2 ± 1.9 kg before for O, $p < 0.01$), corresponding to a weight gain of 26.9 % for GL and 30.3 % for O.

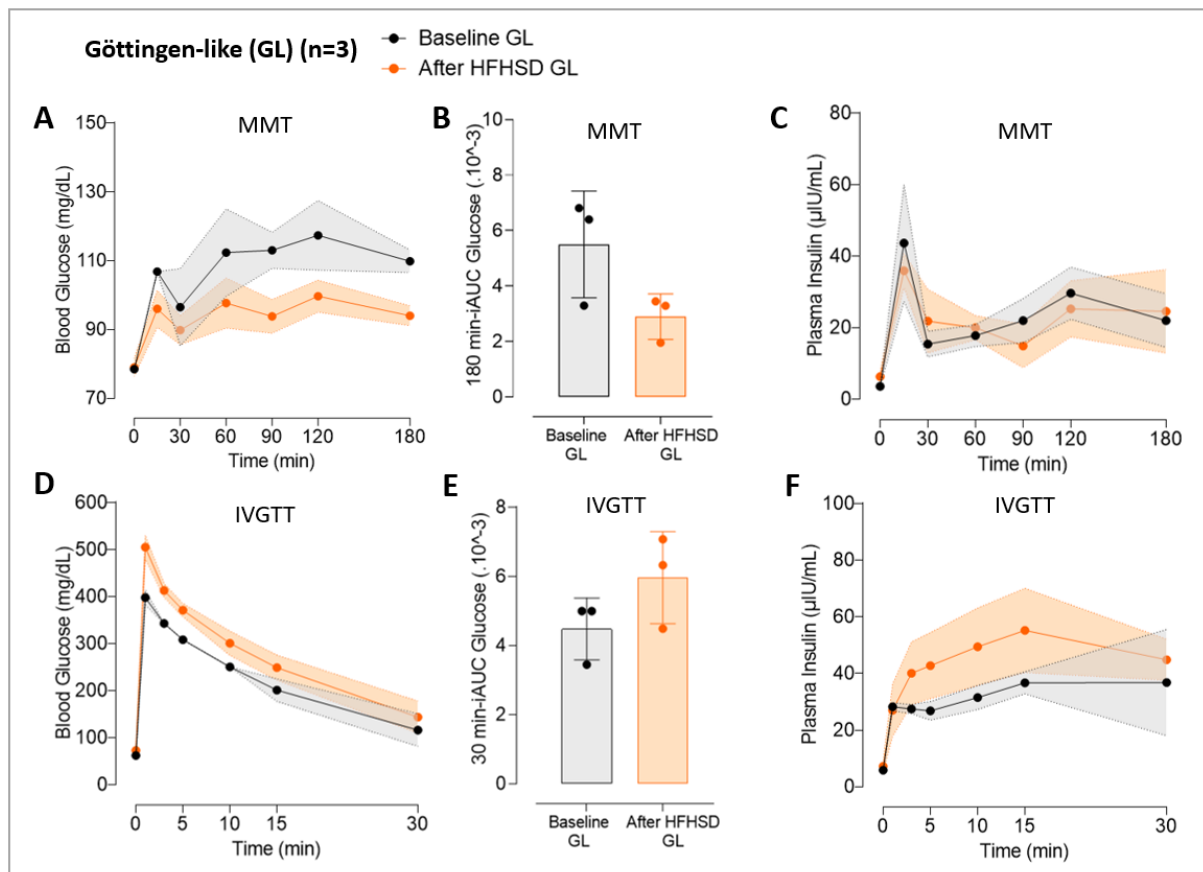


Figure 37: Glucose and insulin response of the Göttingen-like minipig strain to a 2-month high-fat, high-sucrose diet.

(A-C) Response following Mixed Meal Test (MMT) (n=3): (A) Blood Glucose (Mean \pm SEM) and (B) 180 min-incremental area under curve (180 min-iAUC) (Mean \pm SD); (C) Plasma Insulin (Mean \pm SEM).

(D-F) Response following Intravenous Glucose Tolerance Test (IVGTT) (n=3): (D) Blood Glucose (Mean \pm SEM) and (E) 30 min-incremental area under curve (30 min-iAUC) (Mean \pm SD); (F) Plasma Insulin (Mean \pm SEM).

The baseline characteristics were represented in black and those after 2-month high fat high sucrose diet (HFHSD) in orange. Two-Way ANOVA test for repeated measures and Sidak post-hoc test; Paired t-test

Postprandial blood glucose concentrations (**Figure 37A**) and corresponding 180-min iAUC (**Figure 37B**) were generally lower but not significantly following HFHSD, while insulin concentrations (**Figure 37C**) did not differ in Göttingen-like minipigs. The intravenous glucose tolerance test (IVGTT) results for glycemia (**Figure 37D**), its corresponding 30-min iAUC (**Figure 37E**), and insulin (**Figure 37F**) did not change between the two steps.

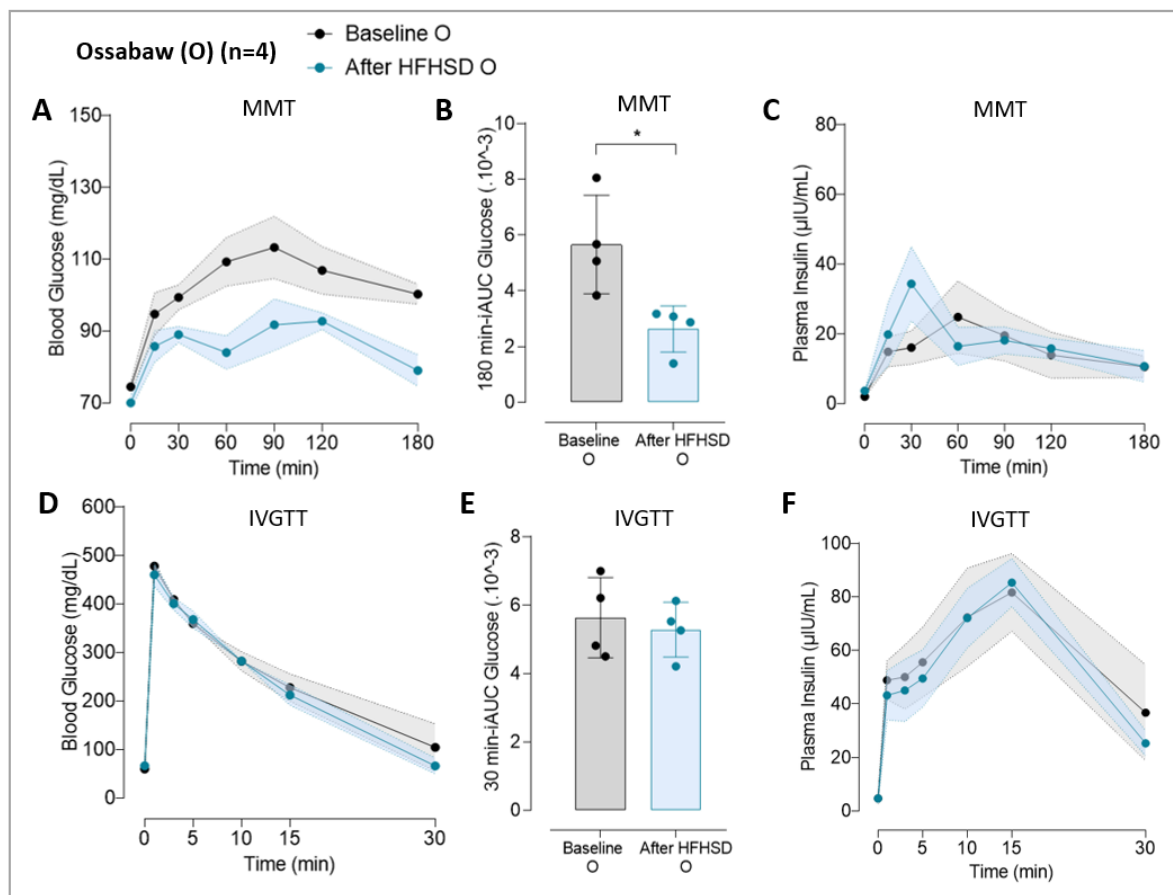


Figure 38: Glucose and insulin response of the Ossabaw minipig strain to a 2-month high-fat, high-sucrose diet.

(A-C) Response following Mixed Meal Test (MMT) (n=4): (A) Blood Glucose (Mean \pm SEM) and (B) 180 min-incremental area under curve (180 min-iAUC) (Mean \pm SD); (C) Plasma Insulin (Mean \pm SEM).

(D-F) Response following Intravenous Glucose Tolerance Test (IVGTT) (n=4): (D) Blood Glucose (Mean \pm SEM) and (E) 30 min-incremental area under curve (30 min-iAUC) (Mean \pm SD); (F) Plasma Insulin (Mean \pm SEM).

The baseline characteristics were represented in black and those after 2-month high fat high sucrose diet (HFHSD) in blue. Two-Way ANOVA test for repeated measures and Sidak post-hoc test; Paired t-test; *p<0.05

After HFHSD, Ossabaw minipigs showed a lower postprandial blood glucose levels (trend) (**Figure 38A**) and corresponding 180-min iAUC (**Figure 38B**) accompanied by a higher insulin peak secretion (trend) (**Figure 38C**). However, during the IVGTT, there were no discernible changes between the glucose

decline (**Figure 38D**), the corresponding 30-min iAUC (**Figure 38E**) and corresponding insulin concentrations (**Figure 38H**).

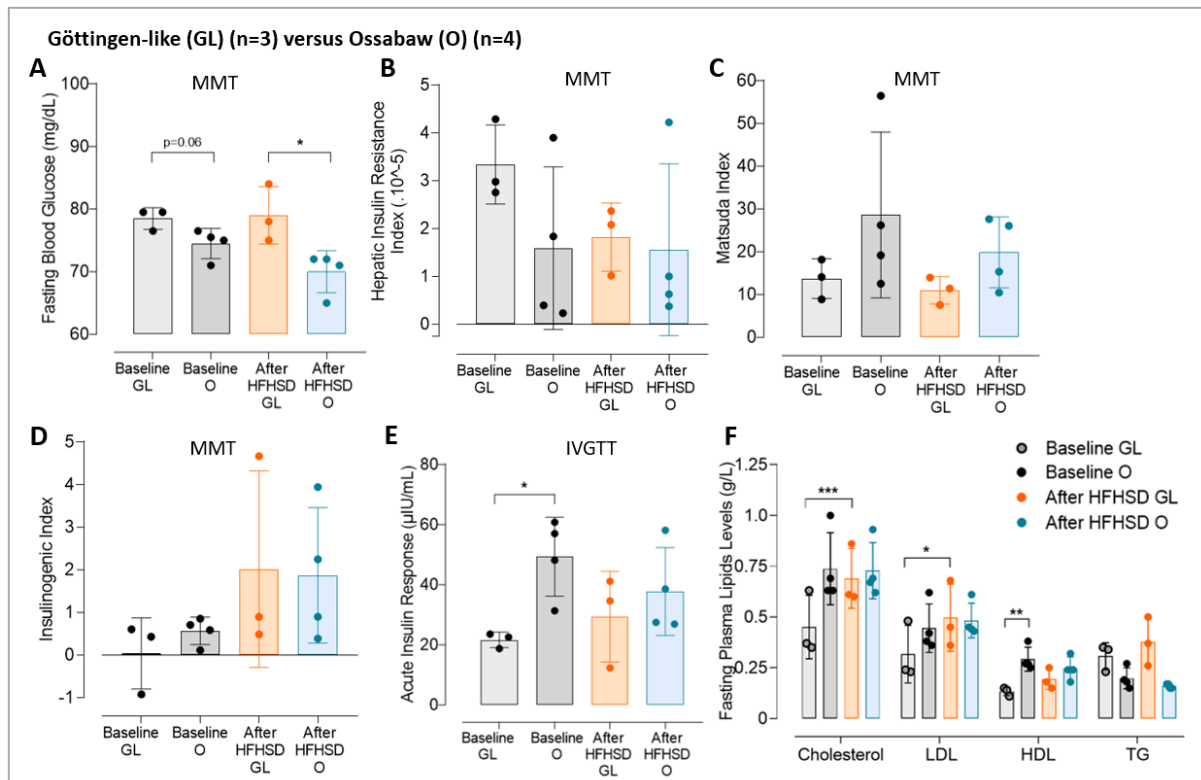


Figure 39: Comparison of the metabolic parameters of the Ossabaw and Göttingen-like strains to a 2-month high-fat, high-sucrose diet.

(A) Fasting Blood Glucose (Mean \pm SD) measured during MMT before (in black) and after (in color) HFHSD in the Göttingen-like (GL, in orange; n=3) and in the Ossabaw (O, blue; n=4) strains.

(B-D) Hepatic Insulin Resistance Index (B), Matsuda Index (C) and Insulinogenic Index (D) (Mean \pm SD) calculated during Mixed Meal Tests (MMT) before (in black) and after (in color) HFHSD in the Göttingen-like (GL, in orange; n=3) and in the Ossabaw (O, blue; n=4) strains.

(E) Acute Insulin Response (Mean \pm SD) calculated during Intravenous Glucose Tolerance Test (IVGTT) before (in black) and after (in color) HFHSD in the Göttingen-like (GL, in orange; n=3) and in the Ossabaw (O, blue; n=4) strains.

(F) Fasting plasma lipid profile (Mean \pm SD) assessed before (in black) and after (in color) HFHSD in the Göttingen-like (GL, in orange; n=3) and in the Ossabaw (O, blue; n=4) strains. Total Chol = total cholesterol; LDL = low-density lipoprotein; HDL = high-density lipoprotein; TG = triglycerides.

Paired or unpaired t-test; *p<0.05, **p<0.01, ***p<0.001.

Fasting blood glucose of the Ossabaw strains appeared lower than Göttingen-like at baseline, and it was significantly lower after HFHSD than those of Göttingen-like (70 ± 3.4 after versus 79 ± 4.6 mg/dL before; p<0.05) (**Figure 39A**). For both strains, there was no change in Hepatic Insulin Resistance Index (**Figure 39B**) and Matsuda Index (**Figure 39C**), although the **Figure 39D** showed a trend of increasing Insulinogenic Index. Compared to Göttingen-like minipigs, Ossabaw minipigs had significantly higher

baseline Acute Insulin Response (49.3 ± 13.1 $\mu\text{U}/\text{mL}$ for O versus 21.7 ± 2.5 $\mu\text{U}/\text{mL}$ for GL, $p < 0.05$) although no discernible alterations were found for any strain following HFHSD (**Figure 39E**).

Ossabaw minipigs presented a higher level in fasting cholesterol at the baseline than Göttingen-like (**Figure 39F**) (total cholesterol: 0.74 ± 0.18 g/L for O versus 0.45 ± 0.16 g/L for GL, not significant; LDL: 0.45 ± 0.12 g/L for O versus 0.32 ± 0.14 g/L for GL, not significant; HDL: 0.29 ± 0.06 g/L for O versus 0.13 ± 0.02 g/L for GL, $p < 0.01$). However, there was no change in the lipid profile after HFHSD in Ossabaw while total cholesterol and LDL levels were significantly increased in Göttingen-like (total cholesterol: 0.69 ± 0.15 g/L after versus 0.45 ± 0.16 g/L before, $p < 0.001$; LDL: 0.50 ± 0.17 g/L after versus 0.32 ± 0.14 g/L before, $p < 0.05$).

These findings indicated that Ossabaw minipigs had a better early insulin response than Göttingen-like minipigs. We thus decided to proceed with our strategy using the Göttingen-like strain.

2. Reduction of Acute Insulin Response after subtotal pancreatectomy in Göttingen-like minipigs

We assessed how a subtotal pancreatectomy affected glucose metabolism in 10 Göttingen-like minipigs (**Figure 40 and 41**).

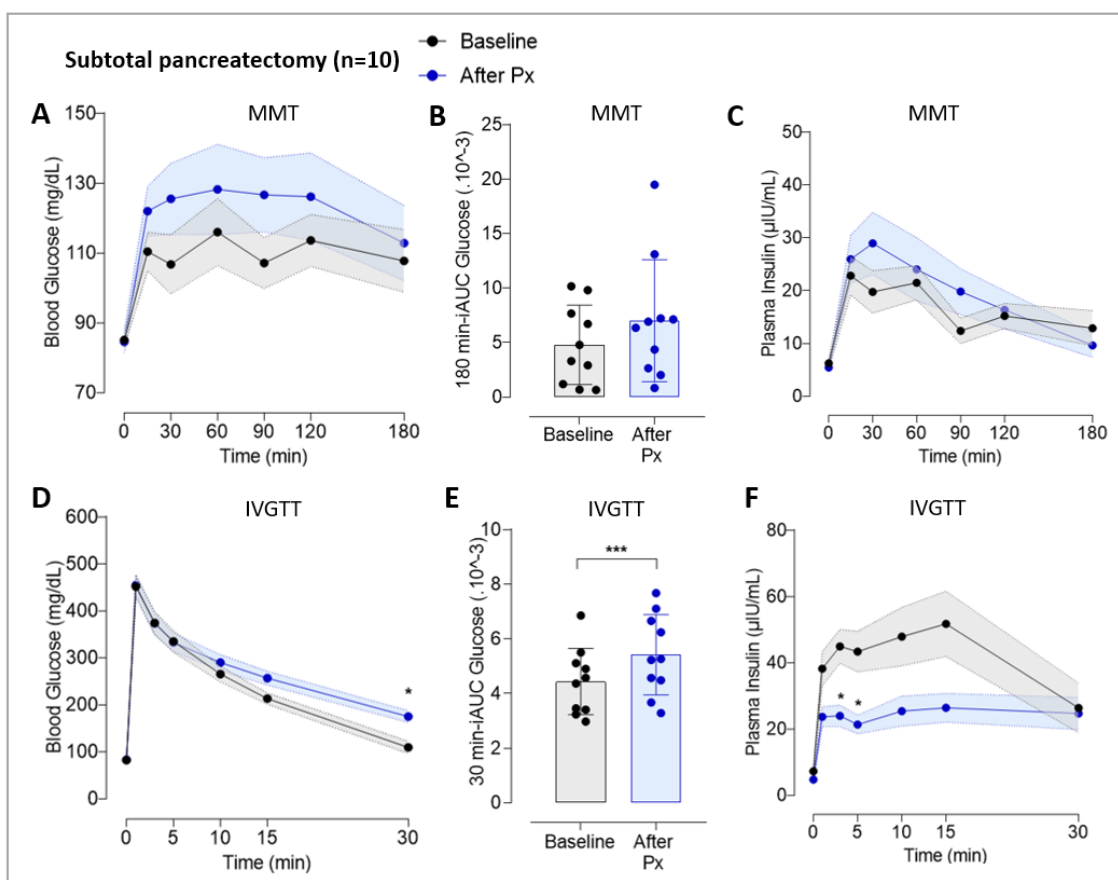


Figure 40: Glucose and insulin response of the Göttingen-like minipig strain to a subtotal pancreatectomy (Px) in Göttingen-like minipigs

(A-C) Response following Mixed Meal Test (MMT) (n=10): (A) Blood Glucose (Mean ± SEM) and (B) 180-min incremental area under curve (180-min iAUC) (Mean ± SD); (C) Plasma Insulin (Mean ± SEM).

(D-F) Response following Intravenous Glucose Tolerance Test (IVGTT) (n=10): (D) Blood Glucose (Mean ± SEM) and (E) 30-min incremental area under curve (30 min-iAUC) (Mean ± SD); (F) Plasma Insulin (Mean ± SEM).

The baseline characteristics were represented in black and those after a 75-% pancreatectomy in blue.

Two-Way ANOVA test for repeated measures and Sidak post-hoc test; Paired t-test; *p<0.05, ***p<0.001.

Mixed Meal Tests did not reveal any appreciable changes in blood glucose (**Figure 40A**), in its corresponding 180-min iAUC (**Figure 40B**) or insulin levels (**Figure 40C**).

When compared to before the intervention, the speed at which the glucose levels declined during the IVGTT following pancreatectomy was slower (blood glucose levels of respectively 175.1 ± 12.4 mg/dL after versus 109.4 ± 13.1 mg/dL before at 30 min, $p<0.05$) (**Figure 40D**). A significant interaction between “time” and “pancreatectomy” was thus reported ($p<0.05$). Consequently, the 30 min-iAUC of blood glucose during IVGTT was significantly increased (5423 ± 1469 after versus 4444 ± 1215 before, $p<0.001$) (**Figure 40E**). The pancreatectomy significantly decreased plasma insulin levels during IVGTT compared to the baseline ($p<0.05$) and especially at 3 and 5 min (respectively 24 ± 3.2 μ U/mL after versus 45 ± 5.1 μ U/mL before and 21 ± 2.8 μ U/mL after versus 43 ± 6.1 μ U/mL) (**Figure 40F**). A significant interaction between “time” and “pancreatectomy” was thus noticed ($p<0.0001$).

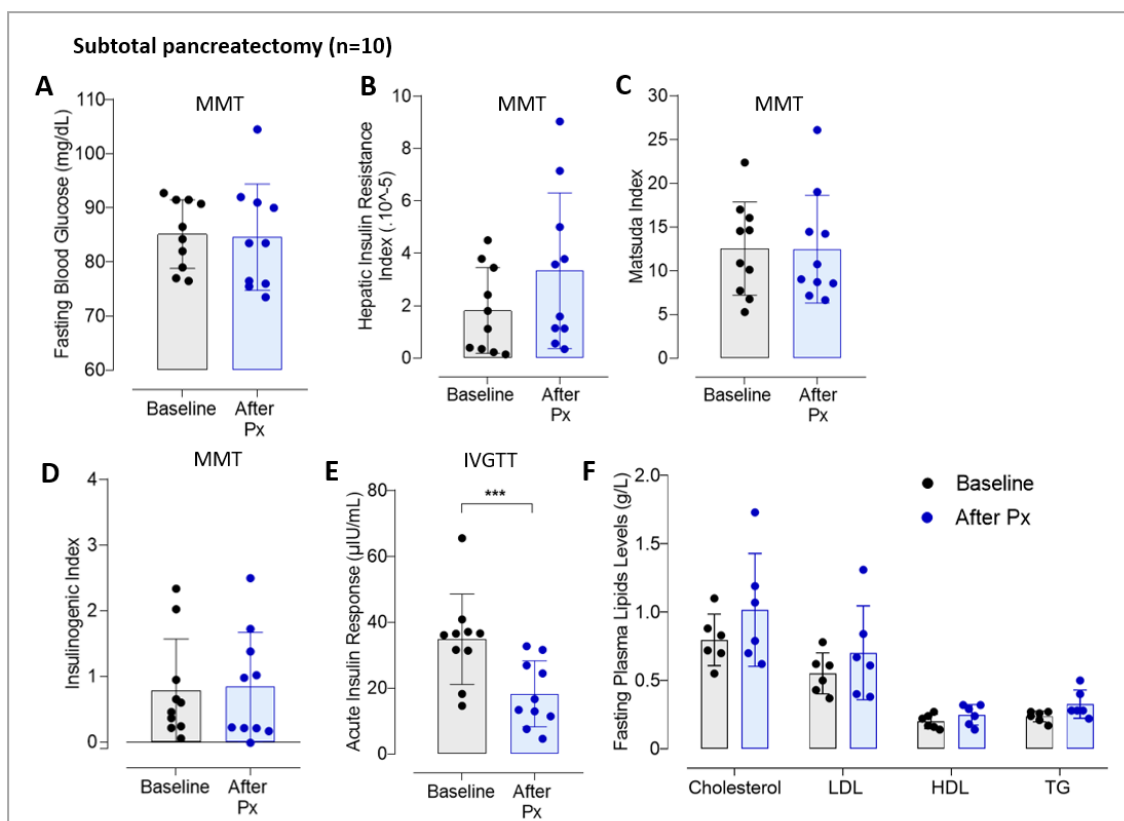


Figure 41: Evolution of the metabolic parameters following a subtotal pancreatectomy (Px) in Göttingen-like minipigs

(A) Fasting Blood Glucose (Mean \pm SD) (n=10) measured during MMT before (in black) and after (in blue) subtotal pancreatectomy

(B-D) Hepatic Insulin Resistance Index (B), Matsuda Index (C) and Insulinogenic Index (D) (Mean \pm SD) (n=10) calculated during Mixed Meal Tests (MMT) before (in black) and after (in blue) subtotal pancreatectomy

(E) Acute Insulin Response (Mean \pm SD) (n=10) calculated during Intravenous Glucose Tolerance Test (IVGTT) before (in black) and after (in blue) subtotal pancreatectomy

(F) Fasting plasma lipid profile (Mean \pm SD) (n=10) assessed before (in black) and after (in blue) subtotal pancreatectomy. Total Chol = total cholesterol; LDL = low-density lipoprotein; HDL = high-density lipoprotein; TG = triglycerides.

Paired t-test; ***p<0.0005.

After the surgical procedure, there was no rise in fasting blood glucose (**Figure 41A**). There was also no change of the Hepatic Insulin Resistance Index (**Figure 41B**), of the Matsuda Index (**Figure 41C**) and of the Insulinogenic Index (**Figure 41D**). However, following pancreatectomy, the Acute Insulin Response was significantly decreased (18.3 ± 10.0 μ IU/mL after versus 34.9 ± 13.7 μ IU/mL before, p<0.0005) (**Figure 41E**). Finally, there was no significant change reported in fasting plasma lipid profile after subtotal pancreatectomy (**Figure 41F**).

3. No significant change in glucose metabolism following the combination of a subtotal pancreatectomy with a 2-month HFHSD in Göttingen-like minipigs

The metabolic phenotypic changes following a subtotal pancreatectomy and two months of HFHSD as an oral energy overload were then examined (**Figure 42 and 43**). Following the protocol, animals gained weight (26.3 ± 5.9 kg after, compared to 21.3 ± 3.6 kg before, p<0.05).

With a more pronounced peak at 30 min and a faster return to baseline following the procedure, postprandial blood glucose dynamics were different from before, even if not significantly (**Figure 42A**). However, there was no significant change in the corresponding 180-min iAUC (**Figure 42B**). Additionally, there was a trend to higher postprandial insulin levels (**Figure 42C**).

The IVGTT revealed no significant changes in glucose tolerance (**Figure 42D**), its corresponding 30-min iAUC (**Figure 42E**) and insulin levels (**Figure 42F**).

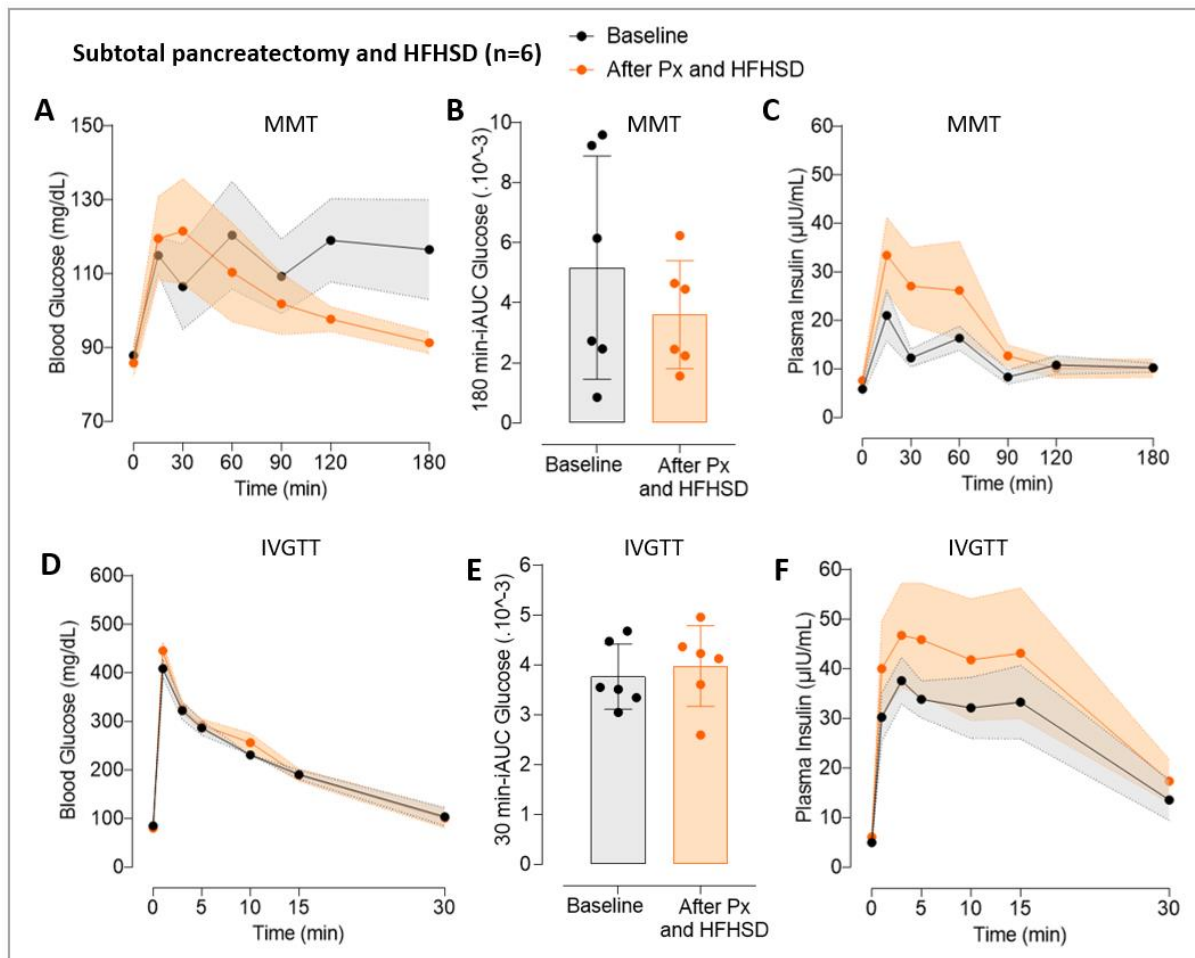


Figure 42: Glucose and insulin response of the Göttingen-like minipig strain to a subtotal pancreatectomy (Px) followed by a 2-months high-fat high-sucrose diet (HFHSD) in Göttingen-like minipigs

(A-C) Response following Mixed Meal Test (MMT) (n=6): (A) Blood Glucose (Mean \pm SEM) and (B) 180-min incremental area under curve (180-min iAUC) (Mean \pm SD); (C) Plasma Insulin (Mean \pm SEM).

(D-F) Response following Intravenous Glucose Tolerance Test (IVGTT) (n=6): (D) Blood Glucose (Mean \pm SEM) and (E) 30-min incremental area under curve (30 min-iAUC) (Mean \pm SD); (F) Plasma Insulin (Mean \pm SEM).

The baseline characteristics were represented in black and those after a 75-% pancreatectomy followed by a 2-months HFHSD in orange.

Two-Way ANOVA test for repeated measures and Sidak post-hoc test; Paired t-test.

Following this approach, no rise in fasting blood glucose (**Figure 43A**) was observed. Additionally, the Hepatic Insulin Resistance Index modestly but not significantly increased (**Figure 43B**). The Matsuda Index was slightly decreased but not significantly (**Figure 43C**) and the Insulinogenic Index (**Figure 43D**) and the Acute Insulin Response (**Figure 43E**) did not significantly change.

Finally, the levels of fasting plasma lipids were globally increased after intervention (**Figure 43F**) (total cholesterol: 1.09 ± 0.2 g/L after versus 0.80 ± 0.19 g/L before, $p < 0.05$; LDL: 0.65 ± 0.12 g/L after versus

0.55 ± 0.15 g/L before, p=0.052; HDL: 0.38 ± 0.18 g/L after versus 0.20 ± 0.05 g/L before, not significant; triglycerides: 0.28 ± 0.07 g/L after versus 0.24 ± 0.04 g/L before, not significant).

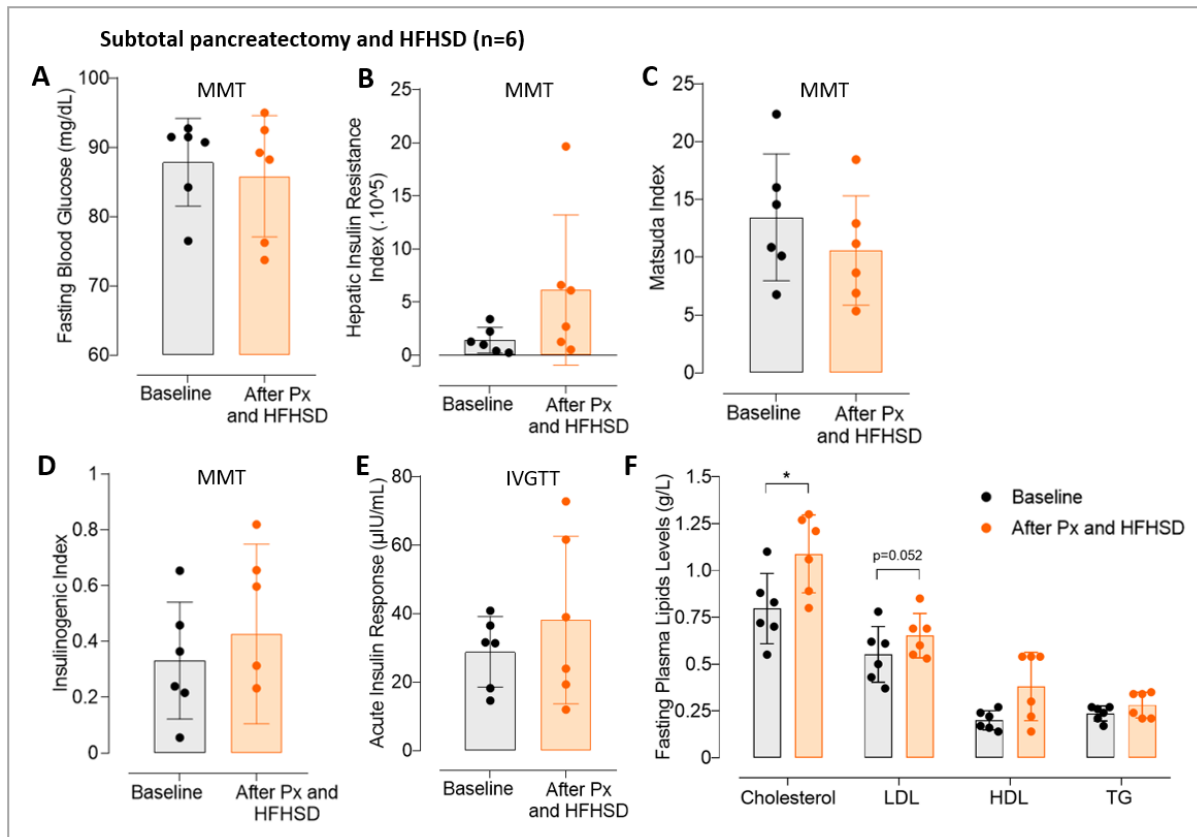


Figure 43: Evolution of the metabolic parameters following a subtotal pancreatectomy (Px) followed by a 2-months high-fat high-sucrose diet (HFHSD) in Göttingen-like minipigs

(A) Fasting Blood Glucose (Mean ± SD) (n=6) measured during MMT before (in black) and after (in orange) a subtotal pancreatectomy followed by a 2-months HFHSD

(B-D) Hepatic Insulin Resistance Index (B), Matsuda Index (C) and Insulinogenic Index (D) (Mean ± SD) (n=6) calculated during Mixed Meal Tests (MMT) before (in black) and after (in orange) a subtotal pancreatectomy followed by a 2-months HFHSD

(E) Acute Insulin Response (Mean ± SD) (n=6) calculated during Intravenous Glucose Tolerance Test (IVGTT) before (in black) and after (in orange) a subtotal pancreatectomy followed by a 2-months HFHSD

(F) Fasting plasma lipid profile (Mean ± SD) (n=6) assessed before (in black) and after (in orange) subtotal pancreatectomy followed by a 2-months HFHSD.

Total Chol = total cholesterol; LDL = low-density lipoprotein; HDL = high-density lipoprotein; TG = triglycerides.

Paired t-test; *p<0.05.

4. Alterations of insulin secretion pattern and insulin resistance after long-term intraportal glucose and lipids infusions in Göttingen-like minipigs

In two groups of minipigs, one without prior pancreatectomy and the other following subtotal pancreatectomy, we infused long-term intraportal glucose and lipids (Figure 44, 45 and 46). Animals

of each group gained a little weight following infusions (35.2 ± 11.4 after versus 28.3 ± 7.4 kg before for Group 1, $p < 0.05$; and 47.4 ± 6.5 kg after versus 41.8 ± 6.7 kg before for Group 2, $p < 0.005$).

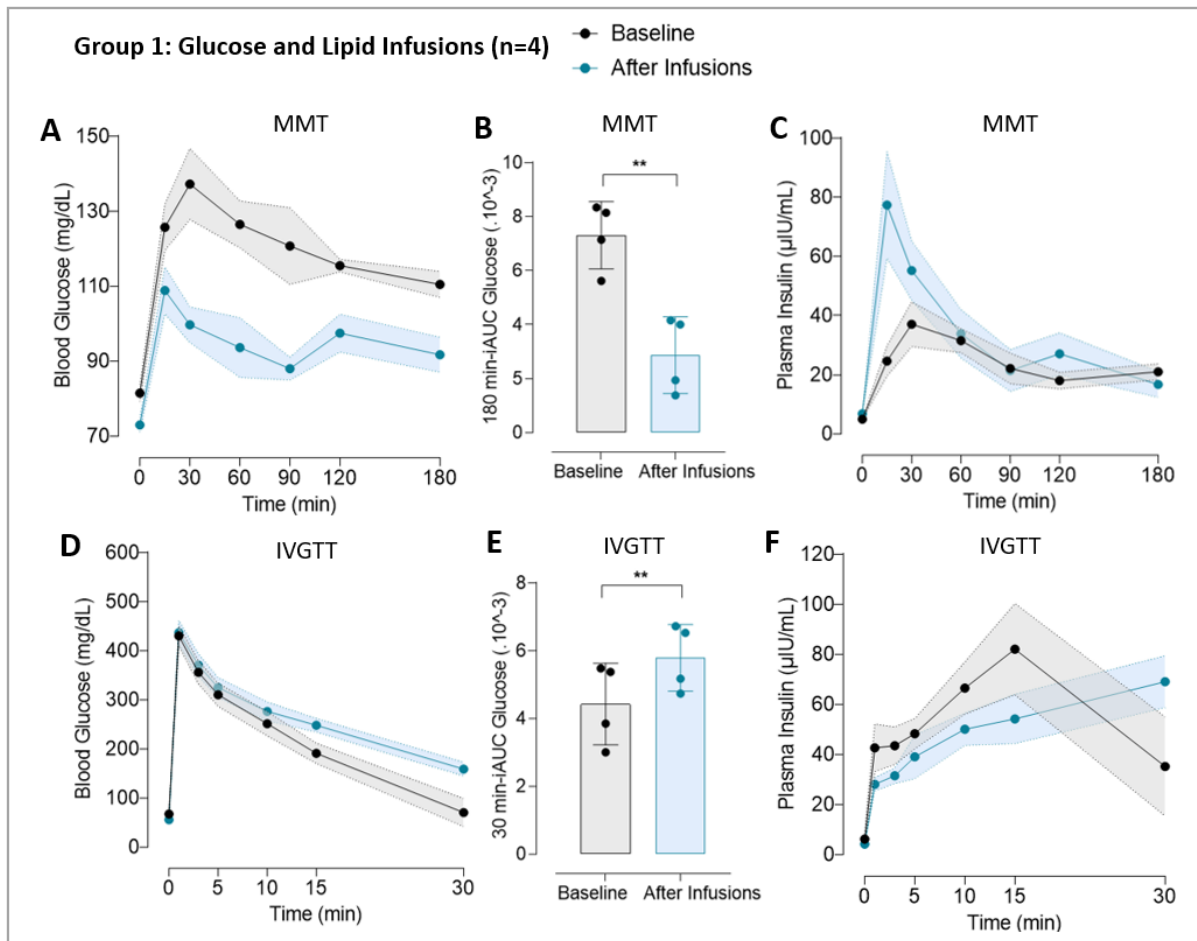


Figure 44: Glucose and insulin response following 3 weeks of intraportal Glucose and Lipid infusions in Göttingen-like minipigs

(A-C) Response following Mixed Meal Test (MMT) (n=4): (A) Blood Glucose (Mean \pm SEM) and (B) 180-min incremental area under curve (180-min iAUC) (Mean \pm SD); (C) Plasma Insulin (Mean \pm SEM).

(D-F) Response following Intravenous Glucose Tolerance Test (IVGTT) (n=4): (D) Blood Glucose (Mean \pm SEM) and (E) 30-min incremental area under curve (30-min iAUC) (Mean \pm SD); (F) Plasma Insulin (Mean \pm SEM).

The baseline characteristics were represented in black and those after intraportal infusions in blue.

Two-Way ANOVA test for repeated measures and Sidak post-hoc test; Paired t-test; ** $p < 0.01$.

Postprandial blood glucose levels of Group 1 were significantly lower compared to the baseline state ($p < 0.005$) (**Figure 44A**) and a significant interaction between “time” and “infusions” was thus noticed ($p < 0.05$). Its corresponding 180 min-iAUC was additionally significantly decreased (2874 ± 1418 after versus 7314 ± 1245 before) (**Figure 44B**). The first 30 minutes showed a rise in plasma insulin levels (77.4 ± 18.0 $\mu\text{U}/\text{mL}$ after infusions at 15 min versus 24.7 ± 5.1 $\mu\text{U}/\text{mL}$ before, and 55.3 ± 10.0 $\mu\text{U}/\text{mL}$ after infusions at 30 min versus 37.1 ± 7.6 $\mu\text{U}/\text{mL}$ before; not significant) and a significant interaction between “time” and “infusions” was discovered ($p < 0.005$) (**Figure 44C**).

Blood glucose levels decreased during IVGTT more slowly than they did before protocol (159.0 ± 14.2 mg/dL after infusions versus 70.4 ± 28.6 mg/dL before at 30 min; not significant) (**Figure 44D**) and its corresponding 30-min iAUC was moreover significantly increased (5793 ± 983 after versus 4431 ± 1206 before) (**Figure 44E**). Moreover, insulin levels globally decreased, with an exception at 30 minutes (**Figure 44F**).

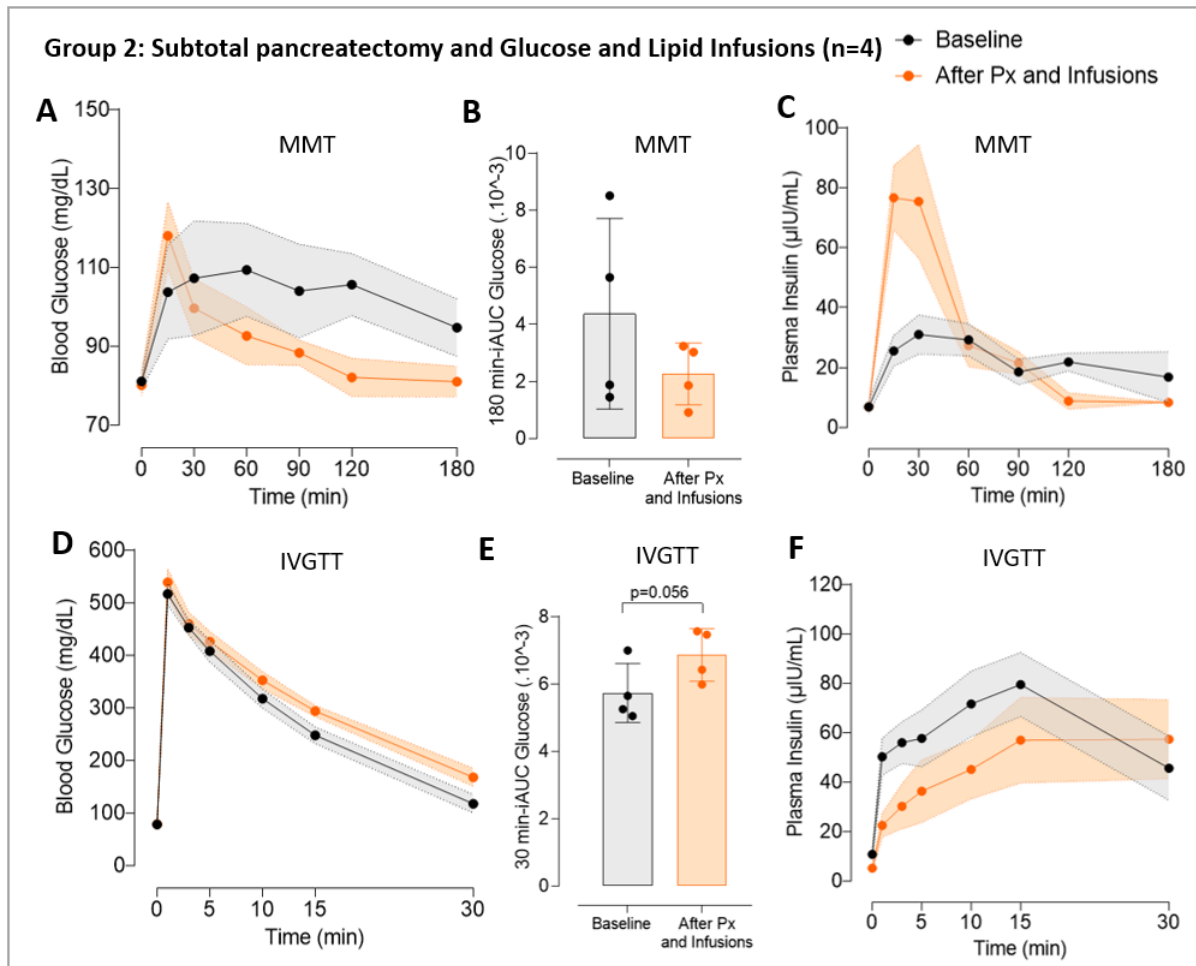


Figure 45: Glucose and insulin response following subtotal pancreatectomy and 3 weeks of intraportal Glucose and Lipid infusions in Göttingen-like minipigs

(A-C) Response following Mixed Meal Test (MMT) (n=4): (A) Blood Glucose (Mean \pm SEM) and (B) 180 min-incremental area under curve (180 min-iAUC) (Mean \pm SD); (C) Plasma Insulin (Mean \pm SEM).

(D-F) Response following Intravenous Glucose Tolerance Test (IVGTT) (n=4): (D) Blood Glucose (Mean \pm SEM) and (E) 30 min-incremental area under curve (30 min-iAUC) (Mean \pm SD); (F) Plasma Insulin (Mean \pm SEM).

The baseline characteristics were represented in black and those after subtotal pancreatectomy and intraportal infusions in orange.

Two-Way ANOVA test for repeated measures and Sidak post-hoc test; Paired t-test.

Following procedure, postprandial blood glucose levels in Group 2 fell globally (**Figure 45A**), similar to Group 1 and a significant interaction between “time” and “intervention” was observed ($p < 0.05$). The corresponding 180-min iAUC was also decreased but not significantly (**Figure 45B**). Plasma insulin

levels rose for the first 30 minutes ($76.7 \pm 10.6 \mu\text{IU/mL}$ after protocol at 15 min versus $25.5 \pm 5.1 \mu\text{IU/mL}$ before, and $75.4 \pm 19.0 \mu\text{IU/mL}$ after protocol at 30 min versus $31.0 \pm 6.5 \mu\text{IU/mL}$ before; not significant) and a significant interaction between “time” and “intervention” was reported ($p < 0.0001$) (Figure 45C).

IVGTT findings after protocol revealed a slower lowering of blood glucose (Figure 45D), associated with an almost significant increase of its corresponding 30-min iAUC (6863 ± 780 after versus 5737 ± 876 before) (Figure 45E). In particular, lower insulin levels with a significant intervention was observed between “time” and “intervention” (Figure 45F).

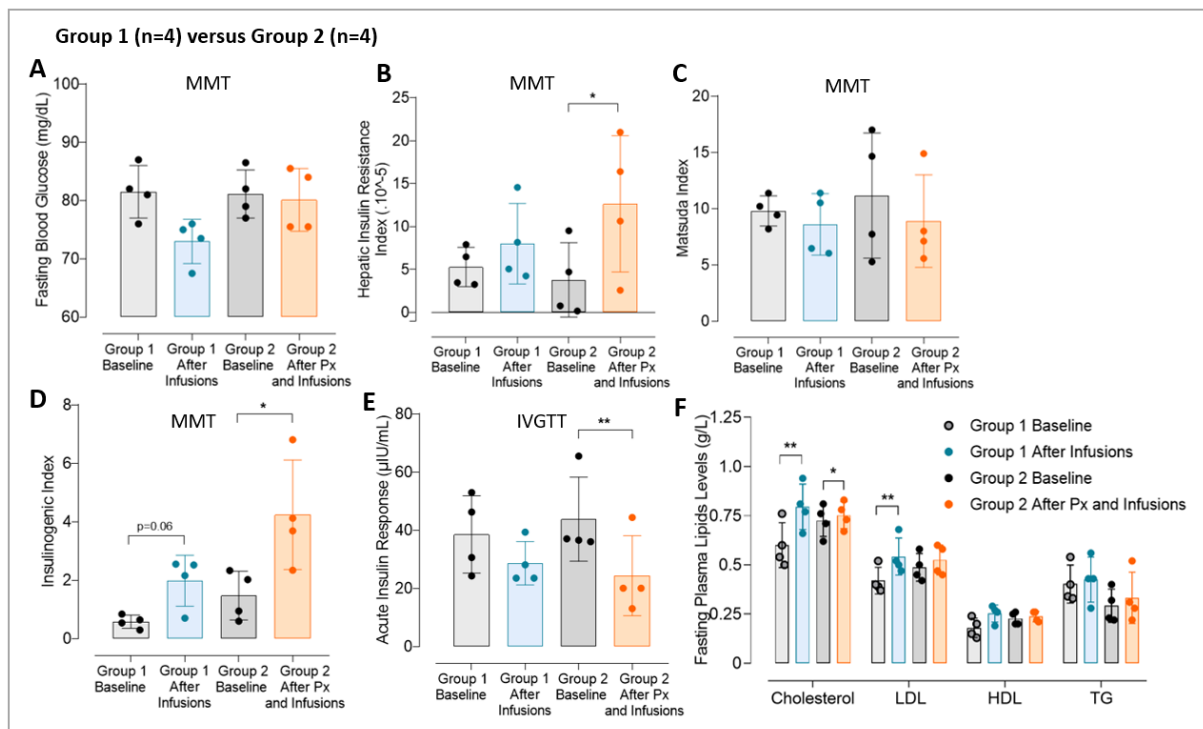


Figure 46: Evolution of the metabolic parameters following 3 weeks of intraportal Glucose and Lipid infusions or a subtotal pancreatectomy (Px) followed by 3 weeks of intraportal Glucose and Lipid infusions in Göttingen-like minipigs

(A) Fasting Blood Glucose (Mean \pm SD) measured during MMT before (in black) and after (in color) intervention in the Group 1 (Infusions, in blue; $n=4$) and in the Group 2 (Px and infusions, in orange; $n=4$).

(B-D) Hepatic Insulin Resistance Index (B), Matsuda Index (C) and Insulinogenic Index (D) (Mean \pm SD) calculated during Mixed Meal Tests (MMT) before (in black) and after (in color) intervention in the Group 1 (Infusions, in blue; $n=4$) and in the Group 2 (Px and infusions, in orange; $n=4$).

(E) Acute Insulin Response (Mean \pm SD) calculated during Intravenous Glucose Tolerance Test (IVGTT) before (in black) and after (in color) intervention in the Group 1 (Infusions, in blue; $n=4$) and in the Group 2 (Px and infusions, in orange; $n=4$).

(F) Fasting plasma lipid profile (Mean \pm SD) assessed before (in black) and after (in color) intervention in the Group 1 (Infusions, in blue; $n=4$) and in the Group 2 (Px and infusions, in orange; $n=4$).

Total Chol = total cholesterol; LDL = low-density lipoprotein; HDL = high-density lipoprotein; TG = triglycerides.

Paired or unpaired t-test; * $p < 0.05$, ** $p < 0.01$.

Whether or not a subtotal pancreatectomy had been performed prior to the intraportal glucose and lipid infusion, no increase in fasting blood glucose was observed (**Figure 46A**). However, an increase in Hepatic Insulin Resistance Index ($\times 10^{-5}$) was also obtained (8.0 ± 4.7 after versus 5.3 ± 2.3 before; not significant, and 12.6 ± 7.9 after versus 3.8 ± 4.3 before; $p < 0.05$, respectively for Group 1 and 2) (**Figure 46B**), but no change in the Matsuda Index was noticed (**Figure 46C**). Both groups showed an increase in the Insulinogenic Index (2.0 ± 0.8 versus 0.59 ± 0.2 ; $p = 0.06$ and 4.2 ± 1.9 versus 1.5 ± 0.8 ; $p < 0.05$, respectively for Group 1 and 2) (**Figure 46D**). Additionally, the Acute Insulin Responses of both groups were reduced (28.7 ± 7.5 after versus 38.6 ± 13.3 before; not significant, and 24.4 ± 13.7 after versus 43.9 ± 14.5 ; $p < 0.005$ before, respectively for Group 1 and 2) (**Figure 46E**).

Finally, fasting plasma levels of total cholesterol and LDL were increased after intervention for both groups (**Figure 46F**) (total cholesterol: 0.80 ± 0.12 g/L after versus 0.60 ± 0.11 g/L before, $p < 0.01$, for Group 1 and 0.75 ± 0.07 g/L after versus 0.73 ± 0.08 g/L before, $p < 0.05$, for Group 2; LDL: 0.54 ± 0.09 g/L after versus 0.42 ± 0.07 g/L before, $p < 0.01$, for Group 1 and 0.53 ± 0.08 g/L after versus 0.49 ± 0.07 g/L before, not significant, for Group 2). HDL and triglycerides levels were not significantly altered after intervention, no matter the group. No significant difference was observed in glucose homeostasis and lipid profile after intervention between Group 1 and Group 2.

IV. Discussion

The main part of the discussion was taken from Goutchtat et al., 2023. Some precisions were added and some parts were reformulated.

1. Summary of the obtained results

In this experimental part of the project, we attempted to develop a preclinical type 2 diabetic pig model in this study in accordance with the World Health Organization definition (glycemia over 126 mg/dL after 8 hours of fasting, verified twice, or over 200 mg/dL following an oral glucose tolerance test) (World Health Organization and International Diabetes Federation, 2006).

In order to determine which strain of pigs was the most suited, we first subjected two distinct strains to a High Fat High Sucrose Diet (HFHSD) for two months. This enabled us to evaluate the metabolic adaptation of each strain to the HFHSD. Both strains responded equally, with Ossabaw having a little better insulin response than Göttingen-like, which justified pursuing the study with Göttingen-like minipigs. During metabolic evaluations, the metabolic response in both strains showed a tendency to an increase in insulin levels, necessitating the introduction of an intervention aimed at reducing pancreas adaptability capacity.

This is why we decided to combine an energy overload with an insulin restriction technique, such as a subtotal pancreatectomy. In the beginning, the effects of a single subtotal pancreatectomy were investigated. In our investigation, subtotal pancreatectomy reduced early insulin secretion while leaving postprandial glycemic response and fasting glycemia unaffected. The subtotal pancreatectomy was performed on a set of pigs combined with 2 months of oral energy overload administered via an HFHSD: there was no change in the metabolism of glucose. Thus, another strategy was considered in moving towards a parenteral energetic overload using chronic intraportal glucose and lipid infusions, whether or not they were associated with a preceding subtotal pancreatectomy. Results showed similar patterns with or without a pancreatectomy, with lower postprandial glycemia values associated with a higher 30-minute insulin peak. A rise in hepatic insulin resistance was also observed, particularly in the group that was subjected to the subtotal pancreatectomy prior to infusions, in addition to this postprandial hyperinsulinism. Finally, during intravenous glucose tolerance testing, a decrease in the first phase of insulin secretion was observed for both groups, with the pancreatectomy group showing significant differences. We were unable to produce a type 2 diabetic minipig model because none of the study groups achieved a fasting hyperglycemia.

2. Ossabaw strain

The results in the Ossabaw strain were unexpected. The HFHSD induced a response that was highly comparable to that of the Göttingen-like strain, with an early insulin secretion that appeared to be even more effective than the Göttingen one in the baseline state.

However, Ossabaw minipigs have a reputation for being the strain that is most susceptible to metabolic syndrome (Dyson et al., 2006; Sturek et al., 2007). In fact, they developed, in the "Ossabaw Georgia island" where they come from, a "thrifty genotype" that enabled them to easily store energy from low-nutritive substrates because of the severe selection pressure imposed by the dry climate of the Ossabaw island. Thus, it is claimed that Ossabaw minipigs serve as a natural model for reproducing the symptoms of type 2 diabetes and the metabolic syndrome, similar to those populations that are predisposed to these diseases naturally (DeFronzo et al., 2015).

However, given that no fasting hyperglycemia could be generated only after a diet in previous research (Newell-Fugate et al., 2017; C. R. Powell et al., 2020; Sham et al., 2014), it would appear that the expression of their metabolic syndrome would be more focused on lipidic dysregulations than disorders of glucose metabolism (Lee et al., 2009; Neeb et al., 2010). Ossabaw fasting lipid levels were much greater than those of the Göttingen-like in our study, particularly in terms of cholesterol, which makes this strain particularly well-suited for the investigation of hypercholesterolemia illnesses (Uceda et al., 2020) but not for studies of diabetes.

We continued the combination protocol, which included a subtotal pancreatectomy, followed by five additional months of HFHSD, in two minipigs of this strain (data not shown). These two minipigs showed no signs of metabolic change, demonstrating that this strain is not susceptible to develop type 2 diabetes.

3. Subtotal pancreatectomy and combination with high-fat high-sucrose diet

The decision to perform a pancreatectomy was made considering the highly variable and toxic effects of streptozotocin (Dufrane et al., 2006) and alloxan (Badin et al., 2018). Additionally, a surgical pancreatic mass excision is easier to control than one caused by toxic chemicals (Ferrer et al., 2008; Renner et al., 2020), which is why this way of generating an insulin deficiency was chosen.

The subsequent impact of the subtotal pancreatectomy on glucose metabolism is unexpectedly modest, with the only discernible change being a reduction in the acute insulin response, which is the first phase of insulin secretion. We also observed that following pancreatectomy, insulin release reached a plateau. Nevertheless, there was no change in insulin secretion throughout the oral glucose challenge. As previously described in this species (Larsen et al., 2004), the loss of pancreatic mass would have been balanced by an increase in glucose and GLP-1 driven insulin secretion per islet. Although we did not measure it in our study, subtotal pancreatectomy may have increased the incretin impact to balance the loss of islet mass.

Contrary to what we expected, the plan to combine a 2-month HFHSD with a subtotal pancreatectomy in order to exceed the capacity of the pancreas for insulin secretion did not result in any phenotypic change. As seen in human islets (Castex et al., 2020), the weight gain brought on by the regimen may have helped to increase the size of the surviving islets and their reactivity to glucose in releasing insulin, serving as a mode of compensation.

4. Long-term intraportal glucose and lipid infusions, preceded or not with a subtotal pancreatectomy

We found the biggest metabolic changes in the minipigs receiving continuous intraportal glucose and lipid infusions. Even while the findings of changes in insulin response were significantly different from the baseline state only in the group with subtotal pancreatectomy prior to infusions, both groups—with or without subtotal pancreatectomy—presented comparable patterns. Therefore, we propose that the pancreatectomy potentialized the impact of infusions.

In conjunction with a decline in the first phase of insulin secretion, we discovered an increase in hepatic insulin resistance and postprandial hyperinsulinism. Because glucose and lipids were infused into the portal vein, they quickly may have caused a hepatic excess in glycogen and triglycerides, which may

have been the source of the hepatic insulin resistance as previously observed in dogs (Everett-Grueter et al., 2006; Warner et al., 2021) and mice (Ito et al., 2013). Furthermore, the administration of parenteral nutrition is known to have major side effects like hepatic steatosis, insulin resistance, and changes in insulin secretion (Alonso et al., 2007; Hagman et al., 2008; Hoy et al., 2007; Stoll et al., 2010), which is why we decided to test this approach in our research. During the sacrifice of these minipigs, a discoloration evocating a hepatic steatosis was macroscopically observed (data not shown).

Additionally, it is now well understood that a decrease in acute insulin response, a marker of change in the first phase of insulin release, constitutes the initial indicator of impaired glucose tolerance (Del Prato and Tiengo, 2001; Marcelli-Tourvieille et al., 2006).

The existence of ectopic triglycerides in the pancreas that were brought on by the intraportal infusions could potentially account for this decline. It is known that ectopic triglycerides have a significant role in the oxidative stress and inflammation that reduce the functionality of pancreatic beta cells (Samuel and Shulman, 2012). Around the abdominal organs during sacrifice, substantial visceral adipose tissue was also macroscopically visible (data not shown). This finding, a potential cause of insulin resistance, might thus be used to explain the postprandial hyperinsulinism. Hepatic insulin resistance was clearly established, while peripheral insulin resistance was not. In particular, the Matsuda Index calculation, which evaluates peripheral insulin sensitivity in humans, did not change after intraportal infusions relative to the initial state. In addition, we did not examine postprandial incretin levels. It would have been interesting to determine whether the observed postprandial hyperinsulinism may be attributed to an increase in GLP-1 concentrations caused by an intestinal adaptation brought on by the intraportal infusions.

Contrary to our predictions, we discovered smaller postprandial hyperglycemia excursions in the groups receiving infusions, along with a tendency for fasting blood glucose to decline. The compensatory hyperinsulinism seen could be the cause of these decreased postprandial glycemic excursions. Additionally, prolonged parenteral feeding is linked to negative effects on the intestine: microbiota dysbiosis (Wang et al., 2023), gut mucosa atrophy (Cerdó et al., 2022) or impairment of enteral bile acids uptake and signaling (Jain et al., 2017, 2012; Zhao et al., 2023) are the main observed complications of total parenteral nutrition. Parenteral nutrition in our situation might have caused intestinal mucosal atrophy, reducing the absorptive capabilities of the intestine and, as a result, reducing the postprandial glucose excursions during the meal test. To the best of our knowledge, no documentation of this mechanism has ever been found in the literature.

In any case, the observed modifications following long-term intraportal glucose and lipid infusions, would look very similar to those intervening early in the beginning of type 2 diabetes, even if no fasting

hyperglycemia was found for these groups. We might have acquired a more severe phenotype if we had continued intraportal infusions for a longer period of time. We did not, however, because of the ethical issues raised by the complicated porcine model.

In addition to these groups, a different one with 4 animals benefited from chronic intraportal glucose infusions exclusively (data not shown), using the same methods as those outlined for the relationship between glucose and lipids. Since no phenotypic alteration was seen following these infusions, we could infer that pigs are a species that are more vulnerable to the effects of lipid-induced oxidative stress than glucose. This theory was not investigated further, and there was no convincing evidence in the literature to back it up. It could have been interesting to further analyze a group that only received intraportal lipid infusions and compare the outcomes to the groups that received both intraportal glucose and lipid infusions. We decided against doing it for ethical reasons.

5. Changes of lipid profile

The lipidic profile of Göttingen-like minipigs was investigated. All groups showed a notable rise in total cholesterol, especially LDL, with the exception of pigs subjected to a single subtotal pancreatectomy. As a result, we were able to develop a minipig model of the metabolic syndrome in the groups receiving continuous intraportal infusions of glucose and lipids. Although the definition of the metabolic syndrome in pigs is still debatable, the key features of this syndrome in humans include visceral obesity, fasting blood glucose levels over 110 mg/dL, insulin resistance, dyscholesterolemia, hypertriglyceridemia, and elevated blood pressure. Metabolic syndrome is defined as the presence of at least three of these criteria (DeFronzo and Ferrannini, 1991), which in our instance were at least visceral obesity, insulin resistance, and dyscholesterolemia.

Type 2 diabetes and metabolic syndrome were frequently confused in many other studies that worked on developing type 2 diabetic pig models. Because of this, some researchers falsely claimed to have a legitimate preclinical minipig model of type 2 diabetes, despite the fact that the World Health Organization strictly defines diabetes as hyperglycemia and not by a variety of signs of insulin resistance.

Minipigs demonstrated both hyperglycemia caused by the use of toxic medication use and obesity with metabolic abnormalities in other studies when HFHSD and streptozotocin were combined (Coelho et al., 2018; von Wilmsky et al., 2016). However, because metabolic disorders and hyperglycemia are in fact interrelated in the genesis of the disease, it was in this case two different independent interventions that produced two phenotypic characteristics independently, raising question on the reliability of this type 2 diabetes paradigm.

6. Early signs of impaired glucose tolerance and insulin resistance only after interventions mimicking intestinal glucose and lipid overabsorption

In order to simulate a diet with high Glycemic Index meals, we used a high-fat high-sucrose diet (HFHSD) for 2 months in some groups of animals in this investigation. Neither combined with a subtotal pancreatectomy nor alone a 2-month HFHSD had a significant impact on glucose homeostasis in the groups that had these treatments.

We only noticed changes in glucose metabolism in the animals that received long-term intraportal glucose and lipid infusions rather than physiological meals, regardless of whether a prior subtotal pancreatectomy had been performed. In other words, only by "bypassing" the intestine with interventions that mimicked intestinal glucose and lipid overabsorption were we able to produce early signs of impaired glucose tolerance and insulin resistance.

First, these findings could let us suppose some genetic factors in pigs limiting intestinal glucose absorption. It was not further investigated in our study, and to the best of our knowledge, it has never been mentioned previously in the pig. However, a previous study in humans identified several intestinal sodium glucose transporter 1 (SGLT1) variants that would be protective against type 2 diabetes and the progression of the metabolic syndrome (Seidelmann et al., 2018). It would be fascinating to see in future research using single cell RNA-seq and proteomic techniques, if these SGLT1 variants are largely present in the pig. This SGLT1 gene may also be a useful target for creating genetically modified pig models and studying the impact on glucose metabolism.

Second, our findings are consistent with the theory that the development of impaired glucose tolerance is caused by an intestinal glucose overabsorption. In fact, whether or not a subtotal pancreatectomy had previously been performed, early symptoms of decreased glucose tolerance were seen. Infusions of intraportal glucose and lipids were able to produce early indicators of decreased glucose tolerance even in the absence of the subtotal pancreatectomy, and the pancreatectomy allowed the potentialization of their effects. In the Group 1 of our study, intestinal glucose and lipid overabsorption occurred before the onset of hepatic insulin resistance and decrease of the acute insulin response. It indicates that it may be the initial catalyst for the development of an impaired glucose tolerance, independent of an initial state of insulin resistance and lack of insulin secretion. Type 2 diabetes would result from intestinal glucose overabsorption when combined with hereditary variables that cause a deficit in insulin sensitivity and secretion.

7. Limitations of the study

We mentioned in a previous paragraph the probably too short duration of the intraportal glucose and lipids infusion to induce a more severe phenotype. In fact, the 3-week duration of the intraportal

infusions was probably too brief to significantly alter the phenotypic and cause type 2 diabetes. The choice of this time was mostly dependent upon our ability to maintain the portal catheter in situ and effective. In fact, maintaining a long-term venous catheter in a pig is technically difficult, particularly when it involves a portal localization. Daily maintenance is required to avoid thrombi from forming and closing the catheter, and a portal localization also involves externally fixing the catheter to the flank of the animal, making it accessible and simple to remove.

Because only castrated males were used in our study, our animal groups were not mixed-gender. This decision was made to reduce the metabolic fluctuations brought on by the reproductive cycles of the females. The ideal solution would have been to medically sterilize the females as well. In contrast to the removal of a testicle, the ovariectomy is a more invasive treatment. Even though it exposed us to the development of a model that was only available for one sex, we did not choose this option for ethical reasons.

We also made the decision to limit the animals in our protocol to adults. To ensure that the weight gain observed was indeed caused by the operation and not by the growth of the pigs, we would like to only perform diabetogenic strategies in animals that have reached the end of their growth. Additionally, the fact that type 2 diabetes primarily affects adults justifies this decision. However, starting the diabetogenic treatments in children rather than adults may have made it simpler to generate a more prominent phenotype. In fact, even while adopting a western diet in adulthood allows the disease to advance, children with poor nutrition-induced obesity are particularly susceptible to develop type 2 diabetes in the future (Velasquez-Mieyer et al., 2005).

Additionally, each minipig that received a diabetogenic intervention was compared to itself at the start of the treatment (Baseline), serving as their "own control." Consequently, there is no proper "control group" in the design of this study, allowing to exclude for example: the potential bias due to the aging of animals during the protocol, the "season effect" or the environmental variations of the housing difficult to control. However, pigs are less susceptible than rodents to environmental changes, and they age very slowly during a 2-month period compared to their 20-year average lifespan. We sought also to limit the number of minipigs included in this research in order to respect the principle of "Reduction" relevant to the use of animals for scientific purposes.

Concerning statistics: the type-II error, associated to statistical analyses, especially t-tests and two-way ANOVA in our case, could have prevented us to highlight differences between strains or interventions, although the estimated minimal number of animals in each group was sufficient to demonstrate an effect.

Finally, to describe the metabolic profile of the pigs, we used human indicators of insulin sensitivity and secretion. Additionally, there is no accurate method for measuring visceral obesity in animals, and no defined standard values exist for defining diabetes, prediabetes, or dyslipidemia in pigs. This is why the metabolic syndrome that we found in Group 2 needs to be assessed in light of these factors.

V. Conclusion

In summary, we were successful in developing a preclinical minipig model with early signs of glucose intolerance and metabolic syndrome, but we were unsuccessful in obtaining a model of type 2 diabetes. The pig continues to be a useful preclinical large animal model for imitating the metabolic syndrome, including insulin resistance, visceral obesity, and dyslipidemia, as we have verified in this work. The minipig, however, has more to contribute as a healthy model, supporting the necessity to choose the proper species for each type of study. The continued difficulty of the pig in achieving a fasting hyperglycemia may prompt us to rethink utilizing it as a translational diabetic subject in accordance with the WHO definition of diabetes mellitus.

Furthermore, we only observed metabolic alterations consistent with the early pathophysiology of the illness when lipid and glucose overabsorption were mimicked, supporting the idea that intestinal glucose overabsorption may be one of the root causes of the development of type 2 diabetes.

The healthy minipig model will be used in the next sections of this thesis to clarify the impact of intestinal glucose absorption on the postprandial glycemic response.

Part 3

Validation of D-Xylose Test as a Relevant Biomarker of Intestinal Glucose Absorption

I. Introduction

The development of a model for measuring intestinal glucose absorption was the main topic of this third section. In fact, intestinal glucose absorption is a variable that is challenging to measure because, at a given time, glycemia is the result of all the entrance and exit flux of glucose through the blood compartment. In addition to intestinal glucose absorption, there are numerous other mechanisms that contribute to glucose homeostasis, such as glucose uptake by tissues or endogenous glucose production. Only the entrance flux of glucose from the intestine needs to be targeted for an accurate quantification of intestinal glucose absorption.

Our intestinal glucose absorption modeling should be accurate, applicable to humans *in vivo*, and able to collect data from large cohorts in order to support our hypothesis and achieve our objectives. This model will be used to better understand the contribution of intestinal glucose absorption on postprandial glycemic response and to achieve precision medicine.

This part of the project was performed in collaboration with the Centre de Recherche en Nutrition Humaine Rhône-Alpes (CRNH) and the Centre de Recherche en informatique Signal et Automatique de Lille (CRISAL).

1. Existing methods of *in vivo* intestinal glucose absorption assessment and limits

1.1 Catheterization of the portal vein and carotid artery

Rerat introduced this technique for the first time in 1980. Due to its close resemblance to human gastrointestinal physiology, the pig was chosen for this study as the species to develop this technique (Rerat, 1980).

The porto-arterial difference in glucose concentration represents a qualitative assessment of its absorption by indicating the level of enrichment of the portal blood draining the whole intestine compared to the afferent arterial blood of the gut. The simultaneous measurement of the blood flow rate in the portal vein allows for a quantitative evaluation of the glucose absorption. By inserting long-term catheters into the carotid/mesenteric artery or portal vein, the artery and portal blood can be collected. Numerous methods, including the electromagnetic flowmeter described by Rerat and the ultrasonic flowmeter (Bach Knudsen et al., 2000; Hooda et al., 2009), can be used to measure the portal blood flow rate.

The intestinal glucose absorption is thus calculated by this equation: $Q(t) = (C_p - C_a) D dt$, where $(C_p - C_a)$ indicates the porto (C_p) - arterial (C_a) differences in glucose concentration, D the portal vein blood flow and Q the amount of glucose absorbed within the time interval dt . This formula can also be transposed for other nutrients.

This quantification only accounts for the apparent glucose absorption rather than the actual glucose uptake because it ignores the ability of the enterocytes to metabolize glucose. The porto-arterial difference would be negative if there was an excess of glucose metabolism by the enterocytes compared to absorption (Rerat, 1980).

The main drawbacks of this approach are the surgical procedures, postoperative management, catheter maintenance, and accurate blood flow measurement. Effectively, measuring blood flow is the essential component of quantitatively measuring glucose absorption. Because electromagnetic flow probes encourage the growth of fibrous tissues between the sensor and the vessel wall, reducing the flow rate abnormally in long-term studies, the use of ultrasonic flowmeters was claimed to be more accurate (Hooda et al., 2009). Due to all of these factors, these methods have only been occasionally used in recent years (Bach Knudsen et al., 2000; Hooda et al., 2009; Noah et al., 2000).

Finally, it cannot be used in clinical research due to ethical considerations, rendering this method useless for future studies.

1.2 Multiple isotopic glucose labeled techniques

1.2.1 Principle

Other methods, which are currently used in humans and involve the use of multiple isotopic tracers of glucose, can also be used to measure intestinal glucose absorption. In these techniques, glycemic balance at a defined time is modeled as the result of the entrance and exit fluxes of glucose in the blood compartment: the rate of appearance of exogenous glucose in the systemic circulation (RaE) and the endogenous glucose production (EGP) constitute the main entrance fluxes, whereas glucose utilization by the organs, also called the rate of disappearance of total glucose (RdT), constitute the main exit fluxes (McMahon et al., 1989). RaE is considered an indirect approximation of intestinal glucose absorption, even if it does not consider splanchnic glucose uptake (Boers et al., 2019).

The global turnover of glucose by the organism can be seen by measuring these rates in humans using stable isotopes of glucose to track the fate of exogenous, endogenous, and total (the sum of exogenous and endogenous) glucose. Two (McMahon et al., 1989; Tricò et al., 2015) or three (Basu et al., 2003; Vella and Rizza, 2009) isotopic tracers of glucose can be involved: ^{13}C -labeled glucose as the ingested tracer during an oral glucose tolerance test (OGTT) and $[3\text{-}^3\text{H}]$ - or $\text{D-[6,6-}^2\text{H}_2]$ -labeled glucose as primed continuous intravenous infusions. The use of a third intravenous glucose tracer involves a different modeling of postprandial glucose turnover, permitting a more accurate measurement of endogenous glucose production (Basu et al., 2003). The kinetics of appearance and disappearance of total glucose are thus tracked using $\text{D-[6,6-}^2\text{H}_2]$ -labeled glucose and those of appearance and disappearance of exogenous glucose using ^{13}C -labeled glucose. The $\text{D-[6,6-}^2\text{H}_2]$ -labeled glucose is given as a continuous

intravenous infusion (following a bolus for a better balance of the tracer in the plasmatic compartment) for the evaluation of the kinetics of total glucose (**Figure 47**). After 120 minutes, the isotopic balance is achieved.

Stable isotopes of glucose have several advantages (Delarue and Beylot, 2007):

- they are safe, due to their non-radioactivity
- they allow to determine at the same time the ratio tracer/tracee and the concentration of the molecule of interest thanks to the simultaneous utilization of an internal standard for analyses
- the isotopic fractionation, which means the preferential utilization of an isotope compared to another during an enzymatic reaction, is almost always negligible for deuterium (^2H) or ^{13}C .

A modified technique entails replacing the oral ^{13}C -labeled glucose with a corn-based plant meal that is naturally high in ^{13}C . In fact, due to the activity of some enzymes during photosynthesis, some plants are more focused on the incorporation of ^{13}C than ^{12}C . They are consequently ^{13}C enriched naturally (O'Leary, 1981). Corn, cane sugar, and succulent plants are examples. Following their consumption, ^{13}C -glucose can be tracked in the plasma. This technique enables the assessment of postprandial glucose fluxes following the intake of carbohydrates with a variable Glycemic Index (Nazare et al., 2010b; Noah et al., 2000; Péronnet et al., 2015; Wachters-Hagedoorn et al., 2006).

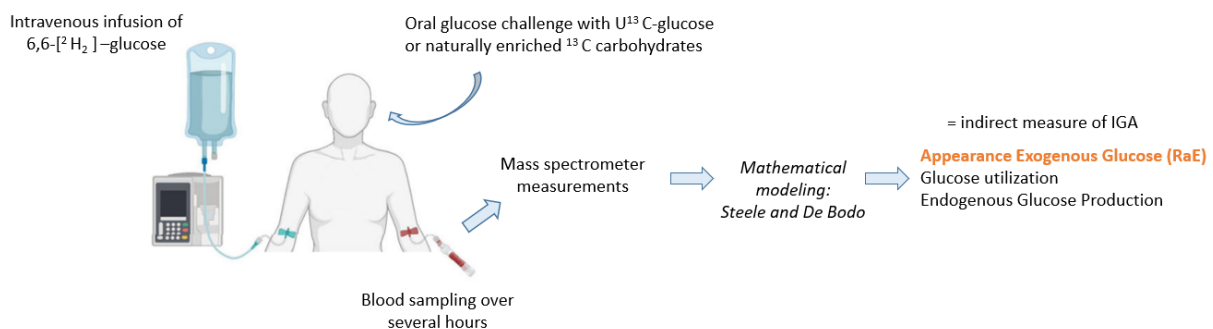


Figure 47: Experimental design of a dual-tracer meal test for intestinal glucose absorption assessment

1.2.2 Analyses

Then, using mass spectrometry coupled to gas chromatography, the plasmatic enrichment of both isotopic tracers of glucose during an oral carbohydrate challenge is determined. Before injection into the gas chromatography column, the plasmatic glucose is subjected to a step of derivatization to become volatile and stable. Following its removal from the gas chromatography column, the derivative glucose molecule is ionized and fragmented, always following the same pattern, into molecular ions and other smaller fragments, which together make up the mass spectrum. Through their entry into a magnet, the various fragments are sorted according to their mass before being collected.

Compared to the more prevalent natural molecule, the stable isotopes of glucose (^2H and ^{13}C) are heavier. The increase in the ratio $M+n/M$ above the level of natural abundance, where M is the mass of the more abundant molecule and $M+n$ is the mass of the heaviest isotopes of this molecule, is an indicator of the enrichment of labeled glucose. Organic or isotopic mass spectrometers thus allow to determine the enrichments, with a limit of detection of 0.5 to 1 % for the organic and a much lower threshold of 0.001 % for the isotopic mass spectrometers (Nazare, 2009).

1.2.3 Calculations

Once the enrichment measure has been determined, all of the rates that constitute the postprandial turnover of glucose are calculated. The rates are thus as follows:

- Rate of appearance of Total glucose (RaT): appearance of glucose ingested and endogenous-produced by the peripheral tissues
- Rate of disappearance of Total glucose (RdT): utilization of glucose, from the meal and endogenous-produced, by the peripheral tissues
- Rate of appearance of Exogenous glucose (RaE): appearance of glucose ingested during a meal in the systemic circulation, approximation of intestinal glucose absorption
- Rate of disappearance of Exogenous glucose (RdE): utilization of glucose, from the meal only, by the peripheral tissues
- Endogenous Glucose Production (EGP): glucose produced by the liver, the kidney or the intestine thanks to gluconeogenesis

Calculations of the rate of appearance of total glucose (RaT) and the rate of disappearance of total glucose (RdT)

RaT and RdT are calculated using the non-steady state of Steele as modified by De Bodo (DeBodo et al., 1963; Steele et al., 1956), using a single-compartmental model and a uniform repartition. RaT and RdT calculations (in mg/kg/min) are based on the enrichment values of plasmatic D-[6,6- $^2\text{H}_2$]-labeled glucose, according to the following formula:

$$\text{RaT} = \frac{F - pV \left[\frac{C_2 + C_1}{2} \right] \left[\frac{IE_2 - IE_1}{t_2 - t_1} \right]}{\frac{IE_2 + IE_1}{2}} - F$$

$$\text{RdT} = \text{RaT} - pV \frac{dC}{dT} = \text{RaT} - pV \frac{C_2 - C_1}{t_2 - t_1}$$

F: perfusion rate of the D-[6,6- $^2\text{H}_2$]-labeled glucose tracer, in mg/kg/min

P: correction factor

V: volume of distribution of glucose in L/kg

C1 and C2: respective glycemia in time t1 and t2 in mg/L

IE1 and IE2: isotopic enrichment at t1 and t2

t1 and t2: two consecutive time of blood collection

Calculations of the rate of appearance of exogenous glucose (RaE) and the rate of disappearance of exogenous glucose (RdE)

The rates of appearance and disappearance of exogenous glucose are evaluated relative to the natural plasmatic enrichment of ¹³C at baseline. The Atom% Excess (APE) is thus the measure (%) of the increase of the isotopic abundance in the sample.

APE ¹³C plasmatic glucose (t) = Atom% ¹³C plasmatic glucose (t) – Atom% ¹³C plasmatic glucose (t0)

RaE and RdE (in mg/kg/min) are thus calculated using the formula of Proietto, following the transposition of the Steele equation (Proietto et al., 1987).

$$RaE = \frac{\left[RaT \times \frac{APE2 + APE1}{2} \right] + \left[pV \times \frac{C1 + C2}{2} \times \frac{APE2 - APE1}{t2 - t1} \right]}{APE \text{ ingested glucose}}$$

$$RdE = RaE - \frac{\left[pV \times \frac{C1 + C2}{2} \times \frac{APE2 - APE1}{t2 - t1} \right]}{APE \text{ ingested glucose}}$$

P: correction factor

V: volume of distribution of glucose in L/kg

C1 and C2: respective glycemia in time t1 and t2 in mg/L

APE1 and APE2: Atom% Excess at t1 and t2 in %

t1 and t2: two consecutive time of blood collection

Calculation of Endogenous Glucose Production (EGP)

Endogenous Glucose Production (EGP) (in mg/kg/min) is calculated as the difference between the rate of appearance of total glucose and the rate of appearance of exogenous glucose: EGP = RaT – RaE.

1.2.4 Limits

The rate of appearance of exogenous glucose (RaE) is thought to be the most accurate in vivo estimate of intestinal glucose absorption that can be used in clinical research.

However, RaE does not totally represent intestinal glucose absorption but rather: the appearance of labeled glucose absorbed by the intestine and that is not captured by the liver during the hepatic first pass; the labeled glucose captured by the liver during different hepatic passages and released later; and the labeled glucose neosynthesized by the liver from labeled lactate produced by peripheral tissues from labeled glucose (Korach-André et al., 2004).

Furthermore, the use of these sophisticated techniques is constrained because they call for expertise and because the analysis can only be done in specialized facilities. In large patient cohorts, multiple glucose labeled techniques cannot be used.

1.3 Positron emission tomography (PET scan)

Positron emission tomography (PET scan) is another technique. This method can be used to evaluate how glucose is distributed throughout the entire organism.

After oral administration of one or several non-metabolized glucose tracers such as α -methyl-4- ^{18}F fluoro-4-deoxy-D-glucopyranoside (Me-4FDG, specific from SGLTs), 2-deoxy-2- ^{18}F fluoro-D-glucose (2-FDG, specific from GLUTs), or 4-deoxy-4- ^{18}F fluoro-D-glucose (4-FDG, substrate for both SGLTs and GLUTs), PET scan allows to record the distribution of tracers throughout the whole organism with high spatial and temporal resolution (Sala-Rabanal et al., 2018). The activity intensity of the tracer at a specific time and area of the body assesses intestinal glucose absorption.

Though particularly well-suited for small animals like rodents (Cavin et al., 2016; Schmitt et al., 2017), quantifying intestinal glucose absorption via PET scan is not adapted to clinical research for this purpose due to ethical considerations.

1.4 3-O-Methyl-D-Glucose (3-OMG)

In vivo intestinal glucose absorption can also be measured using 3-O-Methyl-D-Glucose (3-OMG) as a more straightforward proxy (Pham et al., 2019; Wu et al., 2017).

It is a synthetic glucose analog that is excreted in the urine and actively absorbed in the intestine by SGLT1 and passively by GLUT2 (Erdman et al., 1991; Fordtran, 1962). Following oral administration of a fixed dose of 3-OMG, the plasma concentration of 3-OMG can be determined using gas chromatography-mass spectrometry (Shojaee-Moradie et al., 1996). This method enables the comparison of 3-OMG appearance in the plasma between groups (Kuo et al., 2010a; Nguyen et al., 2016, 2014a) but does not provide an absolute quantification of the rate of glucose absorption because 3-OMG disposal is not estimated (Thazhath et al., 2014).

Since its disposal is not considered, 3-OMG plasmatic levels are not regarded as a validated method of assessment but can nonetheless provide information about intestinal glucose absorption. Additionally, it is an expensive method that requires specialized knowledge due to its plasmatic quantification by mass spectrometry.

2. D-Xylose: a proposed biomarker to assess intestinal glucose absorption in vivo

The in vivo intestinal glucose absorption assessment techniques currently available have limitations. The use of multiple glucose labeled techniques is regarded as the gold-standard intestinal glucose

absorption modeling method that is applicable to humans, but it is technically difficult and does not allow for the collection of data on large patient cohorts, which emphasizes the need for a novel biomarker that is simpler to use. Thus, we suggested D-Xylose as a new proxy for modeling intestinal glucose absorption. D-Xylose is simple to measure in the plasmatic compartment thanks to colorimetric methods (Eberts et al., 1979).

2.1 Intestinal absorption

One review particularly focused on the study of this five-carbon monosaccharide (Craig and Atkinson, 1988). The primary natural sources of D-Xylose are hemicellulose from plants, including hardwood, grasses, cereals, and algae (Petzold-Welcke et al., 2014). However, it is also readily synthesized.

D-Xylose is highly absorbed by the small intestine of many species when they are in a healthy state; its bioavailability was estimated to be approximately 70 % in humans (Craig et al., 1983), 80 % and 95 % in young and old rats, respectively (Yuasa et al., 1995), and more than 95 % in pigs and poultry (Huntley and Patience, 2018a). D-Xylose absorption in the large intestine, however, is essentially negligible (Yuasa et al., 1997). There is little information available about the ability of the microbiota to ferment D-Xylose in the large intestine. Microbiota fermentation in the small intestine is possible but should be negligible. The rate of disappearance of dietary D-Xylose shown above was measured prior to the caecum (Huntley and Patience, 2018a).

The mechanism of intestinal D-Xylose absorption in the literature is in favor of a transport similar to the one of glucose, active by SGLT1 and passive by GLUT2. The uptake of D-Xylose from the intestinal lumen to the enterocyte occurs by the apical SGLT1 transporter but with a lower affinity than the one of D-Glucose (Wright et al., 2011). Additionally, even though D-Xylose does not affect the abundance of GLUT2 at the basal pole (Miyamoto et al., 1993), this transporter allows it to join portal blood system by facilitate diffusion (Koepsell, 2020). As shown *ex vivo* in hamsters (Alvarado, 1966) and rats (Csaky and Lassen, 1964) for low D-Xylose levels in the media, the presence of D-Xylose in the intestinal lumen stimulates the SGLT1 transporters, and its absorption appears to depend on the presence of sodium ions. Furthermore, as demonstrated *ex vivo* in humans, glucose appears to be a competitive inhibitor of D-Xylose intestinal absorption (Rolston and Mathan, 1989). Phlorizin, a SGLT1 inhibitor, has also been shown to inhibit the intestinal transport of D-Xylose in rats (Fujita et al., 1998) as well as pigs (Baud et al., 2016), supporting its mechanism of intestinal transport similar to glucose.

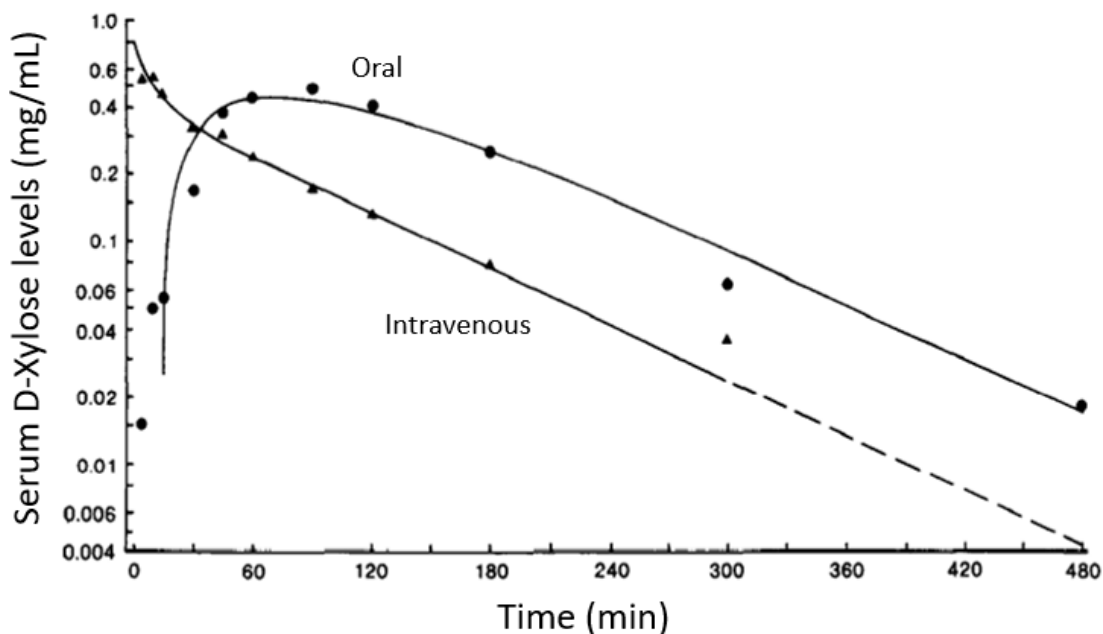


Figure 48: Kinetic analyses of serum D-Xylose concentrations after administering 10-g intravenous (triangles) and 25-g oral (circles) doses to a normal subject. Adapted from (Craig et al., 1998)

The lines are least-squares fits of the measured values shown by the data points.

After oral D-Xylose administration, an absorption lag time of 22 minutes was described in normal subjects, probably reflecting the time required for gastric emptying (Figure 48). The rate constant K_a , reflecting the rate of intestinal absorption, was estimated at 1.03 ± 0.33 /h (Craig et al., 1983) and the absorption half-life time was estimated at 31 ± 12 minutes in normal subjects but seems to be prolonged in patients with uncomplicated renal impairment at 62 ± 23 minutes, although the total extent of D-Xylose absorbed remains unchanged (Worwag et al., 1987).

2.2 Distribution, metabolism and elimination

By administering 10 g of D-xylose intravenously (Figure 48), it was possible to calculate its distribution volume, which was estimated to be 2.3 dL/kg in healthy subjects and 3.2 dL/kg in patients with uncomplicated renal impairment (Worwag et al., 1987). Its distribution volume is thus generally similar to estimates of the extracellular fluid space (Craig and Atkinson, 1988).

The elimination of D-Xylose is essentially renal, with an elimination-phase half-life time calculated at 75 ± 11 minutes in healthy individuals and prolonged at 138 ± 39 minutes in patients with renal impairment (Worwag et al., 1987). Approximately 50 % the total dose of D-Xylose administered is excreted intact in urines, as demonstrated in humans (Christiansen et al., 1959; Huntley and Patience, 2018b; Wyngaarden et al., 1957).

The fate of the remaining D-Xylose is incompletely understood. But approximately 5 % of the administered dose is eliminated intact in bile (Craig and Atkinson, 1988), 15 % is converted to CO_2

(Segal and Foley, 1959) and to D-threitol (a 4-carbon monosaccharide) as the main identified urinary D-Xylose metabolite (Huntley and Patience, 2018b; Pitkänen, 1977). D-Xylose is converted to D-threitol in the liver.

2.3 Clinical use as a qualitative test

D-Xylose urinary levels were initially used in clinical conditions to identify glucose/galactose malabsorption. The initial oral administration of D-xylose ranged from 0.5 to 25 g. However, the dose of 25 g was believed to be more discriminating to detect intestinal malabsorption because abnormal patients could absorb a lower dose more completely despite their disease. Patients with a 5-h urine D-Xylose excretion value less than 5 g after a 25-g oral administration were regarded as having intestinal malabsorption. Because D-Xylose intestinal absorption is independent of pancreatic enzymes, this test was able to distinguish proximal intestinal disease from pancreatic insufficiency. According to studies conducted on adults, the 25-g D-Xylose test has been claimed to be useful for diagnosing proximal malabsorption (Craig and Atkinson, 1988).

The inclusion of D-Xylose serum analyses has since been suggested as a way to improve the accuracy of the test. A number of studies that used the 1-hour serum D-Xylose level were reviewed (Craig and Atkinson, 1988). It was used as a complementary marker to evaluate intestinal malabsorption (Beck et al., 1962; Buts et al., 1978; Finlay et al., 1964). According to Craig and Atkinson, a 1-hour serum D-Xylose value of less than 25 mg/dL in adults was predictive of an abnormal small intestinal biopsy with a sensitivity of 91 % and a specificity of 98 %. Accordingly, serum D-xylose concentrations were thought to be a helpful adjunct to urine measurements in the study of intestinal disturbances (Roberts and Beck, 1960), both in clinical settings and in experimental research (Antunes et al., 2009).

Intestinal malabsorption and proximal intestine enteropathies are now frequently identified using urinary and serum D-Xylose levels as a qualitative test.

2.4 Using D-Xylose as a quantitative biomarker for intestinal glucose absorption assessment?

Even though D-Xylose has historically only been used as a reliable qualitative test to identify malabsorption, some evidence suggests that it may be used as a quantitative method to measure intestinal glucose absorption.

In a study by our team, an *in vivo* experiment carried out on minipigs under general anesthesia clearly showed that D-Xylose is absorbed by the small intestine using the same mechanism as glucose (Baud et al., 2016). In the presence or absence of bile, different mixes of [glucose + D-Xylose] and [glucose + D-Xylose + phlorizin] were administered directly into a jejunal limb, and the plasmatic levels of glucose and D-Xylose were assessed after administration (**Figure 49**). There was no absorption of D-Xylose or glucose in the absence of bile administration into the jejunal limb, but both substrates were

reabsorbed after bile was added. No matter whether bile was present or not, adding phlorizin to the mixture prevented the absorption of glucose and D-Xylose. The primary source of sodium ions needed for absorption is bile. Therefore, this experiment successfully showed that the transport of D-Xylose through the intestinal wall occurs by the active mechanism involving SGLT1 at the apical pole of the enterocytes.

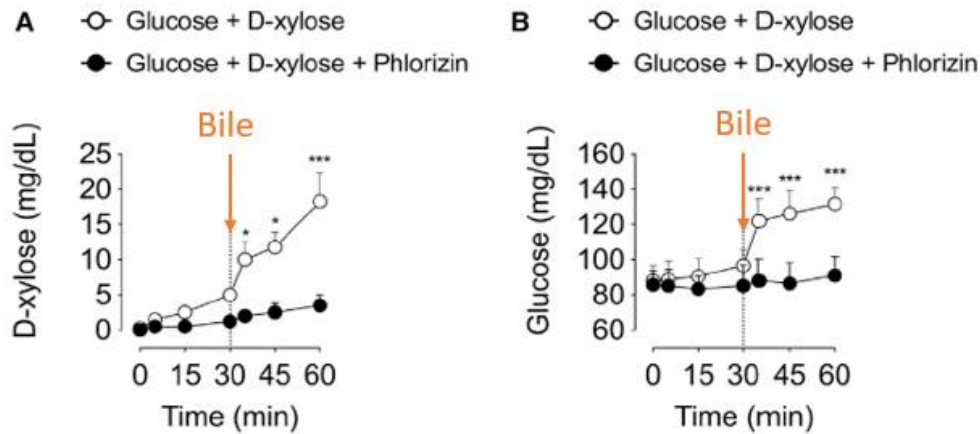


Figure 49: Active transport of D-Xylose across the intestinal wall, similar to the one of glucose. Adapted from (Baud et al., 2016).

Plasma D-Xylose (A) and glucose (B) concentrations following instillation of glucose and D-Xylose into the intestine (white circles, n = 4) or glucose, D-Xylose and phlorizin (black circles, n = 4) before and after administration of the bile (arrow).

The active transport of D-Xylose was shown in another rat study (Fujita et al., 1998) using an oral glucose tolerance test and an oral D-Xylose loading test, without or with co-administration of phlorizin (Figure 50). The study also revealed variations in D-Xylose profiles according to postprandial glycemic response.

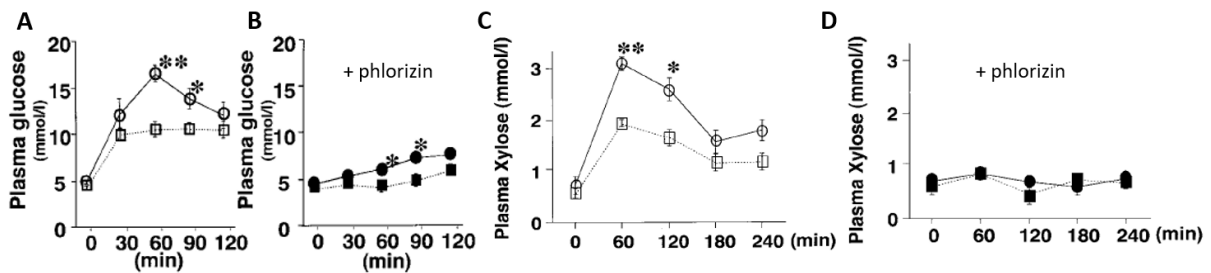


Figure 50: Variation of D-Xylose according to postprandial glycemic response in rats and active transport across the intestinal wall. Adapted from (Fujita et al., 1998).

(A-B) Plasma glucose concentration without phlorizin (A) and with co-administration of phlorizin (B) in rats with obesity (squares, n = 5) or obesity and type 2 diabetes (circles, n = 5).

(C-D) Plasma D-Xylose concentration without phlorizin (C) and with co-administration of phlorizin (D) in rats with obesity (squares, n = 5) or obesity and type 2 diabetes (circles, n = 5).

3. Aims and hypothesis

To resume the previous elements: D-Xylose is thus a five-carbon monosaccharide, actively transported through the intestinal wall via SGLT1 (and passively via GLUT2 at the basal pole) but with a lower affinity than glucose; it is mainly urinary excreted and only partially metabolized; finally, it is easy to measure in the plasmatic compartment thanks to standard colorimetric methods. If the present use of D-Xylose is admitted for detecting intestinal malabsorption, some previous evidence suggests its use as a quantitative marker to assess intestinal glucose absorption *in vivo*.

Thus, we formulated the hypothesis that D-Xylose is a good candidate for assessing *in vivo* intestinal glucose absorption modeling and that it could give the same information as gold-standard glucose labeled methods. D-Xylose would more accurately represent the absorption of complex carbohydrates than glucose (as monosaccharide) because it has a lower affinity for the SGLT1 transporters than glucose does. D-Xylose would also have the benefit of being more easily administered to large patient cohorts.

In this experimental section, we used D-xylose in healthy minipigs to model intestinal glucose absorption. We then compared the results of this model to a gold-standard glucose labeled method that used complex carbohydrates that were naturally ¹³C-enriched to validate its performances.

III. Materials and Methods

1. Ethical statement

This project was approved by the local French Committee of Animal Research and Ethics (CEEA-75, n°#12467 and n°#38311), in accordance with European law (2010/63/EU directive). All the procedures were carried out in the agreed-upon (n°D59-35010) Département Hospitalo-Universitaire de Recherche et d'Enseignement (Dhure) in the Faculty of Medicine in Lille, France.

2. Study design

Using D-Xylose in a minipig model, we developed a model of intestinal glucose absorption in this section of the study. We started by researching and confirming some D-Xylose pharmacokinetics parameters in minipigs, which enabled us to elaborate models for intestinal glucose absorption. The objective of the modeling work was to assess the Rate of Appearance of D-Xylose (Ra D-Xylose). The Rate of Appearance of Exogenous Glucose (RaE Glucose) was determined by a gold-standard dual tracers method utilizing complex carbohydrates that were naturally enriched in ¹³C. We then compared Ra D-Xylose produced by our various model proposals with RaE Glucose obtained by the dual-tracers method.

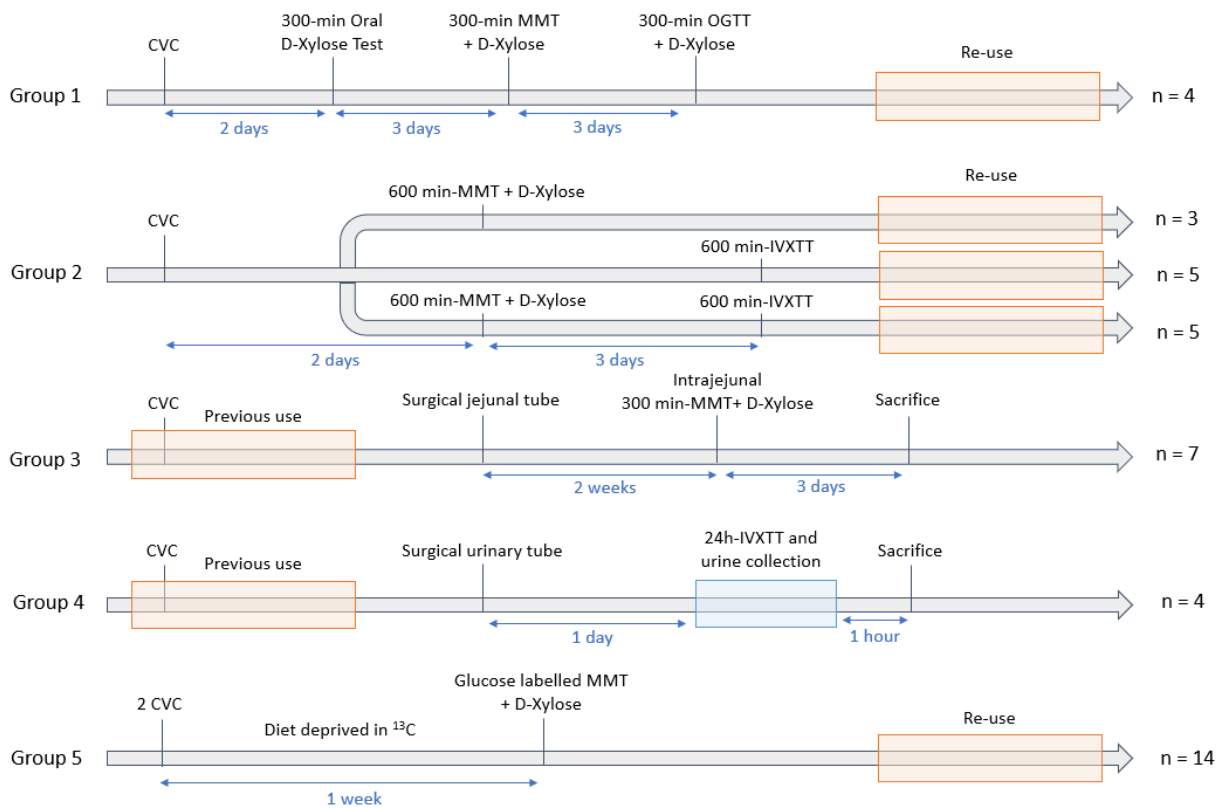


Figure 51: Experimental design of this project

CVC = Central Venous Catheter. MMT = Mixed Meal Test. OGTT = Oral Glucose Tolerance Test. IVXTT = Intravenous D-Xylose Tolerance Test. The orange boxes represent parts of the protocol in which the animals were used for another purpose. The blue box represents the 24h-IVXTT duration.

For this purpose, we constituted 5 groups of animals, as described in **Figure 51**.

In Group 1, we investigated whether D-xylose and glucose might compete with one another for intestinal absorption. The identical minipigs (n=4) were subjected to oral D-Xylose testing singly, mixed meal tests with D-Xylose (MMT), and oral glucose tolerance tests (OGTT) with D-Xylose. The option of using D-Xylose concurrently with a mixed meal test was chosen for the remaining steps of this investigation.

In Group 2, we carried out 600-min MMT (n = 8) and 600-min Intravenous D-Xylose Tolerance Tests (IVXTT) (n = 10) on minipigs to investigate some pharmacokinetics parameters of D-Xylose. Five minipigs in this group received 600 min-MMT and 600 min-IVXTT. To assess the plasma D-Xylose kinetics levels independently of gastric emptying, intrajejunal 300 min-MMT (n=7) were carried out in Group 3. We were able to develop modeling of D-Xylose intestinal absorption thanks to the plasma D-Xylose levels from Groups 2 and 3.

In Group 4, we used IVXTT and urine collection to assess the percentage of intact D-Xylose recovered in urines and its fraction transformed into D-threitol.

In Group 5, we carried out glucose labeled MMT that also contained D-Xylose using naturally ¹³C-enriched complex carbohydrates (n=14).

Animals from Groups 1, 2 and 5 were re-employed in another protocol and animals from Groups 3 and 4 were previously included in another protocol to respect the ethical principle of "Reduction".

3. Animals and housing

A total of 35 healthy minipigs Göttingen-like (24 females and 11 males) weighing 47.9 ± 6.2 kg (Pannier, Wylde, France) were included in this part of the project. All animals were individually housed in conventional conditions with enrichment and benefited from a 15-day acclimatization period. Water was provided *ad libitum* and standard food given twice a day. The composition of food was previously described in Part 2 of the thesis.

4. Surgical procedures

4.1 Anesthesia and analgesia

All the surgical procedures were performed under general anesthesia, after overnight fasting: premedication with a synergistic intramuscular injection of xylazine (3 mg/kg, Paxman®) and ketamine (5 mg/kg, Ketamine 1000®) and then isoflurane relayed (0.5-4 %, Vetflurane®) (Virbac, Carros, France). During the laparotomy procedures, animals were ventilated with assistance at 20 mpm or left with spontaneous ventilation in case of surgeries not involving a laparotomy. Analgesia was assessed by preoperative intramuscular injection of buprenorphine (15 µg/kg, Bupaq®, Virbac) for central catheter and urinary tube implantation. A single application of a fentanyl transdermal solution (1.3 mg/kg, Recuvyra®, Lilly-Elanco, Neuilly-sur-Seine, France) was used to guarantee pain management (Goutchtat et al., 2021) following the jejunal tube implantation and the 80-% intestinal resection.

4.2 Implantation of Central Venous Catheters (CVC)

This procedure was set up in order to refine blood collection during pharmacokinetic and metabolic tests.

The central venous catheters (Hickman® 9.6-F Single-Lumen CV Catheter; Bard Access System, Salt Lake City, UT, USA) were surgically implanted via the jugular external vein according to the procedure previously described in Part 2 of the thesis. The maintenance of the catheters was performed using heparinized saline solution bolus every 48 hours and the catheters were let in place during all the protocol.

Animals undergoing the gold standard glucose labeled meal test had two central venous catheters inserted, one in each external jugular vein, whereas animals undergoing the other pharmacokinetic and metabolic tests had just one catheter.

4.3 Jejunal tube implantation

In order to evaluate the plasma D-Xylose kinetics independently of the rate of gastric emptying, this procedure was carried out to enable delivery of the MMT directly into the jejunum.

After laparotomy, a 6-Fr gastro-duodenal tube (Vygon®, Ecoen, France) was tunnelized through the right flank. Jejunum was opened thirty centimeters distally to the duodenojejunal junction and the gastro-duodenal tube inserted inside on a 15-cm length. A burse suture was performed with non-resorbable thread (Prolene® 4-0, Ethicon, France) and the tube fixed to the intestine by a Cushing overlock on 5 cm. The intestinal limb was then fixed to the abdominal wall in 4 stiches.

The abdominal wall was finally closed in 3 layers by simple overlock: the peritoneum (Polysorb® 2/0, Medtronic, France), the muscular lay (PDS® 1, Ethicon, France) and the skin (Mersilene® 1, Ethicon, France). The external part of the tube was then sutured to the skin (Mersilene® 1, Ethicon, France).

4.4 Surgical implantation of a urinary tube

This procedure was performed in order to collect urinary sample at defined times after intravenous D-Xylose administration.

A minor incision was made in the supra-umbilical region in front of the bladder after the animal was placed in dorsal decubitus. The abdominal cavity was then opened, revealing the urine bladder. After a tunnelization of the tube in the medial plan, the bladder wall was incised at its apical pole, and a CH18-Pezzer tube was introduced. The vesical incision was closed around the tube with a burse suture (Monocryl® 4-0, Ethicon, France).

The abdominal wall was closed in 2 layers: the muscular layer (PDS® 1, Ethicon, France) and the skin (Mersilene® 1, Ethicon, France) and the external part of the Pezzer tube was fixed to the skin with simple points.

5. Pharmacokinetic and standard metabolic tests

5.1 Oral D-Xylose Test

The day before the test, a 16-Fr nasogastric tube was previously implanted under general anesthesia to allow a standard administration of the mix. The oral D-Xylose test was performed on vigil animals, via dissolution of 30 g of D-Xylose (Sigma-Aldrich®, Merck, France) on 200 mL of tap water. The solution was given via the nasogastric tube on a standard 10-minutes period. Blood samples were taken thanks

to the CVC at t=0 (before the administration of the solution), t=15, t=30, t=60, t=90, t=120, t=180, t=240, and t=300 min and collected in fluorinated tubes. They were centrifuged (4000 rpm for 10 min at 4°C) and plasma was isolated and stored at -80°C until analysis.

5.2 Mixed Meal Test with D-Xylose (MMT)

As described for the oral D-Xylose test, the mixed meal test with D-Xylose was administered on vigil animals, via a 16-Fr nasogastric tube previously set up. Standard Meal Tests consisted in 200 mL of liquid oral supplement (Fortimel Energy®, Nutricia, France) and 20 g solid energy bar Ovomaltine® (Ovomaltine, France) containing 13 g of fat, 15 g of protein, 22 g of simple sugars and 49 g of total carbohydrates (990 kJ, 387 kcal), as previously described in the Part 2 of the thesis. D-Xylose was incorporated into the mix at the dose of 30 g. Blood samples were taken thanks to the CVC at t=0, t=15, t=30, t=60, t=90, t=120, t=180 min, t=240, and t=300 min (and t=600 min for 600 min-MMT) and collected in fluorinated tubes. They were centrifuged (4000 rpm for 10 min at 4°C) and plasma was isolated and stored at -80°C until analysis.

5.3 Oral Glucose Tolerance Test with D-Xylose (OGTT)

For the 75-g oral glucose tolerance test, 150 mL of a 50-% glucose solution (G50®, B. Braun, France) were mixed with 150 mL of tap water. D-Xylose was incorporated into the mix at the dose of 30 g. The mix was administered on vigil animals, as previously described, via a 16-Fr nasogastric tube. Blood samples were taken thanks to the CVC at t=0, t=15, t=30, t=60, t=90, t=120, t=180, t=240, and t=300 min and collected in fluorinated tubes. They were centrifuged (4000 rpm for 10 min at 4°C) and plasma was isolated and stored at -80°C until analysis.

5.4 Intrajejunal Mixed Meal Test with D-Xylose

The mixed meal test (MMT) was administered in vigil animals thanks to the jejunal tube previously implanted during a standard 10-min duration period. The composition of the meal was similar to the one of the oral MMT. Blood samples were taken thanks to the CVC at t=0, t=15, t=30, t=60, t=90, t=120, t=180, t=240, and t=300 min and collected in fluorinated tubes. They were centrifuged (4000 rpm for 10 min at 4°C) and plasma was isolated and stored at -80°C until analysis.

5.5 Intravenous D-Xylose Tolerance Test (IVXTT) and urine collection

The intravenous solution of D-Xylose was prepared in dissolving 30 g of D-Xylose into 100 mL of a sterile NaCl 0.9 % solution. This mix was then filtered through a 0.2 µm membrane filter (Rapid-Flow®, Nalgene®, Thermo Scientific®, France) and injected in less than 3 minutes into the central venous catheter on vigil animal. Blood samples were taken in 10 animals at t=0, t=5, t=10, t=15, t=30, t=45, t=60 min, t=90, t=120, t=180, t=300 and t=600 min and collected in fluorinated tubes. They were centrifuged (4000 rpm for 10 min at 4°C) and plasma was isolated and stored at -80°C until analysis.

Urinary samples were taken at t=0, t=180, t=300, and t=24h for 4 more animals that had a urinary tube implanted the day prior. Animals were housed in metabolic cages that allowed for natural miction collection for this purpose. At each predetermined period, the tube was used to collect the residual urine. At each sampling, the total amount of urine generated was assessed.

6. Gold-standard glucose labeled Meal Test with D-Xylose

The glucose labeled Meal Test consisted in a dual-tracer technique with naturally enriched ¹³C-carbohydrates as oral tracer.

The minipigs were given diet deprived in ¹³C enriched carbohydrates the week before the challenge: 5 days of pellets (SAFE®127, SAFE Diets, Augy, France), followed by 2 days of liquid food (Nutrison®, Nutricia, Rueil-Malmaison, France).

After 24 hours of fasting, the vigil minipigs received first (at t=-120 min) a bolus of D-[6,6-²H₂]-glucose (99 % mol enrichment, Microbiological and Pyrogen Tested, Eurisotop, St Aubin, France) as intravenous tracer in saline isotonic solution at 4.004 mg/kg, as previously described (Noah et al., 2000) via one of the central venous catheters. It was then relayed by a continuous infusion at a rate of 0.06 mg/kg/min (Péronnet et al., 2015) delivered by an infusion pump (SK-600II®, Mano Médical, Taden, France) during 120 min before the administration of the meal and then during the 6-hour oral carbohydrates challenge. The pigs received in total 8 hours of infusion. This solution was previously sterilized by filtration through a 0.22 µm Millipore filter (Millex®-GS, Merck-Millipore Ltd, Tullagreen, Ireland).

The meal was made up of 50 g of cornstarch (Maïzena®, Fleur de Maïs®, Unilever, Londres, UK), which was diluted in 400 mL of tap water, cooked for 3 min 30 s at 70°C, and then mixed for one minute. It contained 86 % carbohydrates and had an energetic density of 744 kJ (178 kcal). Via a 21-Fr nasogastric tube that had been set up the day before the labeled meal test when the animals were under general anesthesia, the mixture was given to the vigil animals during 10 minutes. The standard quantity of 30 g D-Xylose (Sigma-Aldrich®, Merck, France) was incorporated into the mix. Blood samples were taken at t=-120, t=0, t=15, t=30, t=60, t=90, t=120, t=180, t=240, t=300 and t=360 min and collected in heparinized, fluorinated and EDTA tubes. They were centrifuged (4000 rpm for 10 min at 4°C) and plasma was isolated and stored at -20°C until analysis for the samples intended to isotopic enrichment measurement and at -80°C for the others.

7. Postprandial glucose turnover evaluation from isotopic enrichment assessment

The evaluation of the postprandial glucose turnover was carried out according to the methodology previously outlined in this Part 3 of the thesis, paragraph I.1.2.

After deproteinization of the samples with perchloric acid, neutralization with potassium carbonate and derivatization of glucose into glucose penta-acetylaldononitrile (Tissot et al., 1990), isotopic ratios of plasma glucose were measured by gas chromatography positive chemical ionization mass spectrometry (GC/EI-MS, GC 6890-MS5973, Agilent Technologies, Massy, France) for $^2\text{H}/\text{H}$ and by GC/C/IRMS (Isoprime, Isoprime Ltd, Cheadle Hulme, UK) for $^{13}\text{C}/^{12}\text{C}$, as previously described (Sauvinet et al., 2009). Isotopic composition for $^{13}\text{C}/^{12}\text{C}$ ratio ($\delta^{13}\text{C}$) was also determined for each constituent of the meal (-13.32 ± 0.60 and -9.24 ± 0.09 ‰ vs PDB respectively for cornstarch and D-Xylose) after enzymatic hydrolysis into glucose for cornstarch.

The non-steady-state equation of Steele (Steele et al., 1956), as modified by De Bodo et al. (DeBodo et al., 1963) was used to compute the Rate of appearance of Total glucose (RaT, mg/kg/min) from the plasmatic $^2\text{H}/\text{H}$ ratio, the Rate of appearance of Exogenous glucose (RaE, mg/kg/min) from the plasmatic $^{13}\text{C}/^{12}\text{C}$ ratio (Proietto et al., 1987), and their corresponding Rate of disappearance of Total and Exogenous glucose (respectively RdT and RdE, mg/kg/min). Endogenous Glucose Production (EGP, mg/kg/min) was calculated as $\text{EGP} = \text{RaT} - \text{RaE}$.

All these analyses were performed in the Centre de Recherche en Nutrition Humaine Rhône-Alpes, in Pierre-Bénite, France, by the group of Julie-Anne Nazare: Valérie Sauvinet, Laure Meiller and Corinne Louche-Pelissier.

8. Other biological procedures

Concerning oral D-Xylose tests, standard mixed meal tests and oral glucose tolerance tests, glycemia was measured on total blood in duplicate using the amperometric glucose oxydase method (Glucose meter Accu-Check Performa[®], Roche, France). For glucose labeled meal tests, plasma glucose was determined by enzymatic hexokinase UV method (C501 Cobas 8000[®], Roche Diagnostics GmbH, Mannheim) with an assay range between 2 and 750 mg/dL, in the Centre de Biologie-Pathologie of Lille University Hospital by the group of Patrice Maboudou.

Plasma D-Xylose levels were determined by a colorimetric method with phloroglucinol (Eberts et al., 1979) by the glycobiology department of the Centre de Biologie-Pathologie of Lille University Hospital.

Plasma and urinary D-threitol levels were determined by the department of Biochimie Métabolique et Cellulaire - Groupe d'étude des glycopathies at the Bichat Hospital, in Paris, France, by Arnaud Bruneel and Anne Barnier. The D-threitol concentrations were measured with electrospray ionization mass spectrometry (ESI-MS) associated with ultra-high-pressure liquid chromatography (UPLC). The separation of D-threitol was performed in isocratic mode (% of H_2O + ammonium acetate (A) and acetonitrile (B) stable in the column). The standard range was elaborated in 7 points between 0 and

500 μ M in diluting 25 mM of D-threitol (Sigma-Aldrich[®], Merck, France) in 10 mL of H₂O. The conditions in the UPLC column (Acquity UPLC BEH Amide 1.7 μ m, 2.1 x 150 mm, Waters[®], United States) were fixed to 10 % of A and 90 % of B between 0 and 5 min and between 9 and 10 min, and to 90 % A and 10 % between 6 and 8 min, with a rate of 0.4 mL/min and a time of retention of D-threitol of 3.5 min. In the mass spectrometer (TQD, Waters[®], United States), the capillary energy was 1 Volt, the cone energy 20 Volts, the collision energy 10 Volts and the desolvation temperature was 450 °C. The electrospray was in negative mode. A volume of 100 μ L of sample was mixed with 400 μ L of an acetonitrile/methanol solution. After centrifugation (4000 rpm/min during 10 min), 5 μ L of the supernatant was collected for analysis.

9. Intestinal Glucose Absorption modeling with D-Xylose

In total, 4 models of intestinal glucose absorption were proposed.

9.1 “Calculation” model

The first model, called “calculation” model, consisted in the conversion of each data of plasma D-Xylose levels (in mg/dL) to rate of appearance of D-Xylose (Ra D-Xylose, in mg/kg/min). This calculation was made according to this formula:

$$\text{Ra D-Xylose (t) (mg/kg/min)} = [\text{Time-derivated plasma D-Xylose (t) (mg/dL/min)} + (k_{\text{elim}} \text{ (/min)} \times \text{Plasma D-Xylose (t) (mg/dL)})] \times \text{volume of distribution of D-Xylose (dL/kg)}$$

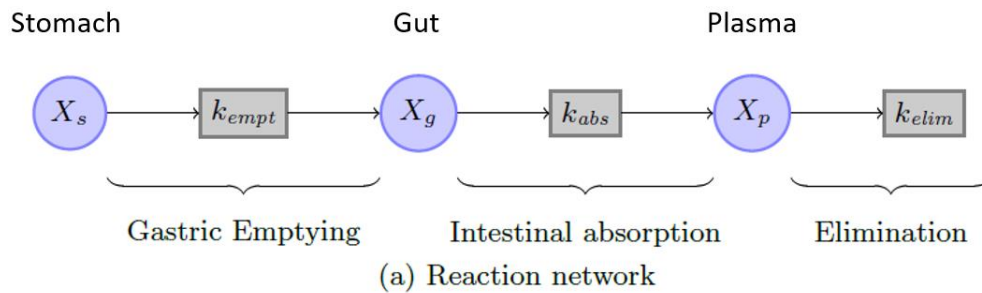
k_{elim} represent the constant of elimination of D-Xylose. It was determined by computational modeling from IVXTT data and fixed at 0.0096 /min. The volume of distribution of D-Xylose, determined for each minipig, was estimated from IVXTT data, in dividing the initial plasma level of D-Xylose following intravenous administration (in mg/dL) by the quantity (30 g) of D-Xylose administered and by the weight of the pig.

9.2 Computational models

The 3 other models were elaborated by the Centre de Recherche en Informatique, Signal et Automatique de Lille, by Cédric Lhoussaine, Danilo Dursoniah and Maxime Folschette.

The computational modeling consisted in using a system of ordinary differential equations for individual parameters estimation. These 3 models were developed using plasma D-Xylose datasets of minipigs collected during IVXTT, oral MMT, and intrajejunal MMT. They allow, thanks to the determination of the k_{abs} parameter relative to intestinal glucose absorption, the prediction of the rate of appearance of D-Xylose (Ra D-Xylose, in mg/kg/min) from experimental plasma D-Xylose levels (in mg/dL). Ra D-Xylose was thus calculated for each of the three models using Visual Studio Code[®] software, the Jupyter[®] computational notebook, and the Julia[®] programming language.

The first computational model, called “simple” model, was elaborated as described in **Figure 52**. The stomach, the gut and the plasma were designed as simple compartments. The rate of gastric emptying, the rate of intestinal absorption, the rate of elimination and bioavailability were the main fluxes defined as interacting between the compartments.



$$\begin{aligned} \dot{X}_s(t) &= -k_{empt} \cdot X_s(t) \\ \dot{X}_g(t) &= k_{empt} \cdot X_s(t) - k_{abs} \cdot X_g(t) \\ \dot{X}_p(t) &= Ra_X(t) - k_{elim} \cdot X_p(t) \\ Ra_X(t) &= k_{abs} \cdot X_g(t) \end{aligned}$$

(b) ODE system

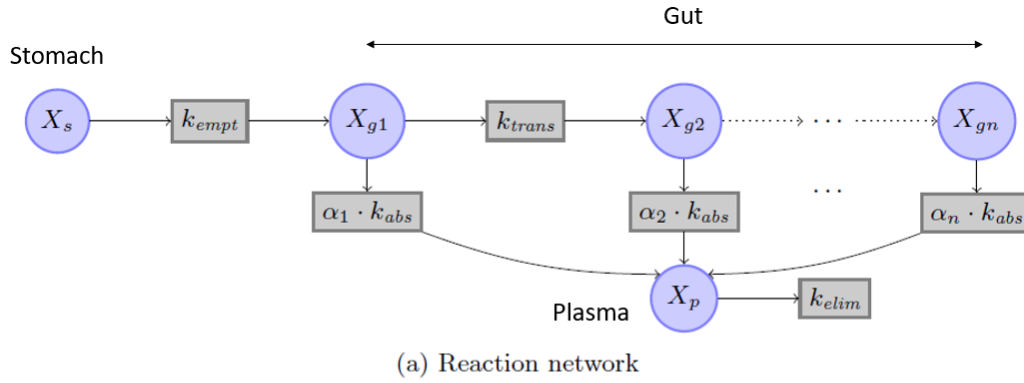
$$\begin{aligned} X_s(0) &= \frac{D_X}{BW \cdot V_{D_X}} \\ X_g(0) &= 0 \\ X_p(0) &= 0 \end{aligned}$$

(c) Initial conditions

Figure 52: “Simple” model proposal for the assessment of the rate of appearance of D-Xylose

$Ra_X(t)$ = Rate of appearance of D-Xylose according to time (mg/kg/min). k_{empt} = rate of D-Xylose gastric emptying (parameter, /min). k_{abs} = rate of D-Xylose intestinal absorption (parameter, /min). k_{elim} = rate of D-Xylose elimination (parameter, /min). $X_s(t)$ = quantity of D-Xylose in the stomach according to time (mg). $X_s(0)$ = quantity of D-Xylose in the stomach at $t=0$ (mg). $X_g(t)$ = quantity of D-Xylose in the gut according to time (mg). $X_g(0)$ = quantity of D-Xylose in the gut at $t=0$ (mg). $X_p(t)$ = quantity of D-Xylose in the plasmatic compartment according to time (mg). $X_p(0)$ = quantity of D-Xylose in the plasmatic compartment at $t=0$ (mg). D_x = administered dose of D-Xylose (mg). BW = Body Weight (kg). V_{dx} = Volume of distribution of D-Xylose (dL/kg). ODE = Ordinary Differential Equations.

The second computational model, called “multi” model, was elaborated as described in **Figure 53**. This multicompartmental design of the gut incorporates the speed of transit and a differential absorption according to fictive different compartment of the small intestine. Thus, the total fraction of D-Xylose absorbed by each intestinal compartment over time was taken into account when calculating the rate of appearance of D-Xylose. The other compartments are designed similarly to the “simple” model.



$$\begin{aligned}
 \dot{X}_s(t) &= -k_{empt} \cdot X_s(t) \\
 \dot{X}_{g1}(t) &= k_{empt} \cdot X_s(t) - (\alpha_1 \cdot k_{abs} + k_{trans}) \cdot X_{g1}(t) \\
 &\vdots \\
 \dot{X}_{gn}(t) &= k_{trans} \cdot X_{gn-1}(t) - \alpha_n \cdot k_{abs} \cdot X_{gn}(t) \\
 \dot{X}_p(t) &= Ra_X(t) - k_{elim} \cdot X_p(t) \\
 Ra_X(t) &= k_{abs} \cdot \left(\sum_{i=1}^n \alpha_i \cdot X_{gi}(t) \right) \text{ and } \sum_{i=1}^n \alpha_i = 1
 \end{aligned}$$

(b) ODE system

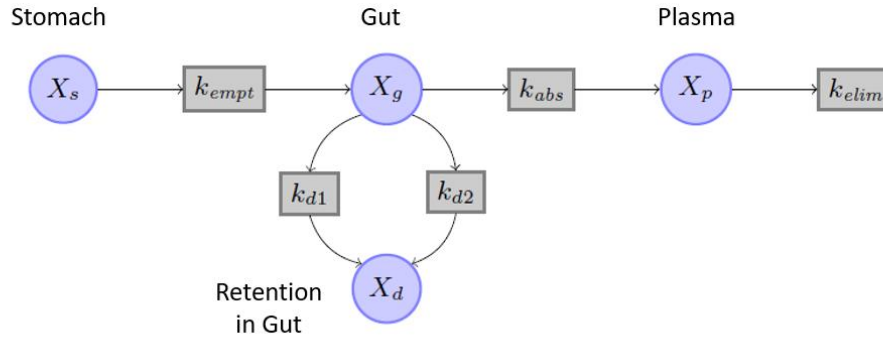
$$\begin{aligned}
 \dot{X}_s(0) &= \frac{D_X}{BW \cdot V_{DX}} \\
 \dot{X}_{g1}(0) &= 0 \\
 &\vdots \\
 \dot{X}_{gn}(0) &= 0 \\
 \dot{X}_p(0) &= 0
 \end{aligned}$$

(c) Initial conditions

Figure 53: “Multi” model proposal for the assessment of the rate of appearance of D-Xylose

$Ra_X(t)$ = Rate of appearance of D-Xylose according to time (mg/kg/min). k_{empt} = rate of D-Xylose gastric emptying (parameter, /min). k_{abs} = rate of D-Xylose intestinal absorption (parameter, /min). k_{elim} = rate of D-Xylose elimination (parameter, /min). k_{trans} = rate of transit (parameter, /min). $X_s(t)$ = quantity of D-Xylose in the stomach according to time (mg). X_{s0} = quantity of D-Xylose in the stomach at $t=0$ (mg). $X_{gi}(t)$ = quantity of D-Xylose in the gut according to time (mg). X_{gi0} = quantity of D-Xylose in the gut at $t=0$ (mg). α_i = coefficient of modulation of k_{abs} for each intestinal subcompartment. $X_p(t)$ = quantity of D-Xylose in the plasmatic compartment according to time (mg). X_{p0} = quantity of D-Xylose in the plasmatic compartment at $t=0$ (mg). D_x = administered dose of D-Xylose (mg). BW = Body Weight (kg). V_{dx} = Volume of distribution of D-Xylose (dL/kg). ODE = Ordinary Differential Equations.

The third computational model, called “retention” model, was elaborated as described in **Figure 54**. A lag time of retention of D-Xylose inside the intestinal lumen was integrated to the “simple” model, corresponding to the time-interval between gastric emptying and intestinal absorption. The other compartments are designed similarly to the “simple” model.



(a) Reaction network

$$\begin{aligned}
 \dot{X}_s(t) &= -k_{empt} \cdot X_s(t) & X_s(0) &= \frac{D_X}{BW \cdot V_{DX}} \\
 \dot{X}_g(t) &= k_{empt} \cdot X_s(t) - (k_{abs} + k_{d1}) \cdot X_g(t) + k_{d2} \cdot X_d(t) & X_g(0) &= 0 \\
 \dot{X}_d(t) &= k_{d1} \cdot X_g(t) - k_{d2} \cdot X_d(t) & X_p(0) &= 0 \\
 \dot{X}_p(t) &= Ra_X(t) - k_{elim} \cdot X_p(t) & X_d(0) &= 0 \\
 Ra_X(t) &= k_{abs} \cdot X_g(t)
 \end{aligned}$$

(b) ODE system

(c) Initial conditions

Figure 54: “Retention” model proposal for the assessment of the rate of appearance of D-Xylose

$Ra_X(t)$ = Rate of appearance of D-Xylose according to time (mg/kg/min). k_{empt} = rate of D-Xylose gastric emptying (parameter, /min). k_{abs} = rate of D-Xylose intestinal absorption (parameter, /min). k_{elim} = rate of D-Xylose elimination (parameter, /min). k_{d1} and k_{d2} = fictive fluxes between the gut and the retention compartment (parameters, /min). $X_s(t)$ = quantity of D-Xylose in the stomach according to time (mg). X_s0 = quantity of D-Xylose in the stomach at $t=0$ (mg). $X_g(t)$ = quantity of D-Xylose in the gut according to time (mg). X_g0 = quantity of D-Xylose in the gut at $t=0$ (mg). $X_d(t)$ = quantity of D-Xylose in the retention compartment according to time (mg). X_d0 = quantity of D-Xylose in the retention compartment at $t=0$ (mg). $X_p(t)$ = quantity of D-Xylose in the plasmatic compartment according to time (mg). X_p0 = quantity of D-Xylose in the plasmatic compartment at $t=0$ (mg). D_x = administered dose of D-Xylose (mg). BW = Body Weight (kg). V_{dx} = Volume of distribution of D-Xylose (dL/kg). ODE = Ordinary Differential Equations.

The bioavailability of D-Xylose was set to 1 (100 %) for each of the three models in accordance with the value previously determined in pigs in the literature (Huntley and Patience, 2018a) and our experimental data. The Elashoff’s gastric emptying kinetic was used to model gastric emptying in the ordinary differential equations system, with β fixed to 1 (Elashoff et al., 1982).

10. Calculations and statistics

As stated, the results were presented as mean \pm SEM for curves and mean \pm SD for histograms. The trapezoidal method was used to calculate areas under the curve (AUC) during a predetermined time after consumption. The graphical visualization was done using GraphPad Prism® 8 program.

Continuous variables were analyzed with paired Student’s t-test. Dynamic variables during meal tests between groups or models were compared using a Two-Way ANOVA or a Mixed-Effects model with

Sidak post-hoc test for multiple comparisons. The presence of interactions between variables were systematically assessed.

Univariate correlations were tested using Pearson coefficients (r). Lin concordance tests were performed to evaluate the concordance between two variables and expressed with 95 % Confidence Interval (CI), using the interpretation of the coefficients of concordance (ccc) of Landis and Koch (Landis and Koch, 1977), according to the method described in (Desquilbet, 2019).

Using RStudio version 4.2.2 and the nlme package, a non-linear mixed model with random intercept was elaborated to predict RaE with D-Xylose appearance. This model was adjusted for weight (in kg), as well as time, that was considered with tail-restricted cubic spline for non-linear effect.

The significance level was established for $p < 0.05$.

III. Results

1. Elements of pharmacokinetics of D-Xylose

First, the existence of a competition between D-Xylose and glucose for intestinal absorption was investigated in performing successively in the same minipigs (Group 1) oral D-Xylose test, Mixed Meal Test (MMT) with D-Xylose and Oral Glucose Tolerance Test (OGTT) with D-Xylose. Results of these tests were presented in **Figure 55**.

There was first no variation of glycemia following oral D-Xylose oral administration on the contrary to following a co-ingestion of MMT or OGTT with D-Xylose, for which postprandial glycemia rose from 77.8 ± 1.5 mg/dL at baseline to 107.1 ± 7.8 mg/dL at 60 min and from 74.4 ± 2.9 mg/dL at baseline to 105.9 ± 13.7 mg/dL at 60 min, respectively for MMT and OGTT (**Figure 55A**).

Secondly, plasma D-Xylose levels were higher when D-Xylose was administered alone, compared to when it was co-administered with MMT or an OGTT, with a significant interaction between the time of the test and groups ($p < 0.005$) (**Figure 55B**). In fact, after singly administration, plasma D-Xylose levels were measured at 39.0 ± 11.8 mg/dL at 30 min and 53.0 ± 9.6 mg/dL at 60 min, compared to 15.8 ± 3.4 mg/dL at 30 min and 25.0 ± 4.7 mg/dL at 60 min for MMT with D-Xylose and 15.0 ± 4.0 mg/dL at 30 min and 22.5 ± 4.7 mg/dL at 60 min for OGTT with D-Xylose.

Moreover, the 300-min areas under the curve (AUC) of plasma D-Xylose were higher when D-Xylose was administered alone compared to when it was co-administered with MMT or an OGTT ($12\,529 \pm 3\,168$ for singly administration compared to $9\,107 \pm 3\,360$ with MMT, $p < 0.05$ and compared to $7\,992 \pm 3\,755$ with OGTT, $p = 0.052$) (**Figure 55C**).

For the next steps of this study, we decided to systematically performed MMT including D-Xylose.

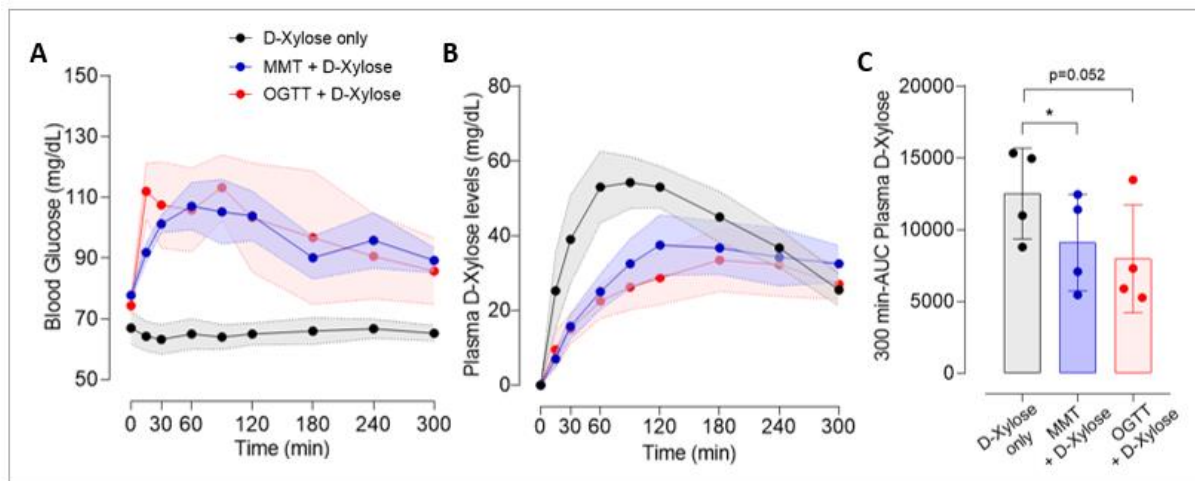


Figure 55: Competition between D-Xylose and glucose for intestinal absorption

(A) Mean of blood glucose levels (Mean \pm SEM, n=4 per group) following oral administration of D-Xylose only (in black), mixed meal test (MMT) with D-Xylose (in blue) and oral glucose tolerance test (OGTT) with D-Xylose (in red)

(B) Mean of plasma D-Xylose levels (Mean \pm SEM, n=4 per group) following oral administration of D-Xylose only (in black), MMT with D-Xylose (in blue) and OGTT with D-Xylose (in red)

(C) Mean of 300-min area under curve (AUC) of plasma D-Xylose (Mean \pm SD, n=4 per group) following oral administration of D-Xylose only (in black), MMT with D-Xylose (in blue) and OGTT with D-Xylose (in red)

Two-Way ANOVA test for repeated measures and Sidak post-hoc test; Paired t-test; *p<0.05

Then, D-Xylose was given to minipigs (Groups 2 and 3) according to several routes of administration in order to determine some parameters of pharmacokinetics. In fact, 600-min oral MMT with D-Xylose, 300-min intrajejunal MMT with D-Xylose and 600-min intravenous D-Xylose tolerance tests (IVXTT) were performed, as shown in **Figure 56**.

After oral administration of MMT with D-Xylose, the mean plasma peak was reached at 90 min, corresponding to a level of 37.3 ± 3.8 mg/dL. D-Xylose levels were almost returned to baseline 600 min after administration (3.4 ± 0.7 mg/dL) (**Figure 56A**). A high interindividual heterogeneity was observed concerning the plasmatic peaks of D-Xylose: 20 mg/dL at 90 min for the pig 3 compared to 50 mg/dL at 90 min for the pig 7 (**Figure 56B**).

After intrajejunal administration of MMT with D-Xylose, the mean plasma peak was reached at 120 min, corresponding to a level of 50.3 ± 1.9 mg/dL (**Figure 56C**). Additionally, variation was seen in the plasmatic peaks of D-Xylose: 42 mg/dL for the pig 3 compared to 56 mg/dL for the pig 4 (**Figure 56D**).

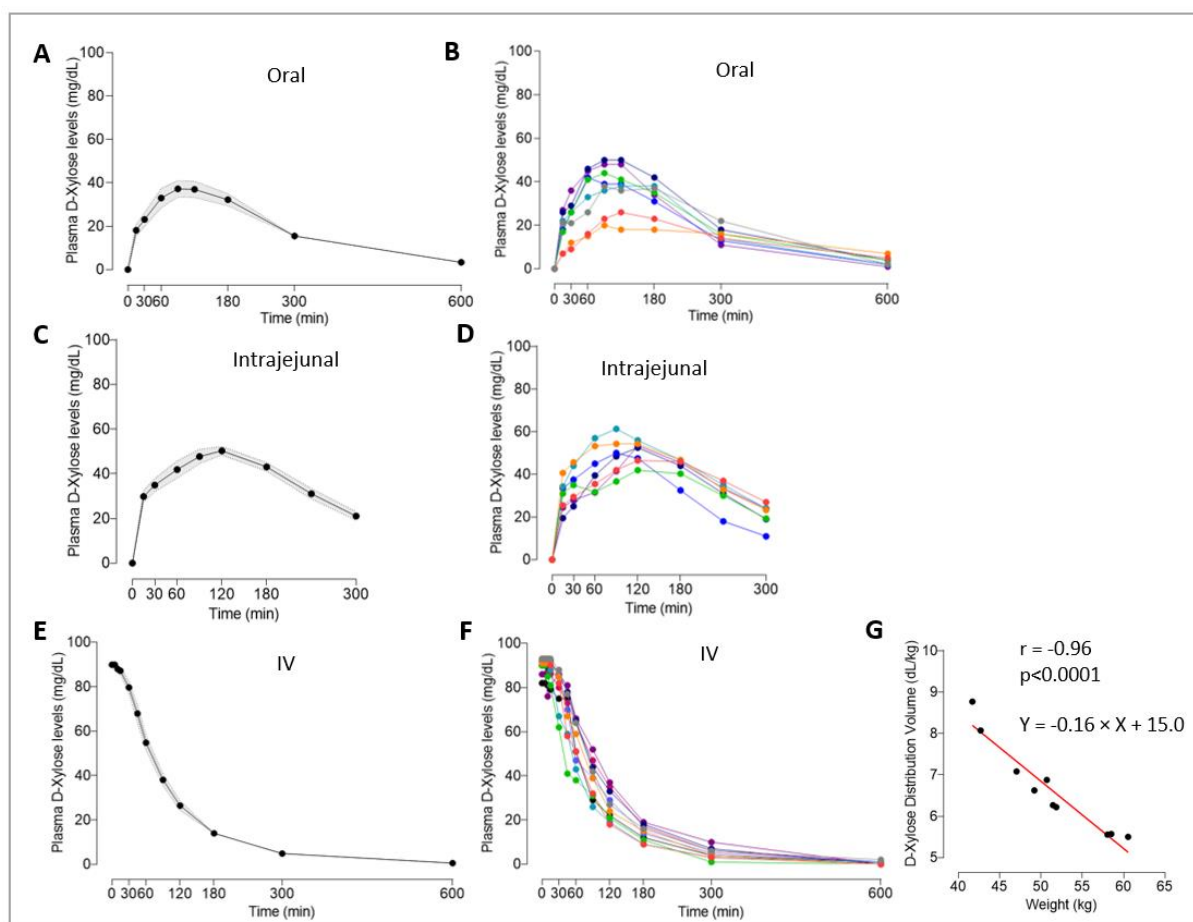


Figure 56: Plasma D-Xylose kinetics according to different routes of administration: oral, jejunal and intravenous

(A-B) Plasma D-Xylose levels following oral mixed meal test (MMT) with D-Xylose: (A) Mean curves (Mean \pm SEM, n=8), (B) Individual curves

(C-D) Plasma D-Xylose levels following intrajejunal mixed meal test (MMT) with D-Xylose: (C) Mean curves (Mean \pm SEM, n=7), (D) Individual curves

(E-F) Plasma D-Xylose levels following intravenous D-Xylose administration: (E) Mean curves (Mean \pm SEM, n=10), (F) Individual curves

(G) Correlation between the volume of distribution of D-Xylose (dL/kg) and the weight (kg)

Correlation with Pearson coefficients: $r = -0.96$, $r^2 = 0.92$, $p < 0.0001$

Following intravenous injection (IVXTT), a declining exponential shape can be seen in the reported drop of plasma D-Xylose (**Figure 56E**). The initial plasma D-Xylose levels after injection were 89.9 ± 1.2 mg/dL and were almost completely returned to baseline at 600 min (0.6 ± 0.2 mg/dL). All minipigs showed a similar decreasing exponential shape of D-Xylose with little interindividual variation (**Figure 56F**). Finally, we found a strong inverse correlation between the volume of distribution of D-Xylose (Vd, in dL/kg) and weight ($r = -0.96$, $r^2 = 0.92$, $p < 0.0001$). We thus found a linear association between Vd and the weight of the pig, according to this formula: $Vd \text{ (dL/kg)} = -0.16 \times \text{weight (kg)} + 15.0$ (**Figure 56G**).

The bioavailability (F) of D-Xylose was also experimentally confirmed on the 5 minipigs using 600-min-MMT with D-Xylose and 600-min-IVXTT as exposed in **Table 2**. The mean bioavailability of D-Xylose was estimated here at $99.40 \pm 0.89 \%$.

Minipig	1	2	3	4	5	Mean \pm SD
Weight (kg)	51.45	51.85	58.05	49.20	47.05	51.52 \pm 4.13
[D-Xylose] _{max} Oral (mg/dL)	38	26	44	50	48	41.20 \pm 9.65
t _{max} Oral (min)	90	120	90	90	90	96.00 \pm 13.42
[D-Xylose] ₀ IV (mg/dL)	93	93	93	92	90	92.20 \pm 1.30
600 min-AUC Oral	12578	8408	12345	14333	11685	11870 \pm 2169
600 min-AUC IV	11520	8520	10105	10388	11858	10478 \pm 1320
F (%)	100	99	100	100	98	99.4 \pm 0.89
Vd (dL/kg)	6.27	6.22	5.56	6.63	7.08	6.35 \pm 0.56

Table 2: Pharmacokinetic parameters of D-Xylose estimated from plasma D-Xylose levels following oral and intravenous administration (n=5)

[D-Xylose]_{max} = maximal peak of D-Xylose level; t_{max} = time for which the maximal peak of D-Xylose was obtained; [D-Xylose]₀ = initial plasma concentration of D-Xylose after intravenous administration; F = bioavailability; Vd = volume of distribution.

Finally, we studied the D-Xylose metabolization and urinary excretion in order to confirm its degree of transformation in other metabolites. D-threitol, as main D-Xylose urinary metabolite, was quantified in the plasmatic compartment and in urines (minipigs of Group 4). Results were presented in **Figure 57**.

Following MMT including D-Xylose, plasma D-threitol levels reached a peak at 300 min of 0.15, 0.22 and 0.24 mmol/L respectively for pig 3, 2 and 1 (**Figure 57A**). However, the mean peak of plasma D-threitol was much lower compared to the mean peak of plasma D-Xylose (**Figure 57B**): it was estimated at 0.21 ± 0.06 mmol/L compared to 3.02 ± 0.28 mmol/L for the mean plasma peak of D-Xylose, thus corresponding to 7 % of the D-Xylose peak. Similarly, plasma D-threitol levels following intravenous administration reached a peak at 120 min for pigs 1 and 2 at respectively 0.17 and 0.27 mmol/L (**Figure 57C**), corresponding to 3 % of the D-Xylose peak (**Figure 57D**).

Following intravenous D-Xylose administration, $37.8 \pm 8.0 \%$ of the quantity of D-Xylose administered was found intact in urines (**Figure 57E**) and $7.2 \pm 2.2 \%$ of the initial dose was converted into D-threitol after 24 hours (**Figure 57F**).

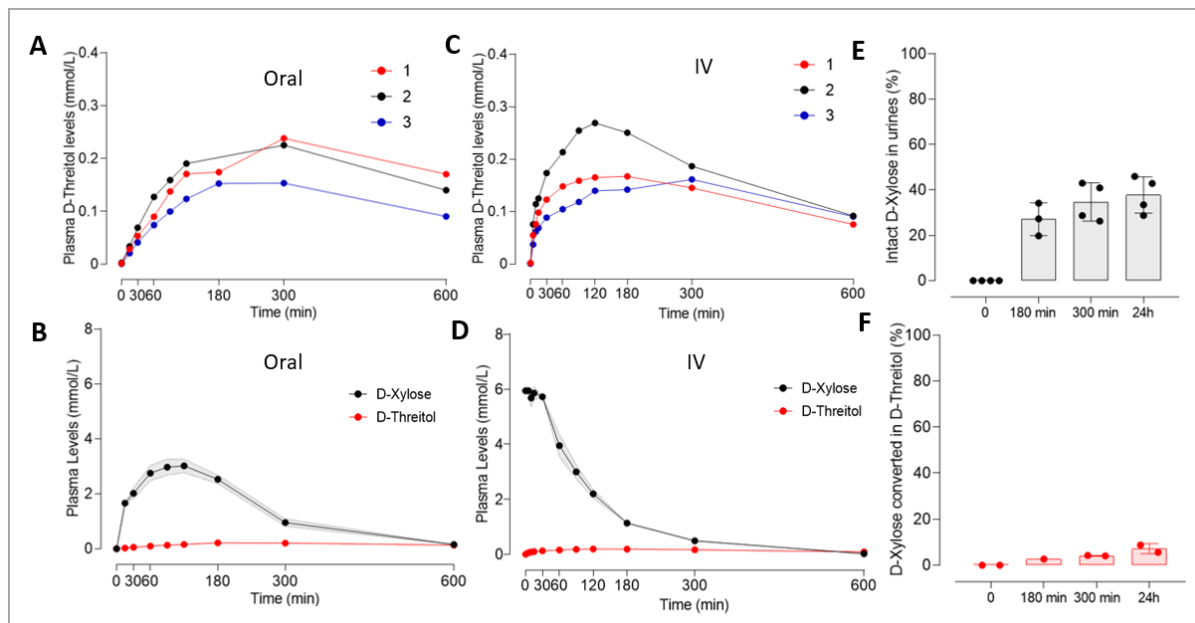


Figure 57: Metabolization and urinary excretion of D-Xylose following oral or intravenous D-Xylose administration

(A-B) Mixed meal test with D-Xylose (n=3): (A) Individual curves of plasma D-threitol levels and (B) Mean curves (Mean \pm SEM) of plasma D-xylose and D-threitol levels.

(C-D) Intravenous D-Xylose tolerance test (IVXTT) (n=3): (C) Individual curves of plasma D-threitol levels and (D) Mean curves (Mean \pm SEM) of plasma D-xylose and D-threitol levels.

(E-F) Urinary excretion of D-Xylose following IVXTT: (E) Fraction of D-Xylose found intact in urines (Mean \pm SD, n=4) and (F) Fraction of D-Xylose converted into D-threitol in urines (Mean \pm SD, n=2).

2. Comparison of the Rate of Appearance of D-Xylose obtained by the proposed models with the Rate of Appearance of Exogenous Glucose obtained by the glucose labeled method in healthy minipigs

The rates of appearance of D-Xylose obtained by the proposed "calculation" and computational models were compared to the rates of appearance of exogenous glucose obtained by the glucose labeled meal test in healthy minipigs in order to assess the performances of the oral D-Xylose test to measure intestinal glucose absorption in vivo (Group 5).

2.1 "Calculation" model in healthy minipigs

Figure 58 shows the comparison of the rate of appearance of D-Xylose (Ra D-Xylose) and their obtained by the "calculation" model with the rate of appearance of Exogenous Glucose (RaE Glucose) obtained by the glucose labeled method, and their corresponding area under the curve (AUC).

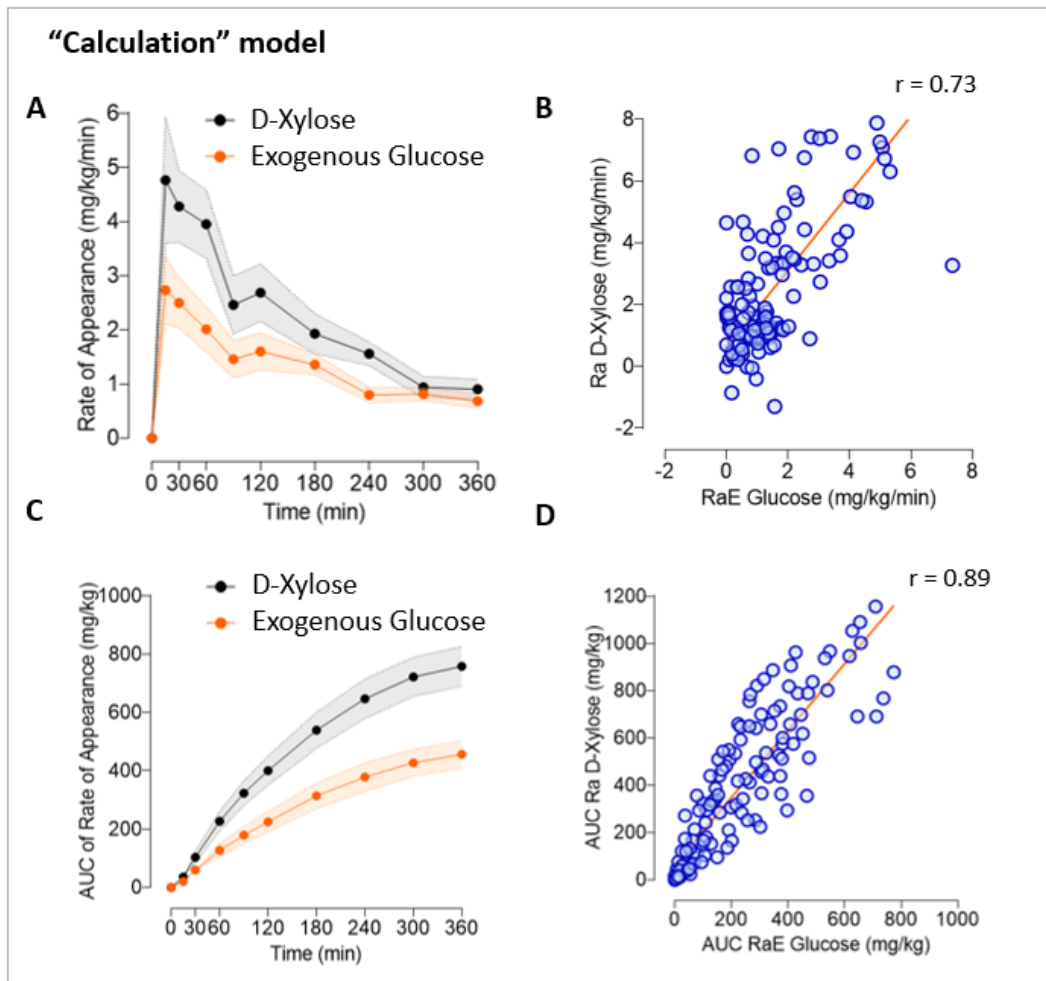


Figure 58: Comparison of the intestinal glucose absorption modeling between the “calculation” model and a gold-standard method with glucose labeled in healthy minipigs

(A) Mean curves (Mean \pm SEM, $n = 14$) of the rate of appearance of D-Xylose (Ra D-Xylose, in black) and the rate of appearance of exogenous glucose (RaE Glucose, in orange) during the labeled meal test.

(B) Concordance between Ra D-Xylose and RaE Glucose.

(C) Mean curves (Mean \pm SEM, $n = 14$) of the area under curve (AUC) of Ra D-Xylose (in black) and the RaE Glucose (in orange) during the labeled meal test.

(D) Concordance between the AUC of Ra D-Xylose and RaE Glucose.

Mixed-effects model and Sidak post-hoc test; r = Pearson coefficient; ccc = Lin concordance coefficient expressed with 95 % confidence interval.

In terms of kinetics and values, the mean curves of Ra D-Xylose and RaE Glucose were comparable, with two primary peaks being obtained for each technique at 15 minutes (2.74 ± 0.62 mg/kg/min for RaE Glucose and 4.76 ± 1.16 mg/kg/min for Ra D-Xylose) and 120 min (1.60 ± 0.34 mg/kg/min for RaE Glucose and 2.69 ± 0.53 mg/kg/min for Ra D-Xylose). (**Figure 58A**). Moreover, Ra D-Xylose obtained by this modeling and RaE Glucose were globally correlated ($r = 0.73$, $p < 0.0001$) (**Figure 58B**).

Additionally, D-Xylose was significant and positive to predict RaE Glucose ($\beta = 0.37$ 95 % CI [0.29, 0.45], $p < 0.0001$) and the prediction of RaE Glucose with Ra D-Xylose was significantly better than without Ra D-Xylose ($p < 0.0001$) (**Table 3**).

The AUC of the Rate of Appearance, which represents the respective amount of D-Xylose and glucose appearing in blood over time (in mg/kg), displayed the same kinetics. (**Figure 58C**). The corresponding AUC of Ra D-Xylose and RaE Glucose were strongly correlated ($r = 0.89$, $p < 0.0001$) (**Figure 58D**).

Model	p value fixed effect	p value "better than without"	Intercept	Estimate Ra D-Xylose
Calculation	<0.0001	<0.0001	1.28 [-0.15; 1.28]	0.37 [0.29; 0.45]
Simple	<0.0001	<0.0001	1.54 [-0.07; 3.10]	0.51 [0.36; 0.67]
Multi	<0.0001	<0.0001	1.50 [0.02; 2.98]	0.58 [0.44; 0.72]
Retention	<0.0001	<0.0001	1.70 [0.11; 3.28]	0.18 [0.13; 0.24]

Table 3: Non-linear mixed model for the rate of appearance of exogenous glucose prediction with D-Xylose performed for each of the proposed model in healthy minipigs

Non-linear mixed model after adjustment on pig, weight and time. The values of the intercept and the estimate of the rate of appearance of D-Xylose (Ra D-Xylose) were expressed with 95 % confidence interval.

2.2 Computational models in healthy minipigs

2.2.1 "Simple" model

Figure 59 shows the comparison of the rate of appearance of D-Xylose (Ra D-Xylose) obtained by the "simple" computational model with the rate of appearance of Exogenous Glucose (RaE Glucose) obtained by the glucose labeled method, and their corresponding AUC.

In terms of kinetics, the mean curves of Ra D-Xylose and RaE Glucose presented the same peak at 15 min (2.74 ± 0.62 mg/kg/min for RaE Glucose and 3.89 ± 0.56 mg/kg/min for Ra D-Xylose). The second peak of RaE Glucose observed at 120 min (1.60 ± 0.34 mg/kg/min) was not noticed for Ra D-Xylose. The statistical comparison between the groups showed a significant interaction between the time of the meal and the method ($p < 0.05$) (**Figure 59A**). Ra D-Xylose obtained by this modeling and RaE Glucose were globally correlated ($r = 0.66$, $p < 0.0001$) and substantially concordant ($ccc = 0.65$ [0.54; 0.73]) (**Figure 59B**).

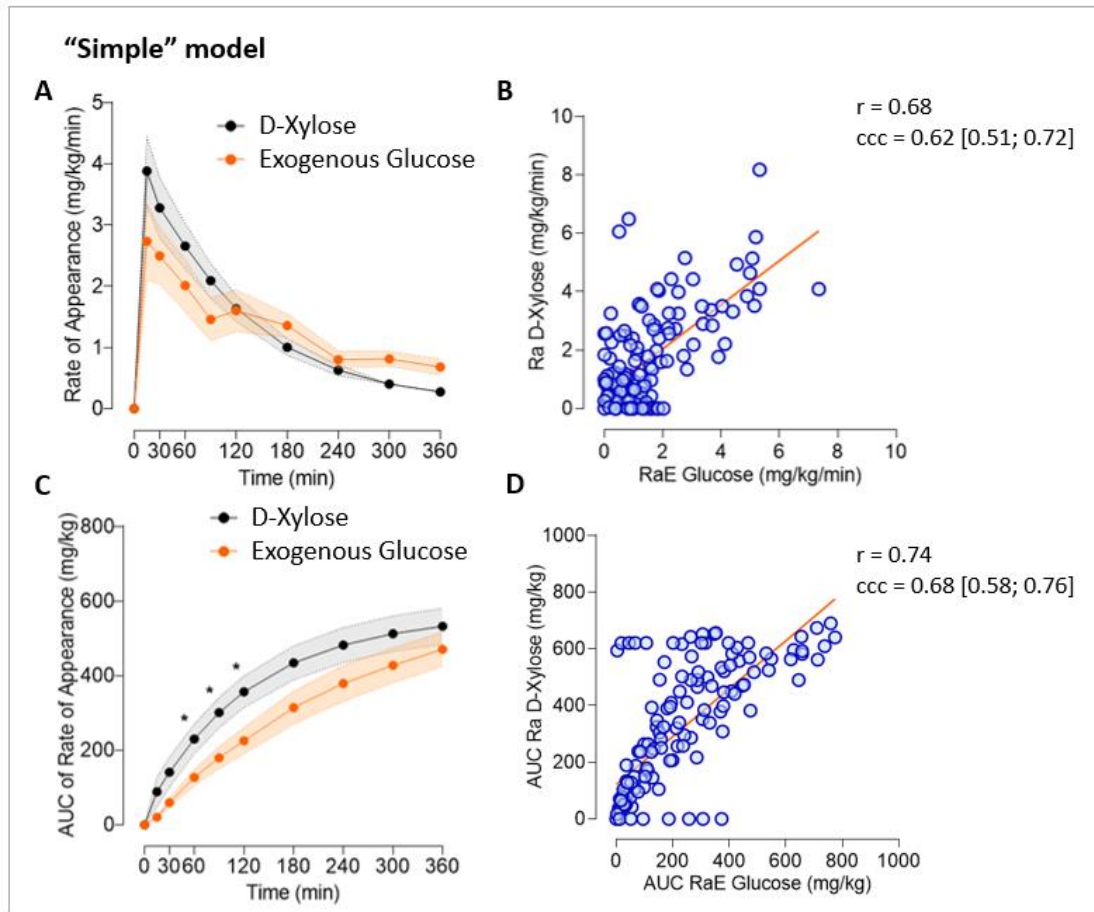


Figure 59: Comparison of the intestinal glucose absorption modeling between the “simple” computational model and a gold-standard method with glucose labeled in healthy minipigs

(A) Mean curves (Mean \pm SEM, n = 14) of the rate of appearance of D-Xylose (Ra D-Xylose, in black) and the rate of appearance of exogenous glucose (RaE Glucose, in orange) during the labeled meal test.

(B) Concordance between Ra D-Xylose and RaE Glucose.

(C) Mean curves (Mean \pm SEM, n = 14) of the area under curve (AUC) of Ra D-Xylose (in black) and the RaE Glucose (in orange) during the labeled meal test.

(D) Concordance between the AUC of Ra D-Xylose and RaE Glucose.

Mixed-effects model and Sidak post-hoc test; * $p < 0.05$; r = Pearson coefficient; ccc = Lin concordance coefficient expressed with 95 % confidence interval.

Additionally, Ra D-Xylose was significant and positive to predict RaE Glucose ($\beta = 0.51$ 95% CI [0.36, 0.67], $p < 0.0001$) and the prediction of RaE Glucose with Ra D-Xylose was significantly better than without Ra D-Xylose ($p < 0.0001$) (**Table 3**).

The AUC of the Rate of Appearance, which represents the amount of D-Xylose and glucose appearing in blood over time (in mg/kg), displayed the same kinetics. However, the AUC of Ra D-Xylose were globally higher than the AUC of RaE Glucose ($p < 0.005$), with an interaction between the method and the time of the meal also significant ($p < 0.005$). More precisely, the AUC of Ra D-Xylose and RaE Glucose

were significantly different ($p < 0.05$) between the times 30 and 120 min (**Figure 59C**). The corresponding AUC of Ra D-Xylose and RaE Glucose were globally correlated ($r = 0.68$, $p < 0.0001$) but moderately concordant ($ccc = 0.57$ [0.40; 0.66]) (**Figure 59D**).

2.2.2 “Multi” model

Figure 60 shows the comparison of the rate of appearance of D-Xylose (Ra D-Xylose) obtained by the “multi” computational model with the rate of appearance of Exogenous Glucose (RaE Glucose) obtained by the glucose labeled method, and their corresponding AUC.

In terms of kinetics, the mean curves of Ra D-Xylose and RaE Glucose presented the same peak at 15 min (2.74 ± 0.62 mg/kg/min for RaE Glucose and 4.09 ± 0.68 mg/kg/min for Ra D-Xylose) and the same bounce between 120 and 180 min (at 120 min: 1.60 ± 0.34 mg/kg/min and 1.56 ± 0.19 mg/kg/min respectively for RaE Glucose and Ra D-Xylose; at 180 min: 1.36 ± 0.19 mg/kg/min and 1.27 ± 0.14 mg/kg/min respectively for RaE Glucose and Ra D-Xylose). The statistical comparison between the groups showed no significant difference between the methods and no significant interaction between the time of the meal and the method (**Figure 60A**). Ra D-Xylose obtained by this modeling and RaE Glucose were globally correlated ($r = 0.70$, $p < 0.0001$) and substantially concordant ($ccc = 0.69$ [0.59; 0.77]) (**Figure 60B**).

Additionally, Ra D-Xylose was significant and positive to predict RaE Glucose ($\beta = 0.58$ 95% CI [0.44, 0.72], $p < 0.0001$) and the prediction of RaE Glucose with Ra D-Xylose was significantly better than without Ra D-Xylose ($p < 0.0001$) (**Table 3**).

The quantity of D-Xylose and glucose appearing in blood according to time (in mg/kg), represented by the AUC of the Rate of Appearance, showed the same kinetics. The AUC of Ra D-Xylose and RaE Glucose were not significantly different between the two methods (**Figure 60C**). The corresponding AUC of Ra D-Xylose and RaE Glucose were globally strongly correlated ($r = 0.84$, $p < 0.0001$) and concordant ($ccc = 0.80$ [0.73; 0.85]) (**Figure 60D**).

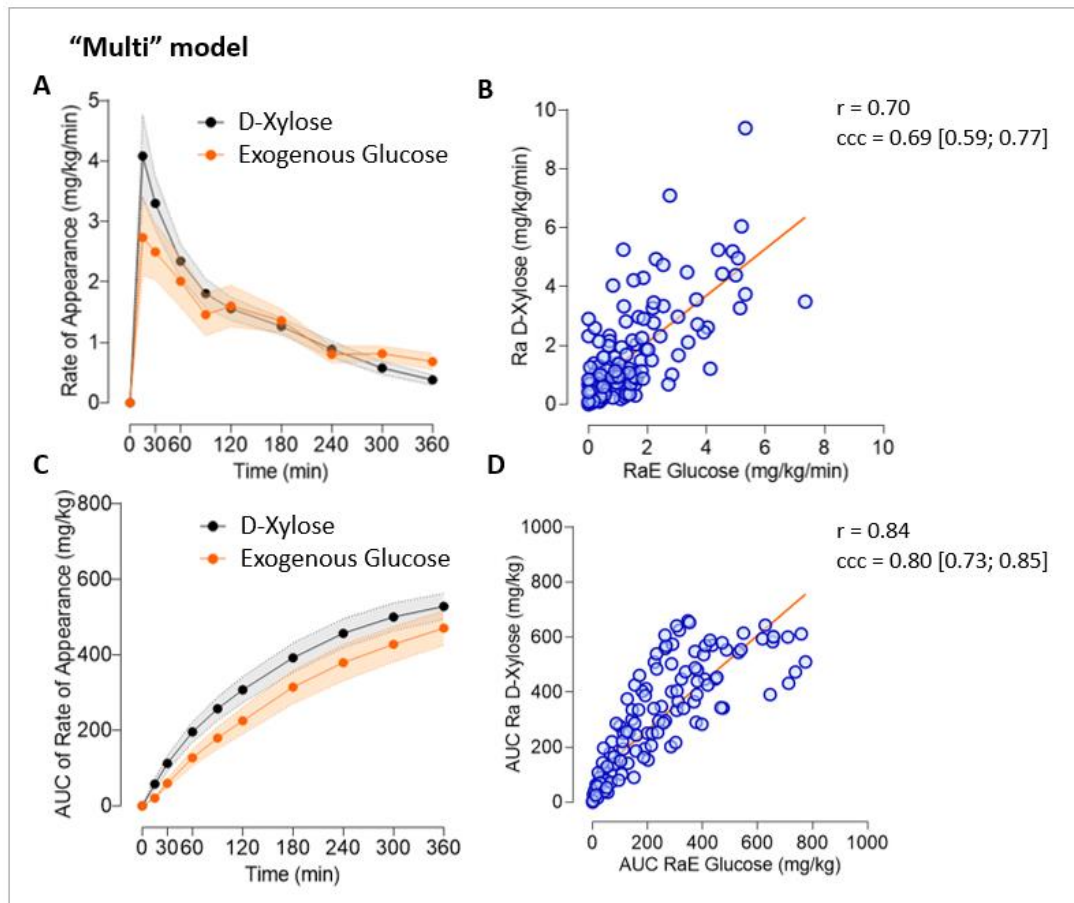


Figure 60: Comparison of the intestinal glucose absorption modeling between the “multi” computational model and a gold-standard method with glucose labeled in healthy minipigs

(A) Mean curves (Mean \pm SEM, n = 14) of the rate of appearance of D-Xylose (Ra D-Xylose, in black) and the rate of appearance of exogenous glucose (RaE Glucose, in orange) during the labeled meal test.

(B) Concordance between Ra D-Xylose and RaE Glucose.

(C) Mean curves (Mean \pm SEM, n = 14) of the area under curve (AUC) of Ra D-Xylose (in black) and the RaE Glucose (in orange) during the labeled meal test.

(D) Concordance between the AUC of Ra D-Xylose and RaE Glucose.

Mixed-effects model and Sidak post-hoc test; r = Pearson coefficient; ccc = Lin concordance coefficient expressed with 95 % confidence interval.

2.2.3 “Retention” model

Figure 61 shows the comparison of the rate of appearance of D-Xylose (Ra D-Xylose) obtained by the “retention” computational model with the rate of appearance of Exogenous Glucose (RaE Glucose) obtained by the glucose labeled method, and their corresponding AUC.

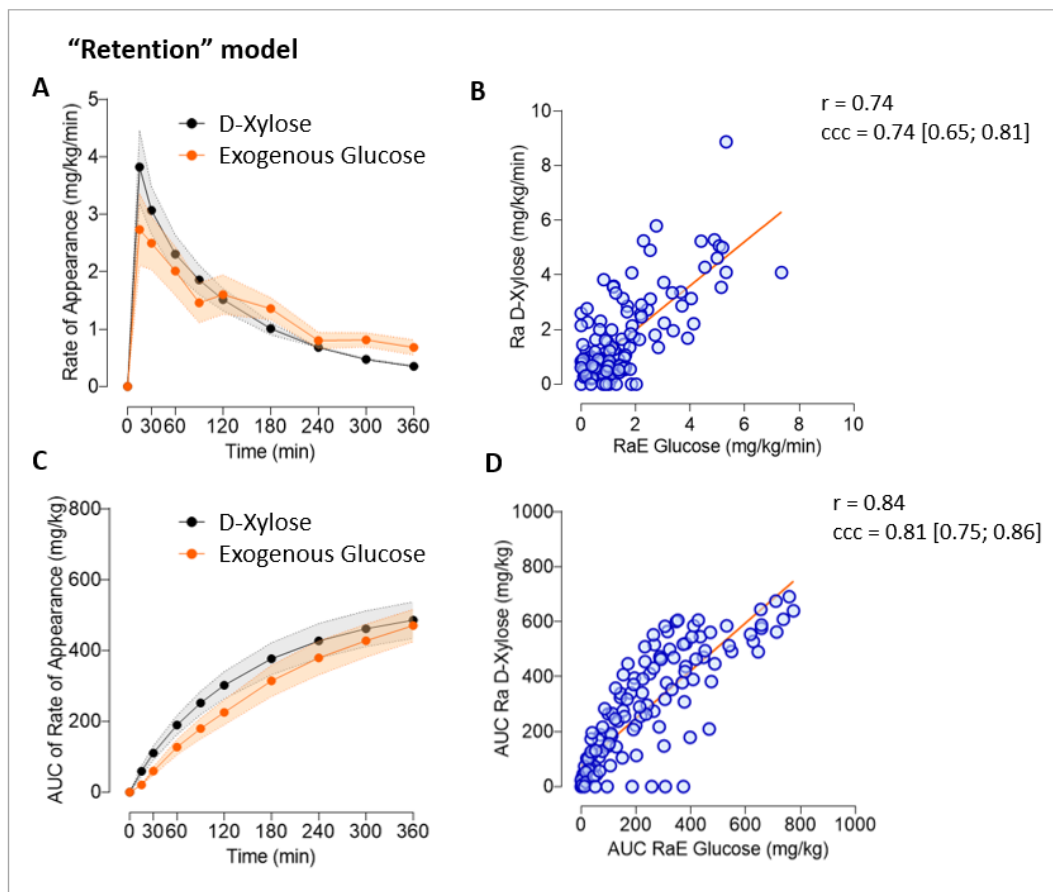


Figure 61: Comparison of the intestinal glucose absorption modeling between the “retention” computational model and a gold-standard method with glucose labeled in healthy minipigs

(A) Mean curves (Mean \pm SEM, n = 14) of the rate of appearance of D-Xylose (Ra D-Xylose, in black) and the rate of appearance of exogenous glucose (RaE Glucose, in orange) during the labeled meal test.

(B) Concordance between Ra D-Xylose and RaE Glucose.

(C) Mean curves (Mean \pm SEM, n = 14) of the area under curve (AUC) of Ra D-Xylose (in black) and the RaE Glucose (in orange) during the labeled meal test.

(D) Concordance between the AUC of Ra D-Xylose and RaE Glucose.

Mixed-effects model and Sidak post-hoc test; r = Pearson coefficient; ccc = Lin concordance coefficient expressed with 95 % confidence interval.

In terms of kinetics, the mean curves of Ra D-Xylose and RaE Glucose presented the same peak at 15 min (2.74 ± 0.62 mg/kg/min for RaE Glucose and 3.83 ± 0.64 mg/kg/min for Ra D-Xylose). The second peak of RaE Glucose observed at 120 min (1.60 ± 0.34 mg/kg/min) was not noticed for Ra D-Xylose. The statistical comparison between the groups showed no global significant differences between Ra D-Xylose and RaE Glucose (**Figure 61A**). Additionally, Ra D-Xylose obtained by this modeling and RaE Glucose were globally correlated ($r = 0.74$, $p < 0.0001$) and substantially concordant ($ccc = 0.74 [0.65; 0.81]$) (**Figure 61B**).

Additionally, Ra D-Xylose was significant and positive to predict RaE Glucose ($\beta = 0.18$ 95% CI [0.13, 0.24], $p < 0.0001$) and the prediction of RaE Glucose with Ra D-Xylose was significantly better than without Ra D-Xylose ($p < 0.0001$) (**Table 3**).

The quantity of D-Xylose and glucose appearing in blood according to time (in mg/kg), represented by the AUC of the Rate of Appearance, showed the same kinetics. The AUC of Ra D-Xylose and RaE Glucose were significantly different ($p < 0.05$) between the times 30 and 120 min (**Figure 61C**). The corresponding AUC of Ra D-Xylose and RaE Glucose were globally correlated ($r = 0.74$, $p < 0.0001$) and substantially concordant ($ccc = 0.68$ [0.58; 0.76]) (**Figure 61D**).

3. Sensibility of each model of systemic appearance of D-Xylose to reflect correctly the differences of Ra Exogenous glucose observed between two minipigs

In order to study the ability of Ra D-Xylose (for each proposed model) to correctly reflect the difference observed between two individuals in comparison with the gold-standard, we generated 14 randomized pairs of minipigs. Between the two minipigs of each pair, we calculated at each time of the meal the difference of Ra D-Xylose, RaE Glucose, AUC Ra D-Xylose and AUC RaE Glucose. We then assess the existence of a concordance between the differences of Ra D-Xylose and RaE Glucose, as for as between those of AUC of Ra D-Xylose and AUC of RaE Glucose respectively (**Figure 62**).

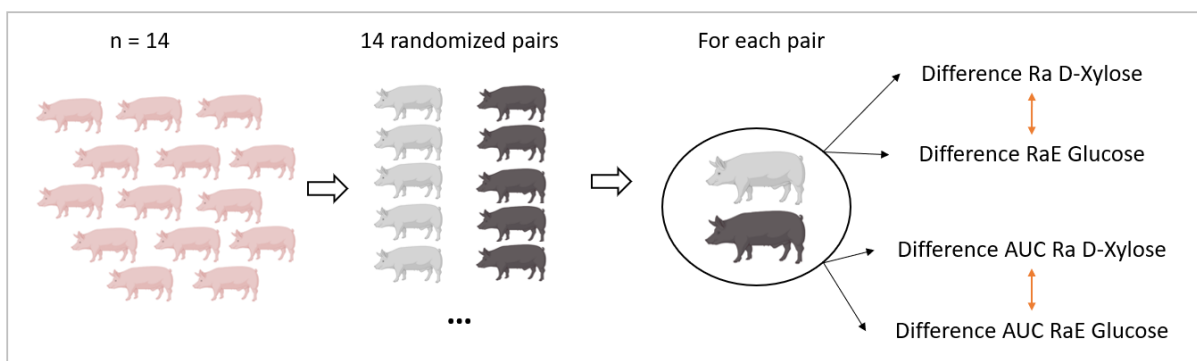


Figure 62: Study of the ability of each proposed model of Ra D-Xylose to correctly reflect the differences observed between two individuals, in comparison with the gold-standard

The differences in each pair between Ra D-Xylose obtained by the “Calculation” model and RaE Glucose obtained by the gold-standard method were correlated ($r = 0.64$, $p < 0.0001$) (**Figure 63A**). The differences of the corresponding AUC were nevertheless substantially correlated ($r = 0.77$, $p < 0.0001$) (**Figure 63B**).

The differences in each pair between Ra D-Xylose obtained by the “Simple” model and RaE Glucose were moderately correlated ($r = 0.60$, $p < 0.0001$) and concordant ($ccc = 0.58$ [0.46; 0.67]) (**Figure 63C**).

Moreover, for this model, the differences of the corresponding AUC were also moderately correlated ($r = 0.53$, $p < 0.0001$) and concordant ($ccc = 0.53$ [0.40; 0.64]) (**Figure 63D**).

The differences in each pair between Ra D-Xylose obtained by the “Multi” model and RaE Glucose were substantially correlated ($r = 0.66$, $p < 0.0001$) and concordant ($ccc = 0.64$ [0.53; 0.72]) (**Figure 63E**). Moreover, for this model, the differences of the corresponding AUC were moderately correlated ($r = 0.55$, $p < 0.0001$) and concordant ($ccc = 0.51$ [0.39; 0.61]) (**Figure 63F**).

Finally, the differences in each pair between Ra D-Xylose obtained by the “Retention” model and RaE Glucose were substantially correlated ($r = 0.73$, $p < 0.0001$) and concordant ($ccc = 0.70$ [0.61; 0.77]) (**Figure 63G**). Moreover, for this model, the differences of the corresponding AUC were also substantially correlated ($r = 0.77$, $p < 0.0001$) and concordant ($ccc = 0.76$ [0.68; 0.82]) (**Figure 63H**).

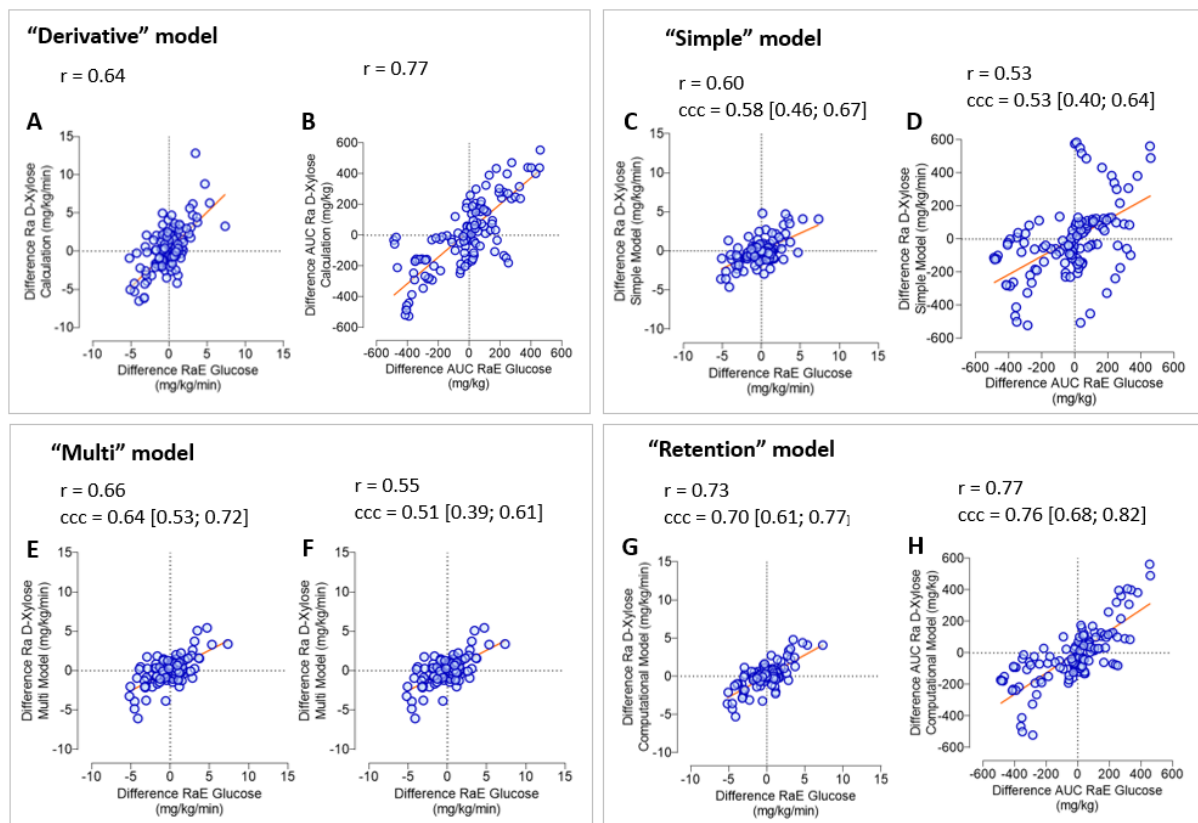


Figure 63: Ability of each proposed model of Ra D-Xylose to correctly reflect the differences observed between two individuals, in comparison with the gold-standard

(A-B) Sensibility to change with the “Calculation” model: Concordance between the difference of (A) Ra D-Xylose and the one of RaE Glucose and of (B) their respective AUC.

(C-D) Sensibility to change with the “Simple” Model: Concordance between the difference of (C) Ra D-Xylose and the one of RaE Glucose and of (D) their respective AUC.

(E-F) Sensibility to change with the “Multi” model: Concordance between the difference of (E) Ra D-Xylose and the one of RaE Glucose and of (F) their respective AUC.

(G-H) Sensibility to change with the "Retention" Model: Concordance between the difference of (G) Ra D-Xylose and the one of RaE Glucose and of (H) their respective AUC.

IV. Discussion

In this thesis section, we created a model to evaluate intestinal glucose absorption *in vivo* with oral D-Xylose test, an easier to use test compared to gold-standard glucose labeled methods.

1. Pharmacokinetic characteristics

In order to suggest the most appropriate modeling, we first reevaluated some of the pharmacokinetic properties of D-Xylose in minipigs. The competition for absorption between D-Xylose and glucose was evaluated. The bioavailability of D-Xylose, its distribution, urinary elimination, as well as the portion that was metabolized, were all quantified.

1.1 Competition with glucose in terms of intestinal absorption

The appearance of plasma D-Xylose was faster when D-Xylose was administered orally alone compared to when it was co-administered with glucose *per se* or with a mixed meal test. This finding suggested a competitive inhibition of intestinal absorption of D-Xylose in the presence of carbohydrates, which is consistent with literature data indicating a greater affinity for SGLT1 for glucose than for D-Xylose (Wright et al., 2011) and with studies demonstrating a competitive inhibition of intestinal absorption of these two substrates (Rolston and Mathan, 1989). Furthermore, because D-Xylose uptake was reduced in the presence of glucose, our data support the intestinal absorption mechanism of D-Xylose through SGLT1 (Baud et al., 2016) even more.

Since there was no discernible difference in the plasma D-Xylose kinetics when D-Xylose was co-administered with a mixed meal test or with glucose alone, it would appear that the type of carbohydrates that were co-administered would not have an impact on the kinetics of absorption.

Next, we opted for a systematic co-administration of D-Xylose (oral or intrajejunal administration) with a meal test. Effectively, our objective would be its inclusion as a biomarker of intestinal glucose absorption in meal tests intended to evaluate the phenotype of patients with obesity or type 2 diabetes. This decision was made to standardize the outcomes after oral administration.

The development of the computational "retention" model also considered this idea of competition by incorporating a latency period for D-Xylose in the intestinal lumen, following gastric emptying but prior to its absorption via glucose transporters. This period corresponds to a time when the SGLT1 transporters would be saturated with glucose and considers the less favorable affinity of D-Xylose for these transporters.

1.2 Bioavailability

Since the plasmatic peak was earlier and higher following intrajejunal administration, in agreement with the data previously exposed (Craig et al., 1983), the results of plasma D-Xylose kinetics following oral and intrajejunal administration allowed us to confirm that the rate of D-Xylose absorption is subjected to the rate of gastric emptying. This factor was also considered in the computational modeling, along with the pharmacokinetic parameter of "gastric emptying" that was determined using the appropriate Elashoff differential equation (Elashoff et al., 1982).

The results obtained after oral and intravenous administration enabled the estimation of the bioavailability of D-Xylose. It was evaluated nearly at 100 % in our study, indicating an almost complete absorption in the pig. According to published data, the bioavailability in pigs was estimated to be over 95 % (Huntley and Patience, 2018a), which is consistent with our calculation.

In contrast to humans, who have a bioavailability of D-Xylose estimated at 70 % (Craig et al., 1983), pigs appear to have a more significant bioavailability. The pig intestine is longer than the one of humans (11 meters compared to 7), which could explain this difference. The D-Xylose bioavailability was then fixed to 100 % (1) in computational modeling.

1.3 Distribution

The initial plasma levels of D-Xylose after intravenous administration made it possible to assess its volume of distribution in minipigs. The mean volume of distribution was thus estimated at 6.35 dL/kg. It has been previously estimated in healthy humans at 2.30 dL/kg (Worwag et al., 1987). Thus, a better distribution would be indicated by the D-Xylose volume of distribution in minipigs being higher than in humans.

Our data showed that the distribution volume varied with weight, with a negative correlation. It is likely that the minipigs used in our study were lighter than the healthy humans involved in the study of Craig and coworkers, which could account for this difference (data not available). Additionally, the volume of distribution of hydrophilic compounds, such as D-Xylose, decreases with fat mass (Zuckerman et al., 2015), which could account for the variation seen in relation to the weight of the animals.

The volume of distribution of D-Xylose varies linearly with weight for animals weighing between 40 and 60 kg, making it simple to estimate for all animals in this range. If we had included animals with a wider range of weights, we might have been able to prove that this evolution was actually sigmoidal. It could have been interesting to also evaluate it in obese animals, but we did not perform it in this study.

Patients with renal impairment were found to have a higher volume of D-Xylose distribution, which was calculated to be 3.20 dL/kg (Worwag et al., 1987). The volume of distribution of D-Xylose will not be affected by renal function in the following phases of our project because the animals will not present renal impairment.

1.4 Elimination

The plasmatic levels of D-Xylose after intravenous administration made it possible to incorporate a pharmacokinetic parameter of "elimination" with the corresponding differential equation in computational modeling. The exponential decreasing shape of the curve highly support the mainly monocompartmental elimination of D-Xylose.

1.5 Metabolization

The total amount of D-Xylose excreted in urine after intravenous administration was measured as well as the metabolization of D-Xylose. The fact that only 40 % of the initial dose of D-Xylose was excreted in urines suggests that the remaining 60 % were either metabolized, transformed, retained in the body, or eliminated in another manner.

The primary urinary excreted D-Xylose metabolite was identified as D-threitol. For this reason, after intravenous administration, we evaluated its plasmatic evolution and urinary excretion. The peak of plasmatic D-threitol represented only 7 % of the plasmatic peak of D-Xylose. Only 7 % of the initially administered dose consistently changed into D-threitol in urine samples. Data of studies revealed a 15 % conversion of D-Xylose into D-threitol (Huntley and Patience, 2018b; Pitkänen, 1977), which was twice as high as our findings. The 60 % of D-Xylose that is not recovered in urine cannot be quantitatively explained by the D-threitol conversion that has been shown to occur.

The metabolization of D-Xylose also produced CO₂, according to data from a prior study (Segal and Foley, 1959). But since CO₂ is also a byproduct of the transformation of D-xylose (5 carbons) into D-threitol (4 carbons), it does not contribute to the metabolization process in any additional ways. Additionally, a D-Xylose fraction that is converted to D-threitol is likely to be eliminated in bile and subsequently in feces (Craig and Atkinson, 1988). Since D-Xylose is a pentose, it may have also been included in the pentose phosphate pathway and used as an energetic substrate by non-bacterial non-yeast organisms, though in small amounts (Moysés et al., 2016). Because D-Xylose is intrinsically integrated with glycosaminoglycans, it serves as the primary component of extracellular matrices as well (Briggs and Hohenester, 2018). The possibility of D-Xylose and vitamin C interconversion pathways was also showed (Cheudjeu, 2020).

In any case, it is not necessary to know the precise fate of D-Xylose in order to model intestinal glucose absorption; the parameters of "elimination", which were determined using the data after intravenous

administration, are sufficient. Moreover, according to the low fraction of D-Xylose transformed into D-threitol by the liver, the hepatic D-Xylose uptake should be negligible, supporting the fact that portal and systemic D-Xylose appearance are close.

2. Intestinal glucose absorption modeling

From the pharmacokinetic characteristics previously determined, 4 different models of intestinal D-Xylose absorption were proposed: 1 model based on calculation and 3 computational models.

The first calculation model that has been suggested involves deriving the levels of D-Xylose from each plasmatic level and the estimation of the constant of elimination of D-Xylose and its volume of distribution. The conversion of each concentration (in mg/dL) to rate of appearance (in mg/kg/min) is thus made possible by this calculation. This modeling has the advantage of being straightforward, simple to process, extrapolable regardless of the groups and conditions, and able to reflect each experimental result. However, it does not allow the individual determination of all the pharmacokinetics parameters, contrary to the 3 other computational models.

In the "Simple" computational model, the main compartments are the stomach, intestine, and plasma, and the different fluxes are gastric emptying, intestinal absorption, and elimination from plasma. The differential equation corresponding to the flux of gastric emptying was elaborated from the kinetics of Elashoff (Elashoff et al., 1982), whereas the other differential equations were elaborated from plasma D-Xylose levels following oral, intrajejunal (intestinal absorption), and intravenous (elimination). The data from this study were used to fix the bioavailability of D-Xylose at 1 (100 %).

The "Multi" computational model extends the "Simple" model but also incorporates a multicompartimental intestine according to Salinari's model (Salinari et al., 2011). We considered the fact that the glucose transporters were not evenly distributed throughout the intestinal tract when developing this model. Following that, the intestinal compartment was divided into n subcompartments, each of which had a different rate of absorption. Additionally, intestinal transit was represented by the flow of sugar from one compartment to the next. In fact, research on humans and rodents revealed that the duodenum contained more glucose transporters than the jejunum and the ileon, making the proximal parts of the intestine more crucial for absorption than the distal ones (Lehmann and Hornby, 2016).

The "Retention" computational model is constructed similarly to the "Simple" model but adds a step of D-Xylose retention in the intestine between the fluxes of gastric emptying and intestinal absorption. This step corresponds to the notion of competition between glucose and D-Xylose that has been

experimentally proven. In fact, we opted to systematically administer D-Xylose in conjunction with the presence of other carbohydrates.

The three computational models are designed to predict Ra D-Xylose (mg/kg/min) from the plasmatic D-Xylose levels (mg/dL). They allow the individual determination of all the pharmacokinetics parameters. They have the advantage of being refined, which really reflects intestinal D-Xylose absorption, but yields "smoother" results than initial experimental data. Additionally, they were developed for a particular animal species (the pig), in a particular setting (in this case, healthy, non-obese, and non-diabetic), and for a specific weight range. As a result, they cannot yet be extended to data from animals or humans who do not respond to these characteristics. There are thus numerous criteria for choosing which model to use depending on the situation, and each modeling type has benefits and drawbacks.

3. Comparison of Ra D-Xylose obtained by each model with RaE Glucose obtained by the gold-standard

After proposing models, we compared the Ra D-Xylose results from each model to the RaE Glucose results from the gold-standard, in a healthy setting, to see if the proposed models were reliable and to determine the interpretive framework for Ra D-Xylose.

A non-linear mixed model adjusted on weight and time of the meal test revealed that Ra D-Xylose was significant and positive to predict RaE Glucose for each of the 4 models. In order to compare Ra D-Xylose and RaE Glucose (which respectively represent the flux of intestinal D-Xylose and glucose absorption), and AUC Ra D-Xylose and AUC RaE Glucose (which represent the load of D-Xylose and glucose absorbed over time) we also performed concordance tests. Among the three computational models, the "Multi" and "Retention" were those presenting the best concordance with the gold-standard. However, the "Retention" model was better than the "Multi" to correctly reflect the differences observed between two pigs in comparison with the gold-standard. This test was not performed for the "Calculation" model because the values between the two methods were too different, even if correlated.

Additionally, the ability of each computational model to fit the intravenous, oral and intrajejunal plasma experimental levels was studied. Both "Multi" and "Retention" models demonstrate good fitting of all the data sets, with low Log-Likelihood Losses (data not shown). Moreover, complementary analyses showed the practical identifiability of the k_{abs} parameter for the "Retention" but not for the "Multi" model, supporting the relevance of using the "Retention" one.

Even though the "Calculation" model to express Ra D-Xylose was less refined compared to computational models, it showed good concordance with RaE Glucose, particularly in terms of the load absorbed.

Consequently, the "Simple" and the "Multi" models have been discarded for the next steps of the study, and only the "Calculation" and the "Retention" have been kept for the expression of Ra D-Xylose.

4. Limitations of the study

4.1 Interpretation framework

By using D-Xylose as a novel biomarker instead of glucose-labeled meal tests using various isotopic tracers, this study enabled the development of several models of intestinal glucose absorption in vivo. The suggested models, particularly the "Calculation" and "Retention" models, are reliable for quantifying intestinal glucose absorption, but require an interpretation framework to prevent misinterpretations. The "Calculation" model is straightforward (especially for the expression of AUC of Ra D-Xylose) and extensible, but does not allow the determination of the pharmacokinetics parameters. All contexts cannot be covered by the "Retention" computational model for the moment and work is still in progress.

4.2 The gold-standard RaE Glucose is only an approximation of intestinal glucose absorption

We validated our models in comparison with the gold-standard dual tracers. However, the variable RaE Glucose calculated with this method is only an indirect approximation of intestinal glucose absorption because it does not consider the hepatic first pass effect. We also demonstrated the ability of D-Xylose of being metabolized but did not assess the D-Xylose first pass hepatic effect. Despite everything, the degree of D-Xylose metabolism is much lower than the degree of glucose metabolism, so we can assume that the first pass effect in the liver should be much lower than that of glucose. This theory could explain why the early 15-min peak of Ra D-Xylose was globally higher than the one of RaE Glucose in our results.

It could have been interesting to compare Ra D-Xylose with the intestinal glucose absorption assessment obtained by the method of catheterization of the portal vein and carotid artery, to take into consideration the absorbed fraction without the liver first pass. However, a pig study compared the dual tracer method and the catheterization method. The findings revealed that the fraction of glucose absorbed calculated by the two methods were not different during the first 240 minutes of the study (Noah et al., 2000), indicating that the approximation underlying RaE Glucose about intestinal glucose absorption assessment is actually very small.

4.3 D-Xylose reflects only the absorption of starch

D-Xylose is a monosaccharide by structure; as a result, it is directly absorbed after being emptied from the stomach rather than being digested. Complex carbohydrates, on the other hand, require digestion before being absorbed as glucose, which is not the case with simple carbohydrates. Thus, structurally distinct carbohydrates were compared. This point is debatable and may help to explain why there is less agreement between the rates of absorption and the amounts absorbed: it is unlikely that the rate of absorption of D-Xylose, which is not subject to digestion but is poorly affine to SGLT1, will be identical to that of glucose derived from starch, which is subject to digestion but is highly affine to SGLT1.

We chose to compare D-Xylose with ¹³C-enriched carbohydrates in this study because of the lower affinity for D-Xylose for SGLT1 than glucose. As a result, D-Xylose can only be used to reflect the absorption of complex carbohydrates like starch because its rate of absorption is unaffected by the type of additional carbohydrates. Due to the different affinities of glucose and D-Xylose for SGLT1 and the ongoing competition between them, its use during an OGTT will not be relevant to reflect the absorption of glucose *per se*. Glucose would be absorbed preferentially compared to D-Xylose.

Additionally, using D-Xylose to study the differences in absorption patterns in relation to carbohydrates with varying availability is not particularly pertinent. And *vice versa*, studies incorporating labeled glucose *per se* in mixed meal tests for the study of complex carbohydrates absorption are similarly unreliable because the RaE Glucose calculated from the labeled glucose is not a true reflection of the complex carbohydrates of the meal (Camastra et al., 2013).

V. Conclusion

In conclusion, we have shown that D-Xylose is an accurate and simple biomarker for evaluating intestinal glucose absorption *in vivo*. Several models were proposed: in a healthy setting, the "Calculation" and "Retention" models demonstrated results that were particularly consistent with the gold-standard method.

According to the study context and the desirable variables to analyze, these models must be used within a rigorous framework, which will influence the selection of the most appropriate model to use. D-Xylose is also more a reflection of complex carbohydrates than it is of glucose itself, so its use is only pertinent with starch-containing meal tests.

After challenging the relevance of D-Xylose test in experimental models, D-Xylose could thus represent a promising tool to better understand the association between intestinal glucose absorption and postprandial glycemic response, in both healthy and metabolically-disease-related contexts.

Part 4

Challenge of the Relevance of D-Xylose Test in Experimental Models

I. Introduction

In Part 1 of the thesis, we first described in detail how glucose homeostasis is ensured in health and what underlying mechanisms are involved in its regulation. The postprandial glycemic response is in fact influenced by a number of factors, including insulin secretion, insulin sensitivity, intestinal glucose absorption and gastric emptying. We also have discussed whether a decrease in insulin secretion, a decrease in insulin sensitivity and an acceleration of gastric emptying have previously been related to postprandial hyperglycemia.

In the previous section of the thesis, we have then demonstrated the equivalence between the systemic appearance of D-Xylose, expressed by several models, and the systemic appearance of glucose obtained by a gold-standard method using isotopic tracers of glucose.

In this present part, we wanted to check how insulin secretion, insulin sensitivity, and gastric emptying also influence the systemic appearance of D-Xylose. Our aims were to challenge our biomarker but also to exclude insulin secretion, insulin sensitivity and gastric emptying as potential confusing factors responsible of D-Xylose appearance variations. **Figure 64** illustrates our issue graphically.

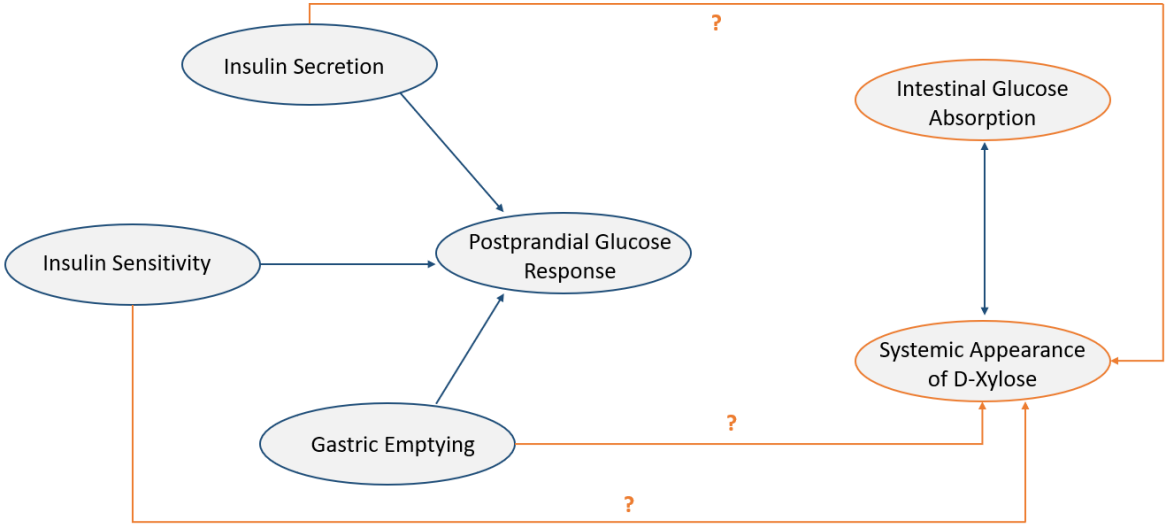


Figure 64: Contribution of insulin secretion, insulin sensitivity and gastric emptying on the systemic appearance of D-Xylose
 ? = relationship between factors still unclear. The orange narrows represent the relationship of interest for this part of the thesis.

We thus formulated the hypothesis that the systemic appearance of D-Xylose is unaffected by insulin secretion and insulin sensitivity. We hypothesized that a rapid gastric emptying affects its appearance but not the total amount of D-Xylose absorbed during a meal, in accordance with the elements previously demonstrated (Horowitz et al., 1993; Chinmay S. Marathe et al., 2015; Wu et al., 2020).

We conducted a number of interventions in separate groups of minipigs that were initially healthy in order to:

- decreasing intestinal glucose absorption
- decreasing insulin secretion
- decreasing insulin sensitivity
- accelerating gastric emptying.

The impact of each intervention on the systemic appearance of D-Xylose was subsequently investigated.

II. Materials and methods

1. Ethical statement

This part of the project was approved by the local French Committee of Animal Research and Ethics (CEEA-75, n°#18915, n°#12467 and n°#38311), in accordance with European law (2010/63/EU directive). All the procedures were carried out in the agreed-upon (n°D59-35010) Département Hospitalo-Universitaire de Recherche et d'Enseignement (Dhure) in the Faculty of Medicine in Lille, France.

2. Study design

This study set out to assess the relative impact of insulin secretion, insulin sensitivity, and gastric emptying on the systemic appearance of D-Xylose. Four distinct groups of animals that were subjected to various manipulations were developed for this objective. In order to respect the ethical principle of Reduction, animals were reused as much as feasible in other protocols.

Figure 65 displays the experimental design of this study.

The animals of the group 1 (n = 8) were subjected to an 80-% intestinal resection, aiming at decrease intestinal glucose absorption. The animals of the groups 2 (n = 10) and 3 (n = 7) were subjected respectively to a subtotal pancreatectomy and a 2-month High-Fat High-Sucrose diet (HFHSD), aiming at respectively decreasing insulin secretion and sensitivity. They were the same animals as those described in the Part 2 of the thesis. Mixed Meal tests (MMT) including D-Xylose were performed before and after each intervention and the evolution of the rate of appearance of D-Xylose (Ra D-Xylose) following each intervention was examined for each group.

The animals of the group 4 (n = 7) underwent MMT with D-Xylose after oral administration (via a nasogastric tube) or intrajejunal administration (after the surgical implantation of a jejunal tube). This group was specifically designed for this purpose, and some data were re-employed in the Part 3 of the

thesis. Ra D-Xylose was then compared in the same minipigs between the oral and intrajejunal administration of the MMT. To smooth out the intraindividual variability concerning the rate of gastric emptying previously described in minipigs (Henze et al., 2018; Suenderhauf et al., 2014), all the MMT were performed in duplicate. Finally, two different doses of D-Xylose were used: the usual 30-g dose (n = 7) and a lower 6-g dose (n = 3), set up to quantitatively spread out the loads of glucose absorbed. In total, 3 of the minipigs were subjected to the meal tests including the two doses.

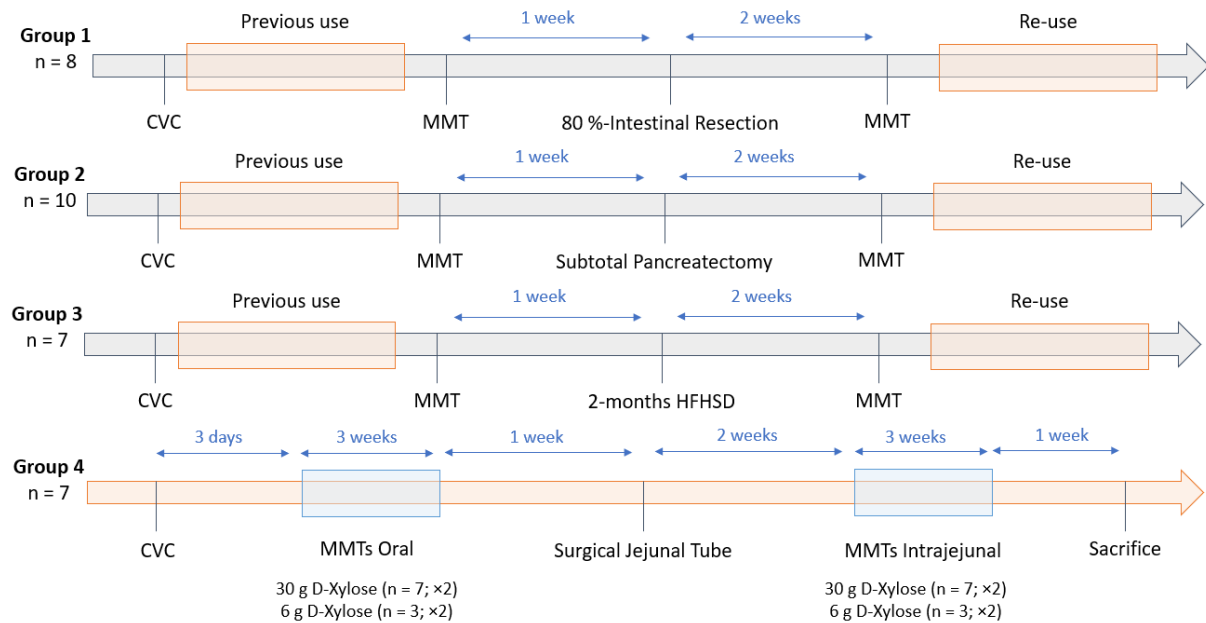


Figure 65: Experimental design of this part of the project

CVC = Central Venous Catheter. MMT = Mixed Meal Test. The orange boxes represent parts of the protocol in which the animals were used for another purpose. The blue boxes represent a 3-weeks period for which the animals were subjected to several MMT. The minipigs in Group 4 (orange arrow) were specifically used for this protocol.

3. Animals and housing

A total of 32 healthy minipigs (28 Göttingen-like and 4 Ossabaw), 24 males and 8 females, weighing 41.2 ± 11.4 kg (Pannier, Wylder, France) were included in this part of the project. As described previously in the thesis, all animals were individually housed in conventional conditions with enrichment and benefited from a 15-day acclimatization period. Water was provided *ad libitum* and standard food given twice a day. The composition of food was previously described in Part 2 of the thesis.

4. Surgical procedures

The surgical procedures were the same as those performed in the Part 2 and Part 3 of the thesis.

4.1 Anesthesia and analgesia

All the surgical procedures were performed under general anesthesia, after overnight fasting: premedication with a synergistic intramuscular injection of xylazine (3 mg/kg, Paxman®) and ketamine (5 mg/kg, Ketamine 1000®) and then isoflurane relayed (0.5-4 %, Vetflurane®) (Virbac, Carros, France). During the laparotomy procedures, animals were ventilated with assistance at 20 mpm or left with spontaneous ventilation in case of surgeries not involving a laparotomy. Analgesia was assessed by preoperative intramuscular injection of buprenorphine (15 µg/kg, Bupaq®, Virbac) for central catheter. A single application of a fentanyl transdermal solution (1.3 mg/kg, Recuvyra®, Lilly-Elanco, Neuilly-sur-Seine, France) was used to guarantee pain management (Goutchtat et al., 2021) following 80-% intestinal resection, the subtotal pancreatectomy and the jejunal tube implantation.

4.2 Implantation of a Central Venous Catheter (CVC)

This procedure was set up in order to refine blood collection during metabolic tests. The central venous catheter (Hickman® 9.6-F Single-Lumen CV Catheter; Bard Access System, Salt Lake City, UT, USA) was surgically implanted via the jugular external vein according to the procedure previously described in Part 2 of the thesis. The maintenance of the catheters was performed using heparinized saline solution bolus every 48 hours and the catheters were let in place during all the protocol.

4.3 Eighty percent-Intestinal resection

This intervention was performed (in Group 1) to decrease intestinal glucose absorption and to evaluate the sensibility to change of D-Xylose in this condition.

A sterile ribbon of known dimensions was used to measure the length of the intestine between the duodenojejunal and ileocecal junctions after the abdominal cavity had been opened. Eighty percent of this intestinal area was then removed, leaving respectively 10 % and 10 % next to the duodenojejunal junction and the ileocecal junction. Intestinal section and anastomosis were performed using staples of respectively 60 and 45 mm (Endo GIA®, Reload with Tri-Staple Technology, Covidien, Boulogne-Billancourt, France,). The anastomosis was then closed (Monocryl® 4-0, Ethicon, France).

The abdominal wall was finally closed in 3 layers by simple overlock: the peritoneum (Polysorb® 2/0, Medtronic, France), the muscular lay (PDS® 1, Ethicon, France) and the skin (Mersilene® 1, Ethicon, France).

4.4 Subtotal pancreatectomy

This intervention was performed (in Group 2) similarly as described in the Part 2 of the thesis. From the tail (splenic lobe) to the head (duodenal lobe), the dissection of the pancreas was carried out. In the retro-portal region, the Winslow pancreas (connecting lobe) was similarly dissected and largely removed. Before section and extraction, ligatures between the splenic and the duodenal lobes were

performed. The connecting lobe was also tightened. As previously stated (Ferrer et al., 2008), the subtotal pancreatectomy involved removing 75 % of the total organ weight.

4.5 Jejunal tube implantation

This procedure was performed (in Group 4), as previously described in the Part 3 of the thesis, in order to elaborate a model without gastric retention, it means with a “maximal” rate of gastric emptying.

After laparotomy, a 6-Fr gastro-duodenal tube (Vygon, Ecoen, France) was tunnelized through the right flank. Jejunum was opened thirty centimeters distally to the duodenojejunal junction and the gastro-duodenal tube inserted inside on a 15-cm length. A burse suture was performed with non-resorbable thread (Prolene® 4-0, Ethicon, France) and the tube fixed to the intestine by a Cushing overlock on 5 cm. The intestinal limb was then fixed to the abdominal wall in 4 stiches.

5. High-Fat High-Sucrose Diet (HFHSD)

Animals of this group (Group 3) were fed with an HFHSD for two months, as previously described in the Part 2 of the thesis. The quantity of 750 g of HFHSD were administered twice a day and contained 61.7 % of carbohydrates, 23.2 % of fats, and 15.1 % of protein. The composition of the HFHSD was detailed in **Table 1**, in the Part 2.

6. Mixed Meal Test (MMT) with D-Xylose

The MMT with D-Xylose were performed as previously described in the Parts 2 and 3 of the thesis, with the same constitution.

For the oral MMT, a 20-g solid energy bar (Ovomaltine®, Nestlé, France) and 200 mL of liquid (Fortimel Energy®, Nutricia, France) were mixed. The dose of 30 g or 6 g of D-Xylose was then added to the mix. The MMT was given *vigil*, for a 10-min period, via a nasogastric tube of 16 Fr that had previously been implanted under general anesthesia during the CVC implantation procedure for the first MMT or the day before for the others MMT. For the intrajejunal MMT, the same mix including 30 g or 6 g of D-Xylose was administered *vigil*, directly via the jejunal tube, for a 10-min period. A minimal 18-hour fast was respected before each MMT.

On EDTA and fluorinated tubes, blood samples were obtained before the MMT was administered (t=0 min) and at various time intervals afterwards (t=15, t=30, t=60, t=90, t=120 and t=180 min). For the Group 4, blood samples were also collected at t=240 and t=300 min. They were centrifuged (4000 rpm for 10 min at 4°C) and plasma was isolated and stored at -80°C until analysis.

For the animals subjected to the partial pancreatectomy (Group 2), an intravenous glucose tolerance test was also performed, as described in the Part 2, for a more accurate assessment of insulin response.

7. Biological procedures

The biological analyses were the similar as previously described in the previous parts of the thesis. The amperometric glucose oxidase method was used to measure the level of glucose in blood (glucometer Accu-Chek Performa[®], Roche, France, or Nova Biomedical StatStrip Xpress[®], DSI, USA). Blood glucose levels were determined instantaneously during each metabolic evaluation. A DXI Access Immunoassay System (Beckman Coulter) with an assay range between 0.3 and 300 μ U/mL was used to measure the plasma insulin concentrations, as previously mentioned (Cook et al., 2010). Plasma D-Xylose levels were determined by a colorimetric method with phloroglucinol (Eberts et al., 1979) by the glycobiology department of the Centre de Biologie-Pathologie of Lille University Hospital.

8. Intestinal glucose absorption modeling with D-Xylose

For Groups 1, 2, and 3, intestinal glucose absorption was modeled using the "Calculation" and "Retention" models for the evaluation of the Rate of Appearance of D-Xylose (Ra D-Xylose). By calculating the Ra D-Xylose time-dependent areas under the curve (AUC), the total amounts of D-Xylose absorbed were calculated.

Only the "Calculation" model was utilized to evaluate Ra D-Xylose for the animals in Group 4 because computational models to estimate intestinal glucose absorption in the context of suppressing gastric retention were not yet available. Calculating the time-dependent AUC of Ra D-Xylose allowed us to estimate the total amounts of D-Xylose absorbed.

9. Calculations and statistics

Results were expressed as mean \pm SEM for curves and mean \pm SD for histograms, as specified. The trapezoidal method was used to calculate areas under the curve (AUC) throughout the specified times following ingestion. The graphical visualization was done using GraphPad Prism[®] 8 program.

Continuous variables were analyzed with paired Student's t-test. Dynamic variables during meal tests between groups or models were compared using a Two-Way ANOVA or a Mixed-Effects model with Sidak post-hoc test for multiple comparisons. The presence of interactions between variables were systematically assessed.

The univariate correlation between the 180-min AUC Ra D-Xylose after Oral administration of the meal and the 180-min AUC Ra D-Xylose after Jejunal administration was tested using the Pearson coefficient (r). The Lin concordance test was performed to evaluate the concordance between these two variables and expressed with 95 % Confidence Interval (CI). The interpretation of the coefficients of concordance (ccc) was performed using the range of Landis and Koch (Landis and Koch, 1977), according to the method described (Desquilbet, 2019).

As described in the Part 2 of the thesis, the peripheral insulin sensitivity was assessed by the calculation of the Matsuda Index (Matsuda and DeFronzo, 1999). The Acute Insulin Response (AIR), which describes the initial phase of insulin production following intravenous glucose stimulation, was computed by subtracting fasting insulin levels from the mean evaluation of plasma insulin levels at 1, 3 and 5 minutes (Hubert et al., 2008, 2005).

III. Results

1. No variation of the systemic appearance of D-Xylose following subtotal pancreatectomy and 2-months High-Fat High-Sucrose Diet

First, we characterized postprandial glucose and insulin response following intestinal resection, subtotal pancreatectomy and a 2-month High-Fat High-Sucrose Diet (HFHSD) in **Figure 66**.

After intestinal resection, blood glucose levels remained globally stable, although we noticed a decrease of the mean glucose concentration at 30 min after intestinal resection (90.1 ± 3.8 mg/dL after versus 104.0 ± 5.5 mg/dL before, not significant) (**Figure 66A**). No significant variation of plasma insulin was shown after intestinal resection (**Figure 66B**) and animals kept the same weight (**Figure 66C**).

After subtotal pancreatectomy, postprandial blood glucose levels were globally slightly increased compared to before intervention, but not significantly (**Figure 66D**). No appreciable changes were revealed in insulin levels (**Figure 66E**) and no loss of weight was observed (**Figure 66F**). However, results from intravenous glucose tolerance tests showed a significant decrease of the Acute Insulin Response (18.3 ± 10.0 μ U/mL after versus 34.9 ± 13.7 μ U/mL before, $p < 0.0005$) (**Figure 66G**).

After HFHSD, minipigs showed a trend of lower postprandial blood glucose levels (**Figure 66H**), accompanied by a trend of higher insulin peak secretion (**Figure 66I**). Animals gained weight following the diet (59.5 ± 5.9 kg after versus 46.4 ± 4.1 kg before, $p < 0.0001$) (**Figure 66J**), accompanied by a decrease of the Matsuda Index (12.9 ± 7.5 after versus 20.0 ± 17.6 before, not significant) (**Figure 66K**).

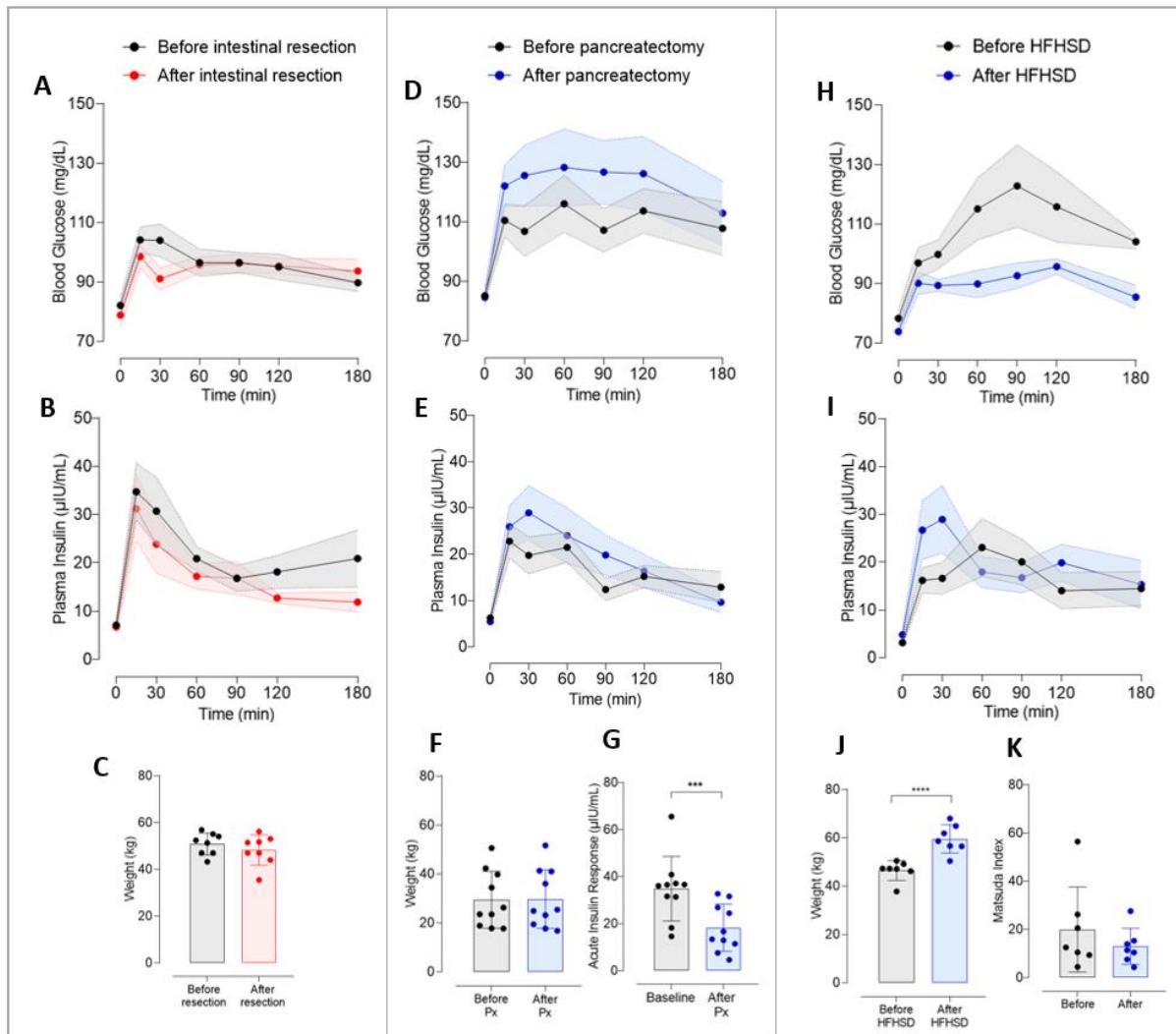


Figure 66: Characterization of postprandial glucose and insulin response following intestinal resection, subtotal pancreatectomy and a 2-months High-Fat High-Sucrose Diet

(A-C) After intestinal resection (n = 8): Evolution of (A) Blood glucose (Mean \pm SEM) and (B) insulin (Mean \pm SEM) during Mixed Meal Tests (MMT). (C) Weight (Mean \pm SD). Before intestinal resection in black and after intestinal resection in red.

(D-G) After subtotal pancreatectomy (n = 10): Evolution of (D) Blood glucose (Mean \pm SEM) and (E) insulin (Mean \pm SEM) during MMT. (F) Weight (Mean \pm SD). (G) Acute insulin response (Mean \pm SD) during intravenous glucose tolerance test. Before subtotal pancreatectomy in black and after subtotal pancreatectomy in blue.

(H-K) After a 2-months High-Fat High-Sucrose Diet (HFHSD) (n = 7): Evolution of (H) Blood glucose (Mean \pm SEM) and (I) insulin (Mean \pm SEM) during Mixed Meal Tests (MMT). (J) Weight (Mean \pm SD). (K) Matsuda Index. Before a 2-months HFHSD in black and after a 2-months HFHSD in blue.

Two-Way ANOVA test for repeated measures and Sidak post-hoc test; Paired t-test; ***p<0.0005; ****p<0.0001

Once the decrease of insulin secretion after subtotal pancreatectomy and the decrease of insulin sensitivity after the 2-month HFHSD characterized, the variation of the rate of appearance of D-Xylose following each intervention was assessed using the “Calculation” and the “Retention” model, and described in **Figure 67** (rates of absorption) and **Figure 68** (loads absorbed).

Using the “Calculation” model, the rate of appearance of D-Xylose (Ra D-Xylose) decreased (trend) after intestinal resection at 30 min (2.87 ± 0.64 mg/kg/min after versus 5.63 ± 0.87 mg/kg/min before) (**Figure 67A**). No appreciable change of Ra D-Xylose was noticed after pancreatectomy ($p = 0.89$) (**Figure 67B**) and after a 2-month HFHSD ($p = 0.49$) (**Figure 67C**).

Using the “Retention” model, we also observed a decrease of Ra D-Xylose values after intestinal resection compared to before, especially at 15 min (2.99 ± 1.61 mg/kg/min after versus 5.29 ± 1.96 mg/kg/min before). A significant interaction ($p < 0.0005$) between the time of the meal test and the intervention was then showed (**Figure 67D**). However, as obtained with the “Derivative” model, no appreciable change of Ra D-Xylose was noticed after pancreatectomy ($p = 0.85$) (**Figure 67E**) and after a 2-month HFHSD ($p = 0.49$) (**Figure 67F**).

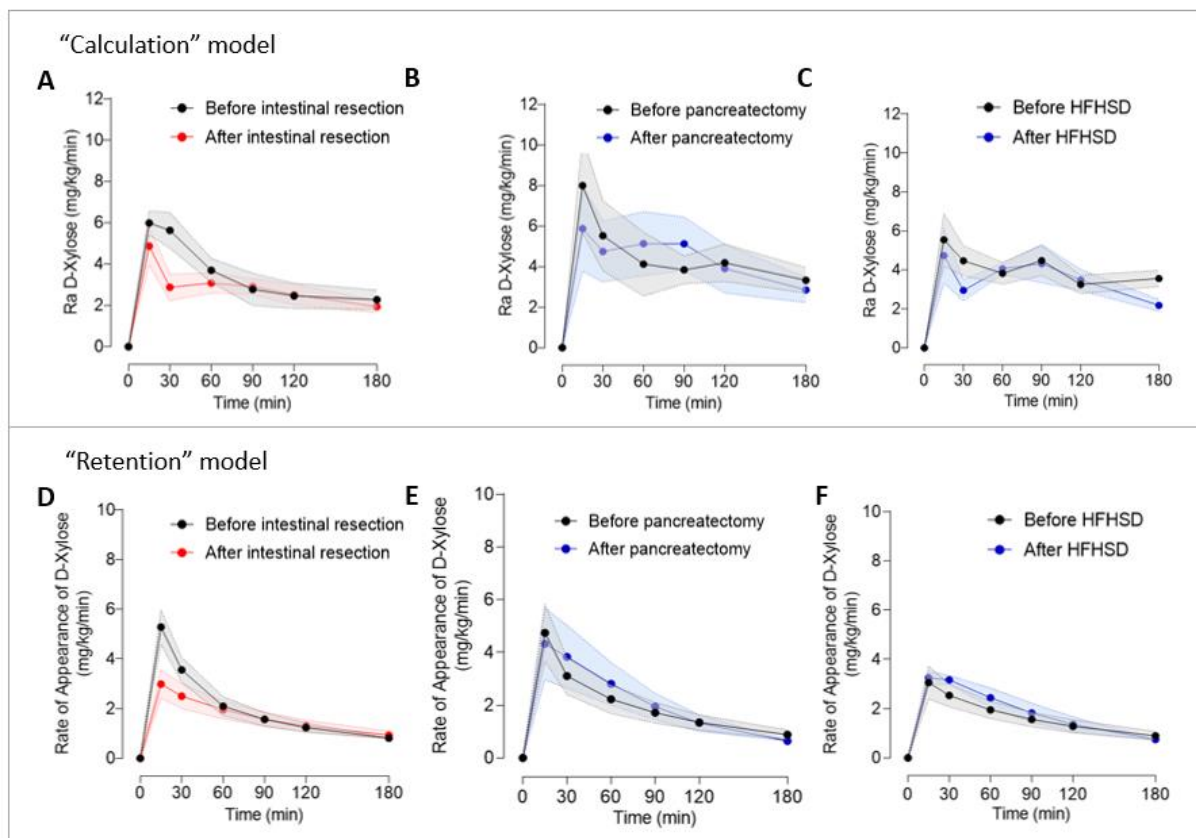


Figure 67: Evolution of the rate of intestinal glucose absorption during a Mixed Meal Test following intestinal resection, subtotal pancreatectomy and a 2-months High-Fat High-Sucrose Diet

(A-C) “Calculation” model: Evolution (Mean \pm SEM) of the rate of appearance of D-Xylose (Ra D-Xylose) during a Mixed Meal Test (MMT) (A) before (in black) and after (in red) intestinal resection ($n = 8$), (B) before (in black) and after (in blue) subtotal pancreatectomy ($n = 10$) and (C) before (in black) and after (in blue) a 2-months High-Fat High Sucrose Diet (HFHSD) ($n = 7$). (D-F) “Retention” model: Evolution (Mean \pm SEM) of Ra D-Xylose during a Mixed Meal Test (MMT) (D) before (in black) and after (in red) intestinal resection ($n = 8$), (E) before (in black) and after (in blue) subtotal pancreatectomy ($n = 10$) and (F) before (in black) and after (in blue) a 2-months HFHSD ($n = 7$).

Two-Way ANOVA test for repeated measures and Sidak post-hoc test

With the “Calculation” model, we found a global decrease of the areas under the curve (AUC) of Ra D-Xylose after intestinal resection with a significant interaction between the time of meal test and the intervention ($p < 0.05$). (**Figure 68A**). On the other hand, the evolution of AUC of Ra D-Xylose according to the time of the meal were not different after subtotal pancreatectomy ($p = 0.91$) (**Figure 68B**) and after a 2-month HFHSD ($p = 0.55$) (**Figure 68C**).

Using the “Retention” model, a trend of decrease of the AUC of Ra D-Xylose according to time was noticed after intestinal resection compared to before, even not significant (**Figure 68D**). On the other hand, those after subtotal pancreatectomy ($p = 0.87$) (**Figure 68E**) and a 2-months HFHSD ($p = 0.87$) (**Figure 68F**) remained totally unchanged.

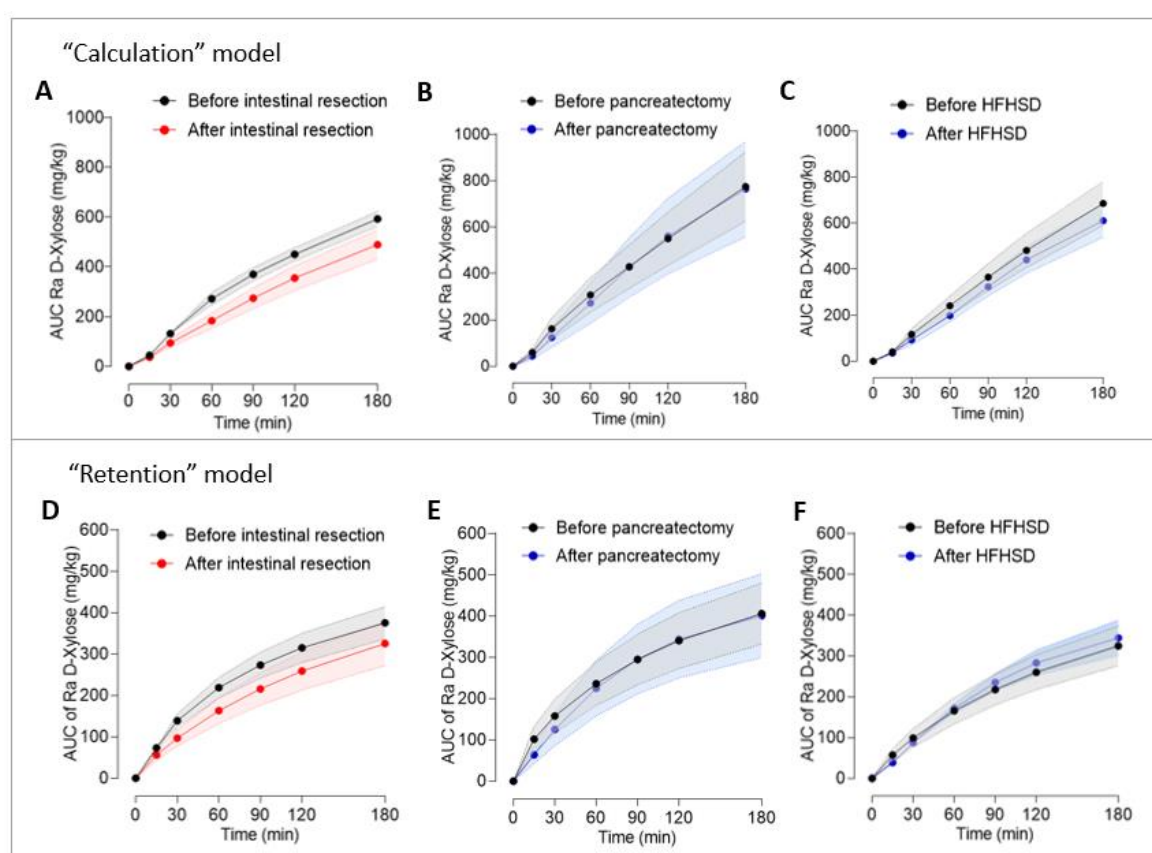


Figure 68: Evolution of the cumulative amount of glucose absorbed during a Mixed Meal Test following intestinal resection, subtotal pancreatectomy and a 2-months High-Fat High-Sucrose Diet

(A-C) “Calculation” model: Evolution (Mean \pm SEM) of the areas under curves (AUC) of the rate of appearance of D-Xylose (Ra D-Xylose) during a Mixed Meal Test (MMT) (A) before (in black) and after (in red) intestinal resection ($n = 8$), (B) before (in black) and after (in blue) subtotal pancreatectomy ($n = 10$) and (C) before (in black) and after (in blue) a 2-months High-Fat High Sucrose Diet (HFHSD) ($n = 7$).

(D-F) “Retention” model: Evolution (Mean \pm SEM) of the AUC of D-Xylose (Ra D-Xylose) during a Mixed Meal Test (MMT) (D) before (in black) and after (in red) intestinal resection ($n = 8$), (E) before (in black) and after (in blue) subtotal pancreatectomy ($n = 10$) and (F) before (in black) and after (in blue) a 2-months HFHSD ($n = 7$).

Two-Way ANOVA test for repeated measures and Sidak post-hoc test

2. Variations of the systemic appearance of D-Xylose consequently to a rapid gastric emptying

We then evaluated the consequences of the suppression of gastric retention on the rate of intestinal glucose absorption, assessed by the “Calculation” model. In others words, we determined if a rapid gastric emptying influenced the pattern of intestinal glucose absorption, in terms of kinetics and loads absorbed (**Figure 69**).

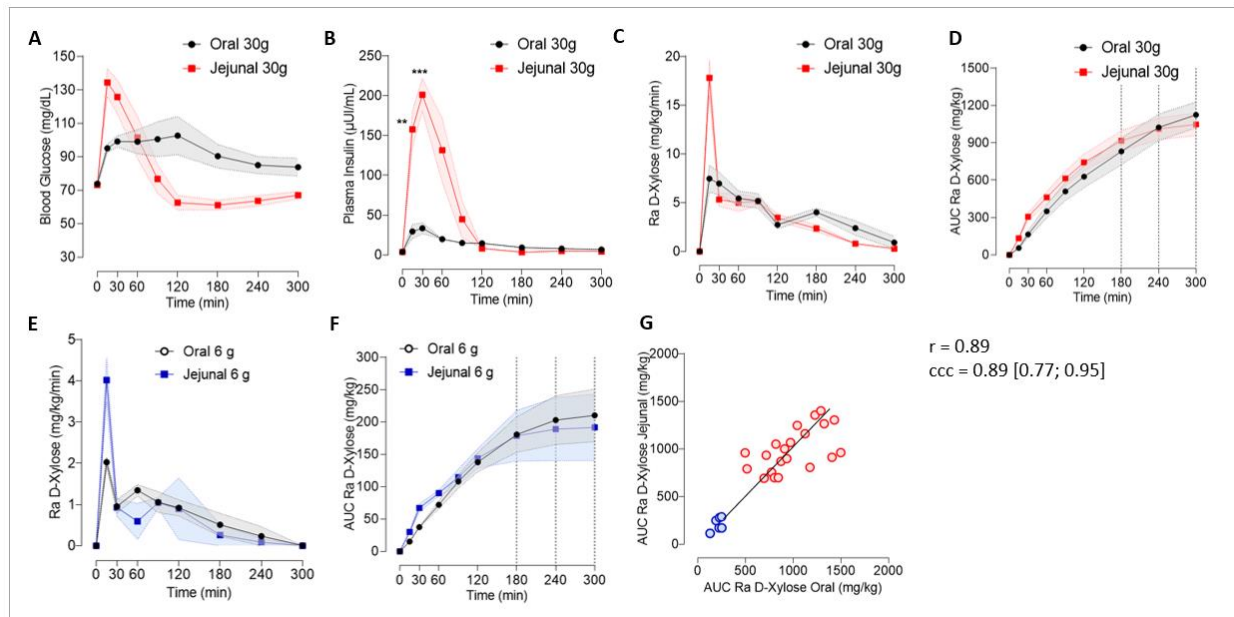


Figure 69: Comparison of the response to a Mixed Meal Test following oral or intrajejunal administration

(A-D) For a 30-g dose of D-Xylose (Mean \pm SEM, n = 7): (A) Blood glucose, (B) plasma insulin, (C) rate of appearance of D-Xylose (Ra D-Xylose) and (D) cumulative areas under curve (AUC) of Ra D-Xylose after oral (in black) or intrajejunal (in red) administration of the Mixed Meal Test (MMT).

(E-F) For a 6-g dose of D-Xylose (Mean \pm SEM, n = 3): (E) Ra D-Xylose following oral (in black) or intrajejunal (in blue) administration of the MMT. (F) Cumulative AUC of Ra D-Xylose following oral (in black) or intrajejunal (in blue) administration of the MMT.

(G) Concordance of AUC of Ra D-Xylose between Oral and Jejunal administration from 180 min: in blue for the 6-g dose and in red for the 30-g dose.

Two-Way ANOVA test for repeated measures and Sidak post-hoc test; **p<0.01; ***p<0.001; r = Pearson coefficient; ccc = Lin concordance coefficient expressed with 95 % confidence interval.

Globally, we showed different shapes of the curves of all the parameters between the two routes of administration of the MMT.

The mean curve of blood glucose formed a high peak on the 90-min period of the meal following intrajejunal administration while its mean curve was smoother on a larger period of 180 min following oral administration. The peak of blood glucose was reached at 15 min after intrajejunal administration (134.4 ± 8.3 mg/dL jejunal versus 95.1 ± 2.4 mg/dL oral) whereas it was reached at 120 min after oral

administration (102.7 ± 11.5 mg/dL oral versus 62.6 ± 4.3 mg/dL jejunal). A significant interaction between the time of the meal test and the route of administration was thus observed ($p < 0.0001$) (**Figure 69A**).

The results of insulin levels also showed a much higher peak following intrajejunal administration compared to oral administration ($p < 0.0005$), with a significant interaction between the time of the meal and the route of administration ($p < 0.0001$). Plasma insulin levels were particularly important at 15 min (157.8 ± 22.9 μ IU/mL jejunal versus 29.6 ± 9.0 μ IU/mL, $p < 0.01$) and 30 min (201.3 ± 20.4 μ IU/mL jejunal versus 33.5 ± 7.0 μ IU/mL, $p < 0.001$) when the meal was given intrajejunal (**Figure 69B**).

Ra D-Xylose was also significantly modified following intrajejunal administration compared to oral administration, with a much higher early peak of Ra D-Xylose, noticeable for the two doses of D-Xylose administered (**Figure 69C and 69E**) (for a 30-g administration: 17.8 ± 1.8 mg/kg/min jejunal versus 7.5 ± 1.4 mg/kg/min oral at 15 min, with a significant interaction between time and group ($p < 0.0001$)).

The cumulative AUC of Ra D-Xylose were higher (trend) in the early steps of the meal following intrajejunal administration compared to oral administration for the two doses of D-Xylose used (**Figure 69D and 69F**). However, the cumulative AUC of Ra D-Xylose from 180 min, it means at the end of the test, were not different (dotted lines). Additionally, they were strongly correlated ($r = 0.89$, $p < 0.0001$) and concordant ($ccc = 0.89$ [0.77; 0.95]) (**Figure 69G**).

IV. Discussion

1. Summary of the obtained results

In this section of the study, we examined the potential effects of insulin secretion, insulin sensitivity, and gastric emptying on the systemic appearance of D-Xylose. These three mechanisms are in fact supposed to affect the pathophysiology of glucose homeostasis. Since we intended to characterize intestinal glucose absorption in patients with various glycemic states in the following section of the work, we first sought to identify any potential sources of uncertainty that might limit the interpretation of the rate of appearance of D-Xylose in the context of postprandial hyperglycemia.

Our results indicated a decrease of the systemic appearance of D-Xylose following intestinal resection. Following a decrease of insulin secretion and sensitivity, no decrease was seen. As a result, interventions that altered insulin secretion and sensitivity had no impact on the systemic appearance of D-Xylose. Additionally, using intrajejunal route of administration to mimic a maximal rate of gastric emptying, we demonstrated that a rapid gastric emptying accelerates the systemic appearance of D-Xylose but not the total amount of D-Xylose absorbed.

2. Interpretation framework

We thus confirmed that impaired insulin secretion and sensitivity are not confusing factors on the interpretation of the systemic appearance of D-Xylose but that a rapid gastric emptying accelerates its rate of appearance.

This last result means that: first, D-Xylose appearance is effectively sensible to gastric emptying; second, the appearance of D-Xylose is time-dependently affected by gastric emptying. In fact, during the earliest steps of a meal test (particularly for the first hour), systemic appearance of D-Xylose cannot be separated from the rate of gastric emptying. For example, if we compare 2 groups and find that one of them has a higher Ra D-Xylose than the other, we will not be able to determine whether this difference is due to a variation in the rate of gastric emptying or a variation specific to the intestine. However, if we examine the total amounts of D-Xylose absorbed over a 180-minute meal period, we can confirm that it is independent of gastric emptying. For instance, if one group presented a higher load of D-Xylose absorbed at this time compared to another, we would be able to confirm that this difference would be caused by a factor specific to the intestine rather than a difference in the rate of gastric emptying.

In any cases, we have demonstrated that variations of the systemic appearance of D-Xylose are specific to the variations of intestinal glucose absorption, and have confirmed that D-Xylose is a good reflect of intestinal glucose absorption.

3. Intestinal resection and decrease of systemic appearance of D-Xylose

It was expected to see a drop in Ra D-Xylose after intestinal resection. However, in contrast to the 80 % of the resected intestine, the estimated 25 % decrease over a 180-minute period was unexpected.

In contrast to the loss of anatomy or function, the decline in the functionality of an organ is not linear. A 70 % loss of anatomy is required for a significant impact on function in organs like the pancreas (Litten-Brown et al., 2010), liver (Guglielmi et al., 2012), or intestine (Scheiner et al., 1965).

Additionally, it would appear that an intestinal adaptation happens after intestinal resection to make up for the lost structure. Four of the minipigs who underwent the 80-% intestinal resection underwent proximal and distal biopsies. The histological findings showed mucosa hypertrophy, which is characterized by an expansion of the villi and crypts. Additionally, quantification analyses of gene expression levels indicated a tendency for SGLT1 expression to increase after resection in comparison to before (**Figures 70 and 71**).

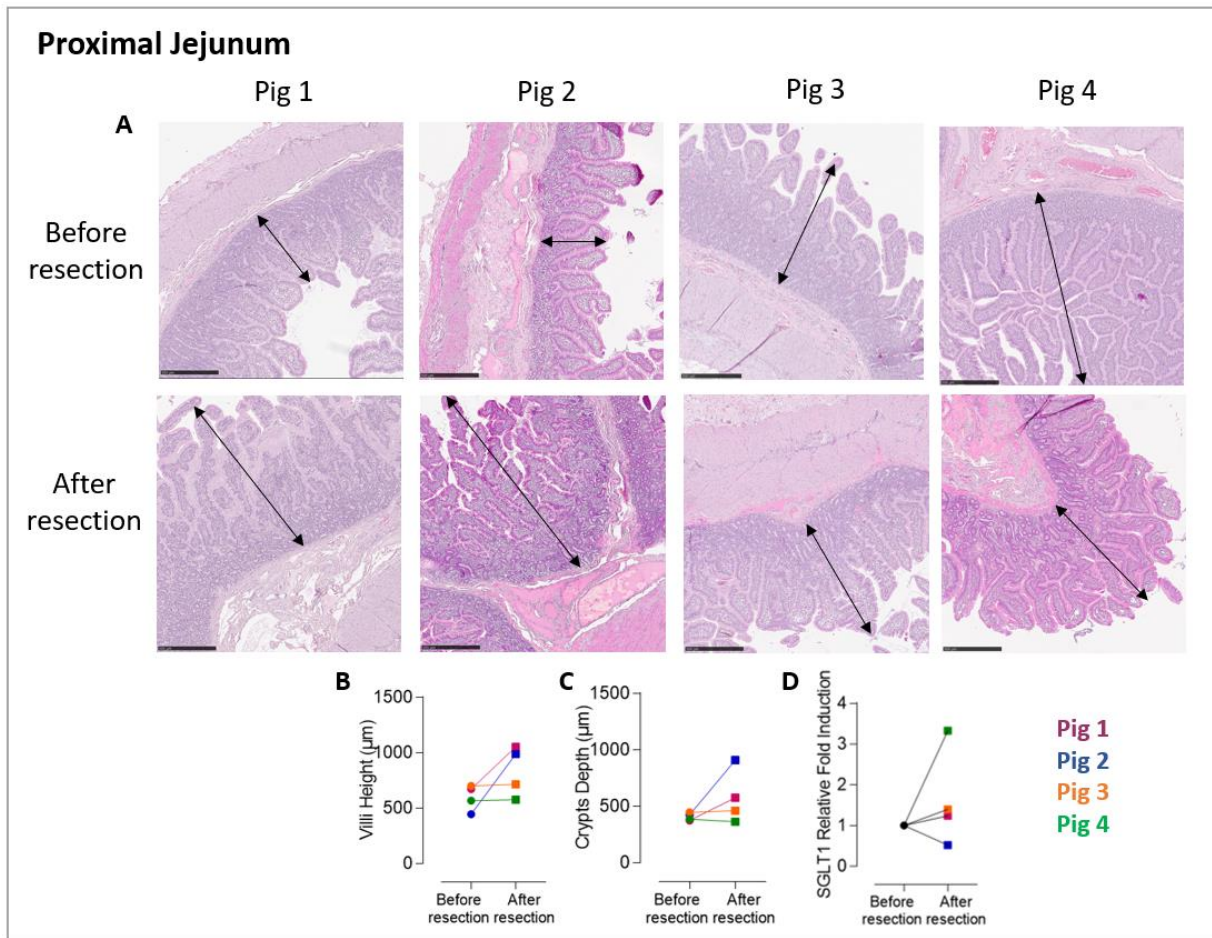


Figure 70: Intestinal adaptation of the proximal jejunum following 80-% intestinal resection

(A) Histological images of the intestinal mucosa for each of the 4 minipigs before and after resection.

(B) Individual villi height, (C) crypts depth and (D) SGLT1 relative fold induction before and after resection.

Hematoxylin-Eosin coloration; magnification 5X; black scale = 500 μm ; black arrow = mucosa thickness

This compensatory hypertrophy of the intestinal mucosa was previously described in rats subjected to gastric bypass in the excluded fraction of the intestine. It was seen in the alimentary limb and was linked to an increase in the expression of the genes responsible for transporting aminoacids (Cavin et al., 2016). This hypertrophy was brought on by the growth of the crypt cells (le Roux et al., 2010) and the expansion of the villi (Stearns et al., 2009), and both of which were absent following sleeve gastrectomy (Mumphrey et al., 2015). Humans were also found to have these modifications (Franquet et al., 2019) and an increase in the expression of glucose transporters has also been observed (Mumphrey et al., 2015; Nguyen et al., 2014b). Additionally, such intestinal modifications were also mentioned previously in rodent models of short bowel syndrome (Berlin et al., 2019; Collantes Pérez et al., 2004).

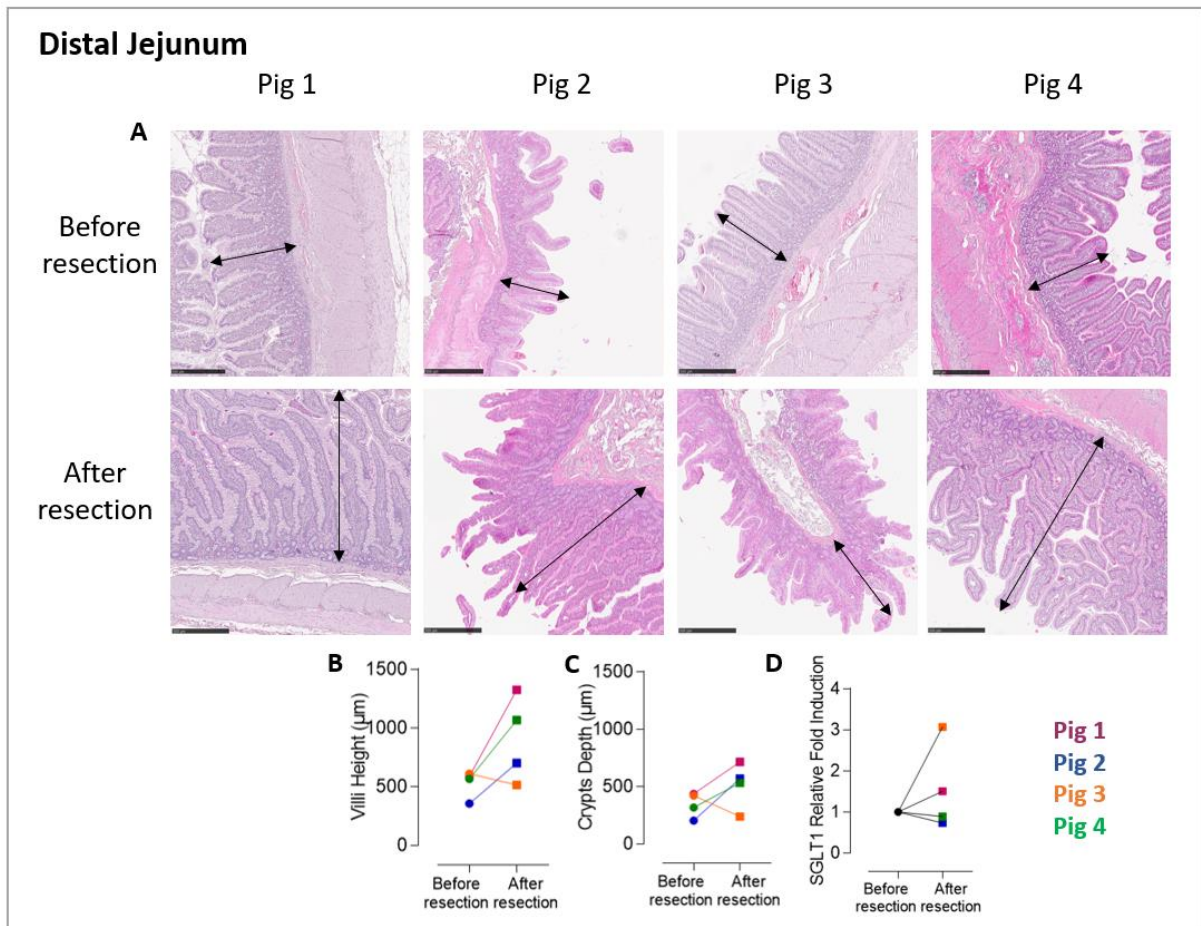


Figure 71: Intestinal adaptation of the distal jejunum following 80% intestinal resection

(A) Histological images of the intestinal mucosa for each of the 4 minipigs before and after resection.

(B) Individual villi height, (C) crypts depth and (D) SGLT1 relative fold induction before and after resection.

Hematoxylin-Eosin coloration; magnification 5X; black scale = 500 µm; black arrow = mucosa thickness

Our findings, in conjunction with these elements from the literature, provide thus evidence to explain the slight decrease in the systemic appearance of D-Xylose that occurs after intestinal resection.

4. No modification of the systemic appearance of D-Xylose after subtotal pancreatectomy and high-fat high-sucrose diet

The findings of our study are consistent with the independence of intestinal glucose absorption from insulin secretion. The presence of insulin receptors in the intestine has been described previously. However, the implication of insulin action in intestinal glucose absorption remains controversial and studies have shown conflicting results about the implication of insulin to increase or decrease intestinal glucose uptake (Costrini et al., 1977; Love and Canavan, 1968; Ussar et al., 2017). This lets us suggest that, if insulin really acts on glucose absorption, its effect would be quantitatively negligible.

However, after the 2-month HFHSD, there was no change in the systemic appearance of D-Xylose. We could have effectively expected an increase following the diet. In fact, a diet rich in sucrose has been

linked to such a mechanism in the past. The increase in intestinal glucose absorption was reached via an increase in SGLT1 content (Dyer et al., 2002; Kishi et al., 1999; Miyamoto et al., 1993).

The pig is a species that is particularly resistant to diabetes, as was exposed in Part 2 of the thesis. Consequently, it is possible that the intestinal adaptation of this species to a high-sucrose diet is different from that of humans. Therefore, it is possible that this species has SGLT1 variants that are hypofunctional and act as protectors against metabolic risk, similar to what Seidelmann et al. have shown in their work on humans (Seidelmann et al., 2018).

5. Intestinal glucose absorption and gastric emptying

Instead of using a drug to speed up gastric emptying, such as metoclopramide (an antagonist of dopamine), the model of suppressing gastric retention through intrajejunal mixed meal tests was chosen (Henze et al., 2018). In fact, by making this choice, we wanted to be free from the potential interindividual variability of response to a pharmacological strategy.

With a glycemic peak that was 2-fold higher and an insulin peak that was 6-fold higher than with oral administration, this model produced a postprandial glucose and insulin response that was very important. The corresponding absorption peak was also 2-fold higher compared to oral administration. These findings confirmed the fundamental significance of gastric retention in the delivery of carbohydrates, into the intestinal lumen and consequently in the appearance of exogenous glucose in the systemic circulation (Wu et al., 2020).

Nutritional approaches have been described as slowing gastric emptying with beneficial consequences on postprandial glycemia, such as: the degree of processing carbohydrates (Hasek et al., 2020); the enrichment in fibers (Hlebowicz et al., 2007); the texture of the meal (Juvonen et al., 2009) particularly thanks to the addition of components increasing the viscosity of the chyme, such as beta glucans (Wolever et al., 2020) or guar gum (Torsdottir et al., 1989); the presence of preload in aminoacids (Du et al., 2018) or whey protein (Hutchison et al., 2015); and the coadministration of lipids (Collier et al., 1984).

In addition to their many other effects, GLP-1 analogs have been used in the development of pharmacological approaches that are said to also slow gastric emptying. By delaying gastric emptying, GLP-1 analogs have been shown to improve postprandial glucose and insulin responses (Jones et al., 2019; Trahair et al., 2015). Amylin or its analogs were also reported to have the same effects (Mayer et al., 2002; Samsom et al., 2000). However, delaying gastric emptying by GLP-1 analogs in type 2 diabetes is controversial because it could lead to early postprandial hypoglycemia with episodes of hyperglycemia in the later stages of the postprandial period.

Is rapid gastric emptying more deleterious for postprandial glucose response than the overall amount of glucose absorbed during a meal? It would appear, according to our results, that gastric emptying has a major influence on the speed of absorption and thus on the value of the peak of postprandial glucose. On the other hand, the nature of the ingested carbohydrates and the number and functionality of the transporters have a great influence on the overall postprandial glucose response (Nazare et al., 2010a; Seidelmann et al., 2018). It would be interesting to study the respective quantitative contribution of gastric emptying, carbohydrates breakdown and glucose transport on intestinal glucose absorption and postprandial glucose response.

The pattern of IGA and postprandial glucose response observed after intrajejunal administration of the meal was similar to the one obtained after sleeve gastrectomy (Chambers et al., 2011; Vigneshwaran et al., 2016b) and RYGB (Nguyen et al., 2014a; Svane et al., 2019; Wang et al., 2012). Although we did not measure the GLP-1 levels after intrajejunal administration, it is very likely that they would rise, as has been demonstrated before (Trahair et al., 2017; Xie et al., 2022). Additionally, a study in healthy minipigs of our group, conducted by Agathe Rémond (data not published) confirmed the important acceleration of the rate of absorption after sleeve gastrectomy but also after sleeve gastrectomy with transit bipartition, in association with a high release in GLP-1 and improvement of postprandial glucose response.

This is why any interest in using dietary or pharmaceutical methods to manage type 2 diabetes by slowing gastric emptying needs to be carefully considered. Undoubtedly, a majorized postprandial glycemic response results from accelerated gastric emptying. But the greatly accelerated gastric emptying brought on by sleeve gastrectomy and RYGB contributes to type 2 diabetes remission through the massive release of GLP-1. Wanting to delay gastric emptying probably is not appropriate in all situations.

6. Limitations of the study

6.1 Inherent limitations to the non-diabetic porcine model

In this research, our goal was to examine how the reduction in insulin secretion and insulin sensitivity affected the systemic appearance of D-Xylose into the intestinal tract. To achieve this, we subjected separate groups of animals to a 2-month HFHSD and a subtotal pancreatectomy. However, the pig is a species that is particularly resistant to type 2 diabetes, as mentioned and shown in Part 2 of the thesis. Only a slight phenotype was obtained for each of the groups here: even though the animals gained weight after the diet, there was only a slight decrease in insulin sensitivity. The acute insulin response was also slightly reduced after subtotal pancreatectomy, but postprandial insulinemia was not affected.

Moreover, the healthy minipig model shows gastric emptying modalities that are somewhat different from those in humans. The time of gastric emptying is longer in Göttingen minipigs compared to humans (40 min compared to 20 minutes for a liquid meal) (Christiansen et al., 2015; Suenderhauf et al., 2014) and the intraindividual variability is also more important in minipigs (Henze et al., 2018; Suenderhauf et al., 2014). This is why we prolonged for Group 4 the fasting to 18 hours instead of 12, in order to be sure that the stomach was completely empty and unaffected by the previous meal at the test. In order to reduce the intraindividual variability of gastric emptying, we also carried out the meal tests in duplicate for this group. Every meal test in this species should ideally be done twice.

6.2 Statistical limits

After intestinal resection, the majority of our results were trends instead of being statistically significant. So, we lacked statistical power to confirm the effect. Additionally, no significant difference was highlighted after subtotal pancreatectomy and diet. The non-quantifiable beta error that underlies these tests of comparison, however, prevents us from drawing any rigorous conclusions about the similarity of these results.

6.3 Computational model not available for data following intrajejunal administration

The results obtained by the two “Calculation” and “Retention” models showed similar trends. Only the “Calculation” model was used to test the impact of accelerated gastric emptying on the pattern of absorption of D-Xylose. In fact, there is currently no adaptation of these computational models that allows for the determination of Ra D-Xylose after intrajejunal administration of the meal.

However, regardless of the computational model, the analysis of the local sensitivity of gastric emptying on the amount of glucose absorbed revealed a non-influence of gastric emptying from 150 minutes after the meal test (data not shown). The findings of this independent analysis, performed by the team of CRISAL, are consistent with our results obtained by the “Calculation” model, demonstrating the non-influence of gastric emptying beyond 180 min of the meal.

6.4 Intrajejunal (not intraduodenal) administration

Instead of being implanted just behind the pylorus, the tube was actually placed in the proximal jejunum, after the duodeno-jejunal junction. As a result, the entire duodenal portion was shifted, and the elaborated model was not totally consistent with a suppression of gastric retention. The duodenum represents only a small fraction of the total intestine. However, it is still possible that if the tube had been inserted directly behind the pylorus, we would have observed a slightly different pattern of D-Xylose absorption. We could have observed a higher peak of Ra D-Xylose because the duodenum is particularly rich in SGLT1 (Lehmann and Hornby, 2016).

This decision was based on the technical simplicity of inserting the jejunal tube into the proximal jejunum as opposed to the proximal duodenum. If the tube had been implanted in this location, there would have been greater risks of altering the release of pancreatic and biliary secretions, and damaging the intestine.

V. Conclusion

In this section, we challenge the relevance of the systemic appearance of D-Xylose in experimental model by decreasing intestinal glucose absorption, insulin secretion and insulin sensitivity and by accelerating the rate of delivery of nutrients into the intestinal lumen. The systemic appearance of D-Xylose was not affected by insulin secretion and sensitivity but exhibited a specific decrease in response to a decrease of intestinal glucose absorption and was also sensitive to the rate of gastric emptying.

However, an accelerated gastric emptying would not result in a rise in the amount of D-Xylose absorbed over the previous 180 minutes. The overall quantity of D-Xylose absorbed could thus be interpreted independently from gastric emptying (**Figure 72**).

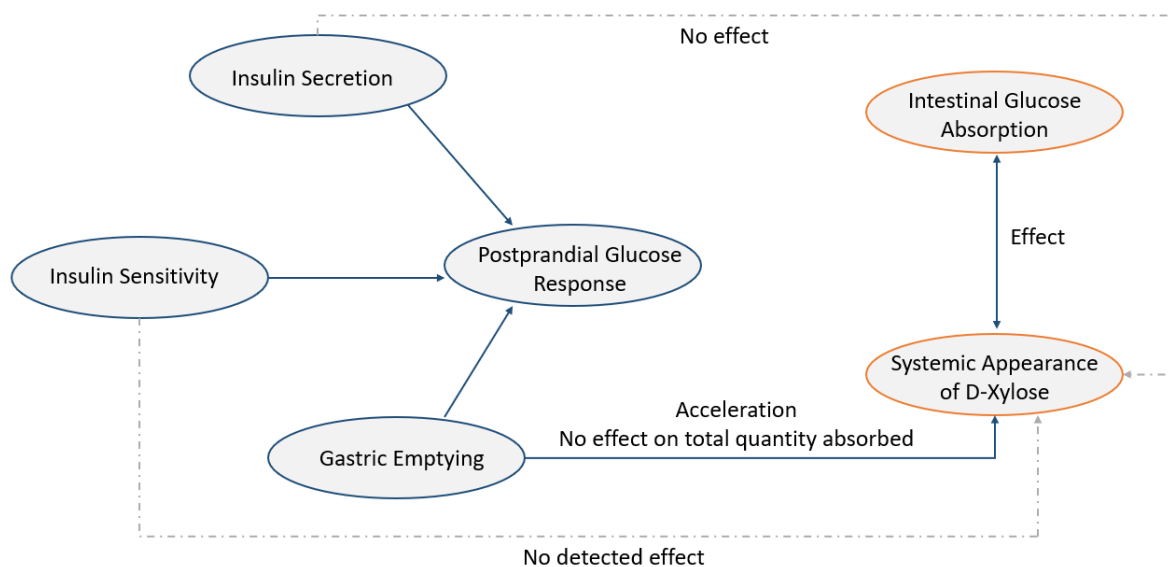


Figure 72: Contribution of insulin secretion, insulin sensitivity, and gastric emptying on the systemic appearance of D-Xylose

The dotted arrows represent an absence of effect.

To resume, we have confirmed the relevance of D-Xylose appearance to specifically identify variations in the pattern of absorption, that make it a relevant biomarker to quantify intestinal glucose absorption. D-Xylose test can thus be used in context of dysglycemia, which is the topic of the final section of the thesis.

Part 5

Exploration of D-Xylose Clinical Value in Glucose Metabolic Disorders

I. Introduction

As previously mentioned, insulin secretion and sensitivity are well-known mechanisms that contribute to the postprandial glucose response in health; therefore, a decrease in insulin secretion and sensitivity are primary pathophysiological factors that lead to the onset of type 2 diabetes (DeFronzo, 2009). Intestinal glucose absorption has been suggested as a potential mechanism related to type 2 diabetes. Furthermore, in healthy non-diabetic subjects, intestinal glucose absorption was shown to be one of the major drivers of the postprandial glucose response, particularly of the 1-hour postload (Fiorentino et al., 2018; Tricò et al., 2019b). However, its impact on postprandial glycaemic response in individuals with type 2 diabetes and impaired glucose tolerance still remained unclear.

In the earlier sections of the thesis, we developed models for measuring intestinal glucose absorption in vivo using D-Xylose as biomarker. We challenged D-Xylose tests in experimental models and confirmed its relevance to specifically quantify variations in intestinal glucose absorption.

The aim of this present part of the study was to explore D-Xylose clinical value in glucose metabolic disorders. For this purpose, we quantified the rate of appearance of D-Xylose in individuals with diverse glycaemic status and associated it with their postprandial glucose response. We wanted thus to confirm the association between D-Xylose absorption and postprandial glucose response. **Figure 73** is a graphical representation of our issue.

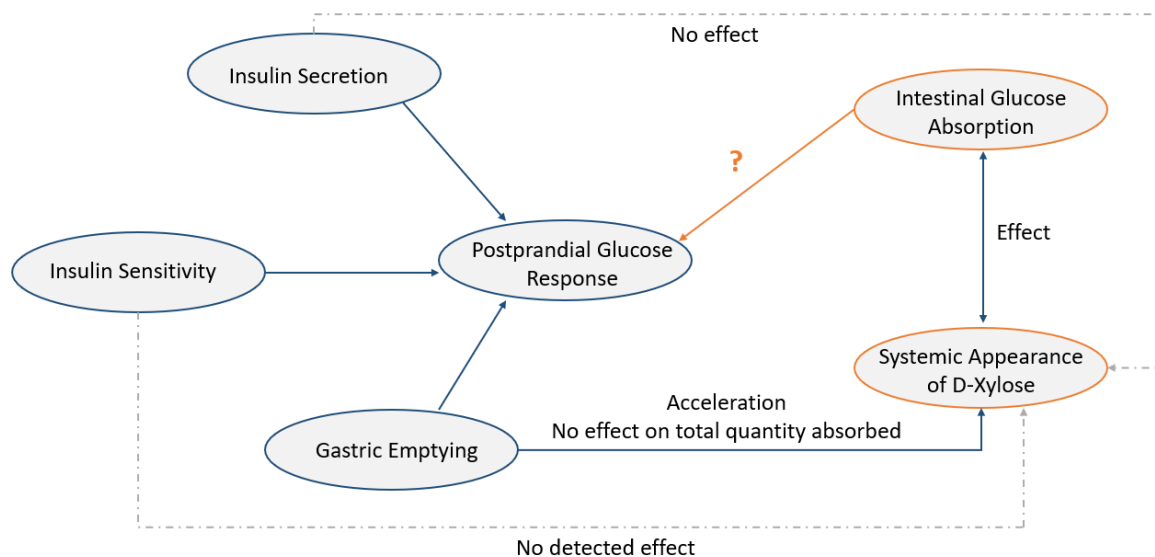


Figure 73: Contribution of insulin secretion, insulin sensitivity, and intestinal glucose absorption on postprandial glycaemic response

? = relationship between factors still unclear. The orange narrows represent the relationship of interest for this part of the thesis.

We further hypothesized that intestinal glucose absorption is a crucial factor in determining postprandial glycemic response, both in people with normal glucose tolerance and those with impaired glucose tolerance, as was shown in healthy subjects (Tricò et al., 2019b). Finally, we suggest its contribution to both early postprandial glycemia and overall postprandial glucose excursion.

We conducted cross-sectional studies on a cohort of healthy minipigs and on the ABOS cohort from the Centre Hospitalier Universitaire de Lille, which was made up of obese patients with varying glycemic status in order to validate our hypothesis.

II. Materials and methods

1. Ethical statement

1.1 Animal cross-sectional study

All the 74 animals of the healthy minipigs cohort belonged to previous preclinical projects (carried out by our laboratory between 2012 and 2021) approved by the local French Committee of Animal Research and Ethics (CEEA-75, authorization n°12467, n°18915 and n°4273), in accordance with European law (2010/63/EU directive). All the procedures were carried out in the agreed-upon (n°D59-35010) Département Hospitalo-Universitaire de Recherche et d'Enseignement (Dhure) in the Faculty of Medicine in Lille, France.

1.2 Clinical cross-sectional study

The cohort of patients was constituted of 158 subjects. All were candidate for metabolic surgery and have been included (between 2006 and 2022) to the Lille University Hospital "Atlas Biologique de l'Obésité Sévère" (ABOS/DIAB-OMICS) cohort, ongoing prospective study aimed at better understanding the determinants of metabolic surgery outcomes. All patients provided a written information and consent form before inclusion. This project benefited from an ethical approval by the Comité de Protection des Personnes Nord Ouest VI (Lille, France) (CP06/49, registration number DGS 2006/0307, Clinical Gov NCT01129297).

2. Animals and housing

A total of 74 healthy minipigs Göttingen-like (20 males and 54 females) weighing 44.5 ± 13.8 kg (Pannier, Wylder, France) were included in this part of the project. As described previously in the thesis, all animals were individually housed in conventional conditions with enrichment and benefited from a 15-day acclimatization period. Water was provided *ad libitum* and standard food given twice a day. The composition of food was previously described in Part 2 of the thesis.

3. Study design

3.1 Animal cross-sectional study

All the minipigs were subjected to an oral Mixed Meal Test (MMT) including D-Xylose. The MMT had the same constitution and was given according to the same modalities as previously described in the thesis and all the minipigs were subjected, 2 days before the MMT, to the implantation of a central venous catheter (CVC) under general anesthesia (see Materials and Methods of Part 2, 3 or 4).

A 20-g solid energy bar (Ovomaltine®, Nestlé, France) and 200 mL of liquid (Fortimel Energy®, Nutricia, France) were mixed. The dose of 30 g of D-Xylose was then added to the mix. The MMT was given *vigil*, after an overnight fasting, for a 10-min period, and via a nasogastric tube of 16 Fr that had previously been implanted under general anesthesia during the CVC implantation procedure. On EDTA and fluorinated tubes, blood samples were obtained before the MMT was administered (t=0 min) and at various time intervals afterwards (t=15, t=30, t=60, t=90, t=120, and t=180 min). They were centrifuged (4000 rpm for 10 min at 4°C) and plasma was isolated and stored at -80°C until analysis.

Since we did not dispose of neither a type 2 diabetes nor an impaired glucose tolerance minipig model, we stratified all the healthy minipigs in 4 quartiles according to the value of their 30 min-Incremental glycemia obtained during the MMT. The respective characteristics of the First Quartile (n = 19), Second Quartile (n = 19), Third Quartile (n = 18) and Last Quartile (n = 18) were presented in the **Table 4**.

3.2 Clinical cross-sectional study

The patients eligible to metabolic surgery included in the ABOS cohort underwent a 180 min-MMT including 30 g of D-Xylose after an overnight fasting. The MMT administered was identical in composition as the one given to the minipigs. Blood samples were collected in dry, fluorinated and EDTA tubes at t=0, t=15, t=30, t=60, t=90, t=120 and t=180 min via a peripheral catheter. Only data from non-operated patients were considered in this work.

Patients were then stratified according to their glycemic status: Obesity and Type 2 Diabetes (T2D, n = 87), Obesity and Impaired Glucose Tolerance (IGT, n = 30) and Obesity and Normal Glucose Tolerance (NG, n = 41). Patients from these groups were compared to a lean group of subjects (Lean, n = 8) constituted of volunteers from the department of General and Endocrine Surgery of the Lille University Hospital. The characteristics of the patients were presented in the **Table 5**.

4. Biological procedures

The biological analyses were the similar as previously described in the previous parts of the thesis. The amperometric glucose oxidase method was used to measure the level of glucose in blood (glucometer Accu-Chek Performa®, Roche, France, or Nova Biomedical StatStrip Xpress®, DSI, USA). Blood glucose

levels were determined instantaneously during each metabolic evaluation. A DXI Access Immunoassay System (Beckman Coulter) with an assay range between 0.3 and 300 μ IU/mL was used to measure the plasma insulin concentrations, as previously mentioned (Cook et al., 2010). Plasma D-Xylose levels were determined by a colorimetric method with phloroglucinol (Eberts et al., 1979) by the glycobiology department of the Centre de Biologie-Pathologie of Lille University Hospital.

5. Intestinal glucose absorption modeling with D-Xylose

The “Calculation” model was used here to assess the Rate of Appearance of D-Xylose (Ra D-Xylose). In fact, no computational model was available yet in humans. The volume of distribution of D-Xylose was determined for each minipig according to its weight. For humans, we used previous data about D-Xylose intravenous administration (Craig and Atkinson, 1988; Fiset and LeBel, 1990) to determine by computational modeling the constant of elimination of D-Xylose (k_{elim}). k_{elim} was then fixed to 0.017 /min in humans. Concerning the volume of distribution, the value of 2.3 dL/kg was implemented for all the patients (Worwag et al., 1987) since it has not been assessed for each subject. The cumulative loads of D-Xylose absorbed were also estimated by the calculation of the time-dependent area under curve (AUC) of Ra D-Xylose.

6. Calculations and statistics

Results were expressed as mean \pm SEM for curves and mean \pm SD for histograms, as specified. Areas under the curve (AUC) were calculated during the defined periods following ingestion by the trapezoidal method. GraphPad Prism[®] 8 software was used for the graphical visualization and calculations.

Continuous variables were analyzed with paired Student’s t-test or Ordinary One-Way ANOVA Tukey’s post-hoc test, as specified. Dynamic variables during meal tests between groups or models were compared using a Two-Way ANOVA or a Mixed-Effects model with Sidak post-hoc test for multiple comparisons. The presence of interactions between variables were systematically assessed.

The peripheral insulin sensitivity was assessed by the calculation of the Matsuda Index (Matsuda and DeFronzo, 1999) (see Part 2).

The assessment of the insulin secretion was performed using the Disposition Index (Utzschneider et al., 2009), corresponding to the ratio between the Insulinogenic Index (IGI) and the Homeostasis Model Assessment of Insulin Resistance (HOMA-IR).

$IGI = [\text{Insulinemia (t = 30)} - \text{Insulinemia (t = 0)}] / [\text{Glycemia (t = 30)} - \text{Glycemia (t = 0)}]$, as previously described (Singh, 2010) (see Part 2).

HOMA-IR = [Glycemia (t=0) (mg/dL) × Insulinemia (t=0) (μUI/mL)]/405, as previously described (Matthews et al., 1985). The HOMA-IR is an index of insulin resistance at a steady state. The relationship between glucose and insulin in the basal state reflects the balance between hepatic glucose output and insulin secretion, which is maintained by a feedback loop between the liver and β-cells.

Disposition Index = IGI/HOMA-IR. It provides thus a reflect of beta cell function adjusted on insulin sensitivity.

Univariate correlations between postprandial glucose response and intestinal glucose absorption were tested using Pearson coefficients. Multivariable linear regression models with intercept were used to examine the independent contribution of intestinal glucose absorption, insulin sensitivity and early insulin secretion on postprandial glycemic response in each case. For multivariate analyses, the variables were centered-reduced.

The significance level was established for p<0.05.

III. Results

1. Variation of intestinal D-Xylose absorption according to glycemic status

Concerning healthy minipigs, all the quartiles were all constituted of more females than males and were not different in terms of weight. Fasting glycemia, fasting insulin, HOMA-IR and the two indexes of insulin secretion Insulinogenic Index and Disposition Index were also not different.

Healthy minipigs (n = 74)	Last Quartile (n = 18)	Third Quartile (n = 18)	Second Quartile (n = 19)	First Quartile (n = 19)
Sex				
Female	12 (67 %)	14 (78 %)	12 (63 %)	17 (89 %)
Male	7 (33 %)	4 (22 %)	7 (37 %)	2 (11 %)
Weight, kg	43.2 (12.8)	49.9 (10.6)	49.8 (14.6)	47.3 (12.2)
Fasting Glycemia, mg/dL	80.1 (12.8)	76.3 (7.9)	77.3 (10.1)	78.1 (10.5)
30 min-Incremental Glycemia, mg/dL	52.7 (11.8)	27.0 (4.8)	11.1 (3.0)	-1.7 (7.9)
60 min-Incremental Glycemia, mg/dL	42.1 (25.5)	28.9 (18.9)	13.1 (12.9)	4.9 (7.9)
180 min-iAUC Glycemia	6781 (2372)	4884 (3265)	2769 (1692)	1834 (1630)
30 min-AUC Ra D-Xylose, mg/kg	223.4 (84.5) *§	190.6 (72.6) *#	92.6 (53.6)	79.3 (80.9)
60 min-AUC Ra D-Xylose, mg/kg	316.2 (113.6) *§	274.6 (98.4) *#	213.3 (106.1)	166.1 (140.6)
180 min-AUC Ra D-Xylose, mg/kg	945.4 (419.9) *§	890.9 (303.3) *#	571.8 (249.7)	441.3 (280.9)
Fasting Insulin, μIU/mL	18.4 (15.0)	17.8 (13.7)	14.8 (11.9)	17.1 (13.6)
HOMA-IR	3.7 (3.0)	3.3 (2.5)	2.9 (2.6)	3.6 (3.5)
Matsuda Index	3.3 (1.0) *§	6.8 (4.7) *#	11.6 (7.0)	12.5 (6.7)
Insulinogenic Index	2.5 (5.6)	1.7 (3.6)	1.1 (2.2)	0.9 (0.7)
Disposition Index	0.5 (0.5)	0.4 (0.3)	0.7 (0.9)	0.7 (1.7)

Table 4: Characteristics of the healthy minipigs according to the stratification in quartiles

Data are expressed in n (%) or mean (SD). (i)AUC = (Incremental) Area Under Curve. Ra D-Xylose = Rate of Appearance of D-Xylose. HOMA-IR = Homeostasis Model Assessment of Insulin Resistance.

Ordinary One-Way ANOVA with Tukey's post-hoc test between quartiles (excepted for incremental of iAUC glycemia); * First vs Last quartile; ° First vs Third quartile; # Second vs Third quartile; § Second vs Last quartile; p<0.05.

The groups differed mainly according to quantity of glucose absorbed during the meal, at 30, 60 and 180 min, with higher quantity absorbed in the Third and Last quartiles (p<0.05). Additionally, the Matsuda Index was lower in these same quartiles (p<0.05) (**Table 4**).

Human subjects (n = 166)	Obesity and Type 2 Diabetes (T2D; n = 87)	Obesity and Impaired Glucose Tolerance (IGT; n = 30)	Obesity and Normal Glucose Tolerance (NG; n = 41)	Lean Subjects (Lean; n = 8)
Sex				
Female	53 (61 %)	21 (70 %)	30 (63 %)	4 (50 %)
Male	34 (39 %)	9 (30 %)	11 (37 %)	4 (50 %)
Type of surgery				
RYGB	61 (70 %)	14 (46 %)	19 (46 %)	NC
SG	12 (14 %)	2 (7 %)	8 (20 %)	NC
AGB	5 (6 %)	2 (7 %)	0 (0 %)	NC
Others	9 (10 %)	12 (40 %)	14 (34 %)	NC
Age, years	49.6 (9.0)	45.6 (11.2)	41.0 (11.6)	38.7 (6.1)
BMI, kg/m ²	45.3 (9.4)	45.7 (7.9)	45.0 (6.1)	22.7 (2.5)
Diabetes duration, years	8.3 (10.6)	NC	NC	NC
Antidiabetic drugs				
Total	78 (90 %)	NC	NC	NC
0	9 (10 %)	NC	NC	NC
1§	32 (37 %)	NC	NC	NC
≥ 2§	19 (22 %)	NC	NC	NC
Insulin	28 (32 %)	NC	NC	NC
HbA1c, %	7.5 (1.5)*#	5.8 (0.3)	5.3 (0.2)	5.5 (0.4)
Fasting Glycemia, mg/dL	164.5 (62.7)*#	102.4 (13.3)°	88.6 (9.9)	83.6 (3.0)
30 min-Incremental Glycemia, mg/dL	38.6 (26.5)*	29.4 (14.9)	19.6 (15.7)	15.7 (15.1)
60 min-Incremental Glycemia, mg/dL	52.4 (25.8)*	33.6 (20.7)°	15.7 (13.2)	9.0 (21.6)
180 min-iAUC Glycemia	10 749 (10 717) *#	4 241 (2 379)	2 798 (1 719)	2 697 (1 306)
30 min-AUC Ra D-Xylose, mg/kg	39.1 (21.8)*	31.5 (13.1)	29.2 (17.8)	25.4 (10.3)
60 min-AUC Ra D-Xylose, mg/kg	98.6 (45.2)*	90.5 (30.0)	74.3 (26.3)	73.7 (26.9)
180 min-AUC Ra D-Xylose, mg/kg	285.1 (89.7)	266.9 (47.4)	250.0 (54.5)	253.3 (41.2)
Fasting Insulin, µUI/mL§	30.1 (35.7)*#	18.7 (10.1)	14.0 (8.5)	3.0 (1.2)
Fasting C-peptide, ng/mL	4.5 (2.2)*	3.7 (1.2)	3.1 (0.96)	1.7 (0.2)
HOMA-IR	10.2 (8.9)*#	4.9 (3.0)	3.1 (2.1)	0.63 (0.23)
Matsuda Index	2.5 (1.5)*	3.7 (2.1)°	6.2 (4.5)	19.3 (7.6)
Insulinogenic Index	0.83 (1.2)#	4.2 (11.2)	3.5 (7.5)	0.17 (2.4)
Disposition Index	0.15 (0.31)	1.3 (4.3)	1.5 (4.3)	0.1 (5.1)
Dyslipidemia	68 (78 %)	17 (57 %)	22 (54 %)	NC
Hypolipidemic treatment	47 (54 %)	6 (20 %)	1 (2 %)	NC
Hypertension	71 (82 %)	20 (67 %)	16 (39 %)	NC
Anti-hypertensive treatment	65 (75 %)	12 (40 %)	9 (22 %)	NC

Table 5: Baseline patients characteristics according to glycemic status stratification in ABOS cohort and compared with a lean group of subjects

Data are expressed in n (%) or mean (SD). RYGB = Roux-en-Y Gastric Bypass. SG = Sleeve Gastrectomy. AGB = Adjustable Gastric Band. (i)AUC = (Incremental) Area Under Curve. § = Patients under insulin treatment were excluded. NC = Not Concerned.

Ordinary One-Way ANOVA with Tukey's post-hoc test between T2D, IGT and NG; *p<0.05 T2D versus NG; °p<0.05 IGT versus NG; #p<0.05 T2D versus IGT.

Concerning humans, there were more females than males in the T2D, IGT and NG groups (respectively 61 %, 70 % and 63 %) whereas the sex ratio was balanced in the Lean group. The patients were aged 49.6 ± 9.0 , 45.6 ± 11.2 , 41.0 ± 11.6 and 38.7 ± 6.1 years respectively in the T2D, IGT, NG and Lean groups. The mean BMI for the patients included in the ABOS cohort was around 45.5 kg/m^2 . The diabetes duration in the T2D groups was 8.3 ± 10.6 years and 90 % of these patients benefited from at least one antidiabetic medication, of which 32 % was insulin. Additionally, 78 %, 57 % and 54 % of the patients belonging respectively to the T2D, IGT and NG groups showed signs of dyslipidemia and 82 % (for T2D), 67 % (for IGT) and 39 % (for NG) exhibited symptoms of hypertension.

The patients of the T2D presented the highest postprandial glycemic excursions at 30, 60 and 180 min ($p<0.0001$), associated with the highest amount of glucose absorbed at 30 ($p<0.05$), 60 ($p<0.005$) and 180 min. They also presented the highest fasting insulin ($p<0.0001$) and a noticeable insulin resistance, as highlighted by the HOMA-IR ($p<0.0001$) and the Matsuda Index ($p<0.0001$), associated with the lowest abilities of insulin secretion, as shown by the Insulinogenic Index ($p<0.05$) and the Disposition Index (**Table 5**).

The evolution of postprandial glucose and insulin response of respectively healthy minipigs and human subjects were described in the **Figure 74**.

As explained previously, the healthy minipigs were stratified in four quartiles according to the value of their 30-min Incremental glycemia. Globally, the minipigs from the highest quartiles showed the highest values of postprandial glycemia whereas those from the lowest showed the lowest values ($p<0.0001$) (**Figure 74A**). Additionally, the highest insulin response was observed in the highest quartiles and the lowest one in the lowest quartiles ($71.2 \pm 11.8 \text{ } \mu\text{IU/mL}$ for the Last Quartile compared to $25.9 \pm 6.9 \text{ } \mu\text{IU/mL}$ for the First Quartile, $p<0.05$), with a significant interaction between the time of the MMT and the insulin levels ($p<0.005$) (**Figure 74B**).

For human subjects, postprandial glucose differed in accordance with the phenotype of the patients ($p<0.0001$). However, no significant difference was observed between the NG and the Lean group (**Figure 74C**). Insulin levels differed according to the glycemic status ($p<0.005$) (**Figure 74D**).

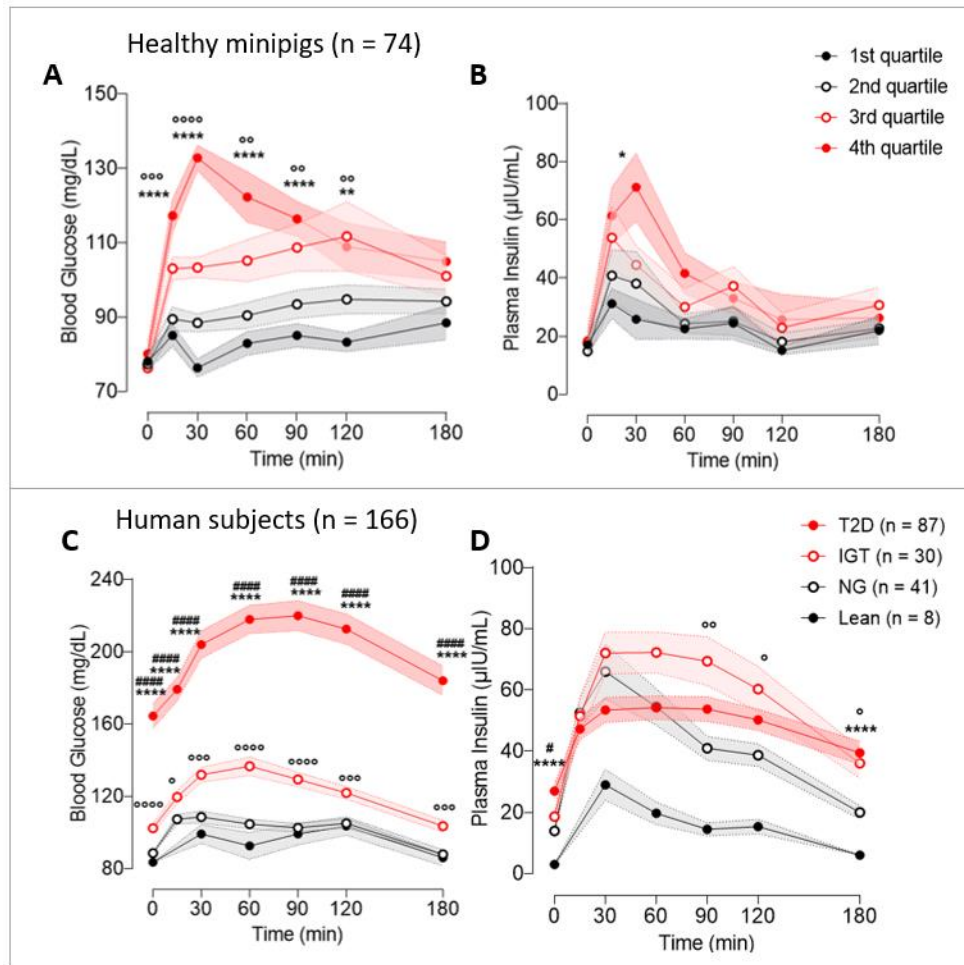


Figure 74: Postprandial glucose and insulin response during a Mixed Meal Test in healthy minipigs and human subjects with different glycaemic status

(A-B) Healthy minipigs (n = 74): (A) Postprandial Glucose (Mean ± SEM) and (B) Insulin (Mean ± SEM) response during the Mixed Meal Test (MMT) according to quartiles.

1st quartile = full black circles (n = 19); 2nd quartile = empty black circles (n = 19); 3rd quartile = empty red circles (n = 18); 4th quartile = full red circles (n = 18). * symbol = 1st quartile versus 4th quartile. ° symbol = 1st quartile versus 3rd quartile. # symbol = 2nd quartile versus 3rd quartile. § symbol = 2nd quartile versus 4th quartile.

(C-D) Human subjects (n = 166) stratified according to their glycaemic status: (C) Postprandial Glucose (Mean ± SEM) and (D) Insulin (Mean ± SEM) response during the MMT.

Lean subjects (Lean; n=8) = full black circles; Patients with Obesity and Normal Glucose Tolerance (NG; n=41) = empty black circles; Patients with Obesity and Impaired Glucose Tolerance (IGT; n=30) = empty red circles; Patients with Obesity and Type 2 Diabetes (T2D; n=87) = full red circles. * symbol = T2D versus NG. ° symbol = IGT versus NG. # symbol = T2D versus IGT

Intestinal glucose absorption pattern was also evaluated in both cohorts of healthy minipigs and human subjects by the assessment of the Rate of Appearance of D-Xylose (Ra D-Xylose) and the area under the curve (AUC) of Ra D-Xylose (**Figure 75**).

In healthy minipigs, Ra D-Xylose values were globally significantly the highest in the highest quartiles ($p < 0.0001$), with a significant interaction between the time of the meal and the quartile ($p < 0.0001$). (Figure 75A).

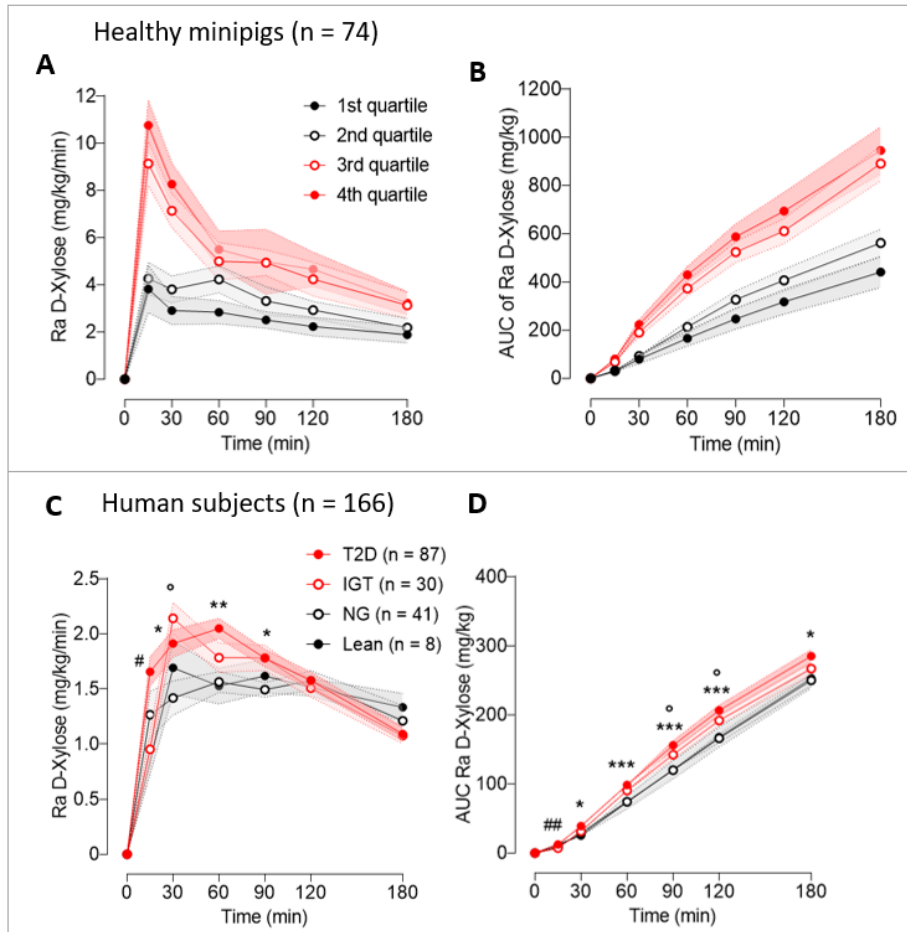


Figure 75: Intestinal glucose absorption pattern during a Mixed Meal Test in healthy minipigs and human subjects with different glycemic status

(A-B) Healthy minipigs (n = 74): (A) Rate of Appearance of D-Xylose (Ra D-Xylose) (Mean \pm SEM), (B) Cumulative area under curve (AUC) of Ra D-Xylose (Mean \pm SEM)

1st quartile = full black circles (n = 19); 2nd quartile = empty black circles (n = 19); 3rd quartile = empty red circles (n = 18); 4th quartile = full red circles (n = 18). * symbol = 1st quartile versus 4th quartile. ° symbol = 1st quartile versus 3rd quartile. # symbol = 2nd quartile versus 3rd quartile. § symbol = 2nd quartile versus 4th quartile.

(C-D) Human subjects (n = 166): (A) Rate of Appearance of D-Xylose (Ra D-Xylose) (Mean \pm SEM), (B) Cumulative area under curve (AUC) of Ra D-Xylose (Mean \pm SEM)

Lean subjects (Lean; n=8) = full black circles; Patients with Obesity and Normal Glucose Tolerance (NG; n=41) = empty black circles; Patients with Obesity and Impaired Glucose Tolerance (IGT; n=30) = empty red circles; Patients with Obesity and Type 2 Diabetes (T2D; n=87) = full red circles. * symbol = T2D versus NG. ° symbol = IGT versus NG. # symbol = T2D versus IGT

Consequently, the corresponding cumulative amount of D-Xylose absorbed during the meal were also the highest in the Last and Third quartiles compared to the Second and the First ($p < 0.0001$), with a significant interaction between the time of the meal and the quartile ($p < 0.0001$) (**Figure 75B**).

In human subjects, we observed higher Ra D-Xylose values in patients from the T2D and the IGT groups compared to those from the NG and the Lean groups, with a significant interaction between the time of the meal and the glycemic status ($p < 0.0001$) (**Figure 75C**).

Consequently, the cumulative amount of D-Xylose absorbed during the meal were also globally higher in T2D and IGT compared to NG and Lean people ($p < 0.005$), with a significant interaction between the time of the meal test and the group ($p < 0.0001$) (**Figure 75D**).

2. Time-dependent association between D-Xylose absorption and postprandial glucose response

We then evaluated the association between the intestinal absorption of D-Xylose and the postprandial glucose response at different time point during the MMT, in healthy minipigs and human subjects with impaired glucose tolerance or type 2 diabetes. The 30-min Incremental Glycemia, the 60-min Incremental Glycemia and the 180 min-iAUC Glycemia were chosen as variables to define postprandial glucose response respectively at 30 min, 60 min, and 180 min. The 30-min AUC, 60-min AUC et 180-min AUC Ra D-Xylose were the variables chosen to represent intestinal D-Xylose absorption respectively at 30 min, 60 min, and 180 min.

To resume, we found a positive association between the postprandial glucose response and intestinal D-Xylose absorption in healthy minipigs and human subjects with impaired glucose tolerance or type 2 diabetes (**Figure 76**).

In healthy minipigs, the 30-min Incremental glycemia was strongly correlated with the amount of D-Xylose absorbed at 30 min ($r = 0.70$, $p < 0.0001$) (**Figure 76A**). The 60-min Incremental glycemia was correlated with the amount of D-Xylose absorbed at 60 min ($r = 0.63$, $p < 0.0001$) (**Figure 76B**). In addition, the 180-min postprandial glycaemic excursion was also positively correlated with the amount of D-Xylose absorbed at 180 min ($r = 0.54$, $p < 0.0001$) (**Figure 76C**).

In subjects with impaired glucose tolerance or type 2 diabetes, we also found a substantial positive correlation between the amount of D-Xylose absorbed at 30 min and the 30-min Incremental glycemia ($r = 0.64$, $p < 0.0001$) (**Figure 76D**) and between the amount of D-Xylose absorbed at 60 min and the 60-min Incremental glycemia ($r = 0.54$, $p < 0.0001$) (**Figure 76E**). However, we found a weak correlation between the amount of D-Xylose absorbed at 180 min and the global 180-min postprandial glycaemic excursion ($r = 0.29$, $p < 0.0001$) (**Figure 76F**).

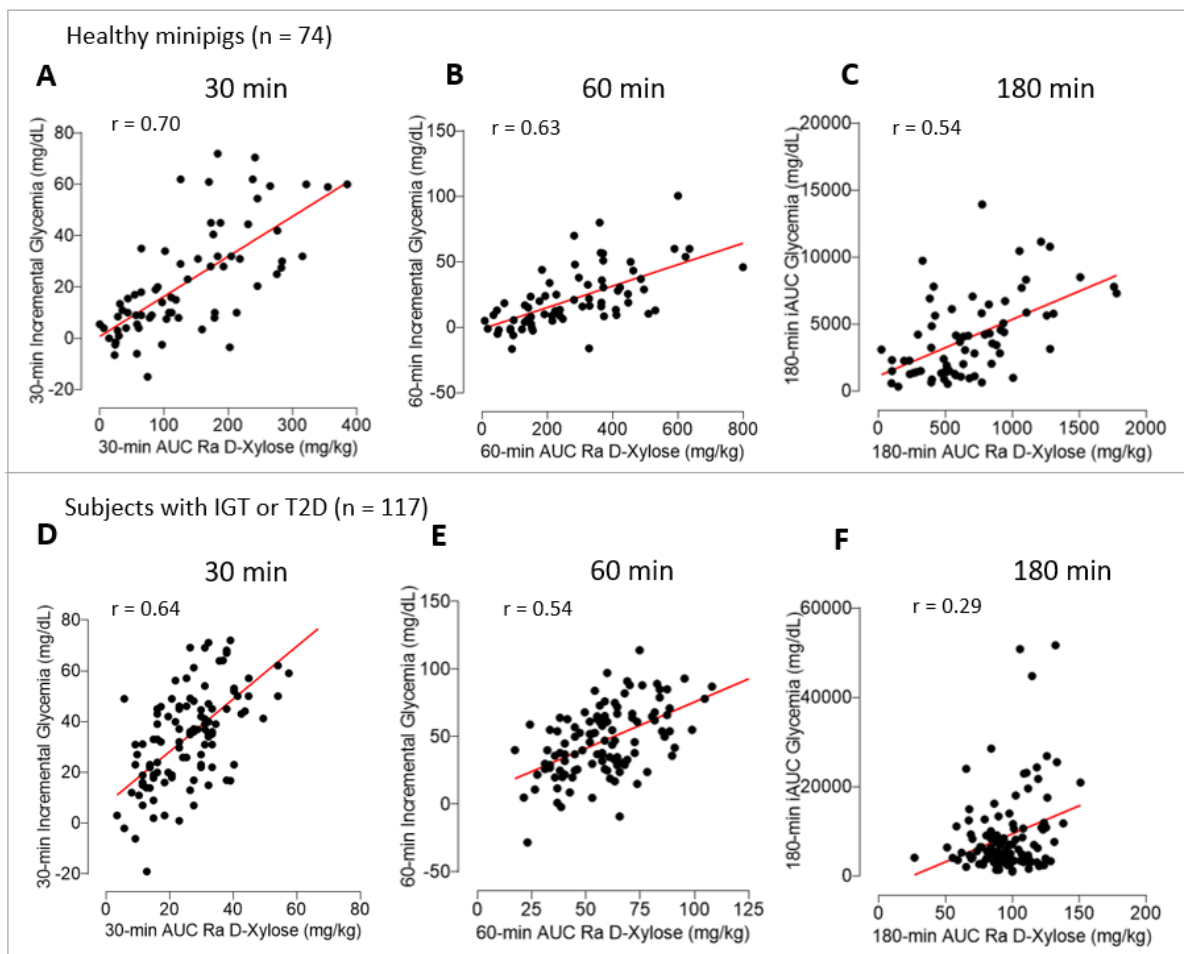


Figure 76: Positive correlations between postprandial glucose response and intestinal glucose absorption in healthy minipigs and human subjects

(A-C) Healthy minipigs (n = 74): Correlations between the postprandial glucose response and the area under curve of the Rate of Appearance of D-Xylose (AUC Ra D-Xylose) at 30 min (r = 0.70), 60 min (r = 0.63) and 180 min (r = 0.54).

(D-F) Subjects with impaired glucose tolerance (IGT) or type 2 diabetes (T2D) (n = 117): Correlations between the postprandial glucose response and the AUC Ra D-Xylose at 30 min (r = 0.64), 60 min (r = 0.54) and 180 min (r = 0.29).

Pearson coefficients, $p < 0.0001$. iAUC = Incremental area under curve.

Finally, we evaluated the respective contribution of insulin sensitivity (with the Matsuda Index), insulin secretion (with the Disposition Index) and intestinal D-Xylose absorption (with the AUC Ra D-Xylose) on postprandial glucose response using multivariate linear regression models in health and impaired glucose tolerance context. Multivariate analyses were thus performed in healthy minipigs and in subjects from IGT or T2D groups (**Figure 77**).

All the estimates of the variables, their corresponding 95 %-confidence interval and p-value as for as the r^2 of the models were exposed in **Table 6**.

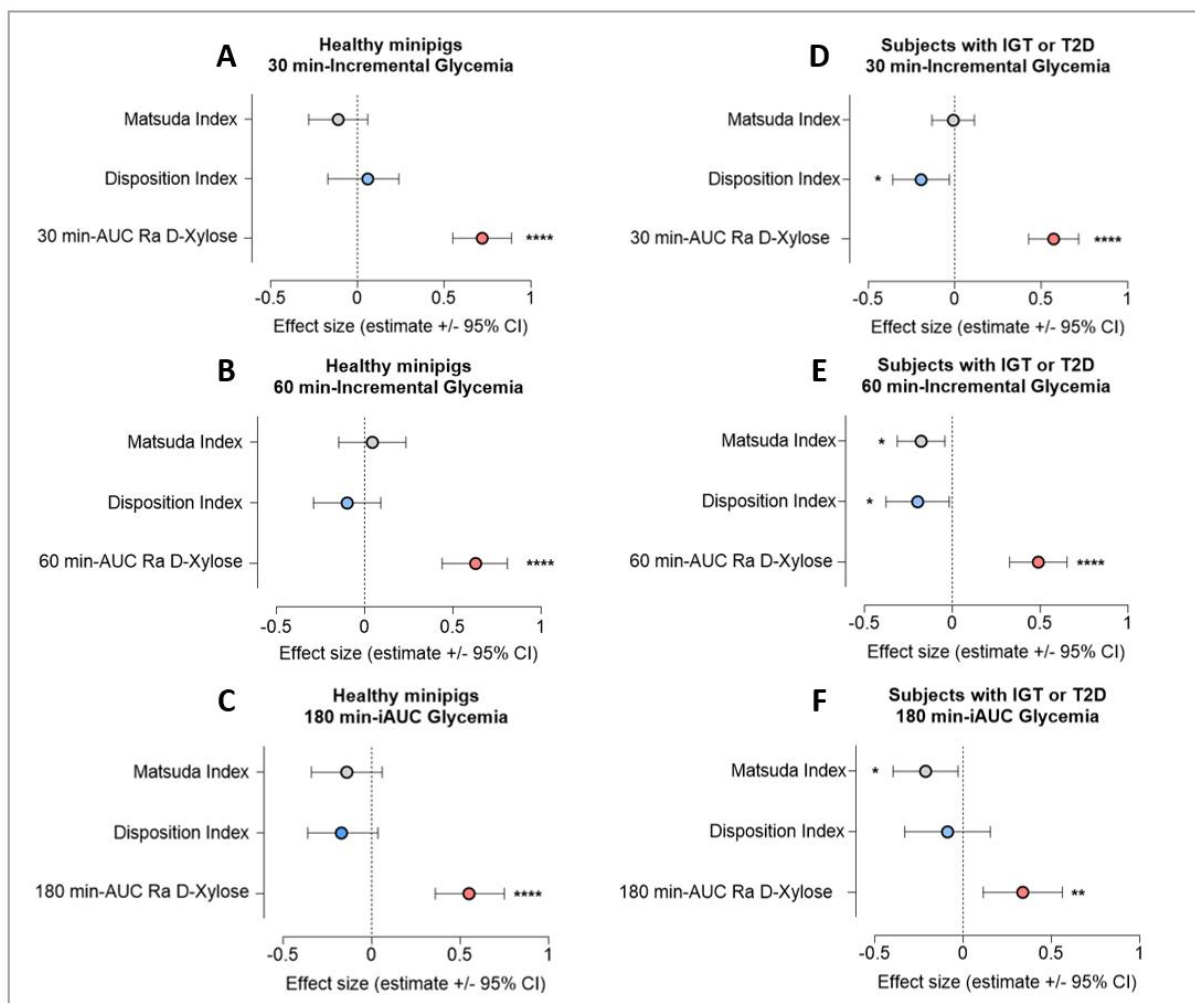


Figure 77: Multivariate Analyses showing the time-dependent contributors of postprandial glycemic response following a Mixed Meal Test in Healthy Minipigs and human Subjects with Impaired Glucose Tolerance or Type 2 Diabetes

(A) Contribution of intestinal glucose absorption (30 min-AUC Ra D-Xylose, red circle), insulin secretion (Disposition Index, blue circle) and insulin sensitivity (Matsuda Index, grey circle) on 30-min postprandial glucose response (30-min Incremental Glycemia) in healthy minipigs (whole-model $r^2=0.51$).

(B) Contribution of intestinal glucose absorption (60-min AUC Ra D-Xylose, red circle), insulin secretion (Disposition Index, blue circle) and insulin sensitivity (Matsuda Index, grey circle) on 60-min postprandial glucose response (60-min Incremental Glycemia) in healthy minipigs (whole-model $r^2=0.41$).

(C) Contribution of intestinal glucose absorption (180-min AUC Ra D-Xylose, red circle), insulin secretion (Disposition Index, blue circle) and insulin sensitivity (Matsuda Index, grey circle) on 180-min postprandial glucose response (180-min iAUC Glycemia) in healthy minipigs (whole-model $r^2=0.36$).

(D) Contribution of intestinal glucose absorption (30-min AUC Ra D-Xylose, red circle), insulin secretion (Disposition Index, blue circle) and insulin sensitivity (Matsuda Index, grey circle) on 30-min postprandial glucose response (30-min Incremental Glycemia) in subjects with Impaired Glucose Tolerance (IGT) or Type 2 Diabetes (T2D) (whole-model $r^2=0.41$).

(E) Contribution of intestinal glucose absorption (60-min AUC Ra D-Xylose, red circle), insulin secretion (Disposition Index, blue circle) and insulin sensitivity (Matsuda Index, grey circle) on 60-min postprandial glucose response (60-min Incremental Glycemia) in subjects with Impaired Glucose Tolerance (IGT) or Type 2 Diabetes (T2D) (whole-model $r^2=0.34$).

(F) Contribution of intestinal glucose absorption (180-min AUC Ra D-Xylose, red circle), insulin secretion (Disposition Index, blue circle) and insulin sensitivity (Matsuda Index, grey circle) on 180-min postprandial glucose response (180-min iAUC Glycemia) in subjects with Impaired Glucose Tolerance (IGT) or Type 2 Diabetes (T2D) (whole-model $r^2=0.16$).

Healthy minipigs (n = 74); Subjects with IGT or T2D (n = 117); iAUC = Incremental Area Under Curve. Multivariable linear regression model with intercept; * $p<0.05$, ** $p<0.005$, **** $p<0.0001$

In healthy minipigs, the 30-min AUC Ra D-Xylose was the only variable significantly associated to the 30-min Incremental Glycemia ($\beta = 0.72$ [0.55; 0.89]; $p<0.0001$; $r^2 = 0.51$) (**Figure 77A**). Similarly, the 60-min AUC Ra D-Xylose was the only variable associated to the 60-min Incremental Glycemia ($\beta = 0.63$ [0.44; 0.81]; $p<0.0001$; $r^2 = 0.41$) (**Figure 77B**) and the 180-min AUC Ra D-Xylose was the only variable associated to the iAUC Glycemia ($\beta = 0.55$ [0.36; 0.75]; $p<0.0001$; $r^2 = 0.36$) (**Figure 77C**).

In subjects with IGT or T2D, two variables were significantly associated to the 30-min Incremental Glycemia ($r^2 = 0.41$): the 30-min AUC Ra D-Xylose ($\beta = 0.57$ [0.42; 0.71]; $p<0.0001$) and the Disposition Index ($\beta = -0.19$ [-0.35; -0.03]; $p<0.05$) (**Figure 77D**). Moreover, all the exposures were contributors of the 60-min Incremental Glycemia ($r^2 = 0.34$): the 60-min AUC Ra D-Xylose ($\beta = 0.49$ [0.33; 0.65]; $p<0.0001$), the Disposition Index ($\beta = -0.19$ [-0.38; -0.02]; $p<0.05$) and the Matsuda Index ($\beta = -0.17$ [-0.31; -0.04]; $p<0.05$) (**Figure 77E**). Finally, the 180-min AUC Ra D-Xylose remained contributors of the 180 min iAUC Glycemia ($\beta = 0.34$ [0.11; 0.56]; $p<0.005$), associated with the Matsuda Index ($\beta = -0.21$ [-0.40; -0.03]; $p<0.05$) ($r^2 = 0.16$) (**Figure 77F**).

	AUC Ra D-Xylose		Disposition Index		Matsuda Index		Intercept		r^2
	Estimate	p-value	Estimate	p-value	Estimate	p-value	Estimate	p-value	
Healthy minipigs									
30 min	0.72 [0.55; 0.89]	<0.0001	0.06 [-0.11; 0.24]	NS	-0.11 [-0.28; 0.06]	NS	0.02 [-0.15; 0.19]	NS	0.51
60 min	0.63 [0.44; 0.81]	<0.0001	-0.10 [-0.29; 0.09]	NS	0.04 [-0.15; 0.23]	NS	0.09 [-0.09; 0.28]	NS	0.41
180 min	0.55 [0.36; 0.75]	<0.0001	-0.17 [-0.36; 0.03]	NS	-0.14 [-0.34; 0.06]	NS	0.01 [-0.18; 0.20]	NS	0.36
IGT/T2D									
30 min	0.57 [0.42; 0.71]	<0.0001	-0.19 [-0.35; -0.03]	<0.05	-0.01 [-0.13; 0.12]	NS	-0.13 [-0.25; 0.00]	<0.05	0.41
60 min	0.49 [0.33; 0.65]	<0.0001	-0.19 [-0.38; -0.02]	<0.05	-0.17 [-0.31; -0.04]	<0.05	0.21 [0.08; 0.35]	<0.005	0.34
180 min	0.34 [0.11; 0.56]	<0.005	-0.09 [-0.33; 0.16]	NS	-0.21 [-0.40; -0.03]	<0.05	-0.06 [-0.24; 0.12]	NS	0.16

Table 6: Multivariate linear regression model describing the time-dependent contribution of intestinal glucose absorption, insulin sensitivity and insulin secretion on postprandial glycemic response in healthy minipigs, all human subjects or subjects with impaired glucose tolerance or type 2 diabetes

Multivariate linear regression model with intercept. Results were expressed with 95 %-confidence interval.

Outcome = Postprandial Glycemic Response at 30 min, 60 min or 180 min. Dependent variables = Intestinal Glucose Absorption (area under curve of Rate of Appearance of D-Xylose (AUC Ra D-Xylose)), Insulin Secretion (Disposition Index) and Insulin Sensitivity (Matsuda Index).

V. Discussion

1. Summary of the obtained results

Using one of our models (the "Calculation" one), we assessed the pattern of intestinal D-Xylose absorption in a cohort of healthy minipigs and in human subjects with varying glycemic status in order to explore its clinical value in glucose metabolic disorders.

Our study showed a positive correlation between postprandial glycemic response and intestinal D-Xylose absorption in healthy minipigs. In patients, the same results were observed: the more altered the glycemic status, the greater the intestinal D-Xylose absorption. In these patients, the important intestinal D-Xylose absorption was not associated with obesity, since the obese patients from the NG group showed similar values compared to the Lean group.

Then, we evaluated the time-dependent correlation between intestinal D-Xylose absorption and postprandial glucose response during the meal in healthy minipigs and dysglycemia. In healthy minipigs, intestinal D-Xylose absorption was the only factor explaining the interindividual variability of postprandial glucose response at any time of the meal. In patients with dysglycemia, intestinal D-Xylose absorption remained associated to postprandial glucose response, at any time. Additionally, the non-negligible co-contribution of the other determinants was totally consistent with the pathophysiology of hyperglycemia: the decrease of insulin secretion would be an explicative factor of an increase in postprandial glucose response only in the early step; the decrease of insulin sensitivity would not be an explicative factor of an increase in postprandial glucose response in the early step but rather in the middle phase and in globality; and finally, intestinal glucose absorption would be an explicative factor of an increase in postprandial glucose response in all the phases, including the overall response, as in healthy individuals.

2. Consistency with the literature data

Only a few studies in the past compared variations of intestinal glucose absorption according to variations in glycemic status. The duodenal SGLT1 level and the postprandial glucose response in healthy individuals were successfully demonstrated to be positively correlated. IGT or T2D patients in particular showed a higher expression (Fiorentino et al., 2017). Another study using oral glucose tolerance tests and isotopic tracers of glucose revealed that subjects with type 2 diabetes had higher peaks of absorption and higher amounts of glucose absorbed than subjects with obesity but not type 2 diabetes (Camastra et al., 2013).

To the best of our knowledge, no study has previously examined how intestinal glucose absorption quantitatively affects the postprandial glucose response in a pathological context. However, because

the peak of insulin secretion occurs at an early stage of the postprandial phase and that the uptake of glucose by the insulin-sensitive tissues takes place in a later step, our results of the multivariate analyses were consistent with the pathophysiological data of the postprandial glucose response (Ferrannini et al., 1985; Taylor et al., 1993).

Additionally, intestinal glucose absorption was shown to be one of the major determinants of the postprandial glucose response at 1 hour as well as at 2 hours in healthy subjects, supporting our findings (Tricò et al., 2019b). This study also highlighted the significant impact of peripheral insulin sensitivity and insulin secretion on the 1-hour postload, which we did not observe in our cohort of minipigs. The modeling was somewhat different because we used clinical indexes to assess beta cell function and insulin sensitivity. Beta cell function was modeled by Tricò and colleagues using the beta cell rate sensitivity (Mari and Ferrannini, 2008), and the calculation of the glucose clearance normalized by the insulin excursion was used to estimate the peripheral insulin sensitivity (Tricò et al., 2015). The Matsuda Index and Disposition Index, which we used as indexes, are more suited to a pathological context, which may be why they were not found to be contributors to the postprandial glucose response in healthy animals.

Our study has an advantage over the one of Tricò and colleagues because we used a mixed meal test rather than a glucose solution, which put us in more physiological conditions. In fact, the Glycemic Index of a meal has a significant impact on intestinal glucose absorption (Péronnet et al., 2015). Our experimental conditions here were similar to those of a physiological meal, allowing us to confidently extrapolate our results to what appears during a usual meal.

3. Intestinal D-Xylose absorption and splanchnic uptake of D-Xylose

The appearance of exogenous glucose in the peripheral circulation includes intestinal glucose absorption minus the splanchnic uptake of glucose. In fact, up to 30 % of the ingested glucose is metabolized by the splanchnic tissues or stored in the liver into glycogen before reaching the peripheral circulation (Abumrad et al., 1982; DeFronzo et al., 1983). Additionally, a decrease in splanchnic glucose uptake has been described in type 2 diabetes (Basu et al., 2001; Ludvik et al., 1997), which may have increased the presence of exogenous glucose in the peripheral circulation, and it was not examined in our cohorts.

In our study, we only measured the portion of D-Xylose metabolized by the liver (7 %) but we did not quantify the splanchnic uptake of D-Xylose (see Part 3 of the thesis). However, this low percentage allowed us to hypothesize that the splanchnic D-Xylose uptake would occur at a much lower rate than the one of glucose. It lets us believe that Ra D-Xylose is actually really close to the rate of intestinal D-Xylose absorption. Consequently, we are confident that, in our study, patients with postprandial

hyperglycemia presented in fact higher intestinal D-Xylose absorption rather than lower splanchnic D-Xylose uptake.

4. Rate of absorption and gastric emptying

It has been yet established that the postprandial glucose response in patients with NG, IGT, and T2D at 30 min during an oral glucose challenge was influenced by the rate of gastric emptying. In patients with IGT and T2D, the rate of gastric emptying also contributed to the postprandial glucose response at 60 min (Chinmay S. Marathe et al., 2015). Furthermore, it is well-known that the rate of gastric emptying is positively correlated to the rate of glucose absorption, contributing to postprandial glucose excursions (Wu et al., 2020).

According to these elements, we could wonder if the accelerated rate of absorption we discovered in some quartiles of minipigs and in patients with IGT and T2D would be due to an accelerated gastric emptying.

In Part 4 of the thesis, we demonstrated that the rate of gastric emptying accelerates the systemic appearance of D-Xylose, but not the total amount absorbed. This means that an accelerated gastric emptying may have contributed to the increase in glucose absorption that was seen in our study at 30 and 60 minutes. However, it would not be the (only) cause because the overall intestinal glucose absorption was also increased (see Part 4).

This phenotype could potentially be explained by an increase in the levels of SGLT1 in the proximal intestine (Fiorentino et al., 2017) or the absence of subjects carrying SGLT1 variants with lower functionalities (Seidelmann et al., 2018). Another investigation in our lab is currently being conducted (by Simon Peschard) to show a causal link between carrying these dysfunctional SGLT1 variants and having a decreased postprandial glucose response. Perhaps the patients in the NG group of our cohort would be numerous carriers of these variants, keeping them from developing diabetes. To the best of our knowledge, these pig variants have not yet been mentioned.

5. Intestinal glucose absorption: an early/causal factor in type 2 diabetes onset?

The findings in the healthy minipigs were especially intriguing because they suggested that intestinal glucose absorption would be the only mechanism explaining the variability of postprandial glucose response, which is not really described in the literature.

It is interesting to note that animals presenting the highest intestinal D-Xylose absorption, and consequently postprandial glucose response, also presented the highest postprandial insulin response. This may explain why the Matsuda Index calculation revealed significant differences between quartiles, suggesting first a lower insulin sensitivity in the highest quartiles.

Previous studies (Bianchi et al., 2013; Jagannathan et al., 2016; Marini et al., 2012) successfully demonstrated that healthy individuals with high postprandial glucose excursions showed signs of alteration of insulin secretion and peripheral insulin sensitivity. But it seems to be the contrary in our case: postprandial insulin response seems to be the consequence of a high postprandial glucose response, due to a high absorption, as is seen after a meal with a high Glycemic Index (Ludwig, 2002). Additionally, we performed the same work but in stratifying the minipigs on D-Xylose absorption instead of incremental glycemia (data not shown). These results showed no significant differences in insulin profil, confirming that intestinal glucose absorption would be the only factor explicating the interindividual variability of postprandial glucose response.

These findings showed that, despite eating a standard meal, there is a significant heterogeneity in the intestinal glucose absorption and consequently, in postprandial glucose response. It thus supports the mechanism of intestinal glucose absorption as a causal determinant responsible for the rise in postprandial glycemc response and thus very early in the progression of type 2 diabetes, before the occurrence of the alteration of insulin sensitivity and secretion, even though the causality relationship was not clearly demonstrated here.

6. Limitations of the study

6.1 Human indexes of insulin sensitivity and secretion in a Minipig model

The use of human indexes of insulin sensitivity (Matsuda Index) and beta cell function (Disposition Index) is one of the limitations of the study. The applicability of these indexes in minipigs has not been proven.

Furthermore, since metabolic disorders in this species are extremely challenging to induce, the notion of insulin resistance and impaired insulin secretion in pigs is relative (see Part 2 of the thesis). This could explain why intestinal glucose absorption is the only explicative factor of the variability in postprandial glucose response in this cohort. The same analysis performed on a larger cohort of healthy humans would be intriguing to investigate. As previously stated (Tricò et al., 2019b), it is likely that human subjects who exhibit a high postprandial glycemc response also exhibit early signs of impaired insulin sensitivity and secretion.

Additionally, rather than assessing insulin secretion and response in relation to time, the Matsuda Index and the Disposition Index reflect a mean state of insulin sensitivity and beta cell function on an entire meal. It keeps these factors steady throughout the meal rather than being time-dependent like intestinal glucose absorption.

6.2 Hepatic insulin sensitivity

In this study, we did not assess hepatic insulin sensitivity. There are not many trustworthy indexes that can measure hepatic insulin sensitivity without using glucose-labeled meal tests.

Abdul-Ghani and colleagues have suggested a different index of hepatic insulin resistance. The 30-min AUC between blood glucose and insulin was multiplied to create the Hepatic Insulin Resistance Index (HIRI) (Abdul-Ghani et al., 2007). Because both the 30-min AUC of glucose and insulin depend on intestinal glucose absorption, it is likely that the HIRI is not entirely specific for hepatic insulin resistance, which would have rendered its use irrelevant for our analyses.

6.3 Splanchnic glucose uptake

As previously stated, because we did not assess it, we cannot completely rule out the possibility that a decrease in splanchnic glucose uptake contributed to the rise in Ra D-Xylose in the minipigs from the highest quartiles and in patients with IGT and T2D.

D-Xylose is thought to be poorly absorbed by the splanchnic tissues, making its occurrence in the bloodstream generally comparable to that of the portal vein. We did not measure this uptake, but a small group of minipigs could have had blood obtained simultaneously during MMT from the portal and external jugular vein to confirm it. Due to the difficulty in collecting blood from the portal vein in vigil animals, we decided against conducting this experiment for ethical reasons.

6.4 Gastric emptying

Furthermore, there was no data on gastric emptying assessment in healthy minipigs or human subjects from our cohorts. As a result, we were unable to evaluate any potential differences in the rate of gastric emptying between the quartiles of minipigs and patient groups. We can exclude its implication for the variations of the amount of glucose absorbed at 180 min between the groups, but not confirm or refute its role concerning the variations observed at 30 and 60 min.

6.5 Causal relationship

Finally, we did not demonstrate in this part of the thesis the existence of a causal relationship between intestinal glucose absorption and type 2 diabetes occurrence, even if it was clearly suspected here.

V. Conclusion

In this section of the thesis, we demonstrated the clinical relevance of using D-Xylose in context of glucose metabolic disorders. We thus confirmed the association between intestinal D-Xylose absorption and postprandial glucose response in health and status with postprandial hyperglycemia.

Independently of insulin sensitivity and secretion, we showed that intestinal glucose absorption was the only determinant of the variations in postprandial glucose response in healthy minipigs at any time of the meal. In addition, intestinal glucose absorption contributed to the early, middle, and overall postprandial glucose responses in patients with an altered glycemic status, in addition to a decline in beta cell function and an increase in insulin sensitivity (**Figure 78**).

Our findings support the causal relationship between high intestinal glucose absorption and high postprandial glucose response, even we did not demonstrate it. In this section, the critical role of intestinal glucose absorption in the pathophysiology of type 2 diabetes was once again reaffirmed. Consequently, we highlighted the relevance of its assessment to better predict the evolution of the disease and to use it as a therapeutic target. Lowering glucose absorption by nutritional, pharmacological, or surgical approaches appears thus as a strategy to be privileged in order to achieve an improvement of postprandial glucose homeostasis.

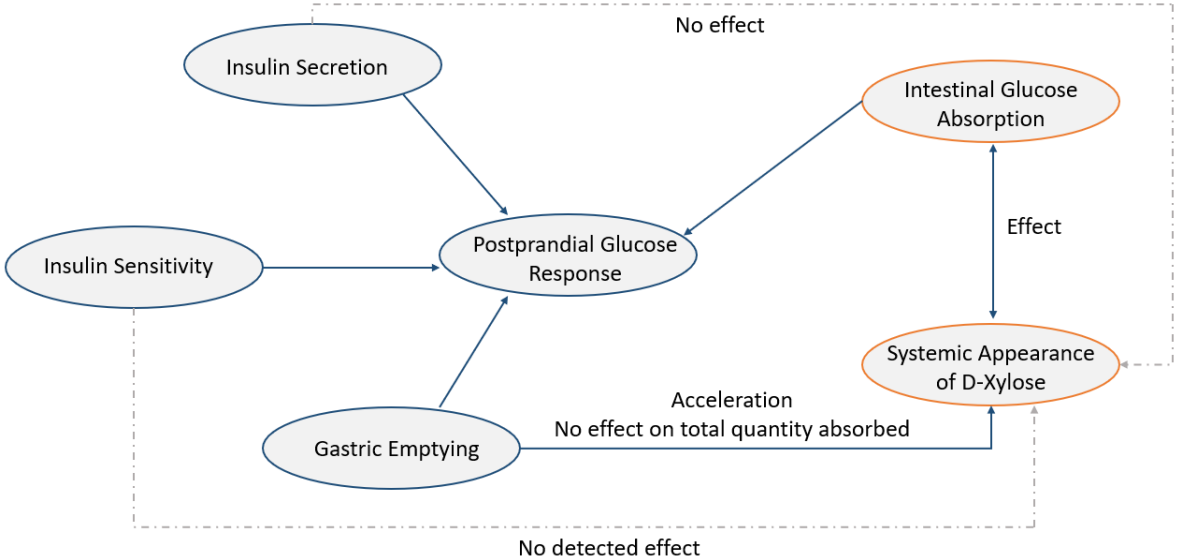


Figure 78: Time-dependent contribution of intestinal glucose absorption, beta cell function and insulin sensitivity on postprandial glucose response in health and impaired glucose tolerance or type 2 diabetes

PGR = Postprandial Glycemic Response; IGT = Impaired Glucose Tolerance; T2D = Type 2 Diabetes. The black arrow represents the positive contribution of a mechanism on postprandial glucose response.

General Conclusion

Intestinal glucose absorption is an important determinant of postprandial glucose response and its routine assessment may inform precision medicine for the prevention and treatment of type 2 diabetes. The subject of the thesis was thus to model intestinal glucose absorption with oral D-Xylose test for confirming its contribution on postprandial glucose response.

We first have presented the supporting evidence from the literature. Secondly, we tried to develop a minipig model of type 2 diabetes, a species particularly resistant to the disease, by combining existing methods with novel approaches. Performing massive overabsorption of glucose and lipids was the only way to obtain a minipig model of metabolic syndrome with first signs of impaired glucose tolerance. These findings therefore support that an increased intestinal glucose absorption would take part to type 2 diabetes pathophysiology, independently of primary insulin resistance and impaired insulin secretion.

Then, we developed and validated new models of in vivo intestinal glucose absorption measurement from oral D-Xylose test in minipigs. Some models are computational and work is still in progress to refine and adapt them to patients with type 2 diabetes.

Moreover, we challenged D-Xylose appearance in experimental models and demonstrated its specificity to show variations in intestinal glucose absorption, confirming it as a reliable biomarker. We particularly showed that a rapid gastric emptying accelerates the rate of absorption, but not the total amount absorbed over a meal, allowing us to rule out gastric emptying as a possible factor in the rising amounts of D-Xylose absorbed over a prolonged meal period.

Finally, we explored D-Xylose clinical value and confirmed the association between intestinal D-Xylose absorption and postprandial glucose response, in health and dysglycemia. We confirmed in health that intestinal D-Xylose absorption is the only explicating factor of the interindividual variability of postprandial glucose response. In impaired glucose tolerance, we confirmed the remaining contribution of intestinal D-Xylose absorption on postprandial hyperglycemia, additionally to impaired insulin secretion and sensitivity, as commonly described.

Although the causal relationship between increased intestinal D-Xylose absorption and dysglycemia was not explored here, we nevertheless demonstrated: a statistically significant positive correlation between intestinal D-Xylose absorption and postprandial glucose response (Part 5); the anteriority of increased intestinal glucose absorption to early signs of impaired glucose tolerance (Part 2); and the independence of intestinal D-Xylose absorption from other mechanistic factors (Part 5).

We did not totally elucidate the contribution of gastric emptying to explain the differences seen on early postprandial glucose response between healthy individual and those with type 2 diabetes but

our data support the existence of intestine-specific factors. It could have been interesting to assess if SGLT1 levels differed according to glycemic status (Fiorentino et al., 2017) and the eventual existence of hypofunctional SGLT1 variants in our cohort associated with lower postprandial glucose response (Seidelmann et al., 2018).

Our research also supported the interest in using 1-hour postprandial glucose as a predictor of type 2 diabetes occurrence (Bergman et al., 2018). The 30-min postprandial glucose concentration may also be a time of interest because: it frequently coincides with the peak of glycemia in healthy individuals; the contribution of intestinal glucose absorption is quantitatively major at this time whatever the glycemic status; and gastric emptying is associated at this time in a similar manner in all the glycemic status (Chinmay S. Marathe et al., 2015).

As perspectives of this study, it remains to totally develop a computational model for intestinal glucose absorption assessment in humans from oral D-Xylose test, allowing the determination of all the pharmacokinetics parameters of postprandial D-Xylose turnover. For this objective, human data following D-Xylose intrajejunal administration are still lacking and are not available from the literature. For this purpose, it thus could be interesting to performed mixed meal tests with D-Xylose in patients benefiting from duodeno- or jejunostomy.

We could additionally confirm the molecular mechanism of D-Xylose absorption by SGLT1 in the apical pole of the enterocytes and by GLUT2 in the basal pole. We have already demonstrated a correlation between the quantity of D-Xylose absorbed at 30 min during a meal test and the jejunal level of expression of SGLT1 in the ABOS cohort ($r = 0.41$, $p < 0.005$, data not shown). Consequently, we could confirm the causal association between the absorption of D-Xylose and the jejunal expression of SGLT1 by mendelian randomization, as previously performed between hypofunctional SGLT1 variants and postprandial glucose response by Seidelmann and coworkers (Seidelmann et al., 2018) and also in our team by Simon Peschard and coworkers. We could also complete these analyses in using in vitro models of intestinal organoïdes or CaCo2 cell lines associated with phlorizin and phloretin, that respectively inhibit SGLT1 and GLUT2 transporters, in order to confirm the transport of D-Xylose by this way. We could also perform mixed meal tests with D-Xylose in in vivo mouse models knout-out for SGLT1 and GLUT2 genes to see if postprandial D-Xylose excursion is effectively blunted in these models.

As other perspective, we could also develop a computational model allowing to determine kinetics of gastric emptying in using oral D-Xylose test. Consequently, we could retrospectively assess gastric emptying in ABOS cohort, definitively dissociate gastric emptying from intestinal absorption and then study the respective quantitative time-dependent contribution of gastric emptying and intestinal glucose absorption on postprandial glucose response.

Finally, D-Xylose could be used for the evaluation of the efficacy of new drugs aiming at inhibiting intestinal glucose absorption, such as metformin (Zubiaga et al., 2023) or selective SGLT1 inhibitors.

In conclusion, assessing intestinal glucose absorption with D-Xylose would therefore be relevant in addition to the early postprandial glucose measurement. This variable would play a discriminant role for type 2 diabetes prediction, diagnosis as well as for personalized therapy. Subjects with high glucose absorption would be especially receptive to nutritional, pharmacological, or surgical therapies that aim at decreasing intestinal glucose absorption, such as SGLT1 inhibitors or metabolic surgery. Consequently, we could envision future research using D-Xylose to assess the impact of dietary, medical, or surgical interventions meant to reduce intestinal glucose absorption and consequently reduce postprandial glucose excursions.

To resume, assessing intestinal glucose absorption in patients with disorders of glucose homeostasis would therefore enable enlarging the therapeutic range to better achieve precision health.

References

- Abbasi, N.N., Purslow, P.P., Tosh, S.M., Bakovic, M., 2016. Oat β -glucan depresses SGLT1- and GLUT2-mediated glucose transport in intestinal epithelial cells (IEC-6). *Nutr Res* 36, 541–552. <https://doi.org/10.1016/j.nutres.2016.02.004>
- Abdul-Ghani, M.A., Abdul-Ghani, T., Ali, N., DeFronzo, R.A., 2008. One-Hour Plasma Glucose Concentration and the Metabolic Syndrome Identify Subjects at High Risk for Future Type 2 Diabetes. *Diabetes Care* 31, 1650–1655. <https://doi.org/10.2337/dc08-0225>
- Abdul-Ghani, M.A., Matsuda, M., Balas, B., DeFronzo, R.A., 2007. Muscle and Liver Insulin Resistance Indexes Derived From the Oral Glucose Tolerance Test. *Diabetes Care* 30, 89–94. <https://doi.org/10.2337/dc06-1519>
- Abudawood, M., 2019. Diabetes and cancer: A comprehensive review. *J Res Med Sci* 24, 94. https://doi.org/10.4103/jrms.JRMS_242_19
- Abumrad, N.N., Cherrington, A.D., Williams, P.E., Lacy, W.W., Rabin, D., 1982. Absorption and disposition of a glucose load in the conscious dog. *American Journal of Physiology-Endocrinology and Metabolism* 242, E398–E406. <https://doi.org/10.1152/ajpendo.1982.242.6.E398>
- Ahlqvist, E., Storm, P., Käräjämäki, A., Martinell, M., Dorkhan, M., Carlsson, A., Vikman, P., Prasad, R.B., Aly, D.M., Almgren, P., Wessman, Y., Shaat, N., Spégel, P., Mulder, H., Lindholm, E., Melander, O., Hansson, O., Malmqvist, U., Lernmark, Å., Lahti, K., Forsén, T., Tuomi, T., Rosengren, A.H., Groop, L., 2018. Novel subgroups of adult-onset diabetes and their association with outcomes: a data-driven cluster analysis of six variables. *The Lancet Diabetes & Endocrinology* 6, 361–369. [https://doi.org/10.1016/S2213-8587\(18\)30051-2](https://doi.org/10.1016/S2213-8587(18)30051-2)
- Ahuja, V., Aronen, P., Pramodkumar, T.A., Looker, H., Chetrit, A., Bloigu, A.H., Juutilainen, A., Bianchi, C., La Sala, L., Anjana, R.M., Pradeepa, R., Venkatesan, U., Jebarani, S., Baskar, V., Fiorentino, T.V., Timpel, P., DeFronzo, R.A., Ceriello, A., Del Prato, S., Abdul-Ghani, M., Keinänen-Kiukaanniemi, S., Dankner, R., Bennett, P.H., Knowler, W.C., Schwarz, P., Sesti, G., Oka, R., Mohan, V., Groop, L., Tuomilehto, J., Ripatti, S., Bergman, M., Tuomi, T., 2021. Accuracy of 1-Hour Plasma Glucose During the Oral Glucose Tolerance Test in Diagnosis of Type 2 Diabetes in Adults: A Meta-analysis. *Diabetes Care* 44, 1062–1069. <https://doi.org/10.2337/dc20-1688>
- Ait-Omar, A., Monteiro-Sepulveda, M., Poitou, C., Le Gall, M., Cotillard, A., Gilet, J., Garbin, K., Houllier, A., Chateau, D., Lacombe, A., Veyrie, N., Hugol, D., Tordjman, J., Magnan, C., Serradas, P., Clement, K., Leturque, A., Brot-Laroche, E., 2011. GLUT2 Accumulation in Enterocyte Apical and Intracellular Membranes: A Study in Morbidly Obese Human Subjects and ob/ob and High Fat-Fed Mice. *Diabetes* 60, 2598–2607. <https://doi.org/10.2337/db10-1740>
- Albaugh, V.L., Banan, B., Ajouz, H., Abumrad, N.N., Flynn, C.R., 2017. Bile acids and bariatric surgery. *Mol Aspects Med* 56, 75–89. <https://doi.org/10.1016/j.mam.2017.04.001>
- Al-Mashhadi, A.L., Poulsen, C.B., von Wachenfeldt, K., Robertson, A.-K., Bentzon, J.F., Nielsen, L.B., Thygesen, J., Tolbod, L.P., Larsen, J.R., Moestrup, S.K., Freundéus, B., Mortensen, B., Drouet, L., Al-Mashhadi, R.H., Falk, E., 2018. Diet-Induced Abdominal Obesity, Metabolic Changes, and Atherosclerosis in Hypercholesterolemic Minipigs. *J Diabetes Res* 2018, 6823193. <https://doi.org/10.1155/2018/6823193>
- Al-Mashhadi, R.H., Sørensen, C.B., Kragh, P.M., Christoffersen, C., Mortensen, M.B., Tolbod, L.P., Thim, T., Du, Y., Li, J., Liu, Y., Moldt, B., Schmidt, M., Vajta, G., Larsen, T., Purup, S., Bolund, L., Nielsen, L.B., Callesen, H., Falk, E., Mikkelsen, J.G., Bentzon, J.F., 2013. Familial hypercholesterolemia and

atherosclerosis in cloned minipigs created by DNA transposition of a human PCSK9 gain-of-function mutant. *Sci Transl Med* 5, 166ra1. <https://doi.org/10.1126/scitranslmed.3004853>

Alonso, L.C., Yokoe, T., Zhang, P., Scott, D.K., Kim, S.K., O'Donnell, C.P., Garcia-Ocana, A., 2007. Glucose Infusion in Mice: A New Model to Induce β -Cell Replication. *Diabetes* 56, 1792–1801. <https://doi.org/10.2337/db06-1513>

Alsalam, W., Ahrén, B., 2019. Insulin and incretin hormone responses to rapid versus slow ingestion of a standardized solid breakfast in healthy subjects. *Endocrinol Diabetes Metab* 2, e00056. <https://doi.org/10.1002/edm2.56>

Alssema, M., Ruijgrok, C., Blaak, E.E., Egli, L., Dussort, P., Vinoy, S., Dekker, J.M., Denise Robertson, M., 2021. Effects of alpha-glucosidase-inhibiting drugs on acute postprandial glucose and insulin responses: a systematic review and meta-analysis. *Nutr Diabetes* 11, 11. <https://doi.org/10.1038/s41387-021-00152-5>

Alvarado, F., 1966. d-xylose active transport in the hamster small intestine. *Biochimica et Biophysica Acta (BBA) - Biophysics including Photosynthesis* 112, 292–306. [https://doi.org/10.1016/0926-6585\(66\)90328-1](https://doi.org/10.1016/0926-6585(66)90328-1)

Alzaid, F., Cheung, H.-M., Preedy, V.R., Sharp, P.A., 2013. Regulation of glucose transporter expression in human intestinal Caco-2 cells following exposure to an anthocyanin-rich berry extract. *PLoS One* 8, e78932. <https://doi.org/10.1371/journal.pone.0078932>

American Diabetes Association, 2017. Pharmacologic Approaches to Glycemic Treatment. *Diabetes Care* 40, S64–S74. <https://doi.org/10.2337/dc17-S011>

American Diabetes Association, 2014. Diagnosis and Classification of Diabetes Mellitus. *Diabetes Care* 37, S81–S90. <https://doi.org/10.2337/dc14-S081>

American Diabetes Association, 2004. Standards of medical care in diabetes. *Diabetes Care* 27, S15–S34.

Aminian, A., Kashyap, S.R., Wolski, K.E., Brethauer, S.A., Kirwan, J.P., Nissen, S.E., Bhatt, D.L., Schauer, P.R., 2021. Patient-reported Outcomes After Metabolic Surgery Versus Medical Therapy for Diabetes: Insights From the STAMPEDE Randomized Trial. *Ann Surg* 274, 524–532. <https://doi.org/10.1097/SLA.0000000000005003>

Anhê, F.F., Zlitni, S., Zhang, S.-Y., Choi, B.S.-Y., Chen, C.Y., Foley, K.P., Barra, N.G., Surette, M.G., Biertho, L., Richard, D., Tchernof, A., Lam, T.K.T., Marette, A., Schertzer, J., 2023. Human gut microbiota after bariatric surgery alters intestinal morphology and glucose absorption in mice independently of obesity. *Gut* 72, 460–471. <https://doi.org/10.1136/gutjnl-2022-328185>

Antunes, D.M.F., da Costa, J.P., Campos, S.M.N., Paschoal, P.O., Garrido, V., Siqueira, M., Teixeira, G.A.P.B., Cardoso, G.P., 2009. The serum D-xylose test as a useful tool to identify malabsorption in rats with antigen specific gut inflammatory reaction. *International Journal of Experimental Pathology* 90, 141–147. <https://doi.org/10.1111/j.1365-2613.2008.00627.x>

Arner, P., 2003. The adipocyte in insulin resistance: key molecules and the impact of the thiazolidinediones. *Trends in Endocrinology and Metabolism* 14, 137–145. [https://doi.org/10.1016/S1043-2760\(03\)00024-9](https://doi.org/10.1016/S1043-2760(03)00024-9)

Ärnlöv, J., Zethelius, B., Risérus, U., Basu, S., Berne, C., Vessby, B., Alftan, G., Helmersson, J., 2009. Serum and dietary β -carotene and α -tocopherol and incidence of type 2 diabetes mellitus in a

community-based study of Swedish men: report from the Uppsala Longitudinal Study of Adult Men (ULSAM) study. *Diabetologia* 52, 97–105. <https://doi.org/10.1007/s00125-008-1189-3>

Atkinson, F.S., Brand-Miller, J.C., Foster-Powell, K., Buyken, A.E., Goletzke, J., 2021. International tables of glycemic index and glycemic load values 2021: a systematic review. *The American Journal of Clinical Nutrition* 114, 1625–1632. <https://doi.org/10.1093/ajcn/nqab233>

Augustin, L.S.A., Kendall, C.W.C., Jenkins, D.J.A., Willett, W.C., Astrup, A., Barclay, A.W., Björck, I., Brand-Miller, J.C., Brighenti, F., Buyken, A.E., Ceriello, A., La Vecchia, C., Livesey, G., Liu, S., Riccardi, G., Rizkalla, S.W., Sievenpiper, J.L., Trichopoulou, A., Wolever, T.M.S., Baer-Sinnott, S., Poli, A., 2015. Glycemic index, glycemic load and glycemic response: An International Scientific Consensus Summit from the International Carbohydrate Quality Consortium (ICQC). *Nutr Metab Cardiovasc Dis* 25, 795–815. <https://doi.org/10.1016/j.numecd.2015.05.005>

Aulinger, B.A., Vahl, T.P., Wilson-Pérez, H.E., Prigeon, R.L., D'Alessio, D.A., 2015. β -Cell Sensitivity to GLP-1 in Healthy Humans Is Variable and Proportional to Insulin Sensitivity. *The Journal of Clinical Endocrinology & Metabolism* 100, 2489–2496. <https://doi.org/10.1210/jc.2014-4009>

Bach Knudsen, K.E., Jorgensen, H., Canibe, N., 2000. Quantification of the absorption of nutrients derived from carbohydrate assimilation: model experiment with catheterised pigs fed on wheat- or oat-based rolls. *British Journal of Nutrition* 84, 449–458. <https://doi.org/10.1017/S0007114500001756>

Badin, J.K., Kole, A., Stivers, B., Progar, V., Paredy, A., Alloosh, M., Sturek, M., 2018. Alloxan-induced diabetes exacerbates coronary atherosclerosis and calcification in Ossabaw miniature swine with metabolic syndrome. *J Transl Med* 16, 58. <https://doi.org/10.1186/s12967-018-1431-9>

Bahne, E., Sun, E.W.L., Young, R.L., Hansen, M., Sonne, D.P., Hansen, J.S., Rohde, U., Liou, A.P., Jackson, M.L., de Fontgalland, D., Rabbitt, P., Hollington, P., Sposato, L., Due, S., Wattchow, D.A., Rehfeld, J.F., Holst, J.J., Keating, D.J., Vilsbøll, T., Knop, F.K., 2018. Metformin-induced glucagon-like peptide-1 secretion contributes to the actions of metformin in type 2 diabetes. *JCI Insight* 3, e93936, 93936. <https://doi.org/10.1172/jci.insight.93936>

Bansal, N., 2015. Prediabetes diagnosis and treatment: A review. *WJD* 6, 296–303. <https://doi.org/10.4239/wjd.v6.i2.296>

Bariatric Clinic, 2021. Introduction to Bariatric Surgery | Bariatric Clinic Singapore | By G & L Surgical. Bariatric Clinic Singapore. URL <https://www.bariatricsurgery.com.sg/introduction-to-bariatric-surgery/> (accessed 9.25.23).

Barrington, P., Chien, J.Y., Showalter, H.D.H., Schneck, K., Cui, S., Tibaldi, F., Ellis, B., Hardy, T.A., 2011. A 5-week study of the pharmacokinetics and pharmacodynamics of LY2189265, a novel, long-acting glucagon-like peptide-1 analogue, in patients with type 2 diabetes. *Diabetes Obes Metab* 13, 426–433. <https://doi.org/10.1111/j.1463-1326.2011.01364.x>

Basu, A., Basu, R., Shah, P., Vella, A., Johnson, C.M., Jensen, M., Nair, K.S., Schwenk, W.F., Rizza, R.A., 2001. Type 2 diabetes impairs splanchnic uptake of glucose but does not alter intestinal glucose absorption during enteral glucose feeding: additional evidence for a defect in hepatic glucokinase activity. *Diabetes* 50, 1351–1362. <https://doi.org/10.2337/diabetes.50.6.1351>

Basu, R., Chandramouli, V., Dicke, B., Landau, B., Rizza, R., 2005. Obesity and Type 2 Diabetes Impair Insulin-Induced Suppression of Glycogenolysis as Well as Gluconeogenesis. *Diabetes* 54, 1942–1948. <https://doi.org/10.2337/diabetes.54.7.1942>

- Basu, R., Di Camillo, B., Toffolo, G., Basu, A., Shah, P., Vella, A., Rizza, R., Cobelli, C., 2003. Use of a novel triple-tracer approach to assess postprandial glucose metabolism. *American Journal of Physiology-Endocrinology and Metabolism* 284, E55–E69. <https://doi.org/10.1152/ajpendo.00190.2001>
- Baud, G., Daoudi, M., Hubert, T., Raverdy, V., Pigeyre, M., Hervieux, E., Devienne, M., Ghunaim, M., Bonner, C., Quenon, A., Pigny, P., Klein, A., Kerr-Conte, J., Gmyr, V., Caiazzo, R., Pattou, F., 2016. Bile Diversion in Roux-en-Y Gastric Bypass Modulates Sodium-Dependent Glucose Intestinal Uptake. *Cell Metabolism* 23, 547–553. <https://doi.org/10.1016/j.cmet.2016.01.018>
- Bauer, P.V., Duca, F.A., Waise, T.M.Z., Rasmussen, B.A., Abraham, M.A., Dranse, H.J., Puri, A., O'Brien, C.A., Lam, T.K.T., 2018. Metformin Alters Upper Small Intestinal Microbiota that Impact a Glucose-SGLT1-Sensing Glucoregulatory Pathway. *Cell Metabolism* 27, 101-117.e5. <https://doi.org/10.1016/j.cmet.2017.09.019>
- Beck, I.T., Rona, S., McKenna, R.D., Kahn, D.S., 1962. Evaluation of 200 D-xylose blood level time curves as an index of intestinal absorption. *Am J Dig Dis* 7, 936–948. <https://doi.org/10.1007/BF02231874>
- Bell, L., Lamport, D.J., Butler, L.T., Williams, C.M., 2017. A study of glycaemic effects following acute anthocyanin-rich blueberry supplementation in healthy young adults. *Food Funct* 8, 3104–3110. <https://doi.org/10.1039/c7fo00724h>
- Benaiges, D., Mas-Lorenzo, A., Goday, A., Ramon, J.M., Chillaron, J.J., Pedro-Botet, J., Flores-Le Roux, J.A., 2015. Laparoscopic sleeve gastrectomy: More than a restrictive bariatric surgery procedure? *WJG* 21, 11804–11814. <https://doi.org/10.3748/wjg.v21.i41.11804>
- Benini, L., Castellani, G., Brighenti, F., Heaton, K.W., Brentegani, M.T., Casiraghi, M.C., Sembenini, C., Pellegrini, N., Fioretta, A., Minniti, G., 1995. Gastric emptying of a solid meal is accelerated by the removal of dietary fibre naturally present in food. *Gut* 36, 825–830. <https://doi.org/10.1136/gut.36.6.825>
- Bergman, M., Chetrit, A., Roth, J., Dankner, R., 2016. One-hour post-load plasma glucose level during the OGTT predicts mortality: observations from the Israel Study of Glucose Intolerance, Obesity and Hypertension. *Diabet. Med.* 33, 1060–1066. <https://doi.org/10.1111/dme.13116>
- Bergman, M., Jagannathan, R., Groop, L., Dankner, R., 2018. Lessons learned from the 1-hour post-load glucose level during OGTT: Current screening recommendations for dysglycaemia should be revised. *Diabetes Metab Res Rev.* 34, 8. <https://doi.org/10.1002/dmrr.2992>
- Berlin, P., Reiner, J., Wobar, J., Bannert, K., Glass, Ä., Walter, M., Bastian, M., Willenberg, H.S., Vollmar, B., Klar, E., Seidler, U., Lamprecht, G., Witte, M., 2019. Villus Growth, Increased Intestinal Epithelial Sodium Selectivity, and Hyperaldosteronism Are Mechanisms of Adaptation in a Murine Model of Short Bowel Syndrome. *Dig Dis Sci* 64, 1158–1170. <https://doi.org/10.1007/s10620-018-5420-x>
- Berne, C., 1996. Hypoglycaemia and gastric emptying. *Diabet Med* 13, S28-30.
- Berry, S.E., Valdes, A.M., Drew, D.A., Asnicar, F., Mazidi, M., Wolf, J., Capdevila, J., Hadjigeorgiou, G., Davies, R., Al Khatib, H., Bonnett, C., Ganesh, S., Bakker, E., Hart, D., Mangino, M., Merino, J., Linenberg, I., Wyatt, P., Ordovas, J.M., Gardner, C.D., Delahanty, L.M., Chan, A.T., Segata, N., Franks, P.W., Spector, T.D., 2020. Human postprandial responses to food and potential for precision nutrition. *Nat Med* 26, 964–973. <https://doi.org/10.1038/s41591-020-0934-0>
- Betsholtz, C., Svensson, V., Rorsman, F., Engström, U., Westermark, G.T., Wilander, E., Johnson, K., Westermark, P., 1989. Islet amyloid polypeptide (IAPP):cDNA cloning and identification of an

amyloidogenic region associated with the species-specific occurrence of age-related diabetes mellitus. *Exp Cell Res* 183, 484–493. [https://doi.org/10.1016/0014-4827\(89\)90407-2](https://doi.org/10.1016/0014-4827(89)90407-2)

Bianchi, C., Miccoli, R., Trombetta, M., Giorgino, F., Frontoni, S., Faloia, E., Marchesini, G., Dolci, M.A., Cavalot, F., Cavallo, G., Leonetti, F., Bonadonna, R.C., Del Prato, S., on behalf of the GENFIEV Investigators, 2013. Elevated 1-Hour Postload Plasma Glucose Levels Identify Subjects With Normal Glucose Tolerance but Impaired β -Cell Function, Insulin Resistance, and Worse Cardiovascular Risk Profile: The GENFIEV Study. *The Journal of Clinical Endocrinology & Metabolism* 98, 2100–2105. <https://doi.org/10.1210/jc.2012-3971>

Bilecik, T., 2019. Metabolic Effects of Sleeve Gastrectomy with Transit Bipartition in Obese Females with Type 2 Diabetes Mellitus: Results After 1-Year Follow-up. *Obesity Surgery* 29. <https://doi.org/10.1007/s11695-018-3603-3>

Blundell, J., 1986. Paradoxical effects of an intense sweetener (aspartame) on appetite. *The Lancet* 327, 1092–1093. [https://doi.org/10.1016/S0140-6736\(86\)91352-8](https://doi.org/10.1016/S0140-6736(86)91352-8)

Bode, G., Clausing, P., Gervais, F., Loegsted, J., Luft, J., Nogues, V., Sims, J., 2010. The utility of the minipig as an animal model in regulatory toxicology. *Journal of Pharmacological and Toxicological Methods* 62, 196–220. <https://doi.org/10.1016/j.vascn.2010.05.009>

Boers, H.M., Alsema, M., Mela, D.J., Peters, H.P.F., Vonk, R.J., Priebe, M.G., 2019. The Rate of Glucose Appearance Is Related to Postprandial Glucose and Insulin Responses in Adults: A Systematic Review and Meta-analysis of Stable Isotope Studies. *The Journal of Nutrition* 149, 1896–1903. <https://doi.org/10.1093/jn/nxz150>

Bollen, P., Ellegaard, L., 1997. The Göttingen Minipig in Pharmacology and Toxicology. *Pharmacology & Toxicology* 80, 3–4. <https://doi.org/10.1111/j.1600-0773.1997.tb01980.x>

Bondia-Pons, I., Nordlund, E., Mattila, I., Katina, K., Aura, A.-M., Kolehmainen, M., Orešič, M., Mykkänen, H., Poutanen, K., 2011. Postprandial differences in the plasma metabolome of healthy Finnish subjects after intake of a sourdough fermented endosperm rye bread versus white wheat bread. *Nutr J* 10, 116. <https://doi.org/10.1186/1475-2891-10-116>

Borgundvaag, E., Mak, J., Kramer, C.K., 2021. Metabolic Impact of Intermittent Fasting in Patients With Type 2 Diabetes Mellitus: A Systematic Review and Meta-analysis of Interventional Studies. *The Journal of Clinical Endocrinology & Metabolism* 106, 902–911. <https://doi.org/10.1210/clinem/dgaa926>

Bozzetto, L., Alderisio, A., Clemente, G., Giorgini, M., Barone, F., Griffo, E., Costabile, G., Vetrani, C., Cipriano, P., Giacco, A., Riccardi, G., Rivellese, A.A., Annuzzi, G., 2019. Gastrointestinal effects of extra-virgin olive oil associated with lower postprandial glycemia in type 1 diabetes. *Clin Nutr* 38, 2645–2651. <https://doi.org/10.1016/j.clnu.2018.11.015>

Bradley, C., 2002. The glitazones: a new treatment for type 2 diabetes mellitus. *Intensive and Critical Care Nursing* 18, 189–191. [https://doi.org/10.1016/S0964-3397\(02\)00010-1](https://doi.org/10.1016/S0964-3397(02)00010-1)

Bradley, D., Conte, C., Mittendorfer, B., Eagon, J.C., Varela, J.E., Fabbrini, E., Gastaldelli, A., Chambers, K.T., Su, X., Okunade, A., Patterson, B.W., Klein, S., 2012. Gastric bypass and banding equally improve insulin sensitivity and β cell function. *J. Clin. Invest.* 122, 4667–4674. <https://doi.org/10.1172/JCI64895>

Brener, W., Hendrix, T.R., McHugh, P.R., 1983. Regulation of the gastric emptying of glucose. *Gastroenterology* 85, 76–82.

- Briggs, D.C., Hohenester, E., 2018. Structural Basis for the Initiation of Glycosaminoglycan Biosynthesis by Human Xylosyltransferase 1. *Structure* 26, 801–809.e3. <https://doi.org/10.1016/j.str.2018.03.014>
- Brubaker, P.L., 1991. Regulation of Intestinal Proglucagon- Derived Peptide Secretion by Intestinal Regulatory Peptides. *Endocrinology* 128, 3175–3182. <https://doi.org/10.1210/endo-128-6-3175>
- Brunetti, A., Chiefari, E., Foti, D., 2014. Recent advances in the molecular genetics of type 2 diabetes mellitus. *WJD* 5, 128–140. <https://doi.org/10.4239/wjd.v5.i2.128>
- Burrin, D., Sangild, P.T., Stoll, B., Thymann, T., Buddington, R., Marini, J., Olutoye, O., Shulman, R.J., 2020. Translational Advances in Pediatric Nutrition and Gastroenterology: New Insights from Pig Models. *Annu. Rev. Anim. Biosci.* 8, 321–354. <https://doi.org/10.1146/annurev-animal-020518-115142>
- Buse, J.B., DeFronzo, R.A., Rosenstock, J., Kim, T., Burns, C., Skare, S., Baron, A., Fineman, M., 2016. The Primary Glucose-Lowering Effect of Metformin Resides in the Gut, Not the Circulation: Results From Short-term Pharmacokinetic and 12-Week Dose-Ranging Studies. *Diabetes Care* 39, 198–205. <https://doi.org/10.2337/dc15-0488>
- Butler, A.E., Janson, J., Bonner-Weir, S., Ritzel, R., Rizza, R.A., Butler, P.C., 2003. Beta Cell Deficit and Increased Beta-Cell Apoptosis in Humans With Type 2 Diabetes. *Diabetes* 52, 102–110. <https://doi.org/10.2337/diabetes.52.1.102>
- Buts, J.-P., Morin, C.L., Roy, C.C., Weber, A., Bonin, A., 1978. One-hour blood xylose test: A reliable index of small bowel function. *The Journal of Pediatrics* 92, 729–733. [https://doi.org/10.1016/S0022-3476\(78\)80138-3](https://doi.org/10.1016/S0022-3476(78)80138-3)
- Buyschaert, M., Bergman, M., Valensi, P., 2022. 1-h post-load plasma glucose for detecting early stages of prediabetes. *Diabetes & Metabolism* 48, 101395. <https://doi.org/10.1016/j.diabet.2022.101395>
- Cabrera, O., Berman, D.M., Kenyon, N.S., Ricordi, C., Berggren, P.-O., Caicedo, A., 2006. The unique cytoarchitecture of human pancreatic islets has implications for islet cell function. *Proceedings of the National Academy of Sciences* 103, 2334–2339. <https://doi.org/10.1073/pnas.0510790103>
- Caiazzo, R., Branche, J., Daoudi, M., Solecki, G., Hubert, T., Quenon, A., Cousin, F., Henin, F., Dalle, V., Noel, S., Vanbiervliet, G., Barthet, M., Pattou, F., 2017. Increased postprandial glucagon-like peptide-1 (GLP-1) production after endoscopic gastrointestinal bypass using the Cousin lumen-apposing stent in a porcine model. *Endoscopy* 50, 14–21. <https://doi.org/10.1055/s-0043-120439>
- Caiazzo, R., Lassailly, G., Leteurtre, E., Baud, G., Verkindt, H., Raverdy, V., Buob, D., Pigeyre, M., Mathurin, P., Pattou, F., 2014. Roux-en-Y Gastric Bypass Versus Adjustable Gastric Banding to Reduce Nonalcoholic Fatty Liver Disease: A 5-Year Controlled Longitudinal Study. *Annals of Surgery* 260, 893–899. <https://doi.org/10.1097/SLA.0000000000000945>
- Callaghan, B.C., Cheng, H.T., Stables, C.L., Smith, A.L., Feldman, E.L., 2012. Diabetic neuropathy: clinical manifestations and current treatments. *The Lancet Neurology* 11, 521–534. [https://doi.org/10.1016/S1474-4422\(12\)70065-0](https://doi.org/10.1016/S1474-4422(12)70065-0)
- Camasta, S., Muscelli, E., Gastaldelli, A., Holst, J.J., Astiarraga, B., Baldi, S., Nannipieri, M., Ciociaro, D., Anselmino, M., Mari, A., Ferrannini, E., 2013. Long-Term Effects of Bariatric Surgery on Meal Disposal and b-Cell Function in Diabetic and Nondiabetic Patients. *Diabetes* 62, 3709–3717. <https://doi.org/10.2337/db13-0321>

- Camastra, S., Palumbo, M., Santini, F., 2022. Nutrients handling after bariatric surgery, the role of gastrointestinal adaptation. *Eat Weight Disord* 27, 449–461. <https://doi.org/10.1007/s40519-021-01194-5>
- Camilleri, M., 2019. Gastrointestinal hormones and regulation of gastric emptying: Current Opinion in *Endocrinology & Diabetes and Obesity* 26, 3–10. <https://doi.org/10.1097/MED.0000000000000448>
- Campbell, J.E., Newgard, C.B., 2021. Mechanisms controlling pancreatic islet cell function in insulin secretion. *Nat Rev Mol Cell Biol* 22, 142–158. <https://doi.org/10.1038/s41580-020-00317-7>
- Carlson, O., Martin, B., Stote, K.S., Golden, E., Maudsley, S., Najjar, S.S., Ferrucci, L., Ingram, D.K., Longo, D.L., Rumpler, W.V., Baer, D.J., Egan, J., Mattson, M.P., 2007. Impact of reduced meal frequency without caloric restriction on glucose regulation in healthy, normal-weight middle-aged men and women. *Metabolism* 56, 1729–1734. <https://doi.org/10.1016/j.metabol.2007.07.018>
- Carpenter, D.O., 2008. Environmental Contaminants as Risk Factors for Developing Diabetes. *Reviews on Environmental Health* 23, 59–74. <https://doi.org/10.1515/REVEH.2008.23.1.59>
- Castex, F., Leroy, J., Broca, C., Mezghenna, K., Duranton, F., Lavallard, V., Lebreton, F., Gross, R., Wojtuszczyk, A., Lajoix, A., 2020. Differential sensitivity of human islets from obese versus lean donors to chronic high glucose or palmitate. *Journal of Diabetes* 12, 532–541. <https://doi.org/10.1111/1753-0407.13026>
- Castro-Acosta, M.L., Lenihan-Geels, G.N., Corpe, C.P., Hall, W.L., 2016. Berries and anthocyanins: promising functional food ingredients with postprandial glycaemia-lowering effects. *Proc Nutr Soc* 75, 342–355. <https://doi.org/10.1017/S0029665116000240>
- Castro-Acosta, M.L., Stone, S.G., Mok, J.E., Mhajan, R.K., Fu, C.-I., Lenihan-Geels, G.N., Corpe, C.P., Hall, W.L., 2017. Apple and blackcurrant polyphenol-rich drinks decrease postprandial glucose, insulin and incretin response to a high-carbohydrate meal in healthy men and women. *J Nutr Biochem* 49, 53–62. <https://doi.org/10.1016/j.jnutbio.2017.07.013>
- Cavin, J.-B., Couvelard, A., Lebtahi, R., Ducroc, R., Arapis, K., Voiteillier, E., Cluzeaud, F., Gillard, L., Hourseau, M., Mikail, N., Ribeiro-Parenti, L., Kapel, N., Marmuse, J.-P., Bado, A., Le Gall, M., 2016. Differences in Alimentary Glucose Absorption and Intestinal Disposal of Blood Glucose After Roux-en-Y Gastric Bypass vs Sleeve Gastrectomy. *Gastroenterology* 150, 454-464.e9. <https://doi.org/10.1053/j.gastro.2015.10.009>
- Cefalo, C.M.A., Cinti, F., Moffa, S., Impronta, F., Sorice, G.P., Mezza, T., Pontecorvi, A., Giaccari, A., 2019. Sotagliflozin, the first dual SGLT inhibitor: current outlook and perspectives. *Cardiovasc Diabetol* 18, 20. <https://doi.org/10.1186/s12933-019-0828-y>
- Cerdó, T., García-Santos, J.A., Rodríguez-Pöhnlein, A., García-Ricobaraza, M., Nieto-Ruiz, A., G. Bermúdez, M., Campoy, C., 2022. Impact of Total Parenteral Nutrition on Gut Microbiota in Pediatric Population Suffering Intestinal Disorders. *Nutrients* 14, 4691. <https://doi.org/10.3390/nu14214691>
- Chaikomin, R., Doran, S., Jones, K.L., Feinle-Bisset, C., O'Donovan, D., Rayner, C.K., Horowitz, M., 2005. Initially more rapid small intestinal glucose delivery increases plasma insulin, GIP, and GLP-1 but does not improve overall glycemia in healthy subjects. *Am J Physiol Endocrinol Metab* 289, E504-507. <https://doi.org/10.1152/ajpendo.00099.2005>
- Chaikomin, R., Wu, K.L., Doran, S., Jones, K.L., Smout, A.J.P.M., Renooij, W., Holloway, R.H., Meyer, J.H., Horowitz, M., Rayner, C.K., 2007. Concurrent duodenal manometric and impedance recording to

evaluate the effects of hyoscine on motility and flow events, glucose absorption, and incretin release. *American Journal of Physiology-Gastrointestinal and Liver Physiology* 292, G1099–G1104. <https://doi.org/10.1152/ajpgi.00519.2006>

Chambers, A.P., Smith, E.P., Begg, D.P., Grayson, B.E., Sisley, S., Greer, T., Sorrell, J., Lemmen, L., LaSance, K., Woods, S.C., Seeley, R.J., D'Alessio, D.A., Sandoval, D.A., 2014. Regulation of gastric emptying rate and its role in nutrient-induced GLP-1 secretion in rats after vertical sleeve gastrectomy. *American Journal of Physiology-Endocrinology and Metabolism* 306, E424–E432. <https://doi.org/10.1152/ajpendo.00469.2013>

Chambers, A.P., Stefater, M.A., Wilson-Perez, H.E., Jessen, L., Sisley, S., Ryan, K.K., Gaitonde, S., Sorrell, J.E., Toure, M., Berger, J., D'Alessio, D.A., Sandoval, D.A., Seeley, R.J., Woods, S.C., 2011. Similar effects of roux-en-Y gastric bypass and vertical sleeve gastrectomy on glucose regulation in rats. *Physiology & Behavior* 105, 120–123. <https://doi.org/10.1016/j.physbeh.2011.05.026>

Chávez-Talavera, O., Baud, G., Spinelli, V., Daoudi, M., Kouach, M., Goossens, J.-F., Vallez, E., Caiazza, R., Ghunaim, M., Hubert, T., Lestavel, S., Tailleux, A., Staels, B., Pattou, F., 2017. Roux-en-Y gastric bypass increases systemic but not portal bile acid concentrations by decreasing hepatic bile acid uptake in minipigs. *Int J Obes (Lond)* 41, 664–668. <https://doi.org/10.1038/ijo.2017.7>

Chávez-Talavera, Oscar, Tailleux, A., Lefebvre, P., Staels, B., 2017. Bile Acid Control of Metabolism and Inflammation in Obesity, Type 2 Diabetes, Dyslipidemia, and Nonalcoholic Fatty Liver Disease. *Gastroenterology* 152, 1679-1694.e3. <https://doi.org/10.1053/j.gastro.2017.01.055>

Cherrington, A.D., Edgerton, D., Sindelar, D.K., 1998. The direct and indirect effects of insulin on hepatic glucose production in vivo. *Diabetologia* 41, 987–996. <https://doi.org/10.1007/s001250051021>

Cheudjeu, A., 2020. Correlation of D-xylose with severity and morbidity-related factors of COVID-19 and possible therapeutic use of D-xylose and antibiotics for COVID-19. *Life Sci* 260, 118335. <https://doi.org/10.1016/j.lfs.2020.118335>

Chiasson, J.-L., Josse, R.G., Gomis, R., Hanefeld, M., Karasik, A., Laakso, M., for The STOP-NIDDM Trial Research Group, 2003. Acarbose Treatment and the Risk of Cardiovascular Disease and Hypertension in Patients With Impaired Glucose Tolerance: The STOP-NIDDM Trial. *JAMA* 290, 486. <https://doi.org/10.1001/jama.290.4.486>

Cho, B., Kim, S.J., Lee, E.-J., Ahn, S.M., Lee, J.S., Ji, D.-Y., Lee, K., Kang, J.-T., 2018. Generation of insulin-deficient piglets by disrupting INS gene using CRISPR/Cas9 system. *Transgenic Res* 27, 289–300. <https://doi.org/10.1007/s11248-018-0074-1>

Christiansen, M.L., Müllertz, A., Garmer, M., Kristensen, J., Jacobsen, J., Abrahamsson, B., Holm, R., 2015. Evaluation of the Use of Göttingen Minipigs to Predict Food Effects on the Oral Absorption of Drugs in Humans. *Journal of Pharmaceutical Sciences* 104, 135–143. <https://doi.org/10.1002/jps.24270>

Christiansen, P.A., Kirsner, J.B., Ablaza, J., 1959. D-xylose and its use in the diagnosis of malabsorptive states. *The American Journal of Medicine* 27, 443–453. [https://doi.org/10.1016/0002-9343\(59\)90010-5](https://doi.org/10.1016/0002-9343(59)90010-5)

Christoffersen, B., Golozoubova, V., Pacini, G., Svendsen, O., Raun, K., 2013. The young göttingen minipig as a model of childhood and adolescent obesity: Influence of diet and gender: The Young Göttingen Minipig. *Obesity* 21, 149–158. <https://doi.org/10.1002/oby.20249>

- Clark, A., Jones, L.C., de Koning, E., Hansen, B.C., Matthews, D.R., 2001. Decreased insulin secretion in type 2 diabetes: a problem of cellular mass or function? *Diabetes* 50, S169. <https://doi.org/10.2337/diabetes.50.2007.S169>
- Clark, A., Wells, C.A., Buley, I.D., Cruickshank, J.K., Vanhegan, R.I., Matthews, D.R., Cooper, G.J., Holman, R.R., Turner, R.C., 1998. Islet amyloid, increased A-cells, reduced B-cells and exocrine fibrosis: quantitative changes in the pancreas in type 2 diabetes. *Diabetes Research* 9, 151–159.
- Coelho, P.G., Pippenger, B., Tovar, N., Koopmans, S.-J., Plana, N.M., Graves, D.T., Engebretson, S., van Beusekom, H.M.M., Oliveira, P.G.F.P., Dard, M., 2018. Effect of Obesity or Metabolic Syndrome and Diabetes on Osseointegration of Dental Implants in a Miniature Swine Model: A Pilot Study. *Journal of Oral and Maxillofacial Surgery* 76, 1677–1687. <https://doi.org/10.1016/j.joms.2018.02.021>
- Coimbra, V.O.R., Crovesy, L., Ribeiro-Alves, M., Faller, A.L.K., Mattos, F., Rosado, E.L., 2022. Gut Microbiota Profile in Adults Undergoing Bariatric Surgery: A Systematic Review. *Nutrients* 14, 4979. <https://doi.org/10.3390/nu14234979>
- Collantes Pérez, J., Prada Oliveira, J.A., Gómez Luy, C., Vallo De Castro, J.J., Verástegui Escolano, C., 2004. A useful experimental model of short bowel syndrome. *J Invest Surg* 17, 9–14. <https://doi.org/10.1080/08941930490269592>
- Collier, G., McLean, A., O’Dea, K., 1984. Effect of co-ingestion of fat on the metabolic responses to slowly and rapidly absorbed carbohydrates. *Diabetologia* 26, 50–54. <https://doi.org/10.1007/BF00252263>
- Cook, P.R., Glenn, C., Armston, A., 2010. Effect of hemolysis on insulin determination by the Beckman Coulter Unicell DXI 800 immunoassay analyzer. *Clinical Biochemistry* 43, 621–622. <https://doi.org/10.1016/j.clinbiochem.2010.01.002>
- Costrini, N.V., Ganeshappa, K.P., Wu, W., Whalen, G.E., Soergel, K.H., 1977. Effect of insulin, glucose, and controlled diabetes mellitus on human jejunal function. *Am J Physiol* 233, E181–187. <https://doi.org/10.1152/ajpendo.1977.233.3.E181>
- Craig, R.M., Atkinson, A.J., 1988. D-Xylose testing: A review. *Gastroenterology* 95, 223–231. [https://doi.org/10.1016/0016-5085\(88\)90318-6](https://doi.org/10.1016/0016-5085(88)90318-6)
- Craig, R.M., Murphy, P., Gibson, T.P., Quintanilla, A., Chao, G.C., Cochrane, C., Patterson, A., Atkinson, A.J., 1983. Kinetic analysis of D-xylose absorption in normal subjects and in patients with chronic renal failure. *J Lab Clin Med* 101, 496–506.
- Csaky, T., Lassen, U., 1964. Active intestinal transport of D-Xylose. *Biochim Biophys Acta* 82, 215–127. [https://doi.org/10.1016/0304-4165\(64\)90041-8](https://doi.org/10.1016/0304-4165(64)90041-8)
- Cui, B.-B., Wang, G.-H., Li, P.-Z., Li, W.-Z., Zhu, L.-Y., Zhu, S.-H., 2021. Long-term outcomes of Roux-en-Y gastric bypass versus medical therapy for patients with type 2 diabetes: a meta-analysis of randomized controlled trials. *Surg Obes Relat Dis* 17, 1334–1343. <https://doi.org/10.1016/j.soard.2021.03.001>
- Davis, B.T., Wang, X.-J., Rohret, J.A., Struzynski, J.T., Merricks, E.P., Bellinger, D.A., Rohret, F.A., Nichols, T.C., Rogers, C.S., 2014. Targeted Disruption of LDLR Causes Hypercholesterolemia and Atherosclerosis in Yucatan Miniature Pigs. *PLoS ONE* 9, e93457. <https://doi.org/10.1371/journal.pone.0093457>
- Deane, A.M., Nguyen, N.Q., Stevens, J.E., Fraser, R.J.L., Holloway, R.H., Besanko, L.K., Burgstad, C., Jones, K.L., Chapman, M.J., Rayner, C.K., Horowitz, M., 2010. Endogenous Glucagon-Like Peptide-1

- Slows Gastric Emptying in Healthy Subjects, Attenuating Postprandial Glycemia. *The Journal of Clinical Endocrinology & Metabolism* 95, 215–221. <https://doi.org/10.1210/jc.2009-1503>
- DeBodo, R.C., Steele, R., Altszuler, N., Dunn, A., Bishop, J.S., 1963. On the hormonal regulation of carbohydrate metabolism; studies with C14 glucose. *Recent Prog Horm Res* 19, 445–488.
- DeFronzo, R.A., 2009. From the Triumvirate to the Ominous Octet: A New Paradigm for the Treatment of Type 2 Diabetes Mellitus. *Diabetes* 58, 773–795. <https://doi.org/10.2337/db09-9028>
- DeFronzo, R.A., Ferrannini, E., 1991. Insulin Resistance: A Multifaceted Syndrome Responsible for NIDDM, Obesity, Hypertension, Dyslipidemia, and Atherosclerotic Cardiovascular Disease. *Diabetes Care* 14, 173–194. <https://doi.org/10.2337/diacare.14.3.173>
- DeFronzo, R.A., Ferrannini, E., Groop, L., Henry, R.R., Herman, W.H., Holst, J.J., Hu, F.B., Kahn, C.R., Raz, I., Shulman, G.I., Simonson, D.C., Testa, M.A., Weiss, R., 2015. Type 2 diabetes mellitus. *Nat Rev Dis Primers* 1, 15019. <https://doi.org/10.1038/nrdp.2015.19>
- DeFronzo, R.A., Ferrannini, E., Hendler, R., Felig, P., Wahren, J., 1983. Regulation of splanchnic and peripheral glucose uptake by insulin and hyperglycemia in man. *Diabetes* 32, 35–45. <https://doi.org/10.2337/diab.32.1.35>
- DeFronzo, R.A., Tripathy, D., 2009. Skeletal Muscle Insulin Resistance Is the Primary Defect in Type 2 Diabetes. *Diabetes Care* 32, S157–S163. <https://doi.org/10.2337/dc09-S302>
- Del Prato, S., Pulizzi, N., 2006. The place of sulfonylureas in the therapy for type 2 diabetes mellitus. *Metabolism* 55, S20–S27. <https://doi.org/10.1016/j.metabol.2006.02.003>
- Del Prato, S., Tiengo, A., 2001. The importance of first-phase insulin secretion: implications for the therapy of type 2 diabetes mellitus. *Diabetes Metab. Res. Rev.* 17, 164–174. <https://doi.org/10.1002/dmrr.198>
- Delarue, J., Beylot, M., 2007. Les traceurs isotopiques stables en nutrition humaine : que peut-on faire avec ? *Cahiers de Nutrition et de Diététique* 42, 324–335. [https://doi.org/10.1016/S0007-9960\(07\)78166-X](https://doi.org/10.1016/S0007-9960(07)78166-X)
- Deng, Y., Chen, Y., Zhang, W., Chen, B., Qiu, X., He, L., Mu, L., Yang, C., Chen, R., 2011. Polysaccharide from *Gynura divaricata* modulates the activities of intestinal disaccharidases in streptozotocin-induced diabetic rats. *Br J Nutr* 106, 1323–1329. <https://doi.org/10.1017/S0007114511001693>
- Desquilbet, L., 2019. Guide pratique de validation statistique de méthodes de mesure : répétabilité, reproductibilité, et concordance.
- Di Ciaula, A., Garruti, G., Lunardi Baccetto, R., Molina-Molina, E., Bonfrate, L., Wang, D.Q.-H., Portincasa, P., 2017. Bile Acid Physiology. *Ann Hepatol* 16, s4–s14. <https://doi.org/10.5604/01.3001.0010.5493>
- Diamond, J.M., Karasov, W.H., Cary, C., Enders, D., Yung, R., 1984. Effect of dietary carbohydrate on monosaccharide uptake by mouse small intestine in vitro. *The Journal of Physiology* 349, 419–440. <https://doi.org/10.1113/jphysiol.1984.sp015165>
- Dimitriadis, G.D., Maratou, E., Kountouri, A., Board, M., Lambadiari, V., 2021. Regulation of Postabsorptive and Postprandial Glucose Metabolism by Insulin-Dependent and Insulin-Independent Mechanisms: An Integrative Approach. *Nutrients* 13, 159. <https://doi.org/10.3390/nu13010159>

- Ding, G.-L., Wang, F.-F., Shu, J., Tian, S., Jiang, Y., Zhang, D., Wang, N., Luo, Q., Zhang, Y., Jin, F., Leung, P.C.K., Sheng, J.-Z., Huang, H.-F., 2012. Transgenerational Glucose Intolerance With Igf2/H19 Epigenetic Alterations in Mouse Islet Induced by Intrauterine Hyperglycemia. *Diabetes* 61, 1133–1142. <https://doi.org/10.2337/db11-1314>
- Dinneen, S., John, G., Robert, R., 1992. Carbohydrate metabolism in non-insulin-dependent diabetes mellitus. *NEJM* 327, 707–713. <https://doi.org/10.1056/NEJM199209033271007>
- Dobbins, R.L., Greenway, F.L., Chen, L., Liu, Y., Breed, S.L., Andrews, S.M., Wald, J.A., Walker, A., Smith, C.D., 2015. Selective sodium-dependent glucose transporter 1 inhibitors block glucose absorption and impair glucose-dependent insulinotropic peptide release. *American Journal of Physiology-Gastrointestinal and Liver Physiology* 308, G946–G954. <https://doi.org/10.1152/ajpgi.00286.2014>
- Dominguez Rieg, J.A., Rieg, T., 2019. What does sodium-glucose co-transporter 1 inhibition add: Prospects for dual inhibition. *Diabetes Obes Metab* 21, 43–52. <https://doi.org/10.1111/dom.13630>
- Du, Y.T., Piscitelli, D., Ahmad, S., Trahair, L.G., Greenfield, J.R., Samocha-Bonet, D., Rayner, C.K., Horowitz, M., Jones, K.L., 2018. Effects of Glutamine on Gastric Emptying of Low- and High-Nutrient Drinks in Healthy Young Subjects-Impact on Glycaemia. *Nutrients* 10, 739. <https://doi.org/10.3390/nu10060739>
- Duchman, S.M., Ryan, A.J., Scheld, H.P., Summers, R.W., Bleiler, T.L., Gisolfi, C.V., 1997. Upper limit for intestinal absorption of a dilute glucose solution in men at rest. *Med Sci Sports Exerc* 29, 482–488. <https://doi.org/10.1097/00005768-199704000-00009>
- Duez, H., Cariou, B., Staels, B., 2012. DPP-4 inhibitors in the treatment of type 2 diabetes. *Biochemical Pharmacology* 83, 823–832. <https://doi.org/10.1016/j.bcp.2011.11.028>
- Dufrane, D., van Steenberghe, M., Guiot, Y., Goebbels, R.-M., Saliez, A., Gianello, P., 2006. Streptozotocin-Induced Diabetes in Large Animals (Pigs/Primates): Role of GLUT2 Transporter and β -cell Plasticity. *Transplantation* 81, 36–45. <https://doi.org/10.1097/01.tp.0000189712.74495.82>
- Dutia, R., Brakoniecki, K., Bunker, P., Paultre, F., Homel, P., Carpentier, A.C., McGinty, J., Laferrère, B., 2014. Limited recovery of β -cell function after gastric bypass despite clinical diabetes remission. *Diabetes* 63, 1214–1223. <https://doi.org/10.2337/db13-1176>
- Duvivier, V., Creusot, S., Broux, O., Helbert, A., Lesage, L., Moreau, K., Lesueur, N., Gerard, L., Lemaitre, K., Provost, N., Hubert, E.-L., Baltauss, T., Brzustowski, A., De Preville, N., Geronimi, J., Adoux, L., Letourneur, F., Hammoutene, A., Valla, D., Paradis, V., Delerive, P., 2022. Characterization and Pharmacological Validation of a Preclinical Model of NASH in Göttingen Minipigs. *J Clin Exp Hepatol* 12, 293–305. <https://doi.org/10.1016/j.jceh.2021.09.001>
- Dyer, J., Vayro, S., King, T.P., Shirazi-Beechey, S.P., 2003. Glucose sensing in the intestinal epithelium. *Eur J Biochem* 270, 3377–3388. <https://doi.org/10.1046/j.1432-1033.2003.03721.x>
- Dyer, J., Wood, I.S., Palejwala, A., Ellis, A., Shirazi-Beechey, S.P., 2002. Expression of monosaccharide transporters in intestine of diabetic humans. *American Journal of Physiology-Gastrointestinal and Liver Physiology* 282, G241–G248. <https://doi.org/10.1152/ajpgi.00310.2001>
- Dyson, M.C., Alloosh, M., Vuchetich, J.P., Mokelke, E.A., Sturek, M., 2006. Components of Metabolic Syndrome and Coronary Artery Disease in Female Ossabaw Swine Fed Excess Atherogenic Diet. *Comparative Medicine* 56, 11.

- Eberts, T.J., Sample, R.H., Glick, M.R., Ellis, G.H., 1979. A simplified, colorimetric micromethod for xylose in serum or urine, with phloroglucinol. *Clinical Chemistry* 25, 1440–1443.
- Ebrahimi, A.G., Hollister-Lock, J., Sullivan, B.A., Tsuchida, R., Bonner-Weir, S., Weir, G.C., 2020. Beta cell identity changes with mild hyperglycemia: Implications for function, growth, and vulnerability. *Molecular Metabolism* 35, 100959. <https://doi.org/10.1016/j.molmet.2020.02.002>
- Efanova, I.B., Zaitsev, S.V., Zhivotovsky, B., Köhler, M., Efendić, S., Orrenius, S., Berggren, P.-O., 1998. Glucose and Tolbutamide Induce Apoptosis in Pancreatic β -Cells. *Journal of Biological Chemistry* 273, 33501–33507. <https://doi.org/10.1074/jbc.273.50.33501>
- Egan, J.M., Margolskee, R.F., 2008. Taste Cells of the Gut and Gastrointestinal Chemosensation. *Molecular Interventions* 8, 78–81. <https://doi.org/10.1124/mi.8.2.5>
- Ehrenkranz, J.R.L., Lewis, N.G., Ronald Kahn, C., Roth, J., 2005. Phlorizin: a review. *Diabetes Metab. Res. Rev.* 21, 31–38. <https://doi.org/10.1002/dmrr.532>
- Elashoff, J.D., Reedy, T.J., Meyer, J.H., 1982. Analysis of gastric emptying data. *Gastroenterology* 83, 1306–1312.
- Elhady, S.S., Alshobaki, N.M., Elfaky, M.A., Koshak, A.E., Alharbi, M., Abdelhameed, R.F.A., Darwish, K.M., 2023. Deciphering Molecular Aspects of Potential α -Glucosidase Inhibitors within *Aspergillus terreus*: A Computational Odyssey of Molecular Docking-Coupled Dynamics Simulations and Pharmacokinetic Profiling. *Metabolites* 13, 942. <https://doi.org/10.3390/metabo13080942>
- Elovaris, R.A., Hajishafiee, M., Ullrich, S.S., Fitzgerald, P.C.E., Lange, K., Horowitz, M., Feinle-Bisset, C., 2021. Intragastric administration of leucine and isoleucine does not reduce the glycaemic response to, or slow gastric emptying of, a carbohydrate-containing drink in type 2 diabetes. *Diabetes Res Clin Pract* 171, 108618. <https://doi.org/10.1016/j.diabres.2020.108618>
- Englyst, H.N., Veenstra, J., Hudson, G.J., 1996. Measurement of rapidly available glucose (RAG) in plant foods: a potential in vitro predictor of the glycaemic response. *British Journal of Nutrition* 75, 327–337. <https://doi.org/10.1079/BJN19960137>
- Ercan, P., El, S.N., 2021. Inhibitory effects of bioaccessible anthocyanins and procyanidins from apple, red grape, cinnamon on α -amylase, α -glucosidase and lipase. *Int J Vitam Nutr Res* 91, 16–24. <https://doi.org/10.1024/0300-9831/a000652>
- Erdman, S.H., Hart, M.H., Park, J.H.Y., Vanderhoof, J.A., 1991. The intestinal absorption of 3-O-Methyl-D-glucose in Methotrexate-Treated Rats: An In Vivo Study of Small Bowel Function. *Journal of Pediatric Gastroenterology and Nutrition* 13, 360–366.
- Eschwege, E., Richard, J.L., Thibault, N., Ducimetière, P., Warnet, J.M., Claude, J.R., Rosselin, G.E., 1985. Coronary heart disease mortality in relation with diabetes, blood glucose and plasma insulin levels. The Paris Prospective Study, ten years later. *Horm Metab Res Suppl* 15, 41–46.
- European Medicines Agency, 2022. Liraglutide: Scientific conclusions and grounds for the variation to the terms of the marketing authorisation(s).
- Everett-Grueter, C., Edgerton, D.S., Donahue, E.P., Vaughan, S., Chu, C.A., Sindelar, D.K., Cherrington, A.D., 2006. The effect of an acute elevation of NEFA concentrations on glucagon-stimulated hepatic glucose output. *American Journal of Physiology-Endocrinology and Metabolism* 291, E449–E459. <https://doi.org/10.1152/ajpendo.00043.2006>

- Farrell, T.L., Ellam, S.L., Forrelli, T., Williamson, G., 2013. Attenuation of glucose transport across Caco-2 cell monolayers by a polyphenol-rich herbal extract: interactions with SGLT1 and GLUT2 transporters. *Biofactors* 39, 448–456. <https://doi.org/10.1002/biof.1090>
- Fatima, K., Farooqui, S.K., Ajaz, I., Ali, S.T., Hashmi, N., Nadeem, S., Ghazi, S.A., Kaleem, S.H., Bozdar, F.S., Noorani, M., 2022. Sleeve gastrectomy versus Roux-en-Y Gastric Bypass for remission of type 2 diabetes mellitus at 1, 3 and 5 years: a systematic review and meta-analysis. *Minerva Gastroenterol (Torino)* 68, 450–458. <https://doi.org/10.23736/S2724-5985.22.03117-5>
- Ferrannini, E., Barrett, E.J., Bevilacqua, S., DeFronzo, R.A., 1983. Effect of fatty acids on glucose production and utilization in man. *J. Clin. Invest.* 72, 1737–1747. <https://doi.org/10.1172/JCI111133>
- Ferrannini, E., Bjorkman, O., Reichard, G.A., Pilo, A., Olsson, M., Wahren, J., DeFronzo, R.A., 1985. The Disposal of an Oral Glucose Load in Healthy Subjects. *Diabetes* 34, 580–588. <https://doi.org/10.2337/diab.34.6.580>
- Ferrannini, E., Mari, A., 2014. β -Cell function in type 2 diabetes. *Metabolism* 63, 1217–1227. <https://doi.org/10.1016/j.metabol.2014.05.012>
- Ferrannini, E., Natali, A., Muscelli, E., Nilsson, P.M., Golay, A., Laakso, M., Beck-Nielsen, H., Mari, A., 2011. Natural history and physiological determinants of changes in glucose tolerance in a non-diabetic population: the RISC Study. *Diabetologia* 54, 1507–1516. <https://doi.org/10.1007/s00125-011-2112-x>
- Ferraris, R.P., Choe, J., Patel, C.R., 2018. Intestinal Absorption of Fructose. *Annu. Rev. Nutr.* 38, 41–67. <https://doi.org/10.1146/annurev-nutr-082117-051707>
- Ferraris, R.P., Yasharpour, S., Lloyd, K.C., Mirzayan, R., Diamond, J.M., 1990. Luminal glucose concentrations in the gut under normal conditions. *American Journal of Physiology-Gastrointestinal and Liver Physiology* 259, G822–G837. <https://doi.org/10.1152/ajpgi.1990.259.5.G822>
- Ferrer, J., Scott, W.E., Weegman, B.P., Suszynski, T.M., Sutherland, D.E.R., Hering, B.J., Papas, K.K., 2008. Pig Pancreas Anatomy: Implications for Pancreas Procurement, Preservation, and Islet Isolation. *Transplantation* 86, 1503–1510. <https://doi.org/10.1097/TP.0b013e31818bfda1>
- Festi, D., Schiumerini, R., Eusebi, L.H., Marasco, G., Taddia, M., Colecchia, A., 2014. Gut microbiota and metabolic syndrome. *WJG* 20, 16079. <https://doi.org/10.3748/wjg.v20.i43.16079>
- Finlay, J.M., Hogarth, J., Wightman, K.J., 1964. A Clinical evaluation of the D-Xylose tolerance test. *Ann Intern Med* 61, 411–422. <https://doi.org/10.7326/0003-4819-61-3-411>
- Fiorentino, T.V., Andreozzi, F., Mannino, G.C., Pedace, E., Perticone, M., Sciacqua, A., Perticone, F., Sesti, G., 2016. One-Hour Postload Hyperglycemia Confers Higher Risk of Hepatic Steatosis to HbA1c-Defined Prediabetic Subjects. *The Journal of Clinical Endocrinology & Metabolism* 101, 4030–4038. <https://doi.org/10.1210/jc.2016-1856>
- Fiorentino, T.V., Marini, M.A., Andreozzi, F., Arturi, F., Succurro, E., Perticone, M., Sciacqua, A., Hribal, M.L., Perticone, F., Sesti, G., 2015. One-Hour Postload Hyperglycemia Is a Stronger Predictor of Type 2 Diabetes Than Impaired Fasting Glucose. *The Journal of Clinical Endocrinology & Metabolism* 100, 3744–3751. <https://doi.org/10.1210/jc.2015-2573>
- Fiorentino, T.V., Marini, M.A., Succurro, E., Andreozzi, F., Perticone, M., Hribal, M.L., Sciacqua, A., Perticone, F., Sesti, G., 2018. One-Hour Postload Hyperglycemia: Implications for Prediction and Prevention of Type 2 Diabetes. *The Journal of Clinical Endocrinology & Metabolism* 103, 3131–3143. <https://doi.org/10.1210/jc.2018-00468>

- Fiorentino, T.V., Succurro, E., Andreozzi, F., Sciacqua, A., Perticone, F., Sesti, G., 2019. One-hour post-load hyperglycemia combined with HbA1c identifies individuals with higher risk of cardiovascular diseases: Cross-sectional data from the CATAMERI study. *Diabetes Metab Res Rev* 35, e3096. <https://doi.org/10.1002/dmrr.3096>
- Fiorentino, T.V., Suraci, E., Arcidiacono, G.P., Cimellaro, A., Mignogna, C., Presta, I., Andreozzi, F., Hribal, M.L., Perticone, F., Donato, G., Luzzza, F., Sesti, G., 2017. Duodenal Sodium/Glucose Cotransporter 1 Expression Under Fasting Conditions Is Associated With Postload Hyperglycemia. *The Journal of Clinical Endocrinology & Metabolism* 102, 3979–3989. <https://doi.org/10.1210/jc.2017-00348>
- Fiorentino, T.V., Suraci, E., De Vito, F., Cimellaro, A., Hribal, M.L., Sciacqua, A., Andreozzi, F., Luzzza, F., Sesti, G., 2021. One-hour post-load hyperglycemia combined with HbA1c identifies individuals with augmented duodenal levels of sodium/glucose co-transporter 1. *Diabetes Research and Clinical Practice* 181, 109094. <https://doi.org/10.1016/j.diabres.2021.109094>
- Fiset, C., LeBel, M., 1990. Influence of the menstrual cycle on the absorption and elimination of D-xylose. *Clin Pharmacol Ther* 48, 529–536. <https://doi.org/10.1038/clpt.1990.189>
- Fitzgerald, P.C.E., Manoliu, B., Herbillon, B., Steinert, R.E., Horowitz, M., Feinle-Bisset, C., 2020. Effects of L-Phenylalanine on Energy Intake and Glycaemia-Impacts on Appetite Perceptions, Gastrointestinal Hormones and Gastric Emptying in Healthy Males. *Nutrients* 12, 1788. <https://doi.org/10.3390/nu12061788>
- Flint, A., Raben, A., Astrup, A., Holst, J.J., 1998. Glucagon-like peptide 1 promotes satiety and suppresses energy intake in humans. *J. Clin. Invest.* 101, 515–520. <https://doi.org/10.1172/JCI990>
- Flynn, C.R., Tamboli, R.A., Antoun, J., Sidani, R.M., Williams, B., Spann, M.D., English, W.J., Welch, E.B., Sundaresan, S., Abumrad, N.N., 2022. Caloric Restriction and Weight Loss Are Primary Factors in the Early Tissue-Specific Metabolic Changes After Bariatric Surgery. *Diabetes Care* 45, 1914–1916. <https://doi.org/10.2337/dc22-0069>
- Fordtran, J.S., 1962. Sugar Absorption Tests, with Special Reference to 3-O-Methyl-d-Glucose and d-Xylose. *Ann Intern Med* 57, 883–891. <https://doi.org/10.7326/0003-4819-57-6-883>
- Foretz, M., Guigas, B., Viollet, B., 2019. Understanding the gluco regulatory mechanisms of metformin in type 2 diabetes mellitus. *Nat Rev Endocrinol* 15, 569–589. <https://doi.org/10.1038/s41574-019-0242-2>
- Forouhi, N.G., Misra, A., Mohan, V., Taylor, R., Yancy, W., 2018. Dietary and nutritional approaches for prevention and management of type 2 diabetes. *BMJ* 361, k2234. <https://doi.org/10.1136/bmj.k2234>
- Franquet, E., Watts, G., Kolodny, G.M., Goldfine, A.B., Patti, M.-E., 2019. PET-CT reveals increased intestinal glucose uptake after gastric surgery. *Surgery for Obesity and Related Diseases* 15, 643–649. <https://doi.org/10.1016/j.soard.2019.01.018>
- Freidenberg, G.R., Henry, R.R., Klein, H.H., Reichart, D.R., Olefsky, J.M., 1987. Decreased kinase activity of insulin receptors from adipocytes of non-insulin-dependent diabetic subjects. *J. Clin. Invest.* 79, 240–250. <https://doi.org/10.1172/JCI112789>
- Fu, Z., Gilbert, E.R., Liu, D., 2014. Regulation of Insulin Synthesis and Secretion and Pancreatic Beta-Cell Dysfunction in Diabetes. *Curr Diabetes Rev* 9, 25–53.

- Fujita, Y., Kojima, H., Hidaka, H., Fujimiya, M., Kashiwagi, A., Kikkawa, R., 1998. Increased intestinal glucose absorption and postprandial hyperglycaemia at the early step of glucose intolerance in Otsuka Long-Evans Tokushima Fatty Rats. *Diabetologia* 41, 1459–1466. <https://doi.org/10.1007/s001250051092>
- Galicia-Garcia, U., Benito-Vicente, A., Jebari, S., Larrea-Sebal, A., Siddiqi, H., Uribe, K.B., Ostolaza, H., Martín, C., 2020. Pathophysiology of Type 2 Diabetes Mellitus. *IJMS* 21, 6275. <https://doi.org/10.3390/ijms21176275>
- Galuska, D., Ryder, J., Kawano, Y., Charron, M.J., Zierath, J.R., 1998. Insulin signaling and glucose transport in insulin resistant skeletal muscle. Special reference to GLUT4 transgenic and GLUT4 knockout mice. *Advances in experimental medicine and biology* 441, 73–85. https://doi.org/10.1007/978-1-4899-1928-1_7
- Garay, M., Balagué, C., Rodríguez-Otero, C., Gonzalo, B., Domenech, A., Pernas, J.C., Gich, I.J., Miñambres, I., Fernández-Ananín, S., Targarona, E.M., 2018. Influence of antrum size on gastric emptying and weight-loss outcomes after laparoscopic sleeve gastrectomy (preliminary analysis of a randomized trial). *Surg Endosc* 32, 2739–2745. <https://doi.org/10.1007/s00464-017-5972-4>
- Gembillo, G., Ingrassiotta, Y., Crisafulli, S., Luxi, N., Siligato, R., Santoro, D., Trifirò, G., 2021. Kidney Disease in Diabetic Patients: From Pathophysiology to Pharmacological Aspects with a Focus on Therapeutic Inertia. *IJMS* 22, 4824. <https://doi.org/10.3390/ijms22094824>
- Gentilcore, D., Chaikomin, R., Jones, K.L., Russo, A., Feinle-Bisset, C., Wishart, J.M., Rayner, C.K., Horowitz, M., 2006. Effects of fat on gastric emptying of and the glycemic, insulin, and incretin responses to a carbohydrate meal in type 2 diabetes. *J Clin Endocrinol Metab* 91, 2062–2067. <https://doi.org/10.1210/jc.2005-2644>
- Gerich, J.E., 2010. Role of the kidney in normal glucose homeostasis and in the hyperglycaemia of diabetes mellitus: therapeutic implications. *Diabetic Medicine* 27, 136–142. <https://doi.org/10.1111/j.1464-5491.2009.02894.x>
- Gerich, J.E., 2000. Physiology of glucose homeostasis. *Diabetes Obes Metab* 2, 345–350. <https://doi.org/10.1046/j.1463-1326.2000.00085.x>
- Gerich, J.E., 1993. Control of glycaemia. *Baillière's Clinical Endocrinology and Metabolism* 7, 551–586. [https://doi.org/10.1016/S0950-351X\(05\)80207-1](https://doi.org/10.1016/S0950-351X(05)80207-1)
- Gerrity, R.G., Natarajan, R., Nadler, J.L., Kimsey, T., 2001. Diabetes-Induced Accelerated Atherosclerosis in Swine. *Diabetes* 50, 1654–1665. <https://doi.org/10.2337/diabetes.50.7.1654>
- Gerstein, H.C., 2006. Why don't pigs get diabetes? Explanations for variations in diabetes susceptibility in human populations living in a diabetogenic environment. *Canadian Medical Association Journal* 174, 25–26. <https://doi.org/10.1503/cmaj.050649>
- Gerstein, H.C., Santaguida, P., Raina, P., Morrison, K.M., Balion, C., Hunt, D., Yazdi, H., Booker, L., 2007. Annual incidence and relative risk of diabetes in people with various categories of dysglycemia: A systematic overview and meta-analysis of prospective studies. *Diabetes Research and Clinical Practice* 78, 305–312. <https://doi.org/10.1016/j.diabres.2007.05.004>
- Giuntini, E.B., Sardá, F.A.H., de Menezes, E.W., 2022. The Effects of Soluble Dietary Fibers on Glycemic Response: An Overview and Futures Perspectives. *Foods* 11, 3934. <https://doi.org/10.3390/foods11233934>

- Gonlachavit, S., Hsu, C.-W., Boden, G.H., Knight, L.C., Maurer, A.H., Fisher, R.S., Parkman, H.P., 2003. Effect of Altering Gastric Emptying on Postprandial Plasma Glucose Concentrations Following a Physiologic Meal in Type-II Diabetic Patients. *Digestive Diseases and Sciences* 48, 10. <https://doi.org/10.1023/a:1022528414264>
- Gonzalez, L.M., Moeser, A.J., Blikslager, A.T., 2015. Porcine models of digestive disease: the future of large animal translational research. *Transl Res* 166, 12–27. <https://doi.org/10.1016/j.trsl.2015.01.004>
- Goodwin, N.C., Ding, Z.-M., Harrison, B.A., Strobel, E.D., Harris, A.L., Smith, M., Thompson, A.Y., Xiong, W., Mseeh, F., Bruce, D.J., Diaz, D., Gopinathan, S., Li, L., O'Neill, E., Thiel, M., Wilson, A.G.E., Carson, K.G., Powell, D.R., Rawlins, D.B., 2017. Discovery of LX2761, a Sodium-Dependent Glucose Cotransporter 1 (SGLT1) Inhibitor Restricted to the Intestinal Lumen, for the Treatment of Diabetes. *J Med Chem* 60, 710–721. <https://doi.org/10.1021/acs.jmedchem.6b01541>
- Gorboulev, V., Schurmann, A., Vallon, V., Kipp, H., Jaschke, A., Klessen, D., Friedrich, A., Scherneck, S., Rieg, T., Cunard, R., Veyhl-Wichmann, M., Srinivasan, A., Balen, D., Breljak, D., Rexhepaj, R., Parker, H.E., Gribble, F.M., Reimann, F., Lang, F., Wiese, S., Sabolic, I., Sendtner, M., Koepsell, H., 2012. Na⁺-D-glucose Cotransporter SGLT1 is Pivotal for Intestinal Glucose Absorption and Glucose-Dependent Incretin Secretion. *Diabetes* 61, 187–196. <https://doi.org/10.2337/db11-1029>
- Gosmanov, A.R., Umpierrez, G.E., 2013. Management of Hyperglycemia During Enteral and Parenteral Nutrition Therapy. *Curr Diab Rep* 13, 155–162. <https://doi.org/10.1007/s11892-012-0335-y>
- Goutchtat, R., Chetboun, M., Wiart, J.-F., Gaulier, J.-M., Pattou, F., Allorge, D., Hubert, T., 2021. Long-Term Analgesia following a Single Application of Fentanyl Transdermal Solution in Pigs. *Eur Surg Res* 62, 115–120. <https://doi.org/10.1159/000516828>
- Goutchtat, R., Quenon, A., Clarisse, M., Delalleau, N., Coddeville, A., Gobert, M., Gmyr, V., Kerr-Conte, J., Pattou, F., Hubert, T., 2023. Effects of subtotal pancreatectomy and long-term glucose and lipid overload on insulin secretion and glucose homeostasis in minipigs. *Endocrinol Diabetes Metab* e425. <https://doi.org/10.1002/edm2.425>
- Gouyon, F., Caillaud, L., Carrière, V., Klein, C., Dalet, V., Citadelle, D., Kellett, G.L., Thorens, B., Leturque, A., Brot-Laroche, E., 2003. Simple-sugar meals target GLUT2 at enterocyte apical membranes to improve sugar absorption: a study in GLUT2-null mice. *The Journal of Physiology* 552, 823–832. <https://doi.org/10.1113/jphysiol.2003.049247>
- Goyal, R.K., 2021. Gastric Emptying Abnormalities in Diabetes Mellitus. *N Engl J Med* 384, 1742–1751. <https://doi.org/10.1056/NEJMra2020927>
- Goyal, R.K., Cristofaro, V., Sullivan, M.P., 2019a. Rapid gastric emptying in diabetes mellitus: Pathophysiology and clinical importance. *Journal of Diabetes and its Complications* 33, 107414. <https://doi.org/10.1016/j.jdiacomp.2019.107414>
- Goyal, R.K., Guo, Y., Mashimo, H., 2019b. Advances in the physiology of gastric emptying. *Neurogastroenterology & Motility* 31, e13546. <https://doi.org/10.1111/nmo.13546>
- Grant, S.F.A., 2019. The TCF7L2 Locus: A Genetic Window Into the Pathogenesis of Type 1 and Type 2 Diabetes. *Diabetes Care* 42, 1624–1629. <https://doi.org/10.2337/dci19-0001>
- Gray, G.M., Ingelfinger, F.J., 1966. Intestinal absorption of sucrose in man: interrelation of hydrolysis and monosaccharide product absorption. *J. Clin. Invest.* 45, 388–398. <https://doi.org/10.1172/JCI105354>

- Gromova, L.V., Fetissov, S.O., Gruzdkov, A.A., 2021. Mechanisms of Glucose Absorption in the Small Intestine in Health and Metabolic Diseases and Their Role in Appetite Regulation. *Nutrients* 13, 2474. <https://doi.org/10.3390/nu13072474>
- Gromova, L.V., Gruzdkov, A.A., 1993. The relative role of different mechanisms of glucose absorption in the small intestine under physiological conditions. *Fiziol Zh Im I M Sechenova* 79, 65–72.
- Guglielmi, A., Ruzzenente, A., Conci, S., Valdegamberi, A., Iacono, C., 2012. How Much Remnant Is Enough in Liver Resection? *Digestive Surgery* 29, 6–17. <https://doi.org/10.1159/000335713>
- Gutierrez, K., Dicks, N., Glanzner, W.G., Agellon, L.B., Bordignon, V., 2015. Efficacy of the porcine species in biomedical research. *Front. Genet.* 6. <https://doi.org/10.3389/fgene.2015.00293>
- Hagman, D.K., Latour, M.G., Chakrabarti, S.K., Fontes, G., Amyot, J., Tremblay, C., Semache, M., Lausier, J.A., Roskens, V., Mirmira, R.G., Jetton, T.L., Poitout, V., 2008. Cyclical and Alternating Infusions of Glucose and Intralipid in Rats Inhibit Insulin Gene Expression and Pdx-1 Binding in Islets. *Diabetes* 57, 424–431. <https://doi.org/10.2337/db07-1285>
- Hai, T., Teng, F., Guo, R., Li, W., Zhou, Q., 2014. One-step generation of knockout pigs by zygote injection of CRISPR/Cas system. *Cell Res* 24, 372–375. <https://doi.org/10.1038/cr.2014.11>
- Halaihel, N., Gerbaud, D., Vasseur, M., Alvarado, F., 1999. Heterogeneity of pig intestinal D-glucose transport systems. *American Journal of Physiology-Cell Physiology* 277, C1130–C1141. <https://doi.org/10.1152/ajpcell.1999.277.6.C1130>
- Halimi, S., 2019. Chirurgie bariatrique : état des lieux en France en 2019. *Médecine des Maladies Métaboliques* 13, 677–686. [https://doi.org/10.1016/S1957-2557\(19\)30210-X](https://doi.org/10.1016/S1957-2557(19)30210-X)
- Hamad, S., Tari, N.R., Mathiyalagan, G., Wright, A.J., 2021. Emulsion acid colloidal stability and droplet crystallinity modulate postprandial gastric emptying and short-term satiety: a randomized, double-blinded, crossover, controlled trial in healthy adult males. *Am J Clin Nutr* 114, 997–1011. <https://doi.org/10.1093/ajcn/nqab116>
- Hammer, R.E., Pursel, V.G., Rexroad, C.E., Wall, R.J., Bolt, D.J., Ebert, K.M., Palmiter, R.D., Brinster, R.L., 1985. Production of transgenic rabbits, sheep and pigs by microinjection. *Nature* 315, 680–683. <https://doi.org/10.1038/315680a0>
- Hara, H., Lin, Y.J., Zhu, X., Tai, H.-C., Ezzelarab, M., Balamarugan, A.N., Bottino, R., Houser, S.L., Cooper, D.K.C., 2008. Safe Induction of Diabetes by High-Dose Streptozotocin in Pigs. *Pancreas* 36, 31–38. <https://doi.org/10.1097/mpa.0b013e3181452886>
- Harris, L.-A., Kayser, B.D., Cefalo, C., Marini, L., Watrous, J.D., Ding, J., Jain, M., McDonald, J.G., Thompson, B.M., Fabbrini, E., Eagon, J.C., Patterson, B.W., Mittendorfer, B., Mingrone, G., Klein, S., 2019. Biliopancreatic Diversion Induces Greater Metabolic Improvement Than Roux-en-Y Gastric Bypass. *Cell Metabolism* 30, 855-864.e3. <https://doi.org/10.1016/j.cmet.2019.09.002>
- Hasan, F.M., Alsahli, M., Gerich, J.E., 2014. SGLT2 inhibitors in the treatment of type 2 diabetes. *Diabetes Research and Clinical Practice* 104, 297–322. <https://doi.org/10.1016/j.diabres.2014.02.014>
- Hasek, L.Y., Phillips, R.J., Hayes, A.M.R., Kinzig, K., Zhang, G., Powley, T.L., Hamaker, B.R., 2020. Carbohydrates designed with different digestion rates modulate gastric emptying response in rats. *Int J Food Sci Nutr* 71, 839–844. <https://doi.org/10.1080/09637486.2020.1738355>
- Haute Autorité de Santé, 2009. Chirurgie de l'obésité - Ce qu'il faut savoir avant de se décider !

- Hayoz, C., Hermann, T., Raptis, D.A., Brönnimann, A., Peterli, R., Zuber, M., 2018. Comparison of metabolic outcomes in patients undergoing laparoscopic roux-en-Y gastric bypass versus sleeve gastrectomy - a systematic review and meta-analysis of randomised controlled trials. *Swiss Med Wkly* 148, w14633. <https://doi.org/10.57187/smw.2018.14633>
- He, Y.-L., Haynes, W., Meyers, C.D., Amer, A., Zhang, Y., Mahling, P., Mendonza, A.E., Ma, S., Chutkow, W., Bachman, E., 2019. The effects of licogliflozin, a dual SGLT1/2 inhibitor, on body weight in obese patients with or without diabetes. *Diabetes Obes Metab* 21, 1311–1321. <https://doi.org/10.1111/dom.13654>
- Hearris, M., Hammond, K., Fell, J., Morton, J., 2018. Regulation of Muscle Glycogen Metabolism during Exercise: Implications for Endurance Performance and Training Adaptations. *Nutrients* 10, 298. <https://doi.org/10.3390/nu10030298>
- Hedberg, J., Sundström, J., Sundbom, M., 2014. Duodenal switch versus Roux-en-Y gastric bypass for morbid obesity: systematic review and meta-analysis of weight results, diabetes resolution and early complications in single-centre comparisons. *Obes Rev* 15, 555–563. <https://doi.org/10.1111/obr.12169>
- Heinke, S., Ludwig, B., Schubert, U., Schmid, J., Kiss, T., Steffen, A., Bornstein, S., Ludwig, S., 2016. Diabetes induction by total pancreatectomy in minipigs with simultaneous splenectomy: a feasible approach for advanced diabetes research. *Xenotransplantation* 23, 405–413. <https://doi.org/10.1111/xen.12255>
- Helke, K.L., Swindle, M.M., 2013. Animal models of toxicology testing: the role of pigs. *Expert Opinion on Drug Metabolism & Toxicology* 9, 127–139. <https://doi.org/10.1517/17425255.2013.739607>
- Henry, C.J., Kaur, B., Quek, R.Y.C., 2020. Chrononutrition in the management of diabetes. *Nutr. Diabetes* 10, 6. <https://doi.org/10.1038/s41387-020-0109-6>
- Henry, C.J.K., Newens, K.J., Lightowler, H.J., 2009. Low-glycaemic index sweetener-based beverages reduce 24-h glucose profiles in healthy adults. *J Hum Nutr Diet* 22, 77–80. <https://doi.org/10.1111/j.1365-277X.2008.00930.x>
- Henze, L.J., Griffin, B.T., Christiansen, M., Bundgaard, C., Langguth, P., Holm, R., 2018. Exploring gastric emptying rate in minipigs: Effect of food type and pre-dosing of metoclopramide. *European Journal of Pharmaceutical Sciences* 118, 183–190. <https://doi.org/10.1016/j.ejps.2018.03.017>
- Herman, M.A., Peroni, O.D., Villoria, J., Schön, M.R., Abumrad, N.A., Blüher, M., Klein, S., Kahn, B.B., 2012. A novel ChREBP isoform in adipose tissue regulates systemic glucose metabolism. *Nature* 484, 333–338. <https://doi.org/10.1038/nature10986>
- Higgins, P.J., Garlick, R.L., Bunn, H.F., 1982. Glycosylated hemoglobin in human and animal red cells. Role of glucose permeability. *Diabetes* 31, 743–748. <https://doi.org/10.2337/diab.31.9.743>
- Himsworth, H.P., 1936. Diabetes mellitus: its differentiation into insulin-sensitive and insulininsensitive types. *Lancet* 227, 127–130. [https://doi.org/10.1016/S0140-6736\(01\)36134-2](https://doi.org/10.1016/S0140-6736(01)36134-2).
- Hinshaw, L., Schiavon, M., Mallad, A., Man, C.D., Basu, R., Bharucha, Adil.E., Cobelli, C., Carter, R.E., Basu, A., Kudva, Y.C., 2014. Effects of delayed gastric emptying on postprandial glucose kinetics, insulin sensitivity, and β -cell function. *Am J Physiol Endocrinol Metab* 307, E494–E502. <https://doi.org/10.1152/ajpendo.00199.2014>

Hjerpsted, J.B., Flint, A., Brooks, A., Axelsen, M.B., Kvist, T., Blundell, J., 2018. Semaglutide improves postprandial glucose and lipid metabolism, and delays first-hour gastric emptying in subjects with obesity. *Diabetes Obes Metab* 20, 610–619. <https://doi.org/10.1111/dom.13120>

Hlebowicz, J., Jönsson, J.M., Lindstedt, S., Björgell, O., Darwich, G., Almér, L.-O., 2009. Effect of commercial rye whole-meal bread on postprandial blood glucose and gastric emptying in healthy subjects. *Nutr J* 8, 26. <https://doi.org/10.1186/1475-2891-8-26>

Hlebowicz, J., Wickenberg, J., Fahlström, R., Björgell, O., Almér, L.-O., Darwiche, G., 2007. Effect of commercial breakfast fibre cereals compared with corn flakes on postprandial blood glucose, gastric emptying and satiety in healthy subjects: a randomized blinded crossover trial. *Nutr J* 6, 22. <https://doi.org/10.1186/1475-2891-6-22>

Hofmann, A., Kessler, B., Ewerling, S., Weppert, M., Vogg, B., Ludwig, H., Stojkovic, M., Boelhaue, M., Brem, G., Wolf, E., Pfeifer, A., 2003. Efficient transgenesis in farm animals by lentiviral vectors. *EMBO Rep* 4, 1054–1060. <https://doi.org/10.1038/sj.embor.7400007>

Holman, R.R., Coleman, R.L., Chan, J.C.N., Chiasson, J.-L., Feng, H., Ge, J., Gerstein, H.C., Gray, R., Huo, Yong, Lang, Z., McMurray, J.J., Rydén, L., Schröder, S., Sun, Yihong, Theodorakis, M.J., Tendera, M., Tucker, L., Tuomilehto, J., Wei, Y., Yang, W., Wang, Duolao, Hu, D., Pan, C., Keenan, J., Milton, J., Doran, Z., Bray, C., Rouleau, J.L., Collier, J., Pocock, S., Standl, E., Swedberg, K., Weng, J., Zhao, D., Petrie, M.C., Connolly, E., Jhund, P., MacDonald, M., Myles, R.C., Bai, R., Li, Jing, Liu, Zhaoping, Liu, Zhenyu, Peng, D., Tong, Q., Wang, Chunxue, Yan, X., Zhang, Yuqing, Zhou, Jingmin, Sattar, N., Fisher, M., Petrie, J.R., Bethel, M.A., Xu, W., Hearn, S., Kappai, A., Su, S.-Y., Liyanage, W., Paul, S., Pozzi, E., Ring, A., Athwal, R., Batra, P., Ferch, A., Groves, N., Kennedy, I., Nawalaniec, O., Patel, Y., Roberts, R., Rush, V., Starrett, J., Tang, Jennifer, Bi, J., Jiang, Z., Wei, H., Wei, X., Zhang, X., Yin, J., Sun, Yu, Hu, R., Liu, Y., Long, J., Long, Y., Qiao, G., Qiao, H., Sun, X., Zhang, Yucheng, Zhou, Jing, Wang, Bangning, Chen, B., Deng, L., Han, X., Hu, T., Hua, Q., Huo, Yanming, Li, Hongmei, Li, Hongwei, Liu, L., Lu, J., Ma, C., Peng, J., Pi, L., Wang, Bin, Wei, G., Yang, M., Zhang, Shuyang, Zhang, L., Zhao, X., Zhou, Y., Shi, L., Wang, M., Wu, L., Han, L., Liao, R., Ran, B., She, Q., Tan, J., Xia, M., Yang, C., Chen, L., Xiong, S., Yu, L., Pu, X., Wang, Yan, Xie, Q., Chen, C., Chen, Jiyan, Dong, Y., Wu, Z., Yuan, Y., Zhou, W., Zhou, S., Chen, Xiaochao, Wu, C., Zhang, A., Li, Zicheng, Lai, S., Yang, J., Wei, J., Kuang, R., Zhao, Z., Zhong, G., Cao, X., Hao, Yuming, Liu, G., Wang, Dongmei, Fang, H., Kong, L., Li, Haitao, Wang, Changqing, Wang, L., Li, Xueqi, Dong, P., Zhang, Shouyan, Liu, Xincan, Zhao, Y., Liu, H., Gu, Y., Liao, Y., Su, X., Wang, Daowen, Wang, H., Yang, B., Guo, Ying, Ouyang, D., Yang, T., Zhang, Yumin, Han, Y., Lin, X., Zhao, R., Man, R., Bian, R., Biao, X., Hasimu, B., Jin, Hui, Liu, P., Yu, J., Zhang, Hang, Xu, C., Guo, Yan, Lv, K., Tao, Y., Xu, X., Yang, Z., Li, Dongye, Qi, C., Zhang, Guohui, Gu, X., Hong, L., Hu, L., Li, Juxiang, Yang, P., Liu, B., Wang, G., Lin, H., Liu, Jun, Zhang, Shuying, Han, P., Jin, Y., Li, L., Li, Zhanquan, Luan, H., Song, M., Xue, L., Hua, Y., Liu, D., Yuan, Zuyi, Ye, J., Gao, F., Feng, J., Wang, A., Ye, S., Li, Xiaoyan, Su, G., Zhang, Shufang, Hou, Z., Jiang, W., Zhou, C., Wang, Yanping, Qi, W., Bao, X., Feng, B., Gong, H., Gu, S., Gu, M., Guo, Xingui, He, B., Huang, Y., Jiang, J., Jiang, Y., Jin, Huigen, Li, Y., Liu, Q., Lu, G., Miao, P., Qin, Y., Wang, Bin, Wang, Yuanming, Wu, S., Xu, Y., Ma, J., Chen, Xiaoping, Liu, Xiumin, Tang, Jianing, Wang, J., Chen, Xiaoping, Tao, J., Zhang, J., Zhang, T., Li, Decai, Du, X., Jiang, T., Lin, J., Lu, C., Ma, H., Gao, B., Guo, Xukun, Li, T., Zheng, S., Li, Zhongcheng, Zhao, S., Qiu, Q., Li, K., Liu, Junming, Tang, B., Yuan, Zhanjun, Zhou, Jianhua, Bai, W., Guo, T., Zhang, Ge, Zhang, Hong, Hao, Yinglu, Fu, G., Tang, L., Chen, Jialun, 2017. Effects of acarbose on cardiovascular and diabetes outcomes in patients with coronary heart disease and impaired glucose tolerance (ACE): a randomised, double-blind, placebo-controlled trial. *The Lancet Diabetes & Endocrinology* 5, 877–886. [https://doi.org/10.1016/S2213-8587\(17\)30309-1](https://doi.org/10.1016/S2213-8587(17)30309-1)

- Holman, R.R., Paul, S.K., Bethel, M.A., Matthews, D.R., Neil, H.A.W., 2008. 10-Year Follow-up of Intensive Glucose Control in Type 2 Diabetes. *N Engl J Med* 359, 1577–1589. <https://doi.org/10.1056/NEJMoa0806470>
- Holst, J.J., 2007. The Physiology of Glucagon-like Peptide 1. *Physiological Reviews* 87, 1409–1439. <https://doi.org/10.1152/physrev.00034.2006>
- Holst, J.J., Gribble, F., Horowitz, M., Rayner, C.K., 2016. Roles of the Gut in Glucose Homeostasis. *Dia Care* 39, 884–892. <https://doi.org/10.2337/dc16-0351>
- Hooda, S., Matte, J.J., Wilkinson, C.W., Zijlstra, R.T., 2009. Technical note: An improved surgical model for the long-term studies of kinetics and quantification of nutrient absorption in swine. *Journal of Animal Science* 87, 2013–2019. <https://doi.org/10.2527/jas.2008-1423>
- Horakova, O., Kroupova, P., Bardova, K., Buresova, J., Janovska, P., Kopecky, J., Rossmeisl, M., 2019. Metformin acutely lowers blood glucose levels by inhibition of intestinal glucose transport. *Sci Rep* 9, 6156. <https://doi.org/10.1038/s41598-019-42531-0>
- Horowitz, M., Edelbroek, M.A.L., Wishart, J.M., Straathof, J.W., 1993. Relationship between oral glucose tolerance and gastric emptying in normal healthy subjects. *Diabetologia* 36, 857–862. <https://doi.org/10.1007/BF00400362>
- Hoy, A.J., Bruce, C.R., Cederberg, A., Turner, N., James, D.E., Cooney, G.J., Kraegen, E.W., 2007. Glucose infusion causes insulin resistance in skeletal muscle of rats without changes in Akt and AS160 phosphorylation. *American Journal of Physiology-Endocrinology and Metabolism* 293, E1358–E1364. <https://doi.org/10.1152/ajpendo.00133.2007>
- Hubert, T., Jany, T., Marcelli-Tourvieille, S., Nunes, B., Gmyr, V., Kerr-Conte, J., Vantyghem, M.-C., Pattou, F., 2005. Acute insulin response of donors is correlated with pancreatic islet isolation outcome in the pig. *Diabetologia* 48, 2069–2073. <https://doi.org/10.1007/s00125-005-1904-2>
- Hubert, T., Strecker, G., Gmyr, V., Arnalsteen, L., Garrigue, D., Ezzouaoui, R., Caiazzo, R., Dezfoulian, G., Averland, B., Vandewalle, B., Vantyghem, M.C., Kerr-Conte, J., Pattou, F., 2008. Acute Insulin Response to Arginine in Deceased Donors Predicts the Outcome of Human Islet Isolation. *Am J Transplant* 8, 872–876. <https://doi.org/10.1111/j.1600-6143.2007.02131.x>
- Hughes, R.L., Alvarado, D.A., Swanson, K.S., Holscher, H.D., 2021. The Prebiotic Potential of Inulin-Type Fructans: A Systematic Review. *Adv Nutr* 13, 492–529. <https://doi.org/10.1093/advances/nmab119>
- Hundal, R.S., Krssak, M., Dufour, S., Laurent, D., Lebon, V., Chandramouli, V., Inzucchi, S.E., Schumann, W.C., Petersen, K.F., Landau, B.R., Shulman, G.I., 2000. Mechanism by which metformin reduces glucose production in type 2 diabetes. *Diabetes* 49, 2063–2069. <https://doi.org/10.2337/diabetes.49.12.2063>
- Hunter, R.W., Hughey, C.C., Lantier, L., Sundelin, E.I., Peggie, M., Zeqiraj, E., Sicheri, F., Jessen, N., Wasserman, D.H., Sakamoto, K., 2018. Metformin reduces liver glucose production by inhibition of fructose-1-6-bisphosphatase. *Nat Med* 24, 1395–1406. <https://doi.org/10.1038/s41591-018-0159-7>
- Huntley, N.F., Patience, J.F., 2018a. Xylose: absorption, fermentation, and post-absorptive metabolism in the pig. *J Animal Sci Biotechnol* 9, 4. <https://doi.org/10.1186/s40104-017-0226-9>
- Huntley, N.F., Patience, J.F., 2018b. Xylose metabolism in the pig. *PLoS ONE* 13, e0205913. <https://doi.org/10.1371/journal.pone.0205913>

Hutchison, A.T., Piscitelli, D., Horowitz, M., Jones, K.L., Clifton, P.M., Standfield, S., Hausken, T., Feinle-Bisset, C., Luscombe-Marsh, N.D., 2015. Acute load-dependent effects of oral whey protein on gastric emptying, gut hormone release, glycemia, appetite, and energy intake in healthy men. *Am J Clin Nutr* 102, 1574–1584. <https://doi.org/10.3945/ajcn.115.117556>

Ikeda, T., Iwata, K., Murakami, H., 2000. Inhibitory effect of metformin on intestinal glucose absorption in the perfused rat intestine. *Biochemical Pharmacology* 59, 887–890. [https://doi.org/10.1016/S0006-2952\(99\)00396-2](https://doi.org/10.1016/S0006-2952(99)00396-2)

International Diabetes Federation, 2021. *IDF Diabetes Atlas 10th edition*.

Inzucchi, S.E., Maggs, D.G., Spollett, G.R., Page, S.L., Rife, F.S., Walton, V., Shulman, G.I., 1998. Efficacy and Metabolic Effects of Metformin and Troglitazone in Type II Diabetes Mellitus. *N Engl J Med* 338, 867–873. <https://doi.org/10.1056/NEJM199803263381303>

Io, F., Gunji, E., Koretsune, H., Kato, K., Sugisaki-Kitano, M., Okumura-Kitajima, L., Kimura, K., Uchida, S., Yamamoto, K., 2019. SGL5213, a novel and potent intestinal SGLT1 inhibitor, suppresses intestinal glucose absorption and enhances plasma GLP-1 and GLP-2 secretion in rats. *Eur J Pharmacol* 853, 136–144. <https://doi.org/10.1016/j.ejphar.2019.03.023>

Ito, K., Hao, L., Wray, A.E., Ross, A.C., 2013. Lipid Emulsion Administered Intravenously or Orally Attenuates Triglyceride Accumulation and Expression of Inflammatory Markers in the Liver of Nonobese Mice Fed Parenteral Nutrition Formula. *The Journal of Nutrition* 143, 253–259. <https://doi.org/10.3945/jn.112.169797>

Jagannathan, R., Sevvick, M.A., Huilin, L., Fink, D., Dankner, R., Chetrit, A., Roth, J., Bergman, M., 2016. Elevated 1-Hour Plasma Glucose Levels are Associated With Dysglycemia, Impaired Beta-Cell Function and Insulin Sensitivity: Pilot Study From a Real World Health Care Setting. *Endocrine* 52, 172–175. <https://doi.org/10.1007/s12020-015-0746-z>

Jain, A.K., Sharma, A., Arora, S., Blumenkamp, K., Jun, I.C., Luong, R., Westrich, D.J., Mittal, A., Buchanan, P.M., Guzman, M.A., Long, J., Neuschwander-Tetri, B.A., Teckman, J., 2017. Preserved Gut Microbial Diversity Accompanies Upregulation of TGR5 and Hepatobiliary Transporters in Bile Acid-Treated Animals Receiving Parenteral Nutrition. *JPEN J Parenter Enteral Nutr* 41, 198–207. <https://doi.org/10.1177/0148607116661838>

Jain, A.K., Stoll, B., Burrin, D.G., Holst, J.J., Moore, D.D., 2012. Enteral bile acid treatment improves parenteral nutrition-related liver disease and intestinal mucosal atrophy in neonatal pigs. *Am J Physiol Gastrointest Liver Physiol* 302, G218–224. <https://doi.org/10.1152/ajpgi.00280.2011>

Jakobsen, J.E., Li, J., Kragh, P.M., Moldt, B., Lin, L., Liu, Y., Schmidt, M., Winther, K.D., Schyth, B.D., Holm, I.E., Vajta, G., Bolund, L., Callesen, H., Jørgensen, A.L., Nielsen, A.L., Mikkelsen, J.G., 2011. Pig transgenesis by Sleeping Beauty DNA transposition. *Transgenic Research* 20, 533–545. <https://doi.org/10.1007/s11248-010-9438-x>

Jalleh, Ryan J., Jones, K.L., Rayner, C.K., Marathe, C.S., Wu, T., Horowitz, M., 2022. Normal and disordered gastric emptying in diabetes: recent insights into (patho)physiology, management and impact on glycaemic control. *Diabetologia*. <https://doi.org/10.1007/s00125-022-05796-1>

Jalleh, Ryan J, Wu, T., Jones, K.L., Rayner, C.K., Horowitz, M., Marathe, C.S., 2022. Relationships of Glucose, GLP-1, and Insulin Secretion With Gastric Emptying After a 75-g Glucose Load in Type 2 Diabetes. *The Journal of Clinical Endocrinology & Metabolism* 107, e3850–e3856. <https://doi.org/10.1210/clinem/dgac330>

- Janah, Kjeldsen, Galsgaard, Winther-Sørensen, Stojanovska, Pedersen, Knop, Holst, Wewer Albrechtsen, 2019. Glucagon Receptor Signaling and Glucagon Resistance. *IJMS* 20, 3314. <https://doi.org/10.3390/ijms20133314>
- Jandhyala, S.M., 2015. Role of the normal gut microbiota. *WJG* 21, 8787. <https://doi.org/10.3748/wjg.v21.i29.8787>
- Jastreboff, A., Aronne, L., Ahmad, N., Wharton, S., Connery, L., Alves, B., Kiyosue, A., Zhang, S., Liu, B., Bunck, M.C., Stefanski, A., SURMON-1 Investigators, 2022. Tirzepatide Once Weekly for the Treatment of Obesity. *N Engl J Med* 387, 205–2016.
- Jenkins, D.J., Wolever, T.M., Taylor, R.H., Barker, H., Fielden, H., Baldwin, J.M., Bowling, A.C., Newman, H.C., Jenkins, A.L., Goff, D.V., 1981. Glycemic index of foods: a physiological basis for carbohydrate exchange. *The American Journal of Clinical Nutrition* 34, 362–366.
- Jennings, A.M., Wilson, R.M., Ward, J.D., 1989. Symptomatic Hypoglycemia in NIDDM Patients Treated With Oral Hypoglycemic Agents. *Diabetes Care* 12, 203–208. <https://doi.org/10.2337/diacare.12.3.203>
- Johansen, T., Hansen, H.S., Richelsen, B., Malmlöf, K., 2001. The Obese Göttingen Minipig as a Model of the Metabolic Syndrome: Dietary Effects on Obesity, Insulin Sensitivity, and Growth Hormone Profile. *Comparative Medicine* 51, 6.
- Jones, K.L., Horowitz, M., Carney, B.I., Wishart, J.M., Guha, S., Green, L., 1996. Gastric Emptying in Early Noninsulin-Dependent Diabetes Mellitus. *The Journal of Nuclear Medicine* 37, 1643–1648.
- Jones, K.L., O'Donovan, D., Horowitz, M., Russo, A., Lei, Y., Hausken, T., 2006. Effects of posture on gastric emptying, transpyloric flow, and hunger after a glucose drink in healthy humans. *Dig Dis Sci* 51, 1331–1338. <https://doi.org/10.1007/s10620-005-9010-3>
- Jones, K.L., Rigda, R.S., Buttfield, M.D.M., Hatzinikolas, S., Pham, H.T., Marathe, C.S., Wu, T., Lange, K., Trahair, L.G., Rayner, C.K., Horowitz, M., 2019. Effects of lixisenatide on postprandial blood pressure, gastric emptying and glycaemia in healthy people and people with type 2 diabetes. *Diabetes Obes Metab* 21, 1158–1167. <https://doi.org/10.1111/dom.13633>
- Jurowich, C.F., Otto, C., Rikkala, P.R., Wagner, N., Vrhovac, I., Sabolić, I., Germer, C.-T., Koepsell, H., 2015. Ileal Interposition in Rats with Experimental Type 2 Like Diabetes Improves Glycemic Control Independently of Glucose Absorption. *Journal of Diabetes Research* 2015, 1–14. <https://doi.org/10.1155/2015/490365>
- Juvonen, K.R., Purhonen, A.-K., Salmenkallio-Marttila, M., Lähteenmäki, L., Laaksonen, D.E., Herzig, K.-H., Uusitupa, M.I.J., Poutanen, K.S., Karhunen, L.J., 2009. Viscosity of oat bran-enriched beverages influences gastrointestinal hormonal responses in healthy humans. *J Nutr* 139, 461–466. <https://doi.org/10.3945/jn.108.099945>
- Kang, J.-D., Kim, H., Jin, L., Guo, Q., Cui, C.-D., Li, W.-X., Kim, S., Kim, J.-S., Yin, X.-J., 2017. Apancreatic pigs cloned using Pdx1-disrupted fibroblasts created via TALEN-mediated mutagenesis. *Oncotarget* 8, 115480–115489. <https://doi.org/10.18632/oncotarget.23301>
- Kanungo, S., Wells, K., Tribett, T., El-Gharbawy, A., 2018. Glycogen metabolism and glycogen storage disorders. *Ann. Transl. Med* 6, 474–474. <https://doi.org/10.21037/atm.2018.10.59>
- Karamanlis, A., Chaikomin, R., Doran, S., Bellon, M., Bartholomeusz, F.D., Wishart, J.M., Jones, K.L., Horowitz, M., Rayner, C.K., 2007. Effects of protein on glycemic and incretin responses and gastric

- emptying after oral glucose in healthy subjects. *Am J Clin Nutr* 86, 1364–1368. <https://doi.org/10.1093/ajcn/86.5.1364>
- Karlsson, F.H., Tremaroli, V., Nookaew, I., Bergström, G., Behre, C.J., Fagerberg, B., Nielsen, J., Bäckhed, F., 2013. Gut metagenome in European women with normal, impaired and diabetic glucose control. *Nature* 498, 99–103. <https://doi.org/10.1038/nature12198>
- Kellett, G.L., Brot-Laroche, E., 2005. Apical GLUT2: A Major Pathway of Intestinal Sugar Absorption. *Diabetes* 54, 3056–3062. <https://doi.org/10.2337/diabetes.54.10.3056>
- Kellett, G.L., Brot-Laroche, E., Mace, O.J., Leturque, A., 2008. Sugar Absorption in the Intestine: The Role of GLUT2. *Annu. Rev. Nutr.* 28, 35–54. <https://doi.org/10.1146/annurev.nutr.28.061807.155518>
- Kelley, D., Mitrakou, A., Marsh, H., Schwenk, F., Benn, J., Sonnenberg, G., Arcangeli, M., Aoki, T., Sorensen, J., Berger, M., 1988. Skeletal muscle glycolysis, oxidation, and storage of an oral glucose load. *J. Clin. Invest.* 81, 1563–1571. <https://doi.org/10.1172/JCI113489>
- Kęska, P., Stadnik, J., Łupawka, A., Michalska, A., 2023. Novel α -Glucosidase Inhibitory Peptides Identified In Silico from Dry-Cured Pork Loins with Probiotics through Peptidomic and Molecular Docking Analysis. *Nutrients* 15, 3539. <https://doi.org/10.3390/nu15163539>
- Kim, J.Y., Goran, M.I., Toledo-Corral, C.M., Weigensberg, M.J., Choi, M., Shaibi, G.Q., 2013. One-Hour Glucose During an Oral Glucose Challenge Prospectively Predicts β -Cell Deterioration and Prediabetes in Obese Hispanic Youth. *Diabetes Care* 36, 1681–1686. <https://doi.org/10.2337/dc12-1861>
- Kindel, T.L., Yoder, S.M., Seeley, R.J., D'Alessio, D.A., Tso, P., 2009. Duodenal-jejunal exclusion improves glucose tolerance in the diabetic, Goto-Kakizaki rat by a GLP-1 receptor-mediated mechanism. *J Gastrointest Surg* 13, 1762–1772. <https://doi.org/10.1007/s11605-009-0912-9>
- Kirwan, J.P., Courcoulas, A.P., Cummings, D.E., Goldfine, A.B., Kashyap, S.R., Simonson, D.C., Arterburn, D.E., Gourash, W.F., Vernon, A.H., Jakicic, J.M., Patti, M.E., Wolski, K., Schauer, P.R., 2022. Diabetes Remission in the Alliance of Randomized Trials of Medicine Versus Metabolic Surgery in Type 2 Diabetes (ARMMS-T2D). *Diabetes Care* 45, 1574–1583. <https://doi.org/10.2337/dc21-2441>
- Kishi, K., Tanaka, T., Igawa, M., Takase, S., Goda, T., 1999. Sucrase-isomaltase and hexose transporter gene expressions are coordinately enhanced by dietary fructose in rat jejunum. *J Nutr* 129, 953–956. <https://doi.org/10.1093/jn/129.5.953>
- Kleinert, M., Clemmensen, C., Hofmann, S.M., Moore, M.C., Renner, S., Woods, S.C., Huypens, P., Beckers, J., de Angelis, M.H., Schürmann, A., Bakhti, M., Klingenspor, M., Heiman, M., Cherrington, A.D., Ristow, M., Lickert, H., Wolf, E., Havel, P.J., Müller, T.D., Tschöp, M.H., 2018. Animal models of obesity and diabetes mellitus. *Nat Rev Endocrinol* 14, 140–162. <https://doi.org/10.1038/nrendo.2017.161>
- Klempel, M.C., Kroeger, C.M., Bhutani, S., Trepanowski, J.F., Varady, K.A., 2012. Intermittent fasting combined with calorie restriction is effective for weight loss and cardio-protection in obese women. *Nutr J* 11, 98. <https://doi.org/10.1186/1475-2891-11-98>
- Koepsell, H., 2020. Glucose transporters in the small intestine in health and disease. *Pflugers Arch - Eur J Physiol* 472, 1207–1248. <https://doi.org/10.1007/s00424-020-02439-5>
- Kolterman, O.G., Reaven, G.M., Olefsky, J.M., 1979. Relationship between in Vivo Insulin Resistance and Decreased Insulin Receptors in Obese Man*. *The Journal of Clinical Endocrinology & Metabolism* 48, 487–494. <https://doi.org/10.1210/jcem-48-3-487>

Kong, F., Qin, Y., Su, Z., Ning, Z., Yu, S., 2018. Optimization of Extraction of Hypoglycemic Ingredients from Grape Seeds and Evaluation of α -Glucosidase and α -Amylase Inhibitory Effects In Vitro. *J Food Sci* 83, 1422–1429. <https://doi.org/10.1111/1750-3841.14150>

König, A., Schwarzingler, B., Stadlbauer, V., Lanzerstorfer, P., Iken, M., Schwarzingler, C., Kolb, P., Schwarzingler, S., Mörwald, K., Brunner, S., Höglinger, O., Weghuber, D., Weghuber, J., 2019. Guava (*Psidium guajava*) Fruit Extract Prepared by Supercritical CO₂ Extraction Inhibits Intestinal Glucose Resorption in a Double-Blind, Randomized Clinical Study. *Nutrients* 11, 1512. <https://doi.org/10.3390/nu11071512>

Koopmans, S.J., Schuurman, T., 2015. Considerations on pig models for appetite, metabolic syndrome and obese type 2 diabetes: From food intake to metabolic disease. *European Journal of Pharmacology* 759, 231–239. <https://doi.org/10.1016/j.ejphar.2015.03.044>

Korach-André, M., Roth, H., Barnoud, D., Péan, M., Péronnet, F., Lerverve, X., 2004. Glucose appearance in the peripheral circulation and liver glucose output in men after a large ¹³C starch meal. *Am J Clin Nutr* 80, 881–886. <https://doi.org/10.1093/ajcn/80.4.881>

Kowalski, G.M., Moore, S.M., Hamley, S., Selathurai, A., Bruce, C.R., 2017. The Effect of Ingested Glucose Dose on the Suppression of Endogenous Glucose Production in Humans. *Diabetes* 66, 2400–2406. <https://doi.org/10.2337/db17-0433>

Krog-Mikkelsen, I., Hels, O., Tetens, I., Holst, J.J., Andersen, J.R., Bukhave, K., 2011. The effects of L-arabinose on intestinal sucrase activity: dose-response studies in vitro and in humans. *Am J Clin Nutr* 94, 472–478. <https://doi.org/10.3945/ajcn.111.014225>

Krassak, M., Brehm, A., Bernroider, E., Anderwald, C., Nowotny, P., Man, C.D., Cobelli, C., Cline, G.W., Shulman, G.I., Waldhäusl, W., Roden, M., 2004. Alterations in Postprandial Hepatic Glycogen Metabolism in Type 2 Diabetes. *Diabetes* 53, 3048–3056. <https://doi.org/10.2337/diabetes.53.12.3048>

Kung, B., Turgeon, S.L., Rioux, L.-E., Anderson, G.H., Wright, A.J., Goff, H.D., 2019. Correlating in vitro digestion viscosities and bioaccessible nutrients of milks containing enhanced protein concentration and normal or modified protein ratio to human trials. *Food Funct* 10, 7687–7696. <https://doi.org/10.1039/c9fo01994d>

Kuo, P., Bellon, M., Wishart, J., Smout, A.J., Holloway, R.H., Fraser, R.J.L., Horowitz, M., Jones, K.L., Rayner, C.K., 2010a. Effects of metoclopramide on duodenal motility and flow events, glucose absorption, and incretin hormone release in response to intraduodenal glucose infusion. *American Journal of Physiology-Gastrointestinal and Liver Physiology* 299, G1326–G1333. <https://doi.org/10.1152/ajpgi.00476.2009>

Kuo, P., Wishart, J.M., Bellon, M., Smout, A.J., Holloway, R.H., Fraser, R.J.L., Horowitz, M., Jones, K.L., Rayner, C.K., 2010b. Effects of physiological hyperglycemia on duodenal motility and flow events, glucose absorption, and incretin secretion in healthy humans. *J Clin Endocrinol Metab* 95, 3893–3900. <https://doi.org/10.1210/jc.2009-2514>

Kuroda, S., Kobashi, Y., Kawamura, M., Kawabe, K., Shiozawa, F., Hamada, M., Shimizu, Y., Okumura-Kitajima, L., Koretsune, H., Kimura, K., Yamamoto, K., Kakinuma, H., 2020. Synthesis and Structure–Activity Relationship of C-Phenyl D-Glucitol (TP0454614) Derivatives as Selective Sodium-Dependent Glucose Cotransporter 1 (SGLT1) Inhibitors. *Chemical and Pharmaceutical Bulletin* 68, 635–652. <https://doi.org/10.1248/cpb.c20-00089>

- Kuusisto, J., Mykkanen, L., Pyorala, K., Laakso, M., 1994. NIDDM and Its Metabolic Control Predict Coronary Heart Disease in Elderly Subjects 43, 960–967. <https://doi.org/10.2337/diab.43.8.960>
- Laferrère, B., 2011. Diabetes remission after bariatric surgery: is it just the incretins? *Int J Obes (Lond)* 35 Suppl 3, S22-25. <https://doi.org/10.1038/ijo.2011.143>
- Laferrère, B., Pattou, F., 2019. A Gut Check Explains Improved Glucose Metabolism after Surgery. *Cell Metabolism* 30, 852–854. <https://doi.org/10.1016/j.cmet.2019.10.002>
- Laferrère, B., Pattou, F., 2018. Weight-Independent Mechanisms of Glucose Control After Roux-en-Y Gastric Bypass. *Front. Endocrinol.* 9, 9. <https://doi.org/10.3389/fendo.2018.00530>
- Landis, J.R., Koch, G.G., 1977. The measurement of observer agreement for categorical data. *Biometrics* 33, 159–174.
- Larsen, M., Elander, M., Sturis, J., Wilken, M., Carr, R., Rolin, B., Pørksen, N., 2002. The conscious Göttingen minipig as a model for studying rapid pulsatile insulin secretion in vivo. *Diabetologia* 45, 1389–1396. <https://doi.org/10.1007/s00125-002-0928-0>
- Larsen, M.O., Juhl, C.B., Pørksen, N., Gotfredsen, C.F., Carr, R.D., Ribel, U., Wilken, M., Rolin, B., 2005. β -Cell function and islet morphology in normal, obese, and obese β -cell mass-reduced Göttingen minipigs. *American Journal of Physiology-Endocrinology and Metabolism* 288, E412–E421. <https://doi.org/10.1152/ajpendo.00352.2004>
- Larsen, M.O., Rolin, B., 2004. Use of the Gottingen Minipig as a Model of Diabetes, with Special Focus on Type 1 Diabetes Research. *ILAR Journal* 45, 303–313. <https://doi.org/10.1093/ilar.45.3.303>
- Larsen, M.O., Rolin, B., Gotfredsen, C.F., Carr, R.D., Holst, J.J., 2004. Reduction of beta cell mass: partial insulin secretory compensation from the residual beta cell population in the nicotinamide-streptozotocin Göttingen minipig after oral glucose in vivo and in the perfused pancreas. *Diabetologia* 47, 1873–1878. <https://doi.org/10.1007/s00125-004-1546-9>
- Larsen, M.O., Rolin, B., Wilken, M., Carr, R.D., Svendsen, O., Bollen, P., 2001. Parameters of glucose and lipid metabolism in the male Göttingen minipig: influence of age, body weight, and breeding family. *Comp Med* 51, 436–442.
- Larsen, M.O., Wilken, M., Gotfredsen, C.F., Carr, R.D., Svendsen, O., Rolin, B., 2002. Mild streptozotocin diabetes in the Göttingen minipig. A novel model of moderate insulin deficiency and diabetes. *American Journal of Physiology-Endocrinology and Metabolism* 282, E1342–E1351. <https://doi.org/10.1152/ajpendo.00564.2001>
- Lartigue, S., Bizais, Y., Bruley des Varannes, S., Murat, A., Pouliquen, B., Galmiche, J.P., 1994. Inter- and intrasubject variability of solid and liquid gastric emptying parameters: A scintigraphic study in healthy subjects and diabetic patients. *Digest Dis Sci* 39, 109–115. <https://doi.org/10.1007/BF02090069>
- Lassailly, G., Caiazzo, R., Ntandja-Wandji, L.-C., Gnemmi, V., Baud, G., Verkindt, H., Ningarhari, M., Louvet, A., Leteurtre, E., Raverdy, V., Dharancy, S., Pattou, F., Mathurin, P., 2020. Bariatric Surgery Provides Long-term Resolution of Nonalcoholic Steatohepatitis and Regression of Fibrosis. *Gastroenterology* 159, 1290-1301.e5. <https://doi.org/10.1053/j.gastro.2020.06.006>
- Le Roux, C.W., Borg, C., Wallis, K., Vincent, R.P., Bueter, M., Goodlad, R., Ghatei, M.A., Patel, A., Bloom, S.R., Aylwin, S.J.B., 2010. Gut hypertrophy after gastric bypass is associated with increased glucagon-like peptide 2 and intestinal crypt cell proliferation. *Ann Surg* 252, 50–56. <https://doi.org/10.1097/SLA.0b013e3181d3d21f>

- Lean, M.E., Leslie, W.S., Barnes, A.C., Brosnahan, N., Thom, G., McCombie, L., Peters, C., Zhyzhneuskaya, S., Al-Mrabeh, A., Hollingsworth, K.G., Rodrigues, A.M., Rehackova, L., Adamson, A.J., Sniehotta, F.F., Mathers, J.C., Ross, H.M., McIlvenna, Y., Stefanetti, R., Trenell, M., Welsh, P., Kean, S., Ford, I., McConnachie, A., Sattar, N., Taylor, R., 2018. Primary care-led weight management for remission of type 2 diabetes (DIRECT): an open-label, cluster-randomised trial. *The Lancet* 391, 541–551. [https://doi.org/10.1016/S0140-6736\(17\)33102-1](https://doi.org/10.1016/S0140-6736(17)33102-1)
- Lee, L., Alloosh, M., Saxena, R., Van Alstine, W., Watkins, B.A., Klaunig, J.E., Sturek, M., Chalasani, N., 2009. Nutritional model of steatohepatitis and metabolic syndrome in the Ossabaw miniature swine. *Hepatology* 50, 56–67. <https://doi.org/10.1002/hep.22904>
- Lee, M.-S., Song, K.-D., Yang, H.-J., Solis, C.D., Kim, S.-H., Lee, W.-K., 2012. Development of a type II diabetic mellitus animal model using Micropig®. *Lab Anim Res* 28, 205–208. <https://doi.org/10.5625/lar.2012.28.3.205>
- Lehmann, A., Hornby, P.J., 2016. Intestinal SGLT1 in metabolic health and disease. *American Journal of Physiology-Gastrointestinal and Liver Physiology* 310, G887–G898. <https://doi.org/10.1152/ajpgi.00068.2016>
- Lema-Perez, L., Garcia-Tirado, J., Builes-Montaño, C., Alvarez, H., 2019. Phenomenological-Based model of human stomach and its role in glucose metabolism. *Journal of Theoretical Biology* 460, 88–100. <https://doi.org/10.1016/j.jtbi.2018.10.024>
- Lenzen, S., 2008. The mechanisms of alloxan- and streptozotocin-induced diabetes. *Diabetologia* 51, 216–226. <https://doi.org/10.1007/s00125-007-0886-7>
- Lenzen, S., Lortz, S., Tiedge, M., 1996. Effect of metformin on SGLT1, GLUT2, and GLUT5 hexose transporter gene expression in small intestine from rats. *Biochem Pharmacol* 51, 893–896. [https://doi.org/10.1016/0006-2952\(95\)02243-0](https://doi.org/10.1016/0006-2952(95)02243-0)
- Levin, R.J., 1994. Digestion and absorption of carbohydrates - from molecules and membranes to humans. *Am J Clin Nutr* 59, 690S-698S. <https://doi.org/10.1093/ajcn/59.3.690S>
- Lewis, G.F., Zinman, B., Groenewoud, Y., Vranic, M., Giacca, A., 1996. Hepatic Glucose Production Is Regulated Both by Direct Hepatic and Extrahepatic Effects of Insulin in Humans. *Diabetes* 45, 454–462. <https://doi.org/10.2337/diab.45.4.454>
- Ley, R., Turnbaugh, P., Klein, S., Gordon, J., 2006. Microbial ecology: human gut microbes associated with obesity. *Nature* 444, 1022–1023. <https://doi.org/10.1038/4441022a>
- Lightowler, H., Thondre, S., Holz, A., Theis, S., 2018. Replacement of glycaemic carbohydrates by inulin-type fructans from chicory (oligofructose, inulin) reduces the postprandial blood glucose and insulin response to foods: report of two double-blind, randomized, controlled trials. *Eur J Nutr* 57, 1259–1268. <https://doi.org/10.1007/s00394-017-1409-z>
- Lim, R.R., Grant, D.G., Olver, T.D., Padilla, J., Czajkowski, A.M., Schnurbusch, T.R., Mohan, R.R., Hainsworth, D.P., Walters, E.M., Chaurasia, S.S., 2018. Young Ossabaw Pigs Fed a Western Diet Exhibit Early Signs of Diabetic Retinopathy. *Invest. Ophthalmol. Vis. Sci.* 59, 2325. <https://doi.org/10.1167/iovs.17-23616>
- Lindberg, M., Astrup, A., 2007. The role of glitazones in management of type 2 diabetes. A DREAM or a nightmare? *Obesity Reviews* 8, 381–384. <https://doi.org/10.1111/j.1467-789X.2007.00399.x>

- Linnebjerg, H., Park, S., Kothare, P.A., Trautmann, M.E., Mace, K., Fineman, M., Wilding, I., Nauck, M., Horowitz, M., 2008. Effect of exenatide on gastric emptying and relationship to postprandial glycemia in type 2 diabetes. *Regulatory Peptides* 151, 123–129. <https://doi.org/10.1016/j.regpep.2008.07.003>
- Litten-Brown, J.C., Corson, A.M., Clarke, L., 2010. Porcine models for the metabolic syndrome, digestive and bone disorders: a general overview. *Animal* 4, 899–920. <https://doi.org/10.1017/S1751731110000200>
- Liu, D., Ma, Z., Zhang, C., Lin, Q., Li, M., Su, K., Li, Y., Wang, H., Zang, Q., Dong, J., 2021. The effects of bariatric surgery on dyslipidemia and insulin resistance in overweight patients with or without type 2 diabetes: a systematic review and network meta-analysis. *Surgery for Obesity and Related Diseases* 17, 1655–1672. <https://doi.org/10.1016/j.soard.2021.04.005>
- Liu, L., Yu, Y.-L., Liu, C., Wang, X.-T., Liu, X.-D., Xie, L., 2011. Insulin deficiency induces abnormal increase in intestinal disaccharidase activities and expression under diabetic states, evidences from in vivo and in vitro study. *Biochemical Pharmacology* 82, 1963–1970. <https://doi.org/10.1016/j.bcp.2011.09.014>
- Liu, L., Yu, Y.-L., Yang, J.-S., Li, Y., Liu, Y.-W., Liang, Y., Liu, X.-D., Xie, L., Wang, G.-J., 2010. Berberine suppresses intestinal disaccharidases with beneficial metabolic effects in diabetic states, evidences from in vivo and in vitro study. *Naunyn-Schmied Arch Pharmacol* 381, 371–381. <https://doi.org/10.1007/s00210-010-0502-0>
- Liu, Y., Wang, Z., Yin, W., Li, Q., Cai, M., Zhang, C., Xiao, J., Hou, H., Li, H., Zu, X., 2007. Severe Insulin Resistance and Moderate Glomerulosclerosis in a Minipig Model Induced by High-Fat/ High-Sucrose/ High-Cholesterol Diet. *Exp. Anim.* 56, 11–20. <https://doi.org/10.1538/expanim.56.11>
- Livesey, G., Taylor, R., Livesey, H.F., Buyken, A.E., Jenkins, D.J.A., Augustin, L.S.A., Sievenpiper, J.L., Barclay, A.W., Liu, S., Wolever, T.M.S., Willett, W.C., Brighenti, F., Salas-Salvadó, J., Björck, I., Rizkalla, S.W., Riccardi, G., Vecchia, C.L., Ceriello, A., Trichopoulou, A., Poli, A., Astrup, A., Kendall, C.W.C., Ha, M.-A., Baer-Sinnott, S., Brand-Miller, J.C., 2019. Dietary Glycemic Index and Load and the Risk of Type 2 Diabetes: Assessment of Causal Relations. *Nutrients* 11, 1436. <https://doi.org/10.3390/nu11061436>
- Livingstone, M.B.E., Redpath, T., Naseer, F., Boyd, A., Martin, M., Finlayson, G., Miras, A.D., Bodnar, Z., Kerrigan, D., Pournaras, D.J., le Roux, C.W., Spector, A.C., Price, R.K., 2022. Food Intake Following Gastric Bypass Surgery: Patients Eat Less but Do Not Eat Differently. *J Nutr* 152, 2319–2332. <https://doi.org/10.1093/jn/nxac164>
- Longnecker, D.S., 2021. Anatomy and Histology of the Pancreas. *Pancreapedia: The Exocrine Pancreas Knowledge Base*. <https://doi.org/10.3998/panc.2021.01>
- Love, A.H.G., Canavan, D.A., 1968. Effects of insulin on intestinal glucose absorption. *The Lancet*, Originally published as Volume 2, Issue 7582 292, 1325–1326. [https://doi.org/10.1016/S0140-6736\(68\)91820-5](https://doi.org/10.1016/S0140-6736(68)91820-5)
- Low Wang, C.C., Lu, L., Leitner, J.W., Sarraf, M., Gianani, R., Draznin, B., Greyson, C.R., Reusch, J.E.B., Schwartz, G.G., 2013. Arterial insulin resistance in Yucatan micropigs with diet-induced obesity and metabolic syndrome. *J Diabetes Complications* 27, 307–315. <https://doi.org/10.1016/j.jdiacomp.2013.02.009>
- Ludvik, B., Nolan, J.J., Roberts, A., Baloga, J., Joyce, M., Bell, J.M., Olefsky, J.M., 1997. Evidence for decreased splanchnic glucose uptake after oral glucose administration in non-insulin-dependent diabetes mellitus. *J Clin Invest* 100, 2354–2361. <https://doi.org/10.1172/JCI119775>

Ludwig, B., Rotem, A., Schmid, J., Weir, G.C., Colton, C.K., Brendel, M.D., Neufeld, T., Block, N.L., Yavriyants, K., Steffen, A., Ludwig, S., Chavakis, T., Reichel, A., Azarov, D., Zimmermann, B., Maimon, S., Balyura, M., Rozenshtein, T., Shabtay, N., Vardi, P., Bloch, K., de Vos, P., Schally, A.V., Bornstein, S.R., Barkai, U., 2012. Improvement of islet function in a bioartificial pancreas by enhanced oxygen supply and growth hormone releasing hormone agonist. *Proceedings of the National Academy of Sciences* 109, 5022–5027. <https://doi.org/10.1073/pnas.1201868109>

Ludwig, D.S., 2002. The Glycemic Index: Physiological Mechanisms Relating to Obesity, Diabetes, and Cardiovascular Disease. *JAMA* 287, 2414. <https://doi.org/10.1001/jama.287.18.2414>

Luna, N.A.B., Mercado-Asis, L.B., 2022. Giving Insulin Is Not a Guessing Game: Insulin Replacement Therapy in Type 2 Diabetes Mellitus. *JMUST* 6, 868–880. <https://doi.org/10.35460/2546-1621.2022-0032>

Lupsa, B.C., Inzucchi, S.E., 2018. Use of SGLT2 inhibitors in type 2 diabetes: weighing the risks and benefits. *Diabetologia* 61, 2118–2125. <https://doi.org/10.1007/s00125-018-4663-6>

Lützhøft, D.O., Sinioja, T., Christoffersen, B.Ø., Jakobsen, R.R., Geng, D., Ahmad, H.F.B., Straarup, E.M., Pedersen, K.-M., Kot, W., Pedersen, H.D., Cirera, S., Hyötyläinen, T., Nielsen, D.S., Hansen, A.K., 2022. Marked gut microbiota dysbiosis and increased imidazole propionate are associated with a NASH Göttingen Minipig model. *BMC Microbiol* 22, 287. <https://doi.org/10.1186/s12866-022-02704-w>

Ma, J., Pilichiewicz, A.N., Feinle-Bisset, C., Wishart, J.M., Jones, K.L., Horowitz, M., Rayner, C.K., 2012. Effects of variations in duodenal glucose load on glycaemic, insulin, and incretin responses in type 2 diabetes. *Diabet Med* 29, 604–608. <https://doi.org/10.1111/j.1464-5491.2011.03496.x>

Madara, J.L., Pappenheimer, J.R., 1987. Structural basis for physiological regulation of paracellular pathways in intestinal epithelia. *J. Membran Biol.* 100, 149–164. <https://doi.org/10.1007/BF02209147>

Maedler, K., Carr, R.D., Bosco, D., Zuellig, R.A., Berney, T., Donath, M.Y., 2005. Sulfonylurea Induced β -Cell Apoptosis in Cultured Human Islets. *The Journal of Clinical Endocrinology & Metabolism* 90, 501–506. <https://doi.org/10.1210/jc.2004-0699>

Magkos, F., Bradley, D., Eagon, J.C., Patterson, B.W., Klein, S., 2016. Effect of Roux-en-Y gastric bypass and laparoscopic adjustable gastric banding on gastrointestinal metabolism of ingested glucose. *The American Journal of Clinical Nutrition* 103, 61–65. <https://doi.org/10.3945/ajcn.115.116111>

Magnuson, B.A., Carakostas, M.C., Moore, N.H., Poulos, S.P., Renwick, A.G., 2016. Biological fate of low-calorie sweeteners. *Nutr Rev* 74, 670–689. <https://doi.org/10.1093/nutrit/nuw032>

Makki, K., Deehan, E.C., Walter, J., Bäckhed, F., 2018. The Impact of Dietary Fiber on Gut Microbiota in Host Health and Disease. *Cell Host & Microbe* 23, 705–715. <https://doi.org/10.1016/j.chom.2018.05.012>

Malunga, L.N., Ames, N., Zhouyao, H., Blewett, H., Thandapilly, S.J., 2021. Beta-Glucan From Barley Attenuates Post-prandial Glycemic Response by Inhibiting the Activities of Glucose Transporters but Not Intestinal Brush Border Enzymes and Amylolysis of Starch. *Front Nutr* 8, 628571. <https://doi.org/10.3389/fnut.2021.628571>

Mambiya, M., Shang, M., Wang, Y., Li, Q., Liu, S., Yang, L., Zhang, Q., Zhang, K., Liu, M., Nie, F., Zeng, F., Liu, W., 2019. The Play of Genes and Non-genetic Factors on Type 2 Diabetes. *Front. Public Health* 7, 349. <https://doi.org/10.3389/fpubh.2019.00349>

- Marathe, C. S., Feinle-Bisset, C., Pilichiewicz, A., Lange, K., Jones, K.L., Rayner, C.K., Kahn, S.E., Horowitz, M., 2015. The duodenal glucose load impacts the oral disposition index in healthy subjects. *Diabet Med* 32, 1500–1503. <https://doi.org/10.1111/dme.12802>
- Marathe, Chinmay S., Horowitz, M., Trahair, L.G., Wishart, J.M., Bound, M., Lange, K., Rayner, C.K., Jones, K.L., 2015. Relationships of Early And Late Glycemic Responses With Gastric Emptying During An Oral Glucose Tolerance Test. *The Journal of Clinical Endocrinology & Metabolism* 100, 3565–3571. <https://doi.org/10.1210/JC.2015-2482>
- Marathe, C.S., Rayner, C.K., Jones, K.L., Horowitz, M., 2013. Relationships Between Gastric Emptying, Postprandial Glycemia, and Incretin Hormones. *Diabetes Care* 36, 1396–1405. <https://doi.org/10.2337/dc12-1609>
- Marcelli-Tourvieille, S., Hubert, T., Pattou, F., Vantyghem, M., 2006. Acute insulin response (AIR): review of protocols and clinical interest in islet transplantation. *Diabetes & Metabolism* 32, 295–303. [https://doi.org/10.1016/S1262-3636\(07\)70283-5](https://doi.org/10.1016/S1262-3636(07)70283-5)
- Marciani, L., Gowland, P.A., Spiller, R.C., Manoj, P., Moore, R.J., Young, P., Al-Sahab, S., Bush, D., Wright, J., Fillery-Travis, A.J., 2000. Gastric Response to Increased Meal Viscosity Assessed by Echo-Planar Magnetic Resonance Imaging in Humans. *The Journal of Nutrition* 130, 122–127. <https://doi.org/10.1093/jn/130.1.122>
- Margolskee, R.F., Dyer, J., Kokrashvili, Z., Salmon, K.S.H., Ilegems, E., Daly, K., Maillet, E.L., Ninomiya, Y., Mosinger, B., Shirazi-Beechey, S.P., 2007. T1R3 and gustducin in gut sense sugars to regulate expression of Na⁺-glucose cotransporter 1. *Proceedings of the National Academy of Sciences* 104, 15075–15080. <https://doi.org/10.1073/pnas.0706678104>
- Mari, A., Ferrannini, E., 2008. Beta-cell function assessment from modelling of oral tests: an effective approach. *Diabetes Obes Metab* 10 Suppl 4, 77–87. <https://doi.org/10.1111/j.1463-1326.2008.00946.x>
- Mari, A., Tura, A., Pacini, G., Kautzky-Willer, A., Ferrannini, E., 2008. Relationships between insulin secretion after intravenous and oral glucose administration in subjects with glucose tolerance ranging from normal to overt diabetes. *Diabetes Medicine* 25, 671–677. <https://doi.org/10.1111/j.1464-5491.2008.02441.x>
- Marini, M.A., Succurro, E., Frontoni, S., Mastroianni, S., Arturi, F., Sciacqua, A., Lauro, R., Hribal, M.L., Perticone, F., Sesti, G., 2012. Insulin sensitivity, β -cell function, and incretin effect in individuals with elevated 1-hour postload plasma glucose levels. *Diabetes Care* 35, 868–872. <https://doi.org/10.2337/dc11-2181>
- Martinussen, C., Bojsen-Møller, K.N., Dirksen, C., Svane, M.S., Kristiansen, V.B., Hartmann, B., Holst, J.J., Madsbad, S., 2019. Augmented GLP-1 Secretion as Seen After Gastric Bypass May Be Obtained by Delaying Carbohydrate Digestion. *The Journal of Clinical Endocrinology & Metabolism* 104, 3233–3244. <https://doi.org/10.1210/jc.2018-02661>
- Matsuda, M., DeFronzo, R.A., 1999. Insulin sensitivity indices obtained from oral glucose tolerance testing: comparison with the euglycemic insulin clamp. *Diabetes Care* 22, 1462–1470. <https://doi.org/10.2337/diacare.22.9.1462>
- Matthews, D.R., Hosker, J.R., Rudenski, A.S., Naylor, B.A., Treacher, D.F., Turner, R.C., 1985. Homeostasis model assessment: insulin resistance and beta cell function from fasting plasma glucose and insulin concentrations in man. *Diabetologia* 28, 412–419. <https://doi.org/10.1007/BF00280883>

- Mattin, L.R., Yau, A.M.W., McIver, V., James, L.J., Evans, G.H., 2018. The Effect of Exercise Intensity on Gastric Emptying Rate, Appetite and Gut Derived Hormone Responses after Consuming a Standardised Semi-Solid Meal in Healthy Males. *Nutrients* 10, 787. <https://doi.org/10.3390/nu10060787>
- Mauranui Clinic, 2023. One Anastomosis Gastric Bypass. Discover Weight Loss. URL <https://www.discoverweightloss.co.nz/one-anastomosis-gastric-bypass-2/> (accessed 9.25.23).
- Mayer, A.-P.T., Durward, A., Turner, C., Skellett, S., Dalton, N., Tibby, S.M., Murdoch, I.A., 2002. Amylin is associated with delayed gastric emptying in critically ill children. *Intensive Care Med* 28, 336–340. <https://doi.org/10.1007/s00134-002-1224-7>
- Mazuy, C., Helleboid, A., Staels, B., Lefebvre, P., 2015. Nuclear bile acid signaling through the farnesoid X receptor. *Cell Mol Life Sci* 72, 1631–1650. <https://doi.org/10.1007/s00018-014-1805-y>
- McCulloch, A., Bansiya, V., Woodward, J.M., 2018. Addition of Insulin to Parenteral Nutrition for Control of Hyperglycemia. *J Parenter Enteral Nutr* 42, 846–854. <https://doi.org/10.1177/0148607117722750>
- McCulloch, D.K., Koerker, D.J., Kahn, S.E., Bonner-Weir, S., Palmer, J.P., 1991. Correlations of In Vivo Beta Cell Function Tests With Beta Cell Mass and Pancreatic Insulin Content in Streptozocin-Administered Baboons. *Diabetes* 40, 673–679. <https://doi.org/10.2337/diab.40.6.673>
- McKnight, L.L., Myrie, S.B., Mackay, D.S., Brunton, J.A., Bertolo, R.F., 2012. Glucose tolerance is affected by visceral adiposity and sex, but not birth weight, in Yucatan miniature pigs. *Appl Physiol Nutr Metab* 37, 106–114. <https://doi.org/10.1139/h11-142>
- McMahon, M., Marsh, H., Rizza, R., 1989. Comparison of the Pattern of Postprandial Carbohydrate Metabolism After Ingestion of a Glucose Drink or a Mixed Meal. *The Journal of Clinical Endocrinology & Metabolism* 68, 647–653. <https://doi.org/10.1210/jcem-68-3-647>
- McRorie, J.W., McKeown, N.M., 2017. Understanding the Physics of Functional Fibers in the Gastrointestinal Tract: An Evidence-Based Approach to Resolving Enduring Misconceptions about Insoluble and Soluble Fiber. *J Acad Nutr Diet* 117, 251–264. <https://doi.org/10.1016/j.jand.2016.09.021>
- Meier, J.J., Breuer, T.G.K., Bonadonna, R.C., Tannapfel, A., Uhl, W., Schmidt, W.E., Schrader, H., Menge, B.A., 2012. Pancreatic diabetes manifests when beta cell area declines by approximately 65% in humans. *Diabetologia* 55, 1346–1354. <https://doi.org/10.1007/s00125-012-2466-8>
- Meier, J.J., Butler, A.E., Saisho, Y., Monchamp, T., Galasso, R., Bhushan, A., Rizza, R.A., Butler, P.C., 2008. β -Cell Replication Is the Primary Mechanism Subserving the Postnatal Expansion of β -Cell Mass in Humans. *Diabetes* 57, 1584–1594. <https://doi.org/10.2337/db07-1369>
- Meier, J.J., Menge, B.A., Breuer, T.G.K., Müller, C.A., Tannapfel, A., Uhl, W., Schmidt, W.E., Schrader, H., 2009. Functional Assessment of Pancreatic β -Cell Area in Humans. *Diabetes* 58, 1595–1603. <https://doi.org/10.2337/db08-1611>
- Meier, J.J., Rosenstock, J., Hincelin-Méry, A., Roy-Duval, C., Delfolie, A., Coester, H.-V., Menge, B.A., Forst, T., Kapitza, C., 2015. Contrasting Effects of Lixisenatide and Liraglutide on Postprandial Glycemic Control, Gastric Emptying, and Safety Parameters in Patients With Type 2 Diabetes on Optimized Insulin Glargine With or Without Metformin: A Randomized, Open-Label Trial. *Diabetes Care* 38, 1263–1273. <https://doi.org/10.2337/dc14-1984>

- Melissas, J., Leventi, A., Klinaki, I., Perisinakis, K., Koukouraki, S., de Bree, E., Karkavitsas, N., 2013. Alterations of Global Gastrointestinal Motility After Sleeve Gastrectomy: A Prospective Study. *Annals of Surgery* 258, 976–982. <https://doi.org/10.1097/SLA.0b013e3182774522>
- Meng, Q., Culnan, D.M., Ahmed, T., Sun, M., Cooney, R.N., 2022. Roux-en-Y gastric bypass alters intestinal glucose transport in the obese Zucker rat. *Front. Endocrinol.* 13, 901984. <https://doi.org/10.3389/fendo.2022.901984>
- Mergenthaler, P., Lindauer, U., Dienel, G.A., Meisel, A., 2013. Sugar for the brain: the role of glucose in physiological and pathological brain function. *Trends in Neurosciences* 36, 587–597. <https://doi.org/10.1016/j.tins.2013.07.001>
- Merino, B., Fernández-Díaz, C.M., Cózar-Castellano, I., Perdomo, G., 2019. Intestinal Fructose and Glucose Metabolism in Health and Disease. *Nutrients* 12, 94. <https://doi.org/10.3390/nu12010094>
- Mingrone, G., Panunzi, S., De Gaetano, A., Guidone, C., Iaconelli, A., Capristo, E., Chamseddine, G., Bornstein, S.R., Rubino, F., 2021. Metabolic surgery versus conventional medical therapy in patients with type 2 diabetes: 10-year follow-up of an open-label, single-centre, randomised controlled trial. *The Lancet* 397, 293–304. [https://doi.org/10.1016/S0140-6736\(20\)32649-0](https://doi.org/10.1016/S0140-6736(20)32649-0)
- Mingrone, G., Panunzi, S., De Gaetano, A., Guidone, C., Iaconelli, A., Leccesi, L., Nanni, G., Pomp, A., Castagneto, M., Ghirlanda, G., Rubino, F., 2012. Bariatric Surgery versus Conventional Medical Therapy for Type 2 Diabetes. *N Engl J Med* 366, 1577–1585. <https://doi.org/10.1056/NEJMoa1200111>
- Mingrone, G., Panunzi, S., De Gaetano, A., Guidone, C., Iaconelli, A., Nanni, G., Castagneto, M., Bornstein, S., Rubino, F., 2015. Bariatric–metabolic surgery versus conventional medical treatment in obese patients with type 2 diabetes: 5 year follow-up of an open-label, single-centre, randomised controlled trial. *The Lancet* 386, 964–973. [https://doi.org/10.1016/S0140-6736\(15\)00075-6](https://doi.org/10.1016/S0140-6736(15)00075-6)
- Miranda, M.A., Macias-Velasco, J.F., Lawson, H.A., 2021. Pancreatic β -cell heterogeneity in health and diabetes: classes, sources, and subtypes. *American Journal of Physiology-Endocrinology and Metabolism* 320, E716–E731. <https://doi.org/10.1152/ajpendo.00649.2020>
- Miras, A.D., Kamocka, A., Purkayastha, S., Moorthy, K., Patel, A., Chahal, H., Frost, G., Bassett, P., Castagnetto-Gissey, L., Coppin, L., Jackson, N., Umpleby, A.M., Bloom, S.R., Tan, T., Ahmed, A.R., Rubino, F., 2021. The Effect of Standard Versus Longer Intestinal Bypass on GLP-1 Regulation and Glucose Metabolism in Patients With Type 2 Diabetes Undergoing Roux-en-Y Gastric Bypass: The Long-Limb Study. *Diabetes Care* 44, 1082–1090. <https://doi.org/10.2337/dc20-0762>
- Mittelman, S.D., Bergman, R.N., 2000. Inhibition of lipolysis causes suppression of endogenous glucose production independent of changes in insulin. *American Journal of Physiology-Endocrinology and Metabolism* 279, E630–E637. <https://doi.org/10.1152/ajpendo.2000.279.3.E630>
- Mittelman, S.D., Fu, Y.Y., Rebrin, K., Steil, G., Bergman, R.N., 1997. Indirect effect of insulin to suppress endogenous glucose production is dominant, even with hyperglucagonemia. *J. Clin. Invest.* 100, 3121–3130. <https://doi.org/10.1172/JCI119867>
- Miyamoto, K., Hase, K., Takagi, T., Fujii, T., Taketani, Y., Minami, H., Oka, T., Nakabou, Y., 1993. Differential responses of intestinal glucose transporter mRNA transcripts to levels of dietary sugars. *Biochemical Journal* 295, 211–215. <https://doi.org/10.1042/bj2950211>

- Modigliani, R., Bernier, J.J., 1971. Absorption of glucose, sodium, and water by the human jejunum studied by intestinal perfusion with a proximal occluding balloon and at variable flow rates. *Gut* 12, 184–193. <https://doi.org/10.1136/gut.12.3.184>
- Monro, J., Mishra, S., Stoklosinski, H., Bentley-Hewitt, K., Hedderley, D., Dinnan, H., Martell, S., 2022. Dietary Fibre and Organic Acids in Kiwifruit Suppress Glycaemic Response Equally by Delaying Absorption—A Randomised Crossover Human Trial with Parallel Analysis of ¹³C-Acetate Uptake. *Nutrients* 14, 3189. <https://doi.org/10.3390/nu14153189>
- Moran, A.W., Al-Rammahi, M.A., Arora, D.K., Batchelor, D.J., Coulter, E.A., Ionescu, C., Bravo, D., Shirazi-Beechey, S.P., 2010. Expression of Na⁺/glucose co-transporter 1 (SGLT1) in the intestine of piglets weaned to different concentrations of dietary carbohydrate. *Br J Nutr* 104, 647–655. <https://doi.org/10.1017/S0007114510000954>
- Moysés, D.N., Reis, V.C.B., Almeida, J.R.M. de, Moraes, L.M.P. de, Torres, F.A.G., 2016. Xylose Fermentation by *Saccharomyces cerevisiae*: Challenges and Prospects. *International Journal of Molecular Sciences* 17, 207. <https://doi.org/10.3390/ijms17030207>
- Müller, M.J., Paschen, U., Seitz, H.J., 1983. Glucose production measured by tracer and balance data in conscious miniature pig. *Am J Physiol* 244, E236–244. <https://doi.org/10.1152/ajpendo.1983.244.3.E236>
- Müller, T.D., Finan, B., Clemmensen, C., DiMarchi, R.D., Tschöp, M.H., 2017. The New Biology and Pharmacology of Glucagon. *Physiological Reviews* 97, 721–766. <https://doi.org/10.1152/physrev.00025.2016>
- Mumphrey, M.B., Hao, Z., Townsend, R.L., Patterson, L.M., Berthoud, H.-R., 2015. Sleeve Gastrectomy Does Not Cause Hypertrophy and Reprogramming of Intestinal Glucose Metabolism in Rats. *OBES SURG* 25, 1468–1473. <https://doi.org/10.1007/s11695-014-1547-9>
- Najjar, A.M., Parsons, P.M., Duncan, A.M., Robinson, L.E., Yada, R.Y., Graham, T.E., 2009. The acute impact of ingestion of breads of varying composition on blood glucose, insulin and incretins following first and second meals. *Br J Nutr* 101, 391–398. <https://doi.org/10.1017/S0007114508003085>
- Nauck, M.A., El-Ouaghli, A., Gabrys, B., Hücking, K., Holst, J.J., Deacon, C.F., Gallwitz, B., Schmidt, W.E., Meier, J.J., 2004. Secretion of incretin hormones (GIP and GLP-1) and incretin effect after oral glucose in first-degree relatives of patients with type 2 diabetes. *Regulatory Peptides* 122, 209–217. <https://doi.org/10.1016/j.regpep.2004.06.020>
- Nauck, M.A., Heimesaat, M.M., Behle, K., Holst, J.J., Nauck, M.S., Ritzel, R., Fner, M.H., Schmiegel, W.H., 2002. Effects of Glucagon-Like Peptide 1 on Counterregulatory Hormone Responses, Cognitive Functions, and Insulin Secretion during Hyperinsulinemic, Stepped Hypoglycemic Clamp Experiments in Healthy Volunteers. *J Clin Endocrinol Metab* 87, 1239–1246. <https://doi.org/10.1210/jcem.87.3.8355>
- Nauck, M.A., Meier, J.J., 2018. Incretin hormones: Their role in health and disease. *Diabetes Obes Metab* 20, 5–21. <https://doi.org/10.1111/dom.13129>
- Nauck, M.A., Quast, D.R., Wefers, J., Meier, J.J., 2021. GLP-1 receptor agonists in the treatment of type 2 diabetes – state-of-the-art. *Molecular Metabolism* 46, 101102. <https://doi.org/10.1016/j.molmet.2020.101102>

- Nazare, J.-A., 2009. Modulation de la phase postprandiale du glucose (Médecine humaine et pathologie). Université Claude Bernard - Lyon I.
- Nazare, J.-A., de Rougemont, A., Normand, S., Sauvinet, V., Sothier, M., Vinoy, S., Désage, M., Laville, M., 2010a. Effect of postprandial modulation of glucose availability: short- and long-term analysis. *Br J Nutr* 103, 1461–1470. <https://doi.org/10.1017/S0007114509993357>
- Nazare, J.-A., de Rougemont, A., Normand, S., Sauvinet, V., Sothier, M., Vinoy, S., Désage, M., Laville, M., 2010b. Effect of postprandial modulation of glucose availability: short- and long-term analysis. *Br J Nutr* 103, 1461–1470. <https://doi.org/10.1017/S0007114509993357>
- Neeb, Z.P., Edwards, J.M., Alloosh, M., Long, X., Mokelke, E.A., Sturek, M., 2010. Metabolic Syndrome and Coronary Artery Disease in Ossabaw Compared with Yucatan Swine. *Comparative Medicine* 60, 16.
- Nergaard, B.J., Leifsson, B.G., Hedenbro, J., Gislason, H., 2014. Gastric Bypass with Long Alimentary Limb or Long Pancreato-Biliary Limb—Long-Term Results on Weight Loss, Resolution of Co-morbidities and Metabolic Parameters. *OBES SURG* 24, 1595–1602. <https://doi.org/10.1007/s11695-014-1245-7>
- Newell-Fugate, A.E., Lenz, K., Skenandore, C., Nowak, R.A., White, B.A., Braundmeier-Fleming, A., 2017. Effects of coconut oil on glycemia, inflammation, and urogenital microbial parameters in female Ossabaw mini-pigs. *PLoS ONE* 12, e0179542. <https://doi.org/10.1371/journal.pone.0179542>
- Neyrinck, A.M., Pachikian, B., Taminiau, B., Daube, G., Frédérick, R., Cani, P.D., Bindels, L.B., Delzenne, N.M., 2016. Intestinal Sucrase as a Novel Target Contributing to the Regulation of Glycemia by Prebiotics. *PLOS ONE* 11, e0160488. <https://doi.org/10.1371/journal.pone.0160488>
- Nguyen, N.Q., Debreceni, T.L., Bambrick, J.E., Bellon, M., Wishart, J., Standfield, S., Rayner, C.K., Horowitz, M., 2014a. Rapid gastric and intestinal transit is a major determinant of changes in blood glucose, intestinal hormones, glucose absorption and postprandial symptoms after gastric bypass: GI Transit and Glycemic Responses after RYGB. *Obesity* 22, 2003–2009. <https://doi.org/10.1002/oby.20791>
- Nguyen, N.Q., Debreceni, T.L., Bambrick, J.E., Chia, B., Deane, A.M., Wittert, G., Rayner, C.K., Horowitz, M., Young, R.L., 2014b. Upregulation of intestinal glucose transporters after Roux-en-Y gastric bypass to prevent carbohydrate malabsorption: Gut Glucose Transporter Changes in RYGB. *Obesity* 22, 2164–2171. <https://doi.org/10.1002/oby.20829>
- Nguyen, N.Q., Debreceni, T.L., Bambrick, J.E., Chia, B., Wishart, J., Deane, A.M., Rayner, C.K., Horowitz, M., Young, R.L., 2015. Accelerated Intestinal Glucose Absorption in Morbidly Obese Humans: Relationship to Glucose Transporters, Incretin Hormones, and Glycemia. *The Journal of Clinical Endocrinology & Metabolism* 100, 968–976. <https://doi.org/10.1210/jc.2014-3144>
- Nguyen, N.Q., Debreceni, T.L., Burgstad, C.M., Neo, M., Bellon, M., Wishart, J.M., Standfield, S., Bartholomeusz, D., Rayner, C.K., Wittert, G., Horowitz, M., 2016. Effects of Fat and Protein Preloads on Pouch Emptying, Intestinal Transit, Glycaemia, Gut Hormones, Glucose Absorption, Blood Pressure and Gastrointestinal Symptoms After Roux-en-Y Gastric Bypass. *OBES SURG* 26, 77–84. <https://doi.org/10.1007/s11695-015-1722-7>
- Noah, L., Krempf, M., Lecannu, G., Maugère, P., Champ, M., 2000. Bioavailability of starch and postprandial changes in splanchnic glucose metabolism in pigs. *American Journal of Physiology-Endocrinology and Metabolism* 278, E181–E188. <https://doi.org/10.1152/ajpendo.2000.278.2.E181>

- Nurjhan, N., Campbell, P.J., Kennedy, F.P., Miles, J.M., Gerich, J.E., 1986. Insulin Dose-Response Characteristics for Suppression of Glycerol Release and Conversion to Glucose in Humans. *Diabetes* 35, 1326–1331. <https://doi.org/10.2337/diab.35.12.1326>
- O'Brien, P.E., Hindle, A., Brennan, L., Skinner, S., Burton, P., Smith, A., Crosthwaite, G., Brown, W., 2019. Long-Term Outcomes After Bariatric Surgery: a Systematic Review and Meta-analysis of Weight Loss at 10 or More Years for All Bariatric Procedures and a Single-Centre Review of 20-Year Outcomes After Adjustable Gastric Banding. *OBES SURG* 29, 3–14. <https://doi.org/10.1007/s11695-018-3525-0>
- Ochoa, M., Malbert, C.-H., Lallès, J.-P., Bobillier, E., Val-Laillet, D., 2014. Effects of chronic intake of starch-, glucose- and fructose-containing diets on eating behaviour in adult minipigs. *Applied Animal Behaviour Science* 157, 61–71. <https://doi.org/10.1016/j.applanim.2014.05.010>
- Ogawa, E., Hosokawa, M., Harada, N., Yamane, S., Hamasaki, A., Toyoda, K., Fujimoto, S., Fujita, Y., Fukuda, K., Tsukiyama, K., Yamada, Y., Seino, Y., Inagaki, N., 2011. The effect of gastric inhibitory polypeptide on intestinal glucose absorption and intestinal motility in mice. *Biochemical and Biophysical Research Communications* 404, 115–120. <https://doi.org/10.1016/j.bbrc.2010.11.077>
- Oguma, T., Nakayama, K., Kuriyama, C., Matsushita, Y., Yoshida, K., Hikida, K., Obokata, N., Tsuda-Tsukimoto, M., Saito, A., Arakawa, K., Ueta, K., Shiotani, M., 2015. Intestinal Sodium Glucose Cotransporter 1 Inhibition Enhances Glucagon-Like Peptide-1 Secretion in Normal and Diabetic Rodents. *J Pharmacol Exp Ther* 354, 279–289. <https://doi.org/10.1124/jpet.115.225508>
- Oh, T.J., Lim, S., Kim, K.M., Moon, J.H., Choi, S.H., Cho, Y.M., Park, K.S., Jang, H., Cho, N.H., 2017. One-hour postload plasma glucose concentration in people with normal glucose homeostasis predicts future diabetes mellitus: a 12-year community-based cohort study. *Clin Endocrinol* 86, 513–519. <https://doi.org/10.1111/cen.13280>
- Ohno, H., Kojima, Y., Harada, H., Abe, Y., Endo, T., Kobayashi, M., 2019. Absorption, disposition, metabolism and excretion of [¹⁴C]mizagliflozin, a novel selective SGLT1 inhibitor, in rats. *Xenobiotica* 49, 463–473. <https://doi.org/10.1080/00498254.2018.1449269>
- Ojo, O., Ojo, O.O., Adebowale, F., Wang, X.-H., 2018. The Effect of Dietary Glycaemic Index on Glycaemia in Patients with Type 2 Diabetes: A Systematic Review and Meta-Analysis of Randomized Controlled Trials. *Nutrients* 10, 373. <https://doi.org/10.3390/nu10030373>
- Oku, T., Murata-Takenoshita, Y., Yamazaki, Y., Shimura, F., Nakamura, S., 2014. D-sorbose inhibits disaccharidase activity and demonstrates suppressive action on postprandial blood levels of glucose and insulin in the rat. *Nutr Res* 34, 961–967. <https://doi.org/10.1016/j.nutres.2014.09.009>
- O'Leary, M.H., 1981. Carbon isotope fractionation in plants. *Phytochemistry* 20, 553–567. [https://doi.org/10.1016/0031-9422\(81\)85134-5](https://doi.org/10.1016/0031-9422(81)85134-5)
- Ortega, R., Valdés, M., Alarcón-Aguilar, F.J., Fortis-Barrera, Á., Barbosa, E., Velazquez, C., Calzada, F., 2022. Antihyperglycemic Effects of *Salvia polystachya* Cav. and Its Terpenoids: α -Glucosidase and SGLT1 Inhibitors. *Plants* 11, 575. <https://doi.org/10.3390/plants11050575>
- Osswald, C., Baumgarten, K., Stümpel, F., Gorboulev, V., Akimjanova, M., Knobloch, K.-P., Horak, I., Kluge, R., Joost, H.-G., Koepsell, H., 2005. Mice without the Regulator Gene *Rsc1A1* Exhibit Increased Na^+ /Glucose Cotransport in Small Intestine and Develop Obesity. *Mol Cell Biol* 25, 78–87. <https://doi.org/10.1128/MCB.25.1.78-87.2005>

- Ota, T., Ishikawa, T., Sakakida, T., Endo, Y., Matsumura, S., Yoshida, J., Hirai, Y., Mizushima, K., Oka, K., Doi, T., Okayama, T., Inoue, K., Kamada, K., Uchiyama, K., Takagi, T., Konishi, H., Naito, Y., Itoh, Y., 2022. Treatment with broad-spectrum antibiotics upregulates SglT1 and induces small intestinal villous hyperplasia in mice. *J. Clin. Biochem. Nutr.* 70, 21–27. <https://doi.org/10.3164/jcfn.21-42>
- Otis, C.R., Wamhoff, B.R., Sturek, M., 2003. Hyperglycemia-Induced Insulin Resistance in Diabetic Dyslipidemic Yucatan Swine. *Comparative Medicine* 53, 53–64.
- Pais, R., Gribble, F.M., Reimann, F., 2016. Stimulation of incretin secreting cells. *Therapeutic Advances in Endocrinology and Metabolism* 7, 24–42. <https://doi.org/10.1177/2042018815618177>
- Pal, A., Rhoads, D.B., Tavakkoli, A., 2019. Portal milieu and the interplay of multiple antidiabetic effects after gastric bypass surgery. *American Journal of Physiology-Gastrointestinal and Liver Physiology* 316, G668–G678. <https://doi.org/10.1152/ajpgi.00389.2018>
- Panasevich, M.R., Meers, G.M., Linden, M.A., Booth, F.W., Perfield, J.W., Fritsche, K.L., Wankhade, U.D., Chintapalli, S.V., Shankar, K., Ibdah, J.A., Rector, R.S., 2018. High-fat, high-fructose, high-cholesterol feeding causes severe NASH and cecal microbiota dysbiosis in juvenile Ossabaw swine. *Am J Physiol Endocrinol Metab* 314, E78–E92. <https://doi.org/10.1152/ajpendo.00015.2017>
- Panepinto, L.M., Phillips, R.W., Westmoreland, N.W., Cleek, J.L., 1982. Influence of Genetics and Diet on the Development of Diabetes in Yucatan Miniature Swine. *The Journal of Nutrition* 112, 2307–2313. <https://doi.org/10.1093/jn/112.12.2307>
- Panepinto, L.M., Phillips, R.W., Wheeler, L.R., Will, D., 1978. The Yucatan miniature pig as a laboratory animal. *Lab Anim Sci* 28, 308–313.
- Pantophlet, A.J., Wopereis, S., Eelderink, C., Vonk, R.J., Stroeve, J.H., Bijlsma, S., van Stee, L., Bobeldijk, I., Priebe, M.G., 2017. Metabolic Profiling Reveals Differences in Plasma Concentrations of Arabinose and Xylose after Consumption of Fiber-Rich Pasta and Wheat Bread with Differential Rates of Systemic Appearance of Exogenous Glucose in Healthy Men. *J Nutr* 147, 152–160. <https://doi.org/10.3945/jn.116.237404>
- Pappenheimer, J.R., 1990. Paracellular intestinal absorption of glucose, creatinine, and mannitol in normal animals: relation to body size. *American Journal of Physiology-Gastrointestinal and Liver Physiology* 259, G290–G299. <https://doi.org/10.1152/ajpgi.1990.259.2.G290>
- Paredes-Flores, M.A., Mohiuddin, S.S., 2023. Biochemistry, Glycogenolysis, in: StatPearls. StatPearls Publishing, Treasure Island (FL).
- Pasmans, K., Meex, R.C.R., Van Loon, L.J.C., Blaak, E.E., 2022. Nutritional strategies to attenuate postprandial glycemic response. *Obesity Reviews* 23. <https://doi.org/10.1111/obr.13486>
- Peddinti, G., Bergman, M., Tuomi, T., Groop, L., 2019. 1-Hour Post-OGTT Glucose Improves the Early Prediction of Type 2 Diabetes by Clinical and Metabolic Markers. *The Journal of Clinical Endocrinology & Metabolism* 104, 1131–1140. <https://doi.org/10.1210/jc.2018-01828>
- Péronnet, F., Meynier, A., Sauvinet, V., Normand, S., Bourdon, E., Mignault, D., St-Pierre, D.H., Laville, M., Rabasa-Lhoret, R., Vinoy, S., 2015. Plasma glucose kinetics and response of insulin and GIP following a cereal breakfast in female subjects: effect of starch digestibility. *Eur J Clin Nutr* 69, 740–745. <https://doi.org/10.1038/ejcn.2015.50>
- Petersen, M.C., Shulman, G.I., 2018. Mechanisms of Insulin Action and Insulin Resistance. *Physiological Reviews* 98, 2133–2223. <https://doi.org/10.1152/physrev.00063.2017>

- Petzold-Welcke, K., Schwikal, K., Daus, S., Heinze, T., 2014. Xylan derivatives and their application potential – Mini-review of own results. *Carbohydrate Polymers, Biopolymers for Life* 100, 80–88. <https://doi.org/10.1016/j.carbpol.2012.11.052>
- Pham, H., Holen, I.S., Phillips, L.K., Hatzinikolas, S., Huynh, L.Q., Wu, T., Hausken, T., Rayner, C.K., Horowitz, M., Jones, K.L., 2019. The Effects of a Whey Protein and Guar Gum-Containing Preload on Gastric Emptying, Glycaemia, Small Intestinal Absorption and Blood Pressure in Healthy Older Subjects. *Nutrients* 11, 2666. <https://doi.org/10.3390/nu11112666>
- Phillips, L.K., Deane, A.M., Jones, K.L., Rayner, C.K., Horowitz, M., 2015. Gastric emptying and glycaemia in health and diabetes mellitus. *Nat Rev Endocrinol* 11, 112–128. <https://doi.org/10.1038/nrendo.2014.202>
- Phillips, W.T., 2006. Gastric emptying in ethnic populations: possible relationship to development of diabetes and metabolic syndrome. *Ethnicity and Disease* 16, 682–692.
- Pierce, W.D., Heth, C.D., Owczarczyk, J.C., Russell, J.C., Proctor, S.D., 2007. Overeating by Young Obesity-prone and Lean Rats Caused by Tastes Associated With Low Energy Foods. *Obesity* 15, 1969–1979. <https://doi.org/10.1038/oby.2007.235>
- Pitkänen, E., 1977. The conversion of d-xylose into d-threitol in patients without liver disease and in patients with portal liver cirrhosis. *Clinica Chimica Acta* 80, 49–54. [https://doi.org/10.1016/0009-8981\(77\)90262-5](https://doi.org/10.1016/0009-8981(77)90262-5)
- Pol, K., Puhmann, M.-L., Mars, M., 2022. Efficacy of L-Arabinose in Lowering Glycemic and Insulinemic Responses: The Modifying Effect of Starch and Fat. *Foods* 11, 157. <https://doi.org/10.3390/foods11020157>
- Powell, C.R., Kim, A., Roth, J., Byrd, J.P., Mohammad, K., Alloosh, M., Vittal, R., Sturek, M., 2020. Ossabaw Pig Demonstrates Detrusor Fibrosis and Detrusor Underactivity Associated with Oxidative Stress in Metabolic Syndrome. *comp med* 70, 329–334. <https://doi.org/10.30802/AALAS-CM-20-000004>
- Powell, D.R., Smith, M., Greer, J., Harris, A., Zhao, S., DaCosta, C., Mseeh, F., Shadoan, M.K., Sands, A., Zambrowicz, B., Ding, Z.-M., 2013. LX4211 increases serum glucagon-like peptide 1 and peptide YY levels by reducing sodium/glucose cotransporter 1 (SGLT1)-mediated absorption of intestinal glucose. *J Pharmacol Exp Ther* 345, 250–259. <https://doi.org/10.1124/jpet.113.203364>
- Powell, D.R., Zambrowicz, B., Morrow, L., Beysen, C., Hompesch, M., Turner, S., Hellerstein, M., Banks, P., Strumph, P., Lapuerta, P., 2020. Sotagliflozin Decreases Postprandial Glucose and Insulin Concentrations by Delaying Intestinal Glucose Absorption. *The Journal of Clinical Endocrinology & Metabolism* 105, e1235–e1249. <https://doi.org/10.1210/clinem/dgz258>
- Proietto, J., Rohner-Jeanrenaud, F., Ionescu, E., Terrettaz, J., Sauter, J.F., Jeanrenaud, B., 1987. Non-steady-state measurement of glucose turnover in rats by using a one-compartment model. *American Journal of Physiology-Endocrinology and Metabolism* 252, E77–E84. <https://doi.org/10.1152/ajpendo.1987.252.1.E77>
- Puhalla, H., 2020. Duodenal Switch Weight Loss Surgery [WWW Document]. General Surgery Gold Coast. URL <https://weightlossoperation.com.au/weight-loss/loop-duodenal-switch-sadi-s-sips/> (accessed 9.25.23).

- Purushothaman, K.-R., Purushothaman, M., Muntner, P., Lento, P.A., O'Connor, W.N., Sharma, S.K., Fuster, V., Moreno, P.R., 2011. Inflammation, neovascularization and intra-plaque hemorrhage are associated with increased reparative collagen content: Implication for plaque progression in diabetic atherosclerosis. *Vasc Med* 16, 103–108. <https://doi.org/10.1177/1358863X11402249>
- Quesada, I., Tudurí, E., Ripoll, C., Nadal, Á., 2008. Physiology of the pancreatic α -cell and glucagon secretion: role in glucose homeostasis and diabetes. *Journal of Endocrinology* 199, 5–19. <https://doi.org/10.1677/JOE-08-0290>
- Ranaivo, H., Zhang, Z., Alligier, M., Van Den Berghe, L., Sothier, M., Lambert-Porcheron, S., Feugier, N., Cuerq, C., Machon, C., Neyrinck, A.M., Seethaler, B., Rodriguez, J., Roumain, M., Muccioli, G.G., Maquet, V., Laville, M., Bischoff, S.C., Walter, J., Delzenne, N.M., Nazare, J.-A., 2022. Chitin-glucan supplementation improved postprandial metabolism and altered gut microbiota in subjects at cardiometabolic risk in a randomized trial. *Sci Rep* 12, 8830. <https://doi.org/10.1038/s41598-022-12920-z>
- Raverdy, V., Cohen, R.V., Caiazzo, R., Verkindt, H., Petry, T.B.Z., Marciniak, C., Legendre, B., Bauvin, P., Chatelain, E., Duhamel, A., Drumez, E., Oukhouya-Daoud, N., Chetboun, M., Baud, G., Ahlqvist, E., Wierup, N., Asplund, O., Laferrère, B., Groop, L., Pattou, F., 2022. Data-driven subgroups of type 2 diabetes, metabolic response, and renal risk profile after bariatric surgery: a retrospective cohort study. *The Lancet Diabetes & Endocrinology* 10, 167–176. [https://doi.org/10.1016/S2213-8587\(22\)00005-5](https://doi.org/10.1016/S2213-8587(22)00005-5)
- Rayner, C.K., Watson, L.E., Phillips, L.K., Lange, K., Bound, M.J., Grivell, J., Wu, T., Jones, K.L., Horowitz, M., Ferrannini, E., Trico, D., Frascerra, S., Mari, A., Natali, A., 2020. Effects of Sustained Treatment With Lixisenatide on Gastric Emptying and Postprandial Glucose Metabolism in Type 2 Diabetes: A Randomized Controlled Trial. *Diabetes Care* 43, 1813–1821. <https://doi.org/10.2337/dc20-0190>
- Rebrin, K., Steil, G.M., Mittelman, S.D., Bergman, R.N., 1996. Causal linkage between insulin suppression of lipolysis and suppression of liver glucose output in dogs. *J. Clin. Invest.* 98, 741–749. <https://doi.org/10.1172/JCI118846>
- Renner, S., Blutke, A., Claus, S., Deeg, C.A., Kemter, E., Merkus, D., Wanke, R., Wolf, E., 2020. Porcine models for studying complications and organ crosstalk in diabetes mellitus. *Cell Tissue Res* 380, 341–378. <https://doi.org/10.1007/s00441-019-03158-9>
- Renner, S., Braun-Reichhart, C., Blutke, A., Herbach, N., Emrich, D., Streckel, E., Wunsch, A., Kessler, B., Kurome, M., Bahr, A., Klymiuk, N., Krebs, S., Puk, O., Nagashima, H., Graw, J., Blum, H., Wanke, R., Wolf, E., 2013. Permanent Neonatal Diabetes in INSC94Y Transgenic Pigs. *Diabetes* 62, 1505–1511. <https://doi.org/10.2337/db12-1065>
- Renner, S., Dobenecker, B., Blutke, A., Zöls, S., Wanke, R., Ritzmann, M., Wolf, E., 2016. Comparative aspects of rodent and nonrodent animal models for mechanistic and translational diabetes research. *Theriogenology* 86, 406–421. <https://doi.org/10.1016/j.theriogenology.2016.04.055>
- Renwick, A.G., Molinary, S.V., 2010. Sweet-taste receptors, low-energy sweeteners, glucose absorption and insulin release. *Br J Nutr* 104, 1415–1420. <https://doi.org/10.1017/S0007114510002540>
- Repin, N., Kay, B.A., Cui, S.W., Wright, A.J., Duncan, A.M., Douglas Goff, H., 2017. Investigation of mechanisms involved in postprandial glycemia and insulinemia attenuation with dietary fibre consumption. *Food Funct* 8, 2142–2154. <https://doi.org/10.1039/c7fo00331e>

- Rerat, A.A., 1980. Some quantitative aspects of protein and carbohydrate absorption in the pig. *Proc. Nutr. Soc.* 39, 177–184. <https://doi.org/10.1017/PNS19800027>
- Reynolds, A., Mann, J., Cummings, J., Winter, N., Mete, E., Te Morenga, L., 2019. Carbohydrate quality and human health: a series of systematic reviews and meta-analyses. *Lancet* 393, 434–445. [https://doi.org/10.1016/S0140-6736\(18\)31809-9](https://doi.org/10.1016/S0140-6736(18)31809-9)
- Risstad, H., Svanevik, M., Kristinsson, J.A., Hjelmæsæth, J., Aasheim, E.T., Hofsø, D., Sjøvik, T.T., Karlsen, T.-I., Fagerland, M.W., Sandbu, R., Mala, T., 2016. Standard vs Distal Roux-en-Y Gastric Bypass in Patients With Body Mass Index 50 to 60: A Double-blind, Randomized Clinical Trial. *JAMA Surg* 151, 1146. <https://doi.org/10.1001/jamasurg.2016.2798>
- Rizza, R.A., Mandarino, L.J., Gerich, J.E., 1981. Dose-response characteristics for effects of insulin on production and utilization of glucose in man. *American Journal of Physiology-Endocrinology and Metabolism* 240, E630–E639. <https://doi.org/10.1152/ajpendo.1981.240.6.E630>
- Robert, M., Espalieu, P., Pelascini, E., Caiazzo, R., Sterkers, A., Khamphommala, L., Poghosyan, T., Chevallier, J.-M., Malherbe, V., Chouillard, E., Reche, F., Torcivia, A., Maucort-Boulch, D., Bin-Dorel, S., Langlois-Jacques, C., Delaunay, D., Pattou, F., Disse, E., 2019. Efficacy and safety of one anastomosis gastric bypass versus Roux-en-Y gastric bypass for obesity (YOMEGA): a multicentre, randomised, open-label, non-inferiority trial. *The Lancet* 393, 1299–1309. [https://doi.org/10.1016/S0140-6736\(19\)30475-1](https://doi.org/10.1016/S0140-6736(19)30475-1)
- Roberts, J.G., Beck, I.T., 1960. D-Xylose blood-level time-curve as an index of intestinal absorption with a description of a simplified method for estimation of blood xylose levels. *Can Med Assoc J* 83, 112–117.
- Roden, M., Weng, J., Eilbracht, J., Delafont, B., Kim, G., Woerle, H.J., Broedl, U.C., 2013. Empagliflozin monotherapy with sitagliptin as an active comparator in patients with type 2 diabetes: a randomised, double-blind, placebo-controlled, phase 3 trial. *The Lancet Diabetes & Endocrinology* 1, 208–219. [https://doi.org/10.1016/S2213-8587\(13\)70084-6](https://doi.org/10.1016/S2213-8587(13)70084-6)
- Rolston, D.D.K., Mathan, V.I., 1989. Xylose transport in the human jejunum. *Digest Dis Sci* 34, 553–558. <https://doi.org/10.1007/BF01536332>
- Rosak, C., Mertes, G., 2012. Critical evaluation of the role of acarbose in the treatment of diabetes: patient considerations. *Diabetes Metab Syndr Obes* 5, 357–367. <https://doi.org/10.2147/DMSO.S28340>
- Rothman, D.L., Magnusson, I., Katz, L.D., Shulman, R.G., Shulman, G.I., 1991. Quantitation of Hepatic Glycogenolysis And Gluconeogenesis in Fasting Humans With ¹³ C NMR. *Science* 254, 573–576. <https://doi.org/10.1126/science.1948033>
- Royal, J.M., Settle, T.L., Bodo, M., Lombardini, E., Kent, M.L., Upp, J., Rothwell, S.W., 2013. Assessment of Postoperative Analgesia after Application of Ultrasound-Guided Regional Anesthesia for Surgery in a Swine Femoral Fracture Model. *Journal of the American Association for Laboratory Animal Science* 52, 12.
- Rubino, F., Forgione, A., Cummings, D.E., Vix, M., Gnuli, D., Mingrone, G., Castagneto, M., Marescaux, J., 2006. The Mechanism of Diabetes Control After Gastrointestinal Bypass Surgery Reveals a Role of the Proximal Small Intestine in the Pathophysiology of Type 2 Diabetes: *Annals of Surgery* 244, 741–749. <https://doi.org/10.1097/01.sla.0000224726.61448.1b>

- Ruiz-Tovar, J., Vorwald, P., Gonzalez-Ramirez, G., Posada, M., Salcedo, G., Llaverro, C., Garcia-Olmo, D., 2019. Impact of Biliopancreatic Limb Length (70 cm vs 120 cm), with Constant 150 cm Alimentary Limb, on Long-Term Weight Loss, Remission of Comorbidities and Supplementation Needs After Roux-En-Y Gastric Bypass: a Prospective Randomized Clinical Trial. *OBES SURG* 29, 2367–2372. <https://doi.org/10.1007/s11695-019-03717-7>
- Russo, A., Stevens, J.E., Chen, R., Gentilcore, D., Burnet, R., Horowitz, M., Jones, K.L., 2005. Insulin-induced hypoglycemia accelerates gastric emptying of solids and liquids in long-standing type 1 diabetes. *J Clin Endocrinol Metab* 90, 4489–4495. <https://doi.org/10.1210/jc.2005-0513>
- Ruud, J., Steculorum, S.M., Brüning, J.C., 2017. Neuronal control of peripheral insulin sensitivity and glucose metabolism. *Nat Commun* 8, 15259. <https://doi.org/10.1038/ncomms15259>
- Sabanayagam, C., Banu, R., Chee, M.L., Lee, R., Wang, Y.X., Tan, G., Jonas, J.B., Lamoureux, E.L., Cheng, C.-Y., Klein, B.E.K., Mitchell, P., Klein, R., Cheung, C.M.G., Wong, T.Y., 2019. Incidence and progression of diabetic retinopathy: a systematic review. *The Lancet Diabetes & Endocrinology* 7, 140–149. [https://doi.org/10.1016/S2213-8587\(18\)30128-1](https://doi.org/10.1016/S2213-8587(18)30128-1)
- Saeidi, N., Meoli, L., Nestoridi, E., Gupta, N.K., Kvas, S., Kucharczyk, J., Bonab, A.A., Fischman, A.J., Yarmush, M.L., Stylopoulos, N., 2013. Reprogramming of Intestinal Glucose Metabolism and Glycemic Control in Rats After Gastric Bypass. *Science* 341, 406–410. <https://doi.org/10.1126/science.1235103>
- Saikat, R., 2016. How is glucose absorbed from the gastrointestinal tract? How are blood glucose levels maintained? | Socratic [WWW Document]. Socratic.org. URL <https://socratic.org/questions/how-is-glucose-absorbed-from-the-gastrointestinal-tract-how-are-blood-glucose-le> (accessed 5.25.23).
- Saisho, Y., 2015. β -cell dysfunction: Its critical role in prevention and management of type 2 diabetes. *WJD* 6, 109–124. <https://doi.org/10.4239/wjd.v6.i1.109>
- Saisho, Y., Butler, A.E., Manesso, E., Elashoff, D., Rizza, R.A., Butler, P.C., 2013. β -Cell Mass and Turnover in Humans. *Diabetes Care* 36, 111–117. <https://doi.org/10.2337/dc12-0421>
- Sakamoto, Y., Sekino, Y., Yamada, E., Ohkubo, H., Higurashi, T., Sakai, E., Iida, H., Hosono, K., Endo, H., Nonaka, T., Ikeda, T., Fujita, K., Yoneda, M., Koide, T., Takahashi, H., Goto, A., Abe, Y., Gotoh, E., Maeda, S., Nakajima, A., Inamori, M., 2011. Mosapride Accelerates the Delayed Gastric Emptying of High-Viscosity Liquids: A Crossover Study Using Continuous Real-Time C Breath Test (BreathID System). *J Neurogastroenterol Motil* 17, 395–401. <https://doi.org/10.5056/jnm.2011.17.4.395>
- Sakar, Y., Meddah, B., Faouzi, M.A., Cherrah, Y., Bado, A., Ducroc, R., 2010. Metformin-induced regulation of the intestinal D-glucose transporters. *J Physiol Pharmacol* 61, 301–307.
- Sala-Rabanal, M., Ghezzi, C., Hirayama, B.A., Kepe, V., Liu, J., Barrio, J.R., Wright, E.M., 2018. Intestinal absorption of glucose in mice as determined by positron emission tomography: Glucose absorption *in vivo*. *J Physiol* 596, 2473–2489. <https://doi.org/10.1113/JP275934>
- Salinari, S., Bertuzzi, A., Mingrone, G., 2011. Intestinal transit of a glucose bolus and incretin kinetics: a mathematical model with application to the oral glucose tolerance test. *American Journal of Physiology-Endocrinology and Metabolism* 300, E955–E965. <https://doi.org/10.1152/ajpendo.00451.2010>
- Sansom, M., Szarka, L.A., Camilleri, M., Vella, A., Zinsmeister, A.R., Rizza, R.A., 2000. Pramlintide, an amylin analog, selectively delays gastric emptying: potential role of vagal inhibition. *Am J Physiol Gastrointest Liver Physiol* 278, G946–951. <https://doi.org/10.1152/ajpgi.2000.278.6.G946>

- Samuel, V.T., Shulman, G.I., 2012. Mechanisms for Insulin Resistance: Common Threads and Missing Links. *Cell* 148, 852–871. <https://doi.org/10.1016/j.cell.2012.02.017>
- Sano, R., Shinozaki, Y., Ohta, T., 2020. Sodium–glucose cotransporters: Functional properties and pharmaceutical potential. *J Diabetes Investig* 11, 770–782. <https://doi.org/10.1111/jdi.13255>
- Sansome, D.J., Xie, C., Veedfald, S., Horowitz, M., Rayner, C.K., Wu, T., 2020. Mechanism of glucose-lowering by metformin in type 2 diabetes: Role of bile acids. *Diabetes Obes Metab* 22, 141–148. <https://doi.org/10.1111/dom.13869>
- Santé publique France, 2021. Le diabète en France : les chiffres 2020 [WWW Document]. URL <https://www.santepubliquefrance.fr/les-actualites/2021/le-diabete-en-france-les-chiffres-2020> (accessed 2.6.23).
- Santé publique France, 2019. Mortalité liée au diabète [WWW Document]. URL <https://www.santepubliquefrance.fr/maladies-et-traumatismes/diabete/mortalite-liee-au-diabete2> (accessed 2.13.23).
- Sato, D., Morino, K., Nakagawa, F., Murata, K., Sekine, O., Beppu, F., Gotoh, N., Ugi, S., Maegawa, H., 2017. Acute Effect of Metformin on Postprandial Hypertriglyceridemia through Delayed Gastric Emptying. *Int J Mol Sci* 18, 1282. <https://doi.org/10.3390/ijms18061282>
- Satsu, H., Shibata, R., Suzuki, H., Kimura, S., Shimizu, M., 2021. Inhibitory Effect of Tangeretin and Cardamonin on Human Intestinal SGLT1 Activity In Vitro and Blood Glucose Levels in Mice In Vivo. *Nutrients* 13, 3382. <https://doi.org/10.3390/nu13103382>
- Sauvinet, V., Gabert, L., Qin, D., Louche-Pélessier, C., Laville, M., Désage, M., 2009. Validation of pentaacetylaldonitrile derivative for dual ² H gas chromatography/mass spectrometry and ¹³ C gas chromatography/combustion/isotope ratio mass spectrometry analysis of glucose: Validation of a glucose derivative for GC/MS and GC/C/IRMS. *Rapid Commun. Mass Spectrom.* 23, 3855–3867. <https://doi.org/10.1002/rcm.4294>
- Scheiner, E., Shils, M.E., Vanamee, P., 1965. Malabsorption Following Massive Intestinal Resection. *The American Journal of Clinical Nutrition* 17, 64–72. <https://doi.org/10.1093/ajcn/17.2.64>
- Schiavon, C.A., Bersch-Ferreira, A.C., Santucci, E.V., Oliveira, J.D., Torreglosa, C.R., Bueno, P.T., Frayha, J.C., Santos, R.N., Damiani, L.P., Noujaim, P.M., Halpern, H., Monteiro, F.L.J., Cohen, R.V., Uchoa, C.H., de Souza, M.G., Amodeo, C., Bortolotto, L., Ikeoka, D., Drager, L.F., Cavalcanti, A.B., Berwanger, O., 2018. Effects of Bariatric Surgery in Obese Patients With Hypertension: The GATEWAY Randomized Trial (Gastric Bypass to Treat Obese Patients With Steady Hypertension). *Circulation* 137, 1132–1142. <https://doi.org/10.1161/CIRCULATIONAHA.117.032130>
- Schirra, J., Katschinski, M., Weidmann, C., Schäfer, T., Wank, U., Arnold, R., Göke, B., 1996. Gastric emptying and release of incretin hormones after glucose ingestion in humans. *J. Clin. Invest.* 97, 92–103. <https://doi.org/10.1172/JCI118411>
- Schloesser, A., Esatbeyoglu, T., Schultheiß, G., Vollert, H., Lüersen, K., Fischer, A., Rimbach, G., 2017. Antidiabetic Properties of an Apple/Kale Extract In Vitro, In Situ, and in Mice Fed a Western-Type Diet. *J Med Food* 20, 846–854. <https://doi.org/10.1089/jmf.2017.0019>
- Schmitt, C.C., Aranas, T., Viel, T., Chateau, D., Le Gall, M., Waligora-Dupriet, A.-J., Melchior, C., Rouxel, O., Kapel, N., Gourcerol, G., Tavitian, B., Lehuen, A., Brot-Laroche, E., Leturque, A., Serradas, P., Grosfeld, A., 2017. Intestinal invalidation of the glucose transporter GLUT2 delays tissue distribution

of glucose and reveals an unexpected role in gut homeostasis. *Molecular Metabolism* 6, 61–72. <https://doi.org/10.1016/j.molmet.2016.10.008>

Schönenberger, K.A., Reber, E., Dürig, C., Baumgartner, A., Efthymiou, A., Huwiler, V.V., Laimer, M., Bally, L., Stanga, Z., 2022. Management of Hyperglycemia in Hospitalized Patients Receiving Parenteral Nutrition. *Frontiers in Clinical Diabetes and Healthcare* 117, 110. <https://doi.org/10.3389/fcdhc.2022.829412>

Schumacher-Petersen, C., Christoffersen, B.Ø., Kirk, R.K., Ludvigsen, T.P., Zois, N.E., Pedersen, H.D., Vyberg, M., Olsen, L.H., 2019. Experimental non-alcoholic steatohepatitis in Göttingen Minipigs: consequences of high fat-fructose-cholesterol diet and diabetes. *J Transl Med* 17, 110. <https://doi.org/10.1186/s12967-019-1854-y>

Schwartz, J.G., McMahan, C.A., Green, G.M., Phillips, W.T., 1995. Gastric emptying in Mexican Americans compared to non-Hispanic whites. *Dig Dis Sci* 40, 624–630. <https://doi.org/10.1007/BF02064382>

Schwartz, M.P., Samsom, M., Renooij, W., van Steenderen, L.W., Benninga, M.A., van Geenen, E.-J.M., van Herwaarden, M.A., de Smet, M.B.M., Smout, A.J.P.M., 2002. Small Bowel Motility Affects Glucose Absorption in a Healthy Man. *Diabetes Care* 25, 1857–1861. <https://doi.org/10.2337/diacare.25.10.1857>

Scognamiglio, R., Avogaro, A., Vigili de Kreutzenberg, S., Negut, C., Palisi, M., Bagolin, E., Tiengo, A., 2002. Effects of Treatment With Sulfonylurea Drugs or Insulin on Ischemia-Induced Myocardial Dysfunction in Type 2 Diabetes. *Diabetes* 51, 808–812. <https://doi.org/10.2337/diabetes.51.3.808>

Segal, S., Foley, J.B., 1959. The metabolic fate of C14 labeled pentoses in man. *J. Clin. Invest.* 38, 407–413. <https://doi.org/10.1172/JCI103815>

Seidemann, S.B., Feofanova, E., Yu, B., Franceschini, N., Claggett, B., Kuokkanen, M., Puolijoki, H., Ebeling, T., Perola, M., Salomaa, V., Shah, A., Coresh, J., Selvin, E., MacRae, C.A., Cheng, S., Boerwinkle, E., Solomon, S.D., 2018. Genetic Variants in SGLT1, Glucose Tolerance, and Cardiometabolic Risk. *Journal of the American College of Cardiology* 72, 1763–1773. <https://doi.org/10.1016/j.jacc.2018.07.061>

Seino, Y., 2011. Understanding the Incretin Effect. *The Journal of Clinical Endocrinology & Metabolism* 96, 934–935. <https://doi.org/10.1210/jc.2011-0329>

Sham, J.G., Simianu, V.V., Wright, A.S., Stewart, S.D., Alloosh, M., Sturek, M., Cummings, D.E., Flum, D.R., 2014. Evaluating the Mechanisms of Improved Glucose Homeostasis after Bariatric Surgery in Ossabaw Miniature Swine. *Journal of Diabetes Research* 2014, 1–7. <https://doi.org/10.1155/2014/526972>

Shojaee-Moradie, F., Jackson, N.C., Jones, R.H., Mallet, A.I., Hovorka, R., Umpleby, A.M., 1996. Quantitative Measurement of 3-O-Methyl-D-glucose by Gas Chromatography-Mass Spectrometry as a Measure of Glucose Transport In Vivo. *J. Mass Spectrom.* 31, 961–966. [https://doi.org/10.1002/\(SICI\)1096-9888\(199609\)31:9<961::AID-JMS359>3.0.CO;2-H](https://doi.org/10.1002/(SICI)1096-9888(199609)31:9<961::AID-JMS359>3.0.CO;2-H)

Shulman, G.I., 2014. Ectopic Fat in Insulin Resistance, Dyslipidemia, and Cardiometabolic Disease. *N Engl J Med* 371, 1131–1141. <https://doi.org/10.1056/NEJMr1011035>

Singh, B., 2010. Surrogate markers of insulin resistance: A review. *WJD* 1, 36–47. <https://doi.org/10.4239/wjd.v1.i2.36>

- Sjöström, L., Lindroos, A.-K., Peltonen, M., Torgerson, J., Bouchard, Carlsson, B., Dahlgren, S., Larsson, B., Narbro, K., Sjöström, C.D., Sullivan, M., Wedel, H., 2004. Lifestyle, Diabetes, and Cardiovascular Risk Factors 10 Years after Bariatric Surgery. *The New England Journal of Medicine* 351, 83–93. <https://doi.org/10.1056/NEJMoa035622>
- Skytte, M.J., Samkani, A., Astrup, A., Frystyk, J., Rehfeld, J.F., Holst, J.J., Madsbad, S., Burling, K., Fenger, M., Thomsen, M.N., Larsen, T.M., Krarup, T., Haugaard, S.B., 2021. Effects of carbohydrate restriction on postprandial glucose metabolism, β -cell function, gut hormone secretion, and satiety in patients with Type 2 diabetes. *American Journal of Physiology-Endocrinology and Metabolism* 320, E7–E18. <https://doi.org/10.1152/ajpendo.00165.2020>
- Smith, K., Taylor, G.S., Allerton, D.M., Brunsgaard, L.H., Bowden Davies, K.A., Stevenson, E.J., West, D.J., 2021. The Postprandial Glycaemic and Hormonal Responses Following the Ingestion of a Novel, Ready-to-Drink Shot Containing a Low Dose of Whey Protein in Centrally Obese and Lean Adult Males: A Randomised Controlled Trial. *Front Endocrinol (Lausanne)* 12, 696977. <https://doi.org/10.3389/fendo.2021.696977>
- Spruijt-Metz, D., O'Reilly, G.A., Cook, L., Page, K.A., Quinn, C., 2014. Behavioral Contributions to the Pathogenesis of Type 2 Diabetes. *Curr Diab Rep* 14, 475. <https://doi.org/10.1007/s11892-014-0475-3>
- Stalmans, W., Bollen, M., Mvumbi, L., 1987. Control of glycogen synthesis in health and disease. *Diabetes Metab. Rev.* 3, 127–161. <https://doi.org/10.1002/dmr.5610030107>
- Stearns, A.T., Balakrishnan, A., Tavakkolizadeh, A., 2009. Impact of Roux-en-Y gastric bypass surgery on rat intestinal glucose transport. *American Journal of Physiology-Gastrointestinal and Liver Physiology* 297, G950–G957. <https://doi.org/10.1152/ajpgi.00253.2009>
- Steele, R., Wall, J.S., de Bodo, R.C., Altszuler, N., 1956. Measurement of Size and Turnover Rate of Body Glucose Pool by the Isotope Dilution Method. *American Journal of Physiology-Legacy Content* 187, 15–24. <https://doi.org/10.1152/ajplegacy.1956.187.1.15>
- Steiner, D.J., Kim, A., Miller, K., Hara, M., 2010. Pancreatic islet plasticity: interspecies comparison of islet architecture and composition. *Islets* 2, 135–145. <https://doi.org/10.4161/isl.2.3.11815>
- Steinert, R.E., Feinle-Bisset, C., Asarian, L., Horowitz, M., Beglinger, C., Geary, N., 2017. Ghrelin, CCK, GLP-1, and PYY(3-36): Secretory Controls and Physiological Roles in Eating and Glycemia in Health, Obesity, and After RYGB. *Physiol Rev* 97, 411–463. <https://doi.org/10.1152/physrev.00031.2014>
- Stenkula, K.G., Erlanson-Albertsson, C., 2018. Adipose cell size: importance in health and disease. *American Journal of Physiology-Regulatory, Integrative and Comparative Physiology* 315, R284–R295. <https://doi.org/10.1152/ajpregu.00257.2017>
- Stenlöf, K., Cefalu, W.T., Kim, K.A., Alba, M., Usiskin, K., Tong, C., Canovatchel, W., Meininger, G., 2013. Efficacy and safety of canagliflozin monotherapy in subjects with type 2 diabetes mellitus inadequately controlled with diet and exercise. *Diabetes, Obesity and Metabolism* 15, 372–382. <https://doi.org/10.1111/dom.12054>
- Stolar, M., 2010. Glycemic Control and Complications in Type 2 Diabetes Mellitus. *The American Journal of Medicine* 123, S3–S11. <https://doi.org/10.1016/j.amjmed.2009.12.004>
- Stoll, B., Horst, D.A., Cui, L., Chang, X., Ellis, K.J., Hadsell, D.L., Suryawan, A., Kurundkar, A., Maheshwari, A., Davis, T.A., Burrin, D.G., 2010. Chronic Parenteral Nutrition Induces Hepatic Inflammation,

- Steatosis, and Insulin Resistance in Neonatal Pigs. *The Journal of Nutrition* 140, 2193–2200. <https://doi.org/10.3945/jn.110.125799>
- Stumvoll, M., Nurjhan, N., Perriello, G., Dailey, G., Gerich, J.E., 1995. Metabolic effects of metformin in non-insulin-dependent diabetes mellitus. *N Engl J Med* 333, 550–554. <https://doi.org/10.1056/NEJM199508313330903>
- Sturek, M., Alloosh, M., Wenzel, J., Byrd, J., Edwards, J., Lloyd, P., Tune, J., March, K., Miller, M., Mokelke, E., Lehr Brisbin, Jr., I., 2007. Ossabaw Island Miniature Swine: Cardiometabolic Syndrome Assessment, in: Michael Swindle, M. (Ed.), *Swine in the Laboratory*. CRC Press, pp. 397–402. <https://doi.org/10.1201/9781420009156.ch18>
- Suenderhauf, C., Tuffin, G., Lorentsen, H., Grimm, H.-P., Flament, C., Parrott, N., 2014. Pharmacokinetics of Paracetamol in Göttingen Minipigs: In Vivo Studies and Modeling to Elucidate Physiological Determinants of Absorption. *Pharmaceutical Research* 31, 2696–2797. <https://doi.org/10.1007/s11095-014-1367-6>
- Sun, H., Wan, S., Wang, X., Xuejin, G., Li, Z., Jiwei, W., Peng, W., Jianbo, Y., 2018. Total parenteral nutrition induces glycometabolic disorders via systemic insulin resistance and hepatic glycogen suppression. *Clinical Nutrition, Abstracts of the 40th ESPEN Congress, Madrid, Spain, 1-4 September 2018* 37, S146–S147. <https://doi.org/10.1016/j.clnu.2018.06.1542>
- Svane, M.S., Bojsen-Møller, K.N., Martinussen, C., Dirksen, C., Madsen, J.L., Reitelsheder, S., Holm, L., Rehfeld, J.F., Kristiansen, V.B., van Hall, G., Holst, J.J., Madsbad, S., 2019. Postprandial Nutrient Handling and Gastrointestinal Hormone Secretion After Roux-en-Y Gastric Bypass vs Sleeve Gastrectomy. *Gastroenterology* 156, 1627–1641.e1. <https://doi.org/10.1053/j.gastro.2019.01.262>
- Swindle, M.M., Makin, A., Herron, A.J., Clubb, F.J., Frazier, K.S., 2012. Swine as Models in Biomedical Research and Toxicology Testing. *Vet Pathol* 49, 344–356. <https://doi.org/10.1177/0300985811402846>
- Szablewski, L., 2011. Glucose Homeostasis – Mechanism and Defects, in: Rigobelo, E. (Ed.), *Diabetes - Damages and Treatments*. InTech. <https://doi.org/10.5772/22905>
- Szkudelski, T., 2001. The mechanism of alloxan and streptozotocin action in B cells of the rat pancreas. *Physiol Res* 50, 537–546.
- Tanaka, K., Kanazawa, I., Yamaguchi, T., Sugimoto, T., 2014. One-hour post-load hyperglycemia by 75g oral glucose tolerance test as a novel risk factor of atherosclerosis. *Endocr J* 61, 329–334. <https://doi.org/10.1507/endocrj.EJ13-0370>
- Taylor, R., Price, T.B., Katz, L.D., Shulman, G., Shulman, G.I., 1993. Direct measurement of change in muscle glycogen concentration after a mixed meal in normal subjects. *American Journal of Physiology Endocrinology and Metabolism* 265, E224–E229. <https://doi.org/10.1152/ajpendo.1993.265.2.E224>
- Telle-Hansen, V.H., Gaundal, L., Høgvard, B., Ulven, S.M., Holven, K.B., Byfuglien, M.G., Måge, I., Knutsen, S.H., Ballance, S., Rieder, A., Rud, I., Myhrstad, M.C.W., 2022. A Three-Day Intervention With Granola Containing Cereal Beta-Glucan Improves Glycemic Response and Changes the Gut Microbiota in Healthy Individuals: A Crossover Study. *Front Nutr* 9, 796362. <https://doi.org/10.3389/fnut.2022.796362>

Thazhath, S.S., Wu, T., Young, R.L., Horowitz, M., Rayner, C.K., 2014. Glucose absorption in small intestinal diseases. *Expert Review of Gastroenterology & Hepatology* 8, 301–312. <https://doi.org/10.1586/17474124.2014.887439>

The Diabetes Control and Complications Trial Research Group, 1993. The effect of intensive treatment of diabetes on the development and progression of long-term complications in insulin-dependent diabetes mellitus. *The New England Journal of Medicine* 329, 977–986. <https://doi.org/10.1056/NEJM199309303291401>

Thomas, M.C., Cooper, M.E., Zimmet, P., 2015. Changing epidemiology of type 2 diabetes mellitus and associated chronic kidney disease. *Nature Reviews Nephrology* 12, 73–81. <https://doi.org/10.1038/nrneph.2015.173>

Thorens, B., 2015. GLUT2, glucose sensing and glucose homeostasis. *Diabetologia* 58, 221–232. <https://doi.org/10.1007/s00125-014-3451-1>

Thorens, B., Mueckler, M., 2010. Glucose transporters in the 21st Century. *American Journal of Physiology-Endocrinology and Metabolism* 298, E141–E145. <https://doi.org/10.1152/ajpendo.00712.2009>

Tissot, S., Normand, S., Guilluy, R., Pachiaudi, C., Beylot, M., Laville, M., Cohen, R., Mornex, R., Riou, J.P., 1990. Use of a new gas chromatograph isotope ratio mass spectrometer to trace exogenous ¹³C labelled glucose at a very low level of enrichment in man. *Diabetologia* 33, 449–456. <https://doi.org/10.1007/BF00405104>

Torsdottir, I., Alpsten, M., Andersson, H., Einarsson, S., 1989. Dietary guar gum effects on postprandial blood glucose, insulin and hydroxyproline in humans. *J Nutr* 119, 1925–1931. <https://doi.org/10.1093/jn/119.12.1925>

Trabelsi, M.-S., Lestavel, S., Staels, B., Collet, X., 2017. Intestinal bile acid receptors are key regulators of glucose homeostasis. *Proc Nutr Soc* 76, 192–202. <https://doi.org/10.1017/S0029665116002834>

Trahair, L.G., Horowitz, M., Stevens, J.E., Feinle-Bisset, C., Standfield, S., Piscitelli, D., Rayner, C.K., Deane, A.M., Jones, K.L., 2015. Effects of exogenous glucagon-like peptide-1 on blood pressure, heart rate, gastric emptying, mesenteric blood flow and glycaemic responses to oral glucose in older individuals with normal glucose tolerance or type 2 diabetes. *Diabetologia* 58, 1769–1778. <https://doi.org/10.1007/s00125-015-3638-0>

Trahair, L.G., Marathe, C.S., Standfield, S., Rayner, C.K., Feinle-Bisset, C., Horowitz, M., Jones, K.L., 2017. Effects of small intestinal glucose on glycaemia, insulinaemia and incretin hormone release are load-dependent in obese subjects. *Int J Obes (Lond)* 41, 225–232. <https://doi.org/10.1038/ijo.2016.202>

Tricò, D., Baldi, S., Tulipani, A., Frascerra, S., Macedo, M.P., Mari, A., Ferrannini, E., Natali, A., 2015. Mechanisms through which a small protein and lipid preload improves glucose tolerance. *Diabetologia* 58, 2503–2512. <https://doi.org/10.1007/s00125-015-3710-9>

Tricò, D., Galderisi, A., Mari, A., Santoro, N., Caprio, S., 2019a. One-hour post-load plasma glucose predicts progression to prediabetes in a multi-ethnic cohort of obese youths. *Diabetes Obes Metab* 21, 1191–1198. <https://doi.org/10.1111/dom.13640>

Tricò, D., Mengozzi, A., Frascerra, S., Scozzaro, M.T., Mari, A., Natali, A., 2019b. Intestinal Glucose Absorption Is a Key Determinant of 1-Hour Postload Plasma Glucose Levels in Nondiabetic Subjects.

The Journal of Clinical Endocrinology & Metabolism 104, 2131–2139. <https://doi.org/10.1210/jc.2018-02166>

Trujillo, J.M., Nuffer, W., Smith, B.A., 2021. GLP-1 receptor agonists: an updated review of head-to-head clinical studies. *Therapeutic Advances in Endocrinology* 12, 204201882199732. <https://doi.org/10.1177/2042018821997320>

Tu, C.-F., Hsu, C.-Y., Lee, M.-H., Jiang, B.-H., Guo, S.-F., Lin, C.-C., Yang, T.-S., 2018. Growing pigs developed different types of diabetes induced by streptozotocin depending on their transcription factor 7-like 2 gene polymorphisms. *Lab Anim Res* 34, 185–194. <https://doi.org/10.5625/lar.2018.34.4.185>

Uceda, D.E., Zhu, X.-Y., Woollard, J.R., Ferguson, C.M., Patras, I., Carlson, D.F., Asirvatham, S.J., Lerman, A., Lerman, L.O., 2020. Accumulation of Pericardial Fat Is Associated With Alterations in Heart Rate Variability Patterns in Hypercholesterolemic Pigs. *Circ: Arrhythmia and Electrophysiology* 13, e007614. <https://doi.org/10.1161/CIRCEP.119.007614>

Ullrich, S.S., Fitzgerald, P.C.E., Giesbertz, P., Steinert, R.E., Horowitz, M., Feinle-Bisset, C., 2018. Effects of Intragastric Administration of Tryptophan on the Blood Glucose Response to a Nutrient Drink and Energy Intake, in Lean and Obese Men. *Nutrients* 10, 463. <https://doi.org/10.3390/nu10040463>

Umeda, L.M., Silva, E.A., Carneiro, G., Arasaki, C.H., Geloneze, B., Zanella, M.T., 2011. Early Improvement in Glycemic Control After Bariatric Surgery and Its Relationships with Insulin, GLP-1, and Glucagon Secretion in Type 2 Diabetic Patients. *OBES SURG* 21, 896–901. <https://doi.org/10.1007/s11695-011-0412-3>

Unger, R.H., 1971. Glucagon and the Insulin:Glucagon Ratio in Diabetes and Other Catabolic Illnesses. *Diabetes* 20, 834–838. <https://doi.org/10.2337/diab.20.12.834>

Urva, S., Coskun, T., Loghin, C., Cui, X., Beebe, E., O'Farrell, L., Briere, D., Benson, C., Nauck, M., Haupt, A., 2020. The novel dual glucosedependent insulinotropic polypeptide and glucagon-like peptide-1 (GLP-1) receptor agonist tirzepatide transiently delays gastric emptying similarly to selective long-acting GLP-1 receptor agonists. *Diabetes Obes Metab* 22, 1886–1891.

Ussar, S., Haering, M.-F., Fujisaka, S., Lutter, D., Lee, K.Y., Li, N., Gerber, G.K., Bry, L., Kahn, C.R., 2017. Regulation of Glucose Uptake and Enteroendocrine Function by the Intestinal Epithelial Insulin Receptor. *Diabetes* 66, 886–896. <https://doi.org/10.2337/db15-1349>

Utzschneider, K.M., Prigeon, R.L., Faulenbach, M.V., Tong, J., Carr, D.B., Boyko, E.J., Leonetti, D.L., McNeely, M.J., Fujimoto, W.Y., Kahn, S.E., 2009. Oral Disposition Index Predicts the Development of Future Diabetes Above and Beyond Fasting and 2-h Glucose Levels. *Diabetes Care* 32, 335–341. <https://doi.org/10.2337/dc08-1478>

Valdés, M., Calzada, F., Mendieta-Wejebe, J.E., Merlín-Lucas, V., Velázquez, C., Barbosa, E., 2020. Antihyperglycemic Effects of *Annona diversifolia* Safford and Its Acyclic Terpenoids: α -Glucosidase and Selective SGLT1 Inhibitors. *Molecules* 25, 3361. <https://doi.org/10.3390/molecules25153361>

Val-Laillet, D., 2019. Review: Impact of food, gut-brain signals and metabolic status on brain activity in the pig model: 10 years of nutrition research using in vivo brain imaging. *Animal* 13, 2699–2713. <https://doi.org/10.1017/S1751731119001745>

van Can, J.G.P., van Loon, L.J.C., Brouns, F., Blaak, E.E., 2012. Reduced glycaemic and insulinaemic responses following trehalose and isomaltulose ingestion: implications for postprandial substrate use

- in impaired glucose-tolerant subjects. *Br J Nutr* 108, 1210–1217. <https://doi.org/10.1017/S0007114511006714>
- van Veldhuisen, S.L., Gorter, T.M., van Woerden, G., de Boer, R.A., Rienstra, M., Hazebroek, E.J., van Veldhuisen, D.J., 2022. Bariatric surgery and cardiovascular disease: a systematic review and meta-analysis. *European Heart Journal* 43, 1955–1969. <https://doi.org/10.1093/eurheartj/ehac071>
- Vandeputte, D., Falony, G., Vieira-Silva, S., Wang, J., Sailer, M., Theis, S., Verbeke, K., Raes, J., 2017. Prebiotic inulin-type fructans induce specific changes in the human gut microbiota. *Gut* 66, 1968–1974. <https://doi.org/10.1136/gutjnl-2016-313271>
- Vega-López, S., Ausman, L.M., Griffith, J.L., Lichtenstein, A.H., 2007. Interindividual Variability and Intra-Individual Reproducibility of Glycemic Index Values for Commercial White Bread. *Diabetes Care* 30, 1412–1417. <https://doi.org/10.2337/dc06-1598>
- Velasquez-Mieyer, P., Perez-Faustinelli, S., Cowan, P.A., 2005. Identifying Children at Risk for Obesity, Type 2 Diabetes, and Cardiovascular Disease. *Diabetes Spectrum* 18, 213–220. <https://doi.org/10.2337/diaspect.18.4.213>
- Vella, A., Rizza, R.A., 2009. Application of Isotopic Techniques Using Constant Specific Activity or Enrichment to the Study of Carbohydrate Metabolism. *Diabetes* 58, 2168–2174. <https://doi.org/10.2337/db09-0318>
- Verhaeghe, R., Zerrweck, C., Hubert, T., Tréchet, B., Gmyr, V., D’Herbomez, M., Pigny, P., Pattou, F., Caiazzo, R., 2014. Gastric Bypass Increases Postprandial Insulin and GLP-1 in Nonobese Minipigs. *Eur Surg Res* 52, 41–49. <https://doi.org/10.1159/000355678>
- Vigneshwaran, B., Wahal, A., Aggarwal, S., Priyadarshini, P., Bhattacharjee, H., Khadgawat, R., Yadav, R., 2016a. Impact of Sleeve Gastrectomy on Type 2 Diabetes Mellitus, Gastric Emptying Time, Glucagon-Like Peptide 1 (GLP-1), Ghrelin and Leptin in Non-morbidly Obese Subjects with BMI 30-35.0 kg/m²: a Prospective Study. *Obes Surg* 26, 2817–2823. <https://doi.org/10.1007/s11695-016-2226-9>
- Vigneshwaran, B., Wahal, A., Aggarwal, S., Priyadarshini, P., Bhattacharjee, H., Khadgawat, R., Yadav, R., 2016b. Impact of Sleeve Gastrectomy on Type 2 Diabetes Mellitus, Gastric Emptying Time, Glucagon-Like Peptide 1 (GLP-1), Ghrelin and Leptin in Non-morbidly Obese Subjects with BMI 30-35.0 kg/m²: a Prospective Study. *Obesity surgery* 26. <https://doi.org/10.1007/s11695-016-2226-9>
- Vlachos, D., Malisova, S., Lindberg, F.A., Karaniki, G., 2020. Glycemic Index (GI) or Glycemic Load (GL) and Dietary Interventions for Optimizing Postprandial Hyperglycemia in Patients with T2 Diabetes: A Review. *Nutrients* 12, 1561. <https://doi.org/10.3390/nu12061561>
- von Wilmowsky, C., Schlegel, K.A., Baran, C., Nkenke, E., Neukam, F.W., Moest, T., 2016. Peri-implant defect regeneration in the diabetic pig: A preclinical study. *Journal of Cranio-Maxillofacial Surgery* 44, 827–834. <https://doi.org/10.1016/j.jcms.2016.04.002>
- Wachters-Hagedoorn, R.E., Priebe, M.G., Heimweg, J.A.J., Heiner, A.M., Englyst, K.N., Holst, Jens.J., Stellaard, F., Vonk, R.J., 2006. The Rate of Intestinal Glucose Absorption Is Correlated with Plasma Glucose-Dependent Insulinotropic Polypeptide Concentrations in Healthy Men. *The Journal of Nutrition* 136, 1511–1516. <https://doi.org/10.1093/jn/136.6.1511>

- Wang, G., Agenor, K., Pizot, J., Kotler, D.P., Harel, Y., Van Der Schueren, B.J., Quercia, I., McGinty, J., Laferrère, B., 2012. Accelerated gastric emptying but no carbohydrate malabsorption 1 year after gastric bypass surgery (GBP). *Obes Surg* 22, 1263–1267. <https://doi.org/10.1007/s11695-012-0656-6>
- Wang, L., Yang, H., Huang, H., Zhang, C., Zuo, H.-X., Xu, P., Niu, Y.-M., Wu, S.-S., 2019. Inulin-type fructans supplementation improves glycemic control for the prediabetes and type 2 diabetes populations: results from a GRADE-assessed systematic review and dose-response meta-analysis of 33 randomized controlled trials. *J Transl Med* 17, 410. <https://doi.org/10.1186/s12967-019-02159-0>
- Wang, P., Sun, H., Maitiabula, G., Zhang, L., Yang, J., Zhang, Y., Gao, X., Li, J., Xue, B., Li, C.-J., Wang, X., 2023. Total parenteral nutrition impairs glucose metabolism by modifying the gut microbiome. *Nat Metab* 5, 331–348. <https://doi.org/10.1038/s42255-023-00744-8>
- Wang, X., Li, Q., Liu, Y., Jiang, H., Chen, W., 2021. Intermittent fasting versus continuous energy-restricted diet for patients with type 2 diabetes mellitus and metabolic syndrome for glycemic control: A systematic review and meta-analysis of randomized controlled trials. *Diabetes Research and Clinical Practice* 179, 109003. <https://doi.org/10.1016/j.diabres.2021.109003>
- Wang, X., Xie, C., Marathe, C.S., Malbert, C.-H., Horowitz, M., Jones, K.L., Rayner, C.K., Sun, Z., Wu, T., 2020. Disparities in gastric emptying and postprandial glycaemia between Han Chinese and Caucasians with type 2 diabetes. *Diabetes Research and Clinical Practice* 159, 107951. <https://doi.org/10.1016/j.diabres.2019.107951>
- Wang, Y., Zhou, X., Xiang, X., Miao, M., 2022. Association of Slowly Digestible Starch Intake with Reduction of Postprandial Glycemic Response: An Update Meta-Analysis. *Foods* 12, 89. <https://doi.org/10.3390/foods12010089>
- Warner, S.O., Wadian, A.M., Smith, M., Farmer, B., Dai, Y., Sheanon, N., Edgerton, D.S., Winnick, J.J., 2021. Liver glycogen-induced enhancements in hypoglycemic counterregulation require neuroglucopenia. *American Journal of Physiology-Endocrinology and Metabolism* 320, E914–E924. <https://doi.org/10.1152/ajpendo.00501.2020>
- Wei, J., Ouyang, H., Wang, Y., Pang, D., Cong, N.X., Wang, T., Leng, B., Li, D., Li, X., Wu, R., Ding, Y., Gao, F., Deng, Y., Liu, B., Li, Z., Lai, L., Feng, H., Liu, G., Deng, X., 2012. Characterization of a hypertriglyceridemic transgenic miniature pig model expressing human apolipoprotein CIII. *FEBS J* 279, 91–99. <https://doi.org/10.1111/j.1742-4658.2011.08401.x>
- Weyer, C., Bogardus, C., Mott, D.M., Pratley, R.E., 1999. The natural history of insulin secretory dysfunction and insulin resistance in the pathogenesis of type 2 diabetes mellitus. *J. Clin. Invest.* 104, 787–794. <https://doi.org/10.1172/JCI7231>
- Wilcock, C., Bailey, C.J., 1991. Reconsideration of inhibitory effect of metformin on intestinal glucose absorption. *J Pharm Pharmacol* 43, 120–121. <https://doi.org/10.1111/j.2042-7158.1991.tb06645.x>
- Woerle, H.-J., Albrecht, M., Linke, R., Zschau, S., Neumann, C., Nicolaus, M., Gerich, J., Göke, B., Schirra, J., 2008. Importance of changes in gastric emptying for postprandial plasma glucose fluxes in healthy humans. *American Journal of Physiology-Endocrinology and Metabolism* 294, E103–E109. <https://doi.org/10.1152/ajpendo.00514.2007>
- Wolever, T.M., Jenkins, D.J., Jenkins, A.L., Josse, R.G., 1991. The glycemic index: methodology and clinical implications. *The American Journal of Clinical Nutrition* 54, 846–854.

- Wolever, T.M., Nuttall, F.Q., Lee, R., Wong, G.S., Josse, R.G., Csima, A., Jenkins, D.J., 1985. Prediction of the Relative Blood Glucose Response of Mixed Meals Using the White Bread Glycemic Index. *Diabetes Care* 8, 418–428. <https://doi.org/10.2337/diacare.8.5.418>
- Wolever, T.M.S., Tosh, S.M., Spruill, S.E., Jenkins, A.L., Ezatagha, A., Duss, R., Johnson, J., Chu, Y., Steinert, R.E., 2020. Increasing oat β -glucan viscosity in a breakfast meal slows gastric emptying and reduces glycemic and insulinemic responses but has no effect on appetite, food intake, or plasma ghrelin and PYY responses in healthy humans: a randomized, placebo-controlled, crossover trial. *The American Journal of Clinical Nutrition* 111, 319–328. <https://doi.org/10.1093/ajcn/nqz285>
- World Health Organization, 2021. Obesity and overweight [WWW Document]. URL <https://www.who.int/news-room/fact-sheets/detail/obesity-and-overweight> (accessed 2.6.23).
- World Health Organization, International Diabetes Federation, 2006. Definition and diagnosis of diabetes mellitus and intermediate hyperglycaemia : report of a WHO/IDF consultation. World Health Organization, Geneva.
- Worwag, E.M., Craig, R.M., Jansyn, E.M., Kirby, D., Hubler, G.L., Atkinson, A.J., 1987. D-Xylose absorption and disposition in patients with moderately impaired renal function. *Clin Pharmacol Ther* 41, 351–357. <https://doi.org/10.1038/clpt.1987.38>
- Wright, E.M., Loo, D.D.F., Hirayama, B.A., 2011. Biology of Human Sodium Glucose Transporters. *Physiological Reviews* 91, 733–794. <https://doi.org/10.1152/physrev.00055.2009>
- Wu, H., Tremaroli, V., Bäckhed, F., 2015. Linking Microbiota to Human Diseases: A Systems Biology Perspective. *Trends in Endocrinology & Metabolism* 26, 758–770. <https://doi.org/10.1016/j.tem.2015.09.011>
- Wu, T., Rayner, C.K., Jones, K.L., Xie, C., Marathe, C., Horowitz, M., 2020. Role of intestinal glucose absorption in glucose tolerance. *Current Opinion in Pharmacology* 55, 116–124. <https://doi.org/10.1016/j.coph.2020.10.017>
- Wu, T., Xie, C., Wu, H., Jones, K.L., Horowitz, M., Rayner, C.K., 2017. Metformin reduces the rate of small intestinal glucose absorption in type 2 diabetes: WU ET AL. *Diabetes Obes Metab* 19, 290–293. <https://doi.org/10.1111/dom.12812>
- Wyngaarden, J.B., Segal, S., Foley, J.B., 1957. Physiological Disposition and Metabolic Fate of Infused Pentoses in Man. *J. Clin. Invest.* 36, 1395–1407. <https://doi.org/10.1172/JCI103539>
- Xie, C., Huang, W., Watson, L.E., Soenen, S., Young, R.L., Jones, K.L., Horowitz, M., Rayner, C.K., Wu, T., 2022. Plasma GLP-1 Response to Oral and Intraduodenal Nutrients in Health and Type 2 Diabetes- Impact on Gastric Emptying. *J Clin Endocrinol Metab* 107, e1643–e1652. <https://doi.org/10.1210/clinem/dgab828>
- Xie, C., Jones, K.L., Rayner, C.K., Wu, T., 2020. Enteroendocrine Hormone Secretion and Metabolic Control: Importance of the Region of the Gut Stimulation. *Pharmaceutics* 12, 790. <https://doi.org/10.3390/pharmaceutics12090790>
- Yahaya, T.O., Yusuf, A.B., Danjuma, J.K., Usman, B.M., Ishiaku, Y.M., 2021. Mechanistic links between vitamin deficiencies and diabetes mellitus: a review. *Egyptian Journal of Basic and Applied Sciences* 8, 189–202. <https://doi.org/10.1080/2314808X.2021.1945395>

- Yan, S., Sun, F., Li, Z., Xiang, J., Ding, Y., Lu, Z., Tian, Y., Chen, H., Zhang, J., Wang, Y., Song, P., Zhou, L., Zheng, S., 2013. Reduction of Intestinal Electrogenic Glucose Absorption After Duodenojejunal Bypass in a Mouse Model. *OBES SURG* 23, 1361–1369. <https://doi.org/10.1007/s11695-013-0954-7>
- Yasutake, H., Goda, T., Takase, S., 1995. Dietary regulation of sucrase-isomaltase gene expression in rat jejunum. *Biochim Biophys Acta* 1243, 270–276. [https://doi.org/10.1016/0304-4165\(94\)00143-I](https://doi.org/10.1016/0304-4165(94)00143-I)
- Yip, R.G.C., Wolfe, M.M., 2000. GIP Biology and Fat Metabolism. *Life Sciences* 66, 91–103. [https://doi.org/10.1016/s0024-3205\(99\)00314-8](https://doi.org/10.1016/s0024-3205(99)00314-8)
- Yoshizane, C., Mizote, A., Yamada, M., Arai, N., Arai, S., Maruta, K., Mitsuzumi, H., Ariyasu, T., Ushio, S., Fukuda, S., 2017. Glycemic, insulinemic and incretin responses after oral trehalose ingestion in healthy subjects. *Nutrition Journal* 16, 9. <https://doi.org/10.1186/s12937-017-0233-x>
- Young, A., Denaro, M., 1998. Roles of amylin in diabetes and in regulation of nutrient load. *Nutrition* 14, 524–527. [https://doi.org/10.1016/s0899-9007\(98\)00044-6](https://doi.org/10.1016/s0899-9007(98)00044-6)
- Young, R.L., Chia, B., Isaacs, N.J., Ma, J., Khoo, J., Wu, T., Horowitz, M., Rayner, C.K., 2013. Disordered Control of Intestinal Sweet Taste Receptor Expression and Glucose Absorption in Type 2 Diabetes. *Diabetes* 62, 3532–3541. <https://doi.org/10.2337/db13-0581>
- Yuasa, H., Kawanishi, K., Watanabe, J., 1995. Effects of Ageing on the Oral Absorption of D-Xylose in Rats. *Journal of Pharmacy and Pharmacology* 47, 576–580. <https://doi.org/10.1111/j.2042-7158.1995.tb05813.x>
- Yuasa, H., Kuno, C., Watanabe, J., 1997. Comparative Assessment of D-Xylose Absorption between Small Intestine and Large Intestine. *Journal of Pharmacy and Pharmacology* 49, 26–29. <https://doi.org/10.1111/j.2042-7158.1997.tb06746.x>
- Zafar, M.I., Mills, K.E., Zheng, J., Regmi, A., Hu, S.Q., Gou, L., Chen, L.-L., 2019. Low-glycemic index diets as an intervention for diabetes: a systematic review and meta-analysis. *The American Journal of Clinical Nutrition* 110, 891–902. <https://doi.org/10.1093/ajcn/nqz149>
- Zambrowicz, B., Freiman, J., Brown, P.M., Frazier, K.S., Turnage, A., Bronner, J., Ruff, D., Shadoan, M., Banks, P., Mseeh, F., Rawlins, D.B., Goodwin, N.C., Mabon, R., Harrison, B.A., Wilson, A., Sands, A., Powell, D.R., 2012. LX4211, a Dual SGLT1/SGLT2 Inhibitor, Improved Glycemic Control in Patients With Type 2 Diabetes in a Randomized, Placebo-Controlled Trial. *Clin Pharmacol Ther* 92, 158–169. <https://doi.org/10.1038/clpt.2012.58>
- Zeevi, D., Korem, T., Zmora, N., Israeli, D., Rothschild, D., Weinberger, A., Ben-Yacov, O., Lador, D., Avnit-Sagi, T., Lotan-Pompan, M., Suez, J., Mahdi, J.A., Matot, E., Malka, G., Kosower, N., Rein, M., Zilberman-Schapira, G., Dohnalová, L., Pevsner-Fischer, M., Bikovsky, R., Halpern, Z., Elinav, E., Segal, E., 2015. Personalized Nutrition by Prediction of Glycemic Responses. *Cell* 163, 1079–1094. <https://doi.org/10.1016/j.cell.2015.11.001>
- Zhang, L., Huang, Y., Wang, M., Guo, Y., Liang, J., Yang, X., Qi, W., Wu, Y., Si, J., Zhu, S., Li, Z., Li, R., Shi, C., Wang, S., Zhang, Q., Tang, Z., Wang, L., Li, K., Fei, J.-F., Lan, G., 2019. Development and Genome Sequencing of a Laboratory-Inbred Miniature Pig Facilitates Study of Human Diabetic Disease. *iScience* 19, 162–176. <https://doi.org/10.1016/j.isci.2019.07.025>
- Zhao, Y., Feng, H., Wang, Y., Jiang, L., Yan, J., Cai, W., 2023. Impaired FXR-CPT1a signaling contributes to parenteral nutrition-induced villus atrophy in short-bowel syndrome. *FASEB J* 37, e22713. <https://doi.org/10.1096/fj.202201527R>

Zhouyao, H., Malunga, L.N., Chu, Y.F., Eck, P., Ames, N., Thandapilly, S.J., 2022. The inhibition of intestinal glucose absorption by oat-derived avenanthramides. *J Food Biochem* 46, e14324. <https://doi.org/10.1111/jfbc.14324>

Zou, X., Ouyang, H., Yu, T., Chen, X., Pang, D., Tang, X., Chen, C., 2019. Preparation of a new type 2 diabetic miniature pig model via the CRISPR/Cas9 system. *Cell Death Dis* 10, 823. <https://doi.org/10.1038/s41419-019-2056-5>

Zubiaga, L., Briand, O., Auger, F., Touche, V., Hubert, T., Thevenet, J., Marciniak, C., Quenon, A., Bonner, C., Peschard, S., Raverdy, V., Daoudi, M., Kerr-Conte, J., Pasquetti, G., Koepsell, H., Zdzieblo, D., Mühlmann, M., Thorens, B., Delzenne, N.D., Bindels, L.B., Deprez, B., Vantghem, M.C., Laferrère, B., Staels, B., Huglo, D., Lestavel, S., Pattou, F., 2023. Oral metformin transiently lowers post-prandial glucose response by reducing the apical expression of sodium-glucose co-transporter 1 in enterocytes. *iScience* 26, 106057. <https://doi.org/10.1016/j.isci.2023.106057>

Zuckerman, M., Greller, H.A., Babu, K.M., 2015. A Review of the Toxicologic Implications of Obesity. *J. Med. Toxicol.* 11, 342–354. <https://doi.org/10.1007/s13181-015-0488-6>

List of communications

Published articles

Related to the subject of the thesis

Effects of subtotal pancreatectomy and long-term glucose and lipid overload on insulin secretion and glucose homeostasis in minipigs.

Goutchtat R, Quenon A, Clarisse M, Delalleau N, Coddeville A, Gobert M, Gmyr V, Kerr-Conte J, Pattou F, Hubert T. *Endocrinol Diabetes Metab.* 2023 Jul;6(4):e425. doi: 10.1002/edm2.425. Epub 2023 May 5. PMID: 37144278; PMCID: PMC10335612.

Related to laboratory animals

Long-Term Analgesia following a Single Application of Fentanyl Transdermal Solution in Pigs.

Goutchtat R*, Chetboun M*, Wiart JF, Gaulier JM, Pattou F, Allorge D, Hubert T. *Eur Surg Res.* 2021;62(2):115-120. doi: 10.1159/000516828. Epub 2021 Jun 24. PMID: 34167112.

Congress communications

Related to the subject of the thesis

Contribution of intestinal glucose absorption in type 2 diabetes onset and progression: retrospective studies in healthy minipigs and obese patients.

R. Goutchtat. 9th Diabetes Research School of the German Center of Diabetes Research (DZD): online lecture series, October 2021. **Oral communication.**

D-Xylose test as a biomarker for glucose intestinal absorption in humans and minipigs.

R. Goutchtat, C. Marciniak, R. Caiazzo, H. Verkindt, A. Quenon, T. Rabier, S. Lapière, V. Raverdy, T. Hubert and F. Pattou. 82nd scientific session of the American Diabetes Association (ADA). New Orleans, June 2022. **Poster.**

Oral D-Xylose plasma appearance as a biomarker for intestinal glucose absorption in minipigs.

R. Goutchtat, C. Marciniak, G. Baud, M. Gobert, V. Vangelder, A. Quenon, A. Dive, M. Pottier, T. Rabier, S. Lapière, V. Raverdy, R. Caiazzo, T. Hubert, F. Pattou. 58th annual meeting of the European Association for the Study of Diabetes (EASD). Stockholm, September 2022. **Oral communication.**

Oral D-Xylose plasma appearance as a biomarker for intestinal glucose absorption in minipigs and humans.

R. Goutchtat, C. Marciniak, A. Quenon, G. Baud, V. Vangelder, M. Gobert, A. Rémond, T. Rabier, S. Lapière, C. Louche-Pélissier, L. Meiller, V. Sauvinet, R. Caiazzo, H. Verkindt, V. Raverdy, J.-A. Nazare, T.

Hubert, F. Pattou. Metabolic Study Surgery Group (MSSG/AFERO) Annual Meeting. Paris, November 2022. **Oral communication.**

Le test oral au D-Xylose comme biomarqueur de l'absorption intestinale du glucose chez le Miniporc et l'Homme

R. Goutchtat, C. Marciniak, A. Quenon, G. Baud, V. Vangelder, M. Gobert, A. Rémond, T. Rabier, S. Lapière, C. Louche-Pélissier, L. Meiller, V. Sauvinet, R. Caiazzo, H. Verkindt, V. Raverdy, J.-A. Nazare, T. Hubert, F. Pattou. Congrès annuel de la société francophone du diabète (SFD). Montpellier, Mars 2023.

Poster.

Contribution of Intestinal Glucose Absorption on Postprandial Glycemic Response: oral D-Xylose plasma appearance as a biomarker for intestinal glucose absorption in minipigs and humans.

R. Goutchtat, C. Marciniak, A. Quenon, G. Baud, V. Vangelder, M. Gobert, A. Rémond, T. Rabier, S. Lapière, C. Louche-Pélissier, L. Meiller, V. Sauvinet, R. Caiazzo, H. Verkindt, V. Raverdy, J.-A. Nazare, T. Hubert, F. Pattou. 55th Congress of the European Society for Surgical Research (ESSR). Lille, June 2023.

Oral communication. Organization committee and moderation of a session.

Intestinal glucose transport, postprandial glucose response, and diabetes.

R. Goutchtat and F. Pattou. 26th Oxford Workshop of the European Association for the Study of Diabetes (EASD). Oxford, August 2023. **Oral communication.**

Related to laboratory animals

Long-term analgesia following single application of a fentanyl transdermal solution in pigs and rats.

R. Goutchtat. 55th Congress of the European Society for Surgical Research (ESSR) and 44th Congress of the Austrian Society for Surgical Research. Innsbruck (virtual), December 2020. **Oral Communication.**

My 3R in 180s: Long-term analgesia following single application of a fentanyl transdermal solution in pigs.

R. Goutchtat. 15th Congress of the Federation of European Laboratory Animal Science Association (FELASA). Marseille, June 2022. **Oral Communication.**

Raffinement des prélèvements et injections de sang : pose de cathéter veineux centraux de longue tenue chez le Porc.

R. Goutchtat, A. Quenon, T. Rabier, S. Lapière, J. François, M. Fourdrinier, A. Dive, F. Stevendart, M. Pottier et T. Hubert. 47^{ème} colloque de l'Association Française des Sciences et Techniques de l'Animal de Laboratoire (AFSTAL). Bordeaux, June 2023. **Oral Communication.**

Long-Term Analgesia following a Single Application of Fentanyl Transdermal Solution in Pigs

Rebecca Goutchtat^a Mikael Chetboun^a Jean-François Wiart^b
Jean-Michel Gaulier^b François Pattou^a Delphine Allorge^b Thomas Hubert^{a, c}

^aUniversité de Lille, Inserm, CHU Lille, Institut Pasteur Lille, Lille, France; ^bCHU Lille, Unité Fonctionnelle de Toxicologie, Lille, France; ^cUniversité de Lille, CHU Lille, Département Hospitalo-Universitaire de Recherche et d'Enseignement (DHURE), Lille, France

© Free Author
Copy - for per-
sonal use only

ANY DISTRIBUTION OF
THIS ARTICLE WITHOUT
WRITTEN CONSENT
FROM S. KARGER AG,
BASEL IS A VIOLATION
OF THE COPYRIGHT.

Written permission to
distribute the PDF will be
granted against payment
of a permission fee,
which is based on the
number of accesses
required. Please contact
permission@karger.com

Keywords

Analgesia · Fentanyl transdermal solution · Pain control · Pig · Surgery

Abstract

Introduction: In animal research, obtaining efficient and constant pain control is regulatory but challenging. The gold standard pain management consists of opioid analgesic administration, such as buprenorphine or fentanyl extended-release patches. However, as in all drugs with a short half-life time, repeated buprenorphine administrations are needed, leading to multiple injections that affect the research protocol. On the other hand, fentanyl patch efficacy is discussed in some species. These elements highlight the need of an optimal formulation of analgesic drugs for laboratory animals. In this study, we investigated how Recuvyra[®], a fentanyl transdermal solution (FTS), validated in dog perioperative pain management, could provide sustained analgesia after a single topical administration in pigs in a surgical context. **Methods:** A total of 11 minipigs were used in this study. As a preliminary experiment, two different doses were tested as a single application on five pigs: two pigs at full dose (2.6 mg/kg) and three pigs at half dose (1.3 mg/kg). Plasma fentanyl

dosages were performed during 4 consecutive days, using liquid chromatography with tandem mass spectrometry detection. The efficacy of FTS was then evaluated in a perioperative period. Six minipigs benefited from a surgical intervention comprising a laparotomy. The FTS was blotted on the skin in a single application 20 min before the surgical incision and plasma fentanyl dosages, clinical examination (body weight, food intake, heart rate, and body temperature) and pain assessment were performed for 7 consecutive days. **Results:** During the preliminary experiment, all fentanyl concentrations reached the minimum effective concentration (MEC) extrapolated in pigs (fentanylemia ≥ 0.2 ng/mL) throughout the 4 days. The half dose was chosen for the next step of the study. After the surgical intervention, all plasma fentanyl concentrations remained above the MEC up to 7 days post administration. Pig clinical examinations and pain evaluations showed efficient and constant pain control at the half dose, and few adverse events were observed. **Discussion and Conclusion:** This study confirms the pharmacological and clinical efficacy of FTS at 1.3 mg/kg in pigs throughout at least 7 postoperative days following laparotomy. The clinical

R. Goutchtat and M. Chetboun contributed equally to this work.

Long-term analgesia following a single application of fentanyl transdermal solution in pigs

Rebecca Goutchtat^{1,*}, Mikael Chetboun^{1,*}, Jean-François Wiart², Jean-Michel Gaulier², François Pattou¹, Delphine Allorge², Thomas Hubert^{1,3,#}

¹Univ. Lille, Inserm, CHU Lille, Institut Pasteur Lille, U1190 - Egid, F-59000 Lille, France

²CHU Lille, Unité Fonctionnelle de Toxicologie, F-59000, Lille, France

³Univ. Lille, CHU Lille, Département Hospitalo-Universitaire de Recherche et d'Enseignement (Dhure), F-59000, Lille, France

** Rebecca Goutchtat and Mikael Chetboun contributed equally to this work*

Short Title: Long-term analgesia with fentanyl in pigs

Corresponding author:

Thomas Hubert, Translational Research for Diabetes, U1190

1 Place de Verdun, F-59045 Lille Cedex – France

+33320627711

thomas.hubert@univ-lille.fr

Number of tables: 0

Number of figures: 3

Word count: 2649 (381 for the abstract and 2268 for the body text)

Key words: Analgesia, Fentanyl transdermal solution, Pain control, Pig, Surgery

Abstract

Introduction

In animal research, obtaining efficient and constant pain control is regulatory but challenging. The gold-standard pain management consists of opioid analgesic administration, such as buprenorphine or fentanyl extended-release patches. However, as in all drugs with a short half-life time, repeated buprenorphine administrations are needed, leading to multiple injections that affect the research protocol. On the other hand, fentanyl patch efficacy is discussed in some species. These elements highlight the need of an optimal formulation of analgesic drugs for laboratory animals. In this study, we investigated how Recuvyra[®], a Fentanyl Transdermal Solution (FTS), validated in dog perioperative pain management, could provide sustained analgesia after a single topical administration in pigs in a surgical context.

Methods

A total of eleven minipigs were used in this study. As a preliminary experiment, two different doses were tested as a single application on 5 pigs: 2 pigs at full dose (2.6 mg/kg) and 3 pigs at half dose (1.3 mg/kg). Plasma fentanyl dosages were performed during 4 consecutive days, using liquid chromatography with tandem mass spectrometry detection. The efficacy of the FTS was then evaluated in a perioperative period. Six minipigs benefited from a surgical intervention comprising a laparotomy. The FTS was blotted on the skin in a single application 20 minutes before the surgical incision and plasma fentanyl dosages, clinical examination (body weight, food intake, heart rate and body temperature) and pain assessment were performed for 7 consecutive days.

Results

During the preliminary experiment, all fentanyl concentrations reached the Minimum Effective Concentration (MEC) extrapolated in pigs (fentanyl_{emia} \geq 0.2 ng/mL) throughout the 4 days. The half dose was chosen for the next step of the study. After the surgical intervention, all the plasma fentanyl concentrations remained above the MEC up to 7 days post-administration. Pig clinical examinations and pain evaluations showed an efficient and constant pain control at the half dose and few adverse events were observed.

Discussion/Conclusion

This study confirms the pharmacological and clinical efficacy of the fentanyl transdermal solution at 1.3 mg/kg in pigs throughout at least 7 postoperative days following laparotomy. Clinical analgesic effect of the FTS appears more efficient and well-tolerated than the one observed with repeated injections of buprenorphine. This analgesic drug formulation could be universally used in animal research to provide optimal perioperative pain management and long-term analgesia.

Body Text

Introduction

Administration of efficient analgesia to research animals is guided by the ethical and regulatory principle of Refinement. The optimal analgesia has to be safe, effective and easy to use. However, obtaining a good and constant pain control without side effects remains challenging.

Gold-standard perioperative pain management consists of opioid analgesic administration. Nonsteroidal anti-inflammatory drugs are good antalgics but opioids have a better effect against pain as analgesics. Moreover, they indeed induce no anti-inflammatory bias compared to them (1).

Buprenorphine is currently the most used opioid analgesic in laboratory rodents and pigs (2,3). However, its efficiency after a single injection at the recommended dose lasts no more than 8-12 hours in different species (4,5). This involves repeated stressful and painful invasive intramuscular injections that can alter biological parameters and cause bias in scientific results (5).

Fentanyl is a strong agonist of μ -opioid receptors with 100-fold superior potency than morphine (6). Transdermal administration systems have been developed, such as extended-release patches, that provide continuous systemic delivery for up to 72 hours (6–9). Its efficacy is discussed in some large mammals, especially in pigs, because of the low adherence to the skin or the risk of ingestion (1,7,9–12).

Recuvyra® (Lilly-Elanco, Neuilly-sur-Seine, France) is a veterinary Fentanyl Transdermal Solution (FTS) validated for topical use in dogs. Drug marketing approval has been validated with efficient analgesia throughout 4 postoperative days with a single application at 2.6 mg/kg (13–16). A single application providing long-term analgesia would be highly beneficial and useful in animal research.

Several previous studies demonstrated the efficacy of this FTS in pain control in rats (17), non-human primates (1,18) and sheep (12). However, no study in pigs has been published yet. Our study consisted in testing the long-term effect of a single dose of FTS in pigs by evaluating its pharmacological and clinical efficacy in order to validate its use in this species.

Materials and Methods

Ethical statement

The protocol was approved by the local French Committee of Animal Research and Ethics (CEEA-75, n° 2019012812135146) according to the European legislation (2010/63/EU directive). All the procedures were performed in the agreed University and Hospital Department for Experimental Research (Dhure) in Lille, France.

Animals and housing

Eleven healthy 1-year adult male (n=6) and female (n=5) minipigs Göttingen-like weighing 39.0 ± 3.7 kg (Pannier, Wylder, France) were used for the study: it is a local strain of minipig crossed more than 30 years ago with the Göttingen strain. All animals were housed and enriched in individual boxes in conventional conditions. Water was provided *ad libitum* and food was given twice a day. The light/dark cycle was 12 hours of light and 12 hours of darkness with a temperature between 19 and 24°C. Pigs benefited from a 15-day acclimatization period.

Study design

A preliminary step (n=5) was first performed to optimize the adequate dose to administrate: two pigs at full dose (2.6 mg/kg) and three pigs at half dose (1.3 mg/kg), as previously described (18). Plasma fentanyl levels were determined. Then, the analgesic effect was studied at half dose in a surgical context of laparotomy (n=6). Plasma fentanyl concentrations, clinical examinations and pain assessments were performed throughout 8 days.

Anaesthesia and surgical interventions

Anaesthesia

All surgical procedures were performed under general anesthesia, after an overnight fasting: premedication with synergistic intramuscular injection of xylazine (3 mg/kg, Sedaxylan®, Dechra Pharmaceutical PLC, France) and ketamine (5 mg/kg, Ketamine 1000®, Virbac, Carros, France), then isoflurane (0.5 to 2%, IsoFlo, Zoetis, Malakoff, France) after endotracheal intubation.

Implantation of a Central Venous Catheter

To allow blood sampling, a Central Venous Catheter (CVC) was surgically applied 1 week before the FTS application. Skin and muscle were incised in the neck area and the external jugular vein was exposed. The catheter (Hickman* 9.6F Single-Lumen CV Catheter, Bard Access System, Salt Lake City, USA) was tunneled across the subcutaneous tissue from the incision zone to the dorsal area of the neck, implanted and fixed to the vein (Vicryl Bobine 2/0, Ethicon, Issy-les-Moulineaux, France). Muscular and cutaneous layers were then closed by simple overlock (respectively Polysorb 2/0, Medtronic, Pont-de-Claix, France and Mersilene 1, Ethicon, Issy-les-Moulineaux, France). Analgesia was assured by a pre-operative intramuscular injection of buprenorphine (15 µg/kg, Bupaq, Virbac, Carros France).

Surgical interventions with laparotomy

The pigs included in this study underwent 2 different surgical interventions including a laparotomy: tissue biopsies for 3 pigs and tissue biopsies associated with a portal vein catheter implantation for 3 pigs. The abdominal wall was then closed by simple overlock in 3 layers: peritoneum and muscles (PDS 1, Ethicon, Issy-les-Moulineaux, France), subcutaneous (Polysorb 2/0, Medtronic, Pont-de-Claix, France) and cutaneous (Mersilene 1, Ethicon, Issy-les-Moulineaux, France). The two same vet surgeons performed the laparotomies, including one with 20 years of surgical practice in this field. These surgical

procedures lasted about 2 hours from the surgical incision to the abdominal wall closure and all the good surgical practices, such as good aseptic conditions, mini-invasive laparotomy, hemostasis management with electrosurgery and analgesics were performed.

Fentanyl application

The FTS was blotted around 45 minutes before the surgical incision on the skin in the dorsal interscapular region. The adequate volume of solution was administrated using the specific micropipette provided.

Daily clinical monitoring and pain assessment

Evolution of body weight, food intake, body temperature and heart rate were evaluated by a veterinary surgeon. Manifestations of narcotization were assessed by using a sedation score scale, as previously described in dogs (14), from 0 (absence of sedation) to 4 (coma). Pain assessment was measured by two out of three evaluators using a visual analogue scale (from 0 to 100) previously established in pigs using 5 different criteria (19): 1/ Level of quietness, 2/ Response to touch, 3/ Ability to ambulate, 4/ Vocalization, 5/ Overall pain level assessment. The higher the score, the more intense the perceived pain. Clinical monitoring and pain assessments were performed 6 hours after the FTS administration, twice a day (9 am and 4 pm) during 3 days, and then once a day (9 am) until the end of the follow-up.

Blood sampling and conservation

Preliminary step: blood samples were collected by the CVC after the FTS administration every hour during the first 8 hours and every morning until day 4. Surgical step: blood sample collection was performed every hour during the first 6 hours and every morning until day 7. Blood was collected into 6-mL lithium-heparin blood tubes, centrifugated at 4000 rpm at 4°C for 10 minutes before the plasma was recovered and stored at -80°C until analysis.

Fentanyl analysis

Pig plasma was pH-adjusted and the analytes were extracted by using a liquid–liquid extraction technique. Analysis was performed using liquid chromatographic separation, positive-ion electrospray and tandem mass spectrometry for detection (limit of detection and quantification are 0.08 and 0.1 ng/mL, respectively).

Results

All pigs remained healthy and no surgical complication appeared during the postoperative period. Some adverse events (hyporeactivity, moderate agitation, tachycardia, hyperthermia, polypnea and ataxia) appeared during the preliminary step (non-operated) and lasted no more than 24 hours. No animal required an antagonization by naloxone.

Preliminary step

Evolution of the fentanyl concentrations at full (2.6 mg/kg) and half (1.3 mg/kg) doses are reported in **Figure 1**. Within the first hour post-administration, plasma fentanyl concentrations reached the Minimum Effective Concentration (MEC) reported in pigs, regardless of the dose (**Figure 1A**). All plasma fentanyl concentrations remained above the MEC during the first 8 hours (**Figure 1A**).

On **Figure 1B**, the evolution of the plasma fentanyl concentration during 4 days post-administration is reported for two pigs: one at full dose and one at half dose. All the values exceeded the MEC during the entire time of the study.

The half dose was thus chosen for the next step of the study.

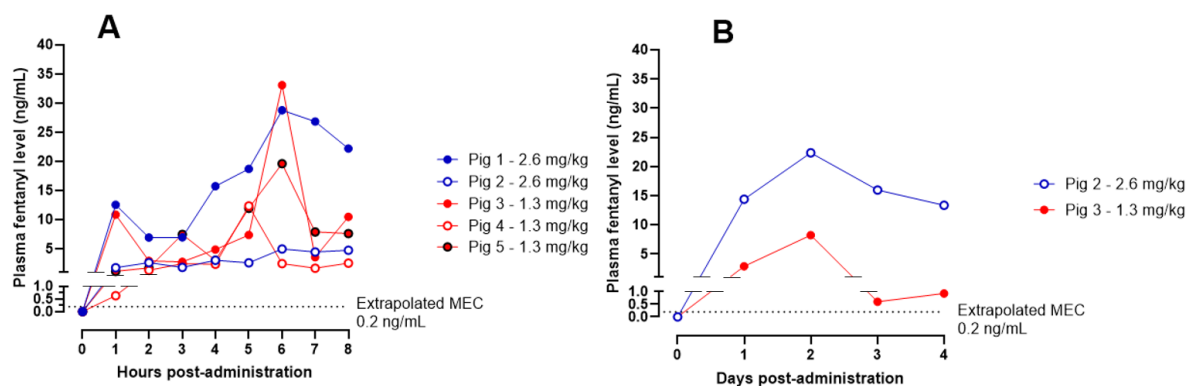


Figure 1: Plasma fentanyl concentrations (ng/mL) during the preliminary step after a single topical application at full (2.6 mg/kg) or half dose (1.3 mg/kg) (n = 5).

(A) During the first eight hours.

(B) During four consecutive days post-administration. The grid line shows the Minimum Effective Concentration (MEC) reported in pigs (0.2 ng/mL).

Perioperative period

Fentanyl concentrations

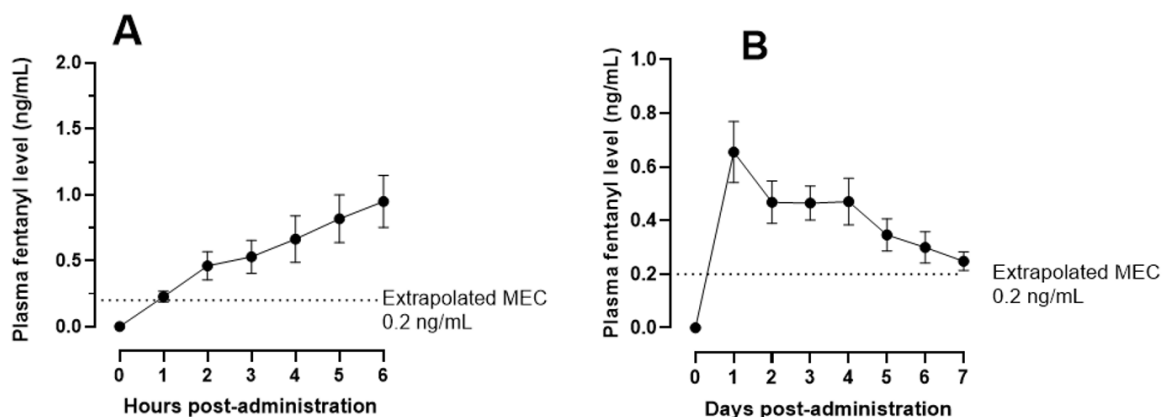


Figure 2: Plasma fentanyl concentrations (ng/mL) during the perioperative period after a single topical administration at half dose (1.3 mg/kg) (n = 6) (Mean ± SEM).

(A) During the first six hours.

(B) During seven consecutive days post-administration. The grid line shows the Minimum Effective Concentration (MEC) reported in pigs (0.2 ng/mL).

All fentanyl measurements were performed following the FTS application at half dose (1.3 mg/kg) and the results (mean \pm SEM) are shown in **Figure 2**. All plasma fentanyl concentrations reached the MEC within the first hour (**Figure 2A**) and remained above the MEC until 4 days post-administration (0.47 ± 0.09 ng/mL), and even up to 7 days (0.25 ± 0.03 ng/mL) (**Figure 2B**).

Clinical parameters

No weight loss was noticed at the end of the study (41.5 ± 3.9 kg vs 41.3 ± 3.6 kg before surgery). Pigs were fasted at day 0 and recovered more than 75% of the initial food intake by day 3 (598 ± 121.5 g vs 775.5 ± 10 g before the surgery). Heart rate and body temperature followed physiological values throughout the whole study. Two pigs had a sedation score of 1 and 4 pigs a score of 0.5 24 hours after the FTS administration. Sedation scores were 0 for all pigs from day 2.

Pain assessment

The surgical procedure was classified as moderate. The pain scores evaluated by the visual analogue scale were subjective, so the sensitivity of the score depends on the sensibility of the evaluator. However, we can considerate the pain as low with a score lower than 30, as moderate with a score between 30 and 60 and as severe with a score higher than 60. Pain score results concerning each of the 5 criteria are shown in Figure 3 (mean \pm SEM). Maximum scores for the criteria 3 and 5 (36 ± 11 and 30 ± 2 , respectively) were achieved 6 hours after the FTS and maximum scores for the criteria 1, 2, and 4 (18 ± 4 , 12 ± 3 and 10 ± 3 , respectively) were observed 24 hours after the surgery (**Figure 3**). From 48 hours after the surgery, all scores were below 14 ± 2 (obtained on criterion 5) (**Figure 3**).

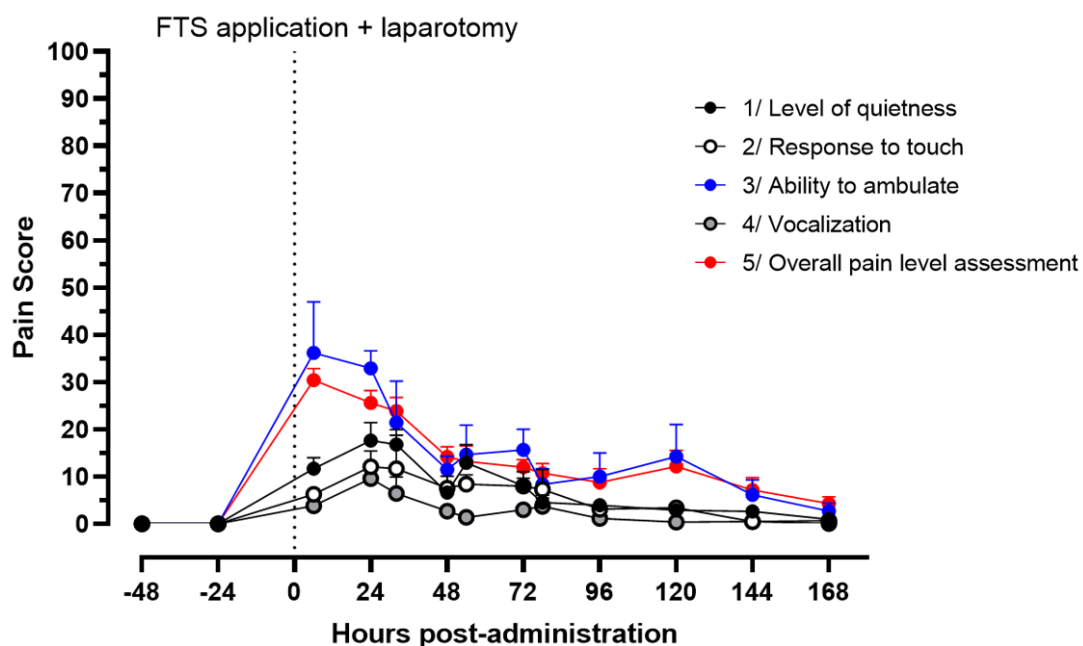


Figure 3: Evolution of the pain scores associated to each criterion defined by the visual analogue scale: Level of quietness, Response to touch, Ability to ambulate, Vocalization, Overall pain assessment, during seven consecutive days post-surgery (n = 6) (Mean ± SEM).

FTS = Fentanyl Transdermal Solution.

Discussion

During the preliminary experiment, our results demonstrated the pharmacological effectiveness of the FTS at full and half doses and determined the choice of using a half dose in pigs. At half dose in the surgical context, all fentanyl concentrations were above the MEC during at least 7 days, which is longer than the minimum analgesic efficacy period described in dogs at full dose (13–16). The postoperative clinical follow-up showed an effective pain management, as indicated by the low scores obtained from the visual pain evaluation and the clinical parameters (no tachycardia or hyperthermia). Moreover, a quick recovery in food intake was also observed.

Only a discrete sedation was observed during the first 24 postoperative hours. At the preliminary step (pigs without surgery), 2 half-dose-treated pigs exhibited a mild agitation leading to tachycardia, polypnea, and moderate hyperthermia associated to hyporeactivity and ataxia. This moderate agitation could be due to a feeling of dysphoria by the pigs, and as generally described in humans (20), when the use of opioids is not appropriate. Without pain, the affinity of opioids for μ 1 receptors decreases. This is why fentanyl comes to fix itself on μ 2 receptors, responsible of the side effects (21). The issue remains about the value of the Minimum Effective Concentration (MEC) of fentanyl in animal species other than dogs (8,9,12). In humans, some studies have discussed the minimum levels of 0.23 (22), 0.63 (6) or 1 ng/mL (23). In dogs, average plasma concentration \geq 0.6 ng/mL is commonly considered as being analgesic (24). In pigs, there is no consensus about the MEC value but some authors proposed an extrapolated therapeutic range. This range was calculated from species for which the MEC is known, considering the variations of several physiological and metabolic parameters. The minimal value of this extrapolated therapeutic range was then estimated at 0.2 ng/mL (8,9). Accordingly, this value was retained for the MEC in the present study.

A high interindividual variability of plasma fentanyl concentrations was noticed independently of the dose at the preliminary step. This variability has already been described in pigs, but also mentioned in other species (7,12). Heterogeneous absorption across the epidermis, dermis, and hypodermis depending on the thickness of the subcutaneous adipose tissue and its vascularization, drug distribution depending on the animal volume and metabolic clearance, as well as the level of animal stress were all suggested to explain this variability (8,25). Lower interindividual variability was observed in our surgical context, but the explanation remains unclear. Moreover, fentanyl concentrations measured in this group were globally lower than those measured after the use of the

same dose (1.3 mg/kg) in the preliminary step. Indeed, the affinity of fentanyl for μ_1 receptors is lower without pain, which may have contributed to increase the circulating concentration in this group (21). Furthermore, fentanyl pharmacokinetic properties can be influenced by changes in hepatic blood flow induced by anesthesia (26), that may have led to a reduction of plasma fentanyl concentrations in operated pigs.

This study presents some limitations. Like all studies in large mammals, the sample size is small. Our study proposed only descriptive results. We noted in our department that the analgesia effect is better with the use of the FTS than with buprenorphine or fentanyl patch. For these ethical reasons, we decided not to compare the analgesic effect of the FTS to buprenorphine injections.

In conclusion, the current study validates the use of a Fentanyl Transdermal Solution Recuvyra® in a single topical application at half dose in pigs. Analgesia was optimized during at least 7 days, confirmed by clinical and visual pain evaluation and plasma fentanyl measurements without adverse effects. This safe and useful formulation could be used universally in many animal research species to provide optimal perioperative pain management and long-term analgesia. Unfortunately, Recuvyra® is no longer available so far because of a too small market. Moreover, there is currently no alternative product as effective and easy to use. This is why there are many expectations concerning an eventual new approval by the European Medical Agency with another laboratory. Discussions are still pending.

Statements

Acknowledgments

The authors warmly thank Martin Fourdrinier, Audrey Quenon, Thibaud Rabier, Sarah Lapière, Arnold Dive, Michel Pottier, Louis Ballet, Franck Stevendart, Christian Sueur, Marion Paurisse, Francis Cherquefosse and Sabrina Decroix (DHURE), as well as Amanda Elledge and Julien Thevenet (U1190).

Statement of Ethics

This present study involving animals was approved by the local French Committee of Animal Research and Ethics (CEEA-75 of Nord-Pas de Calais, France, n° 2019012812135146) according to the European legislation (2010/63/EU directive) and followed the internationally recognized ARRIVE guidelines.

Conflict of Interest Statement

The authors have no conflicts of interest to declare.

Funding sources

The authors want to thank specifically the Lille University Hospital for all dosages and the European Genomic Institute for Diabetes (Egid) for its high and precious contribution to animal disposal and housing.

Author contributions

Rebecca Goutchtat and Mikael Chetboun were in charge of the project design and technical realization and also of the article redaction. Jean-François Wiart performed the plasma fentanyl dosages. Jean-Michel Gaulier and Delphine Allorge were responsible for fentanyl dosages and analysis of the results. François Pattou allowed the financial realization of this project. Thomas Hubert (corresponding author) was at the origin of the project conception and managed it.



References

1. Carlson AM, Iii RK, Fetterer DP, Rico PJ, Bailey EJ. Pharmacokinetics of 2 Formulations of Transdermal Fentanyl in Cynomolgus Macaques. *J Am Assoc Lab Anim Sci.* 2016 Jul;55(4):7.
2. Bradbury AG, Eddleston M, Clutton RE. Pain management in pigs undergoing experimental surgery; a literature review (2012–4). *Br J Anaesth.* 2016 Jan;116(1):37-45.
3. Stokes EL, Flecknell PA, Richardson CA. Reported analgesic and anaesthetic administration to rodents undergoing experimental surgical procedures. *Lab Anim.* 2009 Apr;43(2):149-54.
4. Gades NM, Danneman PJ, Wixson SK, Tolley EA. The magnitude and duration of the analgesic effect of morphine, butorphanol, and buprenorphine in rats and mice. *Contemp Top Lab Anim Sci.* 2000 Mar;39(2):8-13.
5. Harvey-Clark CJ, Gillespie K, Riggs KW. Transdermal fentanyl compared with parenteral buprenorphine in post-surgical pain in swine: a case study. *Lab Anim.* 2000 Oct;34(4):386-98.
6. Nelson L, Schwaner R. Transdermal fentanyl: Pharmacology and toxicology. *J Med Toxicol.* 2009 Dec;5(4):230-41.
7. Malavasi LM, Augustsson H, Jensen-Waern M, Nyman G. The Effect of Transdermal Delivery of Fentanyl on Activity in Growing Pigs. 2005 Jun;46(3):9.
8. Osorio Lujan S, Habre W, Daali Y, Pan Z, Kronen PW. Plasma concentrations of transdermal fentanyl and buprenorphine in pigs (*Sus scrofa domestica*). *Vet Anaesth Analg.* 2017 May;44(3):665-75.
9. Wilkinson A, Thomas M, Morse B. Evaluation of a Transdermal Fentanyl System in Yucatan Miniature Pigs. *Contemp Top Lab Anim Sci.* 2001 May;40(3):12-6.
10. Ahren B, Soma L, Rudy J, Uboh C, Schaer T. Pharmacokinetics of fentanyl administered transdermally and intravenously in sheep. *Am J Vet Res.* 2010 May;71:1127-32.
11. Christou C, Oliver RA, Rawlinson J, Walsh WR. Transdermal fentanyl and its use in ovine surgery. *Res Vet Sci.* 2015 Jun;100:252-6.
12. Jen KY, Dyson MC, Lester PA, Nemzek JA. Pharmacokinetics of a Transdermal Fentanyl Solution in Suffolk Sheep (*Ovis aries*). *J Am Assoc Lab Anim Sci.* 2017 Sep;56(5):8.
13. Freise KJ, Savides MC, Riggs KL, Owens JG, Newbound GC, Clark TP. Pharmacokinetics and dose selection of a novel, long-acting transdermal fentanyl solution in healthy laboratory Beagles: PK of transdermal fentanyl in laboratory dogs. *J Vet Pharmacol Ther.* 2012 Aug;35:21-6.
14. Martinez SA, Wilson MG, Linton DD, Newbound GC, Freise KJ, Lin T-L, et al. The safety and effectiveness of a long-acting transdermal fentanyl solution compared with oxymorphone for the control of postoperative pain in dogs: a randomized, multicentered clinical study. *J Vet Pharmacol Ther.* 2014 Aug;37(4):394-405.

15. Linton DD, Wilson MG, Newbound GC, Freise KJ, Clark TP. The effectiveness of a long-acting transdermal fentanyl solution compared to buprenorphine for the control of postoperative pain in dogs in a randomized, multicentered clinical study: Transdermal fentanyl clinical study. *J Vet Pharmacol Ther.* 2012 Aug;35:53-64.
16. Kukanich B, Clark TP. The history and pharmacology of fentanyl: relevance to a novel, long-acting transdermal fentanyl solution newly approved for use in dogs: Long-acting transdermal fentanyl solution. *J Vet Pharmacol Ther.* 2012 Aug;35:3-19.
17. Clemensen J, Rasmussen LV, Abelson KSP. Transdermal Fentanyl Solution Provides Long-term Analgesia in the Hind-paw Incisional Model of Postoperative Pain in Male Rats. *In Vivo.* 2018 Mar;32(4):713-9.
18. Salyards GW, Lemoy M-J, Knych HK, Hill AE, Christe KL. Pharmacokinetics of a Novel, Transdermal Fentanyl Solution in Rhesus Macaques. *J Am Assoc Lab Anim Sci.* 2017 Jul;56(4):9.
19. Royal JM, Settle TL, Bodo M, Lombardini E, Kent ML, Upp J, et al. Assessment of Postoperative Analgesia after Application of Ultrasound-Guided Regional Anesthesia for Surgery in a Swine Femoral Fracture Model. *J Am Assoc Lab Anim Sci.* 2013 May;52(3):12.
20. Comer SD, Cahill CM. Fentanyl: Receptor pharmacology, abuse potential, and implications for treatment. *Neurosci Biobehav Rev.* 2019 Nov;106:49-57.
21. Deschamps J-Y. Gestion de la douleur chez le chien et le chat. *Med'Com.* Paris; 2010.
22. Gourlay GK, Kowalski SR, Plummer JL, Cousins MJ, Armstrong PJ. Fentanyl Blood Concentration-Analgesic Response Relationship in the Treatment of Postoperative Pain: *Anesth Analg.* 1988 Apr;67(4):329-337.
23. Lane ME. The transdermal delivery of fentanyl. *Eur J Pharm Biopharm.* 2013 Aug;84(3):449-55.
24. Hofmeister EH, Egger CM. Transdermal Fentanyl Patches in Small Animals. *J Am Anim Hosp Assoc.* 2004 Nov;40(6):468-78.
25. Malavasi LM, Nyman G, Augustsson H, Jacobson M, Jensen-Waern M. Effects of epidural morphine and transdermal fentanyl analgesia on physiology and behaviour after abdominal surgery in pigs. *Lab Anim.* 2006 Jan;40(1):16-27.
26. Scholz J, Steinfath M, Schulz M. Clinical pharmacokinetics of alfentanil, fentanyl and sufentanil. An update. *Clin Pharmacokinet.* 1996 Oct;31(4):275-92.

RESEARCH ARTICLE

Effects of subtotal pancreatectomy and long-term glucose and lipid overload on insulin secretion and glucose homeostasis in minipigs

Rébecca Goutchtat¹  | Audrey Quenon^{1,2} | Manon Clarisse³ | Nathalie Delalleau¹ | Anaïs Coddeville¹ | Mathilde Gobert¹ | Valéry Gmyr¹ | Julie Kerr-Conte¹ | François Pattou¹ | Thomas Hubert^{1,2} 

¹Univ. Lille, Inserm, CHU Lille, Institut Pasteur Lille, UFR3S, U1190 – Egid, Lille, France

²Univ. Lille, CHU Lille, UFR3S, Département Hospitalo-Universitaire de Recherche et d'Enseignement (Dhure), Lille, France

³GENFIT, Loos, France

Correspondence

Thomas Hubert, Faculté de Médecine de Lille, Pôle Recherche – 3 étage Ouest, 1 Place de Verdun, 59045 Lille Cedex, France.
Email: thomas.hubert@univ-lille.fr

Funding information

Agence Nationale de la Recherche, Grant/Award Number: ANR-18-CE14-0028-01; Institut National de la Santé et de la Recherche Médicale, Grant/Award Number: Poste d'Accueil Inserm

Abstract

Introduction: Nowadays, there are no strong diabetic pig models, yet they are required for various types of diabetes research. Using cutting-edge techniques, we attempted to develop a type 2 diabetic minipig model in this study by combining a partial pancreatectomy (Px) with an energetic overload administered either orally or parenterally.

Methods: Different groups of minipigs, including Göttingen-like (GL, $n=17$) and Ossabaw (O, $n=4$), were developed. Prior to and following each intervention, metabolic assessments were conducted. First, the metabolic responses of the Göttingen-like ($n=3$) and Ossabaw ($n=4$) strains to a 2-month High-Fat, High-Sucrose diet (HFHSD) were compared. Then, other groups of GL minipigs were established: with a single Px ($n=10$), a Px combined with a 2-month HFHSD ($n=6$), and long-term intraportal glucose and lipid infusions that were either preceded by a Px ($n=4$) or not ($n=4$).

Results: After the 2-month HFHSD, there was no discernible change between the GL and O minipigs. The pancreatectomized group in GL minipigs showed a significantly lower Acute Insulin Response (AIR) (18.3 ± 10.0 IU/mL after Px vs. 34.9 ± 13.7 IU/mL before, $p < .0005$). In both long-term intraportal infusion groups, an increase in the Insulinogenic (IGI) and Hepatic Insulin Resistance Indexes (HIRI) was found with a decrease in the AIR, especially in the pancreatectomized group (IGI: 4.2 ± 1.9 after vs. 1.5 ± 0.8 before, $p < .05$; HIRI ($\times 10^{-5}$): 12.6 ± 7.9 after vs. 3.8 ± 4.3 before, $p < .05$; AIR: 24.4 ± 13.7 μ IU/mL after vs. 43.9 ± 14.5 μ IU/mL before, $p < .005$). Regardless of the group, there was no fasting hyperglycemia.

Conclusions: In this study, we used pancreatectomy followed by long-term intraportal glucose and lipid infusions to develop an original minipig model with metabolic syndrome and early signs of glucose intolerance. We reaffirm the pig's usefulness as a

This is an open access article under the terms of the [Creative Commons Attribution](https://creativecommons.org/licenses/by/4.0/) License, which permits use, distribution and reproduction in any medium, provided the original work is properly cited.

© 2023 The Authors. *Endocrinology, Diabetes & Metabolism* published by John Wiley & Sons Ltd.

preclinical model for the metabolic syndrome but without the fasting hyperglycemia that characterizes diabetes mellitus.

KEYWORDS

energetic overload, hyperglycemia, minipig model, pancreatectomy, type 2 diabetes

1 | INTRODUCTION

Type 2 diabetes, one of the major diseases of the twenty-first century, has an elevated prevalence (10.5% of the global population).¹ The World Health Organization (WHO) defines this disease as reaching a glycemia over 126 mg/dL after 8 h of fasting, twice validated, or over 200 mg/dL following an oral glucose tolerance test.² Currently, it is understood that a variety of pathophysiological processes plays a role in the onset of type 2 diabetes^{1,3}: decrease of insulin secretion, insulin resistance as a result of an imbalanced intake of carbohydrates and lipids and “thrifty genotype”.⁴ Additionally, type 2 diabetes is highly heterogenous and can be divided into five novel subtypes: severe autoimmune diabetes (related to type 1 diabetes), severe insulin-deficient diabetes, severe insulin-resistant diabetes, mild obesity related diabetes and mild-age related diabetes.^{5,6} Due to the disease's polymorphism, type 2 diabetes research needs the appropriate preclinical models in order to better understand pathophysiological pathways and create innovative, effective therapeutic approaches.

The most effective interventional treatment for type 2 diabetes in obese patients nowadays is metabolic surgery,^{7–10} which enables an early diabetes remission independent of weight loss.^{11–14} Current research on metabolic surgery is concentrated on understanding the link between the physiological changes that occur after intervention and the clinical benefit as well as on the development of new methods intended to improve the metabolic phenotype by reducing the associated complications.¹⁵ However, using preclinical models in which the surgical procedure may be easily applied to humans is one of the issues with metabolic surgery research. Porcine models have more translational value than rat models, even if rats are more often employed as preclinical models of metabolic surgery.^{16–19} Pigs are in fact omnivorous and are similar to humans concerning the morphology and the physiology of their gastrointestinal tract, pancreas, propension to obesity and sedentary, metabolic biomarker levels and drug pharmacokinetics,^{20,21} making it a particularly suitable preclinical model for these kinds of studies.

However, the creation of type 2 diabetes itself is the main problem with the preclinical pig model.

Current commercial pigs for meat production are the results of generations of selective breeding that targeted a phenotype able to store energy for later consumption by humans, likely making them protected against the deleterious effects of a “diabetogenic” environment.²² But some minipig strains, such as the Göttingen one, on which the physiology of insulin secretion is similar to humans,^{23,24} or the Ossabaw, recognized to be a natural model of metabolic

syndrome,²⁵ were found to be more susceptible to metabolic issues. Because of this, various studies have attempted in the past to develop preclinical diabetic pig models from these strains. A number of strategies have been tried, including: a surgical strategy involving total or subtotal pancreatectomy, which results in a strong reduction in insulin secretion but has no effect on insulin sensitivity^{26–28}; a chemical strategy involving the use of beta-cell toxins, such as streptozotocin or alloxan, with variable results and significant hepato- and nephrotoxicity^{29–33}; dietary interventions with a High-Fat, High-Sucrose diet, resulting in an insulin-resistant and obesity-related phenotype but not type 2 diabetes^{34–38}; and genetic engineering, which can produce customized pig models^{39–41} but is logistically challenging and may have unintended consequences.⁴² In conclusion, no true type 2 diabetic pig with fasting hyperglycemia and insulin resistance conforming to type 2 diabetes definition has been created so far.

In the current study, we considered additional approaches involving the combination of existing methods: an oral energetic overload (a High-Fat, High-Sucrose diet) and a subtotal pancreatectomy were separately performed and then also combined, intended to outperform the pancreas's regulatory capabilities. A parenteral approach using long-term intraportal glucose and lipid infusions, combined or not with a prior subtotal pancreatectomy, was also attempted. If the parenteral nutrition has already been set up to induce metabolic disorders in a piglet model,^{43,44} it was, to our best knowledge, never tested in the adult pig as an approach to induce type 2 diabetes.

2 | MATERIALS AND METHODS

2.1 | Ethics statement

The local French Committee of Animal Research and Ethics (CEEA-75, n°#18,915), in accordance with European law (2010/63/EU directive), accepted the protocol by approving it in accordance with the widely accepted ARRIVE guidelines. All the procedures were carried out in the agreed-upon (n°D59-35010) Département Hospitalo-Universitaire de Recherche et d'Enseignement (Dhure) in the Faculty of Medicine in Lille, France.

2.2 | Animals and housing

The study included a total of 21 healthy 1-year-old minipigs: 4 Ossabaw minipigs (DTU, Lyngby, Denmark) and 17 Göttingen-like

(Pannier, Wylder, France), weighing respectively 48.2 ± 1.9 kg and 31.7 ± 11.0 kg. Our local minipig strain, called Göttingen-like, was created more than 30 years ago as a consequence of an initial crossing with the Göttingen strain. To limit the metabolic differences related to the female hormonal cycle, only males were included. At the start of the protocol, animals were either surgically castrated or delivered castrated in the animal facility. All animals were housed and enriched in individual boxes in conventional conditions. Water was provided ad libitum and 400 g of standard food (Swine Engrais-F S25/T, Uneal Cooperative) was given twice a day. The composition of the standard diet was detailed in Table 1. The light/dark cycle was 12 h of light and 12 h of darkness with a temperature between 19 and 24°C. Pigs benefited from a 15-day acclimatization period.

2.3 | Study design

In this study, we wanted to create a preclinical pig model of type 2 diabetes that corresponds to the WHO definition.² This led to the combination of a partial pancreatectomy, a surgical method of insulin deprivation, with methods of energetic overload, via oral or intraportal administration. In order to determine which strain of minipigs was most suited for our strategy, we first assessed how both the Göttingen-like strain ($n=3$) and the Ossabaw one ($n=4$) responded to a 2-month High-Fat, High-Sucrose diet (HFHSD). We decided thereafter to discard the Ossabaw strain because Göttingen-like showed a phenotype closer to our expectations. Following this choice, we combined a subtotal pancreatectomy with 2 months of HFHSD in Göttingen-like minipigs ($n=6$). Finally, we explored a different strategy by infusing intraportal glucose and lipids for 3 weeks as a parenteral energetic overload in two groups of Göttingen-like minipigs: in Group 1 ($n=4$), no subtotal pancreatectomy was initially

TABLE 1 Composition (in %) of the standard diet and the High-Fat High-Sucrose (HFHS) diet given to the minipigs.

Composition	Standard diet	HFHS diet
Wheat	10.00	6.25
Barley	34.00	12.00
Wheat bran	25.00	11.14
Soybean cake	6.00	12.00
Sunflower cake	10.00	8.00
Soybean hulls	12.00	8.86
Cornstarch		6.50
Saccharose		20.00
Calcium carbonate	1.30	1.30
Sodium phosphate	0.60	0.60
Sodium chloride	0.60	0.60
Vitamins and minerals	0.50	0.75
Lard		12.00
Energetic density	12.5 kJ/g	20.9 kJ/g

performed; in Group 2 ($n=4$), a subtotal pancreatectomy was performed prior to the energetic overload. The impact of the subtotal pancreatectomy on glucose metabolism in the Göttingen-like strain was simultaneously examined ($n=10$), including the animals subjected to the HFHSD following the pancreatectomy ($n=6$) and those of Group 2 ($n=4$). Figure 1 displays the general design of this research.

2.4 | Surgical procedures

2.4.1 | Anaesthesia and analgesia

Following an overnight fast, all surgical procedures were performed under general anaesthesia. Premedication included intramuscular injections of xylazine (3 mg/kg; Sedaxylan®; Dechra Pharmaceutical PLC, France) and ketamine (5 mg/kg; Ketamine 1000®; Virbac, France), followed by isoflurane after endotracheal intubation (0.5 to 2%; IsoFlo; Zoetis, France). During the laparotomy procedures, animals were ventilated with assistance at 20 mpm or left with spontaneous ventilation. To ensure analgesia, an intramuscular injection of buprenorphine (15 µg/kg, Bupaq®, Virbac, France) for the insertion of a central venous catheter or a single transdermal application of fentanyl (1.3 mg/kg, Recuvyra®, Lilly-Elanco, France) for laparotomy procedures were used.⁴⁵

2.4.2 | Implantation of a central venous catheter (CVC)

The external jugular vein was exposed in the neck region after skin and muscle incision. After venotomy, the catheter (Hickman® 9.6F Single-Lumen CV Catheter, Bard Access System, USA) was inserted and linked to the vein with two ligatures (Vicryl® Bobine 2/0, Ethicon, France). It was tunneled via the subcutaneous tissue from the incision zone to the dorsal area of the neck. Muscular and cutaneous layers were then closed by simple overlock (respectively Polysorb® 2/0, Medtronic, France and Mersilene® 1, Ethicon, France). This catheter remained throughout the duration of the procedure and was kept operational by administering 5 mL of physiological serum that had been heparinized (1 mL heparin at 5000 IU/mL for 250 mL NaCl 0.9%) after each usage or every 2 days if it was not.

2.4.3 | Subtotal pancreatectomy

By reclining the stomach cranially and the intestinal system caudally, the pancreas was made accessible. From the tail to the head, the dissection was carried out (splenic lobe). In the retroportal region, the connecting lobe was similarly dissected and largely removed. Before section and extraction, ligatures between the splenic and the duodenal lobes were performed, and

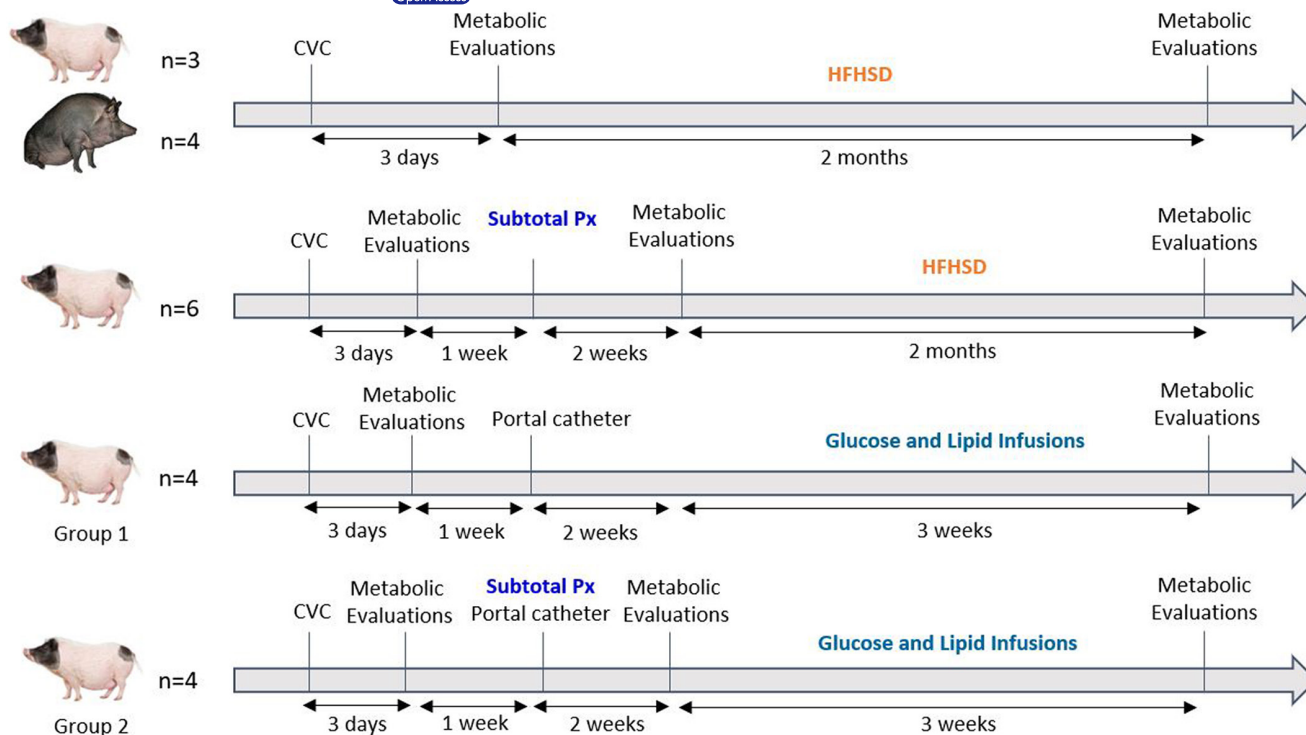


FIGURE 1 Overall study design for each group of animals. CVC, Central Venous Catheter; HFHSD, High-Fat High-Sucrose diet; Px, Pancreatectomy. The fully black minipig represents the Ossabaw strain, while the pink and black ones indicate the Göttingen-like strain. A Mixed Meal Test (MMT) and an Intravenous Glucose Tolerance Test constitute metabolic assessments (IVGTT). Metabolic tests were performed on all minipigs ($n=10$) with subtotal pancreatectomy 2 weeks after the intervention.

the connecting lobe was also tightened. As previously stated,⁴⁶ the subtotal pancreatectomy involved removing 75% of the total organ weight.

2.4.4 | Portal catheter implantation

The spleen was removed from the abdominal cavity after median laparotomy of the supra umbilical region, and the splenic vein was dissected on 2 cm. On the left flank, behind the final rib, the catheter (Hickman® 9.6F Single-Lumen CV Catheter, Bard Access System, USA) was tunneled across the abdominal wall. The catheter was placed following the splenic vein venotomy, advanced through the spleno-mesaraic confluence into the portal vein, and secured to the splenic vein with two ligatures. The layers of the peritoneum, muscles and skin were closed by a simple overlock.

2.4.5 | Surgical castration

Medially between the scrotum and the penile region, cutaneous and subcutaneous tissues were incised after testicles were compressed cranially. Additionally, the tunica vaginalis was cut open to reveal the testis. The cauda epididymis ligament was cut after extraction. Two ligatures were used to ligate the spermatic lead, and it was then

sectioned. Simple overlock was used to seal the tunica vaginalis and scrotum.

2.5 | Energetic overload

2.5.1 | High-Fat High-Sucrose diet (HFHSD)

Animals were fed with a HFHSD for 2 months. The Institut National de Recherche pour l'Agriculture, l'Alimentation et l'Environnement (Inrae, France) determined the food's composition. Seven hundred and fifty grams of HFHSD were administered twice a day and contained 61.7% carbohydrates, 23.2% fats, and 15.1% proteins. The composition of the HFHS diet was detailed in [Table 1](#).

2.5.2 | Intraportal glucose and lipid infusions

Over the period of 3 weeks, the intraportal catheter was used to administer lipid and glucose infusions twice daily for 2 h. A 2-h gap between the bi-daily infusions was observed. Fifty percent glucose (G50®, B. Braun, France) and lipid solution (Intralipid20®, Fresenius Kabi, France) was administered using infusion pumps (SK 600II®, Mano Medical, France) at respective flow rates of 125 mL/h and 63 mL/h. These flow rates were selected in order to maintain each

infusion's glycemia above 500mg/dL. Each infusion was preceded by a 500mg/kg bolus of 50% glucose solution to raise blood glucose levels to more than 500mg/dL within 1 min. All the infusions were performed in an awake animal.

2.6 | Metabolic tests

2.6.1 | Mixed meal tests (MMT)

After a 12-h fast, a 20-g solid energy bar (Ovomaltine®, Nestlé, France) and 200mL of liquid (Fortimel Energy®, Nutricia, France) were mixed and given *vigil* via a nasogastric tube of 16 Fr that had previously been implanted under general anaesthesia during the CVC implantation procedure for the first MMT or the day before for the other MMT. The meal had a 990-kJ energy density and contained 49 g of total carbohydrates, 13 g of fats, and 15 g of proteins. On EDTA and heparinised tubes, blood samples were obtained before the MMT was administered ($t=0$ min) and at various time intervals afterwards ($t=15$, $t=30$, $t=60$, $t=90$, $t=120$, and $t=180$ min).

2.6.2 | Intravenous glucose tolerance test (IVGTT)

Following an overnight fast, a 50-% glucose solution (G50®, B. Braun, France) was intravenously administered into the CVC at a dose of 500mg/kg. On EDTA tubes, blood samples were taken in the awake animal before ($t=0$ min) and following the administration of glucose at $t=1$, $t=3$, $t=5$, $t=10$, $t=15$, and $t=30$ min.

Plasma was collected from each tube, centrifuged at 4000rpm for 10 min at 4°C, and then stored at -80°C until analyses.

2.7 | Biological analyses

The amperometric glucose oxidase method was used to measure the level of glucose in blood (glucometer Accu-Chek Performa®, Roche, France, or Nova Biomedical StatStrip Xpress®, DSI, USA). A DXI Access Immunoassay System (Beckman Coulter) with an assay range between 0.3 and 300 μ IU/mL was used to measure the plasma insulin concentrations, as previously mentioned.⁴⁷ Plasma lipid profile (total cholesterol, LDL, HDL and triglycerides) was assessed using an Abbott Architect C4000® clinical chemistry analyser.

2.8 | Calculations and statistical analyses

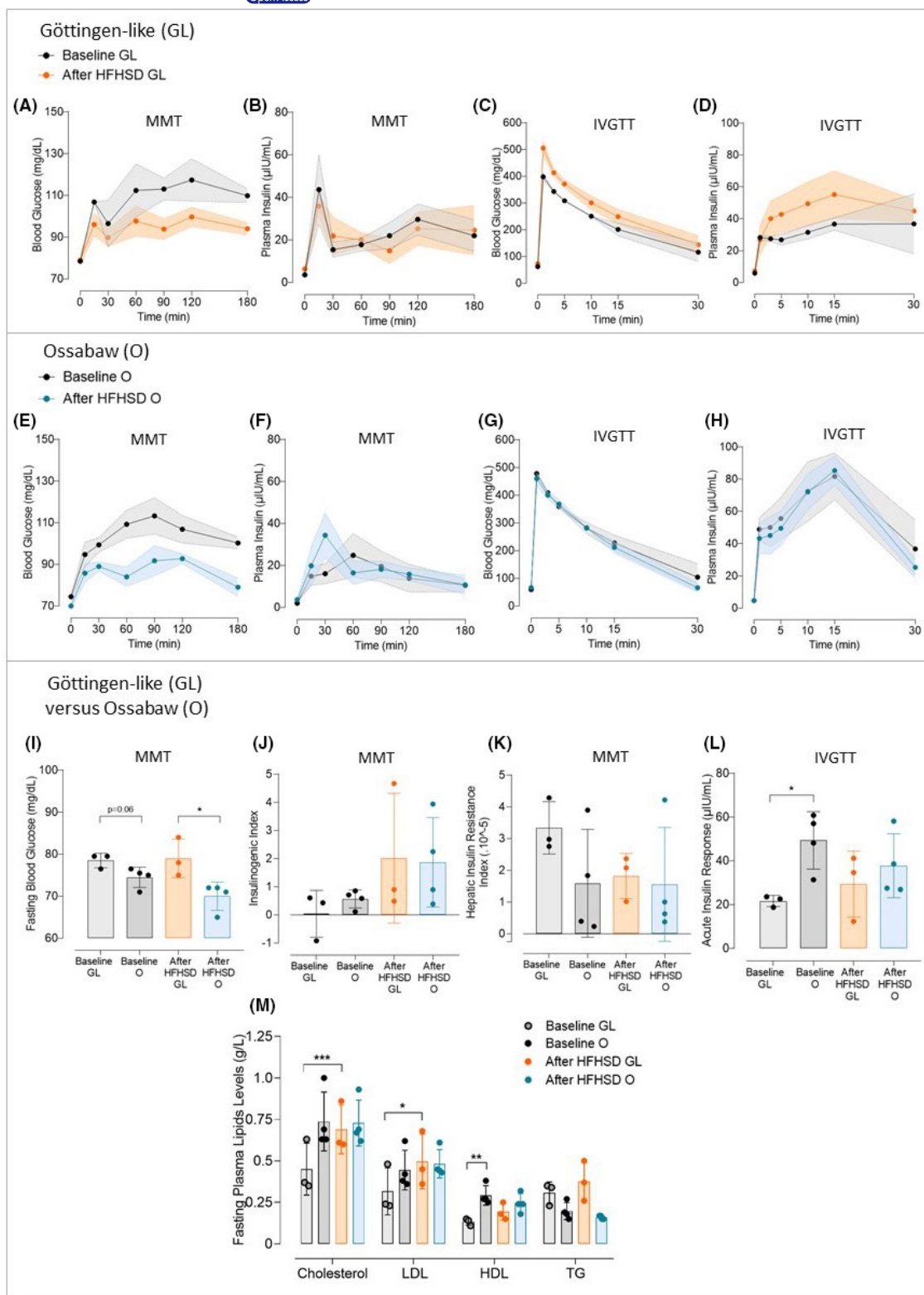
For data analysis, GraphPad Prism v8® software was employed. For curves, the results were expressed as mean \pm SEM, and for histograms, as mean \pm SD. Depending on the situation, paired or unpaired Student's *t*-tests were used to analyse the variables. A Two-Way ANOVA and Sidak post-hoc tests were used to compare blood glucose and plasma insulin levels during the MMT and IVGTT between

the different strains of minipigs or between baseline and after diabetogenic interventions. For each comparison of blood glucose or insulin evolution during metabolic test, the effect of time of the metabolic test (called "time") and strain (Göttingen-like or Ossabaw, called "strain") or diabetogenic intervention ("HFHSD", "pancreatectomy", or "infusions") was systematically assessed. The presence of interaction between "time" and "strain" or "time" and "intervention" was also evaluated. The calculation of Insulinogenic Index was performed to evaluate the postprandial early insulin secretion as described⁴⁸: [Plasma Insulin ($t=30$)-Plasma Insulin ($t=0$)]/[Blood Glucose ($t=30$)-Blood Glucose ($t=0$)], with plasma insulin in μ IU/mL and blood glucose in mg/dL. The hepatic insulin resistance was evaluated thanks to the Hepatic Insulin Resistance Index (HIRI) calculation as previously described,⁴⁹ by multiplication of the first 30-min area under the curve between glucose and insulin concentration during MMT. The Acute Insulin Response (AIR), which describes the initial phase of insulin production following intravenous glucose stimulation, was computed by subtracting fasting insulin levels from the mean evaluation of plasma insulin levels at 1, 3 and 5 min.^{50,51}

3 | RESULTS

3.1 | Choice of the Göttingen-like minipig strain after comparison with Ossabaw

The glucose metabolism of Göttingen-like (GL, $n=3$) and Ossabaw (O, $n=4$) minipigs was compared before and after a 2-month High-Fat High-Sucrose diet (HFHSD) in order to determine which strain was best suited for our procedure (Figure 2). Following the regimen, both strains notably gained weight (55.1 ± 4.3 after vs. 43.4 ± 6.4 kg before for GL, $p < .05$ and 62.8 ± 4.8 after vs. 48.2 ± 1.9 kg before for O, $p < .01$), corresponding to a weight gain of 26.9% for GL and 30.3% for O. Postprandial blood glucose concentrations (Figure 2A) were generally lower but not significantly following HFHSD, while insulin concentrations (Figure 2B) did not differ in Göttingen-like minipigs. The intravenous glucose tolerance test (IVGTT) results for glycemia (Figure 2C) and insulin (Figure 2D) did not change between the two steps. After HFHSD, Ossabaw minipigs showed a trend of lower postprandial blood glucose levels (Figure 2E) accompanied by a trend of higher insulin peak secretion (Figure 2F). However, during the IVGTT, there were no discernible changes between the glucose decline (Figure 2G) and corresponding insulin concentrations (Figure 2H). Ossabaw minipigs' fasting blood glucose appeared lower than Göttingen-like ones at baseline, and it was significantly lower after HFHSD than those of Göttingen-like (70.0 ± 3.4 after vs. 79.0 ± 4.6 mg/dL before; $p < .05$) (Figure 2I). Figure 2J shows a trend of increasing Insulinogenic Index for both strains after HFHSD, although there was no change in Hepatic Insulin Resistance Index (Figure 2K). Compared to Göttingen-like minipigs, Ossabaw minipigs had significantly higher baseline Acute Insulin Response (49.3 ± 13.1 μ IU/mL for O vs. 21.7 ± 2.5 μ IU/mL for GL, $p < .05$) although no discernible alterations were found for any



strain following HFHSD (Figure 2L). Ossabaw minipigs presented a higher level in fasting cholesterol at the baseline than Göttingen-like minipigs (Figure 2M) (total cholesterol: 0.74 ± 0.18 g/L for O vs. 0.45 ± 0.16 g/L for GL, not significant; LDL: 0.45 ± 0.12 g/L for O vs. 0.32 ± 0.14 g/L for GL, not significant; HDL: 0.29 ± 0.06 g/L for O vs.

0.13 ± 0.02 g/L for GL, $p < .01$). However, there was no change in the lipid profile after HFHSD in Ossabaw minipigs while total cholesterol and LDL levels were significantly increased in Göttingen-like minipigs (total cholesterol: 0.69 ± 0.15 g/L after vs. 0.45 ± 0.16 g/L before, $p < .001$; LDL: 0.50 ± 0.17 g/L after vs. 0.32 ± 0.14 g/L before,

FIGURE 2 Comparison of the Ossabaw and Göttingen-like minipig strains' metabolic responses to a 2-month High-Fat, High-Sucrose diet. (A–D) Mean curves (Mean \pm SEM; $n = 3$) of Blood Glucose (A) and Plasma Insulin (B) during Mixed Meal Test (MMT) and Blood Glucose (C) and Plasma Insulin (D) during Intravenous Glucose Tolerance Test (IVGTT) in the Göttingen-like (GL) strain, with the baseline characteristics represented in black and after 2-month High-Fat High-Sucrose diet (HFHSD) in orange. (E–H) Mean curves (Mean \pm SEM; $n = 4$) of Blood Glucose (E) and Plasma Insulin (F) during MMT and Blood Glucose (G) and Plasma Insulin (H) during IVGTT in the Ossabaw (O) strain, with the baseline characteristics represented in black and after HFHSD in blue. (I) Mean Fasting Blood Glucose (Mean \pm SD) measured during MMT before (in black) and after (in colour) HFHSD in the Göttingen-like (GL, in orange; $n = 3$) and in the Ossabaw (O, blue; $n = 4$) strains. (J, K) Mean Insulinogenic Index (J) and Hepatic Insulin Resistance Index (K) (Mean \pm SD) calculated during MMT before (in black) and after (in colour) HFHSD in the Göttingen-like (GL, in orange; $n = 3$) and in the Ossabaw (O, blue; $n = 4$) strains. (L) Mean Acute Insulin Response (Mean \pm SD) calculated during IVGTT before (in black) and after (in colour) HFHSD in the Göttingen-like (GL, in orange; $n = 3$) and in the Ossabaw (O, blue; $n = 4$) strains. (M) Fasting plasma lipid profile (Mean \pm SD) assessed before (in black) and after (in colour) HFHSD in the Göttingen-like (GL, in orange; $n = 3$) and in the Ossabaw (O, blue; $n = 4$) strains. HDL, high-density lipoprotein; LDL, low-density lipoprotein; TG, triglycerides; Total Chol, total cholesterol. Two-Way ANOVA test for repeated measures and Sidak post-hoc test; Paired or unpaired *t*-test; * $p < .05$, ** $p < .01$, *** $p < .001$.

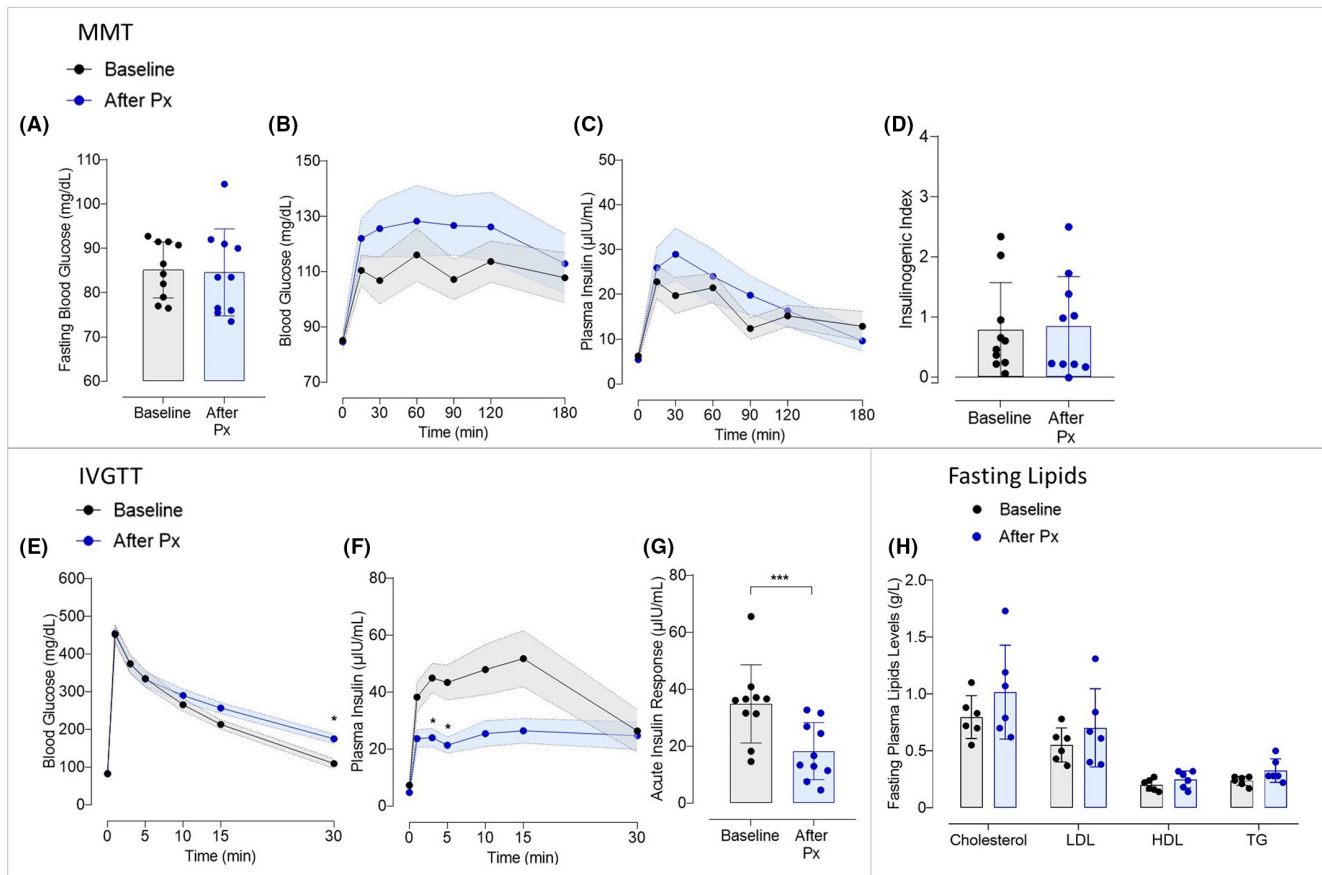


FIGURE 3 Evaluation of the effect of a subtotal pancreatectomy on glucose metabolism in Göttingen-like minipigs. (A) Mean Fasting Blood Glucose (Mean \pm SD; $n = 10$) measured during MMT before (in black) and after (in blue) subtotal pancreatectomy. (B, C) Mean curves (Mean \pm SEM; $n = 10$) of Blood Glucose (B) and Plasma Insulin (C) during MMT before (in black) and after (in blue) subtotal pancreatectomy. (D) Mean Insulinogenic Index (Mean \pm SD; $n = 10$) calculated during MMT before (in black) and after (in blue) subtotal pancreatectomy. (E, F) Mean curves (Mean \pm SEM; $n = 10$) of Blood Glucose (E) and Plasma Insulin (F) during IVGTT before (in black) and after (in blue) subtotal pancreatectomy. (G) Mean Acute Insulin Response (Mean \pm SD; $n = 10$) calculated during IVGTT before (in black) and after (in blue) subtotal pancreatectomy. (H) Fasting plasma lipid profile (Mean \pm SD; $n = 10$) assessed before (in black) and after (in blue) subtotal pancreatectomy. HDL, high-density lipoprotein; LDL, low-density lipoprotein; TG, triglycerides; Total Chol, total cholesterol. Two-Way ANOVA test for repeated measures and Sidak post-hoc test; Paired *t*-test; * $p < .05$, ** $p < .0005$ between baseline and after pancreatectomy.

$p < .05$). These findings indicated that Ossabaw minipigs had a better early insulin response than Göttingen-like minipigs. We thus decided to proceed with our strategy using the Göttingen-like strain.

3.2 | Reduction of acute insulin response after subtotal pancreatectomy in Göttingen-like minipigs

We assessed how a subtotal pancreatectomy affected glucose metabolism (Figure 3). After the surgical procedure, there was no rise in fasting blood glucose (Figure 3A). Mixed Meal Tests did not reveal any appreciable changes in blood glucose (Figure 3B) or insulin levels (Figure 3C). As a result, there was no change in the Insulinogenic Index (Figure 3D). When compared to before the intervention, the speed at which the glucose levels declined during the IVGTT following pancreatectomy was slower (blood glucose levels of respectively 175.1 ± 12.4 mg/dL after vs. 109.4 ± 13.1 mg/dL before at 30 min, $p < .05$) (Figure 3E). A significant interaction between “time” and “pancreatectomy” was thus reported ($p < .05$). Plasma insulin levels during IVGTT were significantly lower after pancreatectomy than at the baseline and especially at 3 and 5 min (respectively 24 ± 3.2 μ U/mL after vs. 45 ± 5.1 μ U/mL before and 21 ± 2.8 μ U/mL after vs. 43 ± 6.1 μ U/mL, $p < .05$) (Figure 3F). A significant interaction between “time” and “pancreatectomy” was thus noticed ($p < .0001$). As a result, following pancreatectomy, the Acute Insulin Response was significantly decreased (18.3 ± 10.0 μ U/mL after vs. 34.9 ± 13.7 μ U/mL before, $p < .0005$) (Figure 3G). Finally, there was no significant change reported in fasting plasma lipid profile after subtotal pancreatectomy (Figure 3H).

3.3 | No significant change in glucose metabolism following the combination of a subtotal pancreatectomy with a 2-month HFHSD in Göttingen-like minipigs

The metabolic phenotypic changes following a subtotal pancreatectomy and 2 months of HFHSD as an oral energy overload were then examined (Figure 4). Following the protocol, animals gained weight (26.3 ± 5.9 kg after, compared to 21.3 ± 3.6 kg before, $p < .05$). Following this approach, no rise in fasting blood glucose (Figure 4A) was observed. With a more pronounced peak at 30 min and a faster return to baseline following the procedure, postprandial blood glucose dynamics were different from before, even if not significantly (Figure 4B). Although there was a trend to higher postprandial insulin levels (Figure 4C), the Insulinogenic Index did not significantly change (Figure 4D). Additionally, the Hepatic Insulin Resistance Index modestly but not significantly increased (Figure 4E). The IVGTT revealed no significant changes in glucose tolerance (Figure 4F), insulin levels (Figure 4G), or Acute Insulin Response (Figure 4H). Finally, the levels of fasting plasma lipids were globally increased after intervention (Figure 4I) (total cholesterol: 1.09 ± 0.20 g/L after vs. 0.80 ± 0.19 g/L before, $p < .05$; LDL: 0.65 ± 0.12 g/L after vs. 0.55 ± 0.15 g/L before, $p = .052$; HDL: 0.38 ± 0.18 g/L after vs. 0.20 ± 0.05 g/L before, not

significant; triglycerides: 0.28 ± 0.07 g/L after vs. 0.24 ± 0.04 g/L before, not significant).

3.4 | Alterations of insulin secretion pattern and insulin resistance after long-term intraportal glucose and lipid infusions in Göttingen-like minipigs

In two groups of minipigs, one without prior pancreatectomy and the other following subtotal pancreatectomy, we infused long-term intraportal glucose and lipid (Figure 5). Animals of each group gained a little weight following infusions (35.2 ± 11.4 after vs. 28.3 ± 7.4 kg before for Group 1, $p < .05$; and 47.4 ± 6.5 kg after vs. 41.8 ± 6.7 kg before for Group 2, $p < .005$). Postprandial blood glucose levels of Group 1 were significantly lower following infusions compared to the baseline state ($p < .005$) (Figure 5A). A significant interaction between “time” and “infusions” was thus noticed ($p < .05$). The first 30-min showed a rise in plasma insulin levels (77.4 ± 18.0 μ U/mL after infusions at 15 min vs. 24.7 ± 5.1 μ U/mL before, and 55.3 ± 10.0 μ U/mL after infusions at 30 min vs. 37.1 ± 7.6 μ U/mL before; not significant) and a significant interaction between “time” and “infusions” was discovered ($p < .005$) (Figure 5B). Blood glucose levels decreased during IVGTT more slowly than they did before protocol (159.0 ± 14.2 mg/dL after infusions vs. 70.4 ± 28.6 mg/dL before at 30 min; not significant) (Figure 5C) and insulin levels globally decreased, with an exception at 30 min (Figure 5D). Following procedure, postprandial blood glucose levels in Group 2 fell globally (Figure 5E), similar to Group 1 and a significant interaction between “time” and “intervention” was observed ($p < .05$). Plasma insulin levels rose for the first 30 min (76.7 ± 10.6 μ U/mL after protocol at 15 min vs. 25.5 ± 5.1 μ U/mL before, and 75.4 ± 19.0 μ U/mL after protocol at 30 min vs. 31.0 ± 6.5 μ U/mL before; not significant) and a significant interaction between “time” and “intervention” was reported ($p < .0001$) (Figure 5F). IVGTT findings after protocol revealed a slower lowering of blood glucose (Figure 5G) and especially lower insulin levels with a significant intervention observed between “time” and “intervention” ($p < .05$) (Figure 5H). Finally, whether or not a subtotal pancreatectomy had been performed prior to the intraportal glucose and lipid infusion, no increase in fasting blood glucose was observed (Figure 5I). However, both groups showed an increase in the Insulinogenic Index (2.0 ± 0.8 vs. 0.59 ± 0.2 ; $p = .06$ and 4.2 ± 1.9 vs. 1.5 ± 0.8 ; $p < .05$, respectively for Groups 1 and 2) (Figure 5J). An increase in Hepatic Insulin Resistance Index ($\times 10^{-5}$) was also obtained (8.0 ± 4.7 after vs. 5.3 ± 2.3 before; not significant, and 12.6 ± 7.9 after vs. 3.8 ± 4.3 before; $p < .05$, respectively for Groups 1 and 2) (Figure 5K). Additionally, both groups' Acute Insulin Responses reduced (28.7 ± 7.5 μ U/mL after vs. 38.6 ± 13.3 μ U/mL before; not significant, and 24.4 ± 13.7 μ U/mL after vs. 43.9 ± 14.5 μ U/mL before; $p < .005$ before, respectively for Groups 1 and 2) (Figure 5L). Finally, fasting plasma levels of total cholesterol and LDL were increased after intervention for both groups (Figure 5M) (total cholesterol: 0.80 ± 0.12 g/L after vs. 0.60 ± 0.11 g/L before, $p < .01$, for Group 1 and 0.75 ± 0.07 g/L after vs. 0.73 ± 0.08 g/L before, $p < .05$, for Group 2; LDL: 0.54 ± 0.09 g/L after vs. 0.42 ± 0.07 g/L

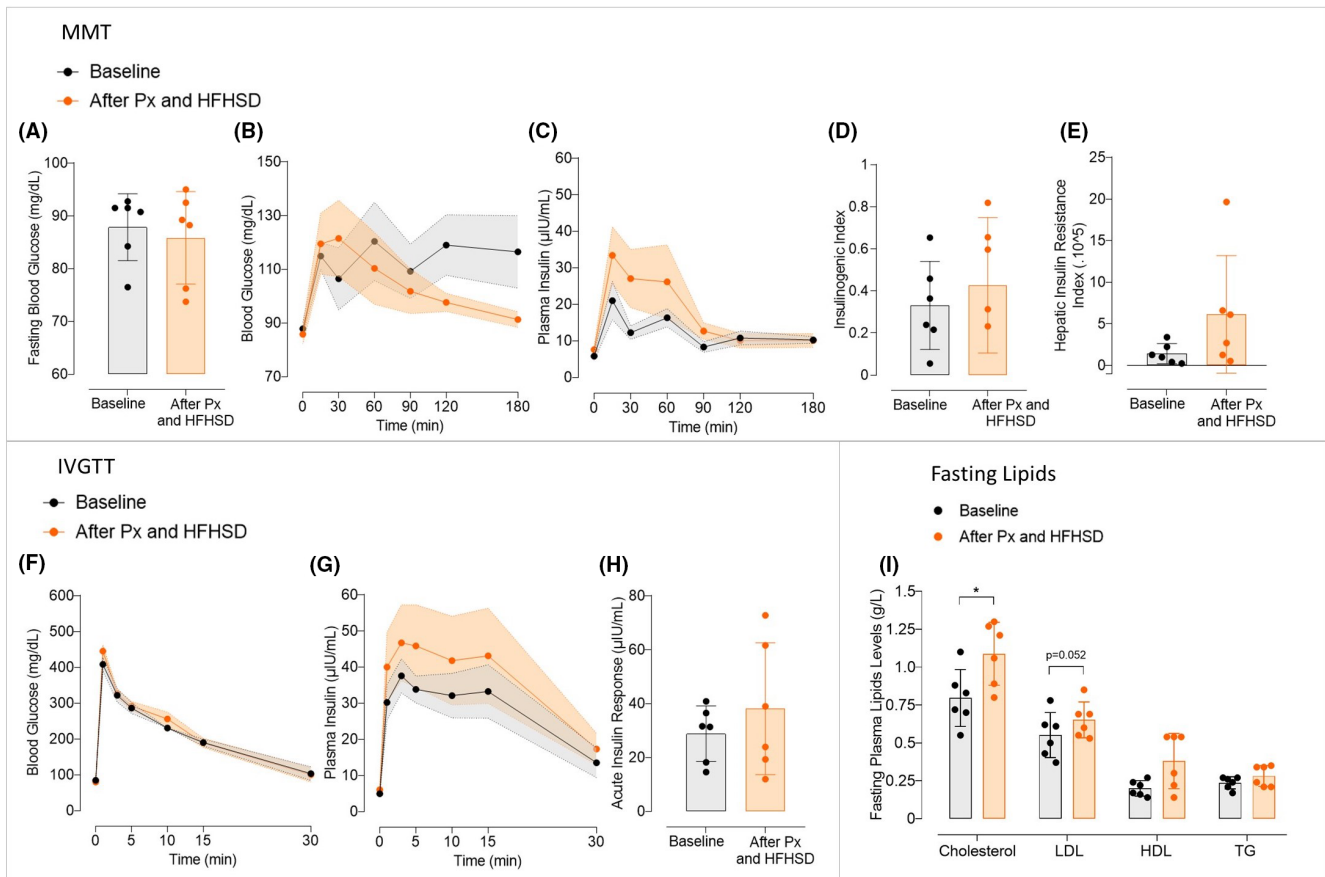


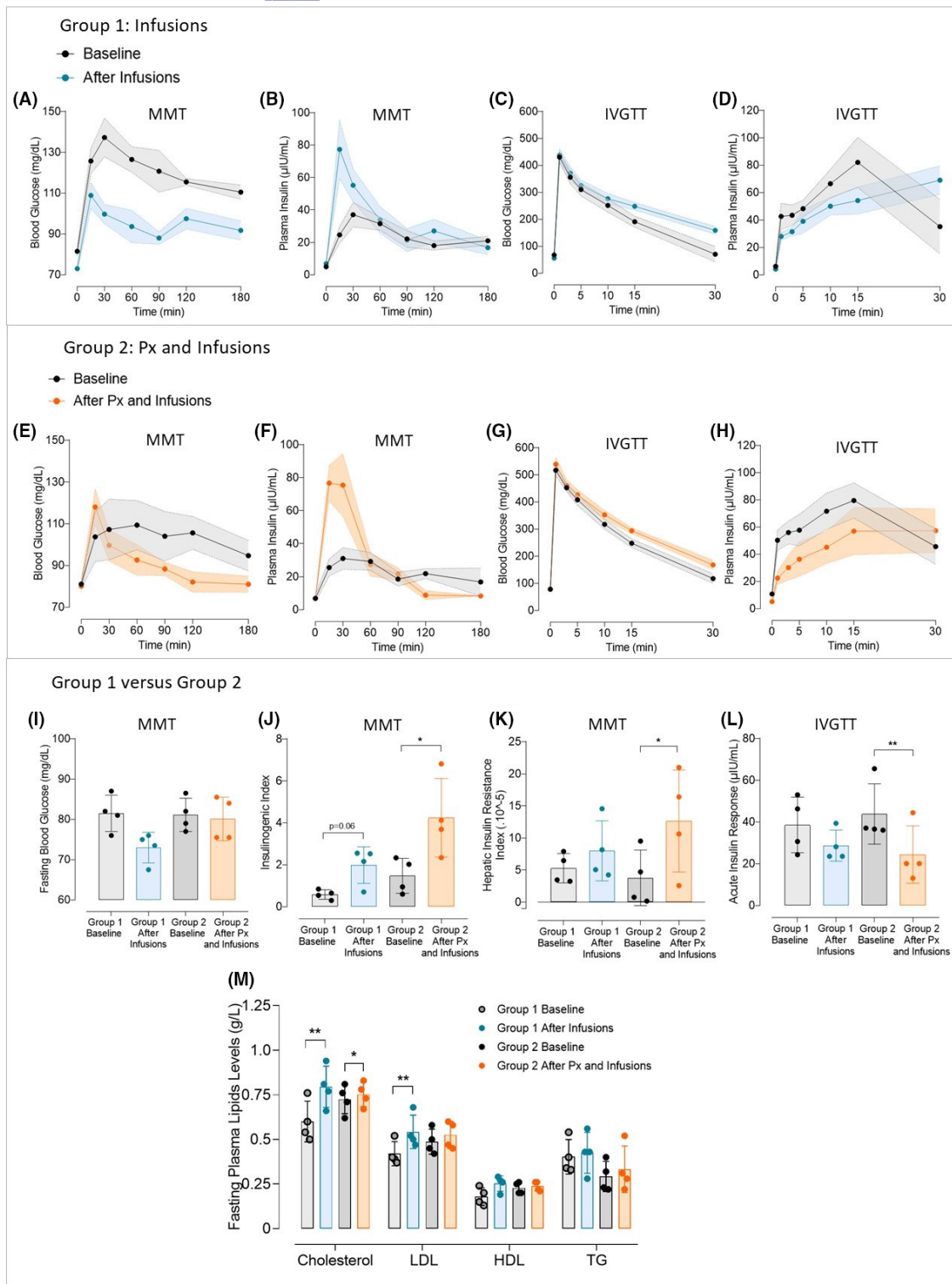
FIGURE 4 Effect of the combination of a subtotal pancreatectomy followed by a 2-month High-Fat High-Sucrose diet on glucose metabolism in Göttingen-like minipigs. (A) Mean Fasting Blood Glucose (Mean \pm SD; $n = 6$) measured during MMT before (in black) and after (in orange) subtotal pancreatectomy followed by a 2-month High-Fat High-Sucrose diet (HFHSD). (B, C) Mean curves (Mean \pm SEM; $n = 6$) of Blood Glucose (A) and Plasma Insulin (B) during MMT before (in black) and after (in orange) subtotal pancreatectomy followed by a 2-month HFHSD. (D, E) Mean Insulinogenic Index (D) and Hepatic Insulin Resistance Index (E) (Mean \pm SD; $n = 6$) calculated during MMT before (in black) and after (in orange) subtotal pancreatectomy followed by a 2-month HFHSD. (F, G) Mean curves (Mean \pm SEM; $n = 6$) of Blood Glucose (F) and Plasma Insulin (G) during IVGTT before (in black) and after (in orange) subtotal pancreatectomy followed by a 2-month HFHSD. (H) Mean Acute Insulin Response (Mean \pm SD; $n = 6$) calculated during IVGTT before (in black) and after (in orange) subtotal pancreatectomy followed by a 2-month HFHSD. (I) Fasting plasma lipid profile (Mean \pm SD; $n = 6$) assessed before (in black) and after (in orange) subtotal pancreatectomy followed by a 2-month HFHSD. HDL, high-density lipoprotein; LDL, low-density lipoprotein; TG, triglycerides; Total Chol, total cholesterol. Two-Way ANOVA test for repeated measures and Sidak post-hoc test; Paired *t*-test; * $p < .05$.

before, $p < .01$, for Group 1 and 0.53 ± 0.08 g/L after vs. 0.49 ± 0.07 g/L before, not significant, for Group 2). HDL and triglycerides levels were not significantly altered after intervention, no matter the group. No significant difference was observed in glucose homeostasis and lipid profile after intervention between Group 1 and Group 2.

4 | DISCUSSION

We attempted to develop a preclinical type 2 diabetic pig model in this study in accordance with the World Health Organization definition (glycemia over 126 mg/dL after 8 h of fasting, verified twice, or over 200 mg/dL following an oral glucose tolerance test).² In order to determine which strain of pigs was the most suited, we first subjected two distinct strains to a High-Fat High-Sucrose diet (HFHSD) for 2 months. This enabled us to evaluate each strain's

metabolic adaptation to the HFHSD. Both strains responded equally, with Ossabaw having a little better insulin response than Göttingen-like, which justified pursuing the study with Göttingen-like minipigs. During metabolic evaluations, the metabolic response in both strains showed a tendency to an increase in insulin levels, necessitating the introduction of an intervention aimed at reducing the capacity of pancreas adaptability. This is why we decided to combine an energy overload with an insulin restriction technique, such as a subtotal pancreatectomy. In the beginning, the effects of a single subtotal pancreatectomy were investigated. In our investigation, subtotal pancreatectomy reduced early insulin secretion while leaving postprandial glycemic response and fasting glycemia unaffected. The subtotal pancreatectomy was performed on a set of pigs combined with 2 months of oral energy overload administered via a HFHSD: there was no change in the metabolism of glucose. Thus, another strategy was considered



in moving towards a parenteral energetic overload using chronic intraportal glucose and lipid infusions, whether or not they were associated with a preceding subtotal pancreatectomy. Results showed similar patterns with or without a pancreatectomy, with lower postprandial glycemia values associated with a higher 30-min insulin peak. A rise in hepatic insulin resistance was also observed, particularly in the group that was subjected to the subtotal pancreatectomy prior to infusions, in addition to this postprandial

hyperinsulinism. Finally, during intravenous glucose tolerance testing, a decrease in the first phase of insulin secretion was observed for both groups, with the pancreatectomy group showing significant differences. We were unable to produce a type 2 diabetic minipig model because none of the study groups achieved a fasting hyperglycemia.

The results in the Ossabaw strain were unexpected. The HFHSD induced a response that was highly comparable to that of the

FIGURE 5 Effect of long-term intraportal glucose and lipid infusions on glucose metabolism in Göttingen-like minipigs, whether or not they are preceded by a subtotal pancreatectomy. (A–D) Mean curves (Mean \pm SEM; $n=4$) of Blood Glucose (A) and Plasma Insulin (B) during Mixed Meal Test (MMT) and Blood Glucose (C) and Plasma Insulin (D) during Intravenous Glucose Tolerance Test (IVGTT) before (in black) and after (in blue) 3 weeks of long-term intraportal glucose and lipids infusions. (E–H) Mean curves (Mean \pm SEM; $n=4$) of Blood Glucose (E) and Plasma Insulin (F) during Mixed Meal Test (MMT) and Blood Glucose (G) and Plasma Insulin (H) during Intravenous Glucose Tolerance Test (IVGTT) before (in black) and after (in orange) the combination of a subtotal pancreatectomy followed by 3 weeks of long-term intraportal glucose and lipid infusions. (I) Mean Fasting Blood Glucose (Mean \pm SD; $n=4$ per group) measured during MMT at the baseline for Group 1 (in light grey) and Group 2 (in dark grey) and after 3 weeks of long-term intraportal glucose and lipid infusions (Group 1, in blue) and after subtotal pancreatectomy followed by 3 weeks of long-term intraportal glucose and lipid infusions (Group 2, in orange). (J, K) Mean Insulinogenic Index (J) and Hepatic Insulin Resistance Index (K) (Mean \pm SD; $n=4$ per group) calculated during MMT at the baseline for Group 1 (in light grey) and Group 2 (in dark grey) and after 3 weeks of long-term intraportal glucose and lipid infusions (Group 1, in blue) and after subtotal pancreatectomy followed by 3 weeks of long-term intraportal glucose and lipid infusions (Group 2, in orange). (L) Mean Acute Insulin Response (Mean \pm SD; $n=4$ per group) calculated during IVGTT at the baseline for Group 1 (in light grey) and Group 2 (in dark grey) and after 3 weeks of long-term intraportal glucose and lipid infusions (Group 1, in blue) and after subtotal pancreatectomy followed by 3 weeks of long term intraportal glucose and lipid infusions (Group 2, in orange). (M) Fasting plasma lipid profile (Mean \pm SD; $n=4$ per group) assessed at the baseline for Group 1 (in light grey) and Group 2 (in dark grey) and after 3 weeks of long-term intraportal glucose and lipid infusions (Group 1, in blue) and after subtotal pancreatectomy followed by 3 weeks of long-term intraportal glucose and lipid infusions (Group 2, in orange). HDL, high-density lipoprotein; LDL, low-density lipoprotein; TG, triglycerides; Total Chol, total cholesterol. Two-Way ANOVA test for repeated measures and Sidak post-hoc test; Paired t-test; * $p < .05$, ** $p < .01$.

Göttingen-like strain, with an early insulin secretion that appeared to be even more effective than the Göttingen one in the baseline state. However, Ossabaw minipigs have a reputation for being the strain that is most susceptible to metabolic syndrome.^{25,52} In fact, they developed, in the “Ossabaw Georgia island” where they come from, a “thrifty genotype” that enabled them to easily store energy from low-nutritive substrates because of the severe selection pressure imposed by the dry climate of the Ossabaw island. Thus, it is claimed that Ossabaw minipigs serve as a natural model for reproducing the symptoms of type 2 diabetes and the metabolic syndrome, similar to those populations that are predisposed to these diseases naturally.³ However, given that no fasting hyperglycemia could be generated only after a diet in previous research,^{53–55} it would appear that the expression of their metabolic syndrome would be more focused on lipidic dysregulations than disorders of glucose metabolism.^{56,57} Fasting lipid levels of Ossabaw minipigs were much greater than those of the Göttingen-like strain in our study, particularly in terms of cholesterol, which makes this strain well-suited for the investigation of hypercholesterolemia illnesses⁵⁸ but not for studies of diabetes. We continued the combination protocol, which included a subtotal pancreatectomy, followed by five more months of HFHSD, in two minipigs of this strain. These two minipigs showed no signs of metabolic change (data not shown), demonstrating that this strain is not susceptible to develop type 2 diabetes.

The decision to perform a pancreatectomy was made considering the highly variable and toxic effects of streptozotocin⁵⁹ and alloxan.⁶⁰ Additionally, a surgical pancreatic mass excision is easier to control than one caused by toxic chemicals,^{42,46} which is why this way of generating an insulin deficiency was chosen. The partial pancreatectomy's subsequent impact on glucose metabolism was unexpectedly modest, with the only discernible change being a reduction in the acute insulin response, which is the first phase of insulin secretion. We also observed that following pancreatectomy, insulin release reached a plateau. Nevertheless, there was no change in insulin secretion throughout the oral glucose challenge. As previously

described in this species,⁶¹ the loss of pancreatic mass would have been balanced by an increase in glucose and GLP-1 driven insulin secretion per islet. Although we did not measure it in our study, subtotal pancreatectomy may have increased the incretin impact to balance the loss of islet mass.

Contrary to what we expected, the plan to combine a 2-month HFHSD with a subtotal pancreatectomy in order to exceed the pancreas's capacity for insulin secretion did not result in any phenotypic change. As seen in human islets,⁶² the weight gain brought on by the diet may have helped to increase the size of the surviving islets and their reactivity to glucose in releasing insulin, serving as a mode of compensation.

We found the biggest metabolic changes in the minipigs receiving continuous intraportal glucose and lipid infusions. Even while the findings of changes in insulin response were significantly different from the baseline state only in the group with a subtotal pancreatectomy prior to infusions, both groups—with or without subtotal pancreatectomy—presented comparable patterns. Therefore, we propose that the pancreatectomy potentialized the impact of infusions. In conjunction with a decline in the first phase of insulin secretion, we discovered an increase in hepatic insulin resistance and postprandial hyperinsulinism. Because glucose and lipids were infused into the portal vein, they may have quickly caused a hepatic excess in glycogen and triglycerides, which may have been the source of the hepatic insulin resistance as previously observed in dogs^{63,64} and mice.⁶⁵ Furthermore, the administration of parenteral nutrition is known to have major side effects like hepatic steatosis, insulin resistance, and changes in insulin secretion,^{43,66–68} which is why we decided to test this approach in our research. During the sacrifice of these minipigs, a discoloration evocating a hepatic steatosis was macroscopically observed (data not shown).

Additionally, it is now well understood that a decrease in acute insulin response, a marker of change in the first phase of insulin release, constitutes the initial indicator of impaired glucose tolerance.^{69,70} The existence of ectopic triglycerides in the pancreas

that were brought on by the intraportal infusions could potentially account for this decline. It is known that ectopic triglycerides have a significant role in the oxidative stress and inflammation that reduce the functionality of pancreatic beta cells.⁷¹ Around the abdominal organs during sacrifice, substantial visceral adipose tissue was also macroscopically visible (data not shown). This finding, a potential cause of insulin resistance, might thus be used to explain the postprandial hyperinsulinism. Hepatic insulin resistance was clearly established, while peripheral insulin resistance was not. In particular, the HOMA-IR and Matsuda Index calculations, which evaluate peripheral insulin sensitivity and resistance in humans, did not change after intraportal infusions relative to the initial state (data not shown). In addition, we did not examine postprandial incretin levels. It would have been interesting to determine whether the observed postprandial hyperinsulinism may be attributed to an increase in GLP-1 concentrations caused by an intestinal adaptation brought on by the intraportal infusions. In any case, the observed modifications would look very similar to those early intervening in the beginning of type 2 diabetes, even if no fasting hyperglycemia or postprandial glucose intolerance were found for these groups. We might have acquired a more severe phenotype if we had continued intraportal infusions for a longer period of time. We did not, however, because of the ethical issues raised by the complicated porcine model.

The lipidic profile of Göttingen-like minipigs was investigated. All groups showed a notable rise in total cholesterol, especially LDL, with the exception of pigs subjected to a single subtotal pancreatectomy. As a result, we were able to develop a minipig model of the metabolic syndrome in the groups receiving continuous intraportal infusions of glucose and lipids. Although the definition of the metabolic syndrome in pigs is still debatable, the key features of this syndrome in humans include visceral obesity, fasting blood glucose levels over 110mg/dL, insulin resistance, dyscholesterolemia, hypertriglyceridemia, and elevated blood pressure. Metabolic syndrome is defined as the presence of at least three of these criteria,⁷² which in our instance were at least visceral obesity, insulin resistance, and dyscholesterolemia. Type 2 diabetes and metabolic syndrome were frequently confused in many other studies that worked on developing type 2 diabetic pig models. Because of this, some researchers falsely claimed to have a legitimate preclinical minipig model of type 2 diabetes, despite the fact that the World Health Organization strictly defines diabetes as hyperglycemia and not by a variety of signs of insulin resistance. Minipigs demonstrated both hyperglycemia caused by the toxic medication's use and obesity with metabolic abnormalities in other studies when HFHSD and streptozotocin were combined.^{73,74} However, because metabolic disorders and hyperglycemia are in reality interrelated in the disease's genesis, it was in this case two different independent interventions that produced two phenotypic characteristics independently, raising question on the reliability of this type 2 diabetes paradigm.

Finally, it is intriguing to note that the only intervention that significantly impacted the way that glucose is metabolized was one in

which we mimicked an intestinal over absorption of glucose and lipids. Previous research suggested that one of the causes of the onset of type 2 diabetes would be an increase in the intestinal glucose absorption rate.^{75,76} Reciprocally, a study identified several intestinal sodium-glucose transporter 1 (SGLT1) variants that would be protective against type 2 diabetes and the progression of the metabolic syndrome.⁷⁷ It would be fascinating to see in future research if these SGLT1 variants are largely present in the pig. Additionally, the associated gene might provide a good target for developing genetically altered pig models and researching the effects on glucose metabolism.

Our study presents some limitations. We mentioned in a previous paragraph the probably too short duration of the intraportal glucose and lipids infusion to induce a more severe phenotype. The type-II error, associated to statistical analyses, could also have prevented us to highlight differences between strains or interventions, although the estimated minimal number of animals in each group was sufficient to demonstrate an effect.

In summary, we were successful in developing a preclinical minipig model with early signs of glucose intolerance and metabolic syndrome, but we were unsuccessful in obtaining a model of type 2 diabetes. Furthermore, the metabolic changes were in line with what had been reported about the disease's early pathogenesis. Thus, the pig continues to be a useful preclinical large animal model for imitating the metabolic syndrome, including insulin resistance, visceral obesity, and dyslipidemia, as we have verified in this work. The minipig, however, has more to contribute as a healthy model, supporting the necessity to choose the proper species for each type of study. The pig's continued difficulty in achieving a fasting hyperglycemia may prompt us to rethink using it as a translational diabetic subject in accordance with the WHO definition of diabetes mellitus.

AUTHOR CONTRIBUTIONS

Rébecca Goutchtat: Conceptualization (equal); data curation (equal); formal analysis (lead); investigation (equal); methodology (equal); project administration (equal); visualization (lead); writing – original draft (lead). **Audrey Quenon:** Data curation (equal); investigation (equal); methodology (equal); project administration (equal). **Manon Clarisse:** Data curation (equal); formal analysis (supporting); investigation (supporting); project administration (supporting). **Nathalie Delalleau:** Investigation (supporting). **Anaïs Coddeville:** Investigation (supporting). **Mathilde Gobert:** Investigation (supporting). **Valéry Gmyr:** Resources (equal); validation (lead); writing – review and editing (equal). **Julie Kerr-Conte:** Conceptualization (supporting); resources (equal); writing – review and editing (supporting). **François Pattou:** Conceptualization (equal); funding acquisition (lead); resources (equal); writing – review and editing (supporting). **Thomas Hubert:** Conceptualization (lead); funding acquisition (equal); investigation (equal); methodology (lead); project administration (supporting); resources (lead); supervision (lead); writing – review and editing (lead).

ACKNOWLEDGMENTS

The authors would like to extend their sincere gratitude to the European Genomic Institute for Diabetes (EGID) for funding this

study, the Institut National de la Santé et de la Recherche Médicale (Inserm) for the "Poste d'Accueil" stipend, the Agence Nationale de Recherche (ANR), all of the members of U1190 for their support, and all of the members of the Département Hospitalo-Universitaire de Recherche et d'Enseignement (Dhure), especially Thibaud Rabier, Sarah Lapière, Arnold Dive, Michel Pottier, Martin Fourdrinier, Louis Ballet, Frank Stevendart and Sabrina Decroix for animal care and Patrice Maboudou from Lille University Hospital for the analyses. Additionally, the authors warmly thank Pierre Bauvin for the statistical consulting and Amanda Elledge for the language reviewing.

FUNDING INFORMATION

The authors warmly thank the European Genomic Institute for Diabetes (EGID) for the funding and its precious contribution for animal disposal and housing, the Institut National de la Santé et de la Recherche Médicale (Inserm) for the stipend "Poste d'Accueil" and the Agence Nationale de Recherche (ANR).

CONFLICT OF INTEREST STATEMENT

The authors declare no conflict of interest.

DATA AVAILABILITY STATEMENT

The data that support the findings of this study are available from the corresponding author upon reasonable request.

ETHICAL APPROVAL

Animals were used in this investigation, which received approval from the local French Committee of Animal Research and Ethics (CEEA-75, n°18,915) in accordance with European law (2010/63/EU directive) and the widely accepted ARRIVE guidelines. The agreed-upon (n°D59-35010) Département Hospitalo-Universitaire de Recherche et d'Enseignement (Dhure) in Lille, France, was where all the procedures were carried out.

ORCID

Rébecca Goutchtat  <https://orcid.org/0000-0003-1880-5950>

Thomas Hubert  <https://orcid.org/0000-0002-5757-6436>

REFERENCES

- Afshin A, Reitsma MB, Murray CJL. Health effects of overweight and obesity in 195 countries over 25 years. *N Engl J Med*. 2017;377(1):13-27.
- World Health Organization, International Diabetes Federation. *Definition and Diagnosis of Diabetes Mellitus and Intermediate Hyperglycaemia: Report of a WHO/IDF Consultation*. World Health Organization; 2006:1-50.
- DeFronzo RA, Ferrannini E, Groop L, et al. Type 2 diabetes mellitus. *Nat Rev Dis Primers*. 2015;1(1):15019.
- Southam L, Soranzo N, Montgomery SB, et al. Is the thrifty genotype hypothesis supported by evidence based on confirmed type 2 diabetes- and obesity-susceptibility variants? *Diabetologia*. 2009;52(9):1846-1851.
- Ahlqvist E, Storm P, Käräjämäki A, et al. Novel subgroups of adult-onset diabetes and their association with outcomes: a data-driven cluster analysis of six variables. *Lancet Diabetes Endocrinol*. 2018;6(5):361-369.
- Raverdy V, Cohen RV, Caiazzo R, et al. Data-driven subgroups of type 2 diabetes, metabolic response, and renal risk profile after bariatric surgery: a retrospective cohort study. *Lancet Diabetes Endocrinol*. 2022;10(3):167-176.
- Schauer PR, Bhatt DL, Kirwan JP, et al. Bariatric surgery versus intensive medical therapy for diabetes — 5-year outcomes. *N Engl J Med*. 2017;376(7):641-651.
- Caiazzo R, Lassailly G, Leteurtre E, et al. Roux-en-Y gastric bypass versus adjustable gastric banding to reduce nonalcoholic fatty liver disease: a 5-year controlled longitudinal study. *Ann Surg*. 2014;260(5):893-899.
- Cummings DE, Arterburn DE, Westbrook EO, et al. Gastric bypass surgery vs intensive lifestyle and medical intervention for type 2 diabetes: the CROSSROADS randomised controlled trial. *Diabetologia*. 2016;59(5):945-953.
- Hofsø D, Fatima F, Borgeraas H, et al. Gastric bypass versus sleeve gastrectomy in patients with type 2 diabetes (Oseberg): a single-Centre, triple-blind, randomised controlled trial. *Lancet Diabetes Endocrinol*. 2019;7(12):912-924.
- LaFerrère B, Pattou F. Weight-independent mechanisms of glucose control after roux-en-Y gastric bypass. *Front Endocrinol*. 2018;9:9.
- Verhaeghe R, Zerrweck C, Hubert T, et al. Gastric bypass increases postprandial insulin and GLP-1 in nonobese minipigs. *Eur Surg Res*. 2014;52(1-2):41-49.
- Holst JJ, Madsbad S, Bojsen-Møller KN, et al. Mechanisms in bariatric surgery: gut hormones, diabetes resolution, and weight loss. *Surg Obes Relat Dis*. 2018;14(5):708-714.
- Marciniak C, Chávez-Talavera O, Caiazzo R, et al. Characterization of one anastomosis gastric bypass and impact of biliary and common limbs on bile acid and postprandial glucose metabolism in a minipig model. *Am J Physiol Endocrinol Metab*. 2021;320(4):E772-E783.
- Buchwald H, Buchwald JN. Metabolic (bariatric and nonbariatric) surgery for type 2 diabetes: a personal perspective review. *Diabetes Care*. 2019;42(2):331-340.
- Lutz TA. The use of rat and mouse models in bariatric surgery experiments. *Front Nutr*. 2016;3:10.
- Dolo PR, Shao Y, Li C, Zhu X, Yao L, Wang H. The effect of gastric bypass with a distal gastric pouch on glucose tolerance and diabetes remission in type 2 diabetes Sprague-Dawley rat model. *Obes Surg*. 2019;29(6):1889-1900.
- Chambers AP, Stefater MA, Wilson-Perez HE, et al. Similar effects of roux-en-Y gastric bypass and vertical sleeve gastrectomy on glucose regulation in rats. *Physiol Behav*. 2011;105(1):120-123.
- Haange SB, Jehmlich N, Krügel U, et al. Gastric bypass surgery in a rat model alters the community structure and functional composition of the intestinal microbiota independently of weight loss. *Microbiome*. 2020;8(1):13.
- Simianu VV, Sham JG, Wright AS, et al. A large animal survival model to evaluate bariatric surgery mechanisms. *Surg Sci*. 2015;6(8):337-345.
- Renner S, Dobenecker B, Blutke A, et al. Comparative aspects of rodent and nonrodent animal models for mechanistic and translational diabetes research. *Theriogenology*. 2016;86(1):406-421.
- Gerstein HC. Why don't pigs get diabetes? Explanations for variations in diabetes susceptibility in human populations living in a diabetogenic environment. *Can Med Assoc J*. 2006;174(1):25-26.
- Larsen MO, Rolin B. Use of the Gottingen minipig as a model of diabetes, with special focus on type 1 diabetes research. *ILAR J*. 2004;45(3):303-313.
- Larsen MO, Elander M, Sturis J, et al. The conscious Göttingen minipig as a model for studying rapid pulsatile insulin secretion in vivo. *Diabetologia*. 2002;45(10):1389-1396.

25. Sturek M, Alloosh M, Wenzel J, et al. Ossabaw Island miniature swine: cardiometabolic syndrome assessment. In: Michael Swindle M, ed. *Swine in the Laboratory*. CRC Press; 2007:397-402.
26. Heinke S, Ludwig B, Schubert U, et al. Diabetes induction by total pancreatectomy in minipigs with simultaneous splenectomy: a feasible approach for advanced diabetes research. *Xenotransplantation*. 2016;23(5):405-413.
27. Kin T, Korbitt GS, Kobayashi T, Dufour JM, Rajotte RV. Reversal of diabetes in pancreatectomized pigs after transplantation of neonatal porcine islets. *Diabetes*. 2005;54(4):1032-1039.
28. Strauss A, Moskalenko V, Tiurbe C, et al. Goettingen minipigs (GMP): comparison of two different models for inducing diabetes. *Diabetol Metab Syndr*. 2012;4(1):7.
29. Larsen MO, Wilken M, Gotfredsen CF, Carr RD, Svendsen O, Rolin B. Mild streptozotocin diabetes in the Göttingen minipig. A novel model of moderate insulin deficiency and diabetes. *Am J Physiol Endocrinol Metab*. 2002;282(6):E1342-E1351.
30. Larsen MO, Rolin B, Ribel U, et al. Valine Pyrrolidide preserves intact glucose-dependent insulinotropic peptide and improves abnormal glucose tolerance in minipigs with reduced β -cell mass. *Exp Diabetes Res*. 2003;4(2):93-105.
31. Hara H, Lin YJ, Zhu X, et al. Safe induction of diabetes by high-dose streptozotocin in pigs. *Pancreas*. 2008;36(1):31-38.
32. Manell EAK, Rydén A, Hedenqvist P, Jacobson M, Jensen-Waern M. Insulin treatment of streptozotocin-induced diabetes re-establishes the patterns in carbohydrate, fat and amino acid metabolisms in growing pigs. *Lab Anim*. 2014;48(3):261-269.
33. Koopmans SJ, Mroz Z, Dekker R, Corbijn H, Ackermans M, Sauerwein H. Association of insulin resistance with hyperglycemia in streptozotocin-diabetic pigs. *Metabolism*. 2006;55(7):960-971.
34. Li SJ, Ding ST, Mersmann HJ, Chu CH, Hsu CD, Chen CY. A nutritional nonalcoholic steatohepatitis minipig model. *J Nutr Biochem*. 2016;28:51-60.
35. Christoffersen B, Golozoubova V, Pacini G, Svendsen O, Raun K. The young göttingen minipig as a model of childhood and adolescent obesity: influence of diet and gender: the young Göttingen minipig. *Obesity*. 2013;21(1):149-158.
36. Johansen T, Hansen HS, Richelsen B, Malmlöf K. The obese Göttingen minipig as a model of the metabolic syndrome: dietary effects on obesity, insulin sensitivity, and growth hormone profile. *Comp Med*. 2001;51(2):6.
37. Liu Y, Yuan J, Xiang L, et al. A high sucrose and high fat diet induced the development of insulin resistance in the skeletal muscle of Bama miniature pigs through the Akt/GLUT4 pathway. *Exp Anim*. 2017;66(4):387-395.
38. Lim RR, Grant DG, Olver TD, et al. Young Ossabaw pigs fed a Western diet exhibit early signs of diabetic retinopathy. *Invest Ophthalmol Vis Sci*. 2018;59(6):2325.
39. Zou X, Ouyang H, Yu T, et al. Preparation of a new type 2 diabetic miniature pig model via the CRISPR/Cas9 system. *Cell Death Dis*. 2019;10(11):823.
40. Backman M, Flenkenthaler F, Blutke A, et al. Multi-omics insights into functional alterations of the liver in insulin-deficient diabetes mellitus. *Mol Metab*. 2019;26:30-44.
41. Blutke A, Renner S, Flenkenthaler F, et al. The Munich MIDY pig biobank – a unique resource for studying organ crosstalk in diabetes. *Mol Metab*. 2017;6(8):931-940.
42. Renner S, Blutke A, Clauss S, et al. Porcine models for studying complications and organ crosstalk in diabetes mellitus. *Cell Tissue Res*. 2020;380(2):341-378.
43. Stoll B, Horst DA, Cui L, et al. Chronic parenteral nutrition induces hepatic inflammation, steatosis, and insulin resistance in neonatal pigs. *J Nutr*. 2010;140(12):2193-2200.
44. Burrin D, Sangild PT, Stoll B, et al. Translational advances in pediatric nutrition and gastroenterology: new insights from pig models. *Annu Rev Anim Biosci*. 2020;8(1):321-354.
45. Goutchtat R, Chetboun M, Wiart JF, et al. Long-term analgesia following a single application of fentanyl transdermal solution in pigs. *Eur Surg Res*. 2021;62(2):115-120.
46. Ferrer J, Scott WE, Weegman BP, et al. Pig pancreas anatomy: implications for pancreas procurement, preservation, and islet isolation. *Transplantation*. 2008;86(11):1503-1510.
47. Cook PR, Glenn C, Armston A. Effect of hemolysis on insulin determination by the Beckman coulter unicell DXI 800 immunoassay analyzer. *Clin Biochem*. 2010;43(6):621-622.
48. Singh B. Surrogate markers of insulin resistance: a review. *WJD*. 2010;1(2):36.
49. Abdul-Ghani MA, Matsuda M, Balas B, DeFronzo RA. Muscle and liver insulin resistance indexes derived from the oral glucose tolerance test. *Diabetes Care*. 2007;30(1):89-94.
50. Hubert T, Jany T, Marcelli-Tourvieille S, et al. Acute insulin response of donors is correlated with pancreatic islet isolation outcome in the pig. *Diabetologia*. 2005;48(10):2069-2073.
51. Hubert T, Strecker G, Gmyr V, et al. Acute insulin response to arginine in deceased donors predicts the outcome of human islet isolation. *Am J Transplant*. 2008;8(4):872-876.
52. Dyson MC, Alloosh M, Vuchetich JP, Mokelke EA, Sturek M. Components of metabolic syndrome and coronary artery disease in female Ossabaw swine fed excess atherogenic diet. *Comp Med*. 2006;56(1):11.
53. Newell-Fugate AE, Lenz K, Skenandore C, Nowak RA, White BA, Braundmeier-Fleming A. Effects of coconut oil on glycemia, inflammation, and urogenital microbial parameters in female Ossabaw mini-pigs. Gonzalez-Bulnes A, ed. *PLoS One*. 2017;12(7):e0179542.
54. Powell CR, Kim A, Roth J, et al. Ossabaw pig demonstrates detrusor fibrosis and detrusor underactivity associated with oxidative stress in metabolic syndrome. *Comp Med*. 2020;70(5):329-334.
55. Sham JG, Simianu VV, Wright AS, et al. Evaluating the mechanisms of improved glucose homeostasis after bariatric surgery in Ossabaw miniature swine. *J Diabetes Res*. 2014;2014:1-7.
56. Lee L, Alloosh M, Saxena R, et al. Nutritional model of steatohepatitis and metabolic syndrome in the Ossabaw miniature swine. *Hepatology*. 2009;50(1):56-67.
57. Neeb ZP, Edwards JM, Alloosh M, Long X, Mokelke EA, Sturek M. Metabolic syndrome and coronary artery disease in Ossabaw compared with Yucatan swine. *Comp Med*. 2010;60(4):16.
58. Uceda DE, Zhu XY, Woollard JR, et al. Accumulation of pericardial fat is associated with alterations in heart rate variability patterns in hypercholesterolemic pigs. *Circ Arrhythm Electrophysiol*. 2020;13(4):e007614.
59. Dufrane D, van Steenberghe M, Guiot Y, Goebbels RM, Saliez A, Gianello P. Streptozotocin-induced diabetes in large animals (pigs/primates): role of GLUT2 transporter and β -cell plasticity. *Transplantation*. 2006;81(1):36-45.
60. Badin JK, Kole A, Stivers B, et al. Alloxan-induced diabetes exacerbates coronary atherosclerosis and calcification in Ossabaw miniature swine with metabolic syndrome. *J Transl Med*. 2018;16(1):58.
61. Larsen MO, Rolin B, Gotfredsen CF, Carr RD, Holst JJ. Reduction of beta cell mass: partial insulin secretory compensation from the residual beta cell population in the nicotinamide-streptozotocin Göttingen minipig after oral glucose in vivo and in the perfused pancreas. *Diabetologia*. 2004;47(11):1873-1878.
62. Castex F, Leroy J, Broca C, et al. Differential sensitivity of human islets from obese versus lean donors to chronic high glucose or palmitate. *J Diabetes*. 2020;12(7):532-541.
63. Everett-Grueter C, Edgerton DS, Donahue EP, et al. The effect of an acute elevation of NEFA concentrations on glucagon-stimulated hepatic glucose output. *Am J Physiol Endocrinol Metab*. 2006;291(3):E449-E459.
64. Warner SO, Wadian AM, Smith M, et al. Liver glycogen-induced enhancements in hypoglycemic counterregulation require

- neuroglucopenia. *Am J Physiol Endocrinol Metab.* 2021;320(5):E914-E924.
65. Ito K, Hao L, Wray AE, Ross AC. Lipid emulsion administered intravenously or orally attenuates triglyceride accumulation and expression of inflammatory markers in the liver of nonobese mice fed parenteral nutrition formula. *J Nutr.* 2013;143(3):253-259.
 66. Alonso LC, Yokoe T, Zhang P, et al. Glucose infusion in mice: a new model to induce β -cell replication. *Diabetes.* 2007;56(7):1792-1801.
 67. Hagman DK, Latour MG, Chakrabarti SK, et al. Cyclical and alternating infusions of glucose and intralipid in rats inhibit insulin gene expression and Pdx-1 binding in islets. *Diabetes.* 2008;57(2):424-431.
 68. Hoy AJ, Bruce CR, Cederberg A, et al. Glucose infusion causes insulin resistance in skeletal muscle of rats without changes in Akt and AS160 phosphorylation. *Am J Physiol Endocrinol Metab.* 2007;293(5):E1358-E1364.
 69. Del Prato S, Tiengo A. The importance of first-phase insulin secretion: implications for the therapy of type 2 diabetes mellitus. *Diabetes Metab Res Rev.* 2001;17(3):164-174.
 70. Marcelli-Tourvieille S, Hubert T, Pattou F, Vantyghem M. Acute insulin response (AIR): review of protocols and clinical interest in islet transplantation. *Diabetes Metab.* 2006;32(4):295-303.
 71. Samuel VT, Shulman GI. Mechanisms for insulin resistance: common threads and missing links. *Cell.* 2012;148(5):852-871.
 72. DeFronzo RA, Ferrannini E. Insulin resistance: a multifaceted syndrome responsible for NIDDM, obesity, hypertension, dyslipidemia, and atherosclerotic cardiovascular disease. *Diabetes Care.* 1991;14(3):173-194.
 73. Coelho PG, Pippenger B, Tovar N, et al. Effect of obesity or metabolic syndrome and diabetes on osseointegration of dental implants in a miniature swine model: a pilot study. *J Oral Maxillofac Surg.* 2018;76(8):1677-1687.
 74. von Wilmsowky C, Schlegel KA, Baran C, Nkenke E, Neukam FW, Moest T. Peri-implant defect regeneration in the diabetic pig: a pre-clinical study. *J Craniomaxillofac Surg.* 2016;44(7):827-834.
 75. Fiorentino TV, Suraci E, Arcidiacono GP, et al. Duodenal sodium/glucose cotransporter 1 expression under fasting conditions is associated with Postload hyperglycemia. *J Clin Endocrinol Metabol.* 2017;102(11):3979-3989.
 76. Tricò D, Mengozzi A, Frascerra S, Scozzaro MT, Mari A, Natali A. Intestinal glucose absorption is a key determinant of 1-hour Postload plasma glucose levels in nondiabetic subjects. *J Clin Endocrinol Metabol.* 2019;104(6):2131-2139.
 77. Seidelmann SB, Feofanova E, Yu B, et al. Genetic variants in SGLT1, glucose tolerance, and cardiometabolic risk. *J Am Coll Cardiol.* 2018;72(15):1763-1773.

How to cite this article: Goutchtat R, Quenon A, Clarisse M, et al. Effects of subtotal pancreatectomy and long-term glucose and lipid overload on insulin secretion and glucose homeostasis in minipigs. *Endocrinol Diab Metab.* 2023;00:e425. doi:[10.1002/edm2.425](https://doi.org/10.1002/edm2.425)